ONTOGENETIC AND STRATIGRAPHIC CRANIAL VARIATION IN THE CERATOPSID DINOSAUR *TRICERATOPS* FROM THE HELL CREEK FORMATION, MONTANA

by

John Benedetto Scannella

A dissertation submitted in partial fulfillment
of the requirements for the degree

of

Doctor of Philosophy

in

Earth Sciences

MONTANA STATE UNIVERSITY
Bozeman, Montana

April 2015

©COPYRIGHT

by

John Benedetto Scannella

2015

All Rights Reserved

ACKNOWLEDGEMENTS

Funding for this research was provided by grants from the Doris O. and Samuel P. Welles Research Fund of the University of California Museum of Paleontology, the Theodore Roosevelt Memorial Fund of the American Museum of Natural History, the Fritz Travel Grant of the Royal Ontario Museum, the Jurassic Foundation, and the Evolving Earth Foundation. Funding for travel to conferences was provided by the North American Paleontological Convention Student Travel Grant, the Society of Vertebrate Paleontology Jackson School of Geosciences Student Member Travel Grant, and the MSU Letters and Science Student Travel Grant. Many thanks also to Dr. Jack Horner, the Museum of the Rockies, the Sands Brothers, and Gerry Ohrstrom for graduate student funding and support. I thank my committee members Dr. Jack Horner, Dr. David Varricchio, Dr. David Roberts, Dr. Mark Goodwin and my graduate representative, Dr. Brendan Mumey, for their support and guidance. Thanks to all the curators, collections managers, graduate students, and volunteers who have permitted me to access their museum collections and displays. I thank my fellow MSU students, the staff and volunteers at the MOR, the MSU Earth Sciences Department, and the many friends I have made through SVP for exciting discussions and help along the way. I thank my parents, Ben and Mae Scannella, for taking me to the AMNH so many times when I was little. Thanks also to Angela Scannella, Regina Johnson, Preston Stewart, P.J. Stewart, and to Fred and Linda Baker. Special thanks to my sister, Christine Stewart, for taking me to the library and helping me take out books about dinosaurs when I was three. Finally, I thank my wife, Kari Scannella, for her love and support throughout the completion of this dissertation.

TABLE OF CONTENTS

1. INTRODUCTION TO DISSERTATION 1

A Brief Review of Early Studies of Ontogeny 2
A Brief Survey of Studies of Dinosaur Cranial Ontogeny 4
A Brief History of *Triceratops* Systematics 12
Triceratops Ontogeny 15
Variation in Stratigraphic Context 16
Summary of Dissertation 18
Literature Cited 23

2. *TOROSAURUS* MARSH, 1891 IS *TRICERATOPS* MARSH, 1889 (CERATOPSIDAE: CHASMOSAURINAE): SYNONYMY THROUGH ONTOGENY 32

Contribution of Author and Co-Authors 32
Manuscript Information Page 33
Abstract 34
Introduction 34
Institutional Abbreviations 35
Materials and Methods 36
Results 37
Ontogenetic Development of Parietal Fenestrae 37
Squamosal Elongation 39
The Ontogenetic Spectrum of *Triceratops* 40
Epiparietal and Episquamosal Variation 43
Osteohistology: a Test of Ontogenetic Hypotheses 45
Discussion 46
Ontogenetic Variation 46
Alternative Hypotheses 47
Implications for Dinosaur Diversity 49
Systematic Paleontology 49
Revised Diagnosis 49
Valid Species 50
Locality and Horizon (YPM 1820) 50
Synonyms 51
"Torosaurus" utahensis Gilmore, 1946 51
Remarks 51
Conclusions 52
Acknowledgments 53
Appendix 2.1: Sample of *Triceratops* Cranial Material Collected by MOR 65
Literature Cited 67

TABLE OF CONTENTS – CONTINUED

3. '*NEDOCERATOPS*': AN EXAMPLE OF A TRANSITIONAL MORPHOLOGY 72

Contribution of Author and Co-Authors 72
Manuscript Information Page 73
Abstract 74
Background 74
Methodology/Principal Findings 74
Conclusions/Significance 75
Introduction 75
Institutional Abbreviations 78
Results 79
Reassessment of USNM 2412 79
Nasal and Nasal Horn 79
Postorbital Horn Cores 80
Parietal Fenestrae 81
Squamosal Morphology 81
Episquamosal Number 82
Discussion 83
Taxonomic Status of '*Nedoceratops hatcheri*' 83
Taxonomic Status of *'Torosaurus latus'* 84
Variation in Epiossification Number and Position 84
The parietal of USNM 2412 as Intermediate between *Triceratops* and *'Torosaurus'* 88
Juvenile '*Torosaurus latus*' 91
Transitional Morphologies and Dinosaur Systematics 93
Conclusions 94
Materials and Methods 96
Acknowledgements 96
References 106

4. A STRATIGRAPHIC SURVEY OF TRICERATOPS LOCALITIES IN THE HELL CREEK FORMATION, NORTHEASTERN MONTANA (2006-2010) 111

Contribution of Author and Co-Authors 111
Manuscript Information Page 112
Abstract 113
Introduction 113
Institutional Abbreviations 116
Materials and Methods 117
Triceratops Localities 118

TABLE OF CONTENTS - CONTINUED

UCMP Locality V88001 (High Ceratopsian): UCMP Specimen 137263 118
UCMP Locality V83224 (Dave's Nose): UCMP Specimen 128561 119
UCMP Locality V88081 (Russell Basin *Triceratops*):
UCMP Specimen 136092 120
UCMP Locality V75046 (Ruben's *Triceratops*):
UCMP Specimen 113697 121
MOR Locality HC-135 (MORT): MOR Specimen 004 122
MOR Locality HC-425 (Afternoon Delight): MOR Specimen 2569 122
MOR Locality HC-531 (Lauren's Trike): MOR Specimen 2938 123
MOR Locality HC-520 (Joe's Half Day Trike): MOR Specimen 2923 123
MOR Locality HC-702 (JD Trike12): MOR Specimen 3056 and
MOR Locality HC-541 (JD Trike14): MOR Specimen 2950 124
MOR Locality HC-426 (Mark's Scavenged Trike): MOR Specimen
2570 and MOR Locality HC-639 (Anky Breaky Heart):
MOR Specimen 3011.....125
MOR Locality HC-430 (Quittin' Time): MOR Specimens
2574 and 2702.....126
MOR Locality HC-521 (Lon's Trike): MOR Specimen 2924 126
MOR Locality HC-571 (Seth's Trike): MOR Specimen 2979 and
MOR Locality HC-543 (TriSarahTops): MOR Specimen 2980.....127
MOR Locality HC-544 (DFJuvieTrike3): MOR Specimen 2951 and
MOR Locality HC-627 (Situ But Sad): MOR Specimen 2999 127
MOR Locality HC-565 (Supernasal): MOR Specimen 2972 and
MOR Locality HC-628 (Ashes Trike): MOR Specimen 3000 128
MOR Locality HC-573 (Three Amigos): MOR Specimen 2982 and
MOR Locality HC-576 (Six O'Clock Trike): MOR Specimen 2985 129
MOR Locality HC-532 (Ducky Tail): MOR Specimen 6648 130
MOR Locality HC-638 (Golden Goose): MOR Specimen 3010.....131
MOR Locality HC-668 (Yoshi's Trike: MOR Specimen 3027 and
MOR Locality HC-682 (Cliffhanger): MOR Specimen 3045 131
MOR Locality HC-716 (Little Horny Devil): MOR Specimen 3064.....132
Discussion and Conclusions 132
Acknowledgments.....134
Appendix 4.1: Catalogued MOR Specimens of *Triceratops* 152
References Cited 159

5. EVOUTIONARY TRENDS IN TRICERATOPS FROM THE
HELL CREEK FORMATION, MONTANA 164

Contribution of Author and Co-Authors.....164
Manuscript Information Page 165

TABLE OF CONTENTS - CONTINUED

Abstract 166
Significance Statement 166
Introduction 167
Results 168
L3 *Triceratops* 169
M3 *Triceratops* 169
U3 *Triceratops* 170
Shifts in Morphology over Time 171
Cladistic and Stratocladistic Analyses 172
Discussion 174
Evolutionary Patterns 174
A Biogeographic Signal? 177
Anagenesis and Cladogenesis 177
Conclusions 179
Materials and Methods 179
Acknowledgments 181
References 187

6. A MORPHOMETRIC ANALYSIS OF CASQUE DEVELOPMENT AND VARIATION IN THE BLACK-CASQUED HORNBILL (*CERATOGYMNA ATRATA*) 192

Contribution of Author and Co-Authors 192
Manuscript Information Page 193
Abstract 194
Introduction 195
Ceratogymna atrata: the Black-casqued Hornbill 197
Materials and Methods 198
Results 200
Relative Growth 200
Multivariate Analyses 201
Discussion 204
Implications for Casque Function 206
Conclusions 210
Acknowledgments 210
Literature Cited 218

7. A MORPHOMETRIC ANALYSIS OF TRENDS IN CRANIAL MORPHOLOGY IN *TRICERATOPS* AND "*TOROSAURUS*" FROM THE HELL CREEK FORMATION, MONTANA 223

Contribution of Author and Co-Authors 223
Manuscript Information Page 224

TABLE OF CONTENTS – CONTINUED

Abstract 225
Introduction 226
Institutional Abbreviations 229
Methods 230
Results 236
Relative Growth 236
Multivariate Analyses 237
Geometric Morphometric Analyses 239
Epinasal 242
Postorbital Horn Cores 243
Squamosal 244
Parietal 245
Nasal 246
Nasal Process of the Premaxilla (NPP) 247
Fisher's Exact Tests 248
Discussion 249
Stratigraphic Trends 249
Ontogenetic trends and the Synonymy of *Triceratops* and "*Torosaurus*" 252
Conclusions 260
Acknowledgments 261
Literature Cited 277

8. CONCLUSIONS 282

Literature Cited 286

REFERENCES CITED 287

APPENDICES 312

APPENDIX A: Supplementary Information for Chapter 5 (SI Text, Figures 5.S1 through 5.S7, Supporting Material References, and Dataset 5.S1) 312
APPENDIX B: Supplementary Information for Chapter 6 (Appendices 6.1 through 6.6) 364
APPENDIX C: Supplementary Information for Chapter 7 (Appendices 7.1 through 7.28) 422

LIST OF TABLES

Table Page

2.1. Ontogenetic trends expressed in the parietal-squamosal frill of *Triceratops*.....63

2.2. Growth stages of *Triceratops* (modified from Horner and Goodwin, 2006).....64

6.1 MANOVA results 217

LIST OF FIGURES

Figure Page

2.1. Development of thin regions of the parietal throughout *Triceratops* ontogeny 55

2.2. *Triceratops* parietal fragment, MOR 2946, showing the histology of the ventral erosion surface 56

2.3. Ontogenetic elongation of the squamosals in *Triceratops*....57

2.4. Squamosal elongation in *Triceratops* 58

2.5. Comparison of AMNH 5116 to "*Torosaurus latus*" specimens 59

2.6. The parietal of *Triceratops* specimen MOR 2923 70

2.7. Osteohistology of an ontogenetic sequence of *Triceratops* postobrial horn cores....61

2.8. The dorsoventrally flattened epoccipitals of "*Torosaurus*" specimen ANSP 15192 reveal ontogenetic maturity 62

3.1. USNM 2412, the holotype and only specimen of '*Nedoceratops hatcheri*'....98

3.2. Nasal horn variation in *Triceratops* 99

3.3. Ventral view of the right half of the parietal of USNM 2412....100

3.4. Dorsal view of the parietal fenestra of USNM 2412 101

3.5. Lateral views of USNM 1201 and USNM 2412....102

3.6. Episquamosal of MOR 2975....103

3.7. Ventral view of the parietal of MOR 1122 104

3.8. Osteohistology of the postorbital horn core of MOR 981 105

LIST OF FIGURES – CONTINUED

Figure Page

4.1. Collection areas for specimens of *Triceratops* discussed in the text, south Fort Peck Lake in Garfield and McCone Counties, Montana 136

4.2. Relative positions of *Triceratops* localities discussed in the text superimposed on a generalized section 137

4.3. The Russell Basin *Triceratops* (UCMP 136092) 138

4.4. Relocating the Russell Basin *Triceratops* quarry (University of California Museum of Paleontology [UCMP] locality V88081) 139

4.5. Ruben's *Triceratops* (University of California Museum of Paleontology [UCMP] locality V75046) 140

4.6. Museum of the Rockies (MOR) Triceratops (MORT; MOR 004), jacketed and awaiting collection in 1981 141

4.7. Correlation of measured sections and Museum of the Rockies (MOR) *Triceratops* localities, ~4.5 km across the Short Creek area (Garfield, county, Fig. 4.1, locality 6) from northwest to southeast 142

4.8. Joe's Half Day Trike (Museum of the Rockies [MOR] locality HC-520) 143

4.9. Fowler discovers JDTrike12 (Museum of the Rockies [MOR] specimen 3056) eroding from a gray mudstone stratigraphically high n the upper unit of the Hell Creek Formation 144

4.10. JDTrike14 (Museum of the Rockies [MOR] locality HC-541) 145

4.11. Correlation of measured sections and Museum of the Rockies (MOR) *Triceratops* localities ~2.5 km across Lost Creek Bay area (Garfield County, Fig. 4.1, locality 5) from north to south 146

LIST OF FIGURES – CONTINUED

Figure Page

4.12. Museum of the Rockies (MOR) locality HC-571 plotted on measured section, Brownie Butte (Garfield County; Fig. 4.1, locality 1). 147

4.13. Seth's Trike (Museum of the Rockies [MOR] locality HC-571) 148

4.14. DFJuvieTrike3 (Museum of the Rockies [MOR] locality HC-544) 149

4.15. Correlation of measured sections and Museum of the Rockies *Triceratops* localities across ~6.5 km of the Pennick Coulee area (Garfield County, Fig. 1, locality 3) from northwest to southeast 150

4.16. Yoshi's Trike (Museum of the Rockies [MOR] locality HC-688) 151

5.1. Stratigraphic placement of HCF *Triceratops* reveals trends in cranial morphology including elongation of the epinasal and change in morphology of the rostrum 183

5.2. Stratigraphic variation in cranial morphology 184

5.3. Results of cladistic analysis of HCF *Triceratops* 185

5.4. Potential patterns of HCF *Triceratops* evolution 186

6.1. Hornbill taxa included in this study 211

6.2. Select measurements and landmarks 212

6.3. Hypothesized male *C. atrata* growth series 213

6.4. Standard major axis (SMA) regression results 214

6.5. Results of linear and geometric morphometric (GM) principal component analysis 215

6.6. Results of UPGMA cluster analyses 216

7.1. Select measurements and landmarks 262

7.2. Standard major axis (SMA) regression results 263

LIST OF FIGURES – CONTINUED

Figure Page

7.3. Results of PCA and cluster analyses of linear dataset 264

7.4. Results of PCA and cluster analyses of GM data for skulls in lateral view 265

7.5. Mean GM shape data for the skull in lateral view 266

7.6. Landmarks for GM analyses of individual bones 267

7.7. PCA of GM shape data for epinasal and postorbital horn cores 268

7.8. Mean GM shape data for epinasals 269

7.9. Mean GM shape data for postorbital horn cores 270

7.10. PCA of GM shape data for squamosals 271

7.11. Mean GM shape data for squamosals 272

7.12. PCA of GM shape data for the parietal, nasal, and nasal process of the premaxilla (NPP) 273

7.13. Mean GM shape data for nasals 274

7.14. The epinasal morphology of MOR 981 275

7.15. Morphology of the anteroventral process of the squamosal 276

ABSTRACT

Hypotheses regarding the taxonomy and systematics of non-avian dinosaurs are based on analyses of morphology. As such, it is critical to assess the potential roles of intraspecific variation in systematic interpretations. Ontogenetic (developmental) change has been found to be a potential contributor to taxonomic confusion in the fossil record of dinosaurs. Similarly, variation between specimens found at different stratigraphic levels should be assessed in order to decipher variation within and between closely related taxa. The chasmosaurine ceratopsid *Triceratops* has had a complicated taxonomic history due to variation in cranial morphology between specimens. Recent work in the uppermost Cretaceous Hell Creek Formation (HCF) has produced a large (n>50) new sample of specimens. Using this data set its possible to reassess variation in *Triceratops* and further explore chasmosaurine paleobiology. Building on previous work on *Triceratops* ontogeny, examination of the parietal-squamosal frill finds that these bones underwent a dramatic transformation late in ontogeny. The short, solid frill of *Triceratops* expanded into a more elongate, thin, fenestrated condition, which had previously been found to characterize the coeval ceratopsid taxon *Torosaurus latus*. This suggests that these taxa are synonymous with *Torosaurus* representing the mature form of *Triceratops* rather than a distinct taxon. Further, *Nedoceratops hatcheri*, which is represented by a single specimen with a small fenestra in the parietal, is hypothesized to represent a transitional morphology between unfenestrated and fully fenestrated (*Torosaurus*) specimens. Detailed locality information for specimens collected over the course of the Hell Creek Project permits for the placement of specimens in stratigraphic context. The two currently recognized species, *T. horridus* and *T. prorsus*, are stratigraphically separated within the HCF and cladistic and stratocladistic analyses are consistent with the evolution of *Triceratops* incorporating anagenetic (transformational) change. Morphometric analyses of the extant archosaur *Ceratogymna atrata* (the Black-casqued hornbill) indicate that enlarged cranial structures function as objects of visual display. Morphometric studies of *Triceratops* further suggest that specimens found lower in the formation may have attained the *Torosaurus* frill morphology through ontogeny, whereas this basal condition became increasingly rare higher in the formation. Morphometric results are also consistent with early divergence between two distinct genera.

CHAPTER ONE

INTRODUCTION TO DISSERTATION

"The remarkable reptiles which the writer recently described, and placed in a new family, the *Ceratopsidæ*, prove to be more and more wonderful as additional specimens are brought to light."

- O.C. Marsh, 1889

The study of non-avian dinosaurs is impeded by the vast stretch of time that separates these living animals from the paleontologists that study them. Attempts to decipher diversity levels in vanished ecosystems may be particularly hindered by an inability to directly observe the creatures in question. Current studies of vertebrate species diversity are largely based on the biological species concept [which states that members of a single species are those which can interbreed and produce fertile offspring (Mayr, 1942)]. As extinct taxa cannot, as of yet, be interbred to determine whether or not they would produce fertile offspring, attempts at taxonomic classification in the fossil record are largely restricted to morphological criteria (see Smith, 1994). This approach is contingent upon an ability to recognize the scope of intraspecific morphological variation in extinct taxa.

The majority of dinosaur taxa are known from one or only a handful of specimens; more often than not these specimens are incomplete. Small sample sizes limit insights into intrapopulation variation, including the changes taxa undergo throughout ontogeny as well as potential evolutionary changes. The importance of understanding variation within and between populations for deciphering evolutionary patterns has been

emphasized and contrasted with typological studies (e.g. Simpson, 1951; Padian and Horner, 2002). As we discover that several dinosaur genera underwent dramatic morphological changes as they matured (e.g. Rozhdestvensky, 1965; Dodson, 1975; Sampson, 1995; Horner and Goodwin, 2006, 2009) and that many of the most extreme changes occurred in the skull (which is considered to be amongst the most diagnostic parts of the skeleton) it becomes apparent that ontogenetic variation may be confused for variation between taxa (e.g. Rozhdestvensky, 1965; Dodson 1975a). This can lead to an inaccurate view of ecological structure and evolutionary relationships. Below is a short review of the role that dinosaur cranial ontogeny has played in the study of these animals.

A Brief Survey of Early Early Studies of Ontogeny

Long before Darwin published *On the Origin of Species* (Darwin, 1859), scientists had discovered that organisms go through a series of morphological changes as they grow. In 345 C.E., Aristotle pioneered the study of embryology by observing the development of chickens in their eggs (Hamburger and Hamilton, 1951; Horner and Gorman, 2009). This initial exploration of embryonic development provided the insight that the developing embryo underwent a dramatic transformation (Hamburger and Hamilton, 1951). Aristotle proposed that developing human embryos similarly underwent radical morphological changes and passed through stages of being inhabited by increasingly "higher" souls - from plant to animal to, ultimately, human (Gould, 1977). This parallel between embryonic development and the relationships between organisms foreshadowed major themes of ontogenetic hypotheses to be expressed in the 19th century (Gould, 1977).

Lorenz Oken, an early 19th century naturalist, proposed that development progressed from simplicity to greater complexity through the addition of structures and that this rule applied to both the development of individual organisms as well as species (Gould, 1977). Two major schools of thought developed on the foundations laid by Oken and his contemporaries once it came into public consciousness that species apparently were not immutable. Karl Ernst von Baer proposed that the embryos of different organisms go through a series of changes from a generalized morphology to more and more specialized morphologies, thus there was some similarity between embryos of all animals earlier in ontogeny. Alternatively, Ernst Haeckel famously proposed that "ontogeny recapitulates phylogeny" - that is, embryos actually go through the adult stages of their ancestors before taking on the morphology of their respective taxa (Gould, 1977). Haeckel's recapitulation hypothesis initially eclipsed Von Baer's theory of embryonic development ("Von Baer's Law"), but it fell out of favor during the "Modern Synthesis" once insights from Mendelian genetics were incorporated into evolutionary studies and revealed that the relationship between ontogeny and evolution was more complex than suggested by the recapitulation hypothesis (Gould, 1977; 1992).

In 1977, Stephen Jay Gould published *Ontogeny and Phylogeny*, a treatise lamenting the abandonment of consideration of the relationships between individual development and the evolution of taxa. Gould acknowledged that Haeckel's 'biogenetic law' was flawed - however, he believed the complete abandonment of the study of relationships between ontogeny and phylogeny was "a classic illustration of the old cliché (particularly relevant here, given the subject matter), of throwing out the baby with the bathwater" (Gould, 1992: 276). Gould suggested that in order to fully understand the

evolutionary history of life on earth, the understanding of a process introduced by Haeckel was critical: "heterochrony." Heterochrony was initially Haeckel's term for events incongruent with recapitulation, however it was later redefined by Gavin de Beer to represent evolutionary changes in developmental timing (de Beer, 1930; Gould, 1977, 2000). As paleontology incorporates both biology and geology, it is a field which is especially suited to explore the interactions between ontogeny and evolution throughout the history of life on Earth.

A Brief Survey of Studies of Dinosaur Cranial Ontogeny

An attempt at analyzing ontogenetic variation in dinosaurs was not possible until a largely complete growth series of a single taxon had been assembled. Though the first juvenile dinosaur was described in 1883 (a juvenile sauropod briefly described by O.C. Marsh [Marsh, 1883]), an extensive dinosaur growth series was not amassed until the famous Gobi expeditions of the American Museum of Natural History (AMNH) in the early 20th century (Brown and Schlaikjer, 1940b). These expeditions are perhaps most celebrated for the discovery of the first nests of dinosaur eggs, which at the time of their discovery were believed to belong to the protoceratopsian dinosaur *Protoceratops andrewsi* (Brown and Schlaikjer, 1940b; Thulborn, 1992). Expeditions by the AMNH in the 1990's would indicate that the true identity of the creator of several of these nests to be the theropod dinosaur *Oviraptor philoceratops* (Norell et al., 1995). However, despite this initial misidentification, the areas of the Gobi which the AMNH crews worked were rich in the remains of *Protoceratops*, and numerous specimens representing a range of ontogenetic stages from babies to adults were collected and returned to New York.

The initial description of *Protoceratops* was based on an incomplete skull which was missing much of the distinctive parietal-squamosal frill (Granger et al., 1923). Brown and Schlaikjer (1940) conducted a more detailed description of *Protoceratops* morphology based on different ontogenetic stages, with special attention given to changes throughout growth. The authors noted that the parietal-squamosal frill expands, the orbit becomes reduced, and the face deepens throughout ontogeny. They stated that "in the development from the young to the old individual, not a single important feature remains constant" (pg. 211). The collection of *Protoceratops* amassed by the AMNH remains one of most studied dinosaur growth series (Dodson, 1976; Thulborn, 1992; Makovicky et al., 2007). However, despite the wealth of information provided by this ontogenetic series, the importance of understanding dinosaur ontogeny for deciphering evolutionary trends was largely overlooked in the literature for several years after the initial *Protoceratops* study.

Rozhdestvenksy (1965) suggested that an understanding of ontogenetic variation was critical to deciphering dinosaur systematics. He pointed out that five species of Late Triassic prosauropods, which had been divided into three genera, actually represented different growth stages of a single species as they were distinguished based on characters related to relative growth. He also suggested that three asian tyrannosaurs (*Tyrannosaurus bataar*, *Tarbosaurus efremovi*, and *Gorgosaurus lancinator*) more likely represented different growth stages of a single tyrannosaur species: *Tarbosaurus bataar*. Rozhdestvensky observed that these taxa had been differentiated primarily by differences in size, relative robustness of the skull, and the number of teeth: characters which have been demonstrated to change throughout ontogeny (Brown and Schlaikjer, 1940). He also

considered dinosaur heterochrony (evolutionary changes in developmental timing, de Beer, 1930; Gould, 1977), noting that: "The extent of growth variation in dinosaurs is sometimes so great that juvenile individuals outwardly look very similar to adults of the preceding species rather than to adult individuals of the species to which they in fact belong. Growth changes are therefore of the greatest importance in determining the scope and boundaries of a species in this group" (Rozhdestvenksy, 1965: 96).

In a landmark study on the implications of cranial ontogeny, Peter Dodson (1975) revealed that the degree of morphological change which occurs in non-avian dinosaurs is comparable to that seen in some extant avian dinosaurs (birds) which retain juvenile morphology until they've achieved 65-80% adult size. This idea had been suggested previously by Nopcsa and Heidsieck (1933) based on the observation that smaller duck-billed dinosaurs which lacked cranial ornamentation exhibited immature bone microstructure. Nopcsa and Heidsieck suggested that cranial ornamentation developed later in ontogeny for the purpose of sexual display. Dodson demonstrated this ontogenetic trend morphometrically and concluded that such stark differences in appearance between individuals could easily lead to juveniles and adults being classified as distinct species rather than growth stages of a single taxon. In the 1975 study, he demonstrated how what were previously considered 12 species of lambeosaurines actually represented growth stages of far fewer taxa (three species representing two genera according to Dodson's study). Lambeosaurines have been the subject of studies in cranial ontogeny since Dodson's seminal work (e.g., Horner and Currie, 1994; Horner and Dobb, 1998; Evans, 2010; Brink et al., 2011). The more conservative cranial morphology of hadrosaurines has not prevented examinations of how these animals changed as they matured (e.g.

Horner, 1983; Horner et al., 1988; Freedman, 2009; Prieto-Marquez, 2010). Recent work on the large hadrosaur *Edmontosaurus* indicate that specimens previously assigned to a separate genus, *Anatotitan*, actually represent large individuals of *Edmontosaurus annectens* (Campione and Evans, 2011).

A small tyrannosaurid skull discovered in the upper Cretaceous deposits of Montana in 1942 was initially classified as a new species of *Gorgosaurus* (*lancensis*) (Gilmore, 1946) and was later placed in its own genus, *Nanotyrannus* (Bakker et al., 1988). This animal was estimated to have an adult length of 3 to 4 meters and so was thought to be a pygmy tyrannosaur. Bakker et al. (1988) noted the apparent fusion of several cranial elements as evidence of its maturity. An analysis of cranial variation in *Tyrannosaurus rex* (Carr, 1999) which took *Nanotyrannus* into consideration shed doubt on its validity. Carr noted that none of the elements which appeared to be fused were actually fused nor was there evidence of those elements being fused in any known tyrannosaurid regardless of ontogenetic stage (Carr, 1999). The differences between *Nanotyrannus* and *T.rex* could be accounted for by relative growth within a taxon; Carr hypothesized that *Nanotyrannus* was actually a juvenile *T.rex*. The synonymy of these two genera halved the known number of tyrannosaurs present in the Latest Cretaceous, though debate still continues over the validity of *Nanotyrannus* (see Larson, 2013).

Perhaps the most extreme changes in cranial morphology throughout ontogeny are found within the Marginocephalia, the clade of ornithischian dinosaurs which includes ceratopsians and pachycephalosaurs. Pachycephalosaurs are an enigmatic clade noted for their thickened fronto-parietal cranial domes (Brown and Schlaikjer, 1943). At least three taxa had been recognized within the upper Cretaceous Hell Creek Formation, among

these are: *Pachycephalosaurus* (Brown and Schlaikjer, 1943) which possessed a large, thickened dome with blunt squamosal nodes; *Stygimoloch* (Galton and Sues, 1983), a slightly smaller pachycephalosaur with a smaller dome and elongate squamosal spikes; and *Dracorex* (Bakker et al., 2006), a small taxon with no cranial dome and elongate squamosal spikes. A reassessment of these taxa incorporating histological analysis of bone microstructure (Horner and Goodwin, 2009) revealed the presence of highly vascularized bone and an open intrafrontal suture within the skull of *Stygimoloch*; indicators of relative immaturity. The tissue within the dome of *Pachycephalosaurus* was denser with less vascularization, suggestive of slower growth typically associated with greater maturity (Francillon-Vieillot et al., 1990; Chinsamy-Turan, 2005; Horner and Goodwin, 2009). The characters which distinguished these taxa appeared to be products of relative growth; *Dracorex* was hypothesized to represent the youngest known *Pachycephalosaurus* growth stage (no dome, long squamosal spikes) and *Pachycephalosaurus* represents the most mature (large dome, squamosal spikes reduced to blunt nodes). In *Pachycephalosaurus*, concurrent with the development of an enlarged fronto-parietal dome is the decrease in size of the squamosal spikes; the resorption of cranial structures throughout ontogeny is also noted in ceratopsians (Sampson, 1995; Sampson et al., 1997; Horner and Goodwin, 2006, 2008; Brown et al., 2009). Recent morphometric studies on the pachycephalosaur *Stegoceras* confirm that the cranial dome enlarged throughout growth in these animals and reveal a high degree of individual variation in cranial features (Schott et al., 2011; Schott and Evans, 2012).

In 1914, Gilmore described a new specimen of centrosaurine ceratopsid from the Two Medicine Formation of Montana. The specimen was named *Brachyceratops*

montanensis; the description of its distinctive generic characters included: "Typically of small size. Skull with facial portion much abbreviated, and deep vertically. Supraorbital horn cores small . . . (parietal) fenestrae of apparently small size . . ." (Gilmore, 1914:2). With ceratopsids being a relatively poorly represented dinosaur family at that time, it is understandable that these features might be considered taxonomically diagnostic. They have since been demonstrated to all be representative of ontogenetic immaturity (Dodson and Currie, 1988; Sampson, 1995; Sampson et al., 1997; Goodwin et al., 2006) and thus the current taxonomic affinities of this taxon are ambiguous due to a lack of morphological features which could be used to reliably diagnose it (McDonald, 2011).

Dodson (1986) described another small centrosaurine specimen from the Judith River of Montana (Figure 6). Among the characters used for the diagnosis of this proposed new taxon, *Avaceratops lammersi*, were the thin, smooth nature of many of the cranial elements and the borders of the frill. Cranial elements were relatively unsculptured, there was no indication of epi-ossifications, and the parietal appeared to be unfenestrated, though Dodson noted "thinning of the parietal in areas where parietal fenestrae may be expected . . . thinning need not imply fenestration. Gilmore . . faced the same problem with *Brachyceratops* . .. he inferred the existence of fenestrae; I infer the presence of a solid frill in *Avaceratops*" (Dodson, 1986: 308). In 1999 a second proposed specimen of *Avaceratops* was described (Penkalski and Dodson, 1999). The second specimen was found within the Judith River Formation, 125 km from the original *Avaceratops* locality. Referral to *Avaceratops* was based on the lack of ornamentation of the parietal, the apparent absence of fenestrae, and a protuberance on the squamosal similar to that seen on the holotype.

The discovery of a large *Centrosaurus* bone bed, containing individuals hypothesized to have died together in a catastrophic event, has yielded a tremendous amount of information on ontogenetic trends within centrosaurines as it apparently preserves representatives of a single population (Currie and Dodson, 1984; Ryan et al., 2001). Studies of this material (e.g. Sampson et al, 1997; Ryan et al., 2001, Frederickson and Tumarkin-Deratzian, 2014) revealed that centrosaurines underwent marked cranial changes throughout ontogeny, with juveniles appearing distinctly different from adults. Based on these studies, *Brachyceratops* and a similar small, enigmatic taxon *Monoclonius*, were classified as *nomen dubia*, immature animals of unknown taxonomic affinities more specific than centrosaurines (Sampson et al., 1997). Aside from a general increase in size, the parietal-squamosal frill changed dramatically throughout ontogeny with the most mature specimens developing enlarged hook-like projections bordering the parietal and epi-ossifications fusing to the lateral and posterior margins (hence the absence of these features in the holotypes of *Brachyceratops* and *Avaceratops* may be due to ontogenetic factors). Ryan et al. (2001) noted that based on comparative studies between taxa, centrosaurine juveniles appeared to be indistinguishable. The distinguishing characters of the parietal-squamosal frill did not appear until relatively late in ontogeny. Brown et al. (2009) mapped changes in surface texture which occur throughout centrosaurine ontogeny. The frills of juvenile individuals exhibit fine striations ("long-grained texture") which correspond to radial canals oriented in the direction of growth (Francillon-Vieillot et al., 1990; Sampson et al., 1997; Carr, 1999; Tumarkin-Deratzian, 2010). More mature specimens reduced the surface area covered by this juvenile texture; the most mature specimens exhibit a mottled/rugose rather than

clearly striated surface texture. Increase in surface area exhibiting the mature parietal surface texture is correlated with expansion of the fenestrae. The most mature individuals exhibit ornamentation (spikes or hooks) bordering the parietal.

Sampson (1995) described two centrosaurine taxa from the Late Cretaceous Two Medicine Formation. The specimens were discovered by Museum of the Rockies field crews in the 1980's and were represented by bone beds at two distinct stratigraphic levels within the formation (Horner et al., 1992). These centrosaurines were significant in that they demonstrated that the nasal ornamentation transformed dramatically throughout ontogeny. Sampson named specimens from the lower stratigraphic section *Einiosaurus procurvicornis* and specimens from the higher section *Achelousaurus horneri*. Both of these taxa possess small, relatively uncurved nasal horns (similar to the morphology seen in *Brachyceratops*) as juveniles. In more mature specimens, the nasal horn is markedly different. In *Einiosaurus*, more mature individuals possess a procurving, hook-like nasal horn. In *Achelousaurus*, the nasal horn appears to have procurved to the point of contact with the front of the skull; the dorsal surface of this 'horn' is extremely rugose, forming a nasal boss.

Until recently, there have been relatively few studies of cranial ontogeny in chasmosaurine ceratopsids. This may be tied to the relatively lower sample sizes (with a few noteable exceptions) available for chasmosaurines. Colbert and Bump (1947) considered variation within the Maastrichtian taxon *Torosaurus latus*, noting that the smallest specimen of this taxon appeared to have a relatively shorter parietal-squamosal frill compared to larger specimens. Lehman (1990; 2007) has described variation in *Agujaceratops* (previously *Chasmosaurus*; see Lucas et al., 2006) *mariscalensis* and

noted two distinct horn core morphologies throughout the sample which were suggested to represent sexual dimorphism.

Godfrey and Holmes (1995) surveyed material which had been assigned to the genus *Chasmosaurus* and noted that as length of the squamosals increased, so did the number of epiossifications on the lateral margin of these elements. A recent review of *Anchiceratops* (Mallon et al., 2011) similarly noted variation in epiossification number and position which may be tied to ontogeny. *Triceratops* is the latest occurring chasmosaurine ceratopsid and the most commonly recovered dinosaur in the latest Cretaceous Hell Creek Formation (Horner et al., 2011). As this taxon represents the subject of the current dissertation, its systematic history is considered in greater detail below.

A Brief History of *Triceratops* Systematics

Ostrom and Wellnhofer (Ostrom and Wellnhofer, 1990) referred to *Triceratops* as an example of "flawed systematics." Since its initial discovery, nearly every variation in morphology between specimens was considered grounds for the erection of a new species of *Triceratops*. Intraspecific, ontogenetic, and sexual variation was rarely taken into account. In fact, even before *Triceratops* was formally named it was a source of taxonomic confusion.

In 1887, George L. Cannon, Jr. sent O.C. Marsh a set of large fossil horn cores found near Denver, Colorado (Dodson, 1996). Marsh described the material as belonging to a new species of extinct giant bison, *Bison "alticornis*." The confusion was due, in large part to the fact that no one had at that point yet discovered a relatively complete

ceratopsian skull. Previously diagnosed species were fragmentary and often based largely on postcranial material. Poor stratigraphic resolution was also responsible for this misidentification. Marsh believed that the Formation which the specimen was collected from was deposited in the Cenozoic Era (Marsh, 1887) .

The discovery of a similar set of horn cores in Montana's Judith River Formation, which Marsh correctly identified as belonging to a dinosaur, "*Ceratops montanus*" (Marsh, 1888), revealed the presence of large horned dinosaurs in the Cretaceous. However, it wasn't until more complete ceratopsian specimens were discovered that Marsh acknowledged that *Bison "alticornis*" was, in fact, a dinosaur. It would turn out to possibly represent the first recorded specimen of *Triceratops* (Hatcher et al., 1907; Dodson, 1996).

In 1889, *Triceratops horridus* was named and described based on a partial skull lacking most of the parietal-squamosal frill. In the same paper that *T. horridus* was named (Marsh, 1889), two other species of *Triceratops* were erected. *Triceratops "flabellatus"* was diagnosed based on a large, relatively complete skull. It was the first ceratopsian specimen which revealed that these animals had large bony crests projecting from their skulls. *Triceratops "galeus"* was named based on much less material, primarily a small nasal horn. This species was erected because the nasal horn was shaped slightly differently than other specimens. In 1890, a skull with a prominent ridge down the midline of its parietal was considered to be a new species, *Triceratops "serratus"*, based on this feature (Marsh, 1890a). In the same paper, *Triceratops prorsus* was erected for a skull with an elongate nasal horn. *Triceratops "sulcatus"* was erected for a specimen in which a pronounced groove was present on the posterior surface of each

postorbital horn core (Marsh, 1890b). *Triceratops "elatus"* was erected for a specimen with a relatively elongate parietal-squamosal frill (Marsh, 1891). *Triceratops "calicornis*" was based on a partial skull with a slightly concave nasal horn (Marsh, 1898). *Triceratops "obtusus*" was the name given to a partial skull with a small, blunt nasal horn (Marsh, 1898). This makes for nine species of *Triceratops* erected by Marsh before his death in 1899 (Dodson, 1996). Marsh also described two species of a new genus of three-horned ceratopsian from the same area of Wyoming as *Triceratops*: *Torosaurus latus* and *Torosaurus gladius* (Marsh, 1891).

In 1905, Marsh's colleague J.B. Hatcher described two new species. *Triceratops "brevicornis*" was erected for a partial skull with relatively short horn cores. In the same paper (Hatcher, 1905), "*Diceratops hatcheri"* was named by R.S. Lull to honor J.B. Hatcher, who didn't have the opportunity to give a name to the specimen before his death. It was placed in a separate genus based on small fenestrae in its parietal-squamosal frill (though Lull suggested these might be pathologic) and the apparent lack of a nasal horn. This skull is the subject of some interest as its taxonomic placement has been the subject of some debate (Forster, 1996; Farke, 2011; Scannella and Horner, 2011; Longrich and Field, 2012). In 1915, Lull named *Triceratops "ingens*" (Lull, 1915) based on a partial skull. This species was erected without a diagnosis or a description (Ostrom and Wellnhofer, 1986; Forster, 1996).

In 1933, Barnum Brown erected *Triceratops "maximus*" (Brown, 1933) based on several dorsal vertebrae which were found to be unusually large. *Triceratops "eurycephalus*" was established for a small skull with an unusually wide parietal-squamosal frill (Schlaikjer, 1935; Ostrom and Wellnhofer, 1986). The most recently

named species of *Triceratops* was *Triceratops "albertensis*," a large partial skull in which the postorbital horn core is directed vertically (Sternberg, 1949).

No fewer than sixteen species of *Triceratops* have been named based on small variations in cranial morphology. The possibility of intraspecific variation accounting for at least some of these morphologies was not addressed at length until Ostrom and Wellnhofer (1986) compared the variation found amongst the type specimens of these species to that found in extant horned mammals. Based on this comparison, they reduced the number of species of *Triceratops* from sixteen to one: *Triceratops horridus*, the type species.

Ten years later, Forster (1996) applied cladistic and morphometric approaches to examine *Triceratops* taxonomy. Her analysis suggested that *Nedoceratops* (= "*Diceratops*") *hatcheri* (Ukrainsky, 2007, 2009; Mateus, 2008) was a distinct genus, rather than a species of *Triceratops*. She also resurrected *Triceratops prorsus*. This is where *Triceratops* taxonomy currently stands, with two valid species (*T. horridus* and *T. prorsus*) though there is still some disagreement over whether or not these taxa are actually distinct (Farke, 1997; Lehman, 1998; Goussard, 2006).

Triceratops Ontogeny

Until recently, the ontogeny of *Triceratops* was unknown aside from the description of small, isolated postorbital horn cores (Brown and Schlaikjer, 1940a; Tokaryk, 1997). The discovery of a partial skull of a small juvenile *Triceratops* revealed that the postorbital horn cores were present at a very early age; suggesting that they functioned primarily as display structures for species recognition or social signaling

(Goodwin et al., 2006; Padian and Horner, 2011a). The multi-institutional Hell Creek Project (HCP), spearheaded by the Museum of the Rockies, is an extensive study of the upper Cretacous Hell Creek Formation which has resulted in the collection over 50 new specimens of *Triceratops*, including representatives of babies, juveniles, subadults, and adults (no eggs or embryos have yet been recovered). The first description of a growth series of *Triceratops* skulls revealed that radical changes in morphology occurred throughout ontogeny (Horner and Goodwin, 2006; 2008). Postorbital horn cores reoriented throughout development, going from straight in the smallest specimens, to posteriorly curved in larger juveniles, to anteriorly curved in the most mature individuals. Concurrent with this was the flattening of the initially triangular epiossifications on the frill margin.

Variation in Stratigraphic Context

A dimension of variation which is often obscured to neontologists is the degree to which morphological features may vary over the course of evolution. Paleontologists are uniquely positioned to make comparisons between specimens found at different stratigraphic levels in order to investigate evolutionary trends. As with studies of ontogenetic change, studies of morphological evolution are facilitated by larger sample sizes. For example, if a taxon is only represented by two specimens which were found stratigraphically separated, it may be difficult to distinguish evolutionary changes from other forms of variation (such as ontogenetic, sexual, or individual).

Sexual dimorphism has been suggested as a source of variation in several dinosaur taxa, including hadrosaurs (Dodson, 1975a) and ceratopsians (Dodson, 1976

[but see Evans et al., 2006]; Lehman, 1990). To date, sexual dimorphism in the sense originally formulated by Darwin (in which a structure is only present or greatly pronounced in one of the sexes, 1859; Padian and Horner, 2011) has not been demonstrated. Suggested instances of dimorphism have generally been restricted to minor proportional differences (see discussions in Knell and Sampson, 2011; Padian and Horner, 2011a, 2011b, 2013; Knell et al., 2013a, 2013b). If such an instance of dimorphism is found in a non-avian dinosaur, it will be necessary to first eliminate the possibility that ontogeny or evolutionary change is the source of variation. This will require detailed stratigraphic data for specimens as well as a large enough sample size to permit study of ontogenetic changes. Ontogenetic and stratigraphic variation represent filters through which data sets can be screened in order to test the hypotheses of new taxa or sexual dimorphs.

Further, the consideration of ontogeny in stratigraphic context can reveal heterochronic trajectories (McKinney and McNamara, 1991). In the absence of precise stratigraphic data, relative position on a phylogenetic tree may be used to infer heterochronic shifts within clades (Long and McNamara, 1997). The fossil record for most groups of dinosaurs is complete enough to allow for some consideration of heterochronic trajectories, at least at course scales. More detailed analyses are only possible with data sets large enough to allow for studies of variation between specimens and stratigraphic data detailed enough to permit precise placement of specimens.

Extensive field studies conducted in the Two Medicine Formation of northwestern Montana allowed for the stratigraphic placement of several dinosaur taxa and revealed apparent evolutionary trends in cranial morphology over time (Horner et al., 1992).

Perhaps the most dramatic hypothesized transformation was that of the centrosaurine ceratopsids found in the upper part of the formation. A stratigraphic succession of ceratopsids exhibits morphological trends which were originally hypothesized to be the product of anagenesis (evolutionary transformation of a lineage through time; Horner et al., 1992). Sampson (1995) in his description of this material, erected the taxa *Einiosaurus* and *Achelousaurus*. Sampson recognized that these taxa underwent dramatic changes in cranial morphology throughout ontogeny but suggested that the hypothesis of anagenetic evolution between the stratigraphically separated taxa would require a larger sample size to confirm, and suggested that cladogenesis (branching evolution) was a more conservative interpretation of the data. More recently, Campione and Evans (2011) explored cranial variation in *Edmontosaurus* and noted that the two currently recognized species (*E. regalis* and *E. annectens*) do not overlap stratigraphically. They suggested two alternative evolutionary scenarios: that these two species were produced by a cladogenetic branching event or, alternatively, that *E. regalis* may have evolved into *E. annectens* through anagenesis. As with the Two Medicine centrosaurines, without stratigraphic context for these specimens the potential to explore the modes of evolution in these animals would remain obscured.

Summary of Dissertation

The large sample of vertebrate fossils collected over the course of the Hell Creek Project (HCP) provides an opportunity to examine trends in morphology throughout the stratigraphic succession of the formation (Horner et al., 2011). As *Triceratops* is the most commonly recovered dinosaur in the formation, representing approximately 40% of

dinosaur skeletons found during a census of taxa in the formation (Horner et al., 2011), it is an ideal starting point to examine morphological variation and trends in the last non-avian dinosaurs. Further, as a ceratopsid, *Triceratops* exhibits interesting "bizarre" cranial structures (horns and frill), the function of which has been the subject of ongoing research and debate (see, for example, Padian and Horner, 2011; Knell and Sampson, 2011).

Horner and Goodwin (2006) noted ontogenetic changes in the shapes of the postorbital horn cores and epiossifications of the parietal-squamosal frill. Chapter Two expands upon this study, and examines ontogenetic trends in the parietal and squamosal. *Triceratops* has been distinguished from the coeval ceratopsid, *Torosaurus latus*, based on the morphology of the parietal-squamosal frill. Whereas *Triceratops* is typically found to exhibit a short, solid parietal-squamosal frill, *Torosaurus* has an expanded frill with a fenestrated parietal. Examination of an ontogenetic series of *Triceratops* frill elements reveals that as *Triceratops* matures, thin regions of bone develop in the parietal. These thin regions initially form on the lateral margins of this element, but as growth proceeds the thin regions are found medial to the lateral margins. In the most mature specimens, these thinning regions are found in the areas of the parietal where specimens of *Torosaurus* have fenestrae. Concurrent with the thinning of the parietal in *Triceratops* is an ontogenetic elongation of the squamosals. The most mature individuals approach the elongate, blade-like morphology seen in *Torosaurus*. Further, examination of the osteohistology of the postorbital horn cores of *Triceratops* and *Torosaurus* reveals a greater degree of secondary remodeling in specimens of *Torosaurus* than is seen in even the largest specimens of *Triceratops*. These lines of evidence suggest that rather than

being a distinct taxon, *Torosaurus latus* actually represents the mature form of *Triceratops*.

Chapter Three examines the morphology of the problematic taxon *Nedoceratops hatcheri*. Recently redescribed by Farke (2011), *Nedoceratops* is distinguished from *Triceratops* (and *Torosaurus*) by the morphology of the parietal-squamosal frill and the horn cores. In light of variation noted in horn core morphology in *Triceratops* and other chasmosaurines, the horn cores of *Nedoceratops* do not appear to be diagnostic. Further, *Nedoceratops* exhibits a small fenestra in the area of the parietal where *Triceratops* has a thin region and *Torosaurus* has a large fenestra. This suggests that rather than being a distinct taxon, *Nedoceratops* may instead represent a transitional morphology between young adult *Triceratops* (with a solid parietal) and the fenestrated condition seen in the most mature individuals (previously referred to *Torosaurus*).

Chapter Four presents the results of a stratigraphic survey of *Triceratops* localities over the course of the HCP, specifically the years 2006 through 2010. Many of the *Triceratops* specimens collected in the late 19th and early 20th centuries (including most of the holotype specimens) had limited stratigraphic information associated with them. Lull (1915) compiled a record of the stratigraphic position of specimens based on the available data, though the precise placement of these specimens has been questioned (Ostrom and Wellnhofer, 1986; Farke, 1997). As such, this chapter presents detailed stratigraphic information for *Triceratops* from the Hell Creek Formation, in order to have this data available for future researchers and also to serve as the foundation for an examination of morphology in stratigraphic context.

Chapter Five presents the results of a detailed study of the cranial morphology of *Triceratops* in stratigraphic context. Forster (1996) recognized two species of *Triceratops*: *T. horridus* and *T. prorsus*. A survey of specimens collected over the HCP reveals that *T. prorsus* appears to be restricted to the upper unit of the formation and *T. horridus* is found lower in the formation. Further, specimens from the upper part of the middle unit of the formation exhibit a combination of *T. horridus* and *T. prorsus* features, which is suggestive of an evolutionary transition between these taxa. Spearman's rank correlation analyses reveal trends in the morphology of the epinasal, nasal, and nasal process of the premaxilla throughout the stratigraphic succession of the Hell Creek Formation. Cladistic and stratocladistic analyses are consistent with the hypothesis that the evolution of *Triceratops* may have incorporated anagenesis, the transformation of a population over time.

Chapter Six explores cranial variation in an extant archosaur which, like *Triceratops*, exhibits 'bizarre' cranial structures: the black-casqued hornbill (*Ceratogymna atrata*). A collection of 33 skulls of *C. atrata*, and six skulls of the sympatric taxa *C. elata* and *Bycanistes albotibialis*, from the Cameroon Province of Africa were the subject of morphometric analyses. Principal Component Analysis indicates that the sexes are easily distinguished by the morphology of cranial ornamentation, but that when these structures are removed from the analyses that sexes (and taxa) overlap in morphospace. This suggests that the cranial casque of these hornbills functions primarily as an object of sexual selection; a secondary role for species recognition is also possible.

Chapter Seven presents the results of morphometric analyses of *Triceratops* from the Hell Creek Formation. This chapter expands upon the findings of Chapter Five by

applying further statistical analyses to the HCP *Triceratops* dataset. Since the hypothesis that *Triceratops* and *Torosaurus* are synonymous was proposed (Scannella and Horner, 2010), this has been a subject of ongoing research and debate (Farke, 2011; Longrich and Field, 2012; Maiorino et al., 2013). Here, morphometric analyses are conducted to further explore and test proposed ontogenetic and evolutionary trends. Specimens collected by other institutions prior to the HCP are incorporated into geometric morphometric analyses of the dataset. Entire skulls are considered as well as elements which have been found to exhibit trends in morphology through ontogeny and/or the stratigraphic succession of the Hell Creek Formation. Results confirm many of the evolutionary trends noted in Chapter Five and suggest that *Triceratops* may have retained immature features of the parietal-squamosal frill longer in ontogeny over the course of its evolution. By the end of the Cretaceous, the *Torosaurus* morphology is rare or absent, and this may indicate that *T. prorsus* did not (or only relatively rarely) expressed the basal conditions of the frill (expanded and fenestrated) very late in ontogeny. Alternatively, *Triceratops* and *Torosaurus* may represent distinct taxa which diverged early in or prior to the deposition of the Hell Creek Formation and *Triceratops* evolved away from the *Torosaurus* morphology over time (*T. horridus* specimens exhibit more *Torosaurus* features than *T. prorsus* do). Removal of horns and frill from analyses causes overlap in morphospace between *Triceratops* and *Torosaurus* specimens (similar to what was observed when casque data was removed from *C. atrata* in Chapter Six), confirming that the shape of these structures differentiate *Triceratops* and *Torosaurus*. This result is consistent with these elements being used for visual display.

Literature Cited

Bakker, R. T., M. Williams, and P. J. Currie. 1988. *Nanotyrannus*, a new genus of pygmy tyrannosaur, from the latest Cretaceous of Montana. Hunteria 1:1–30.

Bakker, R. T., R. M. Sullivan, V. Porter, P. Larson, and S. J. Saulsbury. 2006. *Dracorex hogwartsia*, n. gen., n. sp., a spiked, flat-headed pachycephalosaurid dinosaur from the Upper Cretaceous Hell Creek Formation of South Dakota. New Mexico Museum of Natural History and Science Bulletin 35:331–345.

Brink, K. S., D. K. Zelenitsky, D. C. Evans, F. Therrien, and J. R. Horner. 2011. A sub-adult skull of *Hypacrosaurus stebingeri* (Ornithischia: Lambeosaurinae): anatomy and comparison. Historical Biology 23:63–72.

Brown, B. 1933. A gigantic ceratopsian dinosaur, *Triceratops maximus*, new species. American Museum Novitates, 649: 1-9.

Brown, B., and E. M. Schlaikjer. 1940a. The Origin of ceratopsian horn-cores. American Museum Novitates, 1065: 1-7.

Brown, B., and E. M. Schlaikjer. 1940b. The structure and relationships of *Protoceratops*. Transactions of the New York Academy of Sciences 2:99–100.

Brown, B., and E. M. Schlaikjer. 1943. A study of the troödont dinosaurs, with the description of a new genus and four new species. Bulletin of the AMNH; v. 82, article 5.

Brown, C. M., A. P. Russell, and M. J. Ryan. 2009. Pattern and transition of surficial bone texture of the centrosaurine frill and their ontogenetic and taxonomic implications. Journal of Vertebrate Paleontology 29:132–141.

Campione, N. E., and D. C. Evans. 2011. Cranial Growth and Variation in Edmontosaurs (Dinosauria: Hadrosauridae): Implications for Latest Cretaceous Megaherbivore Diversity in North America. PLoS ONE 6:e25186.

Carr, T. D. 1999. Craniofacial ontogeny in tyrannosauridae (Dinosauria, Coelurosauria). Journal of Vertebrate Paleontology 19:497–520.

Chinsamy-Turan, A. 2005. The Microstructure of Dinosaur Bone: Deciphering Biology with Fine-Scale Techniques. John Wiley & Sons, pp.

Colbert, E. H., and J. D. Bump. 1947. A skull of *Torosaurus* from South Dakota and a revision of the genus. Proceedings of the Academy of Natural Sciences of Philadelphia 93–106.

Currie, P. J., and P. Dodson. 1984. Mass death of a herd of ceratopsian dinosaurs. Third Symposium of Meso− Zoic Terrestrial Ecosystems 52–60.

Darwin, C. 1859. On the origins of species by means of natural selection. London: Murray.

de Beer, G. 1930. Embryology and Evolution. Clarendon Press, Oxford. pp.

Dodson, P. 1976. Quantitative aspects of relative growth and sexual dimorphism in *Protoceratops*. Journal of Paleontology 50:929–940.

Dodson, P. 1986. *Avaceratops lammersi*: a new ceratopsid from the Judith River Formation of Montana. Proceedings of the Academy of Natural Sciences of Philadelphia 305–317.

Dodson, P., and P. J. Currie. 1988. The smallest ceratopsid skull-Judith River Formation of Alberta. Canadian Journal of Earth Sciences 25:926–930.

Dodson, P. 1996. The Horned Dinosaurs. Princeton University Press, Princeton, New Jersey, 346 pp.

Evans, D. C. 2010. Cranial anatomy and systematics of *Hypacrosaurus altispinus*, and a comparative analysis of skull growth in lambeosaurine hadrosaurids (Dinosauria: Ornithischia). Zoological Journal of the Linnean Society 159:398–434.

Evans, D., P. Currie, D. Eberth, and M. Ryan. 2006. High-resolution lambeosaurine dinosaur biostratigraphy, Dinosaur Park Formation: Sexual dimorphism reconsidered. Journal of Vertebrate Paleontology 26 Supplement: 59A.

Farke A.A. 1997. The distribution and taxonomy of *Triceratops*. pp. 47-49 in Dinofest International Proceedings Volume, D.L. Wolberg, E. Stump, G.D. Rosenberg (eds.) Philadephia Academy of Natural Sciences, Philadelphia.

Farke, A. A. 2011. Anatomy and taxonomic status of the chasmosaurine ceratopsid *Nedoceratops hatcheri* from the Upper Cretaceous Lance Formation of Wyoming, U.S.A. PLoS ONE 6:e16196.

Forster, C. A. 1996. Species resolution in *Triceratops*: cladistic and morphometric approaches. Journal of Vertebrate Paleontology 16:259–270.

Francillon-Vieillot, H., V. De Buffrénil, J. Castanet, J. Géraudie, F. J. Meunier, J. Y. Sire, L. Zylberberg, and A. De Ricqlès. 1990. Microstructure and mineralization of vertebrate skeletal tissues. Skeletal Biomineralization: Patterns, Processes and Evolutionary Trends 175–234.

Frederickson, J. A., and A. R. Tumarkin-Deratzian. 2014. Craniofacial ontogeny in *Centrosaurus apertus*. PeerJ 2:e252.

Freedman, E. 2009. Variation in nasal crest size of Brachylophosaurus canadensis (Dinosauria:Hadrosauridae): ontogenetic and stratigraphic implications of a large new specimen from the Judith River Formation of northcentral Montana. Journal of Vertebrate Paleontology 29:99A-100A.

Galton, P. M., and H.-D. Sues. 1983. New data on pachycephalosaurid dinosaurs (Reptilia: Ornithischia) from North America. Canadian Journal of Earth Sciences 20:462–472.

Gilmore, C. W. 1914. A new ceratopian dinosaur from the Upper Cretaceous of Montana, with note on *Hypacrosaurus*. Smithsonian Miscellaneous Collections 63:1-10.

Gilmore, C. W. 1946. New carnivorous dinosaur from the Lance Formation of Montana. Smithsonian Miscellaneous Collections 106: 1-19.

Godfrey, S. J., and R. Holmes. 1995. Cranial morphology and systematics of *Chasmosaurus* (Dinosauria: Ceratopsidae) from the Upper Cretaceous of western Canada. Journal of Vertebrate Paleontology 15:726–742.

Goodwin, M. B., W. A. Clemens, J. R. Horner, and K. Padian. 2006. The smallest known *Triceratops* skull: new observations on ceratopsid cranial anatomy and ontogeny. Journal of Vertebrate Paleontology 26:103–112.

Gould, S. J. 1977. Ontogeny and Phylogeny. The Belknap Press of Harvard University Press, Cambridgen Massachusetts, London England, 501 pp.

Gould, S. J. 1992. Roots: Ontogeny and phylogeny–revisited and reunited. BioEssays 14:275–279.

Gould, S. J. 2000. Of coiled oysters and big brains: how to rescue the terminology of heterochrony, now gone astray. Evolution & Development 2:241–248.

Goussard, F. 2006. The skull of *Triceratops* in the palaeontology gallery, Muséum national d'Histoire naturelle, Paris. Geodiversitas 28:467–476.

Granger, W., W. K. Gregory, and C. P. Berkey. 1923. *Protoceratops andrewsi*, a pre-ceratopsian dinosaur from Mongolia. American Museum Novitates 72: 1-9

Hamburger, V., and H. L. Hamilton. 1951. A series of normal stages in the development of the chick embryo. Journal of Morphology 88:49–92.

Hatcher, J. B. 1905. Two new ceratopsia from the Laramie of Converse County, Wyoming. American Journal of Science 413–419.

Hatcher, J. B., O. C. Marsh, and R. S. Lull. 1907. The Ceratopsia. US Geological Survey Monograph 49:1-300.

Horner, J. R. 1983. Cranial osteology and morphology of the type specimen of *Maiasaura peeblesorum* (Ornithischia: Hadrosauridae), with a discussion of its phylogenetic position. Journal of Vertebrate Paleontology 3:29–38.

Horner, J. R., and P. J. Currie. 1994. Embryonic and neonatal morphology and ontogeny of a new species of *Hypacrosaurus* (Ornithischia, Lambeosauridae) from Montana and Alberta. Dinosaur Eggs and Babies. Cambridge University Press, Cambridge 312–336.

Horner, J. R., and E. Dobb. 1997. Dinosaur Lives. Harpercollins, New York 244 pp.

Horner, J. R., and M. B. Goodwin. 2006. Major cranial changes during *Triceratops* ontogeny. Proceedings of the Royal Society B: Biological Sciences 273:2757–2761.

Horner, J. R., and M. B. Goodwin. 2008. Ontogeny of cranial epi-ossifications in *Triceratops*. Journal of Vertebrate Paleontology 28:134–144.

Horner, J. R., and J. Gorman. 2009. How to Build a Dinosaur: Extinction Doesn't Have to Be Forever. Penguin, pp.

Horner, J. R., and M. B. Goodwin. 2009. Extreme cranial ontogeny in the Upper Cretaceous dinosaur *Pachycephalosaurus*. PLoS One 4:e7626.

Horner, J. R., D. J. Varricchio, and M. B. Goodwin. 1992. Marine transgressions and the evolution of Cretaceous dinosaurs. Nature 358:59–61.

Horner, J. R., and J. Gorman. 1988. Digging Dinosaurs. Workman Pub., 210 pp.

Knell, R. J., and S. Sampson. 2011. Bizarre structures in dinosaurs: species recognition or sexual selection? A response to Padian and Horner. Journal of Zoology 283:18–22.

Knell, R. J., D. Naish, J. L. Tomkins, and D. W. Hone. 2013a. Is sexual selection defined by dimorphism alone? A reply to Padian and Horner. Proc. Zool. Soc. Lond 35:491–562.

Knell, R. J., D. Naish, J. L. Tomkins, and D. W. Hone. 2013b. Sexual selection in prehistoric animals: detection and implications. Trends in Ecology & Evolution 28:38–47.

Larson, P. 2013. The case for *Nanotyrannus*. pp. 15-55 in Tyrannosaurid Paleobiology, J.M. Parrish, R.E. Molnar, P.J. Currie, and E.B. Koppelhus (eds.) Indiana University Press, Bloomington and Indianapolis.

Lehman, T. M. 1990. The ceratopsian subfamily Chasmosaurinae: sexual dimorphism and systematics. pp. 211-230 in *Dinosaur Systematics: Approaches and Perspectives*, Carpenter K, Currie PJ (eds.)Cambridge University Press, New York, New York.

Lehman, T. M. 1998. A gigantic skull and skeleton of the horned dinosaur *Pentaceratops sternbergi* from New Mexico. Journal of Paleontology 894–906.

Lehman, T. M. 2007. Growth and population age structure in the horned dinosaur *Chasmosaurus*. Horns and Beaks: Ceratopsian and Ornithopod Dinosaurs 259–317.

Long, J. A., and K. J. McNamara. 1997. Heterochrony: The key to dinosaur evolution. pp. 113-123 in Dinofest International Proceedings Volume, D.L. Wolberg, E. Stump, G.D. Rosenberg (eds.) Philadephia Academy of Natural Sciences, Philadelphia.

Longrich, N. R., and D. J. Field. 2012. *Torosaurus* is not *Triceratops*: Ontogeny in chasmosaurine ceratopsids as a case study in dinosaur taxonomy. PLoS ONE 7:e32623.

Lucas, S. G., R. M. Sullivan, and A. P. Hunt. 2006. Re-evaluation of *Pentaceratops* and *Chasmosaurus* (Ornithischia: Ceratopsidae) in the Upper Cretaceous of the Western Interior. New Mex Mus Nat Hist Sci Bull 35:367–370.

Lull, R.S. 1915. The mammals and horned dinosaurs of the Lance formation of Niobrara County, Wyoming. American Journal of Science 4: 319–348.

Maiorino, L., A. A. Farke, T. Kotsakis, and P. Piras. 2013. Is *Torosaurus Triceratops*? Geometric morphometric evidence of Late Maastrichtian ceratopsid dinosaurs. PLoS ONE 8:e81608.

Makovicky, P., R. Sadleir, P. Dodson, G. Erickson, and M. Norell. 2007. Life history of *Protoceratops andrewsi* from Bayn Zag, Mongolia. Journal of Vertebrate Paleontology 27:109A–109A.

Mallon, J. C., R. Holmes, D. A. Eberth, M. J. Ryan, and J. S. Anderson. 2011. Variation in the skull of *Anchiceratops* (Dinosauria, Ceratopsidae) from the Horseshoe Canyon Formation (Upper Cretaceous) of Alberta. Journal of Vertebrate Paleontology 31:1047–1071.

Marsh, O. C. 1887. Notice of new fossil mammals. American Journal of Science series 3, 34: 323–331.

Marsh, O. C. 1888. A new family of horned Dinosauria, from the Cretaceous. American Journal of Science, series 3, 36: 477–478.

Marsh, O. C. 1889. Notice of gigantic horned Dinosauria from the Cretaceous. American Journal of Science series 3, 38: 173–176.

Marsh, O. C. 1890a. Description of new dinosaurian reptiles. American Journal of Science s3-39:81–86.

Marsh, O. C. 1890b. Additional characters of the Ceratopsidae, with notice of new Cretaceous dinosaurs. American Journal of Science s3-39:418–426.

Marsh, O. C. 1891. Notice of new vertebrate fossils. American Journal of Science series 3, 42: 265–269.

Marsh, O. C. 1898. New species of Ceratopsia. American Journal of Science, series 4, 6: 92.

Mateus, O. 2008. Two ornithischian dinosaurs renamed: *Microceratops* Bohlin 1953 and *Diceratops* Lull 1905. Journal of Paleontology 82:423.

Mayr, E. 1942. Systematics and the Origin of Species, from the Viewpoint of a Zoologist. Columbia University Press, New York, pp.

McDonald, A. T. 2011. A subadult specimen of *Rubeosaurus ovatus* (Dinosauria: Ceratopsidae), with observations on other ceratopsids from the Two Medicine Formation. PloS One 6:e22710.

McKinney, M. L., and K. J. McNamara. 1991. Heterochrony: the evolution of ontogeny. Plenum Press, New York, 437 pp.

Nopcsa, F. B. and E. Heidsieck 1933. 11. On the histology of-the ribs in immature and half-grown Tracho-dont dinosaurs. Proceedings of the Zoological Society of London 103:221–226.

Norell, M. A., J. M. Clark, L. M. Chiappe, and D. Dashzeveg. 1995. A nesting dinosaur. Nature 378:774–776.

Ostrom, J. P., and Wellnhofer, 1986. The Munich specimen of *Triceratops* with a revision of the genus: Zitteliana 14:111–158.

Ostrom, J. H., and P. Wellnhofer. 1990. *Triceratops*: an example of flawed systematics. Dinosaur Systematics: Perspectives and Approaches. Cambridge University Press, New York 245–254.

Padian, K., and J. R. Horner. 2002. Typology versus transformation in the origin of birds. Trends in Ecology & Evolution 17:120–124.

Padian, K., and J. R. Horner. 2011a. The evolution of "bizarre structures" in dinosaurs: biomechanics, sexual selection, social selection or species recognition? Journal of Zoology 283:3–17.

Padian, K., and J. R. Horner. 2011b. The definition of sexual selection and its implications for dinosaurian biology. Journal of Zoology 283:23–27.

Padian, K., and J. R. Horner. 2013. Misconceptions of sexual selection and species recognition: a response to Knell et al. and to Mendelson and Shaw. Trends in Ecology & Evolution 28:249–250.

Penkalski, P., and P. Dodson. 1999. The morphology and systematics of *Avaceratops*, a primitive horned dinosaur from the Judith River Formation (Late Campanian) of Montana, with the description of a second skull. Journal of Vertebrate Paleontology 19:692–711.

Prieto-Marquez, A. 2010. The braincase and skull roof of *Gryposaurus notabilis* (Dinosauria, Hadrosauridae), with a taxonomic revision of the genus. Journal of Vertebrate Paleontology 30:838–854.

Rozhdestvensky A.K. 1965. Growth changes in Asian dinosaurs and some problems of their taxonomy. Paleontologičeskij žurnal 3: 95-109.

Ryan, M. J., A. P. Russell, D. A. Eberth, and P. J. Currie. 2001. The taphonomy of a *Centrosaurus* (Ornithischia: Certopsidae) bone bed from the Dinosaur Park Formation (Upper Campanian), Alberta, Canada, with comments on cranial ontogeny. Palaios 16:482–506.

Sampson, S. D. 1995. Two new horned dinosaurs from the Upper Cretaceous Two Medicine Formation of Montana; with a phylogenetic analysis of the Centrosaurinae (Ornithischia: Ceratopsidae). Journal of Vertebrate Paleontology 15:743–760.

Sampson, S. D., M. J. Ryan, and D. H. Tanke. 1997. Craniofacial ontogeny in centrosaurine dinosaurs (Ornithischia: Ceratopsidae): taxonomic and behavioral implications. Zoological Journal of the Linnean Society 121:293–337.

Scannella, J. B., and J. R. Horner. 2010. *Torosaurus* Marsh, 1891, is *Triceratops* Marsh, 1889 (Ceratopsidae: Chasmosaurinae): synonymy through ontogeny. Journal of Vertebrate Paleontology 30:1157–1168.

Scannella, J. B., and J. R. Horner. 2011. "*Nedoceratops*": An Example of a Transitional Morphology. PLoS ONE 6:e28705.

Schott, R. K., and D. C. Evans. 2012. Squamosal ontogeny and variation in the pachycephalosaurian dinosaur *Stegoceras validum* Lambe, 1902, from the Dinosaur Park Formation, Alberta. Journal of Vertebrate Paleontology 32:903–913.

Schott, R. K., D. C. Evans, M. B. Goodwin, J. R. Horner, C. M. Brown, and N. R. Longrich. 2011. Cranial Ontogeny in *Stegoceras validum* (Dinosauria: Pachycephalosauria): A quantitative model of pachycephalosaur dome growth and variation. PLoS ONE 6:e21092.

Simpson, G. G. 1951. The species concept. Evolution 5:285–298.

Smith, A. B. 1994. Systematics and the Fossil Record: Documenting Evolutionary Patterns. Blackwell Scientific Publications, Oxford: 223 pp.

Sternberg, C. M. 1949. The Edmonton fauna and description of a new *Triceratops* from the Upper Edmonton Member: phylogeny of the Ceratopsidae. National Museum of Canada Bulletin 113.

Thulborn, R. A. 1992. Nest of the dinosaur *Protoceratops*. Lethaia 25:145–149.

Tokaryk, T. T. 1997. First evidence of juvenile ceratopsians (Reptilia: Ornithischia) from the Frenchman Formation (late Maastrichtian) of Saskatchewan. Canadian Journal of Earth Sciences 34:1401–1404.

Tumarkin-Deratzian, A. R. 2010. Histological evaluation of ontogenetic bone surface texture changes in the frill of *Centrosaurus apertus*. pp. 251-263 in M.J. Ryan, B.J. Chinnery-Allgeier, and D.A. Eberth DA, (eds.) New perspectives on horned dinosaurs. Indiana University Press, Bloomington.

Ukrainsky, A. S. 2007. A new replacement name for *Diceratops* Lull, 1905 (Reptilia: Ornithischia: Ceratopsidae). Zoosystematica Rossica 16:292–291.

Ukrainsky, A. S. 2009. Synonymy of the genera *Nedoceratops* Ukrainsky, 2007 and *Diceratus* Mateus, 2008 (Reptilia: Ornithischia: Ceratopidae). Paleontological Journal 43:116–116.

CHAPTER TWO

TOROSAURUS MARSH, 1891 IS *TRICERATOPS* MARSH, 1889 (CERATOPSIDAE: CHASMOSAURINAE): SYNONYMY THROUGH ONTOGENY

Contribution of Authors and Co-Authors

Manuscript in Chapter 2

Author: John B. Scannella

Contributions: Conceived the study, collected data, analyzed data, interpreted results, and wrote the manuscript.

Co-author: John R. Horner

Contributions: Conceived the study, collected data, analyzed data, interpreted results, and wrote the manuscript.

Manuscript Information Page

John B. Scannella, John R. Horner.
Journal: Journal of Vertebrate Paleontology
Status of Manuscript:
__Prepared for submission to a peer-reviewed journal
___Officially submitted to a peer-reviewed journal
___Accepted by a peer-reviewed journal
_x_Published in a peer-reviewed journal

Published by the Society of Vertebrate Paleontology.
Scannella, J. B., and J. R. Horner. 2010. *Torosaurus* Marsh, 1891, is *Triceratops* Marsh, 1889 (Ceratopsidae: Chasmosaurinae): synonymy through ontogeny. Journal of Vertebrate Paleontology 30:1157–1168.

The following chapter has been published in the Journal of Vertebrate Paleontology and appears in this dissertation with the permission of the Society of Vertebrate Paleontology (http://www.vertpaleo.org). The copyright is held by the Society of Vertebrate Paleontology. Image of YPM 1830 is copyright Yale Peabody Museum.

Abstract

Although they have been considered distinct genera for over a century, ontogenetic analyses reveal that *Triceratops* and '*Torosaurus*' actually represent growth stages of a single genus. Major changes in cranial morphology – including the opening of parietal fenestrae and the elongation of the squamosals - occur rapidly, very late in *Triceratops* ontogeny and result in the characteristic '*Torosaurus*' morphology. This report presents the results of a ten year field study of the dinosaurs of the Hell Creek Formation in Montana and is based on a collection of over 50 specimens of *Triceratops*, including over 30 skulls, which have been amassed in that time, in addition to specimens from numerous other North American museums. This large sample of individuals reveals the full ontogenetic spectrum of *Triceratops*. The synonymy of *Triceratops* and '*Torosaurus*' contributes to an unfolding view of extremely reduced dinosaur diversity just before the end of the Mesozoic Era.

Introduction

Since their discovery in the late 1800s (Marsh, 1889, 1891), *Triceratops* and '*Torosaurus*' (Ceratopsidae; Chasmosaurinae) have been regarded as the last of the horned dinosaurs. *Triceratops* is characterized as having a three-horned face with a rather short parietal-squamosal frill, and a solid, non-fenestrated parietal (Ostrom and Wellnhofer, 1986; Forster, 1996). '*Torosaurus*' is distinguished from *Triceratops* solely on the basis of its expanded, fenestrated parietal-squamosal cranial frill (Sullivan et al.,

2005; Farke, 2007). All other aspects of these animals' remains are indistinguishable (Farke, 2007). *Triceratops* and '*Torosaurus*' are known from the same geological unit, the Hell Creek Formation of Montana and the Dakotas, and equivalent Maastrichtian (latest Cretaceous) age sediments in adjacent states and provinces.

We report here on an analysis of changes in parietal-squamosal morphology in an ontogenetic sequence of *Triceratops*. *'Torosaurus'* specimens were not excluded from this investigation and in all cases were found to exhibit ontogenetic markers of mature individuals, including anteriorly inclined postorbital horn cores, dorsoventrally flattened epoccipitals, and fully developed osteohistologic features (Horner and Goodwin, 2006). Furthermore, transitional features are noted in subadult specimens of *Triceratops* that reveal the ontogenetic trajectory of the genus, culminating in the frill morphology previously considered diagnostic of *"Torosaurus."*

Institutional Abbreviations

AMNH, American Museum of Natural History, New York; ANSP, Academy of Natural Sciences, Philadelphia; BYU, Brigham Young University Earth Science Museum, Provo; FMNH, Field Museum of Natural History, Chicago; LACM, Natural History Museum of Los Angeles County, Los Angeles; MCZ, Museum of Comparative Zoology, Harvard University, Cambridge; MOR, Museum of the Rockies, Bozeman; MPM, Milwaukee Public Museum, Milwaukee; SMM, Science Museum of Minnesota, St. Paul; UCMP, University of California Museum of Paleontology, Berkeley; UND, Paleontology Collection, University of North Dakota, Grand Forks; USNM, National Museum of Natural History, Smithsonian Institution, Washington, D.C.; UWGM,

University of Wisconsin-Madison Geology Museum, Madison; YPM, Yale Peabody Museum, New Haven.

Materials and Methods

This analysis of *Triceratops* cranial morphology is, in part, a result of the Museum of the Rockies' 10-year Hell Creek Project, an attempt to reconstruct the ecosystems of the terminal Cretaceous Hell Creek Formation of Montana and surrounding provinces. The discoveries that are resulting from the Hell Creek Project (e.g., Horner and Padian, 2004; Horner and Goodwin, 2006, 2008, 2009; Horner et al., 2009a; Scannella and Fowler, 2009) emphasize the importance of large-scale field studies in which numerous individuals are collected.

Triceratops is the most commonly recovered dinosaur in the Hell Creek Formation; 40% of dinosaur specimens collected during the course of the Hell Creek Project, including over 30 skulls (Appendix 1) are referable to this genus (Horner, unpublished data). *Triceratops* is represented by various ontogenetic stages, ranging from specimens with skulls less than half a meter in length to skulls that are over two meters in length (Horner and Goodwin, 2006). Most of these specimens have yet to be formally described. "*Torosaurus*," on the other hand, is both rare and generally larger: the smallest known skulls are around two meters in length and the largest approach three meters in length.

The large collection of *Triceratops* cranial material amassed by the MOR was supplemented with the examination of specimens from several North American institutions, including the numerous type specimens at the National Museum of Natural

History and the Yale Peabody Museum. Specimens were placed within the ontogenetic groups (baby, juvenile, subadult, adult) defined by Horner and Goodwin (2006) based on the morphological criteria described therein. This study was not limited to complete skulls; ontogenetic markers (such as shape of the postorbital horn cores and epoccipitals) allow placement of partial specimens into a growth series (Horner and Goodwin, 2006).

Measurements were taken with digital calipers, sliding calipers, or a metric tape measure where appropriate. All measurements were taken at least twice and then averaged. Squamosal length/width was plotted against squamosal length and an exponential least squares regression analysis was performed using Microsoft Excel.

Osteohistology specimens were processed following current techniques (Horner et al. 2009b). Specimens were embedded in polyester resin, sectioned with a diamond powder disk on a precision saw, ground on a lap wheel to achieve the desired optical contrast, and polished.

Results

Ontogenetic Development of Parietal Fenestrae

An ontogenetic series of *Triceratops* skulls reveals that late in ontogeny the ventral surface of the parietal developed thinning regions which we hypothesize are the precursors to fenestrae (Fig. 2.1; Table 2.1). Expansion of parietal fenestrae through ontogeny has been noted in previous studies of ceratopsians (Dodson and Currie, 1988; Brown et al., 2009). Although *Triceratops* has been diagnosed as possessing an extremely thick, solid parietal (Forster, 1996), this thickness is not uniform. The regions

of the parietal that are fenestrated in other chasmosaurines became extremely thin (less than .5 cm thick) as *Triceratops* matured.

Juvenile *Triceratops* possessed subtly thinner regions of the parietal adjacent to the lateral margins, roughly 5-10 cm from the frill's caudal edge. In larger subadult specimens, these thin regions are expanded onto the ventral surface of the parietal and form two prominent fossae (as seen in YPM 1823). These fossae expanded into large, semi-circular depressions that extended medially toward the parietal midline and rostrally toward the supratemporal fenestrae (as seen in MOR 2924, Fig. 2.1B). As the frill continued to grow, the depressions became isolated from the lateral margins of the parietal (MOR 2946, AMNH 970, Fig. 2.1C). The parietal thins abruptly from approximately 2.5 to 3 cm or more at its thickest point near the caudal edge to less than 0.5 cm within the depressions (as exemplified by MOR 2946). These areas are often not fully preserved in specimens of *Triceratops* (e.g., AMNH 56-+*****, MOR 004, MOR 2946, UND 3000), likely due to the inherently fragile nature of the thin bone.

MOR 1122, the most complete skull of "*Torosaurus*," retains a shallow rim bordering the caudal margin of its left parietal fenestra (Fig. 2.1D). The parietal is 2.62 cm thick (measured 2 cm anterior to the caudal margin), intermediate in thickness between the characteristically thick parietal of *Triceratops* and the thinner condition that is typical of '*Torosaurus*' (1 to 2 cm). This allowed for the retention of the "thinning rim" on the ventral surface which is otherwise eliminated by the overall thinning of the parietal. MOR 981, the only other '*Torosaurus*' specimen known to preserve the entire border of a parietal fenestra (parietal thickness 1.9 cm), does not display a similar thickened rim on the ventral surface. The maximum widths of the fenestrae of MOR 1122

are 36.5 cm (left, with thickened rim present) and 49 cm (right). The sole preserved fenestra of MOR 981 has a maximum width of 53 cm.

The osteohistology of the thinning region of the parietal of a young adult *Triceratops* (MOR 2946; Fig. 2.2) reveals that resorption occurs on both the ventral and dorsal surfaces. Multiple erosion surfaces are visible (Fig. 2.2D) indicating that the parietal is extensively remodeled throughout ontogeny.

Squamosal Elongation

Concurrent with the development of parietal fenestrae is the elongation of the squamosals (Figs. 2.3, 2.4). The smallest known *Triceratops* skull (UCMP 154452) possesses extremely short squamosals which are reminiscent of those found in the "short-frilled" centrosaurine ceratopsids (Goodwin et al. 2006; Dodson, 1996; Fig. 2.3A). In contrast to other chasmosaurines in which the squamosals gradually elongate (Lehman, 1990), *Triceratops* is paedomorphic and retains the juvenile morphology throughout most of its development (Fig. 2.3B-F). This retention of relatively short, broad squamosals led to *Triceratops* being grouped with the centrosaurine ceratopsids for many years rather than in its rightful place among the "long-frilled" chasmosaurines (Dodson, 1996; Lull, 1933; Sternberg, 1949). Only very late in *Triceratops* ontogeny do the squamosals become elongate, producing intermediates between the broad, juvenile condition and the blade-like state found in '*Torosaurus*' (Fig. 2.3G, H). These intermediate squamosal morphologies correlate with advanced parietal thinning (see Table 2.1). A thickened squamosal bar forms along the contacts with the parietal in mature specimens (Colbert and Bump, 1947; Farke, 2007).

As seen in Fig. 2.4, *Triceratops* squamosals eventually adopted the morphology previously considered diagnostic of "*Torosaurus*." This is demonstrated by the good correlation between squamosal length and elongation when an exponential least squares regression is performed (R^2=.782). Size, however, is not the most reliable indicator of maturity (see Discussion). '*Torosaurus*' specimen SMM P97.6.1 is noteworthy in its possession of slightly wider squamosals than those of other '*Torosaurus*' specimens. This individual's squamosals are wide rostrally and taper caudally (see Fig. 2.3J) which is consistent with elongation from the immature morphology considered diagnostic of *Triceratops*. Interestingly, a specimen from the Frenchman Formation of Saskatchewan which was originally referred to "*Torosaurus latus*" (Tokaryk, 1986; this has since been contested by Sullivan et al., 2005) exhibits a similar squamosal morphology. This may represent individual or stratigraphic variation (see comments on variation in Discussion).

The Ontogenetic Spectrum of *Triceratops*

The placement of specimens into an ontogenetic spectrum highlights transitional features. AMNH 5116 is a large skull (200 cm skull length, measured from tip of the rostral to the parietal-squamosal contact at caudal frill margin) with extremely narrow squamosals and a fairly thin (2.3 cm, measured 2 cm anterior to the caudal margin) parietal (Fig. 2.5A). The anteriorly inclined postorbital horn cores of AMNH 5116 indicate maturity comparable to that seen in other "adult" *Triceratops* specimens. This individual has been identified as *Triceratops* rather than *'Torosaurus'* because its parietal is unfenestrated. However, close inspection reveals a pronounced sloping of the parietal, from thicker bone near the caudal margin to thinner bone in the regions which are

fenestrated in '*Torosaurus*.' Many '*Torosaurus*' specimens retain a gradual sloping of the parietal in these regions, posterior to the fenestrae, which we hypothesize to be a remnant of the transition from solid frill to perforation (MOR 1122, MPM VP6841, SMM P97.6.1). The sloping of the parietal of AMNH 5116 coincides with a textural change from a striated texture to a more rugose, pebbly surface texture within the areas where fenestrae would be present in '*Torosaurus*' (Fig. 2.5C). A similar textural transition has been noted to occur on the margins of developing parietal fenestrae in centrosaurines (Brown et al., 2009) and represents a transition from the characteristic solid parietal of *Triceratops* to the fenestrated condition found in mature individuals.

Striated frill texture corresponding to visible radial canals is observed in juvenile *Triceratops* (UCMP 154452, MOR 1199, MOR 2569, MOR 2951) as well as other juvenile ceratopsians (Sampson et al., 1997; Brown et al., 2009). It is associated with rapid growth (Francillon-Vieillot et al., 1990; Sampson et al., 1997), the radial vascular canals being oriented in the direction of expansion. Several '*Torosaurus*' specimens have a similar surface texture on their frills, with the striations varying in thickness from being fine to fairly broad, resembling what Tumarkin-Deratzian (2009) refers to as a "grooved" surface texture. Histological examination of a parietal (MOR 981, a large '*Torosaurus*') with striated surface texture reveals that it is associated with the expansion of the frill. The presence of a striated surface texture on the parietal of AMNH 5116 and several '*Torosaurus*' specimens (MOR 981, MPM VP6841, SMM P97.6.1, YPM 1831) which display clear ontogenetic markers of maturity including anteriorly inclined postorbital horn cores and flattened epocciptals, as well as less reliable ontogenetic markers (relatively large size, apparent closure of cranial sutures, see Discussion) suggests that the

late expansion of the frill occurs rapidly, concurrent with overall thinning. AMNH 5116 is a *Triceratops* that died just prior to attainment of the complete '*Torosaurus*' morphology.

The problematic specimen, USNM 2412, has been placed in its own genus "*Nedoceratops*" (Ukrainsky, 2007, 2009); at times it has been the sole representative of "*Diceratus*" (Mateus, 2008), "*Diceratop*s" (Lull, 1905; Hatcher et al., 1907), or its own species of *Triceratops*, "*Triceratops hatcheri*" (Lull, 1933; Ostrom and Wellnhofer, 1986). Suggested autapomorphies of this specimen include the absence of a nasal horn and the presence of a small fenestra in the parietal (Forster, 1996). The apparent absence of an epinasal in this specimen is unlikely to be an autapomorphy as similar nasal horn morphologies are found in *Triceratops* and '*Torosaurus*' specimens (MOR 981, MOR 1122, UCMP 128561, USNM 2410). Alternatively, the epinasal could have been lost in vivo or simply disarticulated from the fossil as a result of taphonomic processes (Horner and Goodwin, 2008). In addition, the specimen shows evidence of severe pathologies (Tanke and Farke, 2007). USNM 2412 possesses dorsoventrally flattened epoccipitals and subtly procurving postorbital horn cores – indicators of ontogenetic maturity. Its elongate squamosals and incipient parietal fenestra are exactly what would be predicted in a *Triceratops* which is transitional between the short, solid subadult frill and the elongate, fenestrated condition found in adults. We consider USNM 2412 an ontogenetically transitional specimen of *Triceratops*.

UWGM 732 is a specimen with anteriorly inclined postorbital horn cores and dorsoventrally flattened epoccipitals. It possesses elongate squamosals (Fig. 2.3I) and a thin parietal (1.5 cm thick measured 2 cm anterior to the caudal margin). However, the

squamosals had yet to develop the thickened squamosal bar that is found in "*Torosaurus latus*" specimens and it is unclear if the parietal was fenestrated at the time of death. We consider UWGM 732 a young adult *Triceratops*. It is interesting to note that the posteriorly curved postorbital horn core of a very small juvenile *Triceratops* was collected from the same site as the larger individual.

Inclusion of '*Torosaurus*' specimens in the examination of *Triceratops* cranial ontogeny highlights transitional morphological features that link these two taxa as ontogenetic stages of the same taxon. As such, the stages of *Triceratops* growth outlined by Horner and Goodwin (2006) must be expanded upon in order to encompass the full ontogenetic spectrum of this genus (Table 2.2). Individuals bearing anteriorly inclined postorbital horn cores and dorsoventrally flattened epoccipitals which have yet to develop the complete '*Torosaurus*' frill morphology (e.g., AMNH 5116, MOR 004, MOR 1625, MOR 2702, USNM 2412) and were previously considered mature adults are revealed to be immature; we will refer to this as the young adult growth stage. '*Torosaurus*' (e.g., MOR 981, MOR 1122, YPM 1830) represents the adult stage of *Triceratops* ontogeny.

Epiparietal and Episquamosal Variation

The epoccipitals (epiparietals and episquamosals) of *Triceratops* undergo dramatic changes in morphology throughout ontogeny (Horner and Goodwin, 2006, 2008). All juvenile specimens possess triangular epoccipitals. As individuals matured the epoccipitals became dorsoventrally flattened onto the frill margin.

Triceratops has previously been diagnosed as possessing an unvarying configuration of five epiparietals, one of which consistently straddles the midline

(Forster, 1996). This character has been used to distinguish *Triceratops* from '*Torosaurus*" and other chasmosaurines (Farke and Williamson, 2006; Farke, 2007). However, several *Triceratops* specimens possess more than five epiparietals (LACM 27428, USNM 2100, Horner and Goodwin, 2008). USNM 1201 was described as possessing six epiparietals without evidence of one on the midline (Hatcher et al., 1907); however this was an inference made from the morphology of the parietal margin and only one epoccipital was found with the specimen. MOR 2923 represents an individual with an unfenestrated parietal in which six epiparietals are clearly preserved, none of which are found on the midline (Fig. 2.6). '*Torosaurus*' specimen MOR 981 preserves only the right half of its parietal, on which three epiparietals are clearly visible. Farke (2007) noted the presence of five parietal marginal undulations, suggesting a total count of 10 epiparietals for this individual. MOR 1122 (previously assigned to '*Torosaurus*') has 12 epiparietals and lacks a midline epiparietal as well. The number and position of epiparietals is variable within *Triceratops* and the greater number found in MOR 981 and MOR 1122 suggests that this number increases throughout ontogeny.

The number of episquamosals is also variable. *Triceratops* has classically been restored with four or five episquamosals per squamosal in addition to one that bridges the parietal/squamosal gap (YPM 1821, YPM 1823). However, MOR 1120 clearly preserves seven episquamosals on its right squamosal; six are preserved on the left squamosal. '*Torosaurus*' specimens (MOR 1122, MPM VP6841) preserve seven episquamosals per squamosal.

Osteohistology: a Test of Ontogenetic Hypotheses

The osteohistology of the postorbital horn cores of *Triceratops* reveal the expected tissue ontogeny seen in other bones (Francillon-Vieillot et al. 1990; Chinsamy-Turan, 2005), in that young *Triceratops* horns are composed of primary tissues, whereas the horns of older individuals are composed of more mature tissues. As seen in Figure 2.7 A-B, the posteriorly curved postorbital horn core of a small juvenile *Triceratops* (comparable in size to MOR 2569; see Fig. 2.3B) is very porous and composed exclusively of primary tissue. The postorbital horn core tissue of a much larger juvenile (orbital horns still arched backward) is slightly less porous and composed of tissues that are mostly primary, but contain some secondary osteons.

The postorbital horn cores of young adult *Triceratop*s skulls approximately 2 meters in length (Fig. 2.7 E-H) have tissues which have been remodeled, but are not yet composed of multigenerational "Haversian" canals. The tissue is still rather spongy, and fibrocytes are abundant and well ordered (Horner and Goodwin, 2009; Horner and Lamm, 2009). Squamosal morphology in these specimens ranges from the broad morphology typical of what were previously considered adult *Triceratops* (MOR 1625) to fairly elongate (MOR 2702; Fig. 2.3G). At this point the parietal has pronounced thinning regions and epoccipitals are dorsoventrally flattened.

The postorbital horn core of a mature *Triceratops* ('*Torosaurus*') is composed of multigenerational dense "Haversian" tissue, indicative of very mature bone (Fig. 2.7 I-J). This histological ontogenetic sequence clearly demonstrates that *Triceratops* which were previously considered to be adults are not as mature as individuals with the expanded,

fenestrated parietal-squamosal frill morphology previously considered diagnostic of '*Torosaurus*'.

Discussion

The radical changes in cranial morphology which occur throughout ceratopsid ontogeny (Sampson, 1995; Horner and Goodwin, 2006) entail that an understanding of ontogenetic development is critical to studies of their paleoecology and systematics. *Triceratops* is paedomorphic relative to other chasmosaurines in that it retains juvenile features (broad squamosals, unfenestrated parietal) until extremely late in ontogeny. A large sample of specimens reveals the full ontogenetic spectrum of *Triceratops*, with intermediate morphologies linking individuals that could easily be mistaken for distinct species without an understanding of the degree of plasticity in the skulls of these animals.

Ontogenetic Variation

It has been suggested that ANSP 15192 is an immature '*Torosaurus*' given its relatively small size (177cm skull length; Colbert and Bump, 1947). However, though it was originally described as not possessing epoccipitals, the epiparietals and episquamosals of ANSP 15192 are indeed preserved and exhibit the mature morphology of being dorsoventrally flattened and fused to the frill border (Fig. 2.8). In fact, all "*Torosaurus latus*" specimens in which the epoccipitals are preserved exhibit this mature morphology (ANSP 15192, MOR 981, MOR 1122, MPM VP6841). No '*Torosaurus*' specimen has posteriorly curving postorbital horn cores, which would be indicative of immaturity (Horner and Goodwin, 2006). To the extent that any '*Torosaurus*' specimens

have a degree of sinuosity to their postorbital horn cores, it falls within the range of variation found in young adult *Triceratops* (as seen in MOR 1604 and UCMP 113697). Interestingly, the postorbital horn cores of several '*Torosaurus*' specimens show signs of pronounced resorption (ANSP 15192, MOR 981, MOR 1122). Remodeling of the postorbital horn cores was still occurring in these mature animals.

Size alone is not a reliable indicator of ontogenetic stage and there is a strong degree of variation in the timing of cranial fusion in *Triceratops* (Horner and Goodwin, 2008). For example, YPM 1822 is a small skull (154cm skull length) in which the cranial sutures appear to be fused. However, it is displayed alongside the much larger skull YPM 1821 (187cm skull length) in which the cranial sutures are open. MOR 2952 is a recently discovered large *Triceratops* in which the 27cm long epinasal has yet to fuse to the nasals. Similarly, the large '*Torosaurus*' MOR 1122 (skull length 255 cm) was discovered with an associated isolated premaxilla that was equivalent in size to its own and yet unfused. BYU 12183 is an extremely large *Triceratops* skull (estimated skull length 250 cm); unfortunately the areas of the parietal which may reveal thinning, incipient fenestrae, or textural transitions are largely reconstructed. Ontogenetic markers (horn core curvature, epoccipital morphology) can be used to group individuals into growth stages, but in ideal situations a combination of factors (including osteohistology, bone texture, sutural fusion, and size) should be considered.

Alternative Hypotheses

Alternative hypotheses to the synonymy of these genera may include the suggestion that '*Torosaurus*' does not conform to the ontogenetic trends observed in

Triceratops. This is unparsimonious given the close phylogenetic relationship proposed for '*Torosaurus*' and *Triceratops* (Dodson *et al*., 2004). Posterior curvature of postorbital horn cores in immature individuals is observed in ceratopsians as primitive as *Zuniceratops* (Wolfe and Kirkland, 1998; Horner and Goodwin, 2006).

Another possibility is that '*Torosaurus*' is a valid genus which is indistinguishable from *Triceratops* until relatively late in ontogeny when its fenestrae develop. Given the geographic and stratigraphic overlap of these animals, ontogeny is far more parsimonious than erecting two distinct genera, particularly since tissue ontogeny reveals that '*Torosaurus*' specimens are more mature than any *Triceratops* specimens, including those previously considered adults. Furthermore, specimens that might otherwise be considered immature '*Torosaurus*' but are here considered transitional ontogenetic stages of *Triceratops* (e.g., AMNH 5116, MCZ 1102, MOR 2702, USNM 2412) all bear ontogenetic indicators of maturity such as anteriorly inclined postorbital horn cores and/or dorsoventrally flattened epoccipitals.

Ostrom and Wellnhofer (1990) suggested that the differences in frill morphology which distinguish "*Torosaurus*" from *Triceratops* may be the result of sexual dimorphism in a single genus. The predictable nature of parietal thinning throughout ontogeny in *Triceratops*, the osteohistological evidence for greater maturity in '*Torosaurus*' specimens, and the lack of strong evidence for sexual dimorphism in non-avian dinosaurs (Padian et al., 2004, Goodwin et al., 2006) argues against this proposal. Sexual dimorphism accounting for differences in size cannot be ruled out at this time.

Implications for Dinosaur Diversity

No centrosaurine material is known from the Hell Creek Formation or adjacent equivalent aged formations. It appears that only the chasmosaurine ceratopsids survived into the latest Maastrichtian (Dodson, 1996). Of this group, *Triceratops* and '*Torosaurus*' were proposed to be the last of their lineages (Sternberg, 1949). The synonymy of these genera diminishes the diversity of ceratopsids in the Hell Creek Formation. Similar synonymizations are occurring for several taxa, including tyrannosaurs (Carr, 1999) and pachycephalosaurs (Horner and Goodwin, 2009), in the latest Cretaceous of North America. These advances show that dinosaur diversity was more depleted than traditionally thought well before the end of the Cretaceous Period.

Systematic Paleontology

Ceratopsia Marsh, 1888

Neoceratopsia Sereno, 1986

Ceratopsidae Marsh, 1888

Chasmosaurinae Lambe, 1915

Triceratops Marsh, 1889

Figure 2.5 A, B

(a) Revised Diagnosis

Skull bears elongate postorbital horn cores (derived from fusion of the postorbitals and prefrontals early in ontogeny) plus a single variable epinasal horn. Epinasal unites the rostral-nasal-premaxillae complex. The shape of the frontal fontanelle

is variable, though generally circular when present; some specimens lack a frontal fontanelle as a result of closure of the frontals and parietal. Parietal-squamosal frill relatively short, broad and fan-like (compared to other chasmosaurine genera). Fenestrated and expanded in mature individuals. Strong undulating midline parietal ridge throughout early ontogeny becomes a broad parietal bar in mature specimens; fenestrae are ovate to nearly circular. Pronounced squamosal bars alongside parietal-squamosal contacts in mature specimens. Epiparietals and episquamosals ornament posterior and lateral margins of the parietal-squamosal frill. Epijugals on the jugal flange fuse the jugal-quadratojugal complex (modified from Ostrom and Wellnhofer, 1986, and Forster, 1996).

(b) Valid Species

Triceratops horridus Marsh, 1889 (type species); holotype: YPM 1820 (Hatcher *et al.* 1907, pl. XXVI, figs. 24, 25, 27); diagnosis same as for genus.

Triceratops prorsus Marsh, 1890; holotype: YPM 1822 (Forster 1996, fig. 9B); diagnosis as per Forster (1996).

T. horridus and *T. prorsus* are stratigraphically separated (Scannella and Fowler, 2009). This finding and its evolutionary, taxonomic, and biogeographic implications will be addressed in detail in a separate manuscript.

(c) Locality and Horizon (YPM 1820)

Section 2, T.36N., R. 64 W. Niobrara County, Wyoming, U.S.A. “About the middle of the upper half of the Lance formation, Late Cretaceous” (Ostrom and Wellnhofer, 1986:156).

(d) Synonyms

Torosaurus latus Marsh, 1891(rediagnosed by Colbert and Bump, 1947; Sullivan et al. 2005; Farke, 2007); *Nedoceratops hatcheri* Lull, 1905; Ukrainsky, 2007 (new combination, *Diceratops* preoccupied) [=*Diceratops hatcheri* Lull, 1905 (original description), *Diceratus hatcheri* Lull, 1905; Mateus, 2008 (new combination, junior subjective synonym)]

(e) "*Torosaurus*" *utahensis* Gilmore, 1946

Chasmosaurine remains from the southern "*Alamosaurus* fauna" (Lehman, 1987) of Utah, New Mexico, and Texas have been referred to *"Torosaurus" utahensis*, however there is still considerable debate by students of ceratopsids over how many of these (largely fragmentary) specimens are actually diagnosable to the genus level (Sullivan et al., 2005; Hunt and Lehman, 2008). The synonymy of *Triceratops* and the type species of '*Torosaurus*' implies that *"Torosaurus" utahensis* is either a species of *Triceratops*, or a different genus; either *Arrhinoceratops* (Parks, 1925), to which it was initially referred by Gilmore (1946), or its own distinct genus. We favor the first hypothesis, but as this southern material was not included in the present study, a further diagnosis of *"Torosaurus" utahensis* is beyond the scope of this paper and will be investigated in a following study.

(f) Remarks

Given the amount of morphological change that occurs throughout the lifespan of an individual, the use of a single type specimen for taxonomic purposes is problematic if the diagnosable characters are not limited to the adult ontogenetic stage. Hence, multiple

ontogenetic stages are easily misinterpreted as distinct taxa (Dodson, 1975). The revised diagnosis of *Triceratops* presented here is based on characters found in a mature individual.

Conclusions

Recognition of the full scope of *Triceratops* ontogeny emphasizes the radical degree of cranial morphological transformation which occurred throughout development. Postorbital horn cores reoriented from being straight, to posteriorly directed, to anteriorly directed correlated with the dorsoventral flattening of epiparietals and episquamosals throughout ontogeny (Horner and Goodwin 2006, 2008). The initially unfenestrated parietal-squamosal frill thickens throughout development, with some specimens reaching a thickness in excess of 6 cm (MOR 2969), before rapidly expanding, thinning, and ultimately adopting the fenestrated condition found in all other chasmosaurines. We hypothesize that these dramatic changes in cranial ornamentation functioned in intraspecific communication, signaling relative maturity.

It is telling that no confirmed juvenile '*Torosaurus*' skulls have been reported. Incorporation of '*Torosaurus*' into the spectrum of *Triceratops* ontogeny explains why '*Torosaurus*' is only known from a few mature individuals in the Hell Creek Formation whereas *Triceratops* is extremely abundant and represented by several growth stages (Horner and Goodwin, 2006). Immature '*Torosaurus*' actually have been known for over a century but have been called *Triceratops*. The fact that the majority of *Triceratops* specimens that have been collected since the initial description of the genus (Marsh, 1889) are not fully mature suggests that either *Triceratops* mortality was fairly high

before full maturity was reached, or adults did not live in the same areas as immature animals.

Ontogenetic analyses of dinosaur morphology highlight transitional features between specimens and suggest that much of the variation previously attributed to taxonomic differences is actually a product of developmental processes (Dodson, 1975). Studies focused on the dinosaur fauna of the Hell Creek Formation are depleting latest Cretaceous dinosaur diversity through ontogenetic synonymies (Horner et al., 2007). As such, a trend of decreasing dinosaur diversity preceding the end of the Mesozoic Era is implied.

Acknowledgments

We are grateful to all of the institutions which permitted access to specimens. Image of YPM 1830 in Figure 2.5 is copyright Peabody Museum of Natural History, Yale University. We thank the MOR field crews as well as Makoshika State Park and Lon Bolick for discovery and collection of specimens. Thanks to C. Ancell, D. Barta, S. Brewer, T. Bridges, N. Carroll, B. Harmon, J. Heuck, P. Hookey, J. Jette, and L. Roberts for preparation of specimens. E. Lamm performed histological preparation. We thank K. Baker, B. Boessenecker, C. Boyd, M. Carrano, P. Dodson, A. Farke, D. Fowler, E. Freedman, M. Goodwin, L. Hall, J. Hartman, M. Holland, F. Jackson, P. Makovicky, M. Pillet, K. Padian, A. Poust, J. Stiegler, D. Varricchio, and H. Woodward for helpful comments, suggestions, and stimulating conversations. H. Woodward produced illustrations. Comments by R. Holmes and two anonymous reviewers improved an early version of the manuscript. Specimen collection was funded primarily by Nathan

Myhrvold. The BLM, USFW, and CMR as well as the Twitchell, Taylor, and Holen families permitted access to lands. Research funding for JBS was provided by the Theodore Roosevelt Memorial Fund of the American Museum of Natural History, the Doris O. and Samuel P. Welles Research Fund of the University of California Museum of Paleontology, and the Sands brothers.

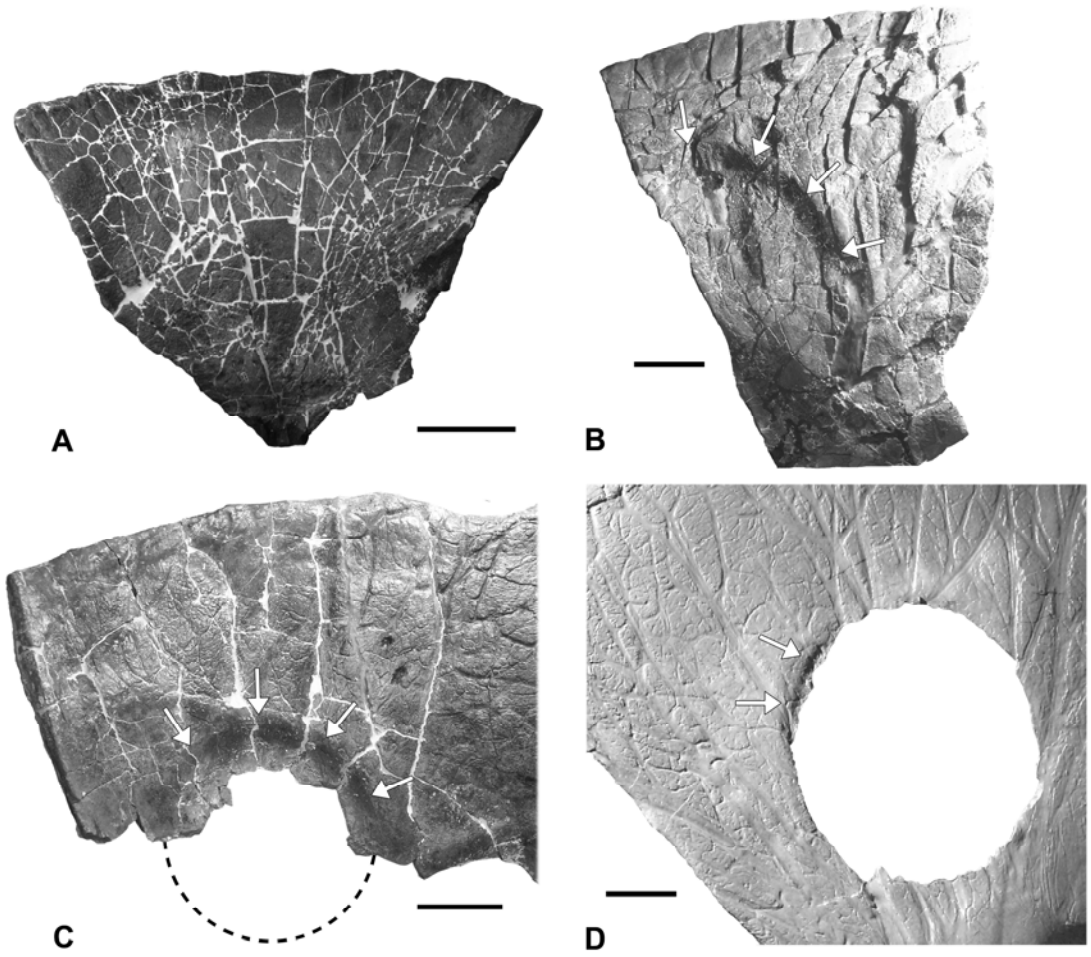


Figure 2.1 Development of thin regions of the parietal throughout *Triceratops* ontogeny. **A**, Ventral view of the parietal of a juvenile *Triceratops*, MOR 2951; **B**, MOR 2924 (left half of parietal). In subadult *Triceratops*, shallow depressions form on the ventral surface of the parietal, adjacent to the lateral margins. These depressions are initially undetectable on the dorsal surface; **C**, MOR 2946 (left half of parietal). As the parietal grows, the shallow regions become isolated from the lateral margins. The parietal is still unperforated at this stage. Dashed line indicates approximate extent of fenestra in "*Torosaurus*"; **D**, MOR 1122. The thinning regions are resorbed late in ontogeny, forming the characteristic fenestrae of "*Torosaurus*." Arrows indicate rim of thinning region on the ventral surface. Scale bars equal 10 cm.

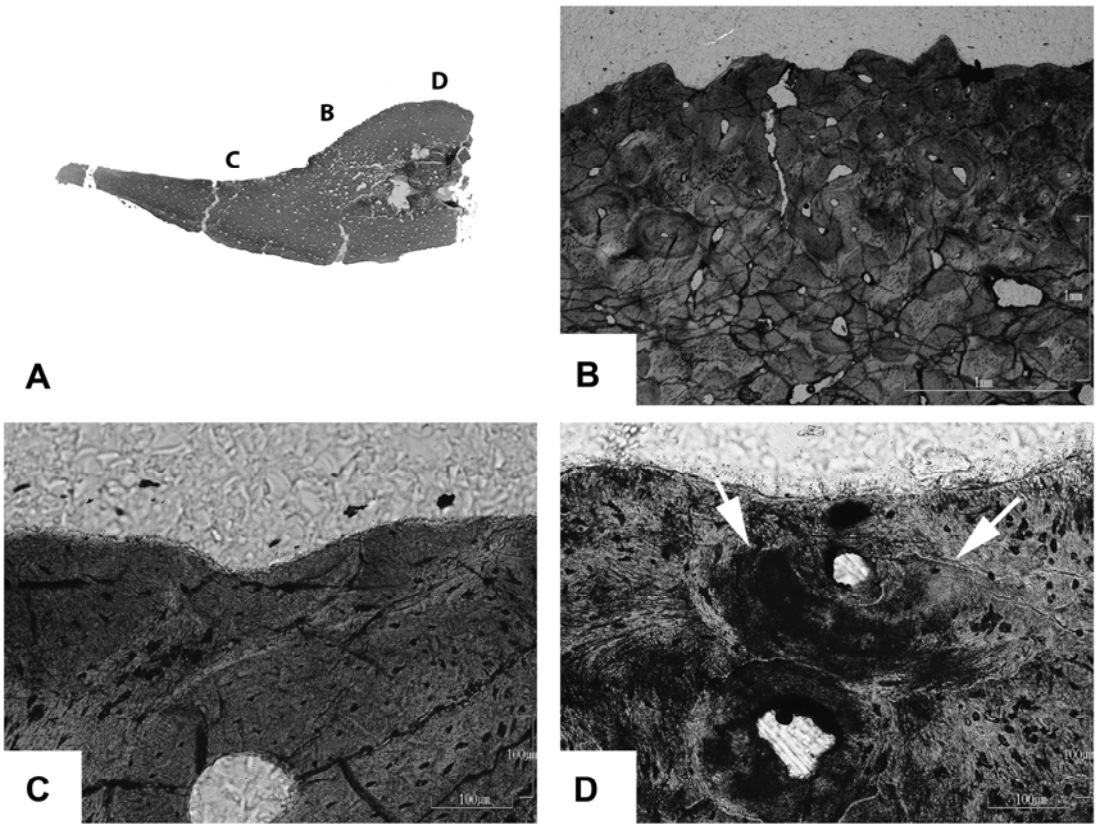


Figure 2.2 *Triceratops* parietal fragment, MOR 2946, showing the histology of the ventral erosion surface. A, view of whole fragment. Ventral surface faces up. Letters show placement of Figures B, C & D. Specimen is 6 cm long; B, Ventral surface of the slope between the thickened and thinned regions of the parietal. Scale bar equals 1 mm; C, Erosion surface of the thinned region showing eroded secondary osteons. Scale bar equals 100 µm; D, Erosion surface of thickened region showing an older erosion surface (arrows) with subsequent deposition. Scale bar equals 100 µm.

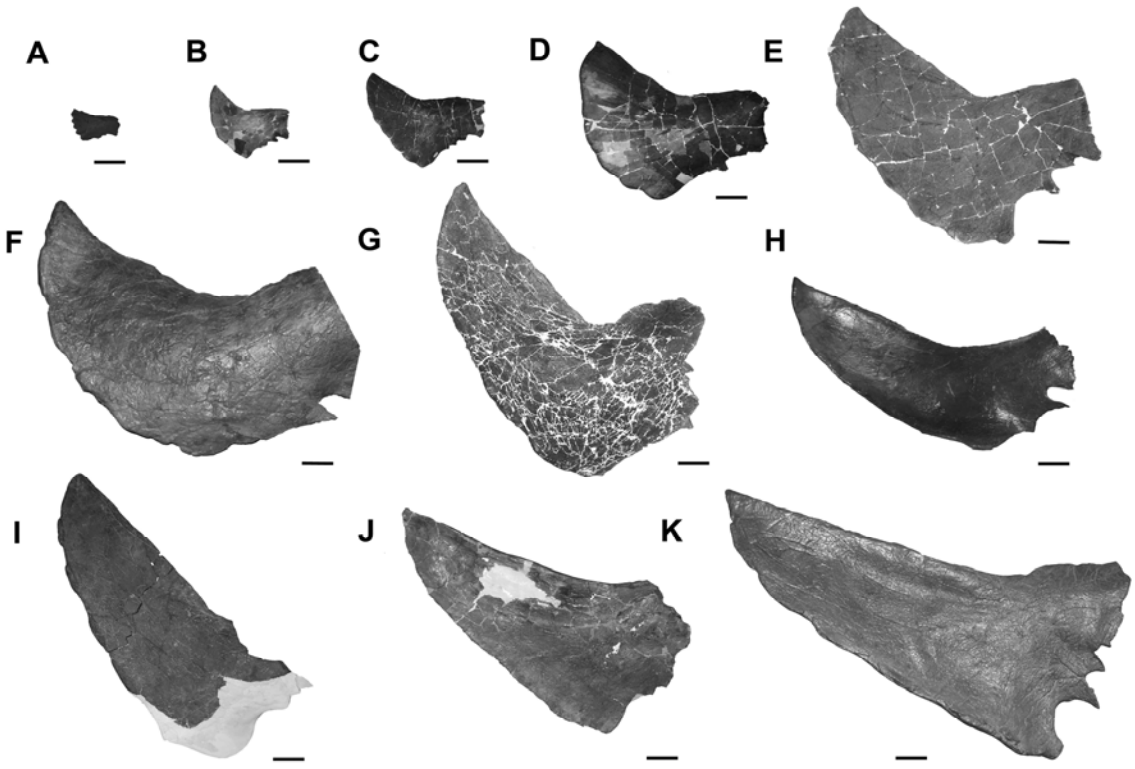


Figure 2.3 Ontogenetic elongation of the squamosals in *Triceratops*. Specimens arranged in hypothesized ontogenetic sequence: A, UCMP 154452; B, MOR 2569; C, MOR 1199; D, MOR 1110; E, MOR 1120; F, MOR 004; G, MOR 2702; H, AMNH 5116; I, UWGM 732; J, "*Torosaurus*" SMM P97.6.1 (image reversed for comparison); K, "*Torosaurus*" MOR 1122. Scale bars equal 10 cm.

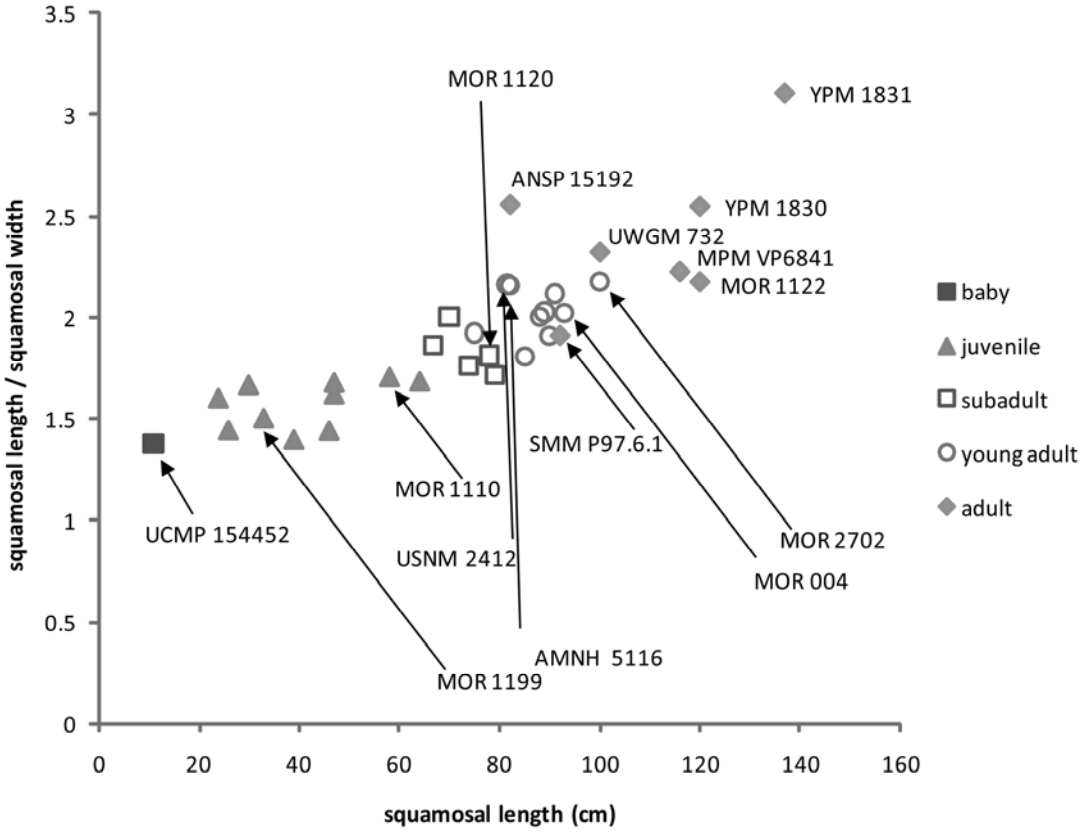


Figure 2.4 Squamosal elongation in *Triceratops*. Growth stages: Baby: UCMP 154452; Juvenile: LACM 149538, MOR 1110, MOR 1199, MOR 2569, MOR 2927, MOR 2928, MOR 2929, MOR 2572, MOR 2951, UCMP 136306; Subadult: MOR 1120, MOR 2923, YPM1821, YPM 1822, YPM 1823; Young adult: AMNH 5116, FMNH P12003, LACM 59049, MOR 004, MOR 1625, MOR 2702, MOR 2942, SMM P60.2.1, UCMP 113697, USNM 2412; UWGM 732*; Adult ("*Torosaurus*"): ANSP 15192, MOR 1122, MPM VP6841, SMM P97.6.1, YPM 1830, YPM 1831. Squamosal length measured from parietal/squamosal contact at caudal frill margin to anterolateral most point of squamosal margin. Squamosal width measured across widest point of squamosal. *Estimate.

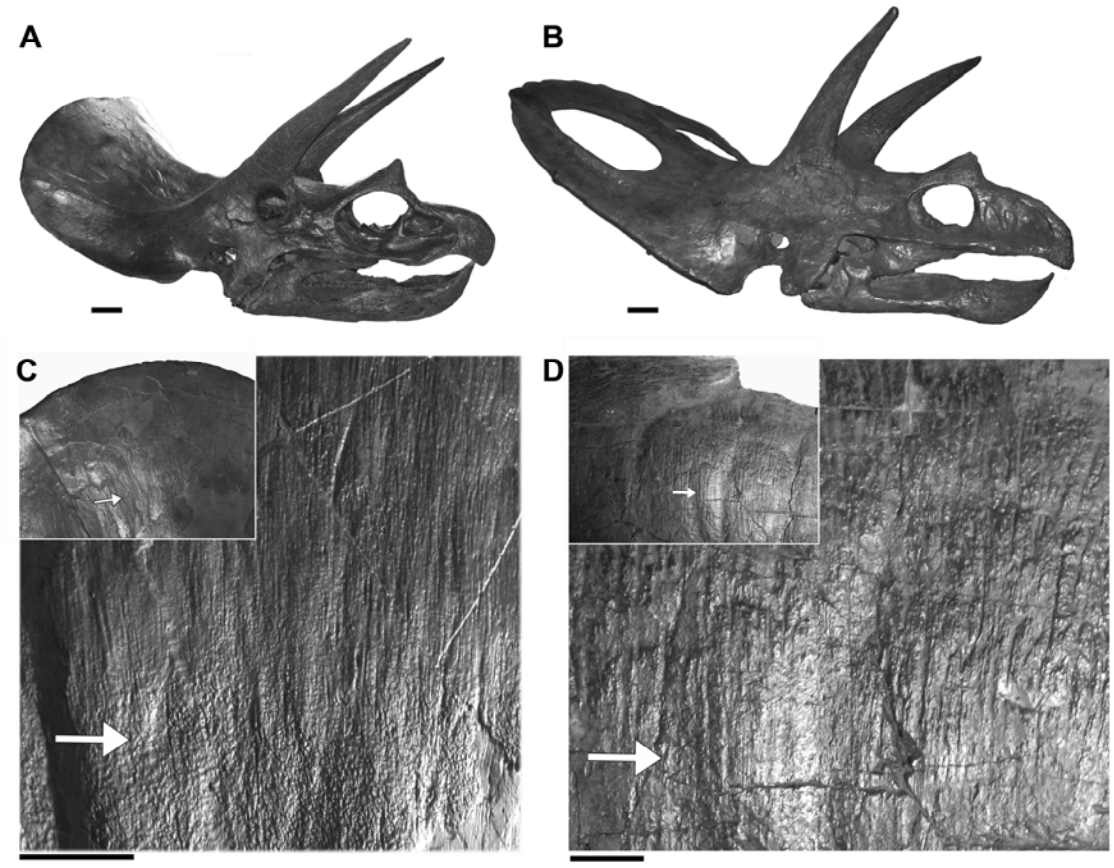


Figure 5. Comparison of AMNH 5116 to "*Torosaurus latus*" specimens. A, AMNH 5116, lower jaw belongs to a separate individual (AMNH 5039). Note anteriorly inclined postorbital horn cores and elongate squamosals. Scale bar equals 10 cm; B, YPM 1830, the type specimen of "*Torosaurus latus*." Scale bar equals 10 cm; C, Close-up of the dorsal surface of the parietal of AMNH 5116 revealing the transition from striated surface texture over the caudal end of the parietal to a pebbly surface texture in the region where the fenestrae will open. Scale bar equals 3 cm; D, Ventral surface of the parietal of "*Torosaurus*" MOR 981, revealing striated surface texture. Scale bar equals 1 cm. Image of YPM 1830 © 2010 Peabody Museum of Natural History, Yale University, used with permission.

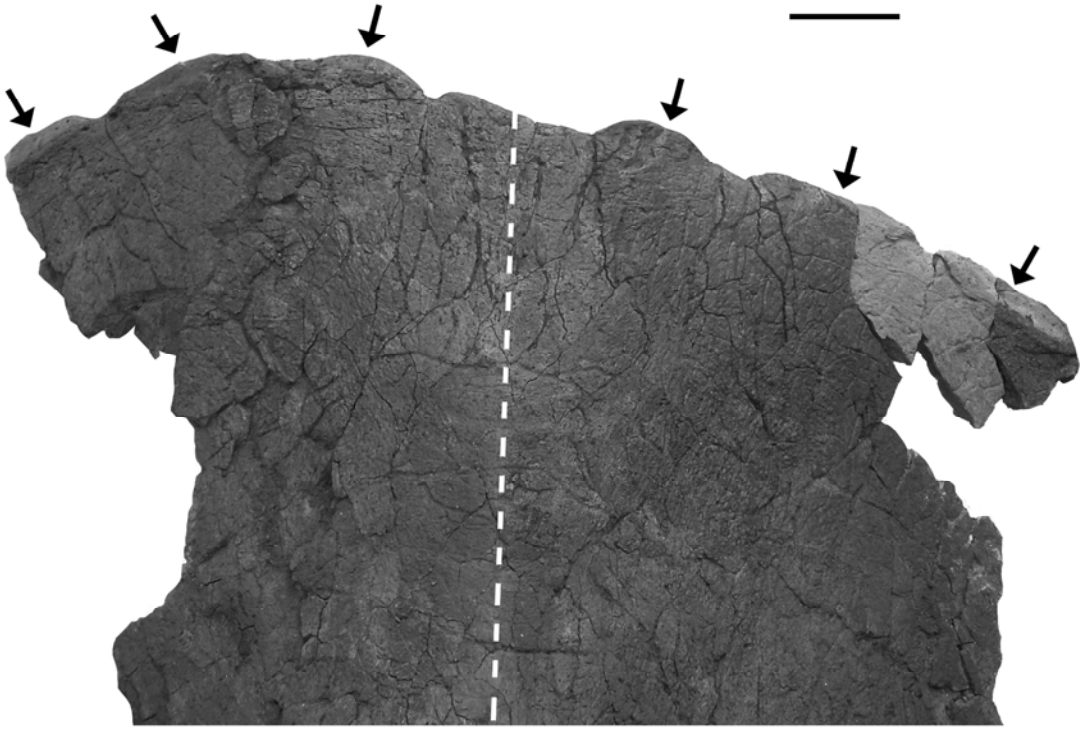


Figure 2.6 The parietal of *Triceratops* specimen MOR 2923 (skull slightly distorted from postmortem crushing). Arrows indicate epiparietals. Dashed line represents the midline. Scale bar equals 10 cm.

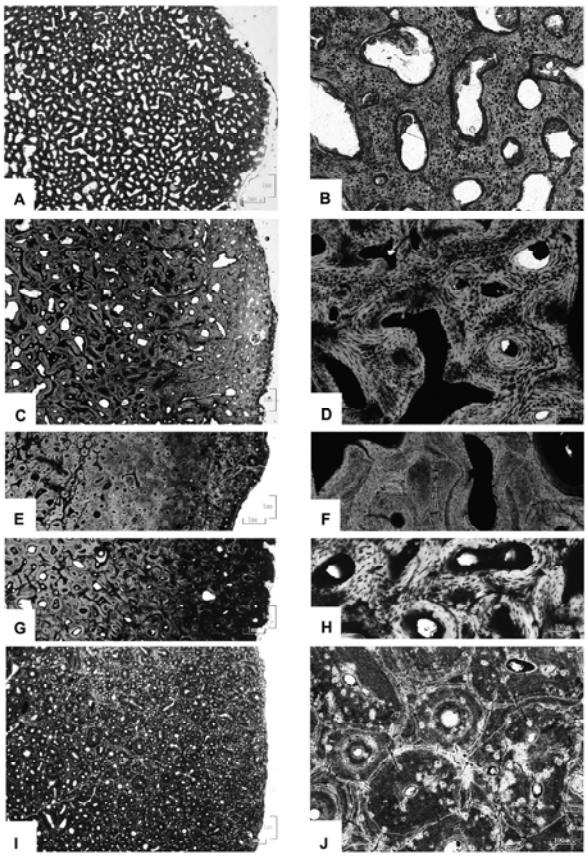


Figure 2.7 Osteohistology of an ontogenetic sequence of *Triceratops* postorbital horn cores. A, UCMP 159233, juvenile postorbital horn core (approximately 20 cm in length, arched backward), transverse section, showing spongy tissue with very high vascularization; B, close-up of A showing that the spongy tissue is entirely primary, indicative of its young age; C, MOR-HYP-P31.Horn1-D2-2, large juvenile postorbital horn core (approximately 50 cm in length, arched backward), transverse section showing spongy tissue with high vascularization; D, close-up of C showing that the spongy tissue is mostly composed of primary tissues with some secondary osteons; E, MOR 1625.Horn1-1, young adult postorbital horn (orbital horns incomplete), transverse section showing compact "Haversian" bone with numerous open erosion rooms and fairly high vascularization; F, close-up of E showing tissue composed of loosely packed "Haversian" systems with large erosion rooms; G, MOR 2702.Horn1-1, young adult postorbital horn core (approximately 55 cm in length arched forward), transverse section, showing dense "Haversian" systems with fairly high vascularization; H, close-up of G showing a tissue composed of loosely packed "Haversian" systems with large erosion rooms; I, MOR 1122.Horn1-2, adult postorbital horn core (approximately 60 cm in length, arched forward), transverse section, showing dense tissue with moderate vascularization; J, close-up of G showing a tissue composed of dense, multigenerational "Haversian" canals, indicative of a mature individual.

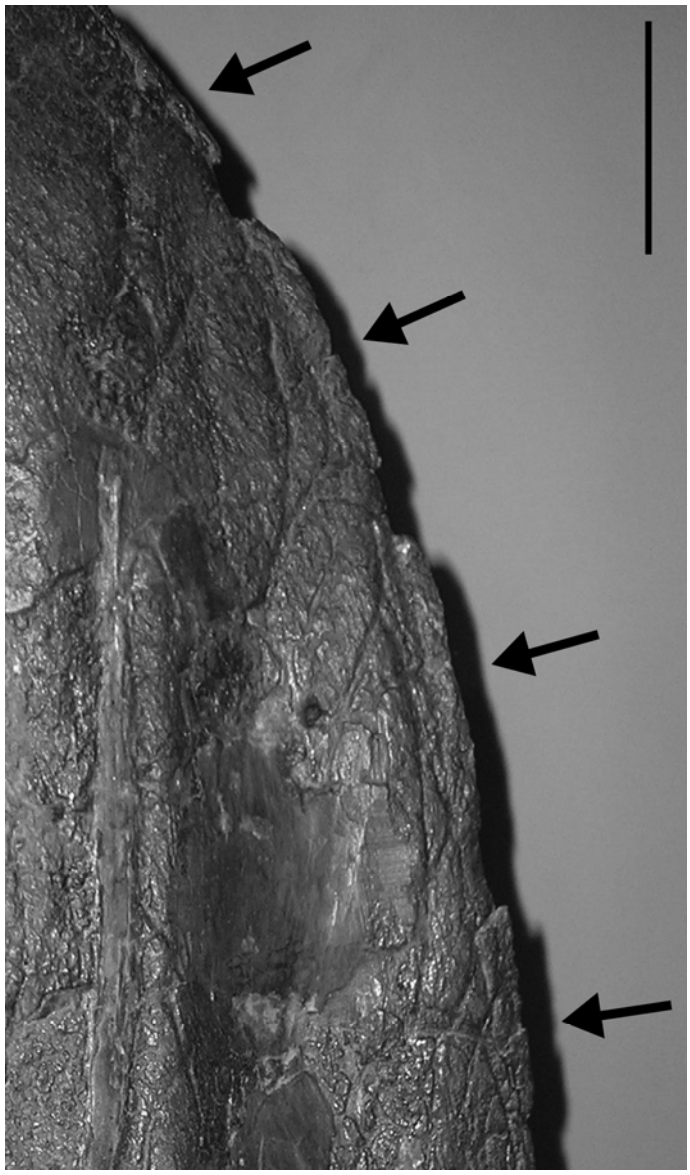


Figure 2.8 The dorsoventrally flattened epoccipitals of "*Torosaurus*" specimen ANSP 15192 reveal ontogenetic maturity. Scale bar equals 10 cm.

Table 2.1 Ontogenetic trends expressed in the parietal-squamosal frill of *Triceratops;* est, estimate; np, not preserved. Ontogenetic trends: A, thinning on lateral margins of parietal; B, depressions along lateral margins on ventral side of parietal; C, ventral depressions isolated from lateral margins of parietal; D, parietal exhibits textural change surrounding incipient fenestrae; E, squamosals elongate; F, fenestrae open. *AMNH970 not measured due to enclosure in display case.**Lateral margins of MOR2702 are not preserved and thus it is unknown if the incipient fenestrae are fully isolated from the margins.

		Parietal	Ontogenetic trends					
Triceratops	Growth stage	length (cm)	A	B	C	D	E	F
UCMP 154452	Baby	12						
MOR 2569	Juvenile	26	x					
MOR 1199	Juvenile	38	x					
MOR 2951	Juvenile	42	x					
UCMP 136306	Juvenile	46	x					
MOR 1110	Juvenile	49	x					
MOR 1120	Subadult	71	np					
YPM 1823	Subadult	64		x				
MOR 2924	Subadult	68		x				
MOR 2950	Subadult	--		x				
MOR 2574	Subadult	--		x				
MOR 1625	Young adult	--		x				
LACM 59049	Young adult	83		x				
AMNH 970	Young adult	--*			x			
MOR 2946	Young adult	--			x			
MOR 2702	Young adult	--			x**		x	
AMNH 5116	Young adult	83				x	x	
USNM 2412	Young adult	71					x	x
UWGM 732	Young adult	--					x	np
SMM P97.6.1	Adult	100(est)					x	x
MOR 981	Adult	116					x	x
YPM 1831	Adult	134(est)					x	x
YPM 1830	Adult	--					x	x
ANSP 15192	Adult	85					x	x
MOR 1122	Adult	125					x	x
MPM VP6841	Adult	107(est)					x	x

Table 2.2 Growth stages of *Triceratops*. Modified from Horner and Goodwin, 2006. np, not preserved; d-v, dorsoventrally compressed.

Growth stage	Example	p.o. Horn orientation (curvature)	Epoccipitals	Squamosals	Parietal
Baby	UCMP 154452	Straight, no curvature	np	Short, broad	Unfenestrated
Juvenile	MOR 1199 MOR 1110	Posterior	Delta-shaped	Short, broad	Unfenestrated
Subadult	MOR 1120	Anterior tip of horn posterior	Delta-shaped	Short, broad	Unfenestrated
Young adult	MOR 004 MOR 1625 MOR 2702	Anterior	d-v	Broad to elongate, no squamosal bar	Unfenestrated to small incipient fenestrae
Adult	MOR 981 MOR 1122	Anterior	d-v	Elongate, squamosal bar present	Fenestrated

Appendix 2.1 Sample of *Triceratops* cranial material collected by the MOR, the majority having been collected since 1999.

Specimen Number	Material	Specimen Number	Material
MOR004	Articulated skull	MOR2436	Partial disarticulated skull
MOR335	Parietal	MOR2551	Partial skull
MOR539	Partial skull	MOR2552	Partial skull
MOR699	Disarticulated skull	MOR2569	Disarticulated skull
MOR965	Partial skull	MOR2570	Partial skull
MOR981	Articulated skull	MOR2572	Squamosal
MOR989	Nasal horn, rostral	MOR2574	Disarticulated skull
MOR1098	Postorbital horn core	MOR2576	Postorbital horn core
MOR1110	Disarticulated skull	MOR2589	Postorbital horn core
MOR1120	Disarticulated skull	MOR2590	Premaxilla
MOR1122	Articulated skull	MOR2597	Partial skull
MOR1199	Disarticulated skull	MOR2702	Partial skull
MOR1604	Articulated skull	MOR2923	Articulated skull
MOR1625	Partial skull	MOR2924	Disarticulated skull

Appendix 2.1 (Continued)

Specimen Number	Material	Specimen Number	Material
MOR2927	Squamosal, postorbital horn core	MOR2958	Postorbital horn core
MOR2928	Squamosal, dentary	MOR 2959	Partial skull
MOR2929	Squamosal	MOR2969	Parietal
MOR2937	Maxilla	MOR 2970	Squamosal
MOR2938	Partial disarticulated skull	MOR2971	Partial disarticulated skull
MOR2942	Squamosal	MOR2972	Partial skull
MOR2945	Dentary	MOR2975	Partial skull
MOR 2946	Parietal, squamosal	MOR2979	Partial skull
MOR2950	Partial skull	MOR2980	Squamosal
MOR2951	Disarticulated skull	MOR2982	Partial disarticulated skull
MOR2952	Partial skull	MOR2984	Partial skull

Literature Cited

Brown, C. M., A. P. Russell, and M. J. Ryan. 2009. Pattern and transition of surfacial bone texture of the centrosaurine frill and their ontogenetic and taxonomic implications. Journal of Vertebrate Paleontology 29:132-141.

Carr, T. D. 1999. Craniofacial ontogeny in tyrannosauridae (Dinosauria, Coelurosauria). Journal of Vertebrate Paleontology 19:497-520.

Chinsamy-Turan, A. 2005. The Microstructure of Dinosaur Bone. Johns Hopkins, Baltimore. 195 pp.

Colbert, E. H., and J. D. Bump. 1947. A skull of *Torosaurus* from South Dakota and a revision of the genus. Proceedings of the Academy of Natural Sciences of Philadelphia 99:93-106.

Dodson, P. 1975. Taxonomic implications of relative growth in lambeosaurine hadrosaurs. Systematic Zoology 24:37-54.

Dodson, P. 1996. The Horned Dinosaurs. Princeton University Press, Princeton, New Jersey, 346 pp.

Dodson, P. and P.J. Currie. 1988. The smallest ceratopsid skull-Judith River Formation of Alberta. Canadian Journal of Earth Sciences 25:926-930.

Dodson, P., C. A. Forster, and S. D. Sampson. 2004. Ceratopsidae; pp. 494-513 in D. B. Weishampel, P. Dodson, and H. Osmólska (eds.), The Dinosauria. Univ. California Press, Berkeley.

Farke, A. A. 2007. Cranial osteology and phylogenetic relationships of the chasmosaurine ceratopsid *Torosaurus latus*; pp. 235-257 in K. Carpenter (ed.), Horns and Beaks: Ceratopsian and Ornithopod Dinosaurs. Indiana University Press, Bloomington and Indianapolis.

Farke, A. A., and T. E. Williamson. 2006. A ceratopsid dinosaur parietal from New Mexico and its implications for ceratopsid biogeography and systematics. Journal of Vertebrate Paleontology 26:1018-1020.

Forster, C. A. 1996. Species resolution in *Triceratops*: cladistic and morphometric approaches. Journal of Vertebrate Paleontology 16:259-270.

Francillon-Vieillot, H., V. de Buffrénil, F. J. Géraudie, J. Y. Meunier, L. Sire, L. Zylberberg, and A. de Ricqlès. 1990. Microstructure and mineralization of vertebrate skeletal tissues; pp. 471-548 in J. G. Carter (ed.), Skeletal

Biomineralization: Patterns, Processes and Evolutionary Trends. Van Nostrand Reinhold, New York.

Gilmore, C. W. 1946. Reptilian fauna of the North Horn Formation of central Utah. U.S. Geological Survey Professional Paper 210C:1-52.

Goodwin, M. B., W. A. Clemens, J. R. Horner, and K. Padian. 2006. The smallest known *Triceratops* skull: new observations on ceratopsid cranial anatomy and ontogeny. Journal of Vertebrate Paleontology 26:103-112.

Hatcher, J. B., O. C. Marsh, and R. S. Lull. 1907. The Ceratopsia. US Geological Survey Monograph 49:1-300.

Horner, J. R., and M. B. Goodwin. 2006. Major cranial changes during *Triceratops* ontogeny. Proceedings of the Royal Society of London B. 273:2757-2761.

Horner, J. R., and M. B. Goodwin. 2008. Ontogeny of cranial epi-ossifications in *Triceratops*. Journal of Vertebrate Paleontology 28:134-144.

Horner, J. R. and M. B. Goodwin. 2009. Extreme cranial ontogeny in the Upper Cretaceous dinosaur *Pachycephalosaurus*. PLoS ONE 4(10): e7626.doi:10.1371/journal.pone. 0007626.

Horner, J.R. and E. T. Lamm. 2009. Metaplasia provided dinosaur skulls extreme morphological plasticity during ontogeny. Journal of Vertebrate Paleontology 29:117A.

Horner, J.R. and K. Padian. 2004. Age and growth dynamics of *Tyrannosaurus rex*. Proceedings of the Royal Society of London B. 271:1875-1880.

Horner, J. R., M. B. Goodwin, and H. N. Woodward. 2007. Synonomy consequences of dinosaur cranial ontogeny. Journal of Vertebrate Paleontology 27:92A.

Horner, J.R., M.B. Goodwin, and N. Myhrvold. 2009a. Hell Creek Formation dinosaur census reveals abundant *Tyrannosaurus*. 9th North American Paleontological Convention Abstracts, Cincinnati Museum Center Scientific Contributions 3: 146.

Horner, J.R., A. de Ricqlès, K. Padian, and R.D. Scheetz. 2009b. Comparative long bone histology and growth of the "hypsilophodontid" dinosaurs *Orodromeus makelai*, *Dryosaurus altus*, and *Tenontosaurus tillettii* (Ornithischia: Eurornithopoda). Journal of Vertebrate Paleontology 29:734-747.

Hunt, R. K., and T. M. Lehman. 2008. Attributes of the ceratopsian dinosaur *Torosaurus*, and new material from the Javelina Formation (Maastrichtian) of Texas. Journal of Paleontology 82:1127-1138.

Lambe, R. S. 1915. On *Eoceratops canadensis*, gen. nov., with remarks on other genera of Cretaceous horned dinosaurs. Geological Survey of Canada Museum Bulletin 12:1-49.

Lehman, T. M. 1987. Late Maastrichtian paleoenvironments and dinosaur biogeography in the western interior of North America. Palaeogeography, Palaeoclimatology, Palaeoecology 60:189-217.

Lehman, T. M. 1990. The ceratopsian subfamily chasmosaurinae: sexual dimorphism and systematics; pp. 211-229 in K. Carpenter and P. J. Currie (eds.), Dinosaur Systematics: Approaches and Perspectives. Cambridge University Press, New York.

Lull, R. 1905. Restoration of the horned dinosaur *Diceratops*. American Journal of Science 20:420-422.

Lull, R. S. 1933. A revision of the Ceratopsia or horned dinosaurs. Yale Peabody Museum of Natural History Memoirs 3:1-178.

Marsh, O. C. 1888. A new family of horned Dinosauria from the Cretaceous. American Journal of Science, series 3:334-336.

Marsh, O. C. 1889. Notice of gigantic horned Dinosauria from the Cretaceous. American Journal of Science, series 3:173-175.

Marsh, O. C. 1890. Description of new dinosaurian reptiles. American Journal of Science, series 3:81-86.

Marsh, O. C. 1891. Notice of new vertebrate fossils. American Journal of Science, series 3:265-269.

Mateus, O. 2008. Two ornithischian dinosaurs renamed: *Microceratops* Bohlin, 1953 and *Diceratops* Lull, 1905. Journal of Paleontology 82: 423.

Ostrom, J. H., and P. Wellnhofer. 1986. The Munich specimen of *Triceratops* with a revision of the genus. Zitteliana 14:111-158.

Ostrom, J. H., and P. Wellnhofer. 1990. *Triceratops*: an example of flawed systematics; pp. 245-254 in K. Carpenter and P. J. Currie (eds.), Dinosaur Systematics: Approaches and Perspectives. Cambridge Univ. Press, New York.

Padian, K., J. R. Horner, and J. Dhaliwal. 2004. Species recognition as the principal cause of bizarre structures in dinosaurs. Journal of Vertebrate Paleontology 24:100A.

Parks, W. A. 1925. *Arrhinoceratops brachyops*, a new genus and species of Ceratopsia from the Edmonton Formation of Alberta. University of Toronto Studies, Geological Series 19:5-15.

Sampson, S.D. 1995. Two new horned dinosaurs from the Upper Cretaceous Two Medicine Formation of Montana; with a phylogenetic analysis of Centrosaurinae (Ornithischia: Ceratopsidae). Journal of Vertebrate Paleontology 15:743-760.

Sampson, S. D., M. J. Ryan, and D. H. Tanke. 1997. Craniofacial ontogeny in centrosaurine dinosaurs (Ornithischia: Ceratopsidae): taxonomic and behavioral implications. Zoological Journal of the Linnean Society 121:293-337.

Scannella, J. B. and D. W. Fowler. 2009. Anagenesis in *Triceratops*: evidence from a newly resolved stratigraphic framework for the Hell Creek Formation. 9th North American Paleontological Convention Abstracts, Cincinnati Museum Center Scientific Contributions 3:148-149.

Sereno, P. C. 1986. Phylogeny of the bird-hipped dinosaurs (Order Ornithischia). National Geographic Society Research 2:234-256.

Sternberg, C. M. 1949. The Edmonton fauna and description of a new *Triceratops* from the Upper Edmonton member; phylogeny of the Ceratopsidae. Annual Report of the National Museum of Canada, Bulletin 113:33-46.

Sullivan, R. M., A. C. Boere, and S. G. Lucas. 2005. Redescription of the ceratopsid dinosaur *Torosaurus utahensis* (Gilmore, 1946) and a revision of the genus. Journal of Paleontology 79:564-582.

Tanke, D.H, and A. A. Farke. 2007. Bone resorption, bone lesions and extra cranial fenestrae in ceratopsid dinosaurs: a preliminary assessment; pp. 319-347 in K. Carpenter (ed.), Horns and Beaks: Ceratopsian and Ornithopod Dinosaurs. Indiana University Press, Bloomington and Indianapolis.

Tokaryk, T.T. 1986. Ceratopsian dinosaurs from the Frenchman Formation (Upper Cretaceous) of Saskatchewan. Canadian Field-Naturalist 100:192-196.

Tumarkin-Deratzian, A.R. 2009. Evaluation of long bone surface textures as ontogenetic indicators in centrosaurine ceratopsids. The Anatomical Record 292:1485-1500.

Ukrainsky, A.S. 2007. A new replacement name for *Diceratops* Lull, 1905 (Reptilia: Ornithischia: Ceratopsidae). Zoosystematica Rossica 16: 292.

Ukrainsky, A.S. 2009. Synonymy of the genera *Nedoceratops* Ukrainsky, 2007 and *Diceratus* Mateus, 2008 (Reptilia: Ornithischia: Ceratopsidae). Paleontologicheskii Zhurnal1: 108.

Wolfe, D.G. and J.I. Kirkland. 1998. *Zuniceratops christopheri* n. gen. & n. sp., a ceratopsian dinosaur from the Moreno Hill Formation (Cretaceous, Turonian) of west-central New Mexico; pp. 303-317 in ed. S.G. Lucas, J.I. Kirkland and J.W. Estep, Lower and Middle Cretaceous Terrestrial Ecosystems vol 14. Albuquerque, NM: New Mexico Museum of Natural History and Science Bulletin.

CHAPTER THREE

'*NEDOCERATOPS*': AN EXAMPLE OF A TRANSITIONAL MORPHOLOGY

Contribution of Authors and Co-Authors

Manuscript in Chapter 3

Author: John B. Scannella

Contributions: conceived and designed the experiments, performed the experiments, analyzed the data, contributed reagents/materials/analysis tools, wrote the paper.

Co-author: John R. Horner

Contributions: conceived and designed the experiments, performed the experiments, analyzed the data, contributed reagents/materials/analysis tools, wrote the paper.

Manuscript Information Page

John B. Scannella, John R. Horner.
Journal: Public Library of Science ONE
Status of Manuscript:
___Prepared for submission to a peer-reviewed journal
___Officially submitted to a peer-reviewed journal
___Accepted by a peer-reviewed journal
_x_Published in a peer-reviewed journal

Published by Public Library of Science
Scannella J. B., and J. R. Horner. 2011. '*Nedoceratops*': An example of a transitional morphology. PLoS ONE 6(12): e28705. doi:10.1371/journal.pone.0028705

The following chapter has been published in the open-access journal PLoS ONE and appears in this dissertation under the terms of the Creative Commons Attribution License.

Abstract

Background

The holotype and only specimen of the chasmosaurine ceratopsid dinosaur '*Nedoceratops hatcheri*' has been the source of considerable taxonomic debate since its initial description. At times it has been referred to its own genus while at others it has been considered synonymous with the contemporaneous chasmosaurine *Triceratops*. Most recently, the debate has focused on whether the specimen represents an intermediate ontogenetic stage between typical young adult *Triceratops* and the proposed mature morphology, which was previously considered to represent a distinct genus, '*Torosaurus*'.

Methodology/Principal Findings

The only specimen of '*Nedoceratops hatcheri*' was examined and the proposed diagnostic features of this taxon were compared with other chasmosaurine ceratopsids. Every suggested autapomorphy of '*Nedoceratops*' is found in specimens of *Triceratops*. In this study, *Triceratops* includes the adult '*Torosaurus*' morphology. The small parietal fenestra and elongate squamosals of *Nedoceratops* are consistent with a transition from a short, solid parietal-squamosal frill to an expanded, fenestrated condition. Objections to this hypothesis regarding the number of episossifications of the frill and alternations of bone surface texture were explored through a combination of comparative osteology and osteohistology. The synonymy of the three taxa was further supported by these investigations.

Conclusions/Significance

The *Triceratops*, '*Torosaurus'*, and '*Nedoceratops'* morphologies represent ontogenetic variation within a single genus of chasmosaurine: *Triceratops*. This study highlights how interpretations of dinosaur paleobiology, biodiversity, and systematics may be affected by ascribing ontogenetic and other intraspecific variation a taxonomic significance.

Introduction

For many years after the description of the first species of *Triceratops* (*T. horridus*; Marsh, 1889), nearly every variation in cranial morphology between specimens was considered sufficient grounds to erect new species. By 1949, as many as 16 species of this genus had been named (Ostrom and Wellnhofer, 1986; Dodson, 1996; Forster, 1996a). After his initial description of *Triceratops*, O.C. Marsh also named two species of a new genus of latest Cretaceous ceratopsid ('*Torosaurus'*), which were found in the same geological formation and geographic area as the *Triceratops* specimens (Marsh, 1891). '*Torosaurus*' differed from *Triceratops* in having an expanded, fenestrated parietal and elongate squamosals. The resultant high number of apparently coeval taxa had major implications for interpretations of dinosaur paleoecology and end-Cretaceous taxonomic diversity (Ostrom and Wellnhofer, 1986).

Ostrom and Wellnhofer (1986, 1990) called attention to the apparent high diversity of *Triceratops* and proposed an alternative hypothesis: that the variation used to

erect all of these taxa was instead simply intraspecific variation within *T. horridus*. They noted similar levels of variation in populations of extant horned mammals. This idea was largely supported by the more recent work of Forster (Forster, 1996a), who found morphometric evidence for only two species of *Triceratops* (*T. horridus* and *T. prorsus*). Ostrom and Wellnhofer (1990) further suggested that '*Torosaurus'* may actually represent sexual dimorphism within *Triceratops*. We recently presented evidence that '*Torosaurus'* instead represents the mature morphology of *Triceratops* (Scannella and Horner, 2010). As *Triceratops* matured, its skull underwent a series of radical transformations: the postorbital horn cores changed orientation, the epiossifications (epoccipitals) bordering the parietal-squamosal frill changed shape, and the frill itself expanded and became fenestrated [Scannella and Horner, 2010; Horner and Goodwin, 2006; Horner and Goodwin, 2008; Horner and Lamm, 2011). The end-product of this transformation was the morphology previously considered to represent a distinct genus: '*Torosaurus*'. Consideration of potential sources of intraspecific variation, including ontogenetic change, has reduced 18 latest Cretaceous ceratopsid taxa to two (*Triceratops horridus* and *Triceratops prorsus*). This produces a dramatically different view of horned dinosaur systematics.

One of the 18 proposed taxa, represented by a single skull (USNM 2412; Figure 3.1), has had a particularly complex taxonomic history. It has at various times been considered a distinct genus ('*Diceratops'*; Forster, 1996a; Lull, 1905), a species of *Triceratops* ('*Triceratops hatcheri'*; Lull, 1933), or variation within *Triceratops horridus* (Ostrom and Wellnhofer, 1986; Lehman, 1998). The genus name '*Diceratops'* was recently found to have been preoccupied and two new names were proposed: '*Diceratus'*

(Mateus, 2008) and '*Nedoceratops'* (Ukrainsky, 2007). '*Nedoceratops'*, being published first, has priority (Ukrainsky, 2009). The prefix 'nedo' is Russian in origin and means 'insufficiency' (Ukrainsky, 2007) – thus, '*Nedoceratops'* roughly translates to 'insufficient horned face.'

USNM 2412 has been considered unusual in that unlike the holotypes of *Triceratops* it expresses a small parietal fenestra and fenestrated squamosals (Lull, 1905). Dodson (1996) noted that the slightly elongate squamosals of USNM 2412 bear a closer resemblance to those of '*Torosaurus*' than to *Triceratops*. The specimen also has a greatly reduced or perhaps absent epinasal (Forster, 1996a). We have previously noted that several of the unusual features of USNM 2412 appear to be intermediate between those seen in *Triceratops* and '*Torosaurus*', and proposed that the specimen represents a *Triceratops* which was beginning to develop the expanded, fenestrated frill characteristic of the mature morphology, '*Torosaurus*' (Scannella and Horner, 2010). Recently, Farke (2011) redescribed USNM 2412 and considers '*Nedoceratops hatcheri'* a valid taxon, stating that its unusual features "may be explained as a whole suite of abnormalities in a single aberrant individual of *Triceratops*, or a suite of autapomorphies characterizing a taxon distinct from *Triceratops* (pg. 6)." Farke favors the latter hypothesis and rejects the hypothesis that '*Torosaurus*' represents a mature *Triceratops* (the Ontogenetic Trajectory Hypothesis [OTH] as he terms it).

The degree to which some proposed dinosaur taxa may or may not actually represent variation (either ontogenetic or individual) within established taxa is debated [e.g. Scannella and Horner, 2010; Farke, 2011; Dodson, 1990; Sampson et al., 1997). Ontogenetically transitional morphologies in the dinosaur fossil record have the potential

to dramatically affect interpretations of taxonomy and systematics (e.g. Scannella and Horner, 2010; Rozhdestvensky, 1965; Dodson, 1975; Horner and Goodwin, 2009; Horner et al., 2011). The taxonomic status of USNM 2412 (as well as '*Torosaurus*' and *Triceratops*) has significant implications for trends in dinosaur diversity preceding the K/Pg boundary.

Here we will demonstrate that every feature of USNM 2412 proposed to be diagnostic of a distinct genus is found within *Triceratops* and thus USNM 2412 more likely reflects variation within *Triceratops*. We also provide further evidence for the synonymy of *Triceratops* and '*Torosaurus*' (by '*Torosaurus*,' we are referring to '*Torosaurus latus*', not '*Torosaurus*' *utahensis* [see Scannella and Horner, 2010]). Finally, we discuss the effect of intraspecific variation on our interpretations of dinosaur paleobiology and systematics.

Institutional Abbreviations.

AMNH, American Museum of Natural History, New York, New York, USA; ANSP, Academy of Natural Sciences of Philadelphia, Pennsylvania, USA; CM, Carnegie Museum, Pittsburgh, Pennsylvania, USA; MOR, Museum of the Rockies, Bozeman, Montana, USA; MPM, Milwaukee Public Museum, Milwaukee, Wisconsin, USA; RTMP, Royal Tyrrell Museum, Drumheller, Alberta, CA; UCMP, University of California Museum of Paleontology, Berkeley, California, USA; USNM, National Museum of Natural History, Washington D.C., USA; YPM, Yale Peabody Museum, New Haven, Connecticut, USA.

Results

Reassessment of USNM 2412

Farke (2011) diagnoses '*Nedoceratops hatcheri*' as follows: "Chasmosaurine ceratopsid with the following autapomorphies: nasal horncore nearly completely undifferentiated from the nasal bone; greater portion of procurved postorbital horncores forms 90 degree angle with tooth row; and parietal fenestrae extremely small (occupying less than five percent of the total surface area of the parietal). *Nedoceratops hatcheri* is distinguished from *Triceratops* spp. in the position of the ventral extremity of the squamosal well above the alveolar process of the maxilla, and in the presence of parietal fenestrae, which are lacking in *Triceratops* species. *Nedoceratops hatcheri* is distinguished from *Torosaurus latus* in squamosal shape (particularly the reduced jugal notch and lack of a thickened medial margin in *N. hatcheri*), and that *N.hatcheri* has extremely reduced parietal fenestrae and a low number of episquamosals relative to *T. latus*. (pg. 4)"

Nasal and Nasal Horn**.** The nasal horn of USNM 2412 is indeed 'nearly completely undifferentiated from the nasal bone', however similar poorly defined nasal horn morphologies are seen in several specimens of *Triceratops* (UCMP 128561, USNM 1208, USNM 4720, MOR 981, MOR 1122; Figure 3.2). The nasal horn of MOR 981 (Figure 3.2D) is particularly unpronounced, yet not quite to the degree observed in USNM 2412. It has been suggested that the epinasal of USNM 2412 was lost either taphonomically or due to pathology (Ostrom and Wellnhofer, 1986; Forster, 1996a;

Horner and Goodwin, 2008). Areas of the anterior nasals are obscured by reconstruction; however there is no clear evidence of breakage indicating a missing epinasal. Farke (2011) suggests that the lack of an open epinasal suture makes it improbable that the epinasal was lost due to trauma in life. However the epinasal is known not to fuse to the underlying nasals until fairly late in ontogeny in some specimens of *Triceratops* (Horner and Goodwin, 2008). If the eipnasal was lost in life and the nasal sutures proceeded to close, there would be no reason to expect an open epinasal suture. For these reasons, the nasal horn morphology of USNM 2412, taken on its own, presents insufficient grounds to distinguish this specimen from *Triceratops*.

Postorbital Horn Cores. The left postorbital horn core is largely reconstructed, yet preserves the base which is slightly anteriorly inclined (Figure 3.1). The right postorbital horn core is more complete, and is fairly erect (varying from the morphology expressed on the left side of the skull) yet procurved. The orientation of the postorbital horn cores undergoes a radical change throughout ontogeny in *Triceratops* (Horner and Goodwin, 2006). In the smallest ('baby') specimens, the postorbital horns are erect, in juveniles they begin to curve posteriorly and then as ontogeny progresses they become procurved. Procurving of the postorbital horn cores indicate that USNM 2412 was a fairly mature individual (see Discussion). Given that the postorbital horn cores transformed so dramatically throughout ontogeny, variation in orientation between specimens is expected. Intraspecific variation in the orientation of the base of the postorbital horn core has been demonstrated in several taxa of chasmosaurine ceratopsids (Lehman, 1990).

Thus, the orientation of horn cores cannot be used to distinguish USNM 2412 from *Triceratops*.

Parietal Fenestrae. Arguably the most intriguing feature of USNM 2412 is the presence of a small parietal fenestra on the right side of the frill (the left half of the parietal is largely unpreserved). Farke (2011) notes no ventral depression surrounding the parietal fenestra of USNM 2412, though acknowledges that the parietal is extremely thin in this region. There is, in fact, a subtle ventral depression around the parietal fenestra of USNM 2412 which conforms to the shape of the fenestra (though it is slightly obscured by the metal framework supporting the skull and not immediately obvious upon observation; Figure 3.3). Also, there is a transition in surface texture surrounding the fenestra (Figure 3.4): the area immediately adjacent to the fenestra is somewhat less rugose than the rest of the parietal (though much of the surface texture is obscured by reconstruction). Parietal fenestrae are unknown in *Triceratops* (exclusive of '*Torosaurus*' specimens) but are found in specimens referred to '*Torosaurus*'. As we previously noted (Scannella and Horner, 2010), if *Triceratops* matured into the morphology previously considered diagnostic of '*Torosaurus*', at some point the parietal fenestrae would open. It is predicted that the fenestrae would start off small and expand in size, as is seen in centrosaurine ontogeny (Sampson et al., 1997; Dodson and Currie, 1988; Brown et al., 2009). Thus, we interpret the small parietal fenestra of USNM 2412 as a product of the parietal thinning which we previously demonstrated (Scannella and Horner, 2010) and not diagnostic of a distinct taxon (see Discussion).

Squamosal Morphology. The ventral extremity of the squamosal of USNM 2412 is positioned above the alveolar process of the maxilla. A similar configuration is seen in several specimens of *Triceratops* (e.g. UCMP 113697; USNM 1201) and is thus not diagnostic of a distinct taxon (Figure 3.5). Similarly, there is considerable variation in the size of the jugal notch formed by the squamosal in *Triceratops* specimens (see Scannella and Horner [2010] Figure 3). Indeed, there is variation in the size of the jugal notch between the left and right side of USNM 2412 (Figure 3.1). This is likely due to pathology (Tanke and Farke, 2007). The lack of a thickened median margin of the squamosal (or 'squamosal bar' (Farke, 2007) exhibited by USNM 2412 is expected until late in ontogeny in *Triceratops* (Scannella and Horner, 2010). The squamosals bear asymmetrical fenestrae which, as Farke (2011) notes, are not reliable for taxonomic purposes. The squamosal morphology of USNM 2412 is here interpreted as representing an intermediate between the short, broad condition typical of immature *Triceratops* and the elongate morphology with a thickened median margin which is found in mature specimens (previously assigned to '*Torosaurus*').

Episquamosal Number. The episquamosal count of USNM 2412 has been estimated as five, with the rostral episquamosals indiscernible due to tight fusion (2011). Alternatively, we suggest that the rostral episquamosals are not preserved in this specimen. Episquamosals are commonly lost taphonomically (Horner and Goodwin, 2008). The number of episquamosals preserved on USNM 2412 cannot be used to distinguish it from *Triceratops* (as noted by Farke [2011]) and as such does not support the hypothesis that this specimen represents a distinct genus.

Discussion

Taxonomic Status of '*Nedoceratops hatcheri*'

All of the features and conditions used to diagnose '*Nedoceratops*' are found in *Triceratops*. The nasal horn, if present, is greatly reduced but given the variation in nasal horn morphology in *Triceratops* (Ostrom and Wellnhofer, 1986; Farke, 2011; Marsh, 1898; Forster, 1993 [contra Cobabe and Fastovsky, 1987]) and the fact that other specimens possess nasal horns which are not much larger than that expressed by USNM 2412, we interpret this as variation within *Triceratops*. Alternatively, as noted above, the epinasal may have been lost in vivo – in which case this feature would not be useful for taxonomic diagnoses. The squamosal morphology (particularly that of the right side of the skull, the left squamosal apparently being pathologic [Tanke and Farke, 2007]) does not fall outside the range of variation found in *Triceratops* (see Scannella and Horner, 2010). The horn cores are procurved yet the right horn core is more erect than is typical in *Triceratops*. A similarly erect horn core is found in the holotype of *Eotriceratops xerinsularis* (RTMP 2002.57.7; [Wu et al., 2007]). We interpret this variation in postorbital horn core orientation as a result of the morphological change which these elements undergo throughout ontogeny (Horner and Goodwin, 2006). Variation between the orientations of the left and right postorbital horn cores in USNM 2412 further suggests that this feature is of limited taxonomic utility. Indeed, even if '*Torosaurus*' is not synonymous with *Triceratops*, the only feature which unambiguously distinguishes '*Nedoceratops*' from *Triceratops* is the small parietal fenestra. However, we think it is

more likely that had the animal not died when it did that this fenestra would have continued to develop and the frill would have continued to expand, resulting in a morphology indistinguishable from mature *Triceratops* (‘*Torosaurus*’).

Taxonomic Status of ‘*Torosaurus latus’*

Radical ontogenetic changes in cranial morphology have been noted in several dinosaur taxa (e.g. Sampson et al., 1997; Dodson, 1975; Horner and Goodwin, 2009; Sampson, 1995; Currie et al., 2008). *Triceratops* underwent a dramatic cranial transformation throughout ontogeny - the postorbital horn cores completely changed orientation and prominent triangular epiossifications of the cranial frill increased in size in juveniles and subadults and then became resorbed and flattened in more mature individuals (Horner and Goodwin, 2006; 2008). We have proposed that the cranial transformation of *Triceratops* included an expansion of the parietal-squamosal cranial frill, ultimately leading to the thin, fenestrated condition previously considered diagnostic of '*Torosaurus latus*' (Scannella and Horner, 2010). The proposed synonymy of *Triceratops* and '*Torosaurus*' (the 'OTH' [Farke, 2011]) has been challenged based on observations about the number and position of epiossifications on the cranial frill and cranial surface texture (Farke, 2011).

Variation in Epiossification Number and Position**.** As Farke notes, *Triceratops* specimens typically express five to seven episquamosals, whereas ‘*Torosaurus*’ specimens have seven (Forster, 1996b; Scannella and Horner, 2010; Farke, 2011). Farke states that “even squamosals from “baby” and juvenile *Triceratops* have between five and seven scallops for attachment of episquamosals . . . corresponding precisely to the

number found in most adult-sized individuals (pg. 7).” This also corresponds to the number of episquamosals found in ‘*Torosaurus*’ specimens (e.g. MOR 1122, MPM VP6841). Thus, variation in episquamosal number does not falsify the OTH. The alternative is to ascribe different species names to specimens with five, six, or seven episquamosals. As the number of episquamosals has been found to vary between the left and right sides of individuals (Scannella and Horner, 2010) and these elements are easily lost taphonomically (Horner and Goodwin, 2008); assigning species names based solely on this criteria would very likely be erroneous.

Triceratops has been diagnosed as possessing both a midline epiparietal and epiossificationswhich span the parietal-squamosal contacts (Forster, 1996a). ‘*Torosaurus*’ specimens, on the other hand, have been found to express evidence for between 10 (MOR 981) and 12 (MOR 1122) epiparietals. These specimens do not express a midline epiparietal or epiossificationsspanning the parietal-squamosal contacts. Thus, if ‘*Torosaurus*’ represents the mature morphology of *Triceratops* it means that a significant reconfiguration of epiparietals occurred throughout ontogeny.

The most complete ‘*Torosaurus*’ parietal is that of MOR 1122, a specimen which clearly expresses 12 epiparietals. Direct comparisons of this specimen to (non-‘*Torosaurus’*) *Triceratops* suggests an increase of at least six epiparietals throughout ontogeny. Is such a transformation feasible? Farke (2011) notes that an addition of epiossifications is apparently not found in ontogenetic series of centrosaurines (though he acknowledges variation by as many as two epiparietals and one episquamosal between juveniles and adults, a difference which he considers individual variation). We question whether direct comparisons of frill epiossifications of chasmosaurines and centrosaurines

are, in this regard, appropriate. In so far as chasmosaurine ceratopsids, Forster et al. (1993) and Godfrey and Holmes (1995) noted an apparent increase in episquamosals throughout ontogeny in *Agujaceratops mariscalensis* and *Chasmosaurus* spp. (respectively). Thus the suggestion of an addition of epiossifications throughout ontogeny in chasmosaurines is by no means unprecedented. These two examples may alternatively be interpreted as individual variation (Farke, 2011).

Triceratops epiossifications undergo dramatic changes in morphology throughout ontogeny (Horner and Goodwin, 2006; 2008). They expand, elongate, and eventually flatten. Forster (1996b) noted that in one specimen of *Triceratops* (CM 1221) these elements 'fuse into a continuous epoccipital rim (pg. 252).' A specimen at the MOR (MOR 2975) exhibits an episquamosal with two peaks, which is suggestive of erosion of the midline of the element and eventual division had elongation continued (Figure 3.6). If the six epiparietals of a (non-'*Torosaurus*') *Triceratops* were each to elongate and divide throughout ontogeny, it would produce 12 epiparietals. Osteohistological studies have already established that dinosaur cranial adornments were capable of dramatic transformations throughout ontogeny (likely due to metaplastic transformation [Horner and Goodwin, 2009; Horner and Lamm, 2011]); continued erosion of the epiossifications to eventually divide the elements is thus not an unfeasible mechanism for the apparent addition of epiossificatons throughout ontogeny which has been previously hypothesized (Lull, 1933; Forster et al., 1993; Godfrey and Holmes, 1995; Scannella and Horner, 2010).

Another factor which must be considered in concert with ontogenetic transformation is stratigraphic variation (Scannella and Fowler, 2009). MOR 1122, which

expresses 12 epiparietals, was collected from the bottom of the Hell Creek Formation in Eastern Montana. No other *Triceratops* specimens have been reported from this low in the formation. MOR 981, originally referred to '*Torosaurus*' (Farke, 2007), was collected from slightly higher in the formation. As Farke (2007) noted, MOR 981 exhibits evidence of only ten epiparietals. MPM VP6841, a large specimen previously referred to '*Torosaurus*' (Johnson and Ostrom, 1995), was collected from significantly higher in the formation (Scannella, 2010). It does not exhibit a complete set of epiparietals, however the one most completely preserved epiparietal is approximately 35 cm in length. Given the total width of this specimen's parietal (204 cm), the maximum number of epiparietals it could have accommodated – assuming no spaces between each epiparietal – is approximately six, a number comparable to that found in specimens of (non-'*Torosaurus*') *Triceratops* (Horner and Goodwin, 2008). There is likely a stratigraphic component to epiparietal count; the count suggested by MPM VP6841 is in agreement with *Triceratops*.

Furthermore, the presence of an epiossification spanning the parietal-squamosal contact, though previously unreported, is clearly present in a specimen of '*Torosaurus*' [ANSP 15192; see Scannella and Horner, 2010 Figure 8]. There is also evidence suggesting a midline epiparietal was present on MOR 1122, though unpreserved: vascular traces on the ventral surface of the parietal appear to lead directly from the anterior region of the parietal to each epiparietal (Figure 3.7). Pronounced vascular traces clearly terminate at the midline of the parietal, suggesting that blood was supplied to a midline epiparietal. If so, this further supports the synonymy of these taxa.

The Parietal of USNM 2412 as Intermediate between *Triceratops* and '*Torosaurus*'. If the parietal-squamosal frill of *Triceratops* eventually adopted the morphology previously considered diagnostic of '*Torosaurus*' through ontogeny, the discovery of intermediate morphologies would be expected. The existence of such intermediate specimens has been previously documented: throughout ontogeny the squamosals elongated and the parietal developed thin regions in the same areas where specimens of '*Torosaurus*' have fenestrae (Scannella and Horner, 2010; Horner and Lamm, 2011). USNM 2412 represents an important specimen in that it exhibits a small parietal fenestra in the same region of the parietal where thin areas (histologically revealed to have been actively becoming thinner at the time of death; [Scannella and Horner, 2010; Horner and Lamm, 2011]) are found in *Triceratops*. We consider these regions 'incipient fenestrae.' Farke suggests that these thin areas were instead areas for muscle attachment (Farke, 2011; Tsuihiji; 2010). As noted above, both a ventral depression and transition in surface texture are found around the parietal fenestra of USNM 2412. A transition in surface texture has been noted around the developing fenestrae of AMNH 5116 [*Triceratops*; Scannella and Horner, 2010] and in centrosaurines (Sampson et al., 1997; Brown et al., 2009). AMNH 5116 expresses a striated surface texture over much of the parietal, and a 'pebbly' surface texture in the regions which we hypothesize represent developing fenestrae. USNM 2412 differs slightly from this, in that no striated texture appears to be present on the parietal (though, as noted, much of the parietal's surface is obscured by reconstruction). Instead

there is a transition from rugose (‘adult’) surface texture to the less rugose texture around the fenestra.

The presence of rugose surface texture on the parietal of USNM 2412 has been noted as evidence of an 'old-adult' ontogenetic status for the specimen (Farke, 2011). Centrosaurine frills appear to have passed through three sequential ontogenetic stages: 1) ‘long-grained’ surface texture in juveniles; 2) mottled surface texture; 3) smooth/rugose ‘adult’ texture (Sampson et al., 1997; Brown et al., 2009; Tumarkin-Deratzian, 2010). Transformation of ceratopsid frill surface texture which does not follow this sequence, or reverts back and forth between these surface textures, has not previously been described (however Ryan and Russell [2005] note a ‘modified long-grain bone texture’ on cranial elements of large *Centrosaurus brinkmani*). It is important to emphasize that surface textures represent expressions of the histological growth and remodeling processes which were occurring at the time of the animal’s death (Francillon-Viellot et al., 1990). ‘Long-grained’ or striated texture, for example, is associated with rapid bone expansion (Francillon-Viellot et al., 1990; Sampson et al., 1997; Brown et al., 2009; Tumarkin-Deratzian, 2010). The parietal of MOR 981 (‘*Torosaurus’*) expresses a striated texture over much of its surface (Scannella and Horner, 2010). Histological examination of this parietal reveals that it was expanding at the time of death (Horner and Lamm, 2011). Based on this observation, it might be predicted that MOR 981 was less mature – perhaps significantly so – than MOR 1122, a ‘*Torosaurus*’ specimen which expresses histological evidence of extreme maturity and exhibits rugose surface texture on its parietal (Scannella and Horner, 2010). However, examination of the osteohistology of the postorbital horn core of MOR 981 reveals extremely dense, multigenerational

'Haversian' tissue indicative of maturity equivalent to that seen in MOR 1122, and greater than that expressed in (non-'*Torosaurus*') *Triceratops* (Figure 3.8). The presence of surface striations indicative of rapid expansion of the parietal in very mature specimens of *Triceratops* ('*Torosaurus*') supports the hypothesis that the short, thickened frill of a young adult *Triceratops* expanded and thinned late in ontogeny.

Farke (2011) notes that surface textures associated with bone resorption, such as those observed on the parietals of *Triceratops* and other ceratopsids, are not unambiguously associated with the formation of fenestrae. This is true, as resorption occurs in all bones – it is a general feature of growth and remodeling (Francillon-Vieillot et al., 1990), thus the presence of mottled surface textures in areas of ceratopsid skulls that do not form fenestrae (such as the parietal midline [Brown et al., 2009]) does not imply the formation of fenestrae but it does indicate that bone resorption was occurring in those areas at the time of death. In areas where fenestrae do form, histological evidence of resorption would be expected and has been demonstrated (Scannella and Horner, 2010; Horner and Lamm, 2011). The histological evidence suggests that reversion from a rugose ('adult') surface texture to a striated texture occurred in *Triceratops*. Therefore, the presence of rugose surficial texture on the parietal of USNM 2412 does not indicate that it had stopped growing, or that its parietal would not have undergone further changes had it not died when it did.

The suggestion that the thin regions of the parietal in *Triceratops* were areas for muscle attachment (Farke, 2011; Tsuihiji; 2010) would be supported by the presence of abundant extrinsic fibers in these areas (Hieronymus, 2006). Examination of the microstructure of these areas in *Triceratops* reveals no evidence of extrinsic fibers and

thus suggests that these were not regions of indirect muscle attachment. However, it is possible there was a direct attachment to the periosteum (Hieronymus, 2006). This is a somewhat more difficult hypothesis to test histologically with fossil material. Significantly, if the cranial ornamentation of marginocephalians developed through metaplastic transformation, as has been suggested (Horner and Lamm, 2011; Horner and Goodwin, 2009), it would indicate the absence of a periosteum at some point in ontogeny and thus direct muscle attachment would be unlikely. Regardless of whether or not there were muscle attachments in these regions at some point in ontogeny, the fact that USNM 2412 exhibits a fenestra within this area of the parietal confirms that resorption leading to eventual fenestration occurred here. We interpret USNM 2412 as a transitional morphology between the solid parietal of immature *Triceratops* and the fenestrated condition of mature individuals (‘*Torosaurus*’).

Juvenile '*Torosaurus latus*'. Until a clearly juvenile ‘*Torosaurus*’ is recovered - with backwards curving postorbital horn cores, delta-shaped epiossifications, elongate squamosals, and a fenestrated parietal – it appears more likely that either: a) juvenile ‘*Torosaurus’* were largely indistinguishable from *Triceratops* and differences in morphology between these two taxa only became apparent later in ontogeny, or b) ‘*Torosaurus*’ and *Triceratops* are synonymous. We favor the latter hypothesis for reasons previously discussed in detail (Scannella and Horner, 2010). An extensive, unbiased survey of the fossils of the Hell Creek Formation resulting in the collection of numerous rare ontogenetic stages of dinosaur taxa failed to recover evidence of juvenile

‘*Torosaurus*’ clearly distinguishable from *Triceratops* (Scannella and Horner, 2010; Goodwin and Horner, 2010; Horner et al., 2011).

Farke (2011) suggests that YPM 1831 (initially described as the holotype of ‘*Torosaurus gladius*’ (Marsh, 1891) may represent a subadult ‘*Torosaurus*.’ He notes that the frill of this specimen exhibits a smooth surface texture, no epiossifications are readily visible, and that several cranial elements are unfused. The frill of YPM 1831 exhibits a striated surface texture similar to that observed in MOR 981. As noted previously (Scannella and Horner, 2010), this surface texture is found in several specimens expressing indicators of ontogenetic maturity. As discussed above, MOR 981 itself exhibits extremely mature bone histology, thus the surface texture of the frill of YPM 1831 does not indicate subadult status. The postorbital horn cores of YPM 1831 are procurved, which is further indicative of ontogenetic maturity. The fact that epiossifications were not fused to the frill margin does not indicate a subadult status as many young adult/adult *Triceratops* do not retain all of their epiossifications (e.g. AMNH 5116, MOR 981, MOR 1122, MOR 2702, MPM VP6841, YPM 1830). As noted previously, epiossifications appear to have been easily lost taphonomically. There is variation in the timing of apparent cranial fusion in *Triceratops* (Scannella and Horner, 2010). Several large specimens exhibit open sutures and unfused cranial elements (e.g. MOR 2702, MOR 2938, MOR 2971) and there are also smaller, less mature specimens in which several sutures of the skull appear closed (e.g. MOR 1120, MOR 3010, YPM 1822). For this reason, apparent cranial fusion is likely one of the least reliable ontogenetic indicators. It is also worth noting that YPM 1831 is, as O.C. Marsh (Marsh,

1892) described it, “gigantic.” For these reasons, it is unlikely that YPM 1831 represents a subadult ‘*Torosaurus*.’

Transitional Morphologies and Dinosaur Systematics

The ongoing dialogue regarding the taxonomic status of USNM 2412 highlights questions of whether suggested autapomorphies for some dinosaur taxa may in fact represent ontogenetic or other intraspecific variation. The potential for dinosaurs of different ontogenetic stages to be mistaken for distinct taxa has been recognized for over half a century (Rozhdestvensky, 1965). In a landmark study, Dodson (1975) demonstrated that lambeosaurines underwent dramatic changes in cranial morphology relatively late in ontogeny. This late stage morphological change was comparable to what is seen in some extant avian dinosaurs (birds) which retain an immature cranial morphology until late in development (Dodson, 1975). As such, specimens of 'adult-sized' dinosaurs may have still undergone considerable changes in morphology had they survived to reach full maturity (e.g. Horner and Goodwin, 2009; Scannella and Horner, 2010; Horner and Lamm, 2011).

Ontogenetically transitional specimens can greatly affect interpretations of dinosaur systematics (e.g. Dodson, 1975; Carr, 1999; Horner and Goodwin, 2009; Carr, 1999; Fowler et al., 2011). The largest, and presumably most mature, dinosaurs are relatively rare in the fossil record and when they are recovered are easily mistaken for new, distinct taxa based on the state of features which transform throughout development (Horner et al., 2011). At the same time, specimens initially described as adults of new, small taxa may actually represent juveniles of other previously described taxa (Bakker et

al., 1988; Carr, 1999; Sereno et al., 2009; Fowler et al., 2011). In the absence of large sample sizes or monospecific bone beds, transitional specimens may be extremely difficult to recognize for what they are. The resulting overestimation of dinosaur diversity may produce an erroneous view of the paleoecology of these animals (Dodson, 1975).

New insights into *Triceratops* ontogeny are the result of a very large sample size produced in part by extensive field exploration of the uppermost Cretaceous Hell Creek Formation (Scannella and Horner, 2010; Horner et al., 2011). Each specimen of *Triceratops* is valuable for insights that may be provided regarding individual, ontogenetic, and stratigraphic variation (Scannella and Horner, 2010). The potential for transitional morphologies to be mistaken for unique taxa underscores the need for large scale field explorations in which numerous specimens of various growth stages are collected in order to test systematic hypotheses and clarify which morphological characters are in fact taxonomically informative.

Conclusions

The evidence thus far collected supports the hypothesis that *Triceratops*, '*Torosaurus'*, and '*Nedoceratops'* are synonymous and that '*Torosaurus'* represents the mature morphology of *Triceratops*. Features suggested to indicate an 'old adult' ontogenetic status for USNM 2412 (rugose surface texture on frill, apparent fusion of cranial elements) are found in non-fully mature *Triceratops* and hence do not indicate that the ontogenetic transformation of USNM 2412 was complete. If anything, the small parietal fenestra found in this specimen supports the hypothesis that it was in the process of transitioning between the classic *Triceratops* and '*Torosaurus*' morphologies. Farke

(2011) states that the hypothesis that USNM 2412 represents a taxon distinct from *Triceratops* would be refuted by "the identification of undisputed specimens of *Triceratops* that . . . preserve a mélange of character-states that are intermediate between known *Triceratops* specimens and *Nedoceratops* (pg. 6)." As we have presented here, there are numerous specimens of *Triceratops* which preserve such character-states in their nasal horn, squamosal, postorbital horn core and frill morphology thus refuting a distinct taxonomic position for '*Nedoceratops.*'

It might be argued that although the individual characters supposedly diagnostic of '*Nedoceratops'* may be found to some degree in specimens of *Triceratops* and '*Torosaurus'*, it is the unique combination of these characters which distinguishes '*Nedoceratops*' as a distinct taxon. But if this is true then nearly every specimen of *Triceratops* is referable to a distinct species and/or genus, for every specimen possesses some unique (if subtle) combination of characters which distinguishes it from others of the same taxon. This is the approach employed by Marsh and others which resulted in the naming of 16 species of *Triceratops* (Ostrom and Wellnhofer, 1986; 1990).

Consideration of the radical nature of ontogenetic change that occurred in marginocephalians (Sampson, 1995; Horner and Goodwin, 2006; 2009; Currie et al., 2008; Scannella and Horner, 2010) is critical to systematic interpretations. Dinosaur specimens representing various transitional growth stages may easily be misinterpreted as distinct taxa (Rozhdestvensky, 1965; Dodson, 1975). The debate which has surrounded USNM 2412 over the last century is inherently tied to the fact that it exhibits many intermediate features, and most likely represents an ontogenetically transitional morphology. Its small parietal fenestra is exactly what is predicted to be present at some

point in *Triceratops* ontogeny as the fenestrae expanded and developed into the '*Torosaurus*' morphology. Even if '*Torosaurus*' were not synonymous with *Triceratops*, it would be more parsimonious to ascribe USNM 2412 to an immature '*Torosaurus'* than to designate it as the holotype of a separate genus.

The synonymy of *Triceratops*, '*Torosaurus'*, and '*Nedoceratops'* reduces perceived latest Cretaceous ceratopsid diversity, and affects our interpretations of these animals' paleoecology. This, along with other ontogenetic synonymies (Carr, 1999; Horner and Goodwin, 2009), also supports the hypothesis that latest Maastrichtian dinosaur diversity was reduced relative to that found earlier in the Cretaceous (Archibald, 1996).

Materials and Methods

The holotpye skull of '*Nedoceratops hatcheri'*, USNM 2412, was examined first-hand in order to compare proposed autapomorphies with the condition expressed in other ceratopsids. Histological samples were prepared as has been previously described (Scannella and Horner, 2010). Specimens were embedded in polyester resin, sectioned with a precision saw, ground to a desired optical contrast using a lap wheel, and polished.

Acknowledgements

We are grateful to M. Carrano and M. Brett-Surman for allowing examination of USNM 2412. D. Brinkman and W. Joyce (YPM), P. Sheehan (MPM), C. Mehling (AMNH), M. Goodwin and P. Holroyd (UCMP), and N. Gilmore (ANSP) provided access to specimens at their respective institutions. D. Fowler provided integral assistance

with the stratigraphic placement of specimens. The MOR provided support. We thank K. Baker, B. Boessenecker, P. Dodson, D. Fowler, L. Freedman, M. Goodwin, L. Hall, S. Keenan, M. Loewen, K. Padian, A.S. Ukrainsky, D. C. Woodruff, and H. Woodward for helpful discussions. E. Lamm provided assistance with histological sectioning. Excavations by the MOR field crews and preparation by C. Ancell, S. Brewer, B. Harmon, P. Hookey, J. Jette, and L. Roberts are gratefully acknowledged. Thoughtful reviews by M. Loewen and two anonymous reviewers improved the manuscript. We would especially like to thank A. Farke for stimulating conversations about USNM 2412 and for making this scientific dialogue particularly enjoyable.



Figure 3.1. USNM 2412, the holotype and only specimen of '*Nedoceratops hatcheri*'. A. Left lateral view. B. Right lateral view. Scale bars equal 10 cm.

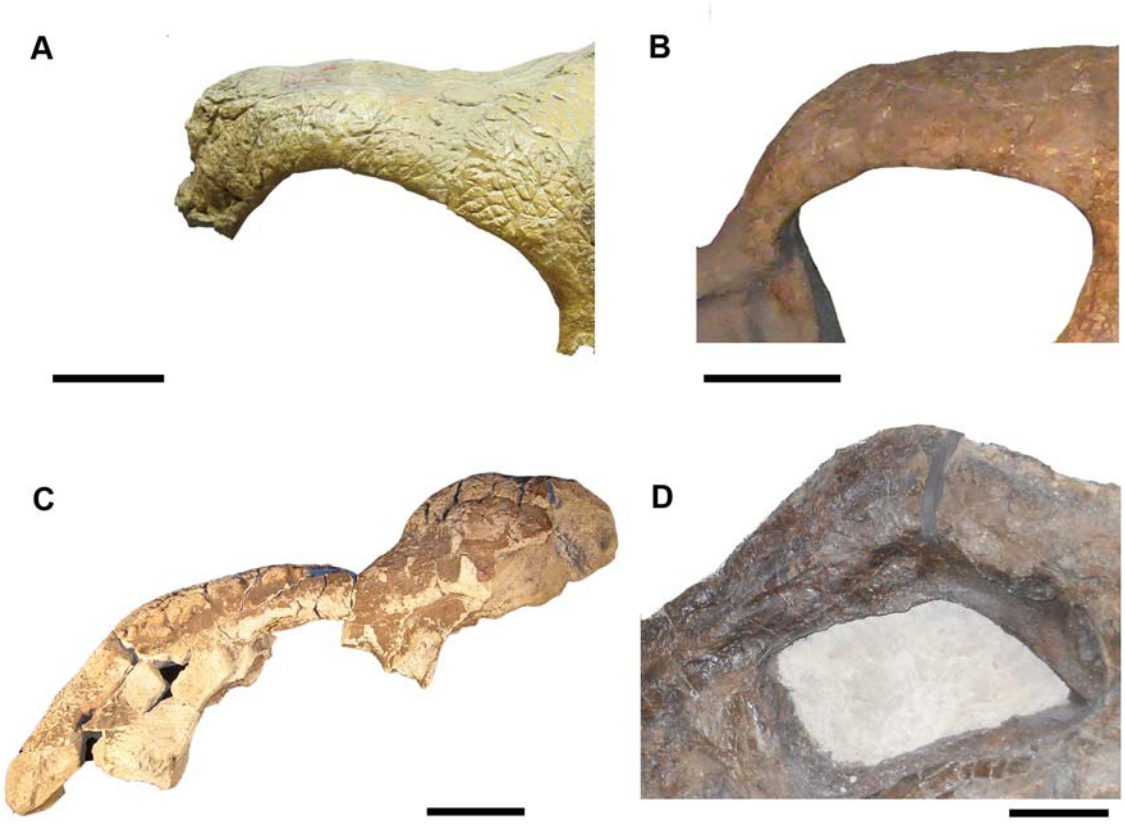


Figure 3.2. Nasal horn variation in *Triceratops*. A. USNM 4720, originally named the holotype of *Triceratops* '*obtusus*.' This specimen preserves a very low, blunt nasal horn. B. USNM 2412, the holotype of '*Nedoceratops hatcheri*.' The nasal horn of this specimen (if present – see discussion) is a low, smooth boss. C. UCMP 128561, originally named the holotype of '*Ugrosaurus olsoni*.' The nasal horn of this specimen is a low rugose boss. D. MOR 981 (previously '*Torosaurus*'). This specimen bears a low boss which is undifferentiated from the nasals. Scale bars equal 10 cm.

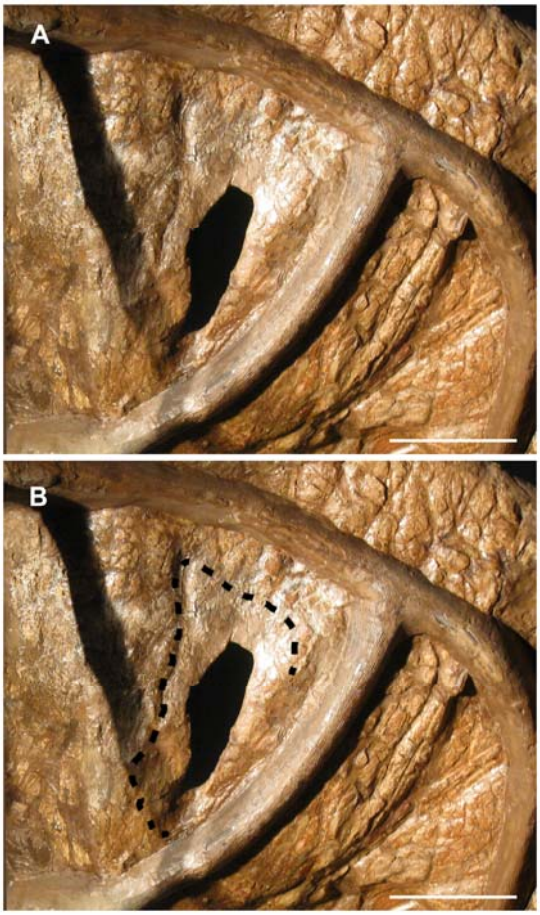


Figure 3.3. Ventral view of the right half of the parietal of USNM 2412. A. When viewed with offset lighting, the rim of a shallow depression surrounding the small fenestra is apparent. B. Extent of the depression is outlined. The area within the outline is markedly thinner than the remainder of the parietal. The extent of the depression is partially obscured by the framework which supports the skull. Scale bars equal 10 cm.

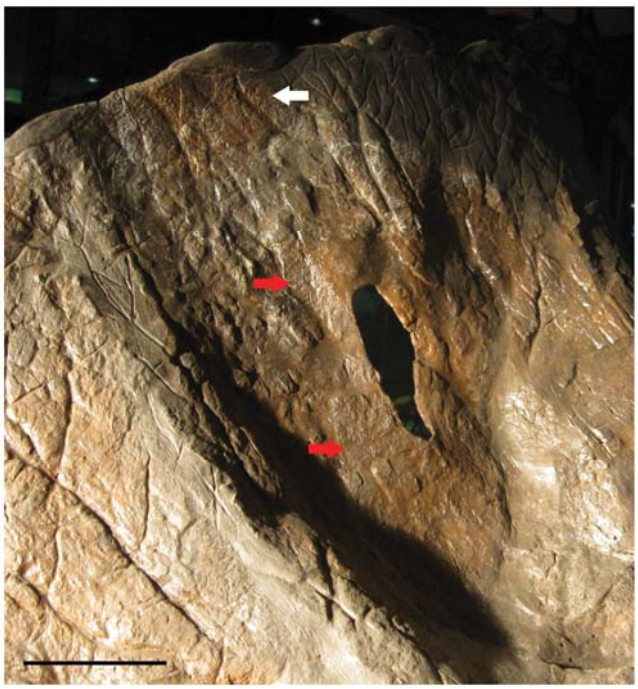


Figure 3.4. Dorsal view of the parietal fenestra of USNM 2412. Although much of the parietal is obscured by reconstruction, a transition in surface texture from the posterior margin (red arrow) to the area immediately adjacent to and surrounding the fenestra (white arrows) is apparent. Scale bar equals 10 cm.

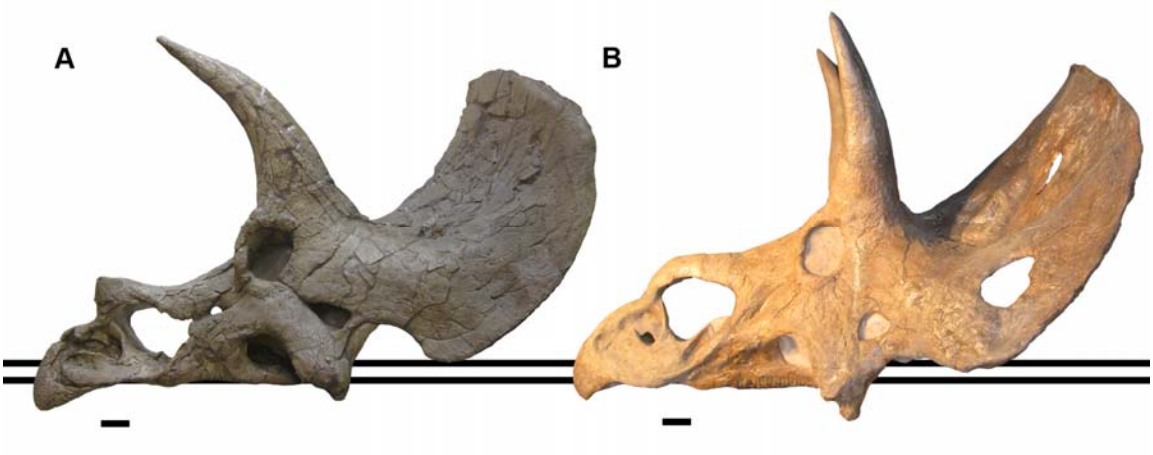


Figure 3.5. Lateral views of USNM 1201 and USNM 2142. A. Left lateral view of USNM 1201, originally named the holotype of *Triceratops* '*elatus*.' Note that the ventral extremity of the squamosal (denoted by upper horizontal line) is positioned well above the alveolar process of the maxilla (denoted by lower horizontal line). B. USNM 2412, right lateral view (reversed for direct comparison with USNM 1201 which only preserves the left side of the skull; the right squamosal of USNM 2412 is more elevated than the left). The alveolar process of the maxilla is positioned on the lower horizontal line, allowing for a direct comparison with USNM 1201. Note that the squamosal is not elevated to the extent found in USNM 1201. The position of the ventral extremity above the alveolar process of the maxilla can thus not be used to distinguish '*Nedoceratops hatcheri'* from *Triceratops*. Scale bars equal 10 cm.

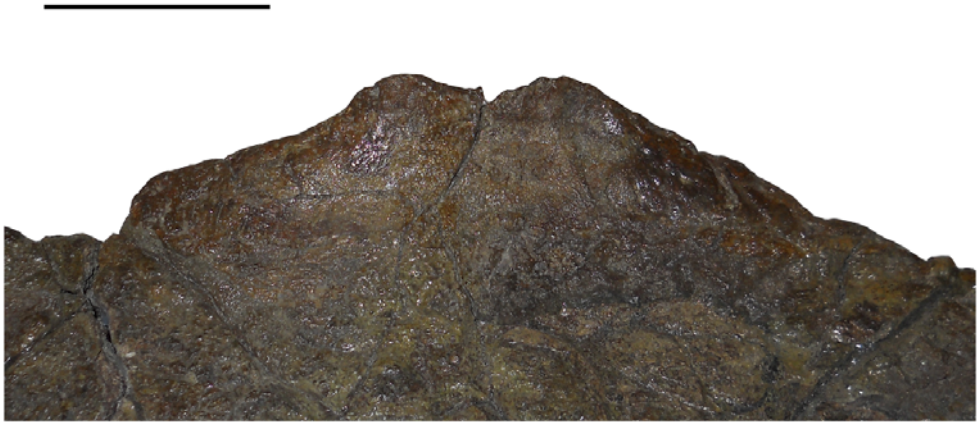


Figure 3.6. Episquamosal of MOR 2975. The presence of two peaks is suggestive of midline erosion. Scale bar equals 5 cm.

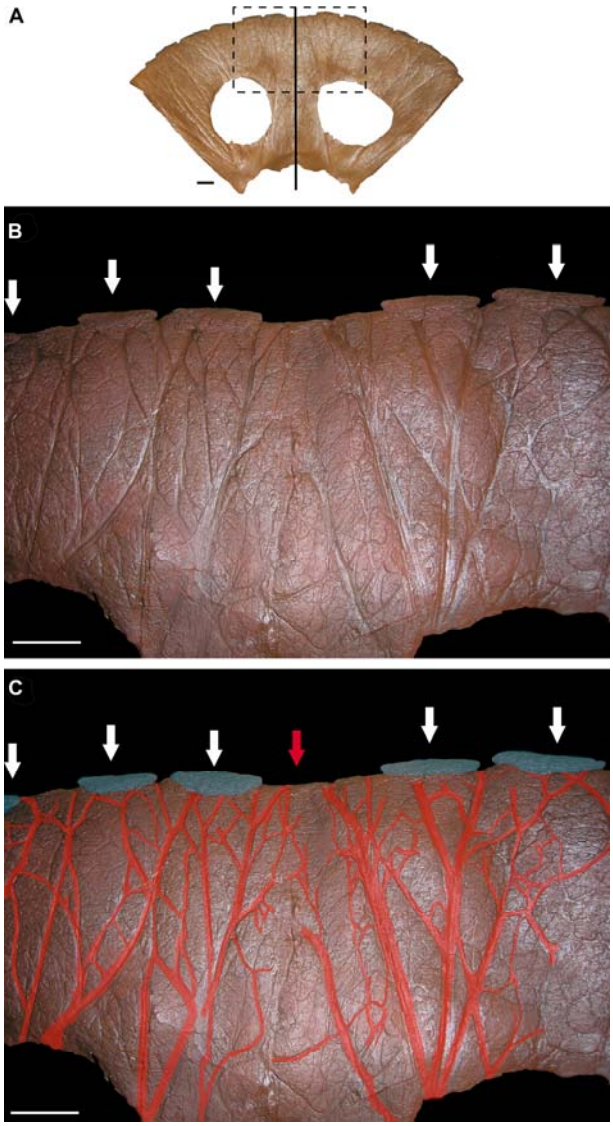


Figure 3.7. Ventral view of the parietal of MOR 1122. A. The entire parietal with midline denoted by vertical line. Dashed rectangle indicates area of interest in B and C. B. Impressed vascular traces are found over the entire ventral surface of the parietal. Epiparietals are indicated by arrows. MOR 1122 does not appear to possess an epiparietal over the midline of the parietal. C. Major vascular traces are highlighted in red. Note that the most prominent vascular traces lead to the epiparietals (highlighted in blue). Two large vascular traces lead to the midline of the parietal (denoted by red arrow), suggesting that an epiparietal occupied this position but was lost taphonomically. Scale bars equal 10 cm.

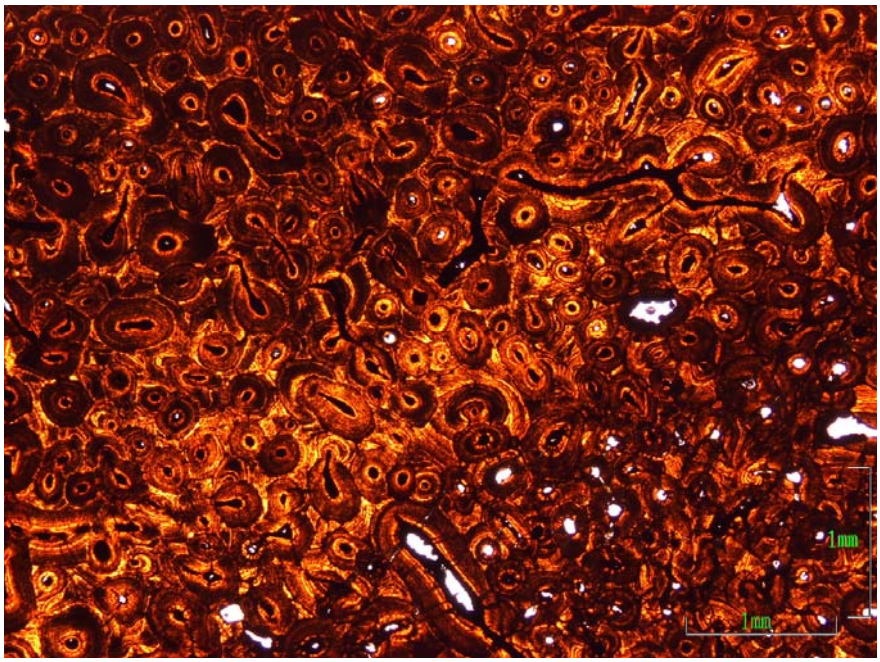


Figure 3.8. Osteohistology of the postorbital horn core of MOR 981. The dense, multigenerational 'Haversian' tissue is indicative of a mature individual.

References

Archibald, D.J. 1996. Dinosaur extinction and the end of an era: what the fossils say. Columbia University Press, New York. 237 p.

Bakker R.T., M. Williams, P.J. Currie. 1988. "*Nanotyrannus*, a new genus of pygmy tyrannosaur, from the latest Cretaceous of Montana." Hunteria 1: 1–30.

Brown, C. M., A. P. Russell, and M. J. Ryan. 2009. Pattern and transition of surfacial bone texture of the centrosaurine frill and their ontogenetic and taxonomic implications. Journal of Vertebrate Paleontology 29:132-141.

Carr, T. D. 1999. Craniofacial ontogeny in tyrannosauridae (Dinosauria, Coelurosauria). Journal of Vertebrate Paleontology 19:497-520.

Cobabe, E.A., and D.E. Fastovsky 1987. *Ugrosaurus olsoni*, a new ceratopsian (Reptilia: Ornithischia) from the Hell Creek Formation of eastern Montana. Journal of Paleontology 61: 148-154.

Currie, P.J., W. Langston, and D.H. Tanke. 2008. A new species of *Pachyrhinosaurus* (Dinosauria, Ceratopsidae) from the Upper Cretaceous of Alberta, Canada; pp. 1-108 in P.J. Currie, W. Langston, D.H. Tanke (eds.), A New Horned Dinosaur from an Upper Cretaceous Bone Bed in Alberta. NRC Research Press, Ottawa, Ontario, Canada.

Dodson, P. 1975. Taxonomic implications of relative growth in lambeosaurine hadrosaurs. Systematic Zoology 24:37-54.

Dodson, P. 1990. On the status of the ceratopsids *Monoclonius* and *Centrosaurus*; pp. 231-243 in K. Carpenter, P.J. Currie, (eds.) Dinosaur systematics: approaches and perspectives. Cambridge University Press, New York.

Dodson, P. 1996. The Horned Dinosaurs. Princeton University Press, Princeton, New Jersey, 346 pp.

Dodson, P. and P.J. Currie. 1988. The smallest ceratopsid skull-Judith River Formation of Alberta. Canadian Journal of Earth Sciences 25:926-930.

Farke, A. A. 2007. Cranial osteology and phylogenetic relationships of the chasmosaurine ceratopsid *Torosaurus latus*; pp. 235-257 in K. Carpenter (ed.), Horns and Beaks: Ceratopsian and Ornithopod Dinosaurs. Indiana University Press, Bloomington and Indianapolis.

Farke, A. A. 2011. Anatomy and taxonomic status of the chasmosaurine ceratopsid *Nedoceratops hatcheri* from the Upper Cretaceous Lance Formation of Wyoming, U.S.A. PLoS ONE 6:e16196.

Forster, C.A. 1993. Taxonomic validity of the ceratopsid dinosaur *Ugrosaurus olsoni* (Cobabe and Fastovsky). Journal of Paleontology 67: 316-318.

Forster, C. A. 1996a. Species resolution in *Triceratops*: cladistic and morphometric approaches. Journal of Vertebrate Paleontology 16:259-270.

Forster, C.A. 1996b. New information on the skull of *Triceratops*. Journal of Vertebrate Paleontology 16: 246-258.

Forster, C.A., P.C. Sereno, T.W. Evans, and T. Rowe. 1993. A complete skull of *Chasmosaurus mariscalensis* (Dinosauria: Ceratopsidae) from the Aguja Formation (Late Campanian) of West Texas. Journal of Vertebrate Paleontology 13: 161-170.

Francillon-Vieillot, H., V. de Buffrénil, F. J. Géraudie, J. Y. Meunier, L. Sire, L. Zylberberg, and A. de Ricqlès. 1990. Microstructure and mineralization of vertebrate skeletal tissues; pp. 471-548 in J. G. Carter (ed.), Skeletal Biomineralization: Patterns, Processes and Evolutionary Trends. Van Nostrand Reinhold, New York.

Fowler, D.W., H.N. Woodward, E.A. Freedman, P.L. Larson, and J.R. Horner. 2011. Reanalysis of "*Raptorex kriegsteini*": a juvenile tyrannosaurid dinosaur from Mongolia. PLoS ONE 6(6): e21376. doi:101371/journalpone.0021376

Godfrey, S. J., and R. Holmes. 1995. Cranial morphology and systematics of *Chasmosaurus* (Dinosauria: Ceratopsidae) from the Upper Cretaceous of western Canada. Journal of Vertebrate Paleontology 15:726–742.

Goodwin M.B., and J.R. Horner. 2010. Historical collecting bias and the fossil record of *Triceratops* in Montana; pp. 551-563 in M.J. Ryan, B.J. Chinnery-Allgeier, and D.A. Eberth DA, (eds.) New perspectives on horned dinosaurs. Bloomington, Indiana University Press.

Hieronymus, T.L. 2006. Quantitative microanatomy of jaw muscle attachment in extant diapsids. Journal of Morphology 267: 954-967.

Horner, J. R., and M. B. Goodwin. 2006. Major cranial changes during *Triceratops* ontogeny. Proceedings of the Royal Society of London B. 273:2757-2761.

Horner, J. R., and M. B. Goodwin. 2008. Ontogeny of cranial epi-ossifications in *Triceratops*. Journal of Vertebrate Paleontology 28:134-144.

Horner, J. R. and M. B. Goodwin. 2009. Extreme cranial ontogeny in the Upper Cretaceous dinosaur *Pachycephalosaurus*. PLoS ONE 4(10): e7626.doi:10.1371/journal.pone. 0007626.

Horner, J.R. and E.T. Lamm. 2011. Ontogeny of the parietal frill of *Triceratops*: a preliminary histological analysis. Comptes Rendus Pelevol 10: 439-452.

Horner, J.R., M.B. Goodwin, and N. Myrhvold. 2011. Dinosaur census reveals abundant *Tyrannosaurus* and rare ontogenetic stages in the Upper Cretaceous Hell Creek Formation (Maastrichtian), Montana, USA. PLoSOne 6(2): e16574. doi:10.1371/journal.pone.0016574.

Johnson, R.E. and J.H. Ostrom. 1995. The forelimb of *Torosaurus* and an analysis of the posture and gait of ceratopsians; pp. 205-218 in J. Thomasson (ed.) Functional Morphology in Vertebrate Paleontology. Cambridge University Press, New York.

Lehman, T. M. 1990. The ceratopsian subfamily chasmosaurinae: sexual dimorphism and systematics; pp. 211-229 in K. Carpenter and P. J. Currie (eds.), Dinosaur Systematics: Approaches and Perspectives. Cambridge University Press, New York.

Lehman, T. M. 1998. A gigantic skull and skeleton of the horned dinosaur *Pentaceratops sternbergi* from New Mexico. Journal of Paleontology 894–906.

Lull R.S. 1905. Restoration of the horned dinosaur *Diceratops*. American Journal of Science 20: 420-422.

Lull R.S. 1933. A revision of the Ceratopsia or horned dinosaurs. Yale Peabody Museum Memoir 3: 1-175.

Marsh, O. C. 1889. Notice of gigantic horned Dinosauria from the Cretaceous. American Journal of Science, series 3:173-175.

Marsh, O. C. 1891. Notice of new vertebrate fossils. American Journal of Science 265–269.

Marsh O.C. 1892. The skull of *Torosaurus.* American Journal of Science 43: 81-84.

Marsh, O. C. 1898. New species of Ceratopsia. American Journal of Science 92.

Mateus, O. 2008. Two ornithischian dinosaurs renamed: *Microceratops* Bohlin, 1953 and *Diceratops* Lull, 1905. Journal of Paleontology 82: 423.

Ostrom, J. H., and P. Wellnhofer. 1986. The Munich specimen of *Triceratops* with a revision of the genus. Zitteliana 14:111-158.

Ostrom, J. H., and P. Wellnhofer. 1990. *Triceratops*: an example of flawed systematics; pp. 245-254 in K. Carpenter and P. J. Currie (eds.), Dinosaur Systematics: Approaches and Perspectives. Cambridge Univ. Press, New York.

Rozhdestvensky A.K. 1965. Growth changes in Asian dinosaurs and some problems of their taxonomy. Paleontologičeskij žurnal 3: 95-109.

Ryan M.J., and A.P. Russell. 2005. A new centrosaurine ceratopsid from the Oldman Formation of Alberta and its implications for centrosaurine taxonomy and systematic. Canadian Journal of Earth Sciences 42: 1369-1387.

Sampson, S.D. 1995. Two new horned dinosaurs from the Upper Cretaceous Two Medicine Formation of Montana; with a phylogenetic analysis of Centrosaurinae (Ornithischia: Ceratopsidae). Journal of Vertebrate Paleontology 15:743-760.

Sampson, S. D., M. J. Ryan, and D. H. Tanke. 1997. Craniofacial ontogeny in centrosaurine dinosaurs (Ornithischia: Ceratopsidae): taxonomic and behavioral implications. Zoological Journal of the Linnean Society 121:293-337.

Scannella, J.B. 2010. *Triceratops*: a model organism for deciphering dinosaur heterochrony. Journal of Vertebrate Paleontology SVP Program and Abstracts Book: 158A.

Scannella, J. B. and D. W. Fowler. 2009. Anagenesis in *Triceratops*: evidence from a newly resolved stratigraphic framework for the Hell Creek Formation. 9th North American Paleontological Convention Abstracts, Cincinnati Museum Center Scientific Contributions 3:148-149.

Scannella, J. B., and J. R. Horner. 2010. *Torosaurus* Marsh, 1891, is *Triceratops* Marsh, 1889 (Ceratopsidae: Chasmosaurinae): synonymy through ontogeny. Journal of Vertebrate Paleontology 30:1157–1168.

Sereno P.C., L. Tan, S.L. Brusatte, H.J. Kriegstein, Zhao X., and K. Cloward. 2009. Tyrannosaurid skeletal design first evolved at small body size. Science 326: 418-422.

Tanke, D.H, and A. A. Farke. 2007. Bone resorption, bone lesions and extra cranial fenestrae in ceratopsid dinosaurs: a preliminary assessment; pp. 319-347 in K.

Carpenter (ed.), Horns and Beaks: Ceratopsian and Ornithopod Dinosaurs. Indiana University Press, Bloomington and Indianapolis.

Tsuihiji, T. 2010. Reconstructions of the axial muscle insertions in the occipital region of dinosaurs: evaluations of past hypotheses on marginocephalia and tyrannosauridae using the Extant Phylogenetic Bracket approach. The Anatomical Record 293:1360-1386.

Tumarkin-Deratzian, A. R. 2010. Histological evaluation of ontogenetic bone surface texture changes in the frill of *Centrosaurus apertus*. New Perspectives on Horned Dinosaurs, the Royal Tyrrell Museum Ceratopsian Symposium 251–263.

Ukrainsky, A.S. 2007. A new replacement name for *Diceratops* Lull, 1905 (Reptilia: Ornithischia: Ceratopsidae). Zoosystematica Rossica 16: 292.

Ukrainsky, A.S. 2009. Synonymy of the genera *Nedoceratops* Ukrainsky, 2007 and *Diceratus* Mateus, 2008 (Reptilia: Ornithischia: Ceratopsidae). Paleontologicheskii Zhurnal1: 108.

Wu X-C., D.B., Brinkman, D.A., Eberth, D.R., Braman. 2007. A new ceratopsid dinosaur (Ornithischia) from the uppermost Horseshoe Canyon Formation (upper Maastrichtian), Alberta, Canada. Canadian Journal of Earth Sciences 44: 1243-1265.

CHAPTER FOUR

A STRATGRAPHIC SURVEY OF *TRICERATOPS* LOCALITIES IN THE HELL CREEK FORMATION, NORTHEASTERN MONTANA (2006-2010)

Contribution of Authors and Co-Authors

Manuscript in Chapter 4

Author: John B. Scannella

Contributions: Conceived the study, collected data, interpreted results, and wrote the manuscript.

Co-author: Denver W. Fowler

Contributions: Conceived the study, collected data, correlated stratigraphic sections, interpreted results, and contributed to the manuscript.

Manuscript Information Page

John B. Scannella, Denver W. Fowler.
Status of Manuscript:
__Prepared for submission to a peer-reviewed journal
___Officially submitted to a peer-reviewed journal
___Accepted by a peer-reviewed journal
_x_Published in a peer-reviewed journal

Published by the Geological Society of America
Scannella J.B., and D.W. Fowler. 2014. A stratigraphic survey of *Triceratops* localities in the Hell Creek Formation, northeastern Montana (2006-2010). pp. 313-332 in Through the End of the Cretaceous in the Type Locality of the Hell Creek Formation in Montana and Adjacent Areas, G.P. Wilson, W.A. Clemens, J.R. Horner, and J.H. Hartman (eds.) Geological Society of America Special Paper, Boulder, Colorado.

The following chapter has been published in the Geological Society of America Special Paper 503 and appears in this dissertation with the permission of the Geological Society of America. The copyright is held by the Geological Society of America.

Abstract

Here we provide a survey of *Triceratops* localities and accompanying stratigraphic data from the Hell Creek Formation of northeastern Montana. The majority of the sites discussed here were relocated or discovered during the last five years of the Hell Creek Project (1999–2010); a multi-institutional effort to record a large volume of faunal, floral, and geologic data on the Hell Creek Formation in order to test evolutionary, paleoecological, and geological hypotheses. *Triceratops* is the most abundant dinosaur in the Hell Creek Formation and one of the most common non-avian dinosaurs of the Upper Cretaceous. It is known from hundreds of specimens, which have been collected since it was first described in 1889. Although these specimens provide a wealth of morphological data on *Triceratops*, many lack detailed stratigraphic information and context. Detailed stratigraphic and contextual data for more than 70 specimens of *Triceratops* collected during the Hell Creek Project make this data set among the most comprehensive for any non-avian dinosaur.

Introduction

It was the famous horned dinosaur *Triceratops* that first called paleontologists to the Hell Creek Formation. W.T. Hornaday, the director of the Bronx Zoölogical Garden, returned from a 1901 hunting trip to eastern Montana with a piece of fossil bone (Brown, 1907). Henry Fairfield Osborn, director of the American Museum of Natural History

(AMNH) and Barnum Brown (AMNH) recognized the fossil as a segment of *Triceratops* horn (Brown, 1907; Dingus and Norell, 2010). By 1901, *Triceratops* was already known from multiple impressive specimens collected from the Lance Formation of Wyoming and broadly contemporaneous Upper Cretaceous formations of Colorado (Hatcher et al., 1907; Ostrom and Wellnhofer, 1986; Carpenter and Young, 2002). The AMNH was seeking an exhibit-quality specimen of *Triceratops* for its dinosaur hall and the Hornaday horn (originally discovered by settler Max Sieber) seemed a promising lead (Dingus and Norell, 2010). Osborn dispatched Barnum Brown to the area, initiating over a century of fossil collecting in the uppermost Cretaceous deposits of eastern Montana. Brown would go on to discover and collect numerous dinosaur fossils from the Hell Creek Formation, including the holotype specimen of *Tyrannosaurus* (Osborn, 1905); however, it was *Triceratops* that he encountered most frequently. "During seven years' work, 1902–1909, in the Hell Creek Beds (Lance) of Montana I identified no less than five hundred fragmentary skulls and innumerable bones referable to this genus" (Brown, 1917, p. 281–282). Lull (1915) presented a stratigraphic survey of specimens of *Triceratops* from the Lance Formation of Wyoming. "I have arranged the skulls in their stratigraphic sequence, based upon all the data available at the present, but taken very largely from a study of the map . . ." (Lull, 1915, p. 341). As Ostrom and Wellnhofer (1986, p. 155) noted: " . . . the precise stratigraphic spacing of these specimens can no longer be established," and it has been difficult to assess the stratigraphic placement of these specimens due to the absence of more precise locality data (Farke, 1997). The detailed stratigraphy of the Hell Creek Formation in Montana is now well understood

(e.g., Flight, 2004; Fowler, 2009; Horner et al., 2011; Hartman et al., 2014), allowing specimens of *Triceratops* to be placed in a high-resolution stratigraphic context.

Taxa known from greater numbers of specimens can reveal more details of systematics and development than those known from a few pristine specimens. *Triceratops* is now one of the best understood of all dinosaur taxa (e.g., Hatcher et al., 1907; Ostrom and Wellnhofer, 1986; Forster, 1996a; 1996b; Horner and Goodwin, 2006; 2008; Scannella and Horner, 2010; Horner and Lamm, 2011). This is, in part, due to the efforts of the Hell Creek Project, a large scale, multi-institutional (Museum of the Rockies [MOR], University of California Museum of Paleontology [UCMP], University of North Dakota [UND]) study of the fauna, flora, and geology of the Hell Creek Formation in northeastern Montana (e.g., Wilson, 2005; Goodwin and Horner, 2010; Horner et al., 2011, this volume). Since the initiation of the Hell Creek Project in 1999, field crews at the MOR alone have collected over 70 new specimens of *Triceratops* (Scannella and Horner, 2010; Horner et al., 2011; Appendix). Dozens more poorly preserved specimens were discovered and recorded in the field but remain uncollected (Horner et al., 2011). Many of the specimens of *Triceratops* collected by the MOR represent previously unrecorded ontogenetic stages, revealing new details of the developmental biology of this animal (Horner and Goodwin, 2006; 2008; Scannella and Horner, 2010).

The MOR now houses one of the largest collection of *Triceratops* in the world, and, significantly, nearly every specimen has detailed locality records associated with it (Horner et al., 2011). In contrast, many of the specimens of *Triceratops* collected in the late nineteenth and early twentieth centuries have very little stratigraphic data associated

with them (Farke, 1997). This makes it difficult to place those specimens in precise stratigraphic position and thus test evolutionary hypotheses in detail. In many cases, fragmentary specimens with stratigraphic data can provide valuable insights unavailable from more complete skulls or skeletons lacking this data (e.g., Pearson et al., 2002; Horner et al., 2011).

Here, we present a review of some significant localities of *Triceratops* either relocated or discovered during the later years of the Hell Creek Project (1999–2010). Firsthand accounts from those who have visited sites can be critical to future quarry relocation (e.g., Tanke, 2010), and, as such, we provide contextual information for sites that we have personally visited (Fig. 1). For each locality, we provide details of the specimen(s) collected, its relative stratigraphic position, and, for many, a stratigraphic section. Precise locality data are on record at the respective institutions. This survey will facilitate reassessment of the stratigraphic positions of these specimens, thus helping to make systematic and evolutionary hypotheses testable now and in the future.

Institutional Abbreviations

AMNH—American Museum of Natural History, New York, New York, USA

MOR—Museum of the Rockies, Bozeman, Montana, USA

MSU—Montana State University, Bozeman, Montana, USA

NCSU—North Carolina State University, Raleigh, North Carolina, USA

UCMP—University of California Museum of Paleontology, Berkeley, California, USA

UND—University of North Dakota, Grand Forks, North Dakota, USA

UW-FDL—University of Wisconsin–Fond du Lac, Fond du Lac, Wisconsin, USA

USNM—National Museum of Natural History, Smithsonian Institution, Washington, D.C., USA

Materials And Methods

The stratigraphy of the Montanan Hell Creek Formation remained poorly resolved until recently (Flight, 2004; Fowler, 2009; Hartman et al., 2014; Horner et al., 2011). Analyses within a stratigraphic framework were largely dependent on finding a nearby exposure of either the top or the bottom of the formation and measuring the distance to that contact (e.g., Wilson, 2005). This methodology, however, does not always allow for reliable placement of specimens recovered from areas in which neither the top nor the bottom contact is exposed in relatively close proximity, nor does it allow for correlation of specimens traced to the bottom contact with specimens that have been traced to the top contact without making the assumption that all exposures of the Hell Creek Formation have a consistent preserved thickness (Fowler, 2009). While the Hell Creek Formation is commonly around 90 m thick in the Fort Peck area (Wilson, 2004), this can vary by 20 m, especially based on the presence or absence of the Basal Sandstone (Brown, 1907; Flight, 2004) or incised Paleocene channels (e.g., 20 m or more removed at Bug Creek; Lofgren, 1995).

The most accurate method of stratigraphic placement of localities is to measure their position relative to the upper and lower formational contacts and stratigraphic unit boundaries (Fig. 4.2; see Hartman et al., 2014; Horner et al., 2011). A sequence stratigraphic interpretation of facies shifts within the Hell Creek Formation is in preparation (Fowler, 2009). The majority of specimens included in this review are placed

stratigraphically relative to nearby exposures of either the upper or lower contacts. Placement relative to unit boundaries increases stratigraphic resolution. Nomenclature for unit boundaries follows Horner et al. (2011; see also Hartman et al., 2014). The Basal Sandstone is an informal name for the sandstone unit that marks the base of the lower unit of the formation. The Jen-rex Sandstone is an informal name for the sandstone unit that marks the base of the middle unit of the formation. The Apex Sandstone is an informal name for the sandstone unit that marks the base of the upper unit; it is typically located ~26–30 m below the Hell Creek–Fort Union formational contact. The 10-Meter Sandstone is the informal name for a sandstone that typically occurs ~10 m below the lower Z-coal.

A 1.5 m Jacob's staff and Brunton compass were used to take stratigraphic sections for *Triceratops* sites discovered by MOR crews during the Hell Creek Project from 2006 through 2010. The lower Z-coal was identified as the lowermost coal in the Fort Union Formation, although the precise stratigraphic position of this horizon can vary (Archibald et al., 1982; Swisher et al., 1993; Turner, 2010). These data were combined with stratigraphic information from the MOR archives as well as locality data for specimens from UCMP.

Triceratops Localities

UCMP Locality V88001 (High Ceratopsian): UCMP Specimen 137263

In 1987, along the southern margin of a local basin in close proximity to exposures of the Fort Union Formation referred to by UCMP and MOR paleontologists

as “the swamp” (for its organic-rich beds containing abundant champsosaurs and crocodiles), Mark Goodwin (UCMP) discovered a disarticulated skull of a subadult *Triceratops* weathering out of a bentonitic, dark-gray mudstone high in the underlying Hell Creek Formation (Goodwin and Horner, 2010). The site, UCMP locality V88001, “High Ceratopsian,” is stratigraphically a few meters below the base of the lower Z-coal, which defines the Hell Creek–Fort Union formational contact and, in this area, approximates the Cretaceous-Paleogene boundary. Crews from the UCMP returned to the site several times over the next few years, collecting a set of postorbital horn cores, much of the parietal-squamosal frill, a pair of unfused nasals, a jugal, and other cranial elements. In 2007, when we visited the locality with Mark Goodwin, a shallow depression was still visible in the mudstone where the skull had been removed. UCMP 137263 was not from a large individual of *Triceratops*, but the crews working the site had been thorough in expanding the quarry. In more recent years, it has been determined that *Triceratops* quarries often need to be expanded significantly to discover if more elements are preserved (Horner et al., 2011). The stratigraphic position of the locality is ~5 m below the lower Z-coal.

UCMP Locality V83224 (Dave’s Nose): UCMP Specimen 128561

UCMP 128561 was originally described as a new genus of latest Cretaceous ceratopsid, “*Ugrosaurus olsoni*” (Cobabe and Fastovsky, 1987). The specimen, which was discovered by David Fastovsky in the summer of 1983, consists of a partial premaxilla and rostral, a partial nasal with a low nasal boss, and fragments of dentary, frill, and postcrania. Forster (1993) found that all the characters used to diagnose UCMP

128561 were within the range of variation seen in *Triceratops* and referred it to *Triceratops* sp.

We visited the site along with Mark Goodwin, Mary Schweitzer (NCSU), and Liz Johnson (NCSU) on 8 July 2007. Because the majority of the fossil material was collected as float, remnants of a quarry were not apparent. Based on maps and field notes, we narrowed the location of the site to a gray-green mudstone on one side of a small tributary. The locality falls within the middle unit of the Hell Creek Formation, roughly 30 m below the local formational contact as initially reported by Cobabe and Fastovsky (1987). The specimen exhibits a nasal boss morphology, which is similar to that seen in several specimens of *Triceratops* (e.g., MOR 981, MOR 1122) from the lower half of the Hell Creek Formation. Similar morphologies are also found in some specimens collected from the Lance Formation, for which detailed stratigraphic data are not available (USNM 2412, USNM 4720). Whether the boss morphology represents the ontogenetic transformation of a pre-existing nasal horn (as is seen in some centrosaurines [Sampson, 1995; Currie et al., 2008]), pathology (Horner and Goodwin, 2008), or individual variation are competing hypotheses that cannot be rejected at this time and are under study by Hell Creek Project participants.

UCMP Locality V88081 (Russell Basin *Triceratops*): UCMP Specimen 136092

In 1981, Dale Russell and Helen Michel discovered UCMP 136092, a nearly complete skull (missing the snout, jaws, and beak). We visited the area with Mark Goodwin and Mary Schweitzer on 10 July 2007. With only the plotted location on a topographic map and the lithologic description, we were unable to locate any remnants of

an old quarry. A deep excavation had not been required to collect the skull, which had been preserved on its side, laterally compressed and covered by very little overburden (W.A. Clemens, pers. comm, 2011; Fig. 4.3). On a previous visit to the UCMP, one of us (Scannella) had examined the jacket of UCMP 136092 and noted the dark gray mudstone partially covering the skull (Fig. 4.3). While in the field and the area of the Russell Basin *Triceratops*, we located a dark gray mudstone horizon and eventually came upon bits of old plaster that we believe are from the original quarry (Fig. 4.4). The quarry was positioned just below a prominent sandstone ~6–10 m below multiple thin organic rich horizons, one of which represents the lower Z-coal (Fig. 4.4, C). As noted by Goodwin and Horner (2010), several other specimens of *Triceratops* were found weathering out of the same mudstone horizon within a kilometer of UCMP locality V88081.

UCMP Locality V75046 (Ruben's *Triceratops*): UCMP Specimen 113697

In 1970, then graduate student John Ruben discovered the skull of a large specimen of *Triceratops* in the Hell Creek Formation in the Bug Creek area of McCone County, Montana (Fig. 5). The stratigraphy in the Bug Creek area is notoriously problematic (Lofgren, 1995). Specifically, the local contact between the Hell Creek and Fort Union formations is obscured by what is now understood to be a Paleocene sandstone channel deposit that formed by incision of latest Cretaceous-aged Hell Creek Formation deposits (Lofgren, 1995).

The *Triceratops* quarry was in a mudstone bed in the saddle of a low set of hills. Upon tracing the beds laterally across the area, we found a thin coal and a dinosaur-bearing sandstone stratigraphically above it that we identified as the Apex Sandstone,

which marks the base of the upper sequence of the Hell Creek Formation (Horner et al., 2011). The lower Z-coal is not present in the area surrounding UCMP locality V75046, likely having been scoured out by a Paleocene channel that incised down some 30 m or more from the Fort Union Formation. UCMP locality V75046 is stratigraphically very high in the middle unit of the Hell Creek Formation, ~6 m below the Apex Sandstone.

MOR Locality HC-135
(MORT): MOR Specimen 004

MOR 004 is a specimen that represents a large individual of *Triceratops* from the upper part of the Hell Creek Formation. It was discovered by Norman Constenius and was collected by Mick Hager in 1981 (Fig. 4.6). MOR 004 was the first specimen of *Triceratops* collected by the MOR. The site name, "MORT," is an acronym for "Museum of the Rockies *Triceratops*." On 12 July 2007, we visited the locality, which is in a sandstone ~6 m stratigraphically below the lower Z-coal. We also located and recorded locality data for several other poorly preserved skulls of *Triceratops* within one half of a kilometer of MOR locality HC-135.

MOR Locality HC-425
(Afternoon Delight): MOR Specimen 2569

In 2006, MOR volunteer Sonya Scarff discovered the partial skull of a very young juvenile *Triceratops* (MOR 2569) in a gray mudstone ~6 m below the top of prominent hill in the Lost Creek Bay area (MOR locality HC-425; "Afternoon Delight"). MOR 2569 is one of the most complete specimens of *Triceratops* known that represents this early stage of ontogeny. Material collected from the locality includes the parietal, squamosals,

a postorbital horn core, quadrates, and a partial maxilla (see Goodwin and Horner, 2010). The locality is in the lower part of the middle unit of the Hell Creek Formation (Fig. 4.1).

MOR Locality HC-531
(Lauren's Trike): MOR Specimen 2938

Lauren Berg discovered a partial skull of *Triceratops* (MOR 2938) weathering out of a gray mudstone roughly 2 m above the base of a small hill (16 July 2007). Among the material collected from the site (MOR locality HC-531) were the nasal horn, a dentary, maxilla, partial parietal, and sections of other cranial bones. MOR locality HC-531 was measured at ~10 m below the lower Z-coal (Fig. 4.7,section 1). The drainage of Short Creek (~200 m south of MOR locality HC-531) is extremely productive, particularly for material of *Triceratops*.

MOR Locality HC-520 (Joe's
Half Day Trike): MOR Specimen 2923

A short distance from MOR locality HC-531, film director Joe Johnston discovered the skull of a large *Triceratops* (MOR 2923). MOR locality HC-520 is stratigraphically slightly lower than MOR locality HC-531; it was found in a prominent sandstone that we believe can be stratigraphically correlated with a sandstone that is typically ~10 m below the lower Z-coal (Fig. 4.7, section 1). The skull was lying with its ventral side up and the underside of the parietal exposed (Fig. 4.8A). Whereas MOR 2938, which was found in mudstone, was disarticulated and three-dimensionally distorted post mortem, MOR 2923 was articulated, largely undistorted, and in excellent condition (Fig. 4.8B). This taphonomic pattern (correlation between lithology and degree of

articulation in specimens of *Triceratops*) was noted by Goodwin and Horner (2010). MOR locality HC-520 also produced a shed *Tyrannosaurus* tooth and leaf impressions.

MOR 2923 preserves six epiparietals adorning the parietal with no evidence of one straddling the midline (Scannella and Horner, 2010). *Triceratops* had previously been described as possessing five epiparietals, one of which caps the midline of the frill (Forster, 1996a; 1996b). It is relatively rare to find all of the epiparietals attached to the parietal margin as they were likely removed during postmortem transport and burial (Horner and Goodwin, 2008). MOR 1122, a specimen of *Triceratops* ("*Torosaurus*" morph; Scannella and Horner, 2010 originally described by Farke, 2007) from the lower part of the Hell Creek Formation (the locality [MOR locality HC-258] is positioned at the bottom of the Basal Sandstone), preserves 12 epiparietals. Whether variation in epiparietal count is indicative of stratigraphic, ontogenetic, or individual variation is a research question currently under study by researchers at the MOR.

MOR Locality HC-702 (JD Trike12):
MOR Specimen 3056 and MOR Locality
HC-541 (JD Trike14): MOR Specimen 2950

In 2007, we encountered numerous specimens of *Triceratops* of varying degrees of preservation. Those in poor shape were recorded and left uncollected in the field. Others that were collected provide information on ontogenetic changes in cranial morphology. MOR 3056 is a squamosal and postorbital horn core of a juvenile *Triceratops* that was exposed on a small gray mudstone bluff ~7 m stratigraphically below the lower Z-coal (Fig. 4.9). MOR 3056, though only represented by two elements, exhibits morphologies that are useful for testing hypotheses about ontogenetic variation

and documenting patterns of growth and development (Horner and Goodwin, 2006; Goodwin and Horner, 2010).

Less than 100 m from MOR locality HC-702, and ~2 m higher in section, we found a partially disarticulated skull of a subadult *Triceratops* (MOR 2950 at MOR locality HC-541; Fig. 4.10) weathering out of a mudstone. This specimen preserves most of a squamosal, section of parietal, braincase, quadrate, frill epiossifications, and epijugal.

MOR Locality HC-426 (Mark's Scavenged Trike): MOR Specimen 2570 and MOR Locality HC-639 (Anky Breaky Heart): MOR Specimen 3011

In 2006, Mark Goodwin discovered MOR specimen 2570, a partial young adult skull, in a gray mudstone (MOR locality HC-426; Mark's Scavenged Trike"; see Goodwin and Horner, 2010). It was found in an area where the formational contacts are not visible. In 2009, we identified the middle to upper depositional unit boundary (Apex Sandstone) in this area and the lower Z-coal ~1.5 miles (2.4 km) farther south. MOR locality HC-426 is ~25 m stratigraphically below the base of the upper unit (Fig. 4.11, section 2).

In 2009, Holly Woodward discovered the partial skull of a *Triceratops* in a low mudstone bluff less than 0.5 km west of MOR locality HC-426. The specimen (MOR 3011) preserves a partial parietal, nasal, epinasal, maxilla and premaxilla. The locality (MOR locality HC-639; "Anky Breaky Heart") is at approximately the same stratigraphic level as MOR locality HC-426 (Fig. 4.11, section 2).

MOR Locality HC-430 (Quittin' Time): MOR Specimens 2574 and 2702

The Quittin' Time Bonebed was discovered by Laura Wilson in 2006. The specimens of *Triceratops* were found in a mudstone 17 m stratigraphically below the lower Z-coal. Collected material includes partial skulls of a juvenile, subadult, and large, young adult *Triceratops*. The taphonomy of this site is discussed in detail by Keenan and Scannella (2014).

MOR Locality HC-521 (Lon's Trike): MOR Specimen 2924

In 2007, Lon Bolick, a retired psychology professor (UW-FDL), discovered a specimen of *Triceratops* north of Jordan near Brownie Butte. The Hell Creek Formation and overlying Fort Union Formation have been extensively studied in this area (e.g., Archibald, 1982; Fastovsky, 1987). Jack Horner (MOR, MSU), who initially inspected the site (MOR locality HC-521), collected a partial braincase that was found as float on the surface of a sandstone horizon from the Apex Sandstone. We later collected the remainder of a nearly complete skull of a subadult *Triceratops* (MOR 2924) as well as much of the right forearm, several vertebrae (including articulated caudals), and ribs. A nearly complete crocodile skull, invertebrates, and palm impressions were also found at the site. MOR 2924 preserves the skull and postcrania of a subadult *Triceratops*. This allows for study of correlations between skull and postcranial morphology in ontogeny. Whereas *Triceratops* cranial material is common in the Hell Creek Formation, associated postcrania are rare (Horner et al., 2011). After the excavation was concluded, an isolated postorbital horn core (MOR 3057 from MOR locality HC-114) as well as other material

of *Triceratops* was discovered in the upper unit of the Hell Creek Formation within one kilometer of MOR locality HC-521.

MOR Locality HC-571 (Seth's Trike):
MOR Specimen 2979 and MOR Locality
HC-543 (TriSarahTops): MOR Specimen 2980

On August 6, 2008, MOR volunteer Seth Bainbridge discovered weathered fossil bone scattered over a hard, gray mudstone in the upper unit of the Hell Creek Formation (Figs. 4.12, 4.13A). In the nearby hill, two *Triceratops* postorbital horn cores were discovered in situ (MOR locality HC-571; "Seth's Trike"; MOR 2979). MOR 2979 consists of a partial skull in good condition, preserving the postorbital horn cores, frontoparietal fontanelle morphology (sensu Farke, 2010), and braincase region as well as pieces of frill and premaxilla (Fig. 4.13B). About a hundred meters east of MOR locality HC-571, Sarah Keenan discovered a site with a poorly preserved specimen of *Triceratops* (MOR locality HC-543; "TriSarahTops"). The best-preserved bone at the site is a squamosal (MOR 2980) that was collected.

MOR Locality HC-544 (DFJuvieTrike3):
MOR Specimen 2951 and MOR Locality
HC-627 (Situ But Sad): MOR Specimen 2999

On 22 June 2008 Fowler discovered the most complete juvenile *Triceratops* so far reported (MOR 2951). The site was named "DFJuvieTrike3" (Fig. 14A). Small bone fragments on the surface of a dark gray mudstone were identified as part of the jugal of a very young *Triceratops* (Fig. 14B). A fragmentary rib was found eroding out of the same horizon. Excavation of MOR locality HC-544 (2008, 2009) produced a nearly complete and well-preserved juvenile skull, along with postcranial material including limb bones,

ribs, vertebrae, a scapula, and an ilium. The specimen was placed at ~4 m stratigraphically above the Apex Sandstone, in the upper unit of the formation (Fig. 4.7, section 3). MOR 2951, which is currently under study, will provide a wealth of information on the ontogeny of the skeleton of *Triceratops*.

Nearly 1.5 km southeast of MOR locality HC-544, Fowler and Michiel Pillet discovered what initially appeared to be the partial parietal of a *Triceratops* weathering out of a mudstone near the base of a small hill. The locality (MOR locality HC-627; "Situ but Sad") was excavated and produced a partial skull from a subadult *Triceratops* (MOR 2999). Most of the posterior of the skull was preserved, including both postorbital horn cores and the braincase. An unfused nasal was also found at the site. MOR locality HC-627 is very high in the upper unit of the Hell Creek Formation (~7 m below the lower Z-coal; Fig. 4.7, section 5).

MOR Locality HC-565 (Supernasal):
MOR Specimen 2972 and MOR Locality
HC-628 (Ashes Trike): MOR Specimen 3000

Several specimens of *Triceratops* were collected from within two kilometers of MOR locality HC-544. On 23 June 2008, Fowler found an isolated large juvenile horn core (MOR 2958; MOR locality HC-500; "DF Juvie-Horncore"). He subsequently discovered a very large nasal horn in the Apex Sandstone (MOR locality HC-565; "Supernasal"; Fig. 4.7, section 3) within 200 km of MOR locality HC-500. In addition to the nasal horn, MOR locality HC-565 produced a partial squamosal, braincase, jugal, and postcranial elements (MOR 2972).

Near MOR locality HC-565, Scannella discovered the partial skull of a large *Triceratops* weathering out of a dark gray mudstone horizon ~14 m stratigraphically below the lower Z-coal (MOR 3000; MOR locality HC-628; "Ashes Trike"; Fig. 4.7, section 2). The locality, which was excavated in 2009, produced a postorbital horn core, partial parietal, squamosal, dentary, and scapula.

MOR Locality HC-573 (Three Amigos):
MOR Specimen 2982 and MOR Locality
HC-576 (Six O'Clock Trike): MOR Specimen 2985

In 2008, Lee Hall discovered a nasal horn weathering out of a dark gray mudstone horizon (MOR 3055; MOR locality HC-1026; "Brown Nose") ~1 km north of Pennick Coulee. The locality is ~100 m away from a partial skeleton of a *Tyrannosaurus* (MOR 2925) found weathering out of a gray mudstone (Hall and Keenan, 2010). MOR 2925 and MOR 3055 occur low in the middle unit of the formation (Fig. 4.15, section 2).

Several more specimens of *Triceratops* were found in this area, the most complete being a partial subadult skeleton discovered by Lee Hall and volunteers Seth Bainbridge and Michael Flowers (MOR 2982; MOR locality HC-573; "Three Amigos"; Fig. 4.15, section 2). MOR 2982 was collected from a dark gray bentonitic mudstone low in the middle unit and consists of a partial skull including postorbital horn core, nasal horn, partial squamosal, midline of the parietal, dentary, rostral, and associated postcrania.

Less than half a kilometer from the *Tyrannosaurus* quarry (MOR locality HC-522), Bob Harmon discovered a large squamosal of a *Triceratops* weathering out of a mudstone horizon. In addition to the squamosal, the site ("Six O'Clock Trike"; MOR locality HC-576) produced a partial parietal, and associated postcrania. This specimen

(MOR 2985) is significant as it occurred ~12 m below MOR locality HC-522 ("Brown Nose"), in the upper part of the lower unit (Fig. 4.15, section 2; see Discussion).

MOR Locality HC-532 (Ducky Tail): MOR Specimen 6648

In 2007, Bob Harmon discovered articulated caudal vertebrae of an *Edmontosaurus* (MOR 2939) leading into a sandstone horizon within the upper unit of the formation. In 2009, during excavation at the locality (MOR locality HC-532; "Ducky Tail"), an MOR crew led by Alessandro Carpana discovered the parietal, squamosal, and ilium of a juvenile *Triceratops* amongst the hadrosaur material.

Several other specimens of *Triceratops* were found within two kilometers of MOR locality HC-532, most notably the complete skull of a large *Triceratops* (MOR 3004; MOR locality HC-633; "The Horn Resounding") discovered by Becky Schaff ~22 m stratigraphically below the Apex Sandstone (Fig. 4.11, section 1). HC-633 also produced some postcranial material. MOR 3004 awaits preparation at the MOR. Less than a hundred meters from MOR locality HC-633, Bobby Ebelhar found a disarticulated skull weathering from a stratigraphically lower dark gray mudstone layer. This site (MOR locality HC-634; "Antsy Trike"; MOR 3005; Fig. 4.11, section 1) produced an unfused nasal, partial parietal, and some postcranial material. Paul Ullmann collected an isolated nasal horn (MOR 3008; MOR locality HC-636; "American Beauty"; Fig. 4.11, section 1) from the base of the Apex Sandstone in this area.

MOR Locality HC-638 (Golden Goose): MOR Specimen 3010

In 2009, Fowler and Bobby Ebelhar discovered an area (~400 m^2) that produced several fragmentary *Triceratops* and was called "Trikey Town". A ~3 m-thick mudstone horizon, produced the majority of the material. The locality produced *Triceratops* from the lower part of the middle unit of the Hell Creek Formation (Fig. 4.11, section 3). MOR 3010 ("Golden Goose"), a partial skull of a small *Triceratops*, was the most complete specimen collected from the area. The quarry (MOR locality HC-638) produced a nasal horn, postorbital horn core, dentary and other more fragmentary material. In addition to *Triceratops*, the area contained a rich fossil macrosite with concentrated remains of several taxa including fish, turtles, crocodiles, and dinosaurs.

MOR Locality HC-668 (Yoshi's Trike): MOR Specimen 3027 and MOR Locality HC-682 (Cliffhanger): MOR Specimen 3045

MOR 3027 is an exquisitely preserved large disarticulated skeleton of *Triceratops* discovered by Yoshi Katsura in 2010. The specimen was collected from a mudstone high in the middle unit of the Hell Creek Formation (~5.5 m stratigraphically below the Apex Sandstone; Fig. 4.15, section 5; Fig. 4.16). Although on the surface the specimen did not look very promising, excavation in 2010 and 2011 revealed one of the most productive MOR *Triceratops* localities (MOR locality HC-668).

Less than half a kilometer from MOR locality HC-668, Yoshi discovered a subadult *Triceratops* weathering out of a mudstone horizon in a shear hillside. This locality (MOR locality HC-682; "Cliffhanger"), like MOR locality HC-668, is positioned

very high in the middle unit (Fig. 4.15, section 5). A disarticulated partial skull (MOR 3045) was collected from the site.

MOR Locality HC-716 (Little Horny Devil): MOR Specimen 3064

MOR 3064 is a partial skull of a small juvenile *Triceratops*, consisting of a brow horn, quadrate, partial squamosal, both jugals, partial quadratojugal, numerous frill epiossifications, and other cranial material. It was discovered by Fowler, Aaron Medford, Nick Resar and Rebecca Cook at the southern end of Pennick Coulee. The specimen was recovered from a horizon ~13 m stratigraphically below the Apex Sandstone (MOR loc HC-716; Fig. 4.15, section 4). MOR 3064 is approximately the size of MOR 2951, which is from above the Apex Sandstone, hence the specimens will facilitate comparison of ontogenetic trajectories between *Triceratops* from the upper middle and lower upper unit of the Hell Creek Formation. Approximately 100 m south of MOR locality HC-717, Fowler discovered a postorbital horn above the Apex Sandstone (MOR 3047; MOR locality HC-697; "Got the Horn"; Fig. 4.15, section 4).

Discussion And Conclusions

Lull (1933: p. 123) stated: “There is infinite variation in all *Triceratops* skulls.” Due to the morphological variability seen among specimens, *Triceratops* has been the source of considerable systematic confusion since its initial description. As many as 16 species of *Triceratops* have been named, many of which are based on the slightest of variations in cranial morphology (Ostrom and Wellnhofer, 1986; 1990; Dodson, 1996). Forster (1996b) argued that the characters that had been used to erect these taxa likely

represented intraspecific variation in only two species: *T. horridus* and *T. prorsus*. Much of the variation found in *Triceratops* is likely due to changes that occurred through ontogeny (Horner and Goodwin, 2006; 2008; Scannella and Horner, 2010). Another important consideration for dinosaur systematics is that morphology may vary with stratigraphy (e.g., Evans et al., 2006). Evolutionary change through the Hell Creek Formation may have contributed to morphological variation seen in *Triceratops* (Scannella and Fowler, 2009).

The database of *Triceratops* specimens compiled during the Hell Creek Project is among the most comprehensive for any non-avian dinosaur in a single study area. It includes not only a large sample of *Triceratops* specimens from multiple ontogenetic stages, but each specimen is accompanied by detailed stratigraphic positional data as well. This stratigraphic survey forms the basis for ongoing research into the evolution of *Triceratops* (e.g., Scannella and Fowler, 2009; Scannella, 2010). From this database, analyses may be able to tease apart the relative contributions of ontogeny and evolution to the morphological variation of *Triceratops* from the Hell Creek Formation. Every specimen of *Triceratops*, whether a complete skull or an isolated epinasal, might hold valuable research information if considered in stratigraphic context. Moreover, this survey suggests that a reliance on holotypes in phlyogenetic analyses may place undue focus on a single morphologic variant and may actually obscure stratigraphic and ontogenetic variation (e.g., Mayr, 1959; Scannella and Horner, 2010).

This survey highlights the importance of targeted fossil collecting within a stratigraphic context. Ideally, an ontogenetic series of *Triceratops* specimens would be collected for each depositional unit of the Hell Creek Formation in order to detail

evolutionary and heterochronic trends (Scannella, 2010). Several specimens of *Triceratops* have been collected from the lower unit of the Hell Creek Formation (Horner et al., 2011), including a nearly complete, disarticulated skull of a subadult (MOR 1120; MOR locality HC-256 [“Getaway Trike”]; see Goodwin and Horner, 2010) and the most complete skull of an adult known (= ”*Torosaurus*”; MOR 1122 [but see also Farke, 2011; Longrich and Field, 2012]); however, sampling of the ontogenetic series for the lower unit remains far less complete than those for the middle and upper units. A small juvenile from this stratigraphic interval, for example, would reveal insights into chasmosaurine heterochrony. Future field work will target the lower part of the Hell Creek Formation in order to increase resolution of trends in *Triceratops* morphological variation.

Acknowledgments

We are especially grateful to Jack Horner for advice, assistance, and constant support. Special thanks also to Mark Goodwin for assistance and encouragement throughout. Carrie Ancell, Susan Brewer, Bob Harmon, Patsy Hookey, Jamie Jette, and Linda Roberts prepared specimens. We thank all of the Museum of the Rockies (MOR) field crews, who contributed to the findings of the Hell Creek Project, and everyone who has discovered or collected a *Triceratops* for the MOR collections. The Twitchell, Taylor, Trumbo, Holen, and Isaacs families granted access to lands. The Bureau of Land Management, U.S. Fish and Wildlife Service, Charles M. Russell National Wildlife Refuge, and the Montana Department of Natural Resources and Conservation granted

collection permits to J. Horner and MOR over the course of the Hell Creek Project. Montana Fish Wildlife and Parks hosted MOR crews during the early years of the Hell Creek Project. Sarah Keenan and Leigha King provided invaluable field assistance. We thank Bill Clemens and Laura Wilson for sharing stratigraphic data. We thank Bobby Boessenecker, Lon Bolick, Bill Clemens, Peter Dodson, David Evans, Andy Farke, Liz Freedman, Mark Goodwin, Lee Hall, Joe Hartman, John Hoganson, Michael Holland, Jack Horner, Mark Loewen, Kevin Padian, Dean Pearson, Kari Scannella, Mary Schweitzer, Darrin Strosnider, Dave Varricchio, Dave Weishampel, Greg Wilson, and Holly Woodward for helpful comments and conversations. Two anonymous reviewers provided helpful comments that improved the manuscript. Editorial comments from Greg Wilson and W.A. Clemens improved the manuscript. Funding was provided by MOR Paleo, the donors to the Hell Creek Project, and the Smithsonian Institution. Grants from the Welles Fund of the University of California Museum of Paleontology to Scannella and Fowler are gratefully acknowledged. We are thankful for North American Paleontological Convention student travel grants (2009).

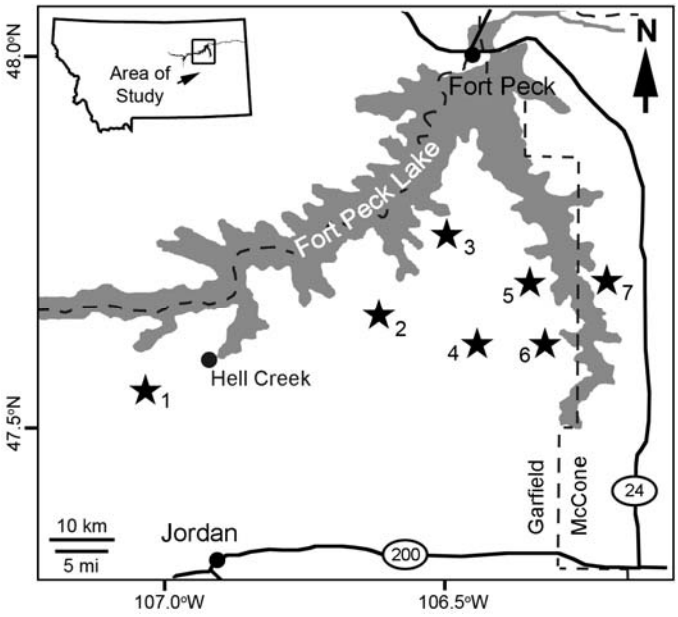


Figure 4.1. Collection areas for specimens of *Triceratops* discussed in the text, south Fort Peck Lake in Garfield and McCone Counties, Montana. 1—Brownie Butte; 2—Gilbert Creek; 3—Pennick Coulee; 4—Lone Tree Creek; 5—Lost Creek; 6—Short Creek; 7—Bug Creek. More detailed locality data are on file at the Museum of the Rockies and are available to qualified researchers upon request.

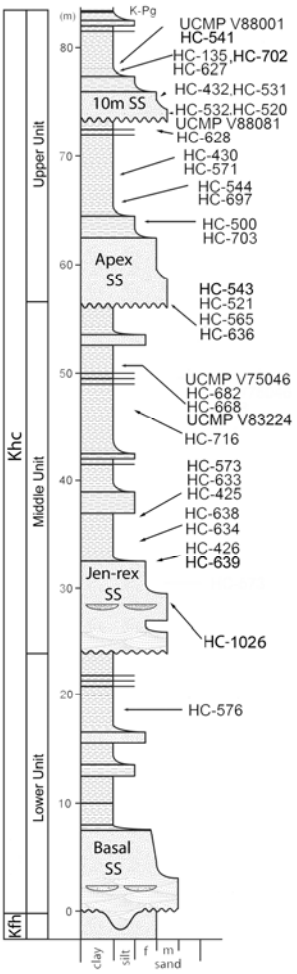


Figure 4.2. Relative positions of *Triceratops* localities discussed in the text superimposed on a generalized section. Localities are plotted based on stratigraphic position, not by facies. Because unit thicknesses vary among outcrops, the relative positions of localities from different sections are approximate at the meter scale. Placement of localities within subunits (e.g., middle unit–upper part; see Appendix) is accurate. Position of the Cretaceous-Paleogene (K-Pg) boundary varies in northern Montana (Turner, 2010). Scale in meters. SS—sandstone. Kfh-Fox Hills Formation. Khc-Hell Creek Formation.



Figure 4.3. The Russell Basin *Triceratops* (University of California Museum of Paleontology [UCMP] 136092), photographed while still under preparation at the UCMP. Right lateral view of skull.

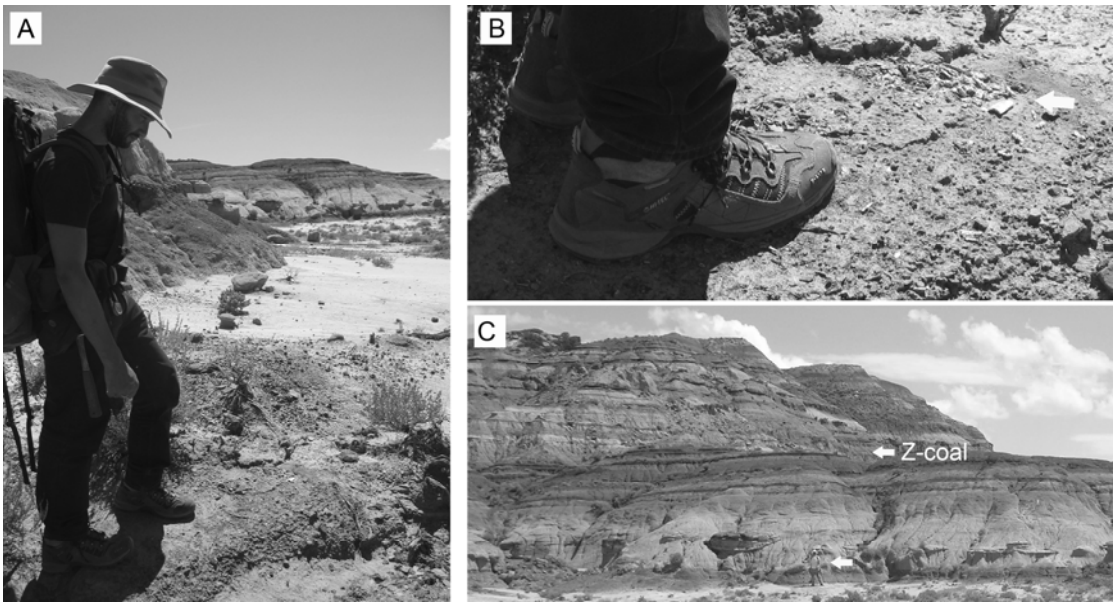


Figure 4.4. Relocating the Russell Basin *Triceratops* quarry (University of California Museum of Paleontology [UCMP] locality V88081). (A) Scannella standing at the site. (B) A small amount of plaster found at the site. (C) Fowler standing just above the stratigraphic level of UCMP locality V88081.

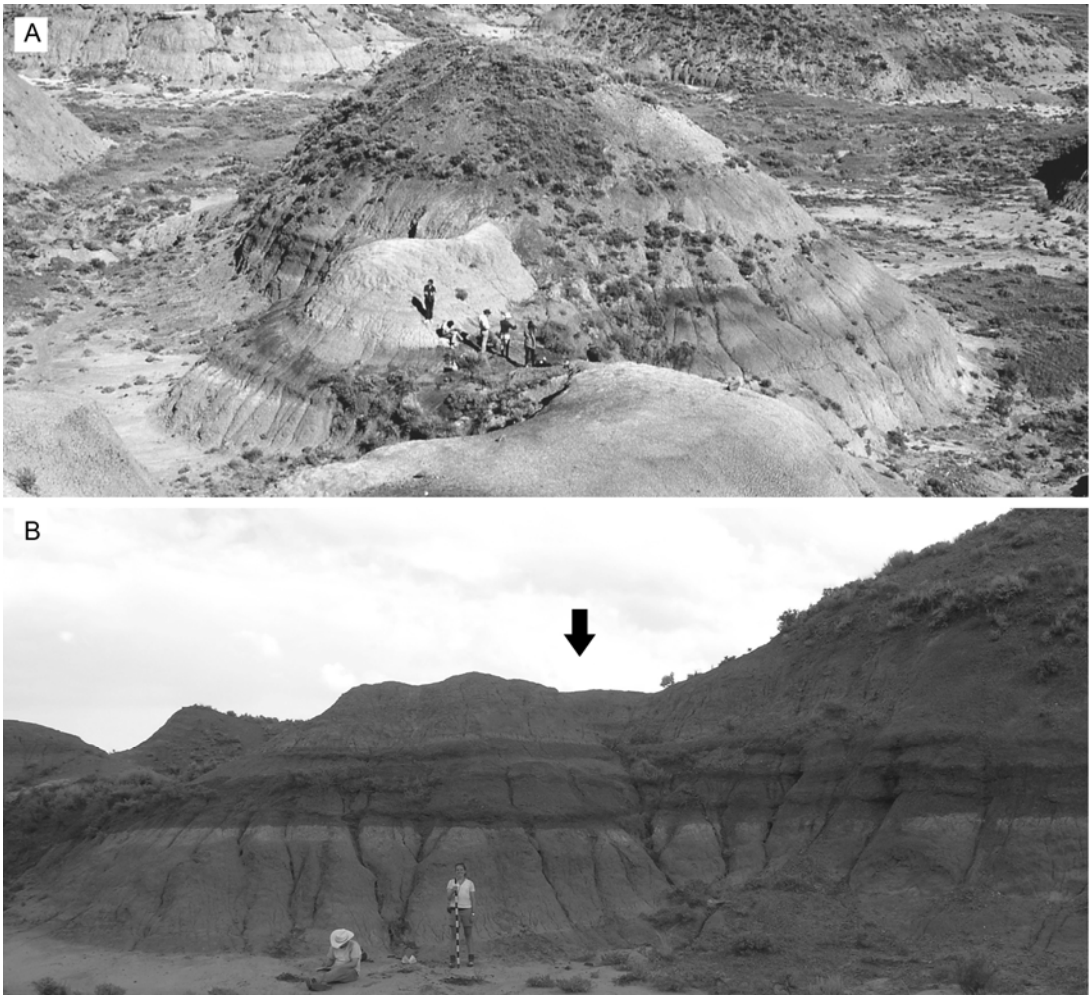


Figure 4.5. Ruben's *Triceratops* (University of California Museum of Paleontology [UCMP] locality V75046). (A) Excavation under way in 1970 (image by J.T. Gregory, courtesy of UCMP). (B) Fowler and Sarah Keenan taking a stratigraphic section at the site in 2007. Arrow indicates quarry site.



Figure 4.6. Museum of the Rockies (MOR) *Triceratops* (MORT; MOR 004), jacketed and awaiting collection in 1981. Note the prominent coals of the Fort Union Formation in the background. Image courtesy of MOR.

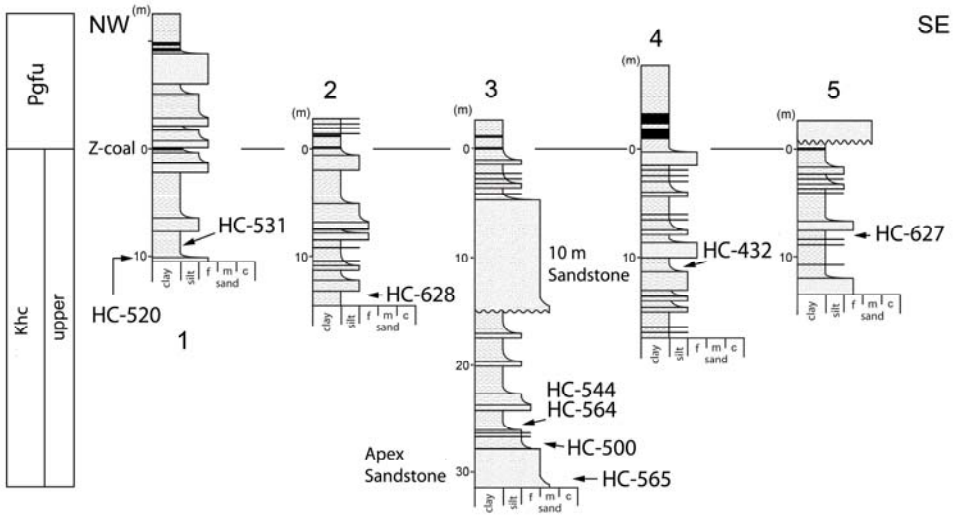


Figure 4.7. Correlation of measured sections and Museum of the Rockies (MOR) *Triceratops* localities, ~4.5 km across the Short Creek area (Garfield County, Fig. 4.1, locality 6) from northwest to southeast. This area includes exposures of the upper part of the Hell Creek Formation (Khc) up to the contact with the Fort Union Formation (Pgfu). Section 1 taken at HC-531. Section 2 taken at HC-628. Section 3 taken at HC-500. Section 4 taken at site HC-432 ("Snap Creek," which produced an isolated nasal horn [Museum of the Rockies (MOR) 2576]). Section 5 taken at site HC-627. Scale in meters.

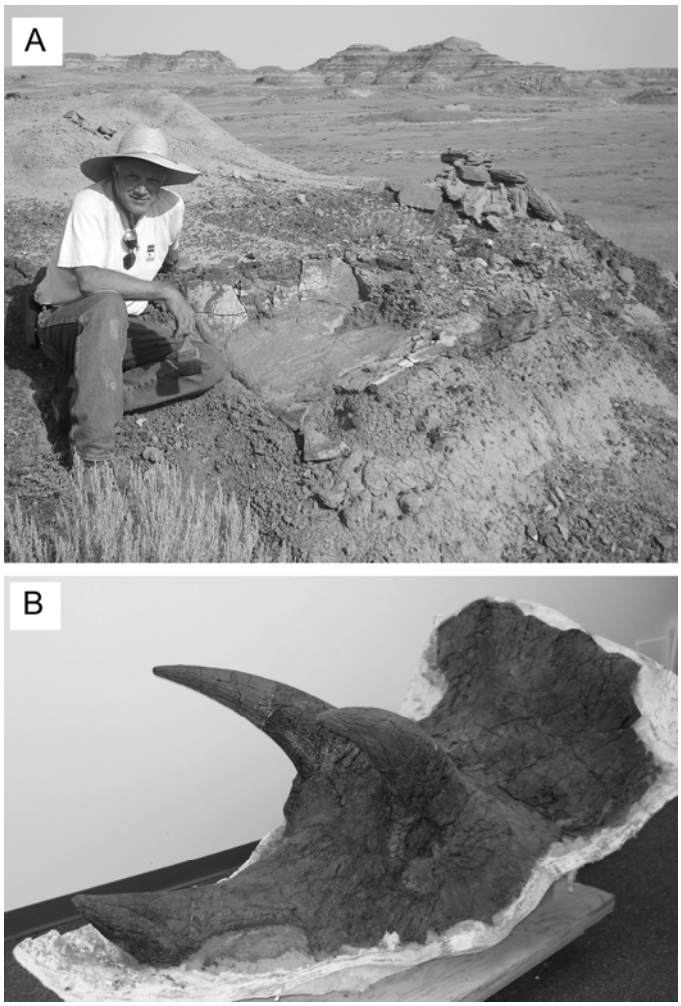


Figure 4.8. Joe's Half Day Trike (Museum of the Rockies [MOR] locality HC-520). (A) Joe Johnston uncovers MOR specimen 2923. It was preserved ventral side up (the ventral surface of its parietal is exposed here) in the 10-Meter Sandstone. The lower Z-coal is exposed in the hills in the background. Image by Kari Scannella, courtesy of MOR. (B) MOR 2923 after preparation. This specimen preserves a nearly complete posterior parietal margin; the remaining pieces are housed in a cabinet in collections at MOR.

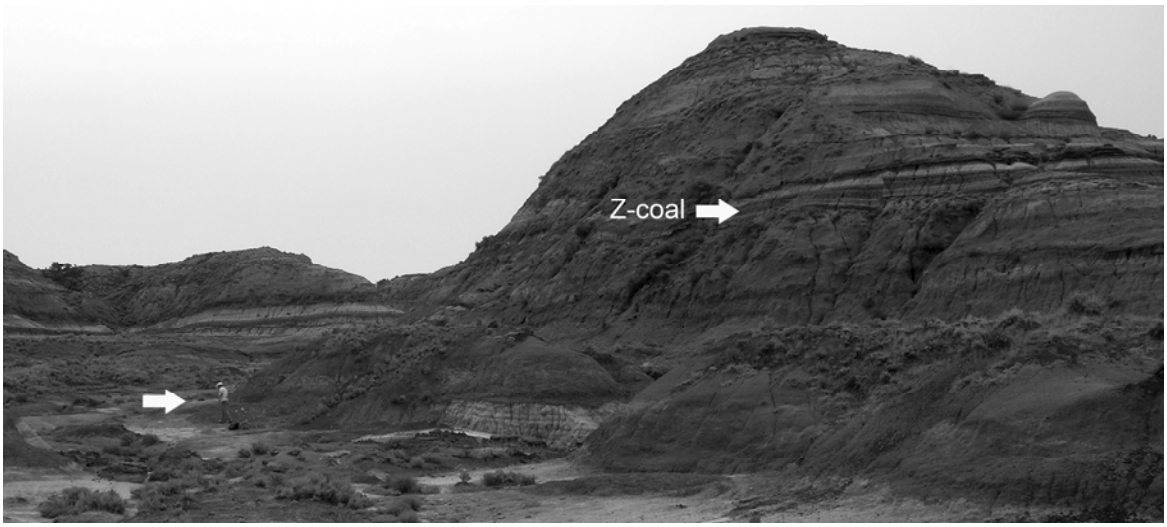


Figure 4.9. Fowler discovers JDTrike12 (Museum of the Rockies [MOR] specimen 3056) eroding from a gray mudstone stratigraphically high in the upper unit of the Hell Creek Formation.

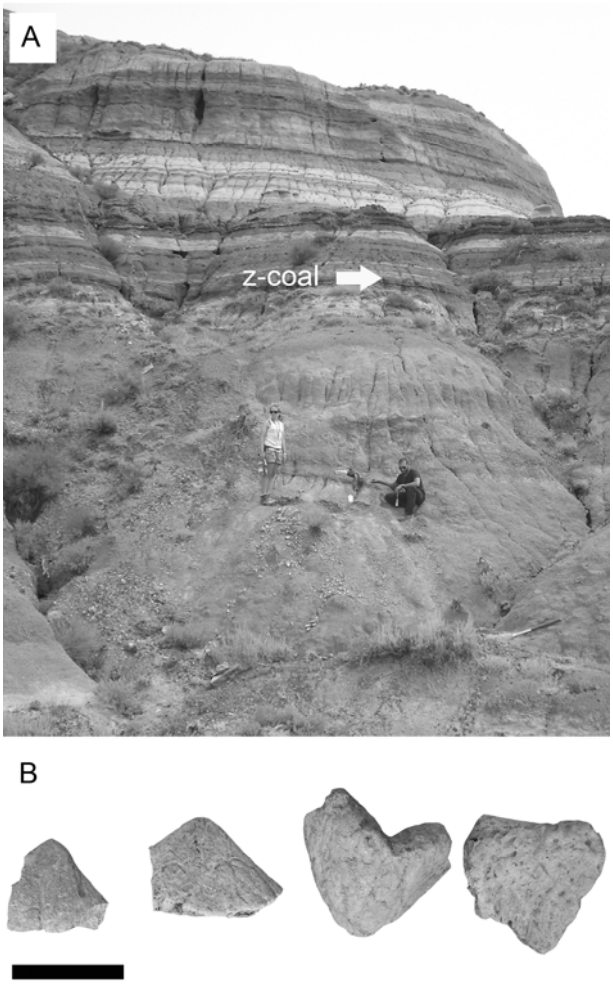


Figure 4.10. JDTrike14 (Museum of the Rockies [MOR] locality HC-541). (A) Scannella and Sarah Keenan at the quarry, only a few meters below the lower Z-coal. (B) Some of the elements originally surface collected from the site, including an epijugal and frill episossification, which provide information on the ontogenetic status of the individual (MOR 2950). The specimen represents a subadult *Triceratops*. Scale bar is 5 cm.

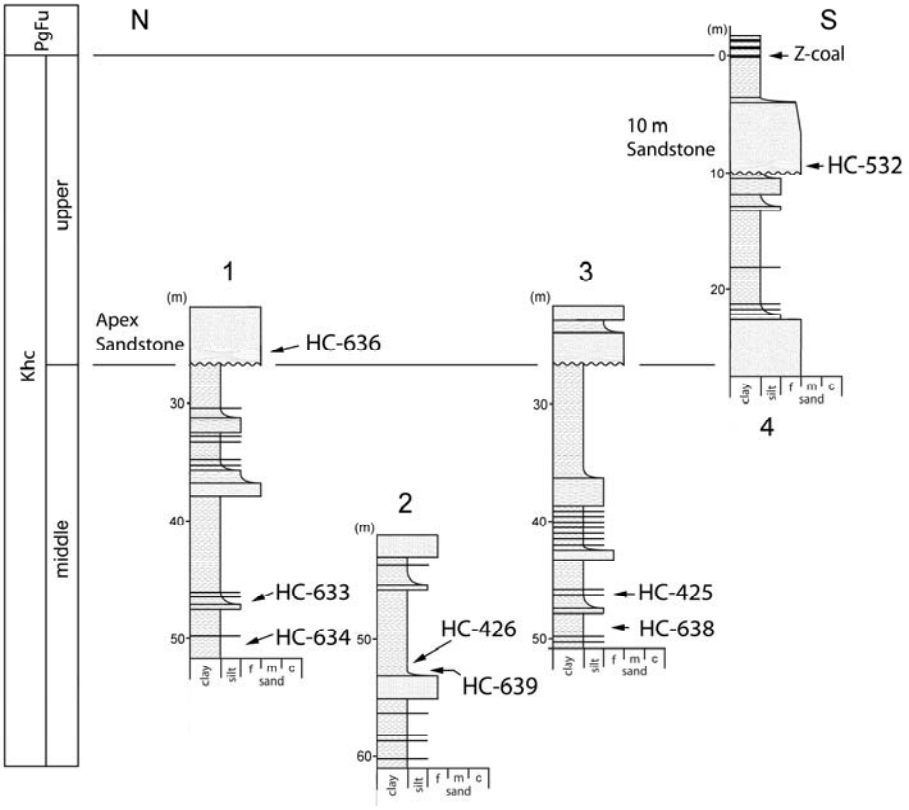


Figure 4.11. Correlation of measured sections and Museum of the Rockies (MOR) *Triceratops* localities ~2.5 km across Lost Creek Bay area (Garfield County, Fig. 1, locality 5) from north to south. This area exposes the lower middle part of the Hell Creek Formation (Khc), up to the contact with the Fort Union Formation (Pgfu). Section 1 taken at HC-633. Section 2 taken at HC-426. Section 3 taken at HC-638. Section 4 taken at HC-532. Scale in meters.

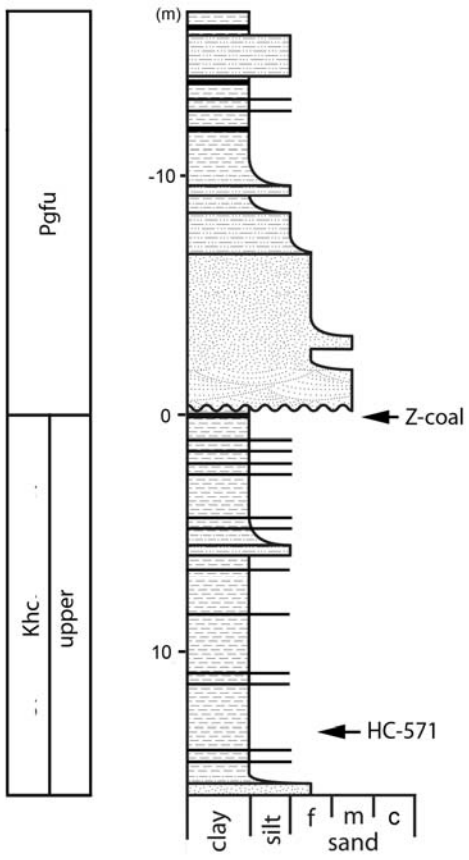


Figure 4.12. Museum of the Rockies (MOR) locality HC-571 plotted on measured section, Brownie Butte (Garfield County; Fig. 1, locality1). This area includes exposures of the upper part of the Hell Creek (Khc) and the lower part of the Fort Union Formations (Pgfu). Scale in meters.

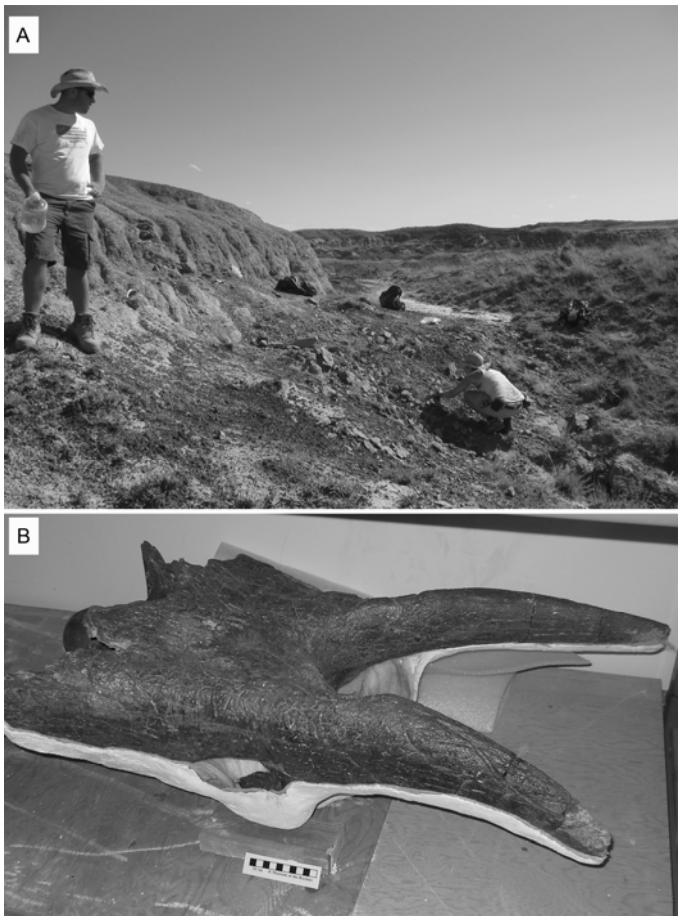


Figure 4.13. Seth's Trike (Museum of the Rockies [MOR] locality HC-571). (A) Seth Bainbridge and Sarah Keenan at the site. (B) MOR 2979 after preparation; additional cranial elements were also recovered from the site.

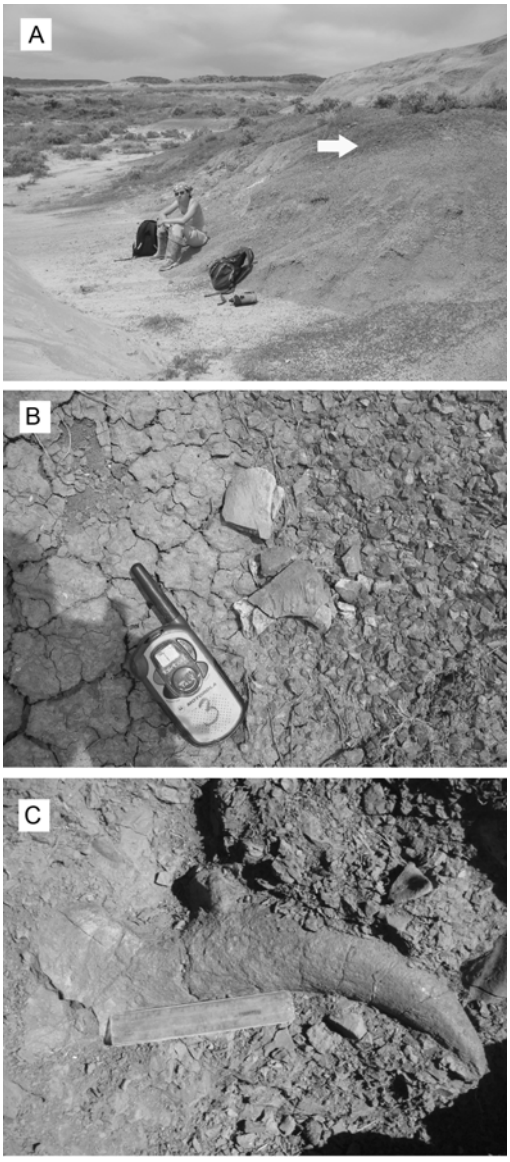


Figure 4.14. DFJuvieTrike3 (Museum of the Rockies [MOR] locality HC-544). (A) Liz Freedman at the site. (B) A partial jugal that was found as float at the site. (C) A left postorbital horn core is exposed during collection of the specimen. MOR 2951 is one of the most complete juvenile specimens of *Triceratops* ever discovered. Ruler is 15 cm in length.

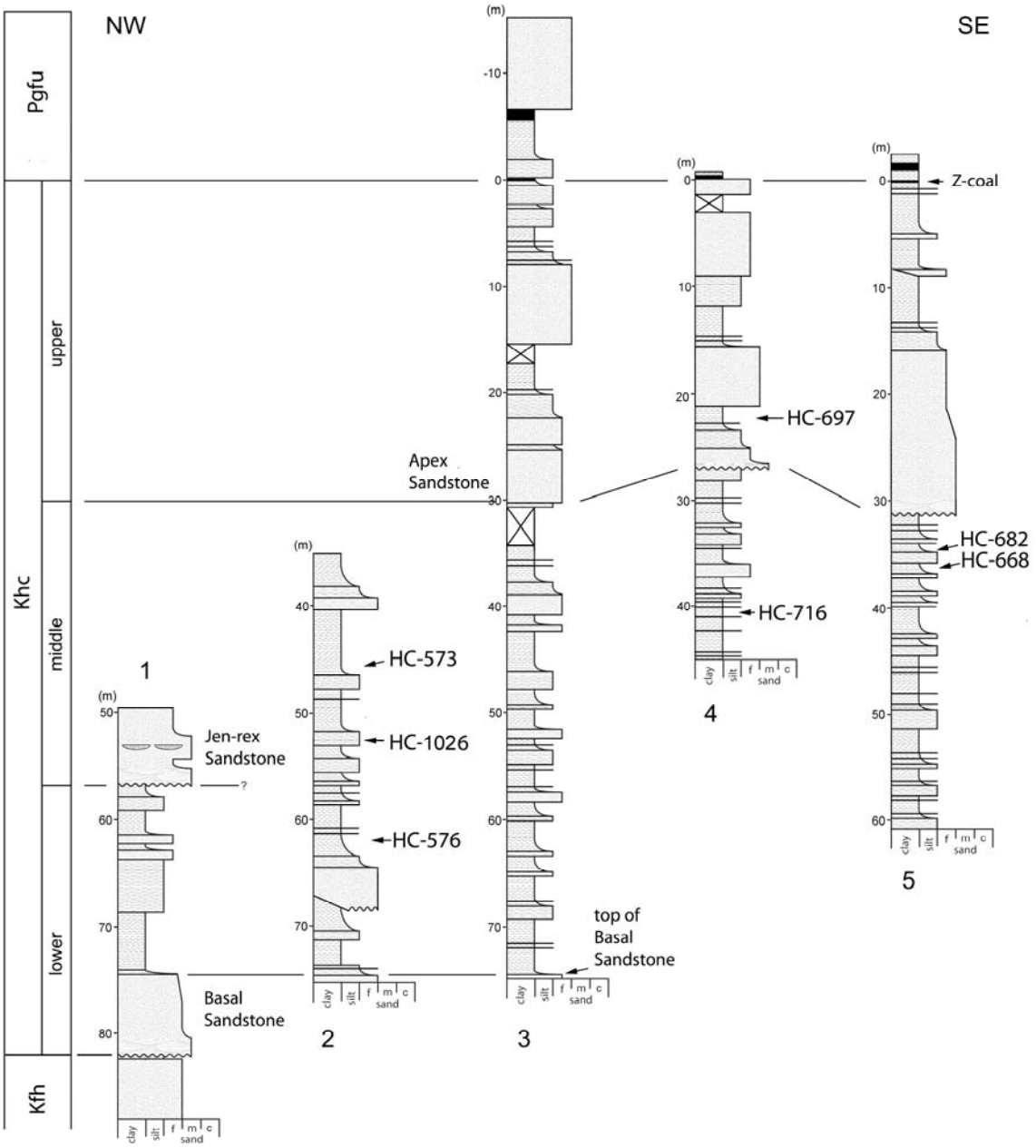


Figure 4.15. Correlation of measured sections and Museum of the Rockies (MOR) *Triceratops* localities across ~6.5 km of the Pennick Coulee area (Garfield County, Fig. 1, locality 3) from northwest to southeast. This area includes a complete section of the Hell Creek Formation (Khc). Section 1 taken at NW Pennick Coulee. Section 2 taken at N Pennick Coulee. Section 3 taken at E Pennick Coulee. Section 4 taken at HC-716. Section 5 taken at HC-668. Scale in meters. Kfh-Fox Hills Formation. Pgfu-Fort Union Formation.



Figure 4.16. Yoshi's Trike (Museum of the Rockies [MOR] locality HC-668). This locality is very high in the middle unit, ~5.5 m below the Apex Sandstone.

APPENDIX 4.1. CATALOGUED MOR SPECIMENS OF *TRICERATOPS* FROM THE HELL CREEK FORMATION

Loc. no.	Spec. no.	Locality	Coll.year	Collector	Unit	Material
HC-135	MOR 004	MORT	1981	M. Hager and crew	Upper unit (upper part)	Articulated skull, distal postorbital horn cores reconstructed
HC-1022	MOR 335	H&M Trike Parietal	1985	J. Horner and R. Makela	Lower unit	Parietal
HC-199	MOR 539	Trumbo Ranch	1987	D. Rasmussen	T.B.D.	Partial disarticulated juvenile skull including postorbital horn cores, right exoccipital
HC-069	MOR 598	Wankel T-Rex	1989	J. Horner	Upper unit	Epinasal
HC-069	MOR 599	Wankel T-Rex	1989	J. Horner	Upper unit	Partial maxilla
HC-196	MOR 622	Engdahl Trike	1989	J. Horner	Upper unit	Partial skull and associated postcranial material; scapula and humerus prepared
HC-085	MOR 652	Maloney Hill N	1990	C. Ancell	Upper unit	Juvenile squamosal
HC-069	MOR 669	Wankel T-Rex	1990	B. Harmon	Upper unit	Partial braincase
HC-069	MOR 670	Wankel T-Rex	1990	B. Harmon	Upper unit	Partial braincase
HC-108	MOR 699	Irv's Triceratops	1991	D. Gabriel	?Lower unit	Skull, lacking nasal horn and associated with postcrania including caudal vertebrae, dorsal vertebrae, pubis, ribs - skull currently on display at Makoshika State Park Visitor Center
HC-172	MOR 799	Bite Trike	1995	K. Olson	T.B.D.	Sacrum
HC-177	MOR 965	Mickey's Trike	1996	B. Harmon and C. Ancell	T.B.D.	Partial skull including nasal horn, sections of parietal and squamosal margin, jugal
HC-192	MOR 966		1996	J. Horner	T.B.D.	Nasal horn
HC-188	MOR 981	TORO I	1991	K. Olson	Lower to lowest middle unit	Articulated skull missing left jugal and left half of frill
HC-191	MOR 987	2/4/Day Site	1997	J. Horner	T.B.D. - 50 ft (15 m) below K-Pg	Partial braincase
HC-193	MOR 989	Pompey	1997	McKinley	T.B.D.	Epinasal, partial rostral
HC-209	MOR 1053	Johnston Lease	1991	P. Leiggi	T.B.D.	Baby postorbital horn core
HC-210	MOR 1059	Howell Lease	1991	Leiggi and Hanson	T.B.D.	Basioccipital and occipital condyle
HC-235	MOR 1098	'Fisk'	1999	B. Harmon	Lower unit	Postorbital horn core
HC-249	MOR 1109	Celestial Clam Bed	1999	B. Harmon and 1999 crew	Lower unit	Fragmentary skeleton including epijugal, vertebra, tooth
HC-250	MOR 1110	SG-5	1999	1999 MOR crew	Upper unit	Disarticulated skull (see Horner and Goodwin, 2006)
HC-256	MOR 1120	Getaway Trike	1999	B. Harmon and crew	Lower unit	Disarticulated skull (see Horner and Goodwin, 2006)

APPENDIX 4.1. CATALOGUED MOR SPECIMENS OF *TRICERATOPS* FROM THE HELL CREEK FORMATION

Loc. no.	Spec. no.	Locality	Coll.year	Collector	Unit	Material
HC-258	MOR 1122	TORO II	2000	B. Harmon, K. Olson, crew	Lower unit	Articulated skull
HC-265	MOR 1129	Coyote Basin	2000	J. Horner	Upper unit	Partial disarticulated skull including postorbital horn core, occipital condyle, and predentary
HC-267	MOR 1133	Larry's BO	2000	L. Boychuk	Lower unit	Basal braincase
HC-283	MOR 1157	#73 Site	2001	M. Goodwin	Lower unit	Braincase
HC-285	MOR 1160	Heaven Site	2001	J. Horner and 2001 crew	Lower unit	Elements of forelimb (associated)
HC-287	MOR 1162	Bandana Site	2001	M. Goodwin and J. Horner	Lower unit	Associated skeletal elements
HC-293	MOR 1167	Celeste's Mag. Micro Site	2001	C. Horner and J. Horner	Lower unit	Juvenile epinasal (see Horner and Goodwin, 2008)
HC-300	MOR 1171	Allard#4	2000	K. Olson	T.B.D.	Braincase
HC-301	MOR 1174	Triceratops Sacrum Site	1995	K. Olson	T.B.D.	Large sacrum, ischia, pubis
HC-308	MOR 1186	Mark's Trike	2002	B. Chinnery and crew	Lower unit	Partial skull - associated postcrania
HC-310	MOR 1188	Triceratopolis	2002	J. Horner	Lower unit	Dorsal vertebrae
HC-317	MOR 1199	Sierra Trike	2003	Sierra College	T.B.D. - ?middle unit	Disarticulated skull - missing epinasal (see Horner and Goodwin, 2006)
HC-376	MOR 1604	Baker Trike	2004	K. Olson	T.B.D. - upper middle/upper	Articulated skull, syncervical
HC-301	MOR 1612	Triceratops Sacrum Site	2005	K. Olson	T.B.D.	Humerus
HC-385	MOR 1625	Haxby Trike	2004	K. Olson and crew	Upper unit	Partial articulated skull including premax/nasal horn/rostrum/partial postorbital horn/squamosal/parietal (see Horner and Goodwin, 2008)
HC-389	MOR 1629	Marge's Trike Tibia	1998	M. Baisch and K. Olson	T.B.D.	Tibia
HC-392	MOR 2551	CSTrike2	2005	N. Peterson and crew	T.B.D. - ?upper/middle unit	Partial skull including nasal horn, nasals, postorbital horn, parietal and associated post crania
HC-393	MOR 2552	BOSH	2004	B. Schaff and crew	Lower unit	Partial skull including postorbital horn, partial parietal, squamosal, frill epiossifications
HC-425	MOR 2569	Afternoon Delight	2006	L. Hall and crew	Middle unit (lower part)	Disarticulated skull including parietal, squamosals, postorbital horn core, jugal, maxilla, quadrates (see Goodwin and Horner, 2010)

APPENDIX 4.1. CATALOGUED MOR SPECIMENS OF *TRICERATOPS* FROM THE HELL CREEK FORMATION

Loc. no.	Spec. no.	Locality	Coll.year	Collector	Unit	Material
HC-426	MOR 2570	Mark's Scavenged Trike	2006	M. Goodwin	Middle unit	Nasal horn, epijugal, pieces of maxilla and frill
HC-428	MOR 2572	Mark's Trike Generation	2006	M. Goodwin	T.B.D.	Juvenile squamosal
HC-430	MOR 2574	Quittin' Time	2006	B. Harmon, N. Peterson and crew	Upper unit (lower part)	Bonebed (see Keenan and Scannella, 2014)
HC-431	MOR 2575	Wagon Coulee North	2004	A. Ballarina	?Lower unit	Nasal horn
HC-432	MOR 2576	Snap Creek	2006	J. Horner	Upper unit (upper part)	Nasal horn
HC-435	MOR 2579	"Twitchell North"	2006	B. Harmon	T.B.D.	Juvenile postorbital horn core
HC-275	MOR 2582	Weird Microsite	2006	J. Horner	Lower unit	Frill epiossifications (see Horner and Goodwin, 2008)
HC-109	MOR 2583	Robert's Microsite	1991	R. Ivens	T.B.D.	Frill epiossification
HC-135	MOR 2584	MORT		J. Horner	Upper unit	Epijugal (see Horner and Goodwin, 2008)
HC-135	MOR 2585	MORT	1982	J. Horner	Upper unit	Epijugal
HC-135	MOR 2586	MORT		J. Horner	Upper unit	Epiossification (see Horner and Goodwin, 2008)
HC-438	MOR 2587	6-12-00-CCH Trike	2000	C. Horner	?Middle unit	Right nasal
HC-439	MOR 2588	7-4-00-CCH Microsite	2000	C. Horner	Lower unit	Frill epiossifications
HC-290	MOR 2589	DK Site	2001	2001 MOR crew	Lower unit	Juvenile postorbital horn core
HC-440	MOR 2590	JRH7-2-05-2	2005	J. Horner	Upper unit	Partial disarticulated premaxilla
HC-441	MOR 2593	Thedford Site	2005	N. Peterson and crew	T.B.D.	Quadrate
HC-442	MOR 2594	Bf9	2004	B. Hendricks	T.B.D.	Frill epiossifications
HC-444	MOR 2597	Mark's Trike II	2006	M. Goodwin	Upper unit	Dentaries, postorbital horn core, frill fragment (see Goodwin and Horner, 2010)

APPENDIX 4.1. CATALOGUED MOR SPECIMENS OF *TRICERATOPS* FROM THE HELL CREEK FORMATION

Loc. no.	Spec. no.	Locality	Coll.year	Collector	Unit	Material
HC-430	MOR 2702	BAB	2006	L. Hall and crew	Upper unit (lower part)	Partial skull including nasal horn, postorbital horns, squamosal, section of parietal, maxilla, dentary, partial premaxilla. From Quittin' Time Bonebed (see Keenan and Scannella, 2014)
HC-448	MOR 2704	"Sand Creek, Dawson"	1993	D. Gabriel	T.B.D.	Large partial jugal with epijugal
HC-280	MOR 2728	"F-Rex"	2001	L. Wilson	Lower unit	Partial right nasal
HC-520	MOR 2923	Joe's Half Day Trike	2007	B. Harmon and crew	Upper unit (upper part)	Articulated skull missing squamosals and lower jaw
HC-521	MOR 2924	Lon's Trike	2007	J. Scannella and D. Fowler	Upper unit (lower part)	Disarticulated skull including nasal horn, squamosal, nasal, premaxilla, partial parietal and associated postcrania including humerus and ulna
HC-525	MOR 2927	Trike Basin	2007	J. Horner	Upper unit	Postorbital horn core and squamosal
HC-525	MOR 2928	Trike Basin	2007	J. Horner	Upper unit	Squamosal and dentary
HC-525	MOR 2929	Trike Basin	2007	J. Horner	Upper unit	Juvenile squamosal
HC-528	MOR 2936	Lazy Bones	2006	G. Sorrentino	Upper unit	Partial disarticulated skull including squamosals, nasal horn, maxilla, braincase
HC-529	MOR 2937	Prospero	2007	S. Keenan	Upper unit (upper part)	Partial dentary, frill fragment, and other material
HC-531	MOR 2938	Lauren's Trike	2007	L. Hall, S. Keenan, and crew	Upper unit (upper part)	Partial skull including nasal horn, maxilla, dentary, partial parietal
HC-535	MOR 2941	Nosy Nasal	2007	L. Hall	Upper unit	Nasal horn, ungual
HC-530	MOR 2942	Doldrums	2007	2007 MOR crew	Upper unit	Squamosal
HC-539	MOR 2945	Too Close	2006	B. Harmon	T.B.D.	Dentary
HC-64	MOR 2946	–	–	Unknown Makoshika State Park	Unknown	Partial parietal and squamosal
HC-541	MOR 2950	JDTrike14	2007	J. Scannella and L. Hall	Upper unit (upper part)	Partial skull including braincase, partial squamosal and parietal
HC-544	MOR 2951	DFJuvieTrike 3	2008	D. Fowler, B. Schaff	Upper unit (lower part)	Nearly complete disarticulated skull and associated postcrania including humerus, femur, ilium, vertebrae, ribs

APPENDIX 4.1. CATALOGUED MOR SPECIMENS OF *TRICERATOPS* FROM THE HELL CREEK FORMATION

Loc. no.	Spec. no.	Locality	Coll.year	Collector	Unit	Material
HC-545	MOR 2952	Homer's Nose	2008	H. Hickam	Upper unit	Partial skull including epinasal, postorbital horn core, frill frag
HC-500	MOR 2958	DF Juvie-Horncore	2008	D. Fowler	Upper unit (lower part)	Juvenile postorbital horn core
HC-551	MOR 2959	Great Googoly Moogoly	2006	J. Scannella, B. Harmon, and crew	?Lower unit	Frill fragments including frill epiossifications, occipital condyle, syncervical
HC-1027	MOR 2965	TrkNas	2007	D. Fowler	Upper unit	Epinasal
HC-563	MOR 2969	Jack's 2008 Parietal	2008	J. Horner	T.B.D.	Juvenile parietal
HC-564	MOR 2971	Crazy Trike	2008	B. Schaff	Upper unit (lower part)	Partial skull including premaxilla, nasal horn, rostral, maxilla, frill
HC-565	MOR 2972	Supernasal	2008	D. Fowler and B. Schaff	Upper unit (lower part)	Partial skull including nasal horn, partial squamosal, braincase
HC-566	MOR 2974	Legs	2005	N. Peterson and crew	Upper unit	Partial limb bones (tibia)
HC-567	MOR 2975	More Frill	2009	B. Schaff and crew	Upper unit	Partial skull including postorbital horn core and squamosals
HC-570	MOR 2978	Greene Trike	2008	–	T.B.D.	Articulated skull with syncervical - missing maxillae, premaxillae, and lower jaw
HC-571	MOR 2979	Seth's Trike	2008	D. Fowler and S. Bainbridge	Upper unit	Partial skull including postorbital horns, maxilla, partial premaxilla - missing much of frill and lower jaws
HC-543	MOR 2980	TriSarahTops	2008	J. Scannella and crew	Upper unit	Squamosal
HC-573	MOR 2982	Three Amigos	2008	L. Hall and crew	Middle unit (lower part)	Partial skull including postorbital horn, nasal and nasal horn, dentary, parietal midline, partial squamosal – and associated postcrania including vertebrae and femur
HC-575	MOR 2984	2 Big	2001	L. Boychuk	Lower unit	Squamosal
HC-576	MOR 2985	6 o'clock Trike	2008	A. Carpana and crew	Lower unit	Squamosal, partial parietal, associated postcrania
HC-579	MOR 2988	Spike the Trike	2008	B. Schaff	Upper unit	Postorbital horn core
HC-622	MOR 2991	Toothburg	2009	P. Ullman	T.B.D.	Includes partial frill, occipital condyle
HC-623	MOR 2992	Halfway Hill	2009	J. Scannella and crew	T.B.D.	Partial squamosal

APPENDIX 4.1. CATALOGUED MOR SPECIMENS OF *TRICERATOPS* FROM THE HELL CREEK FORMATION

Loc. no.	Spec. no.	Locality	Coll.year	Collector	Unit	Material
HC-627	MOR 2999	Situ but Sad	2009	E. Freedman and P. Ullmann	Upper unit (upper part)	Partial skull including parietal, squamosal, braincase and postorbital horns, nasal, maxilla, dentary
HC-628	MOR 3000	Ashes Trike	2009	J. Scannella and crew	Upper unit	Postorbital horn core, parietal, partial squamosal, dentary, scapula
HC-633	MOR 3004	The Horn Resounding	2009	B. Schaff and E. Freedman	Middle unit (lower part)	Skull and associated postcrania
HC-634	MOR 3005	Antsy Trike	2009	P. Ullmann and crew	Middle unit (lower part)	Partial disarticulated skull including parietal and nasal
HC-635	MOR 3006	Warwick's Horn	2009	W. Fowler	Middle unit (lower part)	Postorbital horn core
HC-636	MOR 3008	American Beauty	2009	P. Ullmann	Upper unit (lower part)	Nasal horn
HC-638	MOR 3010	The Golden Goose	2009	J. Scannella and crew	Middle unit (lower part)	Postorbital horn core, nasal horn, dentary
HC-639	MOR 3011	Anky Breaky Heart	2009	H. Woodward and D. Fowler	Middle unit (lower part)	Partial skull including epinasal and parietal
HC-642	MOR 3015	Trash Trike	2009	E. Freedman and crew	Upper unit	Squamosal, partial braincase
HC-643	MOR 3016	Devil's Horns	2009	P. Murphy	Upper unit	Postorbital horn cores and skull frags
HC-668	MOR 3027	Yoshi's Trike	2010	J. Scannella, D. Fowler, E. Freedman	Middle unit (upper part)	Disarticulated skull including nasal horn, squamosal, nasal, premaxilla, partial parietal and associated postcrania
HC-671	MOR 3029	Jared's Trike	2010	D. Fowler and crew	Upper unit (upper part)	Parietal
HC-672	MOR 3030	JDTrike15	2007	J. Scannella and Fowler	Upper unit	Partial postorbital and frill (juvenile)
HC-692	MOR 3041	Joey's Trike	2010	L. Hall and Crew	Upper unit	Partial skull including squamosals and braincase
HC-693	MOR 3042	Ed's Trike	2008	D. Fowler and crew	Upper unit (upper part)	Dentary
HC-694	MOR 3043	GPS Maniac	2009	P. Ullmann	Upper unit	Squamosal
HC-682	MOR 3045	Cliffhanger	2010	M. Pillet, D. Fowler	Middle unit (upper part)	Parietal, squamosal, and other material
HC-696	MOR 3046	Trikey Town 2	2010	J. Scannella and crew	Upper unit	Parietal and dentary

APPENDIX 4.1. CATALOGUED MOR SPECIMENS OF *TRICERATOPS* FROM THE HELL CREEK FORMATION

Loc. no.	Spec. no.	Locality	Coll.year	Collector	Unit	Material
HC-697	MOR 3047	Got the Horn	2010	D. Fowler	Upper unit (lower part)	Postorbital horn core
HC-698	MOR 3048	Wednesday's Trike	2009	J. Scannella and L. Hall	Upper unit	Nasal horn, occipital condyle, other cranial material
HC-699	MOR 3049	Present	2009	P. Ullmann	Upper unit	Nasal horn
HC-700	MOR 3053	PVU Trike	2009	P. Ullmann	Upper unit	Associated material including postorbital horn core
HC-1026	MOR 3055	Brown Nose	2008	L. Hall	Middle unit (lower part)	Nasal horn
HC-702	MOR 3056	JDTrike12	2007	D. Fowler and J. Scannella	Upper unit (upper part)	Juvenile squamosal and postorbital horn core
HC-114	MOR 3057	Brownie Butte Trike	2008	D. Fowler	Upper unit (lower part)	Postorbital horn core
HC-704	MOR 3058	JDExTrike2	2008	J. Scannella and D. Fowler	Middle unit	Partial horn and jugal
HC-1023	MOR 3059	Heck's Horn	2009	C. Heck	Upper unit	Nasal horn
HC-716	MOR 3064	Little Horny Devil	2010	D. Fowler	Middle unit (upper part)	Brow horn, partial squamosal, quadrate, epiossifications, jugals, other cranial
HC-532	MOR 6648	Ducky Tail	2009	A. Carpana and crew	Upper unit (upper part)	Juvenile *Triceratops* parietal and squamosal found among *Edmontosaurus* material
HC-898	MOR 7037	Lost and Found	2008	B. Harmon	Middle unit	Squamosal

Note: All specimens are either *Triceratops* or cf. *Triceratops*. This table does not include specimens that are currently unprepared or housed in off-site storage (as of 2011).

T.B.D.—Precise position relative to unit boundaries to be determined. Specimens have detailed locality data on file at MOR. Loc. no.—Locality number; Spec. no.—Specimen number; Coll. year—Collection year; K-Pg—Cretaceous-Paleogene boundary.

References Cited

Archibald, D.J. 1982. A Study of Mammalia and Geology across the Cretaceous-Tertiary Boundary in Garfield County, Montana. University of California Publications in Geological Sciences 122: 286 p.

Archibald, D.J., R.F. Butler, E.H. Lindsay, W.A. Clemens, and L. Dingus. 1982, Upper Cretaceous–Paleocene biostratigraphy and magnetostratigraphy, Hell Creek and Tullock Formations, northeastern Montana. Geology 10(3): 153–159, doi:10.1130/0091-7613(1982)10<153:UCBAMH>2.0.CO;2.

Brown, B. 1907. The Hell Creek beds of the Upper Cretaceous of Montana: American Museum of Natural History Bulletin 23:823–845.

Brown, B. 1917. A complete skeleton of the horned dinosaur Monoclonius, and a description of a second skeleton showing skin impressions. Bulletin of the American Museum of Natural History 37: 281–306.

Carpenter, K., and D.B. Young. 2002. Late Cretaceous dinosaurs from the Denver Basin, Colorado. Rocky Mountain Geology 37(2): 237–254.

Cobabe, E.A., and D.E. Fastovsky. 1987. *Ugrosaurus olsoni*, a new ceratopsian (Reptilia: Ornithischia) from the Hell Creek Formation of eastern Montana: Journal of Paleontology 61 (1):148–154.

Currie, P.J., W. Langston, and D.H. Tanke. 2008. A new species of *Pachyrhinosaurus* (Dinosauria, Ceratopsidae) from the Upper Cretaceous of Alberta Canada; pp. 1-108 in P.J. Currie, W. Langston, and D.H. Tanke (eds.) A New Horned Dinosaur from an Upper Cretaceous Bone Bed in Alberta. NRC Research Press, Ottawa, Ontario, Canada.

Dingus, L., and M.A. Norell 2010. Barnum Brown: The Man Who Discovered *Tyrannosaurus rex*. University of California Press, Berkeley, California, 368 pp.

Dodson, P. 1996. The Horned Dinosaurs. Princeton University Press, Princeton, New Jersey, 346 pp.

Evans, D., P. Currie, D. Eberth, and M. Ryan. 2006. High-resolution lambeosaurine dinosaur biostratigraphy, Dinosaur Park Formation: Sexual dimorphism reconsidered. Journal of Vertebrate Paleontology 26 Supplement: 59A.

Farke, A.A., 1997, The distribution and taxonomy of *Triceratops* p. 47-79 in Wolberg, D.L., E. Stump, and G.D. Rosenberg (eds.), Dinofest International Proceedings Volume. Philadelphia Academy of Natural Sciences, Philadelphia, Pennsylvania.

Farke, A.A., 2007, Cranial osteology and phylogenetic relationships of the chasmosaurine ceratopsid *Torosaurus latus*,p. 235-257 in Carpenter, K., (ed.), Horns and Beaks: Ceratopsian and Ornithopod Dinosaurs. Indiana University Press, Bloomington, Indiana.

Farke, A.A. 2010. Evolution, homology, and function of the supracranial sinuses in ceratopsian dinosaurs. Journal of Vertebrate Paleontology 30 (5): 1486–1500, doi:10.1080/02724634.2010.501436.

Farke, A.A. 2011. Anatomy and taxonomic status of the chasmosaurine ceratopsid *Nedoceratops hatcheri* from the Upper Cretaceous Lance Formation of Wyoming, U.S.A. PLoS ONE 6:e16196, doi:10.1371/journal.pone.0016196.

Fastovsky, D.E. 1987. Paleoenvironments of vertebrate-bearing strata during the Cretaceous-Paleogene transition, eastern Montana and western North Dakota. Palaios 2: 282–295, doi:10.2307/3514678.

Flight, J.N. 2004. Sequence stratigraphic analysis of the Fox Hills and Hell Creek Formations (Maastrichtian), Eastern Montana and its relationships to dinosaur paleontology [M.S. thesis]: Bozeman, Montana, State University, 164 pp.

Forster, C.A. 1993. Taxonomic validity of the ceratopsid dinosaur *Ugrosaurus olsoni* (Cobabe and Fastovsky). Journal of Paleontology 67(2): 316–318.

Forster, C.A. 1996a. New information on the skull of *Triceratops*. Journal of Vertebrate Paleontology 16(2): 246–258, doi:10.1080/02724634.1996.10011312.

Forster, C.A. 1996b. Species resolution in *Triceratops*: Cladistic and morphometric approaches. Journal of Vertebrate Paleontology 16(2): 259–270, doi:10.1080/02724634.1996.10011313.

Fowler, D.W. 2009. A sequence stratigraphic subdivision of the Hell Creek Formation: Beginnings of a high-resolution regional chronostratigraphic framework for the terminal Cretaceous, p. 136 in Storrs, G.W. (ed.) 9th North American Paleontological Convention Abstracts. University of Cincinnati, Cincinnati Museum Center Scientific Contributions 3, Cincinnati, Ohio.

Goodwin, M.B., and J.R. Horner. 2010. Historical collecting bias and the fossil record of *Triceratops* in Montana, p. 551-564 in Ryan, M.J., Chinnery-Allgeier, B.J., and Eberth, D.A. (eds.), New Perspectives on Horned Dinosaurs: The Royal Tyrrell Museum Ceratopsian Symposium. Indiana University Press, Bloomington, Indiana.

Hall, L., and S. Keenan 2010, Taphonomy of a new specimen of *Tyrannosaurus rex* from the Hell Creek Formation, Montana. Journal of Vertebrate Paleontology: SVP Program and Abstracts Book, v. 30: 100A-101A.

Hartman, J.H., R.D., Butler, M.W., Weiler, K.K., Schumaker. 2014. Context, naming, and formal designation of the Cretaceous Hell Creek Formation lectostratotype, Garfield County, Montana , in Wilson, G.P., Clemens, W.A., Horner, J.R., and Hartman, J.H., eds., Through the End of the Cretaceous in the Type Locality of the Hell Creek Formation in Montana and Adjacent Areas: Geological Society of America Special Paper 503, doi:10.1130/2014.2503(02).

Hatcher, J.B., Marsh, O.C., and Lull, R.S., 1907, The Ceratopsia. U.S. Geological Survey Monograph 49, 300 pp.

Horner, J. R., and M. B. Goodwin. 2006. Major cranial changes during *Triceratops* ontogeny. Proceedings of the Royal Society B: Biological Sciences 273:2757–2761, doi:10.1098/rspb.2006.3643.

Horner, J. R., and M. B. Goodwin. 2008. Ontogeny of cranial epi-ossifications in *Triceratops*. Journal of Vertebrate Paleontology 28:134–144 doi:10.1671/0272-4634(2008)28[134:OOCEIT]2.0.CO;2.

Horner, J. R., and E.-T. Lamm. 2011. Ontogeny of the parietal frill of *Triceratops*: A preliminary histological analysis. Comptes Rendus Palevol 10:439–452 doi:10.1016/j.crpv.2011.04.006.

Horner, J. R., M. B. Goodwin, and N. Myhrvold. 2011. Dinosaur Census Reveals Abundant *Tyrannosaurus* and Rare Ontogenetic Stages in the Upper Cretaceous Hell Creek Formation (Maastrichtian), Montana, USA. PLoS ONE 6:e16574.

Keenan, S.W., and J.B. Scannella. 2014. Paleobiological implications of a *Triceratops* bonebed from the Hell Creek Formation, Garfield County, northeastern Montana, in Wilson, G.P., W.A. Clemens, J.R. Horner, and J.H. Hartman, (eds.) Through the End of the Cretaceous in the Type Locality of the Hell Creek Formation in Montana and Adjacent Areas: Geological Society of America Special Paper 503, doi:10.1130/2014.2503(14).

Lofgren, D.L. 1995. The Bug Creek Problem and the Cretaceous-Tertiary Transition at McGuire Creek, Montana. University of California Publications in Geological Sciences 140, 185 p.

Longrich, N.R., and D.J. Field. 2012. *Torosaurus* is not *Triceratops*: Ontogeny in chasmosaurine ceratopsids as a case study in dinosaur taxonomy: PLoS ONE 7(2) p. e32623, doi:10.1371/journal.pone.0032623.

Lull, R.S. 1915. The mammals and horned dinosaurs of the Lance formation of Niobrara County, Wyoming. American Journal of Science 4: 319–348, doi:10.2475/ajs.s4-40.238.319.

Lull, R.S. 1933. A Revision of the Ceratopsia or Horned Dinosaurs. Yale Peabody Museum of Natural History Memoir 3, 178 pp.

Mayr, E. 1959. Darwin and the evolutionary theory in biology, p. 1-10 in Meggers J., ed., Evolution and Anthropology: A Centennial Appraisal: Anthropological Society of Washington, Washington, D.C.

Osborn, H.F. 1905. *Tyrannosaurus* and other Cretaceous carnivorous dinosaurs. Bulletin of the American Museum of Natural History 22: 475–479.

Ostrom, J.H. and P. Wellnhofer. 1986. The Munich specimen of *Triceratops* with a revision of the genus. Zitteliana 14: 111–158.

Ostrom, J.H., and P. Wellnhofer. 1990. *Triceratops*: An example of flawed systematics, p. 245-254 in Carpenter, K., and Currie, P.J., eds., Dinosaur Systematics: Approaches and Perspectives. Cambridge University Press, New York, New York.

Pearson, D.A., T., Schaefer, K.R., Johnson, D.J., Nichols, and J.P., Hunter. 2002. Vertebrate biostratigraphy of the Hell Creek Formation in southwestern North Dakota and northwestern South Dakota, p. 145-167 in Hartman, J.H., K.R., Johnson, and D.J., Nichols (eds.) The Hell Creek Formation and the Cretaceous-Tertiary Boundary in the Northern Great Plains: An Integrated Continental Record of the End of the Cretaceous. Geological Society of America Special Paper 361.

Sampson, S.D. 1995. Two new horned dinosaurs from the Upper Cretaceous Two Medicine Formation of Montana; with a phylogenetic analysis of the Centrosaurinae (Ornithischia: Ceratopsidae). Journal of Vertebrate Paleontology 15 (4):743–760, doi:10.1080/02724634.1995.10011259.

Scannella, J. 2010. *Triceratops*: A model organism for deciphering dinosaur heterochrony. Journal of Vertebrate Paleontology, SVP Program and Abstracts Book 30 (2): 158A.

Scannella, J.B., and D.W., Fowler. 2009. Anagenesis in *Triceratops*: Evidence from a newly resolved stratigraphic framework for the Hell Creek Formation p. 148-149 in Storrs, G.W. (ed.), 9th North American Paleontological Convention Abstracts. University of Cincinnati, Cincinnati Museum Center Scientific Contributions 3, Cincinnati, Ohio.

Scannella, J.B., and J.R. Horner. 2010. *Torosaurus* Marsh, 1891 is *Triceratops* Marsh, 1889 (Ceratopsidae: Chasmosaurinae): Synonymy through ontogeny. Journal of Vertebrate Paleontology 30(4):1157–1168, doi:10.1080/02724634.2010.483632.

Swisher, C.C., L., Dingus. and R.F., Butler. 1993. 40Ar/39Ar dating and magnetostratigraphic correlation of the terrestrial Cretaceous-Paleogene boundary and Puercan mammal age, Hell Creek-Tullock Formations, eastern Montana. Canadian Journal of Earth Sciences 30(9):1981–1996, doi:10.1139/e93-174.

Tanke, D.H. 2010. Ceratopsian discoveries and work in Alberta, Canada: A historical review and census, in Ryan, M.J., B.J., Chinnery-Allgeier, and D.A., Eberth, (eds.), New Perspectives on Horned Dinosaurs: The Royal Tyrrell Museum Ceratopsian Symposium. Indiana University Press, Bloomington, Indiana, supplemental CD-ROM, 488 pp.

Turner, B.W. 2010. Testing the Local Diachroneity of the Terrestrial Lithostratigraphic KPg Boundary, Northern Montana [M.S. thesis]: Montana State University, Bozeman, Montana, 187 pp.

Wilson, G.P. 2004. A Quantitative Assessment of Evolutionary and Ecological Change in Mammalian Faunas Leading Up To and Across the Cretaceous-Tertiary Boundary, Northeastern Montana [Ph.D. dissertation]: University of California, Berkeley, California, 412 p.

Wilson, G.P. 2005. Mammalian faunal dynamics during the last 1.8 million years of the Cretaceous in Garfield County, Montana. Journal of Mammalian Evolution. 12(1-2): 53–76, doi:10.1007/s10914-005-6943-4.

CHAPTER FIVE

EVOLUTIONARY TRENDS IN *TRICERATOPS* FROM THE HELL CREEK FORMATION, MONTANA

Contribution of Authors and Co-Authors

Manuscript in Chapter 5

Author: John B. Scannella

Contributions: Designed research, performed research, analyzed data, wrote the paper

Co-author: Denver W. Fowler

Contributions: Designed research, performed research, analyzed data, wrote the paper

Co-author: Mark B. Goodwin

Contributions: Designed research, performed research, wrote the paper

Co-author: John R. Horner

Contributions: Designed research, performed research, contributed new reagents/analytic tools

Manuscript Information Page

John B. Scannella, Denver W. Fowler, Mark B. Goodwin, John R. Horner
Journal: Proceedings of the National Academy of Sciences of the United States of America
Status of Manuscript:
__Prepared for submission to a peer-reviewed journal
___Officially submitted to a peer-reviewed journal
___Accepted by a peer-reviewed journal
_x_Published in a peer-reviewed journal

Scannella, J. B., D. W. Fowler, M. B. Goodwin, and J. R. Horner. 2014. Evolutionary trends in *Triceratops* from the Hell Creek Formation, Montana. Proceedings of the National Academy of Sciences 111:10245–10250, doi: 10.1073/pnas.1313334111

The following chapter (and supporting information in Appendix A) has been published in the Proceedings of the National Academy of Sciences of the United States of America.

Abstract

The placement of over 50 skulls of the well-known horned dinosaur *Triceratops* within a stratigraphic framework for the Upper Cretaceous Hell Creek Formation (HCF) of Montana reveals the evolutionary transformation of this genus. Specimens referable to the two recognized morphospecies of *Triceratops*, *T. horridus* and *T. prorsus*, are stratigraphically separated within the HCF with the *T. prorsus* morphology recovered in the upper third of the formation and *T. horridus* found lower in the formation. Hypotheses that these morphospecies represent sexual or ontogenetic variation within a single species are thus untenable. Stratigraphic placement of specimens appears to reveal ancestor-descendant relationships. Transitional morphologies are found in the middle unit of the formation, a finding which is consistent with the evolution of *Triceratops* being characterized by anagenesis, the transformation of a lineage over time. Variation among specimens from this critical stratigraphic zone may indicate a branching event in the *Triceratops* lineage. Purely cladogenetic interpretations of the HCF dataset imply greater diversity within the formation. These findings underscore the critical role of stratigraphic data in deciphering evolutionary patterns in the Dinosauria.

Significance Statement

The deciphering of evolutionary trends in non-avian dinosaurs can be impeded by a combination of small sample sizes, low stratigraphic resolution, and lack of ontogenetic (developmental) details for many taxa. Analysis of a large sample (n>50) of the famous horned dinosaur *Triceratops* from the Hell Creek Formation of Montana incorporates

new stratigraphic and ontogenetic findings to permit the investigation of evolution within this genus. Our research indicates that the two currently recognized species of *Triceratops* (*T. horridus* and *T. prorsus*) are stratigraphically separated and that the evolution of this genus likely incorporated anagenetic (transformational) change. These findings impact interpretations of dinosaur diversity at the end of the Cretaceous and illuminate potential modes of evolution in the Dinosauria.

Introduction

The Hell Creek Project (1999-2010), a multi-institutional survey of the fauna, flora, and geology of the Upper Cretaceous Hell Creek Formation (HCF), provides insights into the paleobiology and evolution of the last non-avian dinosaurs (Horner et al., 2011). *Triceratops* (Ceratopsidae: Chasmosaurinae) is the most abundant dinosaur in the HCF; >50 skulls, including previously unknown or rare growth stages, have been collected throughout the entire formation (spanning ~ 1 to 2 million y) (Hicks et al., 20022) over the course of the Hell Creek Project (Horner and Goodwin, 2006; Horner et al., 2011; Scannella and Horner, 2010; Scannella and Fowler, 2014). The combination of a stratigraphically-controlled robust sample from the entire ~90 meter (m) thick HCF and identification of ontogenetic stages makes *Triceratops* a model organism for testing hypotheses proposed for the modes of dinosaur evolution (e.g. Horner et al., 1992, Sampson, 1995; Sampson and Loewen, 2010).

Since its initial discovery (Marsh, 1889), as many as 16 species of *Triceratops* were named based on variations in cranial morphology (Ostrom and Wellnhofer, 1986; 1990). Forster (1996) recognized only two species, *T. horridus* and *T. prorsus,* based on

cranial features including differences in relative length of the postorbital horn cores (long in *T. horridus* and shorter in *T. prorsus*), morphology of the rostrum (elongate in *T. horridus* and shorter in *T. prorsus*), and closure of the frontoparietal fontanelle (sensu Farke) (2010); open in *T. horridus* and closed in *T. prorsus*). Marsh initially distinguished these two species by the morphology of the nasal horn (Marsh, 1890); the type specimen of *T. horridus* possesses a short, blunt nasal horn whereas the nasal horn in *T. prorsus* is elongate. Whether or not these taxa were largely biogeographically separated or represented ontogenetic variants or sexual dimorphs within a single species has remained unresolved (Ostrom and Wellnhofer, 1986; Dodson, 1996; Forster, 1996; Happ and Morrow, 1996; Farke, 1997; Lehman, 1998; Sampson and Loewen, 2010) . A record of the stratigraphic distribution of *Triceratops* from the Upper Cretaceous Lance Formation of Wyoming compiled by Lull (1915; 1933) suggested that these taxa overlap stratigraphically. However, this assessment was likely based on limited stratigraphic data (Farke, 1997) and "the precise stratigraphic placement of these specimens can no longer be established" (Ostrom and Wellnhofer, p. 155). As such, consideration of morphological variation in a detailed stratigraphic context is necessary to reassess systematic hypotheses.

Results

Stratigraphic placement of *Triceratops* specimens within the HCF reveals previously undocumented shifts in morphology. The HCF is divided into three stratigraphic units: the lower third (L3), middle third (M3), and upper third (U3) (Horner et al., 2011; Hartman et al., 2014). The stratigraphic separation of *Triceratops*

morphospecies is apparent with specimens referable to *T. prorsus* (following Forster) (1996) found in U3 and *T. horridus* only recovered lower in the HCF. Specimens from the upper part of M3 exhibit a combination of *T. horridus* and *T. prorsus* features (Fig. 5.1, SI Text, and Fig. 5.S1).

L3 *Triceratops*.

Triceratops from the lowermost 15-30 m of the HCF (L3) possess either a small nasal horn (Fig. 5.2A; Dataset 5.S1) or a low nasal boss. The boss morphology appears in a large individual that histologically represents a mature specimen [="*Torosaurus*" ontogenetic morph [Scannella and Horner, 2010 (but see also: Farke, 2011; Longrich and Field, 2012; Maiorino et al., 2014); Museum of the Rockies (MOR) specimen 1122) (SI Text)]. The nasal process of the premaxilla (NPP) in L3 *Triceratops* is narrow (Fig. 5.2B andFig. 5.S2) and strongly posteriorly inclined; a pronounced anteromedial process is present on the nasal (Fig. 5.S3). The frontoparietal fontanelle remains open until late in ontogeny (MOR 1122). Specimens from the lower unit of the HCF bear a range of postorbital horn core lengths (ranging from ~ .45 to at least .74 basal-skull length) (Fig. 5.2D and Dataset 5.S1).

M3 *Triceratops*.

The mean nasal-horn length increases through M3 (Figs. 5.1*E* and *F* and Fig. 5.2A). University of California Museum of Paleontology (UCMP) specimen 113697 (collected ~ 6 m below the base of U3) possesses a nasal horn that is elongate (length/width: 2.12) (Dataset 5.S1) but retains a broad posterior surface, giving the horn a subtriangular cross section. Forster (1996) noted that UCMP 113697 exhibits a small

nasal boss posterior to the nasal horn. Disarticulated specimens (e.g. MOR 3027 and MOR 3045) reveal that this protuberance posterior to the epinasal appears to be formed by the combination of a posterior projection on the epinasal (Fig. 5.S4) and the anteriormost nasal. A homologous morphology is observed in specimens from L3 and the lower half of M3 (MOR 1120, MOR 2982, MOR 3010). UCMP 128561, from the upper half of M3, exhibits a low nasal boss (Cobabe and Fastovsky, 1987; Forster, 1993) (*SI Text*). The anteromedial process of the nasal is pronounced in *Triceratops* from M3 and the NPP is more vertically inclined in specimens from upper M3, producing a more convex rostrum morphology which was previously found to characterize *T. prorsus* (Forster, 1996; Longrich and Field, 2012). The frontoparietal fontanelle is open in late stage subadults/young adults (UCMP 113697).

U3 *Triceratops*.

Specimens from U3 exhibit the features Forster (1996) found to characterize *T. prorsus*. U3 *Triceratops* possess an elongate, relatively narrow nasal horn (average length/width > 2) (Fig. 5.2A; Dataset 5.S1). The NPP is more vertically inclined, producing a convex rostrum lacking the low, elongate profile noted in *T. horridus* [although the largest, and presumably oldest, known specimens (e.g. MOR 004 and MOR 1625) exhibit proportionally longer rostra] (Fig. 5.2E and Dataset 5.S1). The NPP is antero-posteriorly expanded and the anteromedial process of the nasal is greatly reduced (Fig. 5.S3) (Horner and Goodwin, 2008). The frontoparietal fontanelle becomes constricted and eventually closed in late stage subadults/young adults (e.g. MOR 2923 and MOR 2979), ontogenetically earlier than in L3 and M3. The postorbital horn cores

are short (< 0.64 basal-skull length) (Fig. 5.2D). Further, U3 *Triceratops* appear to exhibit nasals which are more elongate than *Triceratops* from the lower half of the HCF (Fig. 5.2F and Dataset 5.S1).

Shifts in Morphology over Time.

Epinasals exhibit a directional morphologic trend; average length increases throughout the formation (Fig. 5.2A and Dataset 5.S1) (Spearman's rank coefficient = 0.824, p = 4.15E-07). A protuberance just posterior to the epinasal, observed in specimens from L3 and M3 (Fig. 5.1) is particularly pronounced in UCMP 113697 from the uppermost M3 (Fig. 5.1E). U3 *Triceratops* either do not exhibit this feature or express only a subtle ridge in the homologous location. Concurrent with elongation of the epinasal was an expansion of the NPP (Fig. 5.2B) (Spearman's rank coefficient = -0.969, *P*= 3.74E-06) and an increase in the angle between the NPP and the narial strut of the premaxilla (Fig. 5.2C and Dataset 5.S1) (Spearman's rank coefficient = .802, *P* = .000186). Nasals also become more elongate relative to basal skull length (although only three specimens with complete nasals have thus far been recorded from the lower half of the formation) (Fig 5.2F and Dataset 5.S1) (Spearman's rank coefficient = .804, *P* = .00894).

Postorbital horn-core length appears to be variable throughout L3 and M3 and is consistently short in U3 *Triceratops* (Fig. 5.2D and Dataset 5.S1) [Spearman's rank coefficient is negative (-0.197) and not statistically significant (*P*=0.392)]. Large juvenile U3 *Triceratops* (e.g. MOR 1110) can possess more elongate postorbital horn cores (0.64 basal-skull length). Whereas U3 postorbital horn core length falls within the range of

variation observed lower in the formation (Fig. 5.2D), elongate postorbital horn cores have thus far not been found in post-juvenile stage *Triceratops* from U3. Many large *Triceratops* (e.g. MOR 1122 and MOR 3000) (Scannella and Horner, 2010) exhibit evidence of postorbital horn core resorption, suggesting maximum length is reached earlier in ontogeny. Maximum postorbital horn core length may have been expressed later in development (or for a longer duration) in *Triceratops* from lower in the formation

Triceratops from the upper half of the HCF exhibit a more vertically inclined NPP (Fig. 5.2C), which contributes to a rostrum which appears shorter and more convex in lateral profile (a feature Forster [1996] noted in *T. prorsus*) (). However, we note that a Spearman's rank correlation test found apparent reduction in rostrum length to be statistically insignificant (Spearman rank's coefficient .018, *P*=.966). Large specimens from U3 (e.g. MOR 004) possess a more elongate rostrum relative to basal skull length (Fig. 5.2E and Dataset 5.S1), however the shape of U3 rostra appears to be consistently convex.

Eotriceratops xerinsularis, found in the stratigraphically older uppermost Horseshoe Canyon Formation (~ 68 Ma) (Wu et al., 2007), expresses morphologies (elongate postorbital horn cores, small nasal horn) consistent with its stratigraphic position relative to *Triceratops*.

Cladistic and Stratocladistic Analyses.

Initial cladistic analyses recovered a polytomy of all HCF specimens, with the 50% majority tree producing a succession of *Triceratops* that largely correlates with stratigraphic placement (Fig. 5.S5 and SI Text). Removal of the more fragmentary

material recovered *Torosaurus* specimens as basal to a stratigraphic succession of *Triceratops* including a polytomy of specimens from the upper half of the formation. A similar topology was recovered when specimens not exhibiting codeable features of the parietal squamosal frill were removed from the analysis (Fig. 5.3B). Removal of MOR 2924, a specimen from the base of U3 which does not preserve postorbital horn cores (SI Text), recovers specimens from the upper part of M3 as basal to U3 *Triceratops*.

In the analysis of the most reduced data set, UCMP 113697 and MOR 3027 cluster together (Fig. 5.3C). These specimens exhibit a combination of characters found in *Triceratops* from L3 and M3. The epinasal of UCMP 113697 is morphologically intermediate between L3 and U3 *Triceratops* (the epinasal of MOR 3027 is incomplete). These specimens each exhibit large postorbital horn cores (a feature expressed in some L3 *Triceratops*) and a more vertically inclined NPP (found in U3 *Triceratops*). MOR 3045 is recovered as being more derived than UCMP 113697 and MOR 3027 (Fig. 3) based on its possession of relatively short postorbital horn cores, a more expanded NPP, and a pronounced step bordering the 'incipient fenestrae' (sensu Scannella and Horner, 2010) (SI Text). This specimen exhibits the basal condition of the antero-medial nasal process and expresses a pronounced upturn of the posterior surface of the epinasal, suggesting the presence of a protuberance in life. MOR 3045 exhibits a fairly elongate epinasal (est. length/width: ~ 1.88), with a posterior surface which is broader than is seen in most U3 specimens; and, like UCMP 113697, MOR 3027, and U3 *Triceratops*, exhibits a more vertically inclined NPP.

Stratocladistic analyses, in which specimens were grouped into operational units based on stratigraphic position, were performed in the program StrataPhy (Marcot and

Fox, 2008). *Torosaurus* specimens were initially considered separately from other specimens (see SI Text). Initial results suggested that specimens from the upper half of the HCF represented a sequence of ancestors and descendants but differed on the position of operational units from the lower half of the formation (Fig. 5.S6A). This result was likely influenced by missing data for specimens from the lower half of the formation; no specimens from lower M3 preserve frill characters which can distinguish them from the *Torosaurus* morphology. When *Torosaurus* specimens were incorporated into *Triceratops* operational units, three topologies were produced: a strictly cladogenetic result, a topology in which all operational units except lower M3 were recovered in a transformational sequence, and a topology in which the HCF operational units were recovered in two lineages (an upper L3/lower M3 lineage and an upper M3/U3 lineage) which had diverged at some point in the deposition of L3 (Fig. 5.S6B). Pruning of *Torosaurus* specimens from the dataset produced two topologies which incorporated morphological transformation: one topology in which all HCF operational units fell into a single lineage and another topology presenting two HCF lineages which diverged either in L3 or prior to deposition of the HCF (Fig. 5.S6C).

Discussion

Evolutionary Patterns.

One of the principle questions in evolutionary biology regards the modes of evolution: what evolutionary patterns are preserved in the fossil record and how prominent are these patterns (Simpson, 1944; 1953; Eldredge and Gould, 1972)? Small sample sizes for most non-avian dinosaur taxa complicate the investigation of

evolutionary modes in this group. As such, it is unknown how prominent a role anagenesis (the transformation of lineages over time) (Fig. 5.4A) (e.g. Rensch, 1947; Malmgren et al., 1983; Gingerich, 1985; Macleod, 1991; Benton and Pearson, 2001) played in their evolution or whether the majority of morphologies recorded in the fossil record were a product of cladogenesis (evolution via branching events (Fig. 5.4B-D) (Rensch, 1947; Eldredge and Gould, 1972; Wagner and Erwin, 1995; Benton and Pearson, 2001; Sampson and Loewen, 2010).

Horner et al. (1992) presented evidence for anagenesis in several dinosaur clades within the Cretaceous Two Medicine Formation of Montana. It has been suggested that the sample size presented in that study was too small and that cladogenesis was a more conservative interpretation of the data (Sampson, 1995). A combination of large sample size, ontogenetic resolution, and detailed stratigraphic data makes *Triceratops* an ideal taxon for testing hypotheses regarding evolutionary mode in a non-avian dinosaur.

Restriction of the full *T. prorsus* morphology to U3 renders hypotheses that *T. horridus* and *T. prorsus* represent sexual or ontogenetic variation within a single taxon untenable. *Triceratops* from the upper part of M3 exhibit a combination of features found in L3 and U3 *Triceratops*. This pattern suggests that the evolution of *Triceratops* incorporated anagenesis.

Strict consensus trees produced by cladistic analyses either recover upper M3 specimens in a polytomy with all HCF specimens, in a polytomy of HCF *Triceratops* from the upper half of the formation, or UCMP 113697 and MOR 3027 cluster together whereas MOR 3045 shares more features with U3 *Triceratops* (Fig. 5.3 and Fig. 5.S5).

We will consider four alternative hypotheses for the morphological pattern recorded in the HCF:

i) *T. prorsus* evolved elsewhere and migrated into the HCF, eventually replacing the incumbent HCF *Triceratops* population by the beginning of the deposition of U3. Upper M3 specimens represent early members (or close relatives of) this group that would come to dominate the ecosystem.

ii) Variation between MOR 3045, MOR 3027, and UCMP 113697 represents intraspecific (or intrapopulation) variation. As the HCF *Triceratops* lineage evolved, some individuals expressed more of the features that would eventually dominate the population. Over time, these traits were selected for and characterized U3 *Triceratops*. This is a purely anagenetic scenario.

iii) A bifurcation event is recorded in the HCF and occurred at some point prior to the deposition of U3, resulting in two lineages which differ primarily in the morphology of the epinasal and rostrum (consistent with Forster's diagnoses for *T. horridus* and *T. prorsus*). MOR 3045 represents an early member of a lineage which evolved into U3 *Triceratops*. This scenario incorporates anagenesis (Wagner and Erwin, 1995) and is presented in some trees produced by the stratocladistic analysis (Fig. 5.S6).

iv) The evolution of *Triceratops* was characterized by a series of cladogenetic events that produced at least five taxa over the course of the deposition of the HCF (the L3 clade, the lower M3 clade, the MOR 3027 clade, the MOR 3045 clade, and the U3 clade). This strictly cladogenetic scenario suggests that no *Triceratops* found lower in the HCF underwent evolutionary transformation into forms found higher in the formation.

A Biogeographic Signal?

The Hell Creek Project's stratigraphic record of *Triceratops* is primarily restricted to northeastern Montana. It has been hypothesized that *T. horridus* and *T. prorsus* were largely biogeographically separated, with *T. prorsus* generally restricted to the Hell Creek and Frenchman Formations and *T. horridus* commonly found in the more southern Lance, Laramie, and Denver Formations (Happ and Morrow, 1996; Farke, 1997). However, this suggested biogeographic segregation may represent an artifact of the stratigraphic record. Specimens which have thus far been described from neighboring coeval formations exhibit morphologies consistent with their stratigraphic position relative to the HCF (Tokaryk, 1986; Carpenter and Young, 2002) (SI Text).

Anagenesis and Cladogenesis.

If the morphological trends noted in *Triceratops* were purely the result of cladogenetic branching (consistent with punctuated equilibrium [Eldredge and Gould, 1972) (Fig. 5.4C and D), we would expect to find the full U3 morphology coexisting with *Triceratops* found lower in the formation, or alternatively, specimens exhibiting the L3 morphology in U3. Such specimens have yet to be discovered (SI Text). Specimens from the upper part of M3 exhibit transitional features relative to L3 and U3 *Triceratops*, a pattern consistent with anagenesis.

Some cladistic analyses distinguish MOR 3045 from other upper M3 *Triceratops* based on variation in the length of the postorbital horn cores, width of the NPP, and the thickened regions of the parietal (Fig. 5.3, Fig. 5.S5, and SI Text). *Triceratops* collected from a multi-individual bonebed in U3 (MOR locality no. HC-430; Keenan and

Scannella, 2014) show variable morphology of the premaxillae and parietal between individuals (Fig 5.S2) (). This finding suggests that the variation between upper M3 specimens may represent intrapopulational, not taxonomic, variation (Ostrom and Wellnhofer, 1986). Individuals exhibiting more pronounced U3 character states may have become increasingly abundant in the HCF *Triceratops* population over time until, by the end of the Cretaceous, all *Triceratops* exhibited these character states (Fig. 5.4A). Alternatively, MOR 3045 may represent an early member of a U3 (*T. prorsus*) lineage with MOR 3027 representing a separate lineage. Stratocladistic analyses suggest the possibility of two lineages in the HCF (Fig. 5.4B and 5.S6), however this scenario would require the independent evolution of an enlarged epinasal-nasal protuberance. A purely cladogenetic interpretation of the HCF *Triceratops* dataset suggests the presence of at least five stratigraphically overlapping taxa in the formation (Fig. 5.4C and D). This scenario is possible, but we would argue that interpretations that incorporate populational transformation (anagenesis) are more conservative..

Specimens from upper M3 exhibit a combination of primitive and derived characters, as well as more developed states of characters expressed in L3 *Triceratops*. Forster (1996) noted that, whereas *T. prorsus* exhibited derived characters, no autapomorphic characters were recognized in *T. horridus*. This finding is consistent with the hypothesis that the evolution of *Triceratops* incorporated anagenesis and illustrates the potential difficulties with defining species in evolving populations (Gingerich, 1985; Horner et al., 1992). The HCF dataset underscores the importance of considering morphologies in a populational, rather than typological context (Simpson, 1951).

Conclusions

The documented changes in *Triceratops* morphology occurred over a geologically short interval of time (1-2 million y) (Hicks et al., 2002). High-resolution stratigraphy is necessary for recognizing fine scale evolutionary trends. If cladogenesis is considered the primary mode of dinosaur evolution, a problematic inflation of dinosaur diversity occurs.

Current evidence suggests that the evolution of *Triceratops* incorporated anagenesis as there is currently no evidence for biogeographic segregation of contemporaneous *Triceratops* morphospecies and there is evidence for the morphological transformation of *Triceratops* throughout the HCF. This dataset supports hypotheses that the evolution of other Cretaceous dinosaurs may have incorporated phyletic change (Horner et al., 1992; Evans et al., 2006; Campione and Evans, 2011) and suggests that many speciation events in the dinosaur record may represent bifurcation events within anagenetic lineages (Wagner and Erwin, 1995).

Materials and Methods

Most specimens in this study were placed in section relative to either the upper and /or lower formational contacts, respectively marked by the overlying Fort Union or underlying Fox Hills Formations (Scannella and Fowler, 2014). For some specimens, stratigraphic precision was increased by measuring position relative to marker sandstones (Horner et al., 2011). The base of each unit in the HCF near Fort Peck Lake is marked by a prominent amalgamated channel sandstone that consistently occurs in the same stratigraphic position (Horner et al., 2011). The Basal sand, Jen-rex sand, and Apex

sand mark the bases of the Lower, Middle, and Upper units respectively (Horner et al., 2011; Hartman et al., 2014) (Fig. 5.1*C*). Each sandstone complex fines upwards into overbank mudstones and siltstones. MOR 981 was collected from a mudstone horizon above the basal sandstone; more detailed stratigraphic data is unavailable for this specimen.

The boundary between the C30N and C29R magnetozones occurs either at the base, or in the middle of the Apex sand (base of U3) (Fig. 5.1). Samples taken within the sandstone do not produce a signal, but samples from above the sandstone are of reversed polarity (C29r), while those below are normal polarity (C30n) (Lerbekmo and Braman, 2002; Lecain et al., 2014).

A cladistic analysis of HCF *Triceratops* specimens was conducted in PAUP* 4.0b10 (Swofford, 2003) (SI Text) initially using the heuristic search command with *Arrhinoceratops* (Parks, 1925) designated as the outgroup. The matrix was assembled in Mesquite 2.75 (Maddison and Maddison, 2011) and cladograms were displayed using FigTree (Rambaut, 2012). Analyses were conducted using the random addition sequence (SI Text). The most complete post-juvenile stage specimens were included in the analysis (SI Text; see Campione et al., 2013). Characters found to vary within *Triceratops,* and between *Triceratops* and *Eotriceratops,* (Fig. 5.S7 and SI Text), were included. Strongly ontogenetically influenced characters (e.g. postorbital horn core orientation; frill epiossification shape) were excluded from the analysis, however characters often used to distinguish *Triceratops* and *Torosaurus* (e.g. parietal fenestrae, epiossification position) were retained. Specimens exhibiting multiple character states (e.g. differing numbers of episquamosals on each squamosal) were coded as polymorphic. All characters were left

unordered; maxtrees was set to 250,000. Bremer support indices were calculated using TreeRot v3 (Sorenson and Franzosa, 2007). Analyses of the reduced dataset were conducted using the branch and bound search command. Stratocladistic analyses were performed in the program StrataPhy (Marcot and Fox, 2008) with maxtrees set to 250,000. Specimens with some ambiguity regarding stratigraphic position (MOR 981, MOR 1604, MOR 2978) were excluded from the analysis (SI Text). Spearman's rank correlation analyses were performed in R (R Core Team, 2013) using the 'cor.test' function [cor.test(x,y, method='spear', exact = FALSE)]. Juvenile specimens were excluded from these analyses as were specimens exhibiting significant taphonomic distortion (see Fig. 5.2 and Dataset 5.S1). Additional calculations were performed in Microsoft Office Excel 2007.

Acknowledgments

We thank D. Barta, B. Boessenecker, N. Campione, T. Carr, W. Clemens, W. Clyde, P. Dodson, D. Evans, A. Farke, C. Forster, E. Fowler, J. Frederickson, J. Hartman, L. Hall, J. Hoganson, M. Holland, F. Jackson, S. Keenan, M. Lavin, M. Loewen, J. Mallon, K. Olson, C. Organ, K. Padian, A. Poust, D. Pearson, P. Renne, D. Roberts, K. Scannella, J. Stiegler, D. Varricchio, D. Woodruff, H. Woodward, and B. Zorigt for helpful discussions, without implying their agreement with our conclusions. Comments and suggestions from G. Hunt, P.D. Polly, and three anonymous reviewers were very helpful. Thanks to D. Fox, A. Huttenlocker, and J. Marcot for help using StrataPhy. D. Evans, K. Seymour, and B. Iwama provided access to the holotype of *Arrhinoceratops* at the Royal Ontario Museum. B. Strilisky and G. Housego provided access to the holotype

of *Eotriceratops* at the Royal Tyrrell Museum and additional images of its premaxilla. J. Sertich provided access to specimens at the Denver Museum of Nature and Science. P. Sheehan provided access to and locality data for Milwaukee Publich Museum (MPM) specimen VP6841. R. Scheetz and B. Britt provided access to a cast of Museum of Western Colorado (MWC) specimen 7584 at BYU; W. Clemens shared stratigraphic data for this specimen. The Bureau of Land Management, Charles M. Russell National Wildlife Refuge, and the Department of Natural Resources and Conservation provided access to land under their management and collection permits. We are grateful to the Twitchell, Taylor, Trumbo, Holen, and Isaacs families for land access. We thank the Museum of the Rockies (MOR) volunteers, staff, and all participants in the Hell Creek Project. We thank the MOR and the University of California Museum of Paleontology (UCMP) for support of this research. Funding for the Hell Creek Project was provided by donations from J. Kinsey, C.B. Reynolds, H. Hickam, and Intellectual Ventures. The Windway Foundation and the Smithsonian Institution provided grants (to JRH). UCMP provided funding (to MBG). The Theodore Roosevelt Memorial Fund of the American Museum of Natural History, the Fritz Travel Grant of the Royal Ontario Museum, and the Jurassic Foundation provided grants (to J.B.S.). The Evolving Earth Foundation and the Doris O. and Samuel P. Welles Research Fund of the UCMP provided grants (to J.B.S. and D.W.F.).

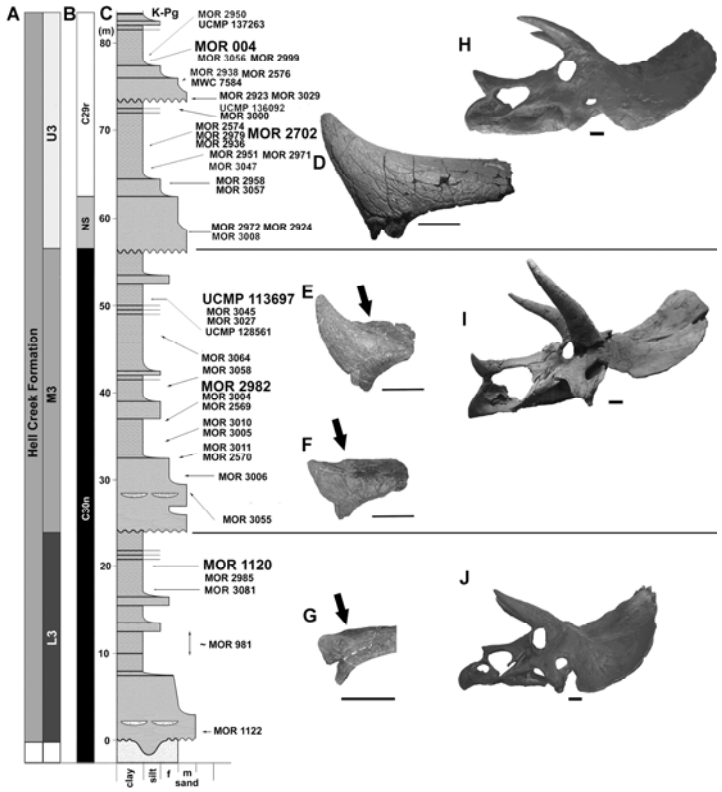


Fig. 5.1. Stratigraphic placement of HCF *Triceratops* reveals trends in cranial morphology including elongation of the epinasal and change in morphology of the rostrum. (*A*) HCF stratigraphic units. (*B*) Magnetostratigraphic correlation (Lerbekmo and Braman, 2002; Lecain et al., 2014); NS: no signal, so precise position of C29R-C30n boundary is unknown. (*C*) Stratigraphic positions of *Triceratops* specimens within a generalized section. Specimens plotted by stratigraphic position, not by facies. Relative position of specimens from different areas are approximate at the meter scale (Scannella and Fowler, 2014). See Horner et al. (2011) and Scannella and Fowler (2014) for further specimens for which more precise position (beyond HCF unit) is to be determined. Scale in meters. (*D*) MOR 2702 nasal horn from U3. (*E*) UCMP 113697 nasal horn from upper part of M3; black arrow indicates epinasal-nasal protuberance. (*F*) MOR 2982 nasal horn from lower part of M3 (image mirrored). (*G*) MOR 1120 nasal horn from L3. (*H*) MOR 004 young adult *Triceratops* skull from U3 (cast; image mirrored). Postorbital horn cores reconstructed to approximate average length of young adult specimens from this unit. (*I*) UCMP 113697 late stage subadult/young adult *Triceratops* skull from the upper part of M3. (*J*) MOR 1120 (cast) subadult *Triceratops* skull from L3. Figure modified from Scannella and Fowler (2014). f, fine sand; m, medium sand (Scale bars: 10 cm).

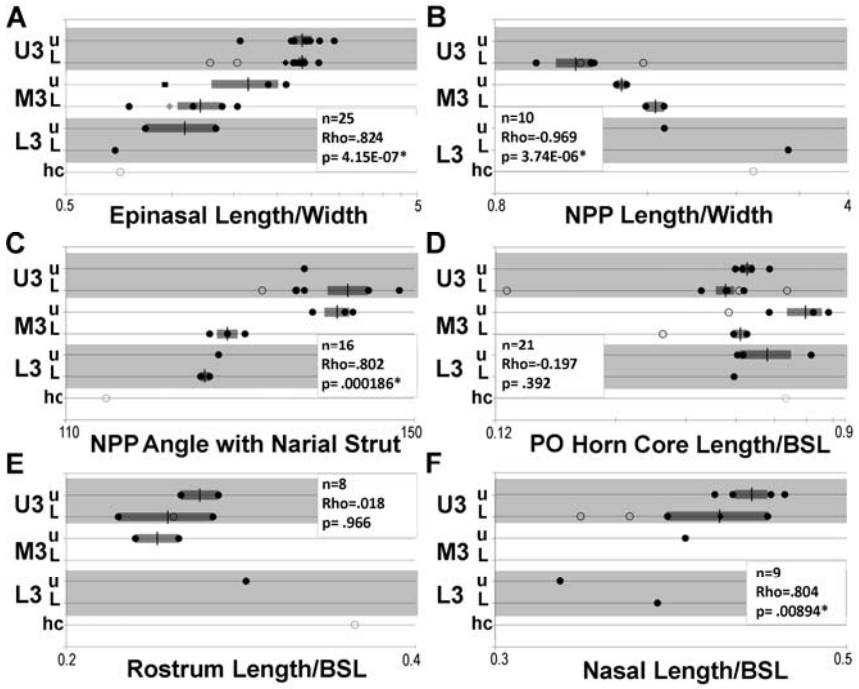


Fig. 5.2. Stratigraphic variation in cranial morphology. Each unit of the HCF is divided into upper and lower sections. For L3, the upper part is here designated as strata above the basal sandstone. For M3, the upper part is here considered the upper 15 m of the unit. The 10-m sandstone and above is here considered the upper section of U3. (*A*) Epinasal length/width. MOR 3011 denoted by a gray diamond as the fragmentary nature of this specimen obscures its ontogenetic status. Square represents UCMP 128561. Results of Spearman's rank correlation analysis in white box. (*B*) Nasal process of the premaxilla (NPP) height/width. *(C*) Angle between the NPP and the narial strut of the premaxilla. (*D*) Postorbital horn core length/basal skull length. Estimated total lengths are used here for postorbital horn core length (see Dataset S1). (*E*) Rostrum length/basal skull length. (*F*) Nasal length/basal skull length. Vertical lines denote the mean (not including juvenile or taphonomically deformed specimens; Dataset S1). Dark gray bars represent standard error. Black rings denote juveniles. Gray ring represents RTMP 2002.57.7. Spearman's rank correlation analyses exclude juveniles and taphonomically distorted specimens (indicated by diamonds). Asterisks indicate statistically significant *P* values. Scale on x-axes are logarithmic.

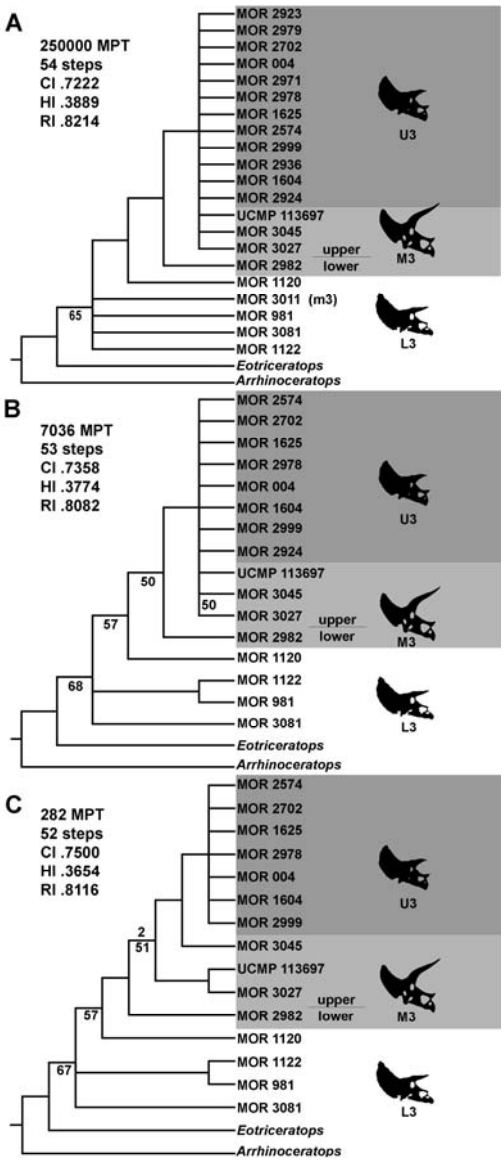


Fig. 5.3. Results of cladistic analysis of HCF *Triceratops*. (*A*) Strict consensus tree produced by analysis of HCF specimens using a heuristic search and multistate coding once the most fragmentary specimens were removed (See SI Text and Fig. S5 for additional results). Bootstrap support values below nodes. Bremer support values greater than 1 above nodes. *Torosaurus* specimens are recovered as basal to a stratigraphic succession of specimens. MOR 3011 does not preserve characters of the parietal-squamosal frill. (SI Text). *(B)* Analysis (multistate coding, branch-and-bound search) excluding specimens that could not be coded for at least 10 cranial characters or characters of the frill. *(C*) Analysis (multistate coding, branch-and-bound search) after removal of MOR 2924 (SI Text).

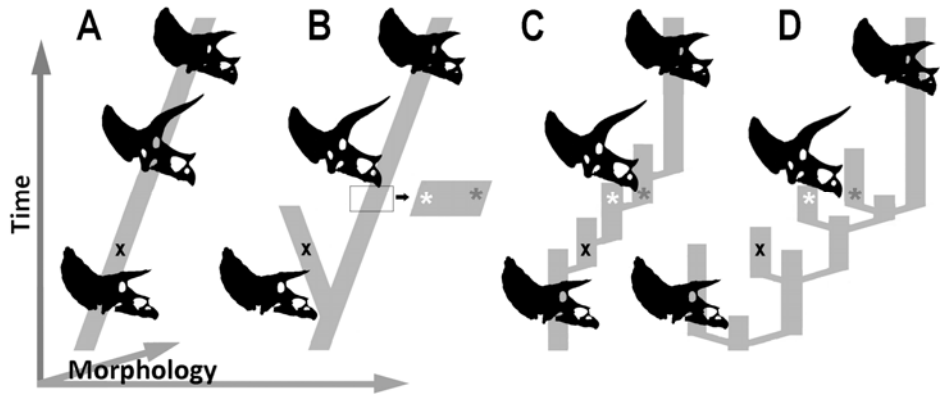


Fig. 5.4. Potential patterns of HCF *Triceratops* evolution. *(A)* Anagenesis, or transformation of a lineage over time. ***(B)*** Bifurcation of an anagenetic lineage in which the ancestor becomes pseudoextinct through evolution (sensu Wagner and Erwin, 1995). Wagner and Erwin (1995) distinguish bifurcation from "true" cladogenesis, which includes no anagenetic component. ***(C,D)*** True cladogenesis implies the coexistence of ancestral and descendant clades for at least a short period of time. The presented modes represent points on a spectrum of potential evolutionary patterns. The gray and white asterisks represent potential positions for MOR 3045 and MOR 3027, respectively; black X represents MOR 2982. X and Y axes represent morphospace.

References

Benton M.J., and P.N. Pearson. 2001. Speciation in the fossil record. Trends in Ecology and Evolution 16(7): 405-411.

Cobabe E.A., and D.E. Fastovsky. 1987. *Ugrosaurus olsoni*, a new ceratopsian (Reptilia: Ornithischia) from the Hell Creek Formation of eastern Montana. Journal of Paleontology 61(1): 148–154.

Campione N.E., and D.C. Evans. 2011. Cranial growth and variation in edmontosaurs (Dinosauria: Hadrosauridae): Implications for Latest Cretaceous megaherbivore diversity in North America. *PLoS ONE* 6(9): e25186. doi:10.1371/journal.pone.0025186

Campione, N.E., K.S. Brink, E.A. Freedman, T. McGarrity, and D.C. Evans. 2013. '*Glishades ericksoni*', an indeterminate juvenile hadrosaurid from the Two Medicine Formation of Montana: implications for hadrosauroid diversity in the latest Cretaceous (Campanian-Maastrichtian) of western North America. Paleobiodiversity and Paleoenvironments 93: 65-75.

Carpenter K., and D.B. Young. 2002. Late Cretaceous dinosaurs from the Denver Basin, Colorado. Rocky Mountain Geology 37(2): 237-254.

Dodson P. 1996. *The Horned Dinosaurs.* Princeton, Princeton University Press.

Eldredge N., and S.J. Gould. 1972. Punctuated equilibria: an alternative to phyletic gradualism. pp. 82-115 in Models in Paleobiology, T.J.M. Schopf (ed.) Freeman, Cooper & Co., San Francisco.

Evans D., P. Currie, D. Eberth, and M. Ryan. 2006. High-resolution lambeosaurine dinosaur biostratigraphy, Dinosaur Park Formation, Alberta: sexual dimorphism reconsidered. Journal of Vertebrate Paleontology 26: 59A.

Farke A.A. 1997. The distribution and taxonomy of Triceratops. pp. 47-49 in Dinofest International Proceedings Volume, D.L. Wolberg, E. Stump, G.D. Rosenberg (eds.) Philadephia Academy of Natural Sciences, Philadelphia.

Farke A.A. 2010. Evolution, homology, and function of the supracranial sinuses in ceratopsian dinosaurs. Journal of Vertebrate Paleontology 30(5): 1486-1500.

Farke A.A. 2011. Anatomy and taxonomic status of the chasmosaurine ceratopsid *Nedoceratops hatcheri* from the Upper Cretaceous Lance Formation of Wyoming, U.S.A. PLoS One 6(1): e16196.doi:10.1371/journal.pone.0016196.

FigTree v 1.4.0. http://tree.bio.ed.ac.uk/software/figtree/

Forster C.A. 1993. Taxonomic validity of the ceratopsid dinosaur *Ugrosaurus olsoni* (Cobabe and Fastovsky). Journal of Paleontology 67(2): 316–318.

Forster C.A. 1996. Species resolution in *Triceratops*: cladistic and morphometric approaches. Journal of Vertebrate Paleontology 16(2): 259-270.

Gingerich P.D. 1985. Species in the fossil record: concepts, trends, and transitions. Paleobiology 11(1): 27-41.

Happ J.W., and C.M. Morrow. 1996. Separation of *Triceratops* (Dinosauria:Ceratopsidae) into two allopatric species by cranial morphology. Journal of Vertebrate Paleontology 16: 40A.

Hartman J.H., R.D. Butler, M.W. Weiler, and K.K. Schumaker. 2014. Context, naming, and formal designation of the Cretaceous Hell Creek Formation lectostratotype, Garfield County, Montana. pp. 89-122 in Through the End of the Cretaceous in the Type Locality of the Hell Creek Formation in Montana and Adjacent Areas. G.P. Wilson, W.A. Clemens, J.R. Horner, and J.H. Hartman (eds.) Geological Society of America Special Paper, Boulder, Colorado.

Hicks J.F., K.R. Johnson, J.D. Obradovich, L. Tauxe, and D. Clark. 2002. Magnetostratigraphy and geochronology of the Hell Creek and basal Fort Union Formations of southwestern North Dakota and a recalibration of the age of the Cretaceous-Tertiary boundary, pp. 35-55 in The Hell Creek Formation and the Cretaceous -Tertiary boundary in the northern Great Plains: an integrated continental record of the end of the Cretaceous, J.H. Hartman, K.R. Johnson, and D.J. Nichols (eds.) Geological Society of America Special Paper 361, Boulder, Colorado.

Horner J.R. and, M.B. Goodwin. 2006. Major cranial changes during *Triceratops* ontogeny. Proceedings of the Royal Society B 273: 2757-2761.

Horner J.R. and, M.B. Goodwin. 2008. Ontogeny of cranial epi-ossifications in *Triceratops*. Journal of Vertebrate Paleontology 28(1): 134–144.

Horner J.R., Varricchio D.J., and M.B. Goodwin. 1992. Marine transgressions and the evolution of Cretaceous dinosaurs. Nature. 358: 59-61.

Horner J.R, M.B. Goodwin, and N. Myhrvold. 2011. Dinosaur census reveals abundant *Tyrannosaurus* and rare ontogenetic stages in the Upper Hell Creek Formation (Maastrichtian), Montana, USA. *PLoS One* 6: e16574 (doi:10.1371/journal.pone.0016574).

Keenan, S.W., and J.B. Scannella. 2014. Paleobiological implications of a *Triceratops* bonebed from the Hell Creek Formation, Garfield County, northeastern Montana, in Wilson, G.P., W.A. Clemens, J.R. Horner, and J.H. Hartman, (eds.) Through the End of the Cretaceous in the Type Locality of the Hell Creek Formation in Montana and Adjacent Areas: Geological Society of America Special Paper 503, doi:10.1130/2014.2503(14).

LeCain R., W. Clyde, G.P. Wilson, and J. Riedel. 2014. Magnetostratigraphy of the Hell Creek and lower Fort Union formations in northeastern Montana. pp. 137-148 in Through the End of the Cretaceous in the Type Locality of the Hell Creek Formation in Montana and Adjacent Areas, G.P. Wilson, W.A. Clemens, J.R. Horner, J.H. Hartman (eds.) Geological Society of America Special Paper, Boulder, Colorado.

Lerbekmo J.F., and D.R. Braman. 2002. Magnetostratigraphic and biostratigraphic correlation of late Campanian and Maastrichtian marine and continental strata from the Red Deer Valley to the Cypress Hills, Alberta, Canada. Canadian Journal of Earth Sciences 39: 539-557.

Lehman T.M. 1998. A gigantic skull and skeleton of the horned dinosaur *Pentaceratops* from New Mexico. Journal of Paleontology 72(5): 894–906.

Longrich N.R., and D.J. Field. 2012. *Torosaurus* Is Not *Triceratops*: Ontogeny in chasmosaurine ceratopsids as a case study in dinosaur taxonomy. PLoS ONE 7(2): e32623.doi:10.1371/journal.pone. 00326

Lull R.S. 1915. The mammals and horned dinosaurs of the Lance formation of Niobrara County, Wyoming. American Journal of Science 4(40): 319-348.

Lull R.S. 1933. A revision of the Ceratopsia or horned dinosaurs. Yale Peabody Museum Memoir 3: 1–175.

Macleod N. 1991. Punctuated anagenesis and the importance of stratigraphy to paleobiology. Paleobiology 17(2): 167-188.

Maddison, W.P., and D.R. Maddison. 2011. Mesquite: a modular system for evolutionary analysis. Version 2.75. http://mesquiteproject.org/

Maiorino L., A.A. Farke, T. Kotsakis, and P. Piras. 2013. Is *Torosaurus Triceratops*? Geometric morphometric evidence of Late Maastrichtian ceratopsid dinosaurs. PLoS ONE 8(11): e81608: doi:10.1371/journal.pone.0081608

Marcot, J.D., and D.L. Fox. 2008. StrataPhy: a new computer program for stratocladistic analysis. Palaeontologica Electronica 11:5A.

Malmgren B.A., W.A. Berggren, and G.P. Lohmann. 1983. Evidence for punctuated gradualism in the Late Neogene *Globorotalia tumida* lineage of planktonic foraminifera. Paleobiology 9(4): 377-389.

Marsh O.C. 1889. Notice of gigantic horned Dinosauria from the Cretaceous. American Journal of Science 3(38): 173-175.

Marsh O.C. 1890. Description of new dinosaurian reptiles. American Journal of Science 3(39): 81-86.

Ostrom J.H., and P. Wellnhofer. 1986. The Munich specimen of *Triceratops* with a revision of the genus. Zitteliana 14: 111-158.

Ostrom, J.H., and P. Wellnhofer. 1990. *Triceratops*: an example of flawed systematics. pp. 245-254 in Dinosaur Systematics: Approaches and Perspectives, K. Carpenter, and P.J. Currie (eds.) Cambridge University Press, New York.

Parks, W.A. 1925. *Arrhinoceratops brachyops*, a new genus and species of Ceratopsia from the Edmonton Formation of Alberta. University of Toronto Studies, Geological Series 19: 5-15.

R Core Team. 2013. R: A language and environment for statistical computing. R Foundation for Statistical Computing, Vienna, Austria. URL http://www.R-project.org/.

Rensch B. 1947. Neure Probleme der Abstammungslehre. Die transspezifische evolution. Ferdinand Enke, Stuttgart.

Sampson S.D. 1995. Two new horned dinosaurs from the Upper Cretaceous Two Medicine Formation of Montana; with a phylogenetic analysis of the Centrosauriane (Ornithischia: Ceratopsidae). Journal of Vertebrate Paleontology 15(4): 743-760.

Sampson S.D., and M.A. Loewen. 2010. Unraveling a radiation: a review of the diversity, stratigraphic distribution, biogeography, and evolution of horned dinosaurs (Ornithischia: Ceratopsidae). pp. 405-427 in New Perspectives on Horned Dinosaurs: The Royal Tyrell Museum Ceratopsian Symposium, M.J. Ryan, B.J. Chinnery-Allgeier, and D.A. Eberth (eds.) Indiana University Press, Bloomington and Indianapolis.

Scannella J.B., and J.R. Horner. 2010. *Torosaurus* Marsh, 1891, is *Triceratops* Marsh, 1889 (Ceratopsidae: Chasmosaurinae): synonymy through ontogeny. Journal of Vertebrate Paleontology 30(4): 1157-1168.

Scannella J.B., and D.W. Fowler. 2014. A stratigraphic survey of *Triceratops* localities in the Hell Creek Formation, northeastern Montana (2006-2010). pp. 313-332 in Through the End of the Cretaceous in the Type Locality of the Hell Creek Formation in Montana and Adjacent Areas, G.P. Wilson, W.A. Clemens, J.R. Horner, and J.H. Hartman (eds.) Geological Society of America Special Paper, Boulder, Colorado.

Simpson G.G. 1944. Tempo and mode in evolution. Columbia University Press, New York.

Simpson G.G. 1951. The species concept. Evolution 5: 285-298.

Simpson G.G. 1953. The major features of evolution. New York, Columbia University Press, New York.

Sorenson M.D., and E.A. Franzosa. 2007. TreeRot, version 3. Boston University, Boston, MA.

Swofford D. L. 2003. PAUP*. Phylogenetic Analysis Using Parsimony (*and Other Methods). Version 4. Sinauer Associates, Sunderland, Massachusetts.

Tokaryk T.T. 1986. Ceratopsian dinosaurs from the Frenchman Formation (Upper Cretaceous) of Saskatchewan. Canadian Field-Naturalist 100(2): 192-196.

Wagner P.J., and D.H. Erwin. 1995. Phylogenetic patterns as tests of speciation models. pp. 87-122 in *New Approaches to Speciation in the Fossil Record*, D.H. Erwin, and R.H. Anstey (eds.) Columbia University Press, New York.

Wu X., D.B. Brinkman, D.A. Eberth, and D.R. Braman.2007. A new ceratopsid dinosaur (Ornithischia) from the uppermost Horseshoe Canyon Formation (upper Maastrichtian), Alberta, Canada. Canadian Journal of Earth Sciences 44: 1243-1265.

CHAPTER SIX

A MORPHOMETRIC ANALYSIS OF CASQUE DEVELOPMENT AND VARIATION IN THE BLACK-CASQUED HORNBILL (*CERATOGYMNA ATRATA*)

Contribution of Authors and Co-Authors

Manuscript in Chapter 6

Author: John B. Scannella

Contributions: Conceived the study, collected data, analyzed data, interpreted results, wrote the manuscript.

Co-author: David W. Roberts

Contributions: Analyzed data, interpreted results, edited drafts of the manuscript.

Co-author: John R. Horner

Contributions: Conceived the study, contributed materials, discussed implications of results, edited drafts of the manuscript.

Manuscript Information Page

John B. Scannella, David W. Roberts, John R. Horner.
Status of Manuscript:
_x_Prepared for submission to a peer-reviewed journal
___Officially submitted to a peer-reviewed journal
___Accepted by a peer-reviewed journal
_ _Published in a peer-reviewed journal

Abstract

The Hornbills (Aves, Bucerotidae) are a diverse clade of extant avian dinosaurs which are found in Africa, Asia, and Oceania. This group is distinguished by an enlarged beak and, in many species, a pronounced cranial casque. In order to explore the development, variation, and possible functions of the casque a morphometric study was conducted on a series of skulls of the Black-casqued Hornbill (*Ceratogymna atrata*) from the Cameroon Province of Africa. *C. atrata* are sexually dimorphic with males exhibitng a larger, more elaborate casque than females. Linear measurements and 2-D geometric morphometric landmark data were collected from 33 skulls of *C. atrata*, as well as specimens of the sympatric taxa *C. elata* and *Bycanistes albotibialis*. Standard major axis regressions indicate strong positive allometry in the casque of *C. atrata*, which appears to first expand dorsally before becoming increasingly anteriorly projected. Principal component analyses segregate sexes, though placement of an immature specimen which does not exhibit mature casque morphology is ambiguous in the analysis of the linear dataset. Multivariate analysis of variation reveals that casque morphology is not only correlated with gender, but also with taxon designation. Removal of casque data from multivariate analyses causes overlap between genders and taxa in skull morphospace. Results suggest that the casque may function primarily as a display structure and likely evolved due to sexual selection. A secondary role in species recognition between closely related taxa is suggested.

Introduction

Among the most distinctive features used to identify and diagnose non-avian dinosaur taxa are the elaborate forms of cranial ornamentation expressed in many clades. Such cranial structures are found in nearly all major non-avian dinosaur clades and are particularly pronounced in the marginocephalians which sport a variety of spikes, enlarged domes, horns, and frills (see, for example, Dodson et al. 2004; Maryanska et al., 2004). The shape and configuration of these structures are often the basis for taxonomic assignments (e.g. Sampson, 1995; Farke, 2011). Several hypotheses have been proposed to explain the persistent reoccurrence of these 'bizarre structures' (sensu Gould, 1974) within the Dinosauria, including functions in defense, thermoregulation, communication, and display (Barrick et al., 1998; Farke, 2014; Padian and Horner, 2011). Recently, debate has focused on the degree to which these structures may have functioned in species recognition or as objects of sexual selection (e.g. Padian and Horner, 2011a; 2011b; 2013; Knell and Sampson, 2011; Knell et al., 2013).

Extant mammals, particularly bovids, are often used as analogues for non-avian dinosaurs which possessed 'bizarre' cranial structures (e.g. Ostrom and Wellnhofer, 1986; 1990). However, members of the dinosaurian extant phylogenetic bracket (EPB; Witmer, 1995) which includes crocodylians and avian dinosaurs (birds) may be more appropriate analogues. Dodson (1975a) briefly discussed casque development in the cassowary (*Casuarius)* for the purpose of comparison with the similarly adorned lambeosaurine hadrosaurs. That study, along with related allometric studies of *Alligator* (Dodson, 1975b) and *Sceloporus* (Dodson, 1975c), quantified skeletal variation in extant groups in

order to illuminate potential sources of variation in non-avian dinosaurs. Dodson emphasized the potential for dramatic cranial transformations throughout ontogeny (a source of potential systematic complications noted by Rozhdestvensky [1965]). Radical cranial transformations are found in multiple non-avian dinosaur taxa exhibiting cranial ornamentation including pachycephalosaurs (Horner and Goodwin, 2009) and ceratopsians (e.g. Sampson, 1995; Horner and Goodwin, 2006; Currie et al., 2008; Scannella and Horner, 2010; Schott et al., 2011).

The cassowary aside, extant dinosaur relatives rarely exhibit osseous cranial ornamentation elaborated to the extent observed in non-avian dinosaurs. A notable exception to this are the hornbills (Family: Bucerotidae; Rafinesque, 1815; Wallace, 1863), a speciose group distributed from western sub-Saharan Africa to the Solomon Islands of Oceania (Kemp, 1995). Many species of hornbill exhibit pronounced cranial casques which are often sexually dimorphic , being larger and more elaborate in males than females. Though sexual dimorphism has been suggested to be present in several non-avian dinosaur taxa (e.g. Dodson, 1975; 1976), proposed differences between sexes are currently restricted to proportional variations as opposed to discrete features which are present in only one sex (Padian and Horner, 2011a; 2011b).

The casque found in hornbills is an exemplar of the ambiguity surrounding 'bizarre' structures, for even in this group of extant animals the possible functions of the casque remains a subject of study. Hypothesized functions include roles in reinforcement of the beak, sound conductance, and display (Alexander et al., 1994; Kemp, 1995; Gamble, 2007, Kinaird and O'Brien, 2007). There are also reports of hornbills engaging in head-butting behavior (Raman, 1998; Cranbrook and Kemp, 1998), suggesting that the

casque functions as a weapon for intraspecific combat. Following the work of Dodson (1975a,b,c) we provide here a morphometric study of casque variation and development in a population of *Ceratogymna atrata* (the Black-casqued Hornbill [Kemp, 1985]) and other sympatric hornbill taxa in order to examine variation in the cranial casque and assess a potential role as an object of display between indiviudals.

Ceratogymna atrata: the Black-casqued Hornbill

Ceratogymna atrata is a large (adult length ~ 60-70 cm) species of hornbill found in western sub-Saharan Africa (Kemp, 1995). The taxon is dimorphic with the sexes exhibiting different cranial colorations (males have black heads with blue coloration around the eyes whereas females have red-brown heads with pale forenecks) and the males sporting more elaborate cranial casques. Females exhibit smaller, less elaborate casques. Both males and females exhibit similar coloration and reduced casque morphology as juveniles with males expressing the adult plumage at the end of the first year (Kemp, 1995). A lifespan of at least 19.5 years has been recorded for a specimen in captivity (Kemp, 1995).

C. atrata inhabits forests and feeds primarily on fruits, berries, and occasional insects (Kemp, 1995). This species is hypothesized to be monogamous (Fry et al., 1988; Kemp, 1995; Stauffer and Smith, 2004), and it is suggested that *C. atrata* may congregate in cooperatively breeding groups in which individuals other than the breeding pair will also help with feeding the young (Kemp, 1995). *C. atrata* nests in trees with the female being sealed inside natural holes. A narrow slit is left as an opening, through which males bring food to the female (Kemp, 1995). Recent studies suggest that during years when

fruit is scarce female *C. atrata* will not seal themselves inside nests and, further, that breeding pairs may forego nesting altogether (Stauffer and Smith, 2004).

The biogeographic range of *C. atrata* overlaps with that of other hornbill species, including the Yellow-Casqued Hornbill (*C. elata*) and the White-Thighed Hornbill (*Bycanistes albotibialis*; Kemp, 1995). These taxa also sport dimorphic cranial ornamentation (Fig. 1B,C). Kemp (1995) reports that *C. atrata* and *C. elata* (as well as the Brown cheeked hornbill [*B. (=C.) cylindricus*], of which *B. albotibialis* was once considered a subspecies) are often found feeding in the same trees.

Materials and Methods

Paleontologists studying extinct taxa are often restricted to analyses of osteology and in much the same way the hornbill sample used in this study is purely osteological. The hornbill skulls examined in this study are in the Osteology Collection at the Museum of the Rockies (MOR) and were acquired through Skulls Unlimited International (Oklahoma City, OK, USA). Thirty-three skulls of *C. atrata*, as well as three skulls each of *C. elata* and *B. albotibialis*, were measured for this analysis. A total of 32 linear measurements was taken from each skull (See Appendices 1,2, and Fig. 2 for measurements taken). All measurements were taken with digital calipers. As casque development and variation is the subject of primary interest in the current study, 10 measurements were taken from the casque. Unfortunately, no age data was available for the specimens used in this analysis. Previous studies of Asian hornbill species have suggested that males may require at least four to five years to fully develop the mature casque morphology (Frith and Douglas, 1978). Further, we note that the current dataset

does not include hatchling-sized individuals and thus cannot explore variation in casques at this very early age. Observations of other taxa suggest that the casque morphology of males and females may be indistinguishable at very early developmental stages (Frith and Douglas, 1978). Though specimens were sexed, we note that MOR-OST 1622 was received labeled as a female *C. atrata* but casque morphology of this individual appears to be consistent with an immature male (Fig. 3D).

Linear measurements were log-transformed in PAST version 2.12 (Hammer et al., 2001) and subjected to standard major axis (SMA, also referred to as reduced major axis [RMA; Schott et al. 2011]) regressions using the lmodel2 package (Legendre, 2013) in the statistical program R (R Core Team, 2013). All SMA results are presented in Appendix 3. Trends were considered isometric if the 95% confidence interval of the slope included 1, positive if the slope was greater than 1, and negative if less than 1. Though sample sizes for the other hornbill taxa were very low (n=3 for each), SMA results were recorded for comparative purposes and as a basis for future studies.

A principal component analysis (PCA) of the variance of log-transformed data was implemented to explore variation within the linear dataset in R. For the PCA analysis, missing values were estimated using the Bayesian Principal Component Analysis (BPCA) method (Oba et al., 2003) in the package pcaMethods (Stacklies et al., 2007). Additionally, a cluster analysis of a Euclidean distance matrix of the linear data was conducted using the UPGMA (Unweighted Pair Group Method with Arithmetic Mean) algorithm. These analyses were first run on the entire dataset and then on a version of the dataset in which all measurements of the casques were removed, in order to explore the role the casque plays on distinguishing sexes and taxa.

As linear measurements may not capture subtle details of variation in the complex shapes of hornbill casques, landmark based geometric morphometric (GM) analyses were conducted based on photographs of the left lateral view of each skull (see also Fabre et al., 2014 for comparisons of linear and GM approaches). Photographs were taken with a J2 model Nikon camera. Thirteen landmarks and 12 semilandmarks were plotted on each skull using the software TPSUtil (Rohlf, 2012) and TPSDig2 (Rohlf, 2012; Fig. 2). PCA analyses were run in R using the package Geomorph (Adams and Otarola-Castillo, 2013). PCAs were conducted on the entire skull as well as in a second analysis in which the three landmarks and 12 semilandmarks which form the outline of the casque and adjoining anterior dorsal surface of the rostrum were removed in order to examine the effect that the shape of the casque and bill had on clustering of individuals in morphospace. Multivariate Analysis of Variance (MANOVA; Anderson, 2001)was performed on the Euclidean distance matrix of the linear and shape data using the 'adonis' function in the vegan package (Oksanen et al., 2013).

Results

Relative Growth

SMA regression analyses of linear measurements reveal positive allometry for all dimensions of the casque relative to basal skull length in *C. atrata* (Appendix 3; Fig. 4). Only two of the measured skull dimensions (orbit length and distance from the jugal-maxilla contact to the pterygoid-palatine contact) exhibit negative allometry. The dataset highlights variation in the casque morphology. The distance from the maxilla/jugal contact to the dorsalmost point of the casque (perpendicular to the jugal bar; hereafter

referred to as posterior casque height) ranges from 73.25 to 84.8 mm in the five smallest male specimens (based on basal skull length; MOR-OST-1622, MOR-OST-285, MOR-OST-1621, MOR-OST-1625, MOR-OST-1627). This range encompasses the value for the largest specimen in the data set (MOR-OST-279; basal skull length 203.5 mm; posterior casque height 81.07 mm). MOR-OST-1631 exhibits the greatest posterior casque height (90.225 mm) despite not being the largest specimen in the sample (basal skull length 187.7 mm).

The smallest males (MOR-OST-1622, BSL 163 mm; MOR-OST-285, BSL 173 mm) express the shortest total casque length (112mm and 116 mm, respectively) whereas MOR-OST-277 possesses a casque which is more than 6 mm longer than that of the largest male (MOR-OST-279; casque length 193.9 mm compared to 200 mm in MOR-OST-277). Unlike other male specimens, the immature individual MOR-OST-1622 exhibits a casque which does not project anterior to its anteriormost contact point with the rostrum. Instead the casque ascends posteriorly, from an initial height of 3.3 mm above the rostrum to a posterior casque height of 73.25 mm. This results in a structure which is strongly anteriorly sloped and markedly different from other male *C. atrata*.

Multivariate Analyses

In a plot of the first two principal components of the PCA of linear measurements (Fig. 5), two distinct clusters of *C. atrata* are apparent; one cluster is constituted by males and the other predominately by females. MOR-OST-1622 , believed to be an immature male individual, groups with the females; this specimen exhibits markedly different cranial ornamentation from other males in the dataset due to the ontogenetic expansion of

the casque (Fig. 3). Approximately 89% of the total variation is captured by the first three axes with 69.45% of the variation explained by the first PC (Appendix 4) and 14.65% explained by PC2. PC1 is strongly associated with dimensions of the cranial casque, the highest loading variables being the posterior casque height (measurement 28), casque width (measurement 27), anterior casque height (measurement 29), and overall casque length (measurement 23; see Appendix 4). All variables exhibit negative loadings aside from the width of the orbit (measurement 14). PC 2 is also strongly associated with casque dimensions, particularly casque width (measurement 27) and the distance from the tip of the beak to the anteriormost point of the casque (measurements 31 and 32). Males of *C. elata* and *B. albotibialis* are distinguished from *C. atrata* along PC2, with *B. albotibialis* falling at the periphery of the *C. atrata* grouping. The female *C. elata* and *B. albotibialis* (n=1 for each) plot relatively close together, but are distinguished from female *C. atrata* along PC2. Larger sample sizes of *C. elata* and *B. albotibialis* will be needed to explore the degree to which these taxa overlap in morphospace, if at all. Removal of measurements of the casque results in male and female *C. atrata* overlapping in morphospace (Fig. 5B) with the strongest loadings associated with the morphology of the dorsal projection of the jugal bar (measurements 21 and 22). Further, all three hornbill taxa overlap when casque measurements are removed from the analysis.

A UPGMA cluster analysis of the Euclidean distance matrix of the linear dataset distinguishes male from female *C. atrata*, but groups the immature MOR-OST-1622 with female specimens (Fig. 6a). The female specimens of *C. elata* and *B. albotibialis* group together, and the remaining male specimens of all taxa are found to be more similar to each other than to the females. Male *C. elata* are recovered just outside a cluster of male

C. atrata whereas MOR-OST-285, a small male *C. atrata* which does not exhibit a strongly anteriorly projecting casque, is suggested to be less similar to other male *C. atrata*. When casque data are removed from the linear dataset, clear distinctions between genders and species are lost.

A MANOVA of the Euclidean distance matrix of the linear dataset indicates a statistically significant correlation between cranial morphology and both the species designation (p-value =.003) and gender (p-value =.001; Table 1) of the hornbills. Approximately 45.18% of the variance in the dataset is explained by gender whereas species explains 12.92%. When measurements of the casques are removed from the dataset, the p-value for gender remains unchanged (p-value=.001) however the R^2 value is greatly reduced indicating that only 23.58% of the variance in the dataset is explained by gender once casques are removed. The R^2 value for species increases slightly when casques are removed (R^2=.1665) and there is a corresponding increase in p-value (.004). both categorical variables have a statistically significant correlation with morphology.

The GM analysis of shape data also distinguishes hornbill taxa and genders. Further, this analysis distinguishes the immature specimen MOR-OST-1622 from female specimens of *C. atrata* in a plot of the first two PCs (Fig. 5C). Approximately 90% of the total variation is captured by the first three axes with 57.91% being captured by the first PC and 24.35% captured by PC2. PC1 is associated with landmarks of the anteriormost beak and casque and position of the jugal bar, quadrate, and dorsal apex of insertion for the M. *adductor mandibulae externus profundus* (following terminology in Quayle et al., 2014) . Positive values of PC2 are associated with the position of the dorsal extent of the casque and the male *C. elata* are clearly distinguished from males of the other two taxa

along this axis (Fig. 5C), whereas in the PCA of linear measurements these specimens were grouped closer to male *C. atrata* specimens. Male *B. albotibialis* are again recovered on the periphery of the male *C. atrata* grouping. Removal of landmarks associated with the casque-beak complex (all beak landmarks aside from the anteriormost point) caused all taxa to overlap in morphospace (Fig. 5D).

UPGMA cluster analysis of the GM dataset recovers the immature MOR-OST-1622 closer to male *C. atrata* than to a cluster of females, however male *B. albotibialis* are suggested to be more similar to the male *C. atrata* group than the immature individual (Fig. 6A). As with the PCA, removal of casque landmarks dissolves resolution between taxa and species (Fig. 6B).

A MANOVA of the GM shape data reveals significant correlations between cranial morphology and gender (p-value = .001) and species (p-value =.001; Table 1). 45.59% of variance is explained by gender whereas 23.75% is explained by species. When casque morphology is removed from the GM analysis, the p-value shows a greater increase for species (p-value=.019) than gender (p-value =.003). Variance explained by gender decreases to only 9.75% and that explained by species is reduced to 11.72%.

Discussion

In male *C. atrata*, development of the casque appears to initiate with a dorsal expansion in the posterior casque region (exemplified by the immature MOR-OST-1622; Fig. 3D) followed by an increase in size of the anterior region of the casque. Smaller males exhibit a relatively antero-posteriorly short casque (e.g. MOR-OST-275, MOR-OST-285; Fig. 3B,C). The largest casques (e.g. MOR-OST-277; Fig. 3A) exhibit a

pronounced anterior extension. Frith and Frith (1978)considered attainment of the mature casque morphology in the Northern Pied Hornbill to be represented by pronounced forward extension over the mandibles and noted hornbills actively rubbing the anterior base of the casque against objects, which further accentuated the prominence of the anterior projection. Results of the SMA regressions indicate that all measured dimensions of the cranial casque exhibit positive allometry in *C. atrata*. The immature specimen MOR-OST-1622 is occasionally recovered among female specimens (e.g. Fig. 4A,B). It is unclear if only male individuals exhibiting the fully mature casque morphology participate in breeding, however the fact that some hornbill taxa require three to five years to attain the mature morphology has been used to suggest the possibility that breeding can occur before the casque is fully developed (Frith and Douglas, 1978). Due to a limited sample size for other hornbill taxa, the current analysis does not indicate whether immature individuals of sympatric taxa exhibit similar casque morphologies at equivalent growth stages.

PCA analyses of both linear and GM data indicate that casque morphology can be used to distinguish the sexes of *C. atrata* once the mature morphology is developed (Fig. 5A,C). Further, it is interesting to note that female *C. atrata* do not overlap females of *C. elata* and *B. albotibialis* in morphospace. This suggests that, based on casque morphology alone, a hornbill can identify a member of the opposite sex of its species (a potential mate) as well as both genders of other hornbill species. The males of the three hornbill taxa are also segregated to some degree in morphospace, with greater segregation apparent in the GM analysis. It appears that not only is it important for

hornbills to be able to visually identify potential mates, but also to recognize individuals which are members of other species.

Removal of casques from the analysis results in a reduction of gender segregation in PCA and cluster analysis results (Fig. 5; 6), indicating that casque shape conveys visual information about gender which is lost in its absence. MANOVA results indicate a dramatic reduction in resolution between genders when casque data are removed from the analysis. The distinction between taxa is also obscured when the casque data are removed.

Implications for Casque Function

Although there is casque variation within a population of *C. atrata*, morphology does not overlap that of sympatric taxa and mature males and females are readily distinguished. This supports hypotheses that the casque conveys visual information (e.g. Kinaird and O'Brien, 2007), particularly between mature individuals. Further work will be needed to access the degree to which the casque is used as a visual cue throughout an individual's ontogeny. The fact that some hornbill taxa have been reported to take up to five years to develop a fully mature casque morphology is suggestive of the various shapes it attains throughout ontogeny (Fig.4) being themselves informative to other hornbills. A similar scenario is proposed for the elaborate cranial transformations which some non-avian dinosaurs underwent throughout growth (see, for example: Dodson, 1975a; Sampson, 1995; Horner and Goodwin, 2006; 2009; Scannella and Horner, 2010).

Strong dimorphism in casque shape indicates that these structures evolved through sexual selection (see Darwin, 1871; Padian and Horner, 2011). Other researchers

have suggested that the casque may have originated as additional support for an elongate bill (Kemp, 1995; Kinaird and O'Brien, 2007). Long-billed avian taxa which do not exhibit enlarged casques (such as kingfishers, storks, and toucans) are suggested to have evolved alternative reinforcements for these structures, or to typically use their bills in ways that do not direct stresses in the same way as hornbills (Kinaird and O'Brien, 2007). Comparative mechanical and functional explorations will help quantify the degree to which the casque plays a role in bill reinforcement, but if an initial thickening of the bill did evolve as structural reinforcement it would be all that was required for that area of the skull to become a subject of selection. Taxa hypothesized to be evolutionarily more basal appear to exhibit smaller casques (Kinarid and O'Brien, 2007) and it has been posited that, as with the famous analogy to the spandrels of San Marco proposed by Gould and Lewontin (1979), the casque of the hornbill may have been greatly elaborated as a biproduct of its presence for a structural purpose (Kinarid and O'Brien, 2007). This scenario may be analogous to that seen in some non-avian dinosaur groups. For example, basal ceratopsians exhibit a parietal-squamosal shelf which may have initially developed as a mechanical adaptation and later evolved into the greatly elaborate frill of derived ceratopsids (Xu et al., 2006; Makovicky and Norell, 2006). We note that the skull of the female *C. elata* in our dataset is larger than any of the female *C. atrata* and yet it has a much smaller cranial casque than those individuals (Compare Fig. 1A and B). This indicates that an enlarged casque is not required for an elongate bill and suggests another role, such as visual display, contributes to the morphology of these structures.

There is some evidence to suggest that the casque plays a role in sound conductance (Alexander et al., 1994) with larger casques producing calls which travel

further throughout dense forests (Kinaird and O'Brien, 2007). We note that hornbill taxa with large casques, such as those examined in the current study, have not converged upon a single, optimal shape for sound conductance, but instead exhibit a wide variety of casque shapes. The casques may be analogous to the cranial crests of lambeosaurine dinosaurs which are hypothesized to have functioned in both nasal resonance and visual display (Evans, 2009).

Head-butting behavior is noted in the only hornbill taxon which exhibits a solid casque, the Helmeted Hornbill (e.g. Shneider, 1945; Cranbrook and Kemp, 1995). All other hornbill taxa possess a largely hollow casque support by thin, bony struts. Head-butting behavior has also been observed in the Great Hornbill (*Buceros bicornis*) which, at times, has been considered congeneric with the Helmeted Hornbill (Raman, 1998). The rarity of these observations suggests that intraspecific combat, though potentially a derived use of a pre-existing structure, was not the primary driver behind the evolution of this bizarre cranial structure.

The diversity of casque shapes exhibited by hornbill taxa suggests that the evolution of the casque may be driven primarily by selection for its utility as a display object. Recent debate has centered on the question of whether 'bizarre' structures in dinosaurs function primarily as objects of sexual selection or species recognition (Padian and Horner, 2011a, 2011b, 2013; Knell and Sampson, 2011; Knell et al., 2013). The dimorphism present in *C. atrata* suggests that the casque evolved due to sexual selection; a hypothesis which is supported by our quantitative assessment of morphology. However, a secondary role as an object of species recognition is not falsified by this study as

hornbill taxa are distinguishable based on shape of the casque though the casque of *C. atrata* appears to be a stronger indicator of gender rather than species.

Correctly identifying conspecifics might be important to prevent hybridization. Hybridization has been reported between subspecies of the Red-Billed hornbill, a genus which, interestingly, does not exhibit a pronounced casque (Delport et al., 2004). However, there is a more recent report of hybridization within the elaborately casqued Great Hornbill (*Buceros bicornis*) and Rhinoceros Hornbill (*Buceros rhinoceros*; Chamutpong et al., 2013). The authors note: "The great and the rhinoceros hornbills resemble one another in their overall body size, appearance, bill and plumage, with similar sexually dimorphic eye colours and black markings on the bill and casque, but with lesser differences in casque shape, colour and size, and in the extent of white on the wing feathers ." (pg. 356). It is possible that these taxa have only diverged relatively recently. Genetic similarity between these closely related (if in fact distinct) species combined with declining numbers of potential mates and changing habitats may allow for or lead to hybridization (Chamutpong et al., 2013). In such a scenario, the ability to hybridize might be advantageous.

The casque is one of a series of potential signals, including plumage color and vocalizations, used by hornbills to convey information to other individuals (Kinaird and O'Brien, 2007). These other signals may amplify the visual information supplied by casque morphology, or may present information on different aspects of the individual to potential mates, rivals, or others (Moller and Pomiankowski, 1993; Curio, 2004). Future studies will further illuminate the degree to which the casque of the hornbill is used to distinguish closely related species. The fact that these taxa are extant will permit for the

type of observations and experiments which are not available to paleobiologists. Comparisons to other, more distantly related avian taxa which exhibit cranial ornamentation, will be most informative.

Conclusions

The casque of *C. atrata* exhibits strong positive allometry. This dimorphic structure likely evolved under sexual selection and may also play a role in distinguishing *C. atrata* from sympatric hornbill taxa. Further studies of extant bird species which exhibit 'bizarre' cranial structures will aid in understanding the function of similar structures in extinct dinosaurs. Current evidence supports hypotheses that these structures were primarily used for communicating visual information between individuals.

Acknowledgments

Thanks to N. Campione, J. Clarke, A. Farke, J. Fearon, E. Ferrer, E. Fowler, M. Goodwin, K. Padian, K. Purens, K. Scannella, R. Schott, D. Strosnider, D. Swiderski, I. Trevethan, D. Varricchio, and M. Zelditch for comments and conversations over the course of this study, without implying their agreement with our conclusions. Funding for this study was provided by Ed and Janet Sands and the Museum of the Rockies Inc.

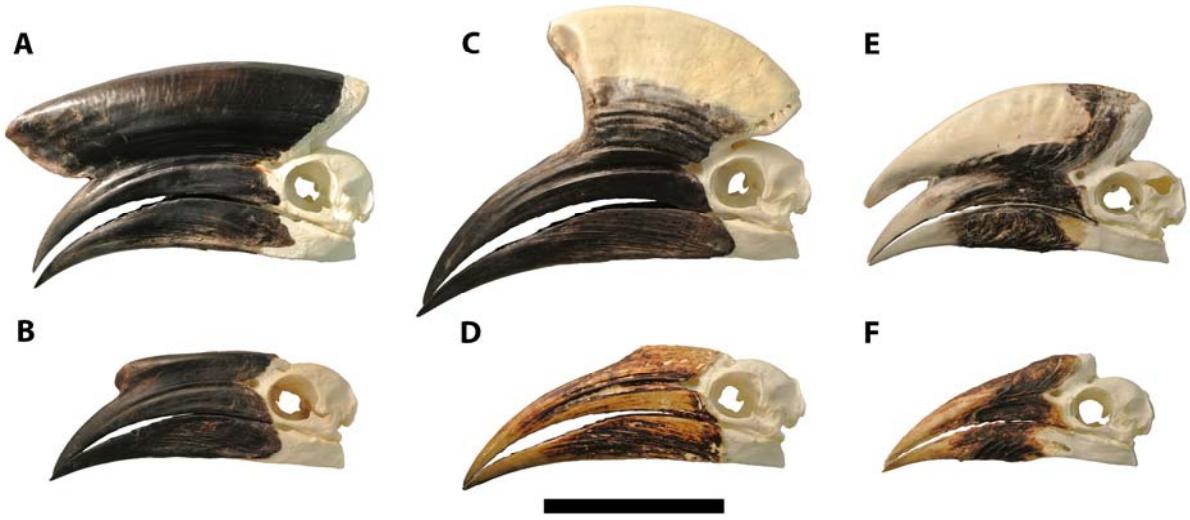


Figure 6.1. Hornbill taxa included in this study. A) *C. atrata* male (MOR-OST-277), B) *C. atrata* female (MOR-OST-259); C) *C. elata* male (MOR-OST-290), D) *C. elata* female (MOR-OST-1634); E) *B. albotibialis* male (MOR-OST-1620); F) *B. albotibialis* female (MOR-OST-1636). Scale, 10 cm.

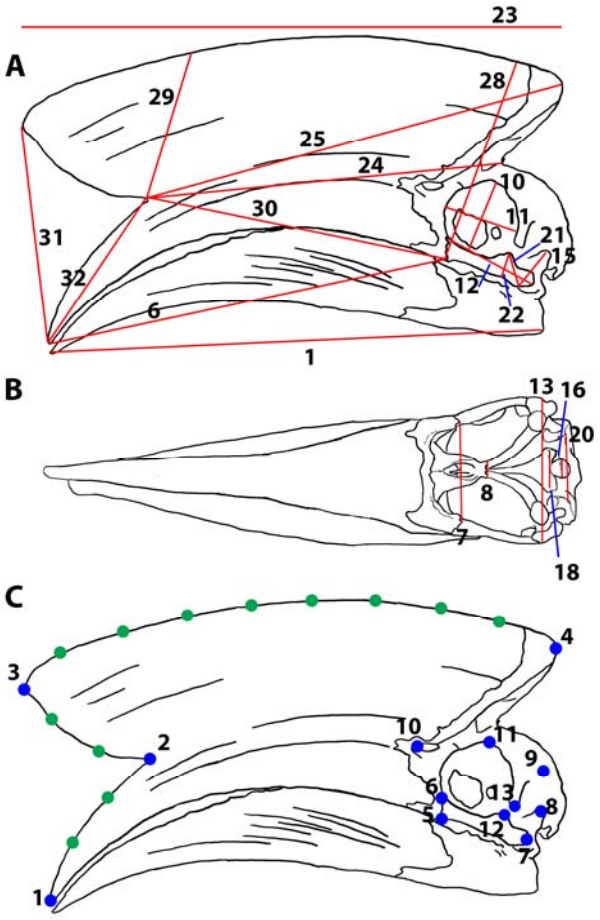


Figure 6.2. Select measurements and landmarks. A) Skull in lateral view showing select linear measurements. B) Skull in ventral view showing select linear measurements. C) Landmark (blue) and semilandmarks (green) used in GM analyses.



Figure 6.3. Hypothesized male *C. atrata* growth series. A) MOR-OST-277. B) MOR-OST-275. C) MOR-OST-285. D) Immature male (MOR-OST-1622). Scale, 10 cm.

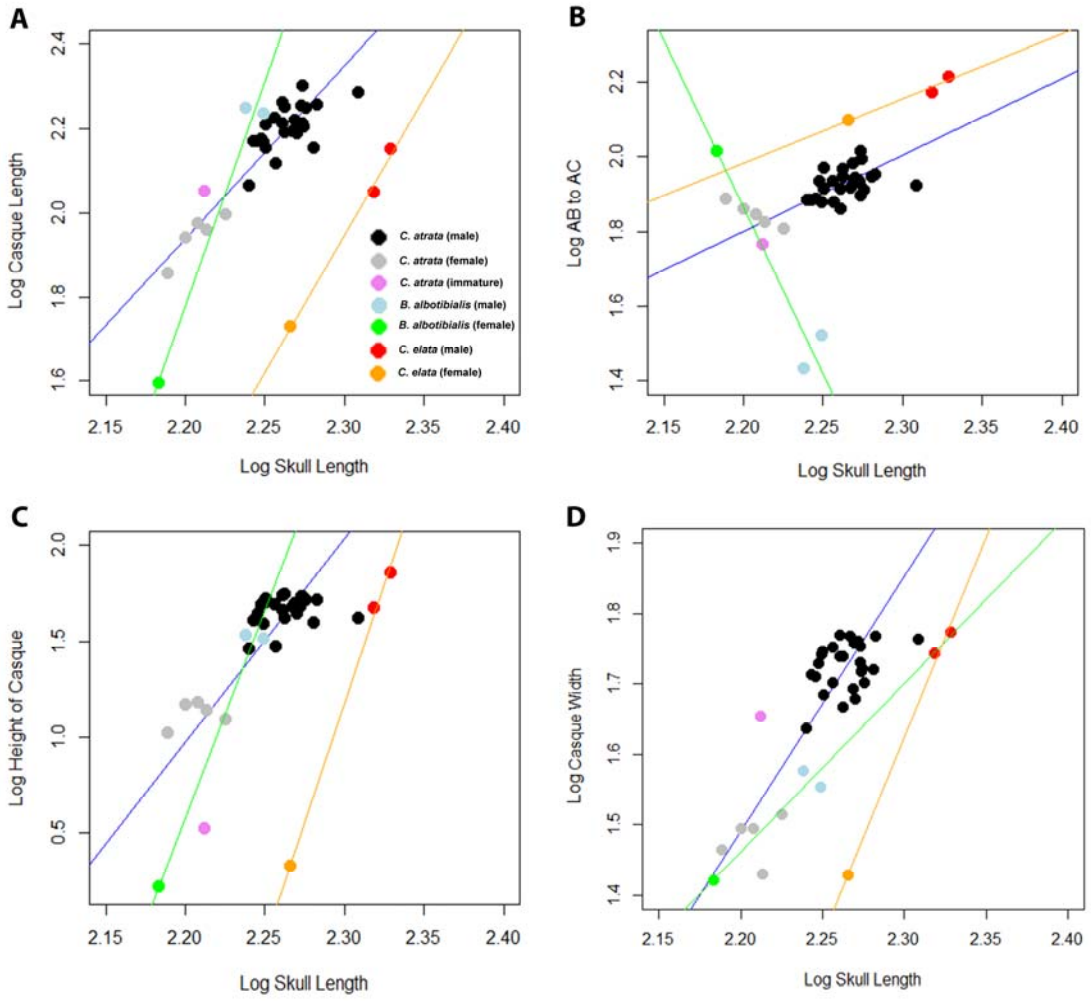


Figure 6.4. Standard major axis (SMA) regression results. Bivariate plots of select cranial measurements against basal skull length. A) Casque Length. B) Anteriormost point of bill (AB) to anteriormost point of casque (AC). C) Casque Height above anteriomost contact with bill. D) Width of casque dorsal to the lacrimal suture along anterior margin of orbit. SMA results presented in Appendix 6.3.

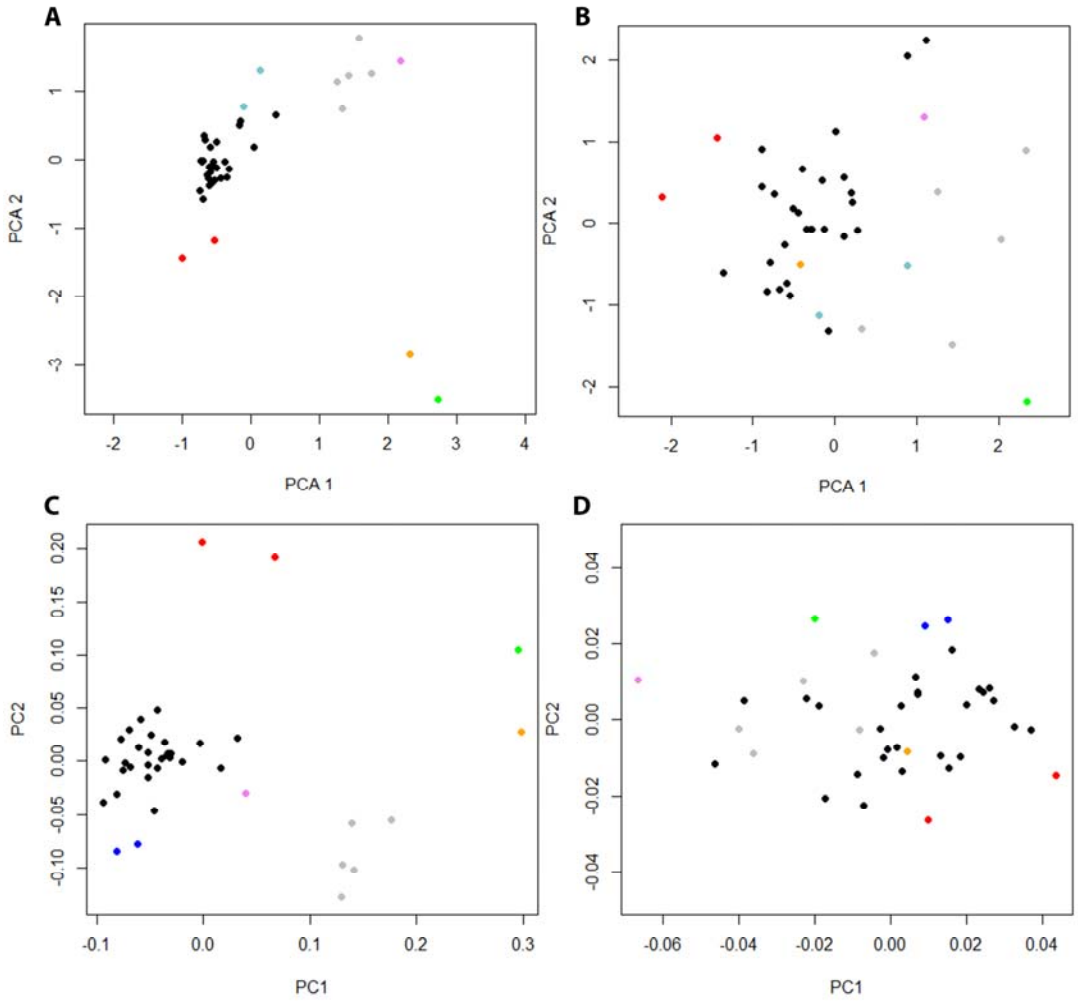


Figure 6.5. Results of linear and geometric morphometric (GM) principal component analysis. A) Results of PCA of log-transformed linear measurements. B) Results of PCA of log-transformed linear measurements after measurements of the casques has been removed. C) Results of GM PCA. D) Results of GM PCA after landmarks and semi-landmarks representing the shape of the casque and dorsal surface of the bill have been removed. Color codes are the same as for Figure 6.4.

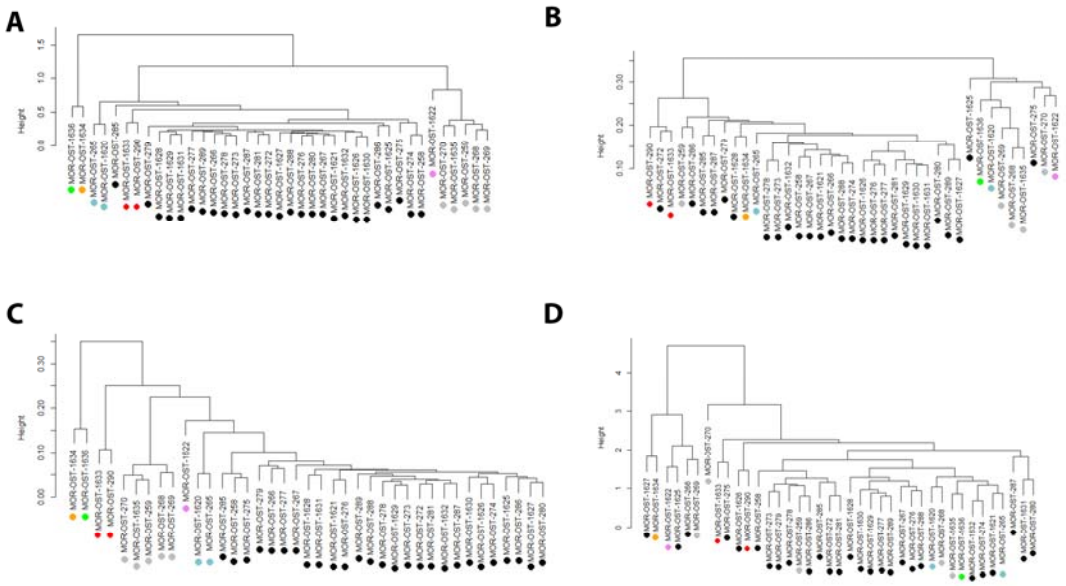


Figure 6.6. Results of UPGMA cluster analyses. A) UPGMA cluster analysis of linear measurements. B) UPGMA cluster analysis of linear measurements with casque measurements removed. C)UPGMA cluster analysis of GM data. C) UPGMA cluster analysis of GM data once landmarks for casque and dorsal surface of bill have been removed. Color codes are the same as for Figure 6.4.

Table 6.1. MANOVA Results.

	Df	Sums of Sqs	Mean Sqs	F. Model	R^2	Pr(>F)	
Linear with casque							
Species	2	1.9989	0.9994	6.961	0.12922	0.003	**
Gender	1	6.9884	6.9884	48.675	0.45179	0.001	***
Species:Gender	2	1.7431	0.8716	6.071	0.11269	0.003	**
Residuals	33	4.7379	0.1436		0.3063		
Total	38	15.4684			1		
Linear without casque							
Species	2	0.24531	0.12266	4.7568	0.16645	0.004	**
Gender	1	0.34753	0.34753	13.4777	0.2358	0.001	***
Species:Gender	2	0.03005	0.01502	0.5827	0.02039	0.77	
Residuals	33	0.85091	0.02579		0.57736		
Total	38	1.4738			1		
GM with casque							
Species	2	0.015566	0.077828	14.406	0.23747	0.001	***
Gender	1	0.29887	0.298869	55.32	0.45595	0.001	***
Species:Gender	1	0.01727	0.017274	3.1997	0.02635	0.071	.
Residuals	34	0.18369	0.005403		0.28023		
Total	38	0.65549			1		
GM without casque							
Species	2	0.005671	0.002836	2.6218	0.11718	0.019	*
Gender	1	0.004716	0.004716	4.3607	0.09745	0.003	**
Species:Gender	1	0.001238	0.001238	1.1447	0.02558	0.28	
Residuals	34	0.036771	0.001082		0.75979		
Total	38	0.048396			1		
Significance Codes:	0'***'	0.001'**'	0.01'*'	0.05'.'	0.1''	1	

Literature Cited

Adams D.C., E. Otarola-Castillo. 2013. geomorph: an R package for the collection and analysis of geometric morphometric shape data. Methods in Ecology and Evolution 4:393-399.

Alexander G.D., D.C. Houston, and M. Campbell. 1994. A possible acoustic function for the casque structure in hornbills (Aves: Bucerotidae). Journal of Zoology 233(1): 57-67.

Anderson M.J. 2001. A new method for non-parametric multivariate analysis of variance. Austral Ecology 26:32-46.

Barrick R.E., M.K. Stoskopf, J.D. Marcot, D.A. Russell, W.J. Showers. 1998. The thermoregulatory functions of the *Triceratops* frill and horns: heat flow measured with oxygen isotopes. Journal of Vertebrate Paleontology *18*(4), 746-750.

Chamutpong S, M. Ponglikitmongkol , W. Charoennitikul, S. Mudsri, P. Poonswad . 2013. Hybridisation in the wild between the Great Hornbill (*Buceros bicornis*) and the Rhinoceros Hornbill (*Buceros rhinoceros*) in Thailand and its genetic assessment. The Raffles Bulletin of Zoology 61(1): 349-358.

Cranbrook Earl of, A.C. Kemp. 1995. Aerial casque-butting by hornbills (Bucerotidae): a correction and an expansion. *Ibis* 137(4): 588-589.

Curio E. 2004. On ornamental maturation of two Philippine hornbill species with a note on physiological colour change. Journal of Ornithology. 145(3): 227-237.

Currie, P.J., W. Langston, and D.H. Tanke. 2008. A new species of *Pachyrhinosaurus* (Dinosauria, Ceratopsidae) from the Upper Cretaceous of Alberta Canada; pp. 1-108 in P.J. Currie, W. Langston, and D.H. Tanke (eds.) A New Horned Dinosaur from an Upper Cretaceous Bone Bed in Alberta. NRC Research Press, Ottawa, Ontario, Canada.

Darwin C. 1871. The Descent of Man and Selection in Relation to Sex. JohnMurray, London.

Delport W., A.C. Kemp, J.W.H. Ferguson. 2004. Structure of an African red-billed hornbill (*Tockus erythrorhynchus rufirostris* and Te *damarensis*) hybrid zone as revealed by morphology, behavior, and breeding biology The Auk 121(2): 565-586.

Dodson P. 1975a. Taxonomic implications of relative growth in lambeosaurine hadrosaurs. Systematic Biology 24(1): 37-54.

Dodson P. 1975b. Functional and ecological significance of relative growth in *Alligator*. Journal of Zoology *175*(3): 315-355.

Dodson P. 1975c. Relative growth in two sympatric species of *Sceloporus*. American Midland Naturalist 94(2): 421-450.

Dodson P. 1976. Quantitative aspects of relative growth and sexual dimorphism in *Protoceratops*. Journal of Paleontology 50(5): 929-940.

Dodson, P., C. A. Forster, and S. D. Sampson. 2004. Ceratopsidae; pp. 494–513 in D. B. Weishampel, P. Dodson, and H. Osmolska (eds.), The Dinosauria. University of California Press, Berkeley, California.

Evans D.C. 2006. Nasal cavity homologies and cranial crest function in lambeosaurine dinosaurs. Paleobiology 32(1): 109-125.

Fabre A.C., R. Cornette, K. Huyghe, D.V. Andrade, A. Herrel. 2014. Linear versus geometric morphometric approaches for the analysis of head shape dimorphism in lizards. Journal of Morphology 275: 1016-1026.

Farke A.A. 2011. Anatomy and taxonomic status of the chasmosaurine ceratopsid *Nedoceratops hatcheri* from the Upper Cretaceous Lance Formation of Wyoming, U.S.A. PLoS One 6(1): e16196.doi:10.1371/journal.pone.0016196.

Farke A.A. 2014. Evaluating combat in ornithischian dinosaurs. Journal of Zoology 292(4): 242-249.

Frith C.B., and V.E. Douglas. 1978. Notes on ten Asian hornbill species (Aves: Bucerotidae); with particular reference to growth and behaviour. Natural History Bulletin of the Siam Society 27: 35-82.

Frith C.B., and D.W. Frith. 1978. Bill growth and development in the Northern Pied Hornbill *Anthracoceros malabaricus*. Avicultural Magazine 84: 20-31.

Keith S., E.K. Urban, and C.H. Fry. 1988. The birds of Africa. Vol. 3. Academic Press, London.

Gamble K.C., and M.S. Dipl. 2007. Internal Anatomy of the Hornbill casque described by radiography, contrast radiography, and computed tomography. Journal of Avian Medicine and Surgery 21 (1): 38-49.

Gill, F.B. 2000. Ornithology. W.H. Freeman and Company. New York. 766pp.

Gould S.J. 1974. The origin and function of'bizarre'structures: antler size and skull size in the 'Irish Elk,' *Megaloceros giganteus*. Evolution 28(2): 191-220.

Gould S.J., and R.C. Lewontin. 1979. The spandrels of San Marco and the Panglossian paradigm: a critique of the adaptationist programme. Proceedings of the Royal Society of London B. 205(1161): 581-598.

Hammer Ø, D.A.T. Harper, and P.D. Ryan. 2001. PAST: Paleontological Statistics software package for education and data analysis. Palaeontologia Electronica 4(1): 9pp.

Horner J.R. and M.B. Goodwin. 2006. Major cranial changes during *Triceratops* ontogeny. Proceedings of the Royal Society of London B. 273: 2757-2761.

Horner J.R. and M.B. Goodwin. 2009. Extreme cranial ontogeny in the Upper Cretaceous dinosaur *Pachycephalosaurus.* PLoS One, 4(10), e7626.

Kemp A. 1995. The Hornbills. Oxford University Press, Oxford, New York, Tokyo: 302 pp.

Knell R.J. and S.D. Sampson. 2011. Bizarre structures in dinosaurs: species recognition or sexual selection? A response to Padian and Horner. Journal of Zoology 283(1): 18-22.

Knell R.J., D. Naish, J.L. Tomkins and D.W. Hone. 2013. Is sexual selection defined by dimorphism alone? A reply to Padian and Horner. Proceedings of the Zoological Society of London (35): 491-562.

Kinnaird M.F. and T.G. O'Brien. 2007. The ecology and conservation of Asian hornbills: farmers of the forest. University of Chicago Press, Chicago and London. 315 pp.

Legendre P. 2013. lmodel2: Model II Regression. R package version 1.7-1. http://CRAN.R-project.org/package=lmodel2

Makovicky P.J. and M.A. Norell. 2006. *Yamaceratops dorngobiensis*, a new primitive ceratopsian (Dinosauria: Ornithischia) from the Cretaceous of Mongolia. American Museum Novitates: 1-42.

Maryanska et al. 2004. Pachycephalosauria; pp. 464–477 in D. B. Weishampel, P. Dodson, and H. Osmolska (eds.), The Dinosauria. University of California Press, Berkeley, California.

Moller A.P. and A. Pomiankowski. 1993. Why have birds got multiple sexual ornaments? Behavioral Ecology and Sociobiology 32(3): 167-176.

Oba S., M.A. Sato, I. Takemasa, M. Monden, K.I. Matsubara and S. Ishii. 2003. A Bayesian missing value estimation method for gene expression profile data. Bioinformatics 19(16): 2088-2096.

Oksanen J., F. Guillaume Blanchet, R. Kindt, P. Legendre, P.R. Minchin, R.B. O'Hara, G.L. Simpson, P. Solymos, M. Henry, H. Stevens and H. Wagner. 2013. vegan: Community Ecology Package. R package version 2.0-7. http://CRAN.R-project.org/package=vegan

Ostrom J.H. and P. Wellnhofer. 1986. The Munich specimen of *Triceratops* with a revision of the genus. *Zitteliana* (14)111-158.

Ostrom J.H. and P. Wellnhofer. 1990. pp. 245-254 in *Dinosaur Systematics: Approaches and Perspectives*, Carpenter K, Currie PJ (eds.)Cambridge University Press, New York, New York.

Padian K. and J.R. Horner. 2011a. The evolution of 'bizarre structures' in dinosaurs: biomechanics, sexual selection, social selection or species recognition? Journal of Zoology 283(1): 3-17.

Padian K. and J.R. Horner. 2011b. The definition of sexual selection and its implications for dinosaurian biology. Journal of Zoology 283(1): 23-27.

Padian K. and J.R. Horner. 2013. Misconceptions of sexual selection and species recognition: a response to Knell et al. and to Mendelson and Shaw. Trends in Ecology and Evolution 28(5): 249-250.

R Core Team 2013. R: A language and environment for statistical computing. R Foundation for Statistical Computing, Vienna, Austria. URL http://www.R-project.org/.

Raman T.R.S. 1998. Aerial casque-butting in the Great Hornbill *Buceros bicornis*. Forktail (13): 123-124.

Rohlf F.J. 2012. TpsUtil. ver. 1.52. Stony Brook, NY. Published by the author.

Rohlf F.J. 2010. TpsDig2 ver 2.16. Stony Brook, NY. Published by the author.

Rozhdestvensky A.K. 1965. [Growth changes in Asian dinosaurs and some problems of their taxonomy]. Paleontologičeskij žurnal 3: 95-109.

Sampson S.D. 1995. Two new horned dinosaurs from the Upper Cretaceous Two Medicine Formation of Montana; with a phylogenetic analysis of the Centrosauriane (Ornithischia: Ceratopsidae). Journal of Vertebrate Paleontology 15: 743-760.

Scannella J.B. and J.R. Horner. 2010. *Torosaurus* Marsh,1891 is *Triceratops* Marsh, 1889 (Ceratopsidae: Chasmosaurinae): synonymy through ontogeny. Journal of Vertebrate Paleontology 30:1157-1168.

Schott R.K., D.C. Evans, M.B. Goodwin, J.R. Horner, C.M. Brown and N.R. Longrich. 2011. Cranial ontogeny in *Stegoceras validum* (Dinosauria: Pachycephalosauria): a quantitative model of pachycephalosaur dome growth and variation. PloS one, 6(6): e21092.

Schneider G. 1945. Rhinoplax vigil (Forst.) und sein Nestling. Vernhandlungen der Naturforschenden Gesellschaft in Basel 61: 1-36.

Stacklies W., H. Redestig, M. Scholz, D. Walther and J. Selbig. 2007. pcaMethods -- a Bioconductor package providing PCA methods for incomplete data. Bioinformatics 23: 1164-1167.

Stauffer D.J. and T.B. Smith TB. 2004. Breeding and nest site characteristics of the Black-casqued Hornbill *Ceratogymna atrata* and White-thighed Hornbill *Ceratogymna cylindricus* in south-central Cameroon. Ostrich-Journal of African Ornithology *75*(3): 79-88.

Wallace A.R. 1863. The Bucerotidae or Hornbills. The Intellectual Observer 3: 309-318.

Witmer L.M. 1995. The extant phylogenetic bracket and the importance of reconstructing soft tissues in fossils. Functional Morphology in Vertebrate Paleontology, 1: 19-33.

Xu X., C.A. Forster, J.M. Clark, J. Mo. 2006. A basal ceratopsian with transitional features from the Late Jurassic of northwestern China. Proceedings of the Royal Society London B. 273(1598): 2135-2140.

CHAPTER SEVEN

A MORPHOMETRIC ANALYSIS OF TRENDS IN CRANIAL MORPHOLOGY IN *TRICERATOPS* AND *"TOROSAURUS"* FROM THE HELL CREEK FORMATION, MONTANA

Contribution of Authors and Co-Authors

Manuscript in Chapter 7

Author: John B. Scannella

Contributions: Conceived the study, collected data, analyzed data, interpreted results, and wrote the manuscript.

Co-author: Kristopher J. S. Purens

Contributions: Analyzed data, interpreted results, wrote the manuscript.

Co-author: John R. Horner

Contributions: Conceived the study, discussed implications of results, edited drafts of the manuscript.

Manuscript Information Page

John B. Scannella, Kristopher J. S. Purens, John R. Horner.
Status of Manuscript:
_x_Prepared for submission to a peer-reviewed journal
___Officially submitted to a peer-reviewed journal
___Accepted by a peer-reviewed journal
___Published in a peer-reviewed journal

Abstract

Triceratops is the most commonly recovered non-avian dinosaur in the upper Cretaceous Hell Creek Formation (HCF) of Montana. Recent analyses based on the large sample of specimens (n>50) collected over the course of the multi-institutional Hell Creek Project (HCP) have provided evidence for ontogenetic and evolutionary trends in the cranial morphology of this taxon. The proposed synonymy of *Triceratops* with the coeval ceratopsid taxon "*Torosaurus latus*" remains a subject of ongoing research and debate. Here, linear and geometric morphometric approaches were taken to further quantify variation in the HCP dataset. Further statistical support is found for stratigraphic trends in the morphology of the epinasal, squamosal, and nasal process of the premaxilla. The scarcity of "*Torosaurus*" specimens in the upper half of the formation and the recovery of these specimens close to or overlapping *Triceratops horridus* (found in the lower half of the HCF) in morphospace is consistent with "*Torosaurus latus*" representing the mature form of *T. horridus*, and suggests that as *Triceratops* evolved it retained the immature (and basal) character states of the parietal-squamosal frill longer in ontogeny. Alternatively, our results are also consistent with the hypothesis that "*Torosaurus*" and *Triceratops* may have diverged early in or prior to deposition of the HCF with *T. horridus* exhibiting more similarities to the "*Torosaurus*" morphology and the *Triceratops* lineage evolving away from the basal condition over the course of the end-Cretaceous, culminating in *T. prorsus* in the upper unit of the HCF.

Introduction

One of the primary goals of paleobiology involves deciphering morphological patterns and trends in the fossil record. As the field moves away from qualitative, typological assessments of taxonomy towards a more rigorous phylogenetic approach, quantitative methods for assessing variation within and between taxa have become increasingly critical (e.g. Padian and Horner, 2002; Hunt and Rabosky, 2014). Intraspecific variation, including that resulting from ontogenetic (developmental) change, can dramatically affect evolutionary and taxonomic interpretations (e.g. (Rozhdestvensky, 1965; Dodson, 1975; Gould, 1977). While non-avian dinosaurs represent one of the most recognized and popular groups of fossil vertebrates, quantitative studies of variation in dinosaurs are often hindered by relatively small sample sizes for many taxa, especially when compared to those which are often available for invertebrates and mammals (see, for example, Gingerich, 1985; Cheetham, 1986). Increasingly, quantitative approaches are being applied to examining variation within dinosaurs as sample sizes increase (e.g. (Dodson, 1975, 1976; Chapman et al., 1981; Forster, 1996; Campione and Evans, 2011; Mallon et al., 2011; Schott et al., 2011; Maiorino et al., 2013).

The chasmosaurine ceratopsid *Triceratops* (Marsh, 1889; Hatcher et al., 1907) has had a particularly complicated taxonomic history, due at least in part to the fact that it is well represented in the upper Cretaceous formations of western North America. Brown (1917) noted that he'd encountered hundreds of fragmentary skulls of this animal over the course of his fieldwork in the upper Cretaceous Hell Creek Formation (HCF) of Montana.

At least 16 species of *Triceratops* have been named since its initial description, based largely on qualitative assessments of cranial variation between specimens (see Ostrom and Wellnhofer, 1986; 1990). In 1996, this number was reduced to two through the application of linear morphometric and cladistic methodologies (Forster, 1996). The currently recognized species, *T. horridus* and *T. prorsus*, are distinguished primarily by the morphology of the rostrum (elongate with a sinusoidal margin in *T. horridus* and more convex in *T. prorsus*) and postorbital horn cores (typically elongate in *T. horridus* and shorter in *T. prorsus* [Forster, 1996]). Marsh initially distinguished these taxa based on the shape of the nasal horn, which is short in the holotype of *T. horridus* and elongate in *T. prorsus* (Marsh, 1890).

Though *Triceratops* is represented by numerous specimens, juvenile *Triceratops* were only rarely recovered (Brown and Schlaikjer, 1940; Tokaryk, 1997), and as such, the range of ontogenetic variation in this genus was largely unknown until relatively recently (Horner and Goodwin, 2006, 2008; Horner et al., 2011; Goodwin and Horner, 2014). Further, studies of variation in *Triceratops* have been hindered by low resolution stratigraphic data associated with many of the specimens collected in the late nineteenth and early twentieth centuries (Ostrom and Wellnhofer, 1986; Farke, 1997; Scannella et al., 2014).

An extensive study of the HCF of Montana (the Hell Creek Project [HCP]) has increased our understanding of the stratigraphy of this formation and resulted in the collection of numerous new fossil specimens, including over 50 new specimens of *Triceratops* (Horner et al., 2011; Scannella and Fowler, 2014). A census of dinosaur taxa

in the formation reveals that 40% of skeletons are referable to *Triceratops*, making it the most commonly recovered dinosaur in the HCF (Horner et al., 2011).

Based largely on data collected over the course of the HCP, Horner and Goodwin (2006) found that as *Triceratops* matured the skull underwent a series of dramatic changes. The orientation of the postorbital horn cores and shape of epiossifications of the parietal-squamosal frill changed throughout growth. Scannella and Horner (2010) further hypothesized that the cranial transformation of *Triceratops* included changes in the shape of the parietal and squamosal bones of the frill at the back of the skull, and that these elements expanded late in ontogeny resulting in the morphology which had been considered diagnostic of the coeval ceratopsid "*Torosaurus latus*" (Marsh, 1891).

The proposed synonymy of *Triceratops* and "*Torosaurus*" has been the subject of ongoing study and debate (see Farke, 2011; Horner and Lamm, 2011; Scannella and Horner, 2011; Longrich and Field, 2012). Most recently, Maiorino et al. (2013) conducted a geometric morphometric study of *Triceratops* skulls and squamosals which suggested that *Triceratops* and "*Torosaurus*" occupied non-overlapping regions of morphospace, and interpreted that as evidence that they are distinct taxa. However, Maiorino et al. (2013) noted that the stratigraphic resolution in their study was limited to the formational level and could not examine variation in a more detailed stratigraphic context.

Scannella et al. (2014) examined details of the cranial morphology of *Triceratops* from the HCF in stratigraphic context and found evidence for the stratigraphic separation of *T. horridus* and *T. prorsus*, with *T. prorsus* recovered in the upper unit of the formation (U3) and *T. horridus* only found lower in the formation. Specimens recovered

from the middle of the formation exhibit a combination of *T. horridus* and *T. prorsus* features, suggesting that the evolution of *Triceratops* may have incorporated anagenetic change.

Building on this previous research, we present here a morphometric analysis of cranial variation in *Triceratops* within the stratigraphic framework of the HCF. Our aim is to further quantify variation in the dataset and test hypotheses which have been proposed regarding the growth and evolution of *Triceratops*, including the hypothesized synonymy of *Triceratops* with "*Torosaurus*".

Institutional Abbreviations

ANSP, Academy of Natural Sciences of Philadelphia, Pennsylvania, USA; AMNH, American Museum of Natural History, New York, New York, USA; BYU, Brigham Young University Earth Science Museum, Provo, Utah, USA: DMNH, Denver Museum of Nature and Science, Denver, Colorado; FMNH, Field Museum of Natural History, Chicago, USA; GMNH, Gumma Museum of Natural History, Gumma, Japan; LACM, Natural History Museum of Los Angeles County, Los Angeles, USA; MNHM, Muséum National d'Histoire Naturelle, Paris, France; MOR, Museum of the Rockies, Bozeman, USA; MPM, Milwaukee Public Museum, Milwaukee, USA; OMNH, Oklahoma Museum of Natural History, Norman, Oklahoma, USA; RTMP, Royal Tyrrell Museum, Drumheller, Alberta, SMM, Science Museum of Minnesota, St. Paul, USA; UCB, University of Colorado Museum of Natural History, Boulder, Colorado; UCMP, University of California Museum of Paleontology, Berkeley, California, USA; USNM,

National Museum of Natural History, Washington D.C., USA; YPM, Yale Peabody Museum, New Haven, Connecticut, USA.

Methods

Cranial variation in the HCF *Triceratops* dataset was explored through both linear and geometric morphometrics (GM). Linear measurements of the skull were subjected to standard major axis (SMA, also referred to as reduced major axis [RMA; Schott et al. 2011] regressions using the lmodel2 package (Legendre, 2013) in the statistical program R (R Core Team, 2013; Figure 7.1; 7.2; Appendix 7.1). Regressions were primarily performed on the proposed diagnostic features of *Triceratops* (nasal horn, postorbital horn cores, squamosal, parietal, rostrum) and additional elements hypothesized to exhibit evolutionary trends in morphology (e.g. nasal process of the premaxilla [NPP], nasal). Regressions were performed relative to basal skull length (BSL) using data presented in Scannella et al. 2014. As the dentary, jugal, occipital condyle, and maxilla were used to estimate BSL for some specimens (see Scannella et al. 2014), these elements were not included in SMA analyses;only specimens for which BSL were known or could be estimated were included in SMA analyses. The estimated BSL for one subadult specimen, MOR 2924, was modified from Scannella et al. 2014; addition of a measurement for maxilla length (45 cm) produced a modified basal skull length estimate of 95.7833 cm. All data were log transformed prior to analyses. Trends were considered isometric if the 95% confidence interval of the slope included 1, positive if the slope was greater than 1, and negative if less than 1.

We first analyzed all specimens from the HCF together, and then performed individual regressions on the data from each stratigraphic unit based on the subdivisions proposed by Horner et al. (2011; the lower unit [L3], middle unit [M3], and upper unit [U3]; see also Hartman et al., 2014). The sample size for L3 is very low, but regressions for this unit were performed for comparative purposes and as a basis for future studies. Following Scannella et al. (2014), elements of the holotype and only know specimen of *Eotriceratops xerinsularis*, which was discovered in the upper Horseshoe Canyon Formation of Alberta and slightly precedes the HCF in time (Wu et al., 2007) were included in analyses.

A principal component analysis (PCA) of the variance of log-transformed data was implemented on the entire linear data set which is composed of 17 cranial measurements (see Figure 7.3A and Appendix 7.2). The specimens in the linear PCA analysis (n=25) represent those with the least missing data for the measured dimensions. MOR 2982, MOR 3010, and MOR 3064 from M3 were included in the analysis despite a relatively large amount of missing data per specimen in order to increase representation of individuals from this stratigraphic zone. Linear measurements presented in Scannella et al. 2014 were used for the PCA analysis, with the addition of measurements of the length and width of the parietal, height and width of the orbit, transverse width at the orbit, and width of the squamosal (Appendix 7.3). Due to missing data for the majority of specimens, length of the maxilla was not included in this analysis. Estimates of postorbital horn core length presented in Scannella et al. 2014, however, were included as the postorbital horn cores are one of the primary elements of interest in this analysis and the majority of horn cores have broken tips (see Appendix 7.2). Linear dimensions which

were not preserved were estimated using the Bayesian Principal Component Analysis (BPCA) method (Oba et al., 2003) in the package pcaMethods (Stacklies et al., 2007). Measurements were either taken from the better preserved side of the skull or were taken from both sides of the skull and averaged. A PCA was then conducted with measurements of the horns and frill (parietal and squamosal) removed, to examine the effect of these elements on distinguishing groupings of specimens (following Dodson, 1993 and Maiorino et al. 2013; Figure 7.3B). Additionally, cluster analyses of the Euclidean distance matrix of the linear data were conducted using the UPGMA (Unweighted Pair Group Method with Arithmetic Mean) algorithm. These analyses were first run on the entire dataset (Figure 7.3C) and then on a version of the dataset in which measurements pertaining to the horns and frill were removed (Figure 7.3D; Appendix 7.4). Due to missing data, specimens with the fewest preserved elements were pruned from the cluster analyses (Figure 7.2).

In order to capture subtleties of shape which may not be apparent in linear measurements, landmark based geometric morphometric (GM) analyses were conducted. 19 landmarks and 16 semilandmarks were digitized on photographs of articulated skulls in lateral view (Figure 7.1). Landmarks were chosen in order to capture shape variation in morphological features which have been found to undergo changes throughout ontogeny (e.g. postorbital horn cores, squamosal) and throughout the stratigraphic succession of the HCF (epinasal, nasal, nasal process of the premaxilla [NPP]), and also based on consistency of occurrence in specimens. Landmarks differ slightly from those used by Maiorino et al. (2013), the major difference being the addition of further landmarks for the postorbital horn cores, nasal, and NPP, as well as removal of landmarks missing in

most specimens or obscured by fusion (see Appendix 7.2). Only articulated skulls or reconstructions with minimal taphonomic distortion or missing landmarks were included. UCMP 154452 and MOR 2569, for example, were excluded from the skull analysis as the major features of the premaxilla, epinasal, and nasals are all reconstructed for these specimens. Similarly, the large specimen MOR 004 was excluded as apparent fusion and preservation of the dentary in close contact with the maxilla obscures the shape of the oral margin. MOR 1199 and MOR 3027 were included in this analysis, though we note that the epinasal is reconstructed for each of these specimens. The reconstructed size of the epinasal of MOR 3027 (which preserves the base of the epinasal) is based on other specimens from the same stratigraphic zone (the upper half of M3). Similarly, MOR 1122 was included in the analysis, though we note that the postorbital horn cores in this specimen are partially reconstructed. The initial dataset was expanded by including specimens not collected or relocated during the HCP. This allows for comparison with specimens which have been highlighted in previous studies of ontogeny in Maastrichtian chasmosaurines. We note that in nearly all cases the stratigraphic position of these specimens relative to HCP specimens remains to be determined. Analysis of the entire skull was conducted with and without horns and frill, as was done for the linear data set (Figure 7.4; Appendix 7.5; 7.6).

To further examine details of variation in *Triceratops* and in order to include specimens which had to be excluded from the skull analysis due to missing landmarks, GM analyses were conducted on individual cranial bones. The epinasal, postorbital horns, squamosal, parietal, nasal, and NPP (Figures 7.6-7.13) were selected for these analyses as these elements are well represented in the HCP dataset and have been hypothesized to

undergo ontogenetic and evolutionary change within *Triceratops*. In the instance of paired elements (e.g. squamosals), the better preserved side was used for the GM analysis. For specimens in which both sides were well preserved, the left side was arbitrarily selected for the individual bone analyses.

The majority of photographs were taken (by JBS) using a Nikon 1 J2 camera, though some images (primarily those of non MOR specimens) were taken using different cameras or were from the literature (Appendix 7.7). The number and position of landmarks is recorded in Figure 7.1 and Appendix 7.3. Landmarks and semilandmarks were plotted on each photograph using the software TPSUtil (Rohlf, 2012) and TPSDig2 (Rohlf, 2012; Fig. 7.3). PCA analyses were run in R using the package Geomorph (Adams and Otárola-Castillo, 2013). Landmarks were placed at the furthest extent of the element which was preserved; thus, some elements, primarily postorbital horn cores which are often missing the very tip, were likely slightly longer in life. However, we were interested in capturing the major shape changes (such as horn curvature) through growth, and thus did not exclude these elements from the analyses. In the analysis of epinasal shape, the position of one landmark on MOR 2923 was estimated due to the anteriormost base of the horn being missing. The very tip of the epinasal of MOR 1120 is missing but was likely within 1 cm of the preserved extent of this bone. Removal of these specimens from the dataset did not substantially alter the results. In instances where the margin of the squamosal was damaged, the curvature of the margin was followed to allow for placement of semilandmarks.

Analysis of Variance (ANOVA) and Multivariate Analysis of Variance (MANOVA; Anderson, 2001) were performed on the Euclidean distance matrices of the

linear data and the GM shape data using the 'adonis' function in the vegan package (Oksanen et al., 2013; Appendices 8-10). Each data set was analyzed relative to numeric representations of ontogenetic stage and stratigraphic position in order to test for directional morphologic trends. Ontogenetic stages were determined based on criteria outlined in Horner and Goodwin (2006) and Scannella and Horner (2010) and include: 'baby' (=1) [represented by one specimen, UCMP 154452 (Goodwin et al. 2006)], 'juvenile' [=2], 'subadult'[=3], 'young adult' [=4], and 'toromorph'[=5]). Analyses of the GM dataset were also conducted with "*Torosaurus"* specimens removed. Following Horner et al.(2011), stratigraphic levels were L3 (=1), M3 (=2), and U3 (=3). In analyses where *Eotriceratops* was included, the Horseshoe Canyon Formation was considered numerically equal to "0". Permutation MANOVA of the shape data was conducted to test the relationship of shape to 1. centroid size and 2. stratigraphic position. Additional analyses of the entire skull tested the relationship of shape to ontogenetic tage and stratigraphic position. As permutation MANOVA is conducted on the distance matrix it avoids potential issues with arbitrary dimension reduction which occur in PCA. Further, least squares regressions were performed on shape data relative to size in order to explore potential allometry in the GM datasets (Appendix 7.11).

A Fisher's exact test (Fisher, 1922) was performed to explore the possibility that the lack of immature specimens exhibiting the "*Torosaurus"* morphology in the fossil record may be due to chance. This analysis is more inclusive as it allows inclusion of damaged and mildly deformed specimens. Data from the recent study of *Triceratops* and "*Torosaurus"* by Longrich and Field (2012) were also included in this analysis, treating their Phase I & II growth stages as our juvenile or subadult and their Phase III as our

adult, excepting in cases where we had personally examined those specimens and ranked them by the criteria outlined in Scannella and Horner (2010). The analysis was then conducted using the ontogenetic rankings of Longrich and Field (2012) for all specimens which were included in that study. The apparent scarcity of "*Torosaurus"* specimens in the upper half of the formation (noted by Scannella et al., 2014) was also tested using a Fisher's exact test (Appendix 7.12; 7.13). Specimen factors and landmark data for GM analyses are listed in Appendices 7.14 through 7.28.

Results

Relative Growth

SMA regression analyses of linear measurements reveal positive allometry for all dimensions of the skull with the exception of the height and width of the orbit, which exhibit negative allometry (Figure 7.2; Appendix 7.1). When the data are examined at the level of each stratigraphic unit within the HCF, all analyses conducted on specimens from the lower unit (L3) suggest isometric growth; however this result is likely tied to the extremely small sample sizes for this unit (n=3-4, see Appendix 7.1).

Squamosal width relative to basal skull length is recovered as isometric in specimens from U3, whereas squamosal length exhibits positive allometry. These dimensions are both positively allometric in specimens from M3, as well as in the dataset when examined as a whole. Definitive specimens exhibiting the "*Torosaurus"* frill morphology are currently unknown from M3 and U3 (see Discussion). *Triceratops* from these units exhibit positive allometry in the width of the parietal (M3: n=4, U3: n=6) but isometric scaling in the length of this element (M3: n=3; U3: n=6). We note that only

three specimens from M3 are represented and this result may be tied to this low sample size. Whereas the length of the rostrum exhibits positive allometry overall, when the analysis is limited to specimens from U3 (n=5) , isometric growth is indicated.

Multivariate Analyses

In a plot of the first two principal components of the PCA of linear measurements (Figure 7.3A), specimens are largely separated along PC1 according to ontogenetic stage though there is overlap between subadults and young adults. Approximately 98% of the total variation is captured by the first three axes with 82.13% of the variation explained by the first PC (Appendix 7.4) and 12.7% explained by PC2. PC1 is strongly associated with postorbital horn length, squamosal length, and parietal width. The strongest loading along PC2 is epinasal length, which has been suggested to increase throughout the HCF (Scannella et al. 2014). As such, more mature specimens from U3, which exhibit the longest epinasals in the dataset, cluster together. Specimens exhibiting the "*Torosaurus"* morphology (MOR 981, MOR 1122, MOR 3081) were all recovered from relatively low in the formation (see Scannella et al. 2014) and cluster together, close in morphospace to a subadult from L3 (MOR 1120) and a young adult from the lower part of the middle formation (MOR 3010). The young adult specimen UCMP 136092 from U3 is recovered among subadults from M3 and U3, however this specimen does not preserve an epinasal.

When measurements of the horns and frill are removed from the analysis (Figure 7.3B), specimens remain largely segregated according to ontogenetic stage along PC1, however "*Torosaurus"* specimens overlap *Triceratops* in morphospace. All loadings on PC1 are negative and within a relatively small range (-.1 to -.16), indicating that these

variables are strongly correlated. Also, juvenile specimens form two distinct groupings which are separated along PC2 which is strongly associated with rostrum and nasal length, with the smallest (and presumably youngest) individual (UCMP 154452) recovered with juveniles from M3 (MOR 2569 and MOR 3064) on the positive side of PC2 whereas juveniles from U3 (MOR 2951, MOR 1110) and a specimen for which stratigraphic position is to be determined (MOR 1199) are recovered on the negative end of PC2. We note that juveniles recovered on the positive side of PC2 do not preserve nasals or rostra and thus this result is based on the estimates produced by BPCA.

A UPGMA cluster analysis of the Euclidean distance matrix of the linear dataset recovers clusters largely consistent with ontogenetic stage (Figure 7.3C). The base of the dendrogram branches into two primary clusters, one composed of the smallest juvenile specimens and the other composed of all other specimens. The remaining juveniles (MOR 1110 and UCMP 136306) are recovered together within a cluster of non-"*Torosaurus"* specimens from the lower half of the formation, with the exception of MOR 2999 which is found in this group. This may be due to missing data for this specimen as it does not preserver either an epinasal or rostrum. The remaining specimens are divided into two clusters, one composed of all "*Torosaurus"* specimens and the other composed of young adults from U3 with subadults from the upper half of the formation (MOR 3045, MOR 2924, MOR 2574). MOR 3027 (a subadult) and UCMP 113697 (a young adult) are recovered together. These specimens along with the smaller MOR 3045 were collected in the upper part of M3 and have been found to exhibit a combination of morphologies typically seen higher and lower in the formation. The results presented by this dendrogram are consistent with those of Scannella et al. 2014 in

that these specimens are recovered as morphologically closer to specimens from U3 than those from the lower half of the formation. When data for the horns and frill are removed from the linear dataset (Figure 7.3D), a similar pattern is recovered with all juveniles clustered together and MOR 1120, from L3, falling outside of a group of specimens from higher in the formation (but being linked to an U3 specimen that is missing an epinasal and rostrum [UCMP 136092]). MOR 004, a large young adult from U3, and MOR 1122 ("*Torosaurus"* from L3) are recovered together to the exclusion of other specimens.

MANOVA of the Euclidean distance matrix of the linear dataset (Appendix 7.8) finds support for a directional trend in cranial morphology (p-value =9.999e-05) throughout ontogeny, but a significant trend throughout the stratigraphic levels of the HCF is not recovered (p-value = .106). Approximately 54% of the variance in the dataset is explained by ontogenetic stage whereas stratigraphic level explains approximately 5%. When specimens which exhibit the "*Torosaurus"* morphology are removed from the analysis, similar results are attained (Appendix 7.8). Removal of measurements of the horns and frill still recovers a directional trend throughout ontogeny (p-value =.0006) and the p-value for stratigraphy increases from .106 to .808.

Geometric Morphometric Analyses

The initial GM analysis of the skull in lateral view recovered groupings largely consistent with ontogeny (Figure 7.4). Approximately 90% of the variation was explained by the first 5 principal components with PC1 accounting for approximately 34% of variation and 20% being explained by PC2. High positive values along PC1 are associated with posteriorly curved postorbital horn cores, which are present in juvenile

Triceratops. Strongly anteriorly inclined postorbital horn cores exhibit low values along PC1. All specimens from U3 of the HCF exhibit positive values along PC1, as do specimens which have previously referred to *T. prorsus* (YPM 1822, LACM 59049; Forster, 1996). USNM 4928, the holotype of *T. 'calicornis'* (Marsh, 1898) is also recovered on the positive end of PC1. MOR 1120 and MOR 1122, each from L3, are recovered on the negative end of PC1, but are separated along PC2, which is strongly associated with the shape of the squamosal. MOR 3027, from the upper half of M3 is recovered on the negative end of PC1, but relatively close to the axis. Removal of landmarks of the horns and frill recovers USNM 4928 on the negative end of PC1, which is consistent with its referral to *T. horridus* by Forster (1996; Figure 7.4B). MOR 3027 moves to the positive side of PC1 and plots close to specimens of *T. prorsus* (YPM 1822 and LACM 59049). The "*Torosaurus"* specimen MOR 1122 clusters closely with AMNH FARB 5116 and DMNH epv. 48617, both of which have been referred *to T. horridus* by previous researchers (e.g. Forster, 1996; Maiorino et al., 2013).

UPGMA cluster analysis of the GM skull dataset recovers specimens from L3 (MOR 1120 and MOR 1122) together with AMNH FARB 5116 (Figure 7.4C). The two smallest juveniles (MOR 1199 and MOR 2951) cluster together, outside of a group containing the holotype of *T. prorsus* (YPM 1822), as well as LACM 59049, and MOR 3027 which is recovered just outside of these two *T. prorsus* specimens. MOR 1110, a juvenile *T. prorsus*, is recovered outside of the MOR 3027-*T. prorsus* group. This is consistent with the recovery of MOR 3027 close to or within *T. prorsus* in the study by Scannella et al. (2014). USNM 4928 is found at the base of this group and DMNH epv. 48617 is found outside of the MOR 1199-*T. prorsus* cluster. Removal of horns and frill

from the data (Figure 7.4D) forms a cluster of MOR 1122, AMNH FARB 5116, and DMNH epv. 48617. MOR 1120 clusters with a juvenile from U3 (MOR 2951) and the MOR 3027-*T. prorsus* group remains together, but USNM 4928 falls to the very base of the dendrogram along with the small juvenile MOR 1199.

A permutation MANOVA of the GM shape data reveals a significant correlation between skull shape and size (p-value =.0236) but not ontogenetic stage (p-value =.1113; Appendix 7.9). Removal of the "*Torosaurus"*, MOR 1122 from the dataset recovers a similar result with size being a significant factor in skull shape (p-value =.0434) but a higher p-value (.253) is recovered for the relationship between shape and ontogenetic stage. When specimens for which stratigraphic position remains to be determined are removed from the analysis, a significant relationship between shape and stratigraphic position (p-value =.04167) is recovered, though we note the sample size for this analysis is very low (n=5) and that this relationship is not found to be statistically significant when stratigraphy and size are analyzed together.

When permutation MANOVA is used to test the relationship of shape to ontogenetic stage and stratigraphic position (Appendix 7.9), a significant relationship between shape and ontogenetic stage is recovered (p-value = .04167), however this correlation is lost when the horns and frill are removed from the analysis (p-value =.2) and the p-value for the relationship between shape and stratigraphic position increases from .14167 to .7167. A least squares regression confirms a significant correlation between shape and size in the data set (p-value =.04) which is also recovered when the horns and frill are removed (p-value=.012). This relationship is lost, however, when the

analysis is limited to specimens from the HCF (see Appendix 7.11). Again, this may be tied to the resulting low sample size.

Epinasal

The first three principal components of a PCA performed on shape data for the epinasals capture approximately 95% of the total variation, with 79.44% being explained by the first PC (Figure 7.7A). Positive PC1 values are associated with elongate epinasals whereas negative values are associated with shorter epinasals. All specimens from the upper unit of the HCF exhibit positive values for PC1 whereas all specimens from the lower unit have negative values (see Figure 7.7A). Both short and elongate epinasals are found in the middle unit, consistent with the findings of Scannella et al. (2014). Juveniles are generally clustered close to 0.0 along PC1 and we note that U3 juveniles are associated with positive values for PC1 whereas MOR 1167, a juvenile from L3, exhibits a negative value for PC1. "*Torosaurus"* specimens are recovered among *Triceratops*, with the majority of specimens associated with negative values along PC1. YPM 1831 expresses a relatively more elongate epinasal, and is recovered among juvenile specimens from U3.

MANOVA finds support for directionality in epinasal shape throughout the stratigraphic succession of the HCF (p=1e-04; see Appendix 7.10), which is consistent with the findings of Scannella et al. (2014). Shape of the epinasal does not exhibit a statistically significant relationship with ontogenetic stage (p-value =.1527), though a relationship with size is recovered (p=1e-04). A regression of epinasal shape on size

further corroborates a relationship between size and shape (p-value=.004; Appendix 7.11).

Postorbital Horn Cores

The first three principal components of a PCA performed on shape data for the postorbital horn cores capture approximately 97% of the total variation (Figure 7.7B). Positive PC1 values are associated with posteriorly curved horn cores whereas negative values represent more anteriorly curved horn cores. Specimens with the lowest PC1 values are largely post-subadult stage specimens, though MOR 3027 and USNM 1201 exhibit fairly elongate, anteriorly arched postorbital horns relative to other individuals of a similar ontogenetic stage. Variation is noted in the shape of "*Torosaurus*" horn cores (MOR 981 and ANSP 15192), which overlap *Triceratops* in morphospace; the horn core of ANSP 15192 is not as anteriorly curved as that of MOR 981. The smallest known specimen of *Triceratops* (UCMP 154452) falls well outside the range of variation seen in other specimens (along PC2) due to the relatively large distance between the anterior base of postorbital horn core and the dorsalmost point of the orbit.

Horner and Goodwin (2006) noted that the shape of the postorbital horn cores changed as *Triceratops* matured. This trend is clear in the plot of mean postorbital horn shape through ontogeny (Figure 7.9). MANOVA results confirm a relationship between horn core shape and both size and ontogenetic stage (see Appendix 7.10). However, a statistically significant relationship between shape and stratigraphic position was not recovered, which is consistent with the findings of Scannella et al. (2014) who noted variability in horn core length in the lower and middle units of the HCF. Regressions of

postorbital horn core shape on size further indicate positive allometry (p-value: .004; Appendix 7.11).

Squamosal

The first three principal components of a PCA performed on shape data for the squamosal capture approximately 90% of the total variation with approximately 70% explained by PC1 (Figure 7.10). Positive values of PC1 are associated with broader squamosals which possess a more convex lateral margin whereas negative values are associated with elongate squamosals with a relatively straight lateral margin. Negative PC2 values are associated with a strongly convex anterior margin of the squamosal; positive values are associated with a relatively straight anterior margin. Longrich and Field (2012) suggested that *T. prorsus* exhibited a more convex lateral margin of the squamosal than specimens referred to *T. horridus*. In the current analysis, there is no clear separation between specimens exhibiting the *T. horridus* and *T. prorsus* morphologies along PC1. Specimens from L3 are restricted to the negative side of PC2, which is consistent with the findings of Scannella et al. (2014) that specimens found lower in the HCF tend to exhibit a more pronounced anteroventral process. Non-"*Torosaurus*" specimens which exhibit the most elongate squamosals include individuals which have been referred to *T. prorsus* (LACM 54909) and *T. horridus* (AMNH FARB 5116). Recovery of these specimens relatively close to specimens which have been referred to "*Torosaurus*" is consistent with the findings of Maiorino et al. (2013) despite slightly different landmark placement between analyses (see Appendix 7.1). These non-"*Torosaurus*" specimens with more elongate squamosals plot higher along PC2 than

"*Torosaurus"* specimens. The stratigraphic positions of these specimens remains to be determined.

Permutation MANOVA recovers a significant relationship between squamosal shape and both size (p-value = .0461) and stratigraphic position (.0301; Appendix 7.10). When "*Torosaurus"* specimens are removed from the analysis, a significant trend throughout stratigraphy is still recovered (p-value =.0473) but the relationship with size is no longer significant (p-value=.6607). ANOVA recovers a significant relationship between squamosal shape and ontogenetic stage when "*Torosaurus"* specimens are included (p-value =1e-04) as well as when they are removed from the analysis (p-value=.0278). Least squares regression recovers a significant relationship between squamosal shape and size when the entire dataset is analyzed (p-value =.044; Appendix 7.11), however this relationship is not found to be significant when the analysis is restricted to the reduced dataset of specimens specimens with detailed stratigraphic data.

Parietal

The first three principal components of a PCA performed on shape data for the parietal capture approximately 96% of the total variation with approximately 81% explained by PC1 (Figure 7.12). Positive values of PC1 are associated with a relatively narrow parietal whereas negative values are associated with a wider parietal. Negative values along PC2 are associated with a more convex posterior margin of the parietal in which the posteriormost parietal-squamosal contact is located anterior to the posterior margin at the midline of the parietal (Figure 7.12A). Juveniles exhibit a range of parietal shapes whereas all post-juvenile specimens from the upper half of the formation (MOR

004, MOR 2999, MOR 3027) exhibit a positive position along PC2 whereas post-juvenile specimens from the L3 (MOR 1120, MOR 1122) exhibit a negative position along PC2.

MANOVA does not recover a significant relationship between parietal shape and ontogenetic stage, stratigraphic position, or size (Appendix 7.10). When MOR 1122 is removed from the analysis, the p-value for the relationship between shape and ontogeny increases from .09091 to .3502. Least squares regressions recover a significant relationship between shape and size (Appendix 7.11).

Nasal

The first three principal components of a PCA performed on shape data for the nasal capture approximately 93% of the total variation with approximately 62% explained by PC1 (Figure 7.12B). Positive values of PC1 are associated with a greater distance between the anterior and posteriormost contacts of the nasal with the epinasal. Negative values of PC2 are associated with a more convex lateral margin of the nasal. Post-juvenile staged specimens from the upper half of the formation exhibit positive positions along PC2, whereas specimens from the lower half of the formation exhibit negative positions along this axis, along with specimens which have previously been referred to *T. horridus*. MOR 1122 is separated from other specimens based on the large distance between the anterior and posteriormost contacts of the nasal with epinasal. This may be due to the epinasals overgrowth of the nasals, forming a low rugose boss (see Farke, 2007). The other "*Torosaurus*" specimen included in this analysis (ANSP 15192) is recovered among specimens which have been referred to *T. horridus* (AMNH 5116, DMNH epv48617, YPM 1820) and MOR 3005, a fragmentary specimen from M3 which

exhibits relatively thin sections of frill and thus may represent the "*Torosaurus*" morphology (Scannella et al. 2014). ANOVA recovers a significant trend in nasal shape throughout ontogeny (p-value=.0013) but not throughout the strata of the HCF (p-value =.2519). A permutation MANOVA used to test the relationship between nasal shape and 1. size and 2. stratigraphic position does not recover support of a significant relationship with either of these variables. Least squares regression also does not indicate a relationship between size and shape of the nasal (Appendix 7.11).

Nasal Process of the Premaxilla (NPP)

The first three principal components of a PCA performed on shape data for the nasal capture approximately 96% of the total variation with approximately 53% explained by PC1 (Figure 7.12C). Positive values of PC1 are associated with the posteriormost point of the dorsal margin of NPP being oriented strongly posterior to the base of the articulation with the anterolateral process of the nasal. Positive values of PC2 are associated with a shorter distance between the anterior and posteriormost points of the dorsal margin of the NPP. MOR 1122-7-22-00-1, a premaxilla from the basal sandstone of the HCF, is separated from other HCF specimens. This specimen currently represents the stratigraphically lowest occurring NPP recovered during the HCP. It is closest in morphospace to RTMP 2002.57.7, the holotype of *Eotriceratops* from the slightly stratigraphically lower Horseshoe Canyon Formation of Alberta (Wu et al. 2007), which is consistent with its low stratigraphic position. Specimens are arrayed diagonally through the PCA plot (Figure 7.10) and we note that all specimens below this diagonal exhibit a relatively wide NPP whereas those above it exhibit a narrower NPP. MOR 3027, from

upper M3, is the highest stratigraphic occurrence thus far of a narrow NPP. The sample size is relatively low for this analysis as NPPs are often incomplete, however we note that even incomplete specimens which were not included in this analysis (e.g. MOR 2936,MOR 8663) exhibit morphologies consistent with the trend of more elongate, narrow NPPs recovered lower in stratigraphic succession and shorter, wide NPPs recovered higher in section. ANOVA recovers a significant relationship between NPP shape and stratigraphic position (p-value = .0037). Permutation MANOVA to test the relationship between shape and centroid size and stratigraphic position, recovers a significant relationship with size (p-value =.0203) but not stratigraphic position (Appendix 7.10). Least squares regression confirms a significant relationship between shape and size (Appendix 7.11).

Fisher's Exact Tests

Results of the Fisher's exact test to examine whether the apparent absence of immature "*Torosaurus"* was due to chance recovered a p-value of .022, suggesting that the absence of juveniles and subadults is unusual (Appendix 7.12). When the criteria for assessment of ontogenetic stages is changed to that of Longrich and Field (2012; in which YPM 1831 is a subadult "*Torosaurus"*) a p-value of .071 hints at a difference in biological reality between these groups of specimens. The Fisher's exact test performed to examine the scarcity of "*Torosaurus"* in the upper half of the formation recovers a p-value of .0128, suggesting that this pattern in the fossil record is likely not a result of chance.

Discussion

Stratigraphic Trends

The results of these analyses are largely consistent with the trends in cranial morphology through the succession of HCF strata that were noted by Scannella et al. (2014). Significant stratigraphic trends are indicated in the skull (when considered as a whole in both the linear dataset and stratigraphic dataset), epinasal, squamosal, and NPP (Appendix 7.10). Higher p-values are recovered for the relationship between nasal morphology and stratigraphic level, though we note that specimens found lower in the formation do appear to exhibit a more arched lateral margin of the nasal, as suggested by Scannella et al. (2014; Figure 7.13). than specimens found higher in section, though a clear stratigraphic trend is not detected. Postorbital horns exhibit variable lengths in the lower and middle units of the HCF and appear to be consistently short in post-juvenile stage individuals from U3.

Scannella et al. (2014) noted that specimens exhibiting the "*Torosaurus"* morphology were recovered from the lower half of the formation. MPM VP6841 appears to be from the upper half of the formation based on study of topographic maps (Scannella et al. 2014), but this has yet to be confirmed. If this stratigraphic placement is correct, it would appear to represent the latest occurrence of a specimen referred to "*Torosaurus"* in the HCF of Montana thus far. MOR 1122, MOR 2984 (a specimen too incomplete for inclusion in these morphometric analyses), and MOR 3081 are all recovered from L3, MOR 1122 being collected from the very bottom of L3 (Horner et al., 2011; Scannella and Fowler, 2014; Scannella et al., 2014). The precise stratigraphic placement of MOR

981 (Farke, 2007) is yet to be determined, but it was recovered from a mudstone above the base of the formation (Scannella et al., 2014). MOR 3005, a fragmentary specimen which preserves thin sections of frill was found in the lower part of M3. Given the extensive nature of the HCP census of the formation's paleofauna, the apparent absence (or at least extreme rarity) of specimens exhibiting the "*Torosaurus"* morphology from the upper half of the formation is striking. A Fisher's exact test of the stratigraphic occurrence of "*Torosaurus"* specimens indicates that the absence of confirmed specimens from high in the formation is likely not a result of chance (p-value =.0128). All of the specimens with confirmed stratigraphic positions exhibit morphologies consistent with stratigraphic trends noted in *Triceratops*, including a short nasal horn and narrow, posteriorly inclined NPP. The largest anteroventral projections of the squamosal are found in specimens (MOR 1120, MOR 1122) from the lower unit of the formation as well.

Even when *"Torosaurus"* specimens are removed from analyses, significant stratigraphic trends are still indicated for the epinasal and squamosal (NPP results did not change as no specimens were removed from the analysis; Appendix 7.10). Interestingly, we note that when measurements/landmarks pertaining to the horns and parietal-squamosal frill of the skull are removed from the skull analyses, R^2, the proportion of variation explained by the independent variable, drops from .077 to .015 in the linear dataset, and from .231 to .130 in the GM dataset. This coincides to a dramatic increase in p-value for the relationship with stratigraphic level (from .056 to .5 in the permutation MANOVA of the linear dataset, and from .142 to .717 for the GM dataset). This shows that the horns and frill are the primary features which change through stratigraphy, and is

consistent with the findings of Horner et al. (1992) in that features which have been suggested to primarily be ornamental change through successive strata. These features were initially suggested to be objects of sexual display, but more recent work has focused discussion on the definition of sexual dimorphism in relation to whether these cranial structures are subjects of sexual display or function primarily in species recognition (see, for example, Knell and Sampson, 2011; Padian and Horner, 2011a, 2011b; see Farke et al., 2009 and Farke, 2014 for alternative interpretations of the function of horns and frills in ceratopsids).

Similar results of the PCA and cluster analyses are recovered for the skull datasets (linear and GM) with and without horns and the parietal-squamosal frill. This is consistent with a taxonomic signal being present in the skull (as noted by Forster, 1996). MOR 3027, a specimen suggested to be intermediate between *T. horridus* and *T. prorsus* (Scannella et al., 2014), is recovered amongst *T. horridus* specimens (AMNH FARB 5116, MOR 1120) in the initial analysis of the linear dataset and then amongst *T. prorsus* when these cranial elements are removed from the analysis (Figure 7.3). It is recovered amongst *T. prorsus* in both versions of the GM cluster analysis (Figure 7.4), consistent with its being grouped with specimens from U3 in cladistic analyses of specimens (Scannella et al., 2014). Other specimens from upper M3 (MOR 3045, UCMP 113697) could not be included in the GM analysis of skulls in lateral view as they are currently either disarticulated (MOR 3045) or do not exhibit all landmarks (UCMP 113697); these specimens are recovered among *T. prorsus* in the cluster analyses of linear skull data (Figure 7.3C,D).

These specimens exhibit several features typically not seen in specimens from U3 (*T. prorsus*). MOR 3027, which is stratigraphically the lowest of the three, has a narrow NPP (the highest stratigraphic occurrence, thus far, of this feature). Both MOR 3027 and UCMP 113697 exhibit postorbital horn cores that are more elongate than any thus far recovered in U3. MOR 3045 appears to be the most *T.prorsus*-like of the three specimens, but even this individual exhibits subtle differences from U3 specimens in the nasal and premaxilla (see Scannella et al. 2014). The identification of details of cranial morphology which appear to vary stratigraphically in *Triceratops* invite a reassessment of these features in the holotype specimens of *Triceratops* before these seemingly intermediate, or transitional, specimens are assigned taxonomic identities.

Ontogenetic Trends and the Synonymy of *Triceratops* and "*Torosaurus*"

The width of the parietal, an element of particular interest in studies of *Triceratops* ontogeny (Scannella and Horner, 2010; Horner and Lamm, 2011), relative to length tends to increase throughout growth. The parietal of the smallest known *Triceratops* (UCMP 154452) exhibits a length to width (L/W) ratio of .92 whereas MOR 3027 exhibits a L/W ratio of .74 and MOR 004, a large young adult, the L/W ratio is approximately .7. In MOR 1122, a specimen with a fenestrated parietal, the length to width ratio is .63. This tendency for more mature individuals to exhibit a wider parietal is highlighted in the GM PCA plot of parietal shape (Figure 7.12A). However, no significant relationship is recovered between parietal shape and either centroid size or ontogenetic stage (Appendix 7.10). The parietal exhibits positive allometry in both length and width when the entire HCF dataset is analyzed (Appendix 7.1), but when specimens

from M3 and U3 (which do not include specimens exhibiting the "*Torosaurus"* morphology) are considered separately, isometric growth is suggested. This is consistent with either a lengthening in the parietal late in ontogeny (as hypothesized by Scannella and Horner, 2010) or different patterns of growth suggestive of distinct taxa (as suggested by Longrich and Field, 2012; Maiorino et al. 2013).

Longrich and Field (2012) found evidence for ontogenetic overlap between *Triceratops* and "*Torosaurus"* based on a cladistic study of cranial features in individual specimens. We note, however, the assessment of maturity in that study was based largely on the degree of apparent cranial fusion observed in specimens. The timing of cranial fusion appears to vary in the HCP dataset (Scannella and Horner, 2011) and the degree to which it can be used to assess maturity in non-avian dinosaurs is the subject of research currently in progress (Bailleul et al., 2013). Maiorino et al (2013) found separation between specimens referred to *Triceratops* and "*Torosaurus"* in morphospace through examination of the entire skull in lateral view (with and without the frill), and the squamosal. In both the linear and GM analyses of skull shape in lateral view in the current analysis, "*Torosaurus"* specimens are initially recovered just outside of the other specimens, but overlaps them in morphospace once horns and frill are removed from the analysis. Currently, it appears that at least in so far as overall shape of cranial elements, morphologic separation between "*Torosaurus"* and *Triceratops* is primarily tied to the morphology of the parietal and squamosal (as noted by Farke, 2007) with other elements overlapping *Triceratops* in morphospace. The nasal analysis separates MOR 1122 from other specimens, but as noted above this may be tied to the enlarged nasal boss of this specimen. The nasal of ANSP 15192 is recovered among *T. horridus* specimens (Figure

7.12B). The full NPP morphology of "*Torosaurus"* specimens is currently unknown: no unfused NPP is currently know from a specimen collected from the HCF which exhibits a fenestrated parietal. MOR 1122-7-22-00-1 was found in association with a "*Torosaurus"* specimen (MOR 1122), but cannot be directly compared to that individual because the full NPP morphology of MOR 1122 is unknown due to fusion with the nasals and epinasal. ANSP 15192 exhibits an elongate NPP which is fused to the nasals, but appears to be consistent with the morphology observed in specimens which have been referred to *T. horridus*.

Whereas most "*Torosaurus"* specimens exhibit a relatively short epinasal, the epinasal of YPM 1831 approaches that of *Triceratops* from U3 (*T. prorsus*) and overlaps juveniles from this stratigraphic zone (Figure 7.7A). Scannella et al. (2014) suggested that development of a nasal boss may be ontogenetic, occurring in the most mature individuals. The development of a nasal boss throughout ontogeny occurs in some centrosaurine ceratopsids (Sampson, 1995; Currie et al., 2008). Farke (2011) and Longrich and Field (2012) suggested that YPM 1831 represents a subadult specimen of "*Torosaurus"*, and its more elongate epinasal horn could be consistent with a younger ontogenetic status. However, we note that non-boss like nasal horns are observed in other specimens exhibiting the "*Torosaurus"* morphology, which exhibit flattened epiossifications and other indicators of maturity (e.g. MOR 3081).Therefore, this could reflect individual variation, or YPM 1831 may have been recovered relatively higher in the stratigraphic section than other specimens, which would be consistent with the trend in epinasal shape noted in *Triceratops* from the HCF. The stratigraphic position of YPM 1831 relative to the HCF remains to be determined.

MOR 981, a large specimen referred to "*Torosaurus"* (Farke, 2007), was excluded from the GM analysis of epinasals as the anterior margin of the nasal horn is obscured by a rugose ossification that extends from the base of the epinasal down the dorsal margin of the premaxilla towards the rostral, a distance of over 20 cm (Figure 7.14). As such, it is unclear where the epinasal ends, and even whether or not the entirety of this structure is composed of the epinasal or if other elements (rostral, nasal) are involved. As one of the largest specimens in the dataset (basal skull length =129.5 cm) with very mature postorbital horn core osteohistology (Scannella and Horner, 2008) this rugosity anterior to the nasal boss may be indicative of the most mature individuals (or the most mature individuals from low in the stratigraphic succession). We note that this mature individual exhibits unfused episquamosals and a clear sutural division between the posterior prong of the premaxilla and the maxilla (Figure 7.14). This further suggests that the degree of cranial fusion may not be indicative of maturity in chasmosaurine ceratopsids (Scannella and Horner, 2011).

As noted by Horner and Goodwin (2006), postorbital horn cores exhibit an ontogenetic trend of progressing from posteriorly curved in juveniles to more anteriorly inclined in more mature individuals. Though this trend is largely consistent, this analysis highlights variation in the shapes of the horn cores of post-juvenile stage individudals. Some subadult individuals (MOR 3027, USNM 1201) exhibit more anteriorly arched postorbital horn cores than more mature individuals (e.g LACM 59049). ANSP 15192, which is currently the smallest known specimen which has been referred to "*Torosaurus"*, overlaps subadult specimens in horn core morphology in that the horn cores are not strongly arched forward (Figure 7.7B). Despite its small size, this specimen

exhibits indicators of being an adult and further highlights size variation in mature specimens (see Scannella and Horner, 2010; Longrich and Field, 2012).

The squamosal has been hypothesized to elongate throughout growth, ultimately producing the narrow morphology found in "*Torosaurus*" (Scannella and Horner, 2010) or, alternatively, to be a feature which distinguishes these taxa (Longrich and Field, 2012; Maiorino et al., 2013). Further, the relative convexity of the lateral margin of the squamosal has been suggested to distinguish *T. horridus* from *T. prorsus* (Longrich and Field, 2012). We note that in the PCA of squamosal shape data (Figure 7.10), some juveniles, including the smallest known *Triceratops* (UCMP 154452), have a straighter lateral margin of the squamosal than more mature individuals whereas all "*Torosaurus*" specimens express a relatively straight lateral margin. Some larger *Triceratops* specimens approach "*Torosaurus*" specimens in terms of the shape of the squamosal. In this analysis, AMNH FARB 5116 and DMNH epv.48617 exhibit squamosals which are closest to "*Torosaurus*" specimens along PC1. LACM 59049, a *T. prorsus* specimen (Forster, 1996), approaches the "*Torosaurus*" cluster along PC1, suggesting that this species is not restricted to a more convex squamosal as hypothesized by Longrich and Field.

We note that "*Torosaurus*" specimen YPM 1831 is further from other "*Torosaurus*" specimens along PC1 than the other "*Torosaurus*" specimens are from several non-fenestrated *Triceratops* specimens. Further, we note that the only specimen of "*Nedoceratops*" (USNM 2412) exhibits a squamosal morphology that is slightly straighter lateral margin than the majority of young adult *Triceratops*, but not to the extent revealed in "*Torosaurus*" specimens and some large unfenestrated *Triceratops*

(e.g. AMNH FARB 5116, LACM 59049). As has been noted previously (e.g. Farke, 2011; Longrich and Field, 2012), the squamosals of USNM 2412 appear to be pathologic and, as such, the degree to which this may affect the morphology of the anteroventral process of the squamosal is undetermined.

This analysis finds that squamosals of "*Torosaurus"* specimens are separated along PC2 from most large specimens which approach them along PC1 (e.g. AMNH FARB 5116; DMNH epv. 48617), which is largely driven by the shape of the anterior margin of the squamosal. Sullivan et al. (2005) suggested that the restricted otic notch produced by the anterior projection of the squamosal was a diagnostic feature of "*Torosaurus"*; however a pronounced anteroventral projection is seen in other taxa, including *Arrhinoceratops* (see Mallon et al., 2014; Scannella et al., 2014). Scannella et al. (2014) reported that the anteroventral projection of the squamosal tended to be more pronounced in specimens from lower in the formation (e.g. MOR 1120) becoming reduced in specimens recovered higher in section (e.g. MOR 2702; Figure 7.11). This feature was also found to vary between the right and left side of some individuals (e.g. MOR 2999). It is interesting that the *T. horridus* specimens which approach the "*Torosaurus"* cluster along PC1 (AMNH FARB 5116, DMNH epv58617) exhibit a relatively reduced anteroventral projection of the squamosal relative to "*Torosaurus"* specimens, but not as reduced as some specimens recovered from the upper unit of the HCF (see Figure 7.15). The stratigraphic provenance of these two specimens relative to "*Torosaurus"* specimens are unknown. The pronounced anteroventral projection may be a feature which develops late in ontogeny (this feature appears to vary in size in *Arrhinoceratops* [see Mallon et al., 2014]), or it may be more pronounced (or develop

earlier in ontogeny) in specimens found lower in the stratigraphic succession. Alternatively, if "*Torosaurus"* is a distinct taxon, the combination of an elongate squamosal with a straight lateral margin and pronounced anteroventral process could be exhibited in "*Torosaurus"*, and approached but not realized in *Triceratops*.

As noted above, the relative abundance of "*Torosaurus"* specimens from low in the HCF does not appear to be a result of chance. Similarly, the results of the Fisher's exact test to examine the apparent absence of immature "*Torosaurus"* (Appendix 7.12) suggests that the hypothesis that "*Torosaurus"* represents the mature growth stage of *Triceratops* is consistent with the current data, given the absence of immature individuals. The scarcity of "*Torosaurus"* in the upper half of the formation combined with the morphometric evidence for these specimens being morphologically most similar to *T. horridus*, suggests the possibility of *Triceratops* becoming increasingly paedomorphic (or paedotypic, following Reilly et al., 1997; see Maiorino et al. 2013) over the course of the HCF's deposition. Scannella et al. (2014) noted differences in the morphology of the regions of the parietal which are hypothesized to fenestrate in *Triceratops* in specimens recovered from different stratigraphic levels of the HCF. In this scenario, an expanded and fenestrated frill is expressed late in ontogeny in *T. horridus*, but becomes increasingly rare over the course of the end-Cretaceous. The current data are consistent with this scenario. Alternatively, *Triceratops* may have diverged from "*Torosaurus"* low in or before the start of the HCF, and thus more basal specimens (*T. horridus*) are closer morphologically to "*Torosaurus"*, which is a rare taxon in the HCF. Both of these scenarios would explain why some specimens of *T. horridus* appear to be more "*Torosaurus"*-like in morphology whereas *T. prorsus* superficially appears to be

very different in morphology (see Longrich and Field, 2012 their Figure 1). The relative rarity of "*Torosaurus"* adults, and their being primarily confined to the lower strata of the HCF, could also be explained by many other possibilities, such as "*Torosaurus"* inhabiting a different environment with only occasional visits to the region captured in the HCF, and only then by adults. As noted by Scannella and Horner (2010), immature "*Torosaurus"* could be mistaken for *Triceratops* if the parietal remained unfenestrated until relatively late in ontogeny. Other circumstances could explain these results, and a broad array of hypotheses should be on the table at this point to explain the statistical peculiarities we observe.

Ostrom and Wellnhofer (1990) suggested that "*Torosaurus"* may represent the male sex of *Triceratops*. This is certainly possible, and would be consistent with dimorphism in prominent cranial structures identifying sexes (see Darwin, 1871; Padian and Horner, 2011b; but see also Knell et al., 2013). An examination of cranial variation in the sexually dimorphic hornbills of the Cameroon Province of Africa (Scannella et al., *In prep*) which, like ceratopsid dinosaurs exhibit pronounced cranial structures, found that removal of cranial ornamentation caused previously segregated sexes and taxa to overlap in morphospace. We note that removal of the horns and frill in the present analysis produced overlap between *Triceratops* and "*Torosaurus"* (Figures 7.2 and 7.3), but given the findings of Scannella et al. (*In prep*) these results, while consistent with those for a sexually dimorphic archosaur are also consistent with these structures being primarily used for species recognition between taxa (see Padian and Horner, 2011a). The possibility of dimorphism should be investigated further, and may very well be contributing to the complexity of the system examined here.

Conclusions

Further statistical support is found for proposed stratigraphic trends in *Triceratops* cranial morphology related to the epinasal, squamosal, and NPP (Scannella et al., 2014). The postorbital horns, nasal, and squamosal exhibit trends in morphology through ontogeny though variation in shape is noted in each of these elements. The scarcity of specimens exhibiting the "*Torosaurus"* morphology in the upper half of the HCF, as well as the apparent absence of juveniles are statistically significant suggesting that these findings are not a result of chance. "*Torosaurus"* specimens are closer in morphospace to specimens referred to *T. horridus,* and overlap these specimens when the horns and parietal-squamosal frill are removed from analyses. Differences in morphospace occupied by the squamosals of *Triceratops* and "*Torosaurus"* (consistent with the findings of Maiorino et al., 2013) are highlighted, though the full "*Torosaurus"* morphology is approached by some specimens of *Triceratops*. The results of these analyses are consistent with the hypotheses that: 1) "*Torosaurus"* represents the mature form of *T. horridus* and the expression of *Torosaurus* features (e.g. expanded frill, fenestrated parietal) became increasingly rare over the course of the HCF, perhaps indicating paedotypy in *Triceratops*; or 2) *Triceratops* and "*Torosaurus"* diverged early in or before the deposition of the HCF and more basal *Triceratops* (*T. horridus*) share more features with "*Torosaurus"*, but as *Triceratops* evolved it diverged further away from the "*Torosaurus"* morphology, ultimately giving rise to *T. prorsus* in the upper part of the HCF.

Acknowledgments

We are grateful to members of the Hell Creek Project field crews, especially D. Fowler, M. Goodwin, and R. Harmon, and all of the field volunteers who have participated in this study of the end-Cretaceous in Montana. Thank you to the preparators in the MOR paleo lab, especially C. Ancell, S. Brewer, R. Harmon, P. Hookey, J. Jette, K. Scannella, B. Phillips, and L. Roberts. For access to collections and specimens in their care we are thankful to N. Gilmore (ANSP), M. Norell and C. Mehling (AMNH), B. Britts and R. Scheetz (BYU), P. Makovicky and W. Simpson (FMNH), J. Sertich (DMNH), L. Chiappe and A. Farrell (LACM), P. Sheehan (MPM), B. Strilisky and G. Housego (RTMP), B. Erickson (SMM), T. Culver and L. Wilson (UCB), M. Carrano and M. Brett-Surman (USNM), W. Joyce and D. Brinkman (YPM). JBS thanks L. Wilson for providing a room in Boulder. For discussions regarding morphometrics, we are grateful to J. Fearon, E. Ferrer, E. Fowler, M. Goodwin, N. Campione, and R. Schott. Thanks also to A. Bailleul, R. Boik, P. Dodson, A. Farke, D. Fowler, M. Goodwin, M. Holland, N. Longrich, L. Maiorino, D. Roberts, S. Sampson, K. Scannella, I. Trevethan, D. Varricchio, and D.C. Woodruff for conversations over the course of this study, without implying their agreement with our conclusions. Funding for this study was provided in part by grants from the Theodore Roosevelt Memorial Fund of the AMNH, the Doris O. and Samuel P. Welles Fund of the UCMP, the Jurassic Foundation, and the Evolving Earth Foundation to JBS. Additional funding provided by the Museum of the Rockies Inc.

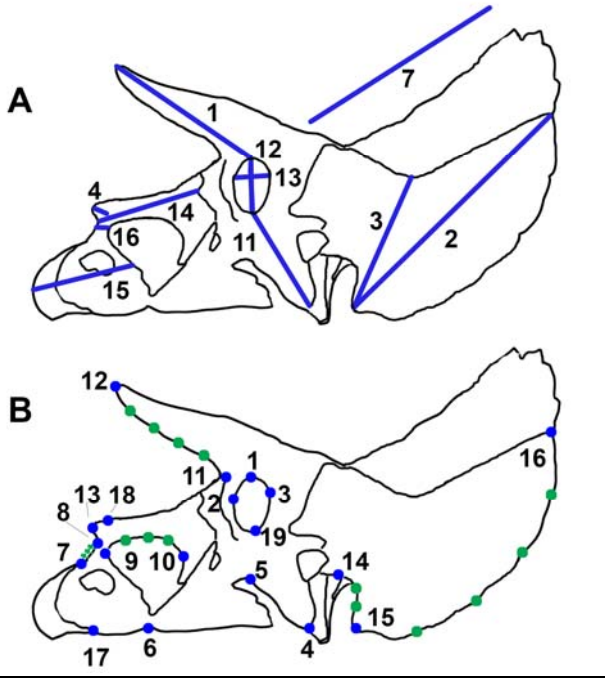


Figure 7.1. Select measurements and landmarks. A) Skull in lateral view showing select linear measurements. B) Landmarks (blue) and semilandmarks (green) used in GM analyses. Measurement and landmark descriptions presented in Appendix 7.2.

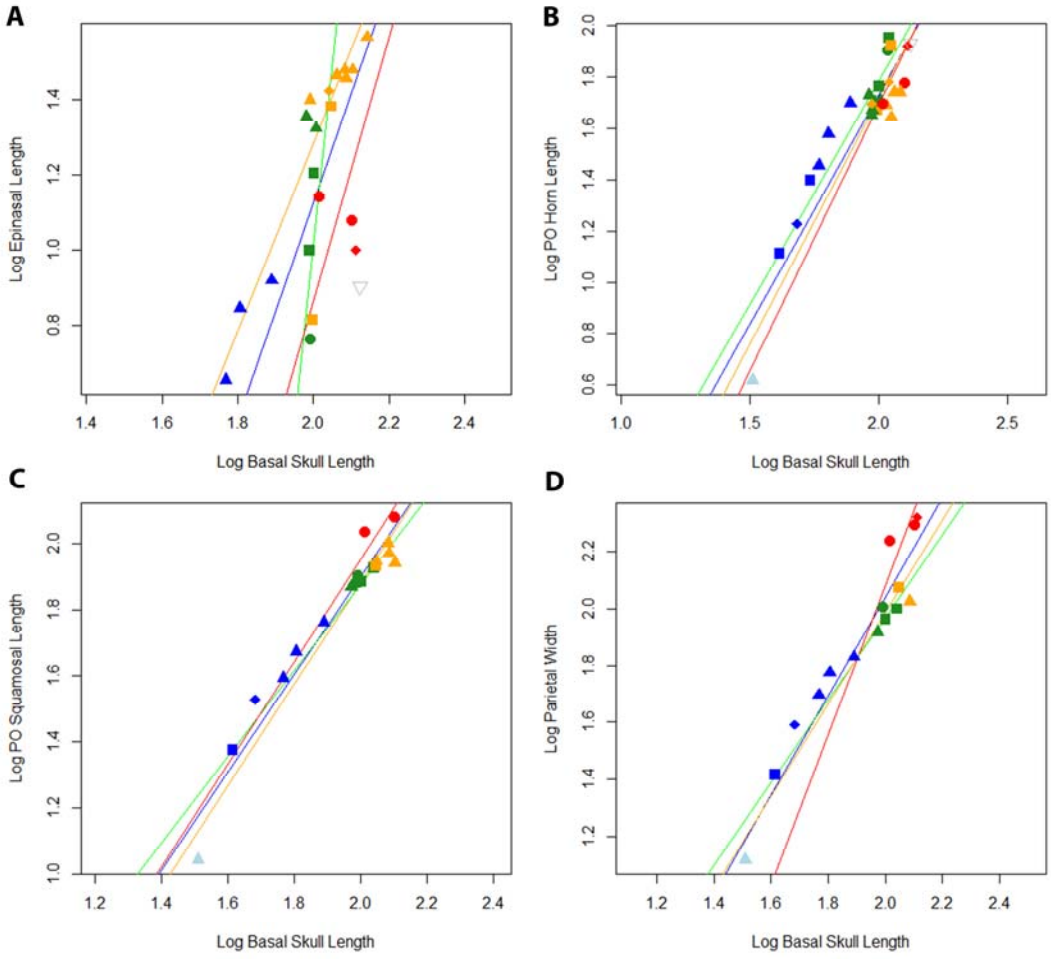


Figure 7.2. Standard major axis (SMA) regression results. Bivariate plots of select cranial measurements against basal skull length. A) Epinasal length. B) Postorbital horn core length. C) Squamosal length. D) Parietal width. Circle=L3; Square=M3; Triangle =U3; Diamond =to be determined; Inverted triangle =RTMP 2002.57.7. Light blue = baby, blue=juvenile, green=subadult, orange=young adult (*Triceratops*), red=adult (=*Torosaurus*). Full SMA results presented in Appendix 7.1.

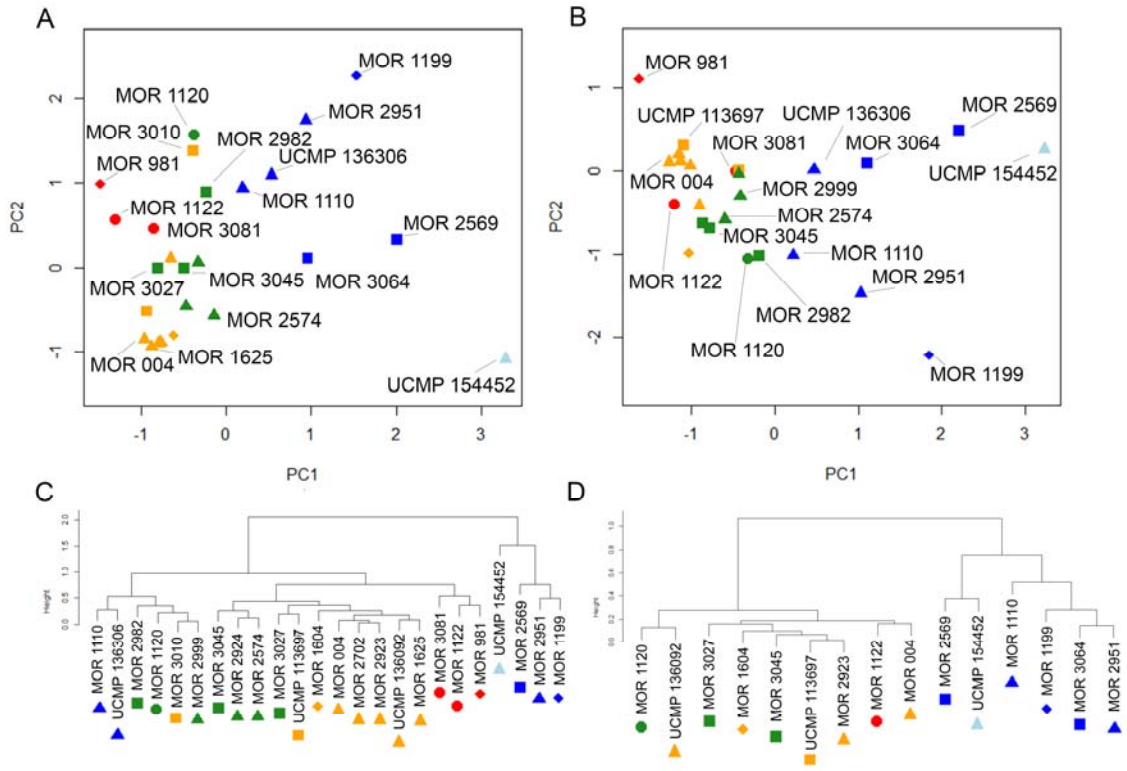


Figure 7.3. Results of PCA and cluster analyses of linear dataset. A) PCA of linear measurements. B) PCA of linear dataset when measurements of horns and frill are removed. C) UPGMA cluster analysis of linear dataset. D) UPGMA cluster analysis of linear dataset when horns and frill are removed. Color/shape codes are the same as for Figure 7.2.

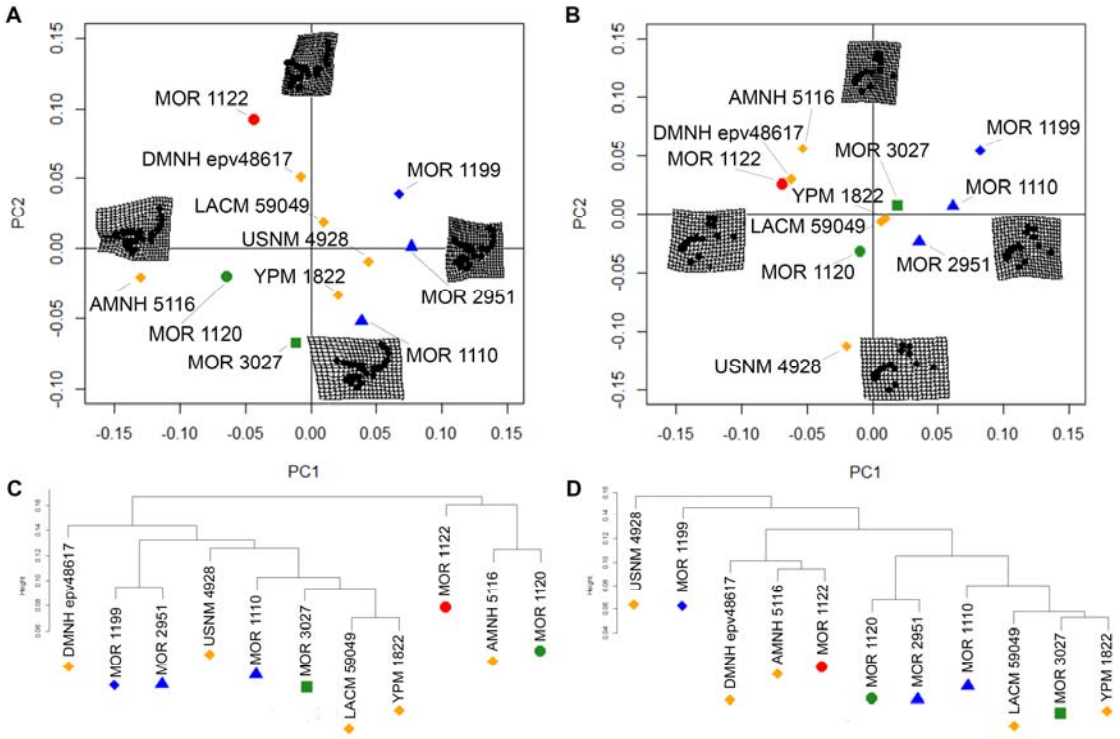


Figure 7.4. Results of PCA and cluster analyses of GM data for skulls in lateral view . A) PCA of GM shape data for skulls in lateral view. B) PCA of GM shape data for skulls in lateral view when horns and frill are removed. C) UPGMA cluster analysis of GM dataset. D) UPGMA cluster analysis of GM dataset for skulls in lateral view when horns and frill are removed. Color/shape codes are the same as for Figure 7.2.

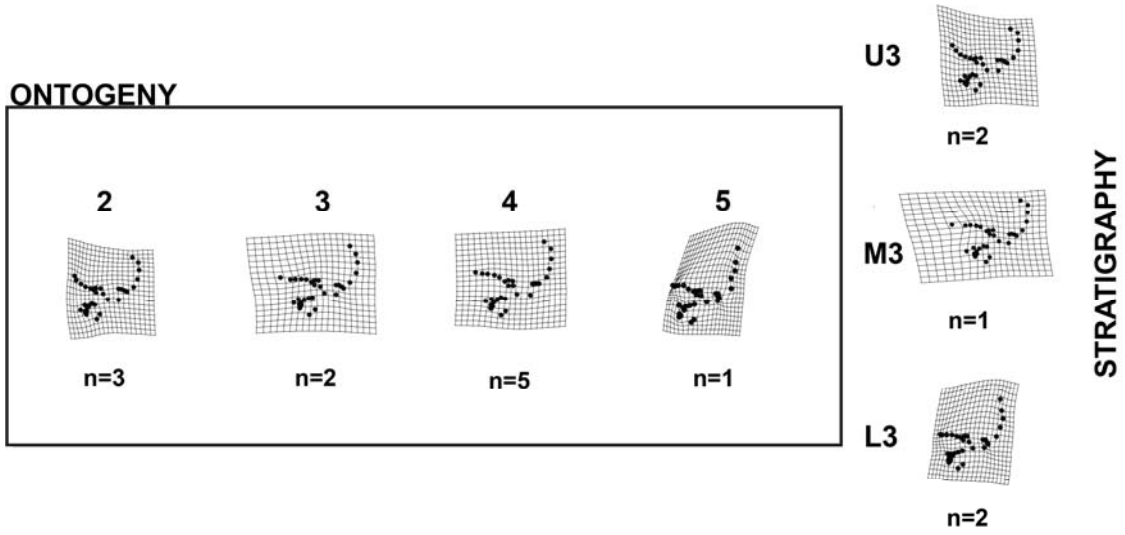


Figure 7.5. Mean GM shape data for the skull in lateral view. Mean shape for each ontogenetic stage (2=juvenile; 3=subadult; 4=young adult; 5="*Torosaurus*") and stratigraphic level of the HCF.

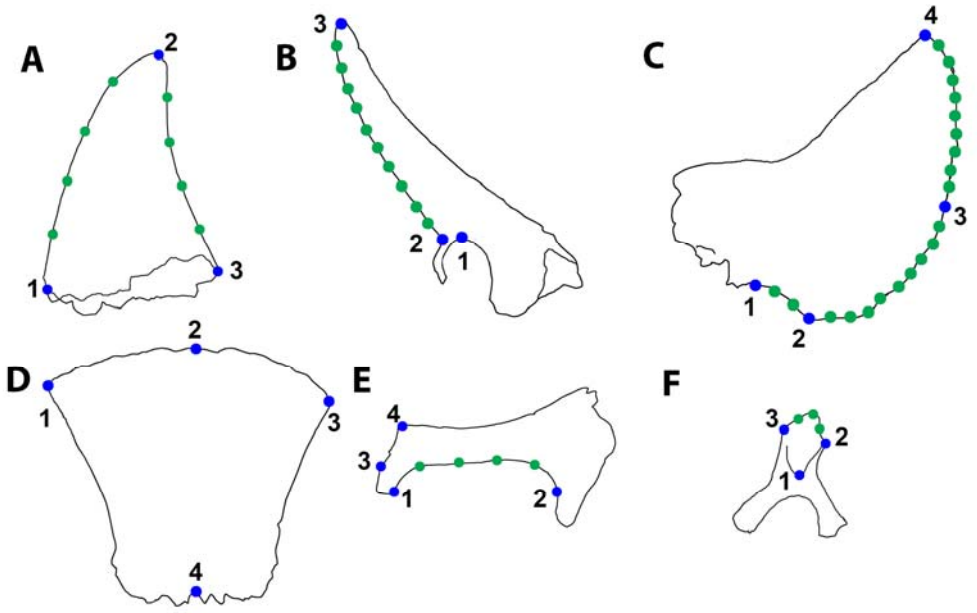


Figure 7.6. Landmarks for GM analyses of individual bones. A) Landmarks for the epinasal. B) Landmarks for the postorbital horn core. C) Landmarks for the squamosal. D) Landmarks for the parietal. E) Landmarks for the nasal. F) Landmarks for the nasal process of the premaxilla (NPP).

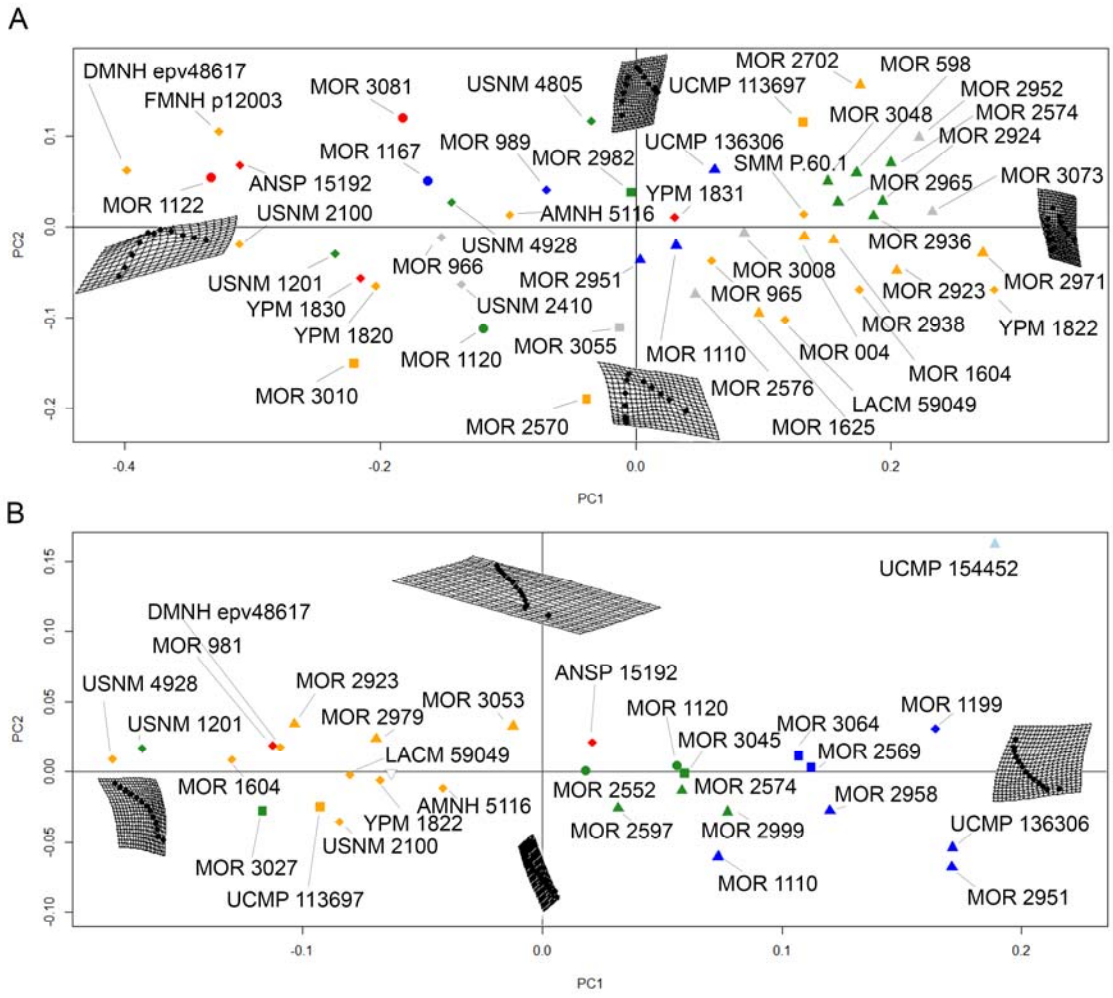


Figure 7.7. PCA of GM shape data for epinasal and postorbital horn cores. A) PCA of epinasals. B) PCA of postorbital horn cores. Colors/shapes are the same as for Figure 7.2; grey = ontogenetic stage to be determined.

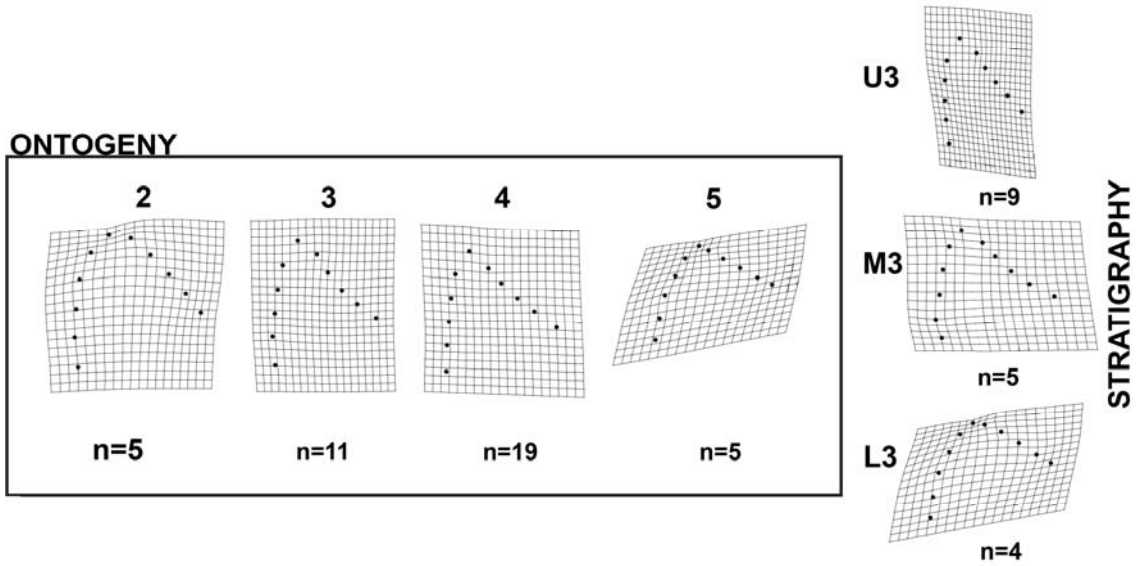


Figure 7.8. Mean GM shape data for epinasals. Mean shape for each ontogenetic stage (2=juvenile; 3=subadult; 4=young adult; 5="*Torosaurus"*) and mean shape for each stratigraphic level of the HCF.

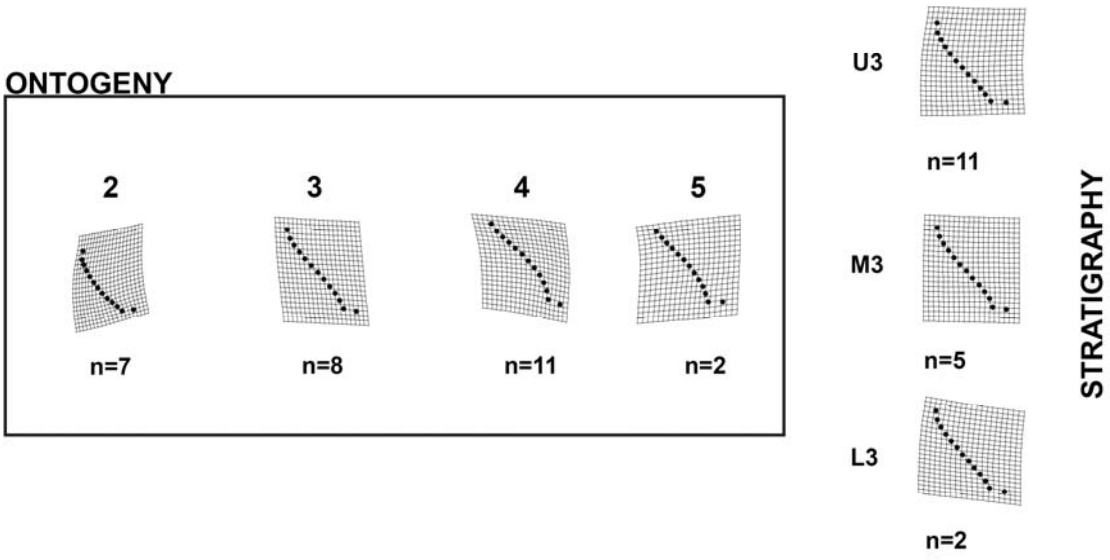


Figure 7.9. Mean GM shape data for postorbital horn cores. Mean shape for each ontogenetic stage (2=juvenile; 3=subadult; 4=young adult; 5="*Torosaurus*") and mean shape for each stratigraphic level of the HCF.

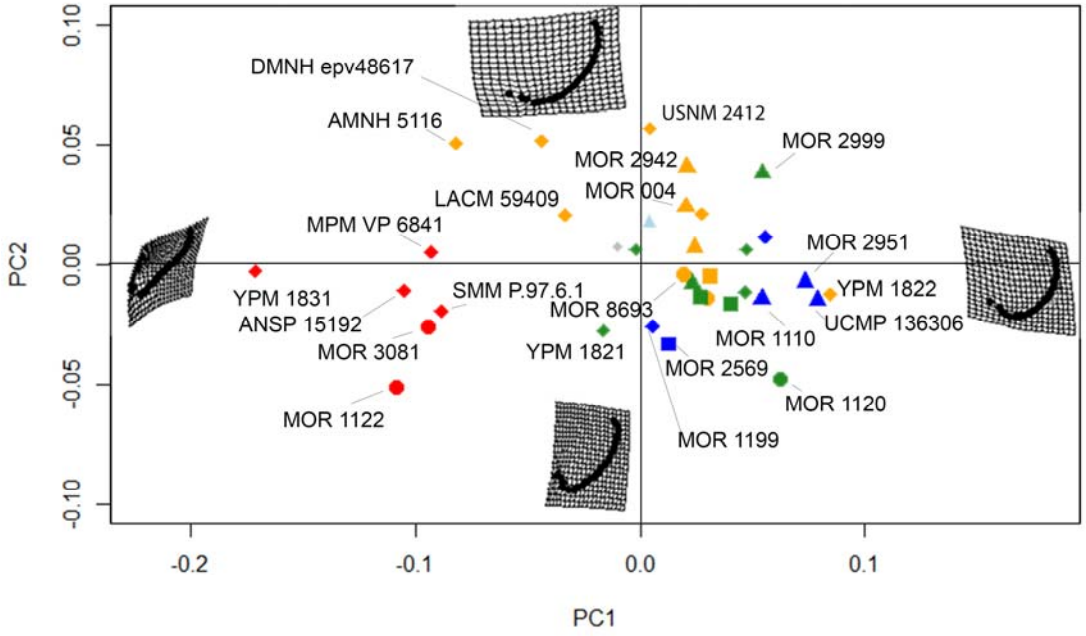


Figure 7.10. PCA of GM shape data for squamosals. Colors/shapes are the same as for Figure 7.2; grey = ontogenetic stage to be determined.

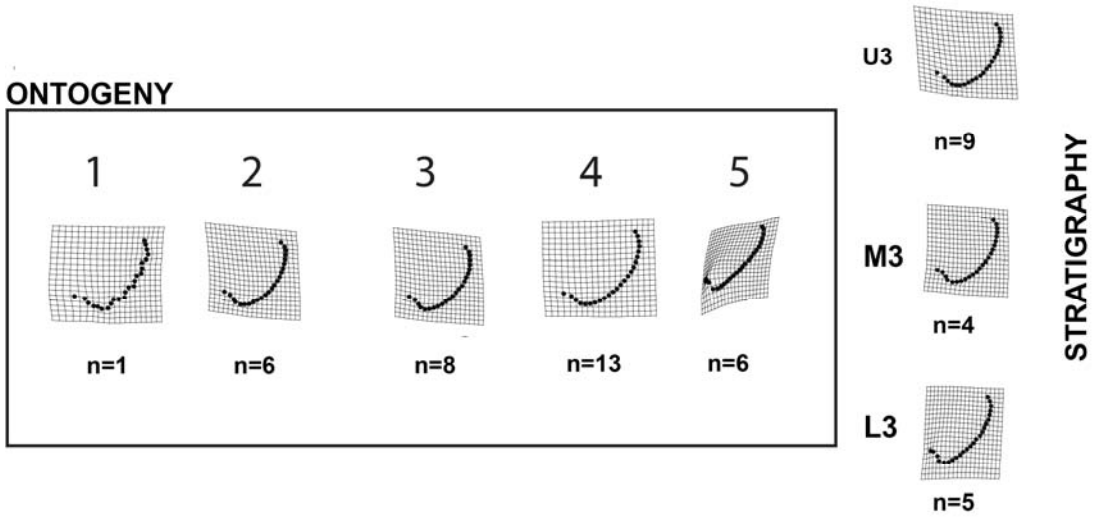


Figure 7.11. Mean GM shape data for squamosals. Mean shape for each ontogenetic stage (2=juvenile; 3=subadult; 4=young adult; 5="*Torosaurus"*) and mean shape for each stratigraphic level of the HCF.

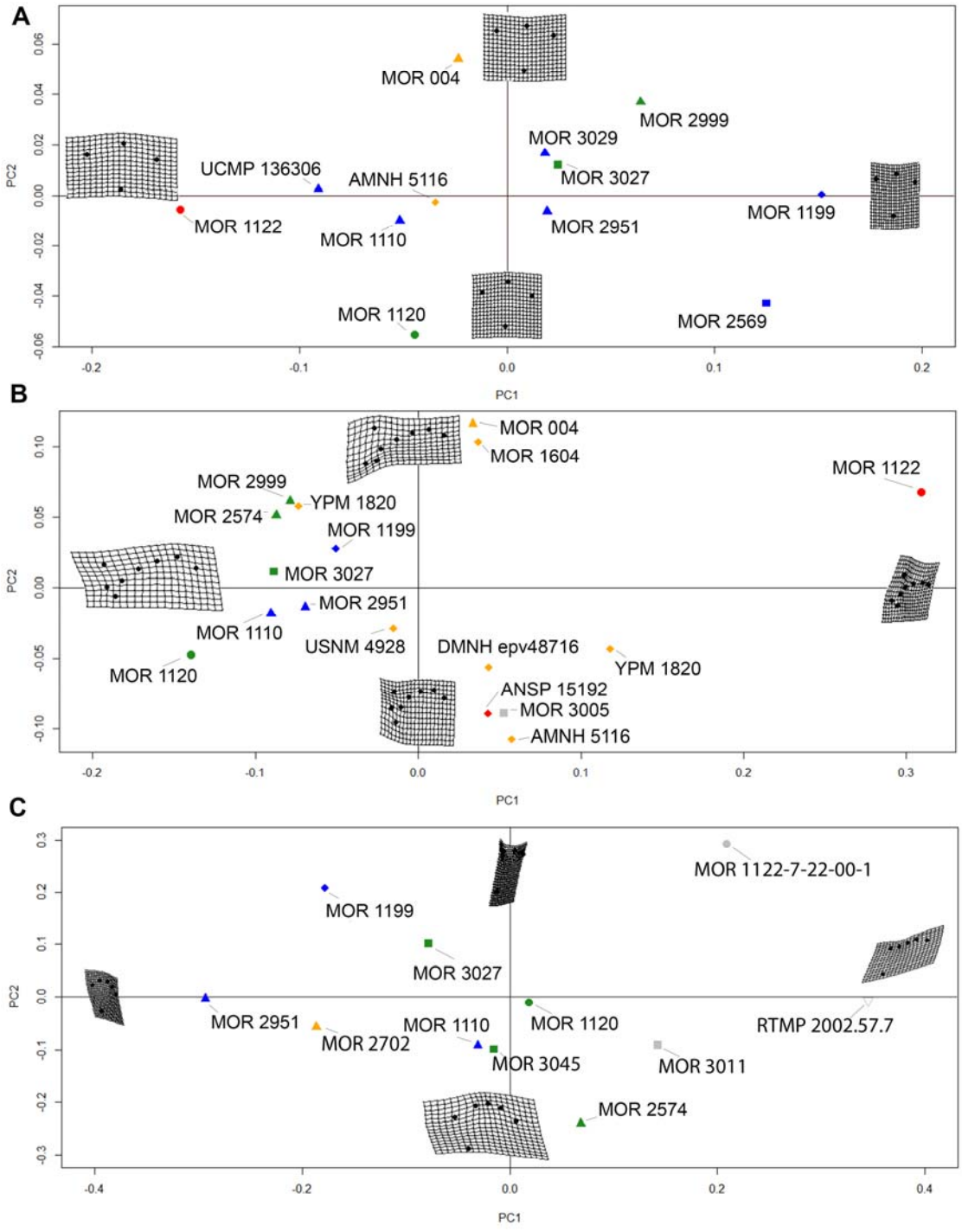


Figure 7.12. PCA of GM shape data for the parietal, nasal, and nasal process of the premaxilla (NPP). A) PCA of the parietal. B) PCA of nasals. C) PCA of NPPs. Colors/shapes are the same as for Figure 7.2; grey = ontogenetic stage to be determined.

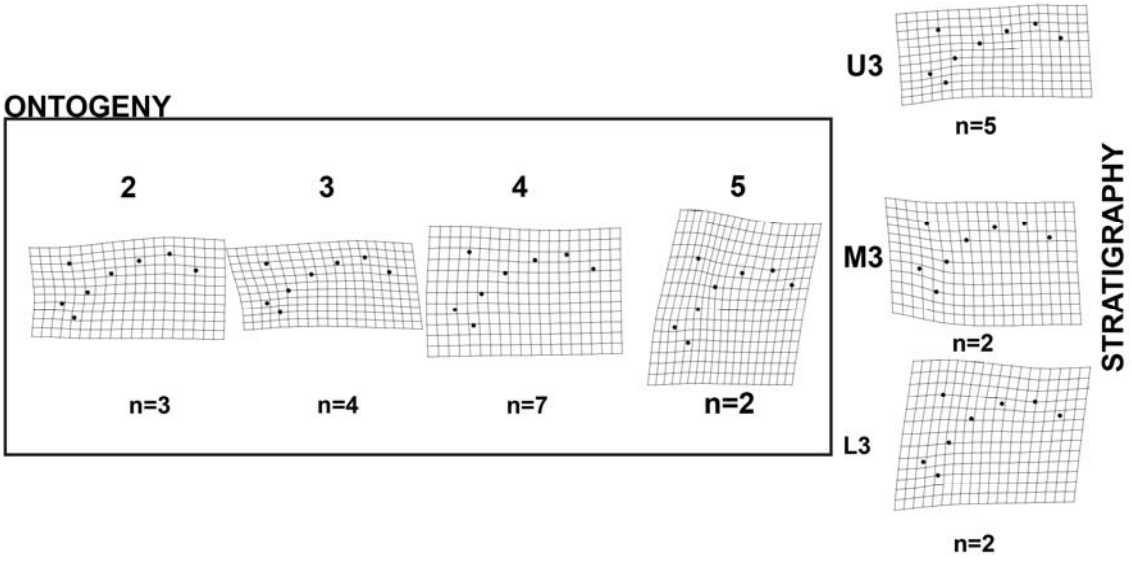


Figure 7.13. Mean GM shape data for nasals. Mean shape for each ontogenetic stage (2=juvenile; 3=subadult; 4=young adult; 5="*Torosaurus"*) and mean shape for each stratigraphic level of the HCF.

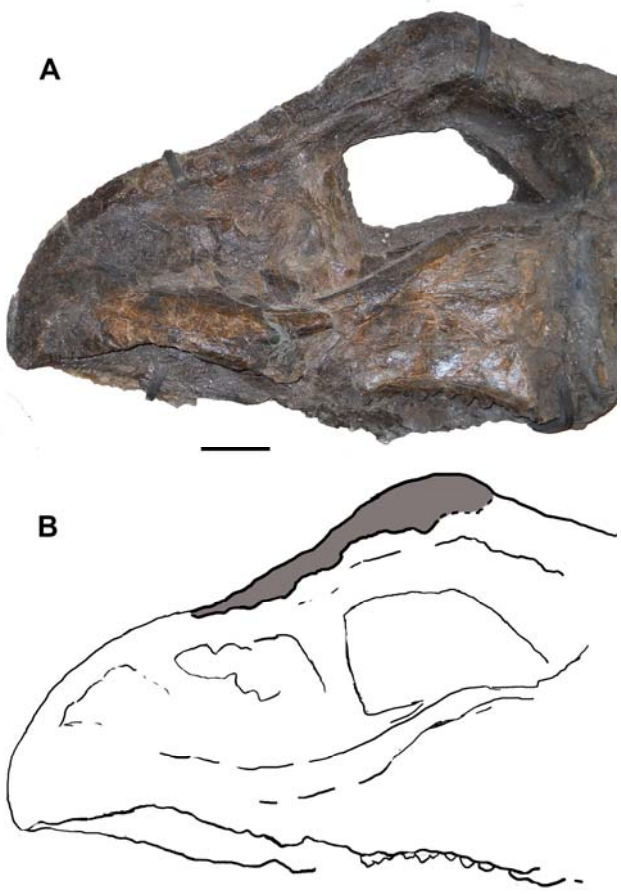


Figure 7.14. The epinasal morphology of MOR 981. A) Rostrum of MOR 981 in lateral view. B) Line drawing of rostrum highlighting the morphology of the epinasal, which appears to extend anteriorly towards the rostral. Scale bar, 10 cm.

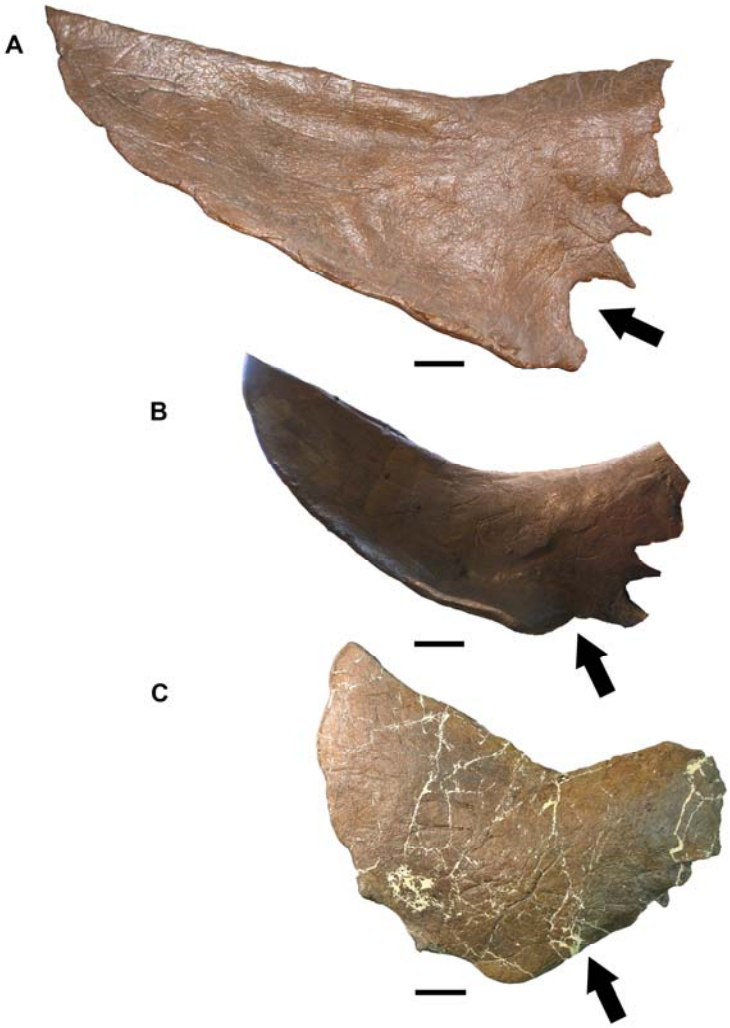


Figure 7.15. Morphology of the anteroventral process of the squamosal. A) MOR 1122 from L3 of the HCF. Arrow indicates strongly concave anterior margin of the squamosal. B) AMNH FARB 5116 from the Lance Formation of Wyoming; stratigraphic position relative to the HCF to be determined. The specimen exhibits an anteroventral projection of the squamosal which is not as pronounced as specimens referred to "*Torosaurus*" (e.g. MOR 1122). C) MOR 2999 form U3 of the HCF. The anterior margin of this squamosal is nearly straight. Scale bars, 10 cm.

Literature Cited

Adams, D. C., and E. Otárola-Castillo. 2013. geomorph: an R package for the collection and analysis of geometric morphometric shape data. Methods in Ecology and Evolution 4:393–399.

Bailleul, A., J. Scannella, and J. Horner. 2013. Ontogeny of cranial sutures in *Alligator mississippiensis*: implications for maturity assessment in non-avian dinosaurs. Journal of Vertebrate Paleontology 81A.

Brown, B. 1917. A Complete Skeleton of the Horned Dinosaur *Monoclonius*, and Description of a Second Skeleton Showing Skin Impressions. order of the Trustees, American Museum of Natural History, pp.

Brown, D. B., and D. E. M. Schlaikjer. 1940. The structure and relationships of *Protoceratops*. Transactions of the New York Academy of Sciences 2:99–100.

Campione, N. E., and D. C. Evans. 2011. Cranial Growth and Variation in Edmontosaurs (Dinosauria: Hadrosauridae): Implications for Latest Cretaceous Megaherbivore Diversity in North America. PLoS ONE 6:e25186.

Chapman, R. E., P. M. Galton, J. J. Sepkoski Jr, and W. P. Wall. 1981. A morphometric study of the cranium of the pachycephalosaurid dinosaur *Stegoceras*. Journal of Paleontology 608–618.

Cheetham, A. H. 1986. Tempo of evolution in a Neogene bryozoan: rates of morphologic change within and across species boundaries. Paleobiology 190–202.

Currie, P. J., W. Langston Jr, and D. H. Tanke. 2008. A new species of *Pachyrhinosaurus* (Dinosauria, Ceratopsidae) from the Upper Cretaceous of Alberta, Canada. A New Horned Dinosaur from an Upper Cretaceous Bone Bed in Alberta. Edited by PJ Currie, W. Langston, Jr., and DH Tanke. NRC Research Press, Ottawa 1–108.

Darwin, C. 1871. Sexual selection and the descent of man. Murray, London.

Dodson, P. 1975. Taxonomic Implications of Relative growth in Lambeosaurine Hadrosaurs. Systematic Biology 24:37–54.

Dodson, P. 1976. Quantitative Aspects of Relative Growth and Sexual Dimorphism in *Protoceratops*. Journal of Paleontology 50:929–940.

Dodson, P. 1993. Comparative craniology of the Ceratopsia. American Journal of Science 293:200–200.

Farke A.A. 1997. The distribution and taxonomy of *Triceratops*. pp. 47-49 in Dinofest International Proceedings Volume, D.L. Wolberg, E. Stump, G.D. Rosenberg (eds.) Philadephia Academy of Natural Sciences, Philadelphia.

Farke, A. A. 2007. Cranial osteology and phylogenetic relationships of the chasmosaurine ceratopsid Torosaurus latus. Horns and Beaks: Ceratopsian and Ornithopod Dinosaurs 235–257.

Farke, A. A. 2011. Anatomy and Taxonomic Status of the Chasmosaurine Ceratopsid *Nedoceratops hatcheri* from the Upper Cretaceous Lance Formation of Wyoming, U.S.A. PLoS ONE 6:e16196.

Farke, A. A. 2014. Evaluating combat in ornithischian dinosaurs. Journal of Zoology 292:242–249.

Farke, A. A., E. D. Wolff, and D. H. Tanke. 2009. Evidence of combat in *Triceratops*. PloS One 4:e4252.

Fisher, R. A. 1922. On the interpretation of $\chi 2$ from contingency tables, and the calculation of P. Journal of the Royal Statistical Society 87–94.

Forster, C. A. 1996. Species resolution in *Triceratops*: cladistic and morphometric approaches. Journal of Vertebrate Paleontology 16:259–270.

Gingerich, P. D. 1985. Species in the fossil record: concepts, trends, and transitions. Paleobiology 27–41.

Goodwin, M. B., and J. R. Horner. 2014. Cranial morphology of a juvenile *Triceratops* skull from the Hell Creek Formation, McCone County, Montana, with comments on the fossil record of ontogenetically younger skulls. Geological Society of America Special Papers 503:333–347.

Gould, S. J. 1977. Ontogeny and Phylogeny. Harvard University Press, pp.

Hartman, J. H., R. D. Butler, M. W. Weiler, and K. K. Schumaker. 2014. Context, naming, and formal designation of the Cretaceous Hell Creek Formation lectostratotype, Garfield County, Montana. Geological Society of America Special Papers 503:89–121.

Hatcher, J. B., H. F. Osborn, and O. C. Marsh. 1907. The Ceratopsia. USGS Monograph 49, 300 pp.

Horner, J. R., and M. B. Goodwin. 2006. Major cranial changes during *Triceratops* ontogeny. Proceedings of the Royal Society B: Biological Sciences 273:2757–2761.

Horner, J. R., and M. B. Goodwin. 2008. Ontogeny of cranial epi-ossifications in *Triceratops*. Journal of Vertebrate Paleontology 28:134–144.

Horner, J. R., and E.-T. Lamm. 2011. Ontogeny of the parietal frill of *Triceratops*: A preliminary histological analysis. Comptes Rendus Palevol 10:439–452.

Horner, J. R., D. J. Varricchio, and M. B. Goodwin. 1992. Marine transgressions and the evolution of Cretaceous dinosaurs. Nature 358:59–61.

Horner, J. R., M. B. Goodwin, and N. Myhrvold. 2011. Dinosaur Census Reveals Abundant *Tyrannosaurus* and Rare Ontogenetic Stages in the Upper Cretaceous Hell Creek Formation (Maastrichtian), Montana, USA. PLoS ONE 6:e16574.

Hunt, G., and D. L. Rabosky. 2014. Phenotypic Evolution in Fossil Species: Pattern and Process. Annual Review of Earth and Planetary Sciences 42:421–441.

Knell, R. J., and S. Sampson. 2011. Bizarre structures in dinosaurs: species recognition or sexual selection? A response to Padian and Horner. Journal of Zoology 283:18–22.

Knell, R. J., D. Naish, J. L. Tomkins, and D. W. Hone. 2013. Is sexual selection defined by dimorphism alone? A reply to Padian and Horner. Proc. Zool. Soc. Lond 35:491–562.

Longrich, N. R., and D. J. Field. 2012. *Torosaurus* Is Not *Triceratops*: Ontogeny in Chasmosaurine Ceratopsids as a Case Study in Dinosaur Taxonomy. PLoS ONE 7:e32623.

Maiorino, L., A. A. Farke, T. Kotsakis, and P. Piras. 2013. Is *Torosaurus Triceratops*? Geometric Morphometric Evidence of Late Maastrichtian Ceratopsid Dinosaurs. PLoS ONE 8:e81608.

Mallon, J. C., R. Holmes, D. A. Eberth, M. J. Ryan, and J. S. Anderson. 2011. Variation in the skull of *Anchiceratops* (Dinosauria, Ceratopsidae) from the Horseshoe Canyon Formation (Upper Cretaceous) of Alberta. Journal of Vertebrate Paleontology 31:1047–1071.

Mallon, J. C., R. Holmes, J. S. Anderson, A. A. Farke, D. C. Evans, and H.-D. Sues. 2014. New information on the rare horned dinosaur *Arrhinoceratops brachyops* (Ornithischia: Ceratopsidae) from the Upper Cretaceous of Alberta, Canada. Canadian Journal of Earth Sciences 51:618–634.

Marsh, O. C. 1889. Notice of gigantic horned Dinosauria from the Cretaceous. American Journal of Science 173–176.

Marsh, O. C. 1890. Description of new dinosaurian reptiles. American Journal of Science s3-39:81–86.

Marsh, O. C. 1891. Notice of new vertebrate fossils. American Journal of Science 265–269.

Oba, S., M. Sato, I. Takemasa, M. Monden, K. Matsubara, and S. Ishii. 2003. A Bayesian missing value estimation method for gene expression profile data. Bioinformatics 19:2088–2096.

Ostrom, J. P., and Wellnhofer, 1986. The Munich Specimen of *Triceratops* with a Revision of the Genus: Zitteliana 14:111–158.

Ostrom, J. H., and P. Wellnhofer. 1990. *Triceratops*: an example of flawed systematics. Dinosaur Systematics: Perspectives and Approaches. Cambridge University Press, New York 245–254.

Padian, K., and J. R. Horner. 2002. Typology versus transformation in the origin of birds. Trends in Ecology & Evolution 17:120–124.

Padian, K., and J. R. Horner. 2011a. The evolution of "bizarre structures" in dinosaurs: biomechanics, sexual selection, social selection or species recognition? Journal of Zoology 283:3–17.

Padian, K., and J. R. Horner. 2011b. The definition of sexual selection and its implications for dinosaurian biology. Journal of Zoology 283:23–27.

Reilly, S. M., E. O. Wiley, and D. J. Meinhardt. 1997. An integrative approach to heterochrony: the distinction between interspecific and intraspecific phenomena. Biological Journal of the Linnean Society 60:119–143.

Rohlf, F. J. 2012. tpsDig, Digitize Landmarks and Outlines, Version 2.16. Department of Ecology and Evolution, State University of New York at Stony Brook. pp.

Rozhdestvensky, A. K. 1965. Growth changes in Asian dinosaurs and some problems of their taxonomy. Paleontologičeskij Žurnal 3:95–109.

Sampson, S. D. 1995. Two new horned dinosaurs from the Upper Cretaceous Two Medicine Formation of Montana; with a phylogenetic analysis of the Centrosaurinae (Ornithischia: Ceratopsidae). Journal of Vertebrate Paleontology 15:743–760.

Scannella, J. B., and J. R. Horner. 2010. *Torosaurus* Marsh, 1891, is *Triceratops* Marsh, 1889 (Ceratopsidae: Chasmosaurinae): synonymy through ontogeny. Journal of Vertebrate Paleontology 30:1157–1168.

Scannella, J. B., and J. R. Horner. 2011. "*Nedoceratops*": An Example of a Transitional Morphology. PLoS ONE 6:e28705.

Scannella, J. B., and D. W. Fowler. 2014. A stratigraphic survey of *Triceratops* localities in the Hell Creek Formation, northeastern Montana (2006–2010). Geological Society of America Special Papers 503:313–332.

Scannella, J. B., D. W. Fowler, M. B. Goodwin, and J. R. Horner. 2014. Evolutionary trends in *Triceratops* from the Hell Creek Formation, Montana. Proceedings of the National Academy of Sciences 111:10245–10250.

Scannella, J.B., D. W. Roberts, and J.R. Horner. *In prep*. A morphometric analysis of casque development and variation in the Black-casqued Hornbill (*Ceratogymna atrata*)

Schott, R. K., D. C. Evans, M. B. Goodwin, J. R. Horner, C. M. Brown, and N. R. Longrich. 2011. Cranial Ontogeny in *Stegoceras validum* (Dinosauria: Pachycephalosauria): A Quantitative Model of Pachycephalosaur Dome Growth and Variation. PLoS ONE 6:e21092.

Stacklies, W., H. Redestig, M. Scholz, D. Walther, and J. Selbig. 2007. pcaMethods—a bioconductor package providing PCA methods for incomplete data. Bioinformatics 23:1164–1167.

Sullivan, R. M., A. C. Boere, and S. G. Lucas. 2005. Redescription of the ceratopsid dinosaur *Torosaurus utahensis* (Gilmore, 1946) and a revision of the genus. Journal Information 79.

Tokaryk, T. T. 1997. First evidence of juvenile ceratopsians (Reptilia: Ornithischia) from the Frenchman Formation (late Maastrichtian) of Saskatchewan. Canadian Journal of Earth Sciences 34:1401–1404.

Wu, X., D. B. Brinkman, D. A. Eberth, and D. R. Braman. 2007. A new ceratopsid dinosaur (Ornithischia) from the uppermost Horseshoe Canyon Formation (upper Maastrichtian), Alberta, Canada. Canadian Journal of Earth Sciences 44:1243–1265.

CHAPTER EIGHT

CONCLUSIONS

Studies of dinosaur paleobiology are dependent on an understanding of the factors which contribute to morphological variation in these animals. In 1990, Ostrom and Wellnhofer referred to the chasmosaurine ceratopsid *Triceratops* as "an example of flawed systematics" as 16 species of *Triceratops* had been named at that point, based primarily on variations in cranial morphology between specimens. They suggested that most, if not all, of this variation was actually intraspecific, and reduced 16 species to one: *Triceratops horridus*. A few years later, Forster (1996) found cladistic and quantitative evidence for two species: *T. horridus* and *T. prorsus*. However, the morphology of juvenile *Triceratops* was largely unknown until 2006 when Goodwin et al. (2006) described the first "baby" *Triceratops* skull and Horner and Goodwin (2006) described the first ontogenetic series for *Triceratops*. These studies revealed that *Triceratops* underwent a dramatic, previously unrecognized transformation throughout growth. In addition to unrecognized ontogenetic changes, stratigraphic resolution for the *Triceratops* holotypes was largely limited (Ostrom and Wellnhofer, 1986) thus obscuring the degree to which variation between specimens might be tied to differing stratigraphic positions.

This dissertation examined ontogenetic and stratigraphic variation in *Triceratops*, the most commonly recovered dinosaur in the upper Cretaceous Hell Creek Formation (HCF) of Montana, based largely on specimens collected over the course of the multi-institutional Hell Creek Project (Horner et al., 2011). While largely consistent with the findings of Forster (1996), this work explored the roles of ontogeny and change

throughout the stratigraphic succession of the HCF in interpretations of variation. Building on the work of Horner and Goodwin, it was found that the ontogenetic transformation of *Triceratops* continued late in growth, with the parietal-squamosal frill ultimately adopting the morphology previously considered to diagnose *Torosaurus latus*. Further, the holotype and only specimen of *Nedoceratops hatcheri* was hypothesized to represent a transitional morphology between unfenestrated and fenestrated specimens (however, see Farke, 2011; Longrich and Field, 2012, and Maiorino et al., 2013 for alternative views). These proposed synonymies suggest reduced ceratopsid diversity just prior to the K-Pg extinction event.

The deciphering of potential evolutionary modes in dinosaurs is often difficult or impossible due to low sample sizes and reduced stratigraphic resolution. Given this, relationships between closely related taxa are often hypothesized to be cladogenetic (due to an evolutionary branching event) in nature. By examining *Triceratops* specimens in stratigraphic context it was found that the two currently recognized species are stratigraphically separated in the HCF, with only *T. prorsus* being present in the upper unit of the formation. The data suggest that *T. horridus* may have evolved into *T. prorsus* over time through anagenesis (the transformation of a lineage over time). Continued analyses and studies will be able to further test this hypothesis, but the ability to explore this subject in detail is due in large part to the rich fossil record for *Triceratops* and stratigraphic resolution for the HCF. *Triceratops* suggests that in order to decipher details of evolution, variation through stratigraphy will be critical to explore in other dinosaur taxa as sample sizes increase.

Whereas extant horned mammals are often used as an analogue for *Triceratops* (e.g. Ostrom and Wellnhofer, 1986); examination of cranial variation in an extant archosaur (*Ceratogymna atrata*) finds that cranial ornamentation likely functions primarily as a visual cue to other individuals. Also, the ability to distinguish sexes is greatly reduced once cranial ornaments are removed from analyses. In *Triceratops*, cranial ornaments (horns and frill) are the elements which undergo the most dramatic changes throughout growth. This is suggestive of these elements being used as visual signals (Horner and Goodwin, 2006), and - as in *C. atrata* - resolution between specimens (representing different species and growth stages) is reduced when cranial ornaments are removed from the analysis. Further, morphometric analysis suggest that *Triceratops* may have retained immature morphologies (such as a short, unfenestrated parietal-squamosal frill) later in ontogeny as it evolved. Alternatively, morphometric results are also consistent with *Triceratops* and *Torosaurus* being distinct taxa and the exhibiting of *Torosaurus*-like morphologies in *T. horridus* being due to *T. horridus* being recovered stratigraphically lower, perhaps closer in time to the divergence between these two taxa. Further testing of these hypotheses will only increase our resolution of how variation between specimens contributes to chasmosaurine taxonomy.

Triceratops is an ideal subject for studies of morphological variation due to its being extremely commonly recovered in the uppermost Cretaceous deposits of western North America, being represented by several growth stages, and being found throughout the stratigraphic succession of a formation for which the stratigraphy is now well understood. After over 120 years of study, we are still gleaning new insights into dinosaur paleobiology from this animal. As sample sizes and stratigraphic resolution for

other non-avian dinosaur taxa increase, studies of *Triceratops* suggest that quantitative analyses of variation throughout ontogeny and stratrigraphic successions will be critical to deciphering evolutionary patterns and processes in the fossil record.

Literature Cited

Farke, A. A. 2011. Anatomy and taxonomic status of the chasmosaurine ceratopsid *Nedoceratops hatcheri* from the Upper Cretaceous Lance Formation of Wyoming, U.S.A. PLoS ONE 6:e16196.

Forster, C. A. 1996. Species resolution in *Triceratops*: cladistic and morphometric approaches. Journal of Vertebrate Paleontology 16:259–270.

Goodwin, M. B., W. A. Clemens, J. R. Horner, and K. Padian. 2006. The smallest known *Triceratops* skull: new observations on ceratopsid cranial anatomy and ontogeny. Journal of Vertebrate Paleontology 26:103–112.

Horner, J. R., and M. B. Goodwin. 2006. Major cranial changes during *Triceratops* ontogeny. Proceedings of the Royal Society B: Biological Sciences 273:2757–2761.

Horner, J. R., M. B. Goodwin, and N. Myhrvold. 2011. Dinosaur Census Reveals Abundant *Tyrannosaurus* and Rare Ontogenetic Stages in the Upper Cretaceous Hell Creek Formation (Maastrichtian), Montana, USA. PLoS ONE 6:e16574.

Longrich, N. R., and D. J. Field. 2012. *Torosaurus* is not *Triceratops*: Ontogeny in chasmosaurine ceratopsids as a case study in dinosaur taxonomy. PLoS ONE 7:e32623.

Maiorino, L., A. A. Farke, T. Kotsakis, and P. Piras. 2013. Is *Torosaurus Triceratops*? Geometric morphometric evidence of Late Maastrichtian ceratopsid dinosaurs. PLoS ONE 8:e81608.

Ostrom, J. P., and Wellnhofer, 1986. The Munich specimen of *Triceratops* with a revision of the genus: Zitteliana 14:111–158.

Ostrom, J. H., and P. Wellnhofer. 1990. *Triceratops*: an example of flawed systematics. Dinosaur Systematics: Perspectives and Approaches. Cambridge University Press, New York 245–254.

REFERENCES CITED

Adams, D. C., and E. Otárola-Castillo. 2013. geomorph: an R package for the collection and analysis of geometric morphometric shape data. Methods in Ecology and Evolution 4:393–399.

Alexander G.D., D.C. Houston, and M. Campbell. 1994. A possible acoustic function for the casque structure in hornbills (Aves: Bucerotidae). Journal of Zoology 233(1): 57-67.

Anderson J. 1999. Occipital condyle in the ceratopsian dinosaur *Triceratops*, with comments on body size variation. Contributions from the Museum of Paleontology University of Michigan 30(8): 215-231.

Anderson M.J. 2001. A new method for non-parametric multivariate analysis of variance. Austral Ecology 26:32-46.

Archibald, D.J. 1982. A Study of Mammalia and Geology across the Cretaceous-Tertiary Boundary in Garfield County, Montana. University of California Publications in Geological Sciences 122: 286 p.

Archibald, D.J. 1996. Dinosaur extinction and the end of an era: what the fossils say. Columbia University Press, New York. 237 p.

Archibald, D.J., R.F. Butler, E.H. Lindsay, W.A. Clemens, and L. Dingus. 1982. Upper Cretaceous–Paleocene biostratigraphy and magnetostratigraphy, Hell Creek and Tullock Formations, northeastern Montana. Geology 10(3): 153–159, doi:10.1130/0091-7613(1982)10<153:UCBAMH>2.0.CO;2.

Bailleul, A., J. Scannella, and J. Horner. 2013. Ontogeny of cranial sutures in *Alligator mississippiensis*: implications for maturity assessment in non-avian dinosaurs. Journal of Vertebrate Paleontology 81A.

Bakker, R. T., M. Williams, and P. J. Currie. 1988. *Nanotyrannus*, a new genus of pygmy tyrannosaur, from the latest Cretaceous of Montana. Hunteria 1:1–30.

Bakker, R. T., R. M. Sullivan, V. Porter, P. Larson, and S. J. Saulsbury. 2006. *Dracorex hogwartsia,* n. gen., n. sp., a spiked, flat-headed pachycephalosaurid dinosaur from the Upper Cretaceous Hell Creek Formation of South Dakota. New Mexico Museum of Natural History and Science Bulletin 35:331–345.

Barrick R.E., M.K. Stoskopf, J.D. Marcot, D.A. Russell, W.J. Showers. 1998. The thermoregulatory functions of the *Triceratops* frill and horns: heat flow measured with oxygen isotopes. Journal of Vertebrate Paleontology 18(4), 746-750.

Benton M.J., and P.N. Pearson. 2001. Speciation in the fossil record. Trends in Ecology and Evolution 16(7): 405-411.

Brink, K. S., D. K. Zelenitsky, D. C. Evans, F. Therrien, and J. R. Horner. 2011. A sub-adult skull of *Hypacrosaurus stebingeri* (Ornithischia: Lambeosaurinae): anatomy and comparison. Historical Biology 23:63–72.

Brown, B. 1907. The Hell Creek beds of the Upper Cretaceous of Montana: American Museum of Natural History Bulletin 23:823–845.

Brown, B. 1917. A complete skeleton of the horned dinosaur *Monoclonius*, and a description of a second skeleton showing skin impressions. Bulletin of the American Museum of Natural History 37: 281–306.

Brown, B. 1933. A gigantic ceratopsian dinosaur, *Triceratops maximus*, new species. American Museum Novitates, 649: 1-9.

Brown, B., and E. M. Schlaikjer. 1940a. The Origin of ceratopsian horn-cores. American Museum Novitates, 1065: 1-7.

Brown, B., and E. M. Schlaikjer. 1940b. The structure and relationships of *Protoceratops*. Transactions of the New York Academy of Sciences 2:133–265.

Brown, B., and E. M. Schlaikjer. 1943. A study of the troödont dinosaurs, with the description of a new genus and four new species. Bulletin of the AMNH; v. 82, article 5.

Brown, C. M., A. P. Russell, and M. J. Ryan. 2009. Pattern and transition of surfacial bone texture of the centrosaurine frill and their ontogenetic and taxonomic implications. Journal of Vertebrate Paleontology 29:132-141.

Campione N.E., and R.R. Reisz. 2010. *Varanops brevirostris* (Eupelycosauria: Varanopidae) from the Lower Permian of Texas, with discussion of varanopid morphology and interrelationships. Journal of Vertebrate Paleontology 30(3):724-746.

Campione, N. E., and D. C. Evans. 2011. Cranial Growth and Variation in Edmontosaurs (Dinosauria: Hadrosauridae): Implications for Latest Cretaceous Megaherbivore Diversity in North America. PLoS ONE 6:e25186.

Campione, N.E., K.S. Brink, E.A. Freedman, T. McGarrity, and D.C. Evans. 2013. *'Glishades ericksoni*', an indeterminate juvenile hadrosaurid from the Two Medicine Formation of Montana: implications for hadrosauroid diversity in the

latest Cretaceous (Campanian-Maastrichtian) of western North America. Paleobiodiversity and Paleoenvironments 93: 65-75.

Carpenter K., and D.B. Young. 2002. Late Cretaceous dinosaurs from the Denver Basin, Colorado. Rocky Mountain Geology 37(2): 237-254.

Carr, T. D. 1999. Craniofacial ontogeny in tyrannosauridae (Dinosauria, Coelurosauria). Journal of Vertebrate Paleontology 19:497-520.

Chamutpong S, M. Ponglikitmongkol , W. Charoennitikul, S. Mudsri, P. Poonswad . 2013. Hybridisation in the wild between the Great Hornbill (*Buceros bicornis*) and the Rhinoceros Hornbill (*Buceros rhinoceros)* in Thailand and its genetic assessment. The Raffles Bulletin of Zoology 61(1): 349-358.

Chapman, R. E., P. M. Galton, J. J. Sepkoski Jr, and W. P. Wall. 1981. A morphometric study of the cranium of the pachycephalosaurid dinosaur *Stegoceras*. Journal of Paleontology 608–618.

Cheetham, A. H. 1986. Tempo of evolution in a Neogene bryozoan: rates of morphologic change within and across species boundaries. Paleobiology 190–202.

Chinsamy-Turan, A. 2005. The Microstructure of Dinosaur Bone: Deciphering Biology with Fine-Scale Techniques. Johns Hopkins University Press, 195 pp.

Cobabe E.A., and D.E. Fastovsky. 1987. *Ugrosaurus olsoni*, a new ceratopsian (Reptilia: Ornithischia) from the Hell Creek Formation of eastern Montana. Journal of Paleontology 61(1): 148–154.

Colbert, E. H., and J. D. Bump. 1947. A skull of *Torosaurus* from South Dakota and a revision of the genus. Proceedings of the Academy of Natural Sciences of Philadelphia 93–106.

Cranbrook Earl of, A.C. Kemp. 1995. Aerial casque-butting by hornbills (Bucerotidae): a correction and an expansion. Ibis 137(4): 588-589.

Curio E. 2004. On ornamental maturation of two Philippine hornbill species with a note on physiological colour change. Journal of Ornithology. 145(3): 227-237.

Currie, P. J., and P. Dodson. 1984. Mass death of a herd of ceratopsian dinosaurs. Third Symposium of Mesozoic Terrestrial Ecosystems 52–60.

Currie, P.J., W. Langston, and D.H. Tanke. 2008. A new species of *Pachyrhinosaurus* (Dinosauria, Ceratopsidae) from the Upper Cretaceous of Alberta, Canada; pp. 1-

108 in P.J. Currie, W. Langston, D.H. Tanke (eds.), A New Horned Dinosaur from an Upper Cretaceous Bone Bed in Alberta. NRC Research Press, Ottawa, Ontario, Canada.

Darwin C. 1871. The Descent of Man and Selection in Relation to Sex. JohnMurray, London.

Darwin, C. 1859. On the origins of species by means of natural selection. London: Murray.

de Beer, G. 1930. Embryology and Evolution. Clarendon Press, Oxford. pp.

Delport W., A.C. Kemp, J.W.H. Ferguson. 2004. Structure of an African red-billed hornbill (*Tockus erythrorhynchus rufirostris* and *Te damarensis*) hybrid zone as revealed by morphology, behavior, and breeding biology The Auk 121(2): 565-586.

Dingus, L., and M.A. Norell 2010. Barnum Brown: The Man Who Discovered *Tyrannosaurus rex*. University of California Press, Berkeley, California, 368 pp.

Dodson P. 1975a. Taxonomic implications of relative growth in lambeosaurine hadrosaurs. Systematic Biology 24(1): 37-54.

Dodson P. 1975b. Functional and ecological significance of relative growth in *Alligator*. Journal of Zoology 175(3): 315-355.

Dodson P. 1975c. Relative growth in two sympatric species of *Sceloporus*. American Midland Naturalist 94(2): 421-450.

Dodson P. 1976. Quantitative aspects of relative growth and sexual dimorphism in *Protoceratops*. Journal of Paleontology 50(5): 929-940.

Dodson, P. 1986. *Avaceratops lammersi*: a new ceratopsid from the Judith River Formation of Montana. Proceedings of the Academy of Natural Sciences of Philadelphia 305–317.

Dodson, P. 1990. On the status of the ceratopsids *Monoclonius* and *Centrosaurus*; pp. 231-243 in K. Carpenter, P.J. Currie, (eds.) Dinosaur systematics: approaches and perspectives. Cambridge University Press, New York.

Dodson, P. 1993. Comparative craniology of the Ceratopsia. American Journal of Science 293:200–200.

Dodson, P. 1996. The Horned Dinosaurs. Princeton University Press, Princeton, New Jersey, 346 pp.

Dodson, P. and P.J. Currie. 1988. The smallest ceratopsid skull-Judith River Formation of Alberta. Canadian Journal of Earth Sciences 25:926-930.

Dodson, P., C. A. Forster, and S. D. Sampson. 2004. Ceratopsidae; pp. 494–513 in D. B. Weishampel, P. Dodson, and H. Osmolska (eds.), The Dinosauria. University of California Press, Berkeley, California.

Eldredge N., and S.J. Gould. 1972. Punctuated equilibria: an alternative to phyletic gradualism. pp. 82-115 in Models in Paleobiology, T.J.M. Schopf (ed.) Freeman, Cooper & Co., San Francisco.

Evans D.C. 2006. Nasal cavity homologies and cranial crest function in lambeosaurine dinosaurs. Paleobiology 32(1): 109-125.

Evans, D. C. 2010. Cranial anatomy and systematics of *Hypacrosaurus altispinus*, and a comparative analysis of skull growth in lambeosaurine hadrosaurids (Dinosauria: Ornithischia). Zoological Journal of the Linnean Society 159:398–434.

Evans D., P. Currie, D. Eberth, and M. Ryan. 2006. High-resolution lambeosaurine dinosaur biostratigraphy, Dinosaur Park Formation, Alberta: sexual dimorphism reconsidered. Journal of Vertebrate Paleontology 26: 59A.

Fabre A.C., R. Cornette, K. Huyghe, D.V. Andrade, A. Herrel. 2014. Linear versus geometric morphometric approaches for the analysis of head shape dimorphism in lizards. Journal of Morphology 275: 1016-1026.

Farke A.A. 1997. The distribution and taxonomy of *Triceratops*. pp. 47-49 in Dinofest International Proceedings Volume, D.L. Wolberg, E. Stump, G.D. Rosenberg (eds.) Philadephia Academy of Natural Sciences, Philadelphia.

Farke, A. A. 2007. Cranial osteology and phylogenetic relationships of the chasmosaurine ceratopsid *Torosaurus latus*; pp. 235-257 in K. Carpenter (ed.), Horns and Beaks: Ceratopsian and Ornithopod Dinosaurs. Indiana University Press, Bloomington and Indianapolis.

Farke A.A. 2010. Evolution, homology, and function of the supracranial sinuses in ceratopsian dinosaurs. Journal of Vertebrate Paleontology 30(5): 1486-1500.

Farke A.A. 2011. Anatomy and taxonomic status of the chasmosaurine ceratopsid *Nedoceratops hatcheri* from the Upper Cretaceous Lance Formation of Wyoming, U.S.A. PLoS One 6(1): e16196.doi:10.1371/journal.pone.0016196.

Farke A.A. 2014. Evaluating combat in ornithischian dinosaurs. Journal of Zoology 292(4): 242-249.

Farke, A. A. 2014. Evaluating combat in ornithischian dinosaurs. Journal of Zoology 292:242–249.

Farke, A. A., and T. E. Williamson. 2006. A ceratopsid dinosaur parietal from New Mexico and its implications for ceratopsid biogeography and systematics. Journal of Vertebrate Paleontology 26:1018-1020.

Farke, A. A., E. D. Wolff, and D. H. Tanke. 2009. Evidence of combat in *Triceratops*. PloS One 4:e4252.

Farke, A. A., M.J. Ryan, P.M. Barrett, D.H., Tanke, D. R. Braman, M.A. Loewen, and M.R. Graham. 2011. A new centrosaurine from the Late Cretaceous of Alberta, Canada, and the evolution of parietal ornamentation in horned dinosaurs. Acta Palaeontologica Polonica 56(4): 691-702

Fastovsky, D.E. 1987. Paleoenvironments of vertebrate-bearing strata during the Cretaceous-Paleogene transition, eastern Montana and western North Dakota. Palaios 2: 282–295, doi:10.2307/3514678.

Felsenstein J. 1985. Confidence limits on phylogenies: an approach using the bootstrap. Evolution 39(4): 783-791.

FigTree v 1.4.0. http://tree.bio.ed.ac.uk/software/figtree/

Fisher D.C. 1994. Stratocladistics: morphological and temporal patterns and their relation to phylogenetic process pp. 133-171 in Interpreting the hierarchy of nature: from systematic patterns to evolutionary process theories, L. Grande, and O. Rieppel (eds.) Academic Press, San Diego, California.

Fisher D.C. 2008. Stratocladistics: integrating temporal data and character data in phylogenetic inference. Annual Revieve of Ecology, Evolution, and Systematics (39): 365-385.

Fisher, R. A. 1922. On the interpretation of $\chi 2$ from contingency tables, and the calculation of P. Journal of the Royal Statistical Society 87–94.

Flight, J.N. 2004. Sequence stratigraphic analysis of the Fox Hills and Hell Creek Formations (Maastrichtian), Eastern Montana and its relationships to dinosaur paleontology [M.S. thesis]: Bozeman, Montana, State University, 164 pp.

Forster, C.A. 1990. The cranial morphology and systematics of *Triceratops* with a preliminary analysis of ceratopsid phylogeny. PhD dissertation. University of Pennsylvania. Philadelphia. PA.

Forster C.A. 1993. Taxonomic validity of the ceratopsid dinosaur *Ugrosaurus olsoni* (Cobabe and Fastovsky). Journal of Paleontology 67(2): 316–318.

Forster, C. A. 1996a. Species resolution in *Triceratops*: cladistic and morphometric approaches. Journal of Vertebrate Paleontology 16(2):259–270.

Forster, C.A. 1996b. New information on the skull of *Triceratops*. Journal of Vertebrate Paleontology 16: 246-258.

Forster, C.A., P.C. Sereno, T.W. Evans, and T. Rowe. 1993. A complete skull of *Chasmosaurus mariscalensis* (Dinosauria: Ceratopsidae) from the Aguja Formation (Late Campanian) of West Texas. Journal of Vertebrate Paleontology 13: 161-170.

Fowler D.W., J.B. Scannella, and J.R. Horner. 2011. Reassessing ceratopsid diversity using unified frames of reference. Journal of Vertebrate Paleontology 31(5): 111A.

Fowler, D.W. 2009. A sequence stratigraphic subdivision of the Hell Creek Formation: Beginnings of a high-resolution regional chronostratigraphic framework for the terminal Cretaceous, p. 136 in Storrs, G.W. (ed.) 9th North American Paleontological Convention Abstracts. University of Cincinnati, Cincinnati Museum Center Scientific Contributions 3, Cincinnati, Ohio.

Fowler, D.W., H.N. Woodward, E.A. Freedman, P.L. Larson, and J.R. Horner. 2011. Reanalysis of "*Raptorex kriegsteini*": a juvenile tyrannosaurid dinosaur from Mongolia. PLoS ONE 6(6): e21376. doi:101371/journalpone.0021376

Francillon-Vieillot, H., V. de Buffrénil, F. J. Géraudie, J. Y. Meunier, L. Sire, L. Zylberberg, and A. de Ricqlès. 1990. Microstructure and mineralization of vertebrate skeletal tissues; pp. 471-548 in J. G. Carter (ed.), Skeletal Biomineralization: Patterns, Processes and Evolutionary Trends. Van Nostrand Reinhold, New York.

Frederickson J.A., and A.R. Tumarkin-Deratzian. 2014. Craniofacial ontogeny *in Centrosaurus apertus*. PeerJ 2:e252; DOI 10.7717/peerj.252

Freedman, E. 2009. Variation in nasal crest size of *Brachylophosaurus canadensis* (Dinosauria:Hadrosauridae): ontogenetic and stratigraphic implications of a large new specimen from the Judith River Formation of northcentral Montana. Journal of Vertebrate Paleontology 29:99A-100A.

Frith C.B., and V.E. Douglas. 1978. Notes on ten Asian hornbill species (Aves: Bucerotidae); with particular reference to growth and behaviour. Natural History Bulletin of the Siam Society 27: 35-82.

Frith C.B., and D.W. Frith. 1978. Bill growth and development in the Northern Pied Hornbill *Anthracoceros malabaricus*. Avicultural Magazine 84: 20-31.

Fujiwara S., and Y. Takakuwa. 2011. A sub-adult growth stage indicated in the degree of suture co-ossification in *Triceratops*. Bulletin of Gumma Museum of Natural History 15: 1-17.

Galton, P. M., and H.-D. Sues. 1983. New data on pachycephalosaurid dinosaurs (Reptilia: Ornithischia) from North America. Canadian Journal of Earth Sciences 20:462–472.

Gamble K.C., and M.S. Dipl. 2007. Internal Anatomy of the Hornbill casque described by radiography, contrast radiography, and computed tomography. Journal of Avian Medicine and Surgery 21 (1): 38-49.

Gates T.A., and S.D. Sampson. 2007. A new species of *Gryposaurus* (Dinosauria: Hadrosauridae) from the Late Campanian Kaiparowits Formation, southern Utah, USA. Zoological Journal of the Linnean Society 151: 351-376.

Gill, F.B. 2000. Ornithology. W.H. Freeman and Company. New York. 766pp.

Gilmore, C. W. 1914. A new ceratopian dinosaur from the Upper Cretaceous of Montana, with note on *Hypacrosaurus*. Smithsonian Miscellaneous Collections 63:1-10.

Gilmore, C. W. 1946. New carnivorous dinosaur from the Lance Formation of Montana. Smithsonian Miscellaneous Collections 106: 1-19.

Gilmore, C. W. 1946. Reptilian fauna of the North Horn Formation of central Utah. U.S. Geological Survey Professional Paper 210C:1-52.

Gingerich P.D. 1985. Species in the fossil record: concepts, trends, and transitions. Paleobiology 11(1): 27-41.

Godfrey, S. J., and R. Holmes. 1995. Cranial morphology and systematics of *Chasmosaurus* (Dinosauria: Ceratopsidae) from the Upper Cretaceous of western Canada. Journal of Vertebrate Paleontology 15:726–742.

Goodwin M.B., and J.R. Horner. 2010. Historical collecting bias and the fossil record of *Triceratops* in Montana; pp. 551-563 in M.J. Ryan, B.J. Chinnery-Allgeier, and D.A. Eberth DA, (eds.) New perspectives on horned dinosaurs. Bloomington, Indiana University Press.

Goodwin, M. B., and J. R. Horner. 2014. Cranial morphology of a juvenile *Triceratops* skull from the Hell Creek Formation, McCone County, Montana, with comments on the fossil record of ontogenetically younger skulls. Geological Society of America Special Papers 503:333–347.

Goodwin, M. B., W. A. Clemens, J. R. Horner, and K. Padian. 2006. The smallest known *Triceratops* skull: new observations on ceratopsid cranial anatomy and ontogeny. Journal of Vertebrate Paleontology 26:103–112.

Gould S.J. 1974.The origin and function of 'bizarre' structures: antler size and skull size in the 'Irish Elk,' Megaloceros giganteus. Evolution 28(2): 191-220.

Gould, S. J. 1977. Ontogeny and Phylogeny. The Belknap Press of Harvard University Press, Cambridge Massachusetts, London England. 501 pp.

Gould, S. J. 1992. Roots: Ontogeny and phylogeny–revisited and reunited. BioEssays 14:275–279.

Gould, S. J. 2000. Of coiled oysters and big brains: how to rescue the terminology of heterochrony, now gone astray. Evolution & Development 2:241–248.

Gould S.J., and R.C. Lewontin. 1979. The spandrels of San Marco and the Panglossian paradigm: a critique of the adaptationist programme. Proceedings of the Royal Society of London B. 205(1161): 581-598.

Goussard, F. 2006. The skull of *Triceratops* in the palaeontology gallery, Muséum national d'Histoire naturelle, Paris. Geodiversitas 28:467–476.

Granger, W., W. K. Gregory, and C. P. Berkey. 1923. *Protoceratops andrewsi*, a pre-ceratopsian dinosaur from Mongolia. American Museum Novitates 72: 1-9

Hall, L., and S. Keenan 2010, Taphonomy of a new specimen of *Tyrannosaurus rex* from the Hell Creek Formation, Montana. Journal of Vertebrate Paleontology: SVP Program and Abstracts Book, v. 30: 100A-101A.

Hamburger, V., and H. L. Hamilton. 1951. A series of normal stages in the development of the chick embryo. Journal of Morphology 88:49–92.

Hammer Ø, D.A.T. Harper, and P.D. Ryan. 2001. PAST: Paleontological Statistics software package for education and data analysis. Palaeontologia Electronica 4(1): 9pp.

Happ J.W., and C.M. Morrow. 1996. Separation of *Triceratops* (Dinosauria:Ceratopsidae) into two allopatric species by cranial morphology. Journal of Vertebrate Paleontology 16: 40A.

Hartman J.H., R.D. Butler, M.W. Weiler, and K.K. Schumaker. 2014. Context, naming, and formal designation of the Cretaceous Hell Creek Formation lectostratotype, Garfield County, Montana. pp. 89-122 in Through the End of the Cretaceous in the Type Locality of the Hell Creek Formation in Montana and Adjacent Areas. G.P. Wilson, W.A. Clemens, J.R. Horner, and J.H. Hartman (eds.) Geological Society of America Special Paper, Boulder, Colorado.

Hatcher, J. B. 1905. Two new ceratopsia from the Laramie of Converse County, Wyoming. American Journal of Science 413–419.

Hatcher, J. B., O. C. Marsh, and R. S. Lull. 1907. The Ceratopsia. US Geological Survey Monograph 49:1-300.

Hicks J.F., K.R. Johnson, J.D. Obradovich, L. Tauxe, and D. Clark. 2002. Magnetostratigraphy and geochronology of the Hell Creek and basal Fort Union Formations of southwestern North Dakota and a recalibration of the age of the Cretaceous-Tertiary boundary, pp. 35-55 in The Hell Creek Formation and the Cretaceous -Tertiary boundary in the northern Great Plains: an integrated continental record of the end of the Cretaceous, J.H. Hartman, K.R. Johnson, and D.J. Nichols (eds.) Geological Society of America Special Paper 361, Boulder, Colorado.

Hicks J.F., K.R. Johnson, J.D. Obradovich, D.P. Miggins, and L. Tauxe. 2003. Magnetostratigraphy of Upper Cretaceous (Maastrichtian) to lower Eocene strata of the Denver Basin, Colorado. Rocky Mountain Geology 38: 1-27.

Hieronymus, T.L. 2006. Quantitative microanatomy of jaw muscle attachment in extant diapsids. Journal of Morphology 267: 954-967.

Holmes R.B., C. Forster, M. Ryan, K.M. Shepherd. 2001. A new species of *Chasmosaurus* (Dinosauria:Ceratopsia) from the Dinosaur Park Formation of Southern Alberta. Canadian Journal of Earth Sciences 38: 1423-1438.

Horner, J. R. 1983. Cranial osteology and morphology of the type specimen of *Maiasaura peeblesorum* (Ornithischia: Hadrosauridae), with a discussion of its phylogenetic position. Journal of Vertebrate Paleontology 3:29–38.

Horner, J. R., and E. Dobb. 1997. Dinosaur Lives. HarperCollins, New York 244pp.

Horner, J. R., and P. J. Currie. 1994. Embryonic and neonatal morphology and ontogeny of a new species of *Hypacrosaurus* (Ornithischia, Lambeosauridae) from Montana and Alberta. Dinosaur Eggs and Babies. Cambridge University Press, Cambridge 312–336.

Horner J.R. and M.B. Goodwin. 2006. Major cranial changes during *Triceratops* ontogeny. Proceedings of the Royal Society of London B. 273: 2757-2761.

Horner J.R. and, M.B. Goodwin. 2008. Ontogeny of cranial epi-ossifications in *Triceratops*. Journal of Vertebrate Paleontology 28(1): 134–144.

Horner J.R. and M.B. Goodwin. 2009. Extreme cranial ontogeny in the Upper Cretaceous dinosaur *Pachycephalosaurus*. PLoS One, 4(10), e7626.

Horner, J. R., and J. Gorman. 1988. Digging Dinosaurs. Workman Pub., 210 pp.

Horner, J. R., and J. Gorman. 2009. How to Build a Dinosaur: Extinction Doesn't Have to Be Forever. Penguin, pp.

Horner, J.R. and E. T. Lamm. 2009. Metaplasia provided dinosaur skulls extreme morphological plasticity during ontogeny. Journal of Vertebrate Paleontology 29:117A.

Horner, J.R. and E.T. Lamm. 2011. Ontogeny of the parietal frill of *Triceratops*: a preliminary histological analysis. Comptes Rendus Pelevol 10: 439-452.

Horner, J.R. and K. Padian. 2004. Age and growth dynamics of *Tyrannosaurus rex*. Proceedings of the Royal Society of London B. 271:1875-1880.

Horner J.R., Varricchio D.J., and M.B. Goodwin. 1992. Marine transgressions and the evolution of Cretaceous dinosaurs. Nature. 358: 59-61.

Horner, J. R., M. B. Goodwin, and H. N. Woodward. 2007. Synonomy consequences of dinosaur cranial ontogeny. Journal of Vertebrate Paleontology 27:92A.

Horner, J.R., A. de Ricqlès, K. Padian, and R.D. Scheetz. 2009. Comparative long bone histology and growth of the "hypsilophodontid" dinosaurs *Orodromeus makelai, Dryosaurus altus,* and *Tenontosaurus tillettii* (Ornithischia: Eurornithopoda). Journal of Vertebrate Paleontology 29:734-747.

Horner, J.R., M.B. Goodwin, and N. Myhrvold. 2009. Hell Creek Formation dinosaur census reveals abundant *Tyrannosaurus*. 9th North American Paleontological Convention Abstracts, Cincinnati Museum Center Scientific Contributions 3: 146.

Horner J.R, M.B. Goodwin, and N. Myhrvold. 2011. Dinosaur census reveals abundant *Tyrannosaurus* and rare ontogenetic stages in the Upper Hell Creek Formation (Maastrichtian), Montana, USA. PLoS One 6: e16574(doi:10.1371/journal.pone.0016574).

Hunt, R. K., and T. M. Lehman. 2008. Attributes of the ceratopsian dinosaur *Torosaurus*, and new material from the Javelina Formation (Maastrichtian) of Texas. Journal of Paleontology 82:1127-1138.

Hunt, G., and D. L. Rabosky. 2014. Phenotypic Evolution in Fossil Species: Pattern and Process. Annual Review of Earth and Planetary Sciences 42:421–441.

Johnson, R.E. and J.H. Ostrom. 1995. The forelimb of *Torosaurus* and an analysis of the posture and gait of ceratopsians; pp. 205-218 in J. Thomasson (ed.) Functional Morphology in Vertebrate Paleontology. Cambridge University Press, New York.

Keenan, S.W., and J.B. Scannella. 2014. Paleobiological implications of a *Triceratops* bonebed from the Hell Creek Formation, Garfield County, northeastern Montana, in Wilson, G.P., W.A. Clemens, J.R. Horner, and J.H. Hartman, (eds.) Through the End of the Cretaceous in the Type Locality of the Hell Creek Formation in Montana and Adjacent Areas: Geological Society of America Special Paper 503, doi:10.1130/2014.2503(14).

Keith S., E.K. Urban, and C.H. Fry. 1988. The birds of Africa. Vol. 3. Academic Press, London.

Kemp A. 1995. The Hornbills: Bucerotiformes. Oxford University Press, Oxford, New York, Tokyo: 302 pp.

Kinnaird M.F. and T.G. O'Brien. 2007. The ecology and conservation of Asian hornbills: farmers of the forest. University of Chicago Press, Chicago and London: 315 pp.

Knell R.J. and S.D. Sampson. 2011. Bizarre structures in dinosaurs: species recognition or sexual selection? A response to Padian and Horner. Journal of Zoology 283(1): 18-22.

Knell, R. J., D. Naish, J. L. Tomkins, and D. W. Hone. 2013a. Is sexual selection defined by dimorphism alone? A reply to Padian and Horner. Proceedings of the Zoological Society of London(35):491–562.

Knell, R. J., D. Naish, J. L. Tomkins, and D. W. Hone. 2013b. Sexual selection in prehistoric animals: detection and implications. Trends in Ecology & Evolution 28:38–47.

Lambe, R. S. 1915. On *Eoceratops canadensis*, gen. nov., with remarks on other genera of Cretaceous horned dinosaurs. Geological Survey of Canada Museum Bulletin 12:1-49.

Larson, P. 2013. The case for *Nanotyrannus*. pp. 15-54 in J.M. Parrish, R.E. Molnar, P.J. Currie, and E.B. Koppelhus (eds.)Tyrannosaurid Paleobiology , Indiana University Press.

Lawson, D.A. 1976. *Tyrannosaurus* and *Torosaurus*, Maestrichtian dinosaurs from Trans-Pecos, Texas. Journal of Paleontology 50(1): 158-164.

LeCain R., W. Clyde, G.P. Wilson, and J. Riedel. 2014. Magnetostratigraphy of the Hell Creek and lower Fort Union formations in northeastern Montana. pp. 137-148 in Through the End of the Cretaceous in the Type Locality of the Hell Creek Formation in Montana and Adjacent Areas, G.P. Wilson, W.A. Clemens, J.R. Horner, J.H. Hartman (eds.) Geological Society of America Special Paper, Boulder, Colorado.

Legendre P. 2013. lmodel2: Model II Regression. R package version 1.7-1. http://CRAN.R-project.org/package=lmodel2

Lehman, T. M. 1987. Late Maastrichtian paleoenvironments and dinosaur biogeography in the western interior of North America. Palaeogeography, Palaeoclimatology, Palaeoecology 60:189-217.

Lehman, T. M. 1990. The ceratopsian subfamily chasmosaurinae: sexual dimorphism and systematics; pp. 211-229 in K. Carpenter and P. J. Currie (eds.), Dinosaur Systematics: Approaches and Perspectives. Cambridge University Press, New York.

Lehman T.M. 1998. A gigantic skull and skeleton of the horned dinosaur *Pentaceratops* sternbergi from New Mexico. Journal of Paleontology 72(5): 894-906.

Lehman, T. M. 2007. Growth and population age structure in the horned dinosaur *Chasmosaurus*. Horns and Beaks: Ceratopsian and Ornithopod Dinosaurs 259–317.

Lerbekmo J.F. 1999. Magnetostratigraphy of the Canadian continental drilling program Cretaceous-Tertiary (K-T) boundary project core holes, western Canada. Canadian Journal of Earth Sciences 36: 705-715.

Lerbekmo J.F. 2009. Glacioeustatic sea level fall marking the base of supercycle TA-1 at 66.5 Ma recored by the kaolinization of the Whitemud Formation and the Colgate Member of the Fox Hills Formation. Marine and Petroleum Geology 26: 1299-1303.

Lerbekmo J.F., and D.R. Braman. 2002. Magnetostratigraphic and biostratigraphic correlation of late Campanian and Maastrichtian marine and continental strata from the Red Deer Valley to the Cypress Hills, Alberta, Canada. Canadian Journal of Earth Sciences 39: 539-557.

Lofgren, D.L. 1995. The Bug Creek Problem and the Cretaceous-Tertiary Transition at McGuire Creek, Montana. University of California Publications in Geological Sciences 140, 185 p.

Long, J. A., and K. J. McNamara. 1997. Heterochrony: The key to dinosaur evolution. pp. 113-123 in Dinofest International Proceedings Volume, D.L. Wolberg, E. Stump, G.D. Rosenberg (eds.) Philadephia Academy of Natural Sciences, Philadelphia.

Longrich N. R. 2010. *Mojoceratops perifania,* a new chasmosaurine ceratopsid from the Late Campanian of Western Canada. Journal of Paleontology 84(4): 681-694.

Longrich N. R. 2011. *Titanoceratops ouranos*, a giant horned dinosaur from the late Campanian of New Mexico. Cretaceous Research 32:264-276.

Longrich, N. R., and D. J. Field. 2012. *Torosaurus* is not *Triceratops*: Ontogeny in chasmosaurine ceratopsids as a case study in dinosaur taxonomy. PLoS ONE 7:e32623.

Lucas, S. G., R. M. Sullivan, and A. P. Hunt. 2006. Re-evaluation of *Pentaceratops* and *Chasmosaurus* (Ornithischia: Ceratopsidae) in the Upper Cretaceous of the Western Interior. New Mex Mus Nat Hist Sci Bull 35:367–370.

Lull, R. 1905. Restoration of the horned dinosaur *Diceratops*. American Journal of Science 20:420-422.

Lull R.S. 1915. The mammals and horned dinosaurs of the Lance formation of Niobrara County, Wyoming. American Journal of Science 4(40): 319-348.

Lull, R. S. 1933. A revision of the Ceratopsia or horned dinosaurs. Yale Peabody Museum of Natural History Memoirs 3:1-178.

Macleod N. 1991. Punctuated anagenesis and the importance of stratigraphy to paleobiology. Paleobiology 17(2): 167-188.

Maddison, W.P., and D.R. Maddison. 2011. Mesquite: a modular system for evolutionary analysis. Version 2.75. http://mesquiteproject.org/

Maiorino, L., A. A. Farke, T. Kotsakis, and P. Piras. 2013. Is *Torosaurus Triceratops*? Geometric morphometric evidence of Late Maastrichtian ceratopsid dinosaurs. PLoS ONE 8:e81608.

Makovicky P.J. and M.A. Norell. 2006. *Yamaceratops dorngobiensis*, a new primitive ceratopsian (Dinosauria: Ornithischia) from the Cretaceous of Mongolia. American Museum Novitates: 1-42.

Makovicky, P., R. Sadleir, P. Dodson, G. Erickson, and M. Norell. 2007. Life history of *Protoceratops andrewsi* from Bayn Zag, Mongolia. Journal of Vertebrate Paleontology 27:109A–109A.

Mallon, J. C., R. Holmes, D. A. Eberth, M. J. Ryan, and J. S. Anderson. 2011. Variation in the skull of *Anchiceratops* (Dinosauria, Ceratopsidae) from the Horseshoe Canyon Formation (Upper Cretaceous) of Alberta. Journal of Vertebrate Paleontology 31:1047–1071.

Mallon, J. C., R. Holmes, J. S. Anderson, A. A. Farke, D. C. Evans, and H.-D. Sues. 2014. New information on the rare horned dinosaur *Arrhinoceratops brachyops* (Ornithischia: Ceratopsidae) from the Upper Cretaceous of Alberta, Canada. Canadian Journal of Earth Sciences 51:618–634.

Malmgren B.A., W.A. Berggren, and G.P. Lohmann. 1983. Evidence for punctuated gradualism in the Late Neogene Globorotalia tumida lineage of planktonic foraminifera. Paleobiology 9(4): 377-389.

Marcot J. D., and D. L. Fox. 2008. StrataPhy: a new computer program for stratocladistic analysis. Palaeontologica Electronica 11:5A.

Marsh, O. C. 1887. Notice of new fossil mammals. American Journal of Science series 3, 34: 323–331.

Marsh, O. C. 1888. A new family of horned Dinosauria, from the Cretaceous. American Journal of Science, series 3, 36: 477–478.

Marsh, O. C. 1889. Notice of gigantic horned Dinosauria from the Cretaceous. American Journal of Science series 3, 38: 173–176.

Marsh, O. C. 1890a. Description of new dinosaurian reptiles. American Journal of Science s3-39:81–86.

Marsh, O. C. 1890b. Additional characters of the Ceratopsidae, with notice of new Cretaceous dinosaurs. American Journal of Science s3-39:418–426.

Marsh, O. C. 1891. Notice of new vertebrate fossils. American Journal of Science series 3, 42: 265–269.

Marsh O.C. 1892. The skull of *Torosaurus*. American Journal of Science 43: 81-84.

Marsh, O. C. 1898. New species of Ceratopsia. American Journal of Science, series 4, 6: 92.

Maryanska et al. 2004. Pachycephalosauria; pp. 464–477 in D. B. Weishampel, P. Dodson, and H. Osmolska (eds.), The Dinosauria. University of California Press, Berkeley, California.

Mateus, O. 2008. Two ornithischian dinosaurs renamed: *Microceratops* Bohlin, 1953 and *Diceratops* Lull, 1905. Journal of Paleontology 82: 423.

Mayr, E. 1942. Systematics and the Origin of Species, from the Viewpoint of a Zoologist. Columbia University Press, New York, pp.

Mayr, E. 1959. Darwin and the evolutionary theory in biology, p. 1-10 in Meggers J., ed., Evolution and Anthropology: A Centennial Appraisal: Anthropological Society of Washington, Washington, D.C.

McDonald, A. T. 2011. A subadult specimen of *Rubeosaurus ovatus* (Dinosauria: Ceratopsidae), with observations on other ceratopsids from the Two Medicine Formation. PloS One 6:e22710.

McDonald A. T., D. G. Wolfe, and J. I. Kirkland. 2010. A new basal hadrosauroid (Dinosauria: Ornithopoda) from the Turonian of New Mexico. Journal of Vertebrate Paleontology 3(3): 799–812.

McKinney, M. L., and K. J. McNamara. 1991. Heterochrony: the evolution of ontogeny. Plenum Press, New York, 437 pp.

Moller A.P. and A. Pomiankowski. 1993. Why have birds got multiple sexual ornaments? Behavioral Ecology and Sociobiology 32(3): 167-176.

Nopcsa, F. B. and E. Heidsieck 1933. 11. On the histology of-the ribs in immature and half-grown Tracho-dont dinosaurs. Proceedings of the Zoological Society of London 103:221–226.

Norell, M. A., J. M. Clark, L. M. Chiappe, and D. Dashzeveg. 1995. A nesting dinosaur. Nature 378:774–776.

Oba S., M.A. Sato, I. Takemasa, M. Monden, K.I. Matsubara and S. Ishii. 2003. A Bayesian missing value estimation method for gene expression profile data. Bioinformatics 19(16): 2088- 2096.

Oksanen J., F. Guillaume Blanchet, R. Kindt, P. Legendre, P.R. Minchin, R.B. O'Hara, G.L. Simpson, P. Solymos, M. Henry, H. Stevens and H. Wagner. 2013. vegan: Community Ecology Package. R package version 2.0-7. http://CRAN.R-project.org/package=vegan

O'Leary M. A., and S. G. Kaufman. 2008. MorphoBank 2.5: Web application for morphological phylogenetics and taxonomy, http://www.morphobank.org.

Osborn, H.F. 1905. *Tyrannosaurus* and other Cretaceous carnivorous dinosaurs. Bulletin of the American Museum of Natural History 22: 475–479.

Ostrom, J. P., and Wellnhofer, 1986. The Munich specimen of *Triceratops* with a revision of the genus: Zitteliana 14:111–158.

Ostrom, J. H., and P. Wellnhofer. 1990. *Triceratops*: an example of flawed systematics; pp. 245-254 in K. Carpenter and P. J. Currie (eds.), Dinosaur Systematics: Approaches and Perspectives. Cambridge Univ. Press, New York.

Ott C. J., and P. L. Larson. 2010. A new, small ceratopsian dinosaur from the latest Cretaceous Hell Creek Formation, northwest South Dakota, United States: a preliminary description pp. 203-218 in New Perspectives on Horned Dinosaurs: The Royal Tyrell Museum Ceratopsian Symposium, M. J. Ryan,

B. J. Chinnery-Allgeier, and D. A. Eberth (eds.) Indiana University Press, Bloomington and Indianapolis.

Padian, K., and J. R. Horner. 2002. Typology versus transformation in the origin of birds. Trends in Ecology & Evolution 17:120–124.

Padian K. and J.R. Horner. 2011a. The evolution of 'bizarre structures' in dinosaurs: biomechanics, sexual selection, social selection or species recognition? Journal of Zoology 283(1): 3-17.

Padian K. and J.R. Horner. 2011b. The definition of sexual selection and its implications for dinosaurian biology. Journal of Zoology 283(1): 23-27.

Padian, K., and J. R. Horner. 2013. Misconceptions of sexual selection and species recognition: a response to Knell et al. and to Mendelson and Shaw. Trends in Ecology & Evolution 28:249–250.

Padian, K., J. R. Horner, and J. Dhaliwal. 2004. Species recognition as the principal cause of bizarre structures in dinosaurs. Journal of Vertebrate Paleontology 24:100A.

Pardo J. D., A. K. Huttenlocker, and J. D. Marcot. 2008. Stratocladistics and evaluation of evolutionary modes in the fossil record: an example from the ammonite genus Semiformiceras. Palaeontology. 51(4): 767-773.

Parks, W.A. 1925. *Arrhinoceratops brachyops*, a new genus and species of Ceratopsia from the Edmonton Formation of Alberta. University of Toronto Studies, Geological Series 19: 5-15.

Pearson, D.A., T., Schaefer, K.R., Johnson, D.J., Nichols, and J.P., Hunter. 2002. Vertebrate biostratigraphy of the Hell Creek Formation in southwestern North Dakota and northwestern South Dakota, p. 145-167 in Hartman, J.H., K.R., Johnson, and D.J., Nichols (eds.) The Hell Creek Formation and the Cretaceous-Tertiary Boundary in the Northern Great Plains: An Integrated Continental Record of the End of the Cretaceous. Geological Society of America Special Paper 361.

Penkalski, P., and P. Dodson. 1999. The morphology and systematics of *Avaceratops*, a primitive horned dinosaur from the Judith River Formation (Late Campanian) of Montana, with the description of a second skull. Journal of Vertebrate Paleontology 19:692–711.

Pleijel F. 1995. On character coding for phylogeny reconstruction. Cladistics. 11:309-315.

Polly P. D. 1997. Ancestry and species definition in paleontology: stratocladistic analysis of Paleocene-Eocene Viverravidae (Mammalia, Carnivora) from Wyoming. Contributions from the Museum of Paleontology University of Michigan 30(1): 1-53.

Prieto-Marquez, A. 2010. The braincase and skull roof of *Gryposaurus notabilis* (Dinosauria, Hadrosauridae), with a taxonomic revision of the genus. Journal of Vertebrate Paleontology 30:838–854.

R Core Team 2013. R: A language and environment for statistical computing. R Foundation for Statistical Computing, Vienna, Austria. URL http://www.R-project.org/.

Raman T.R.S. 1998. Aerial casque-butting in the Great Hornbill *Buceros bicornis*. Forktail (13): 123-124.

Raynolds R. G., and K. R. Johnson. 2003. Synopsis of the stratigraphy and paleontology of the uppermost Cretaceous and lower Tertiary strata in the Denver Basin, Colorado. Rocky Mountain Geology 38: 171-181.

Reilly, S. M., E. O. Wiley, and D. J. Meinhardt. 1997. An integrative approach to heterochrony: the distinction between interspecific and intraspecific phenomena. Biological Journal of the Linnean Society 60:119–143.

Rensch B. 1947. Neure Probleme der Abstammungslehre. Die transspezifische evolution. Ferdinand Enke, Stuttgart.

Rohlf F.J. 2010. TpsDig2 ver 2.16. Stony Brook, NY. Published by the author.

Rohlf F.J. 2012. TpsUtil. ver. 1.52. Stony Brook, NY. Published by the author.

Rook D. L., and J. P. Hunter. 2011. Phylogeny of the Taeniodonta: evidence from dental characters and stratigraphy. Journal of Vertebrate Paleontology 31(2): 422-427.

Rozhdestvensky A.K. 1965. [Growth changes in Asian dinosaurs and some problems of their taxonomy]. Paleontologičeskij žurnal 3: 95-109.

Ryan M.J., and A.P. Russell. 2005. A new centrosaurine ceratopsid from the Oldman Formation of Alberta and its implications for centrosaurine taxonomy and systematic. Canadian Journal of Earth Sciences 42: 1369-1387.

Ryan, M. J., A. P. Russell, D. A. Eberth, and P. J. Currie. 2001. The taphonomy of a *Centrosaurus* (Ornithischia: Certopsidae) bone bed from the Dinosaur Park Formation (Upper Campanian), Alberta, Canada, with comments on cranial ontogeny. Palaios 16:482–506.

Sampson S. D. , M. A. Loewen, A. A. Farke, E. M. Roberts, C. A. Forster, J. A. Smith, and A. L. Titus. 2010. New horned dinosaurs from Utah provide evidence for intracontinental dinosaur endemism. PLoS ONE 5(9): e12292.doi:10.1371/journal.pone.0012292.

Sampson S.D. 1995. Two new horned dinosaurs from the Upper Cretaceous Two Medicine Formation of Montana; with a phylogenetic analysis of the Centrosauriane (Ornithischia: Ceratopsidae). Journal of Vertebrate Paleontology 15: 743-760.

Sampson S.D., and M.A. Loewen. 2010. Unraveling a radiation: a review of the diversity, stratigraphic distribution, biogeography, and evolution of horned dinosaurs (Ornithischia: Ceratopsidae). pp. 405-427 in New Perspectives on Horned Dinosaurs: The Royal Tyrell Museum Ceratopsian Symposium, M.J. Ryan, B.J. Chinnery-Allgeier, and D.A. Eberth (eds.) Indiana University Press, Bloomington and Indianapolis.

Sampson, S. D., M. J. Ryan, and D. H. Tanke. 1997. Craniofacial ontogeny in centrosaurine dinosaurs (Ornithischia: Ceratopsidae): taxonomic and behavioral implications. Zoological Journal of the Linnean Society 121:293–337.

Scannella, J. 2010. *Triceratops*: A model organism for deciphering dinosaur heterochrony. Journal of Vertebrate Paleontology, SVP Program and Abstracts Book 30 (2): 158A.

Scannella, J.B., and D.W., Fowler. 2009. Anagenesis in *Triceratops*: Evidence from a newly resolved stratigraphic framework for the Hell Creek Formation p. 148-149 in Storrs, G.W. (ed.), 9th North American Paleontological Convention Abstracts. University of Cincinnati, Cincinnati Museum Center Scientific Contributions 3, Cincinnati, Ohio.

Scannella J.B., and D.W. Fowler. 2014. A stratigraphic survey of *Triceratops* localities in the Hell Creek Formation, northeastern Montana (2006-2010). pp. 313-332 in Through the End of the Cretaceous in the Type Locality of the Hell Creek Formation in Montana and Adjacent Areas, G.P. Wilson, W.A. Clemens, J.R.

Horner, and J.H. Hartman (eds.) Geological Society of America Special Paper, Boulder, Colorado.

Scannella J. B., and J.R. Horner. 2010. *Torosaurus* Marsh, 1891, is *Triceratops* Marsh, 1889 (Ceratopsidae: Chasmosaurinae): synonymy through ontogeny. Journal of Vertebrate Paleontology 30(4): 1157-1168.

Scannella J. B., and J. R. Horner. 2011. '*Nedoceratops*': An example of a transitional morphology. PLoS ONE 6(12): e28705. doi:10.1371/journal.pone.0028705

Scannella, J. B., and D. W. Fowler. 2014. A stratigraphic survey of *Triceratops* localities in the Hell Creek Formation, northeastern Montana (2006–2010). Geological Society of America Special Papers 503:313–332.

Scannella, J. B., D. W. Fowler, M. B. Goodwin, and J. R. Horner. 2014. Evolutionary trends in *Triceratops* from the Hell Creek Formation, Montana. Proceedings of the National Academy of Sciences 111:10245–10250.

Scannella, J.B., D. W. Roberts, and J.R. Horner. In prep. A morphometric analysis of casque development and variation in the Black-casqued Hornbill (*Ceratogymna atrata*)

Schneider G. 1945. *Rhinoplax vigil* (Forst.) und sein Nestling. Vernhandlungen der Naturforschenden Gesellschaft in Basel 61: 1-36.

Schott R.K., D.C. Evans, M.B. Goodwin, J.R. Horner, C.M. Brown and N.R. Longrich. 2011. Cranial ontogeny in *Stegoceras validum* (Dinosauria: Pachycephalosauria): a quantitative model of pachycephalosaur dome growth and variation. PloS one, 6(6): e21092.

Schott, R. K., and D. C. Evans. 2012. Squamosal ontogeny and variation in the pachycephalosaurian dinosaur *Stegoceras validum* Lambe, 1902, from the Dinosaur Park Formation, Alberta. Journal of Vertebrate Paleontology 32:903–913.

Sereno P.C., L. Tan, S.L. Brusatte, H.J. Kriegstein, Zhao X., and K. Cloward. 2009. Tyrannosaurid skeletal design first evolved at small body size. Science 326: 418-422.

Sereno, P. C. 1986. Phylogeny of the bird-hipped dinosaurs (Order Ornithischia). National Geographic Society Research 2:234-256.

Simpson G.G. 1944. Tempo and mode in evolution. Columbia University Press, New York.

Simpson G.G. 1951. The species concept. Evolution 5: 285-298.

Simpson G.G. 1953. The major features of evolution. New York, Columbia University Press, New York: 434 pp.

Smith, A. B. 1994. Systematics and the Fossil Record: Documenting Evolutionary Patterns. Blackwell Scientific Publications, Oxford: 223 pp.

Sorenson, M. D. , and E. A. Franzosa. 2007. TreeRot, version 3. Boston University, Boston, MA.

Stacklies, W., H. Redestig, M. Scholz, D. Walther, and J. Selbig. 2007. pcaMethods—a bioconductor package providing PCA methods for incomplete data. Bioinformatics 23:1164–1167.

Stauffer D.J. and T.B. Smith TB. 2004. Breeding and nest site characteristics of the Black-casqued Hornbill *Ceratogymna atrata* and White-thighed Hornbill *Ceratogymna cylindricus* in south-central Cameroon. Ostrich-Journal of African Ornithology 75(3): 79-88.

Sternberg, C. M. 1949. The Edmonton fauna and description of a new *Triceratops* from the Upper Edmonton member; phylogeny of the Ceratopsidae. Annual Report of the National Museum of Canada, Bulletin 113:33-46.

Sullivan, R. M., A. C. Boere, and S. G. Lucas. 2005. Redescription of the ceratopsid dinosaur *Torosaurus utahensis* (Gilmore, 1946) and a revision of the genus. Journal of Paleontology 79(3):564–582.

Sullivan, R. M., and S. G. Lucas. 2010. A new chasmosaurine (Ceratopsidae, Dinosauria) from the Upper Cretaceous Ojo Alamo Formation (Naashoibito Member), San Juan Basin, New Mexico, pp. 169-180 in New Perspectives on Horned Dinosaurs: The Royal Tyrell Museum Ceratopsian Symposium, M. J. Ryan, B. J. Chinnery-Allgeier, and D. A. Eberth (eds.) Indiana University Press, Indiana University Press.

Swisher, C.C., L., Dingus. and R.F., Butler. 1993. 40Ar/39Ar dating and magnetostratigraphic correlation of the terrestrial Cretaceous-Paleogene boundary and Puercan mammal age, Hell Creek-Tullock Formations, eastern Montana. Canadian Journal of Earth Sciences 30(9):1981–1996, doi:10.1139/e93-174.

Swofford D. L. 2003. PAUP*. Phylogenetic Analysis Using Parsimony (*and Other Methods). Version 4. Sinauer Associates, Sunderland, Massachusetts.

Tanke, D.H. 2010. Ceratopsian discoveries and work in Alberta, Canada: A historical review and census, in Ryan, M.J., B.J., Chinnery-Allgeier, and D.A., Eberth, (eds.), New Perspectives on Horned Dinosaurs: The Royal Tyrrell Museum Ceratopsian Symposium. Indiana University Press, Bloomington, Indiana, supplemental CD-ROM, 488 pp.

Tanke, D.H, and A. A. Farke. 2007. Bone resorption, bone lesions and extra cranial fenestrae in ceratopsid dinosaurs: a preliminary assessment; pp. 319-347 in K. Carpenter (ed.), Horns and Beaks: Ceratopsian and Ornithopod Dinosaurs. Indiana University Press, Bloomington and Indianapolis.

Thulborn, R. A. 1992. Nest of the dinosaur Protoceratops. Lethaia 25:145–149.

Tokaryk T.T. 1986. Ceratopsian dinosaurs from the Frenchman Formation (Upper Cretaceous) of Saskatchewan. Canadian Field-Naturalist 100(2): 192-196.

Tokaryk, T. T. 1997. First evidence of juvenile ceratopsians (Reptilia: Ornithischia) from the Frenchman Formation (late Maastrichtian) of Saskatchewan. Canadian Journal of Earth Sciences 34:1401–1404.

Tsuihiji, T. 2010. Reconstructions of the axial muscle insertions in the occipital region of dinosaurs: evaluations of past hypotheses on marginocephalia and tyrannosauridae using the Extant Phylogenetic Bracket approach. The Anatomical Record 293:1360-1386.

Tumarkin-Deratzian, A.R. 2009. Evaluation of long bone surface textures as ontogenetic indicators in centrosaurine ceratopsids. The Anatomical Record 292:1485-1500.

Tumarkin-Deratzian, A. R. 2010. Histological evaluation of ontogenetic bone surface texture changes in the frill of *Centrosaurus apertus*. pp. 251-263 in M.J. Ryan, B.J. Chinnery-Allgeier, and D.A. Eberth DA, (eds.) New perspectives on horned dinosaurs. Indiana University Press, Bloomington.

Turner, B.W. 2010. Testing the Local Diachroneity of the Terrestrial Lithostratigraphic KPg Boundary, Northern Montana [M.S. thesis]: Montana State University, Bozeman, Montana, 187 pp.

Ukrainsky, A.S. 2007. A new replacement name for *Diceratops* Lull, 1905 (Reptilia: Ornithischia: Ceratopsidae). Zoosystematica Rossica 16: 292.

Ukrainsky, A.S. 2009. Synonymy of the genera *Nedoceratops* Ukrainsky, 2007 and *Diceratus* Mateus, 2008 (Reptilia: Ornithischia: Ceratopsidae). Paleontologicheskii Zhurnal1: 108.

Wagner P.J., and D.H. Erwin. 1995. Phylogenetic patterns as tests of speciation models. pp. 87- 122 in New Approaches to Speciation in the Fossil Record, D.H. Erwin, and R.H. Anstey (eds.) Columbia University Press, New York.

Wallace A.R. 1863. The Bucerotidae or Hornbills. The Intellectual Observer 3: 309-318.

Wilson, G.P. 2004. A Quantitative Assessment of Evolutionary and Ecological Change in Mammalian Faunas Leading Up To and Across the Cretaceous-Tertiary Boundary, Northeastern Montana [Ph.D. dissertation]: University of California, Berkeley, California, 412 p.

Wilson, G.P. 2005. Mammalian faunal dynamics during the last 1.8 million years of the Cretaceous in Garfield County, Montana. Journal of Mammalian Evolution. 12(1-2): 53–76, doi:10.1007/s10914-005-6943-4.

Witmer L.M. 1995. The extant phylogenetic bracket and the importance of reconstructing soft tissues in fossils. Functional Morphology in Vertebrate Paleontology, 1: 19-33.

Wolfe, D.G. and J.I. Kirkland. 1998. *Zuniceratops christopheri* n. gen. & n. sp., a ceratopsian dinosaur from the Moreno Hill Formation (Cretaceous, Turonian) of west-central New Mexico; pp. 303-317 in ed. S.G. Lucas, J.I. Kirkland and J.W. Estep, Lower and Middle Cretaceous Terrestrial Ecosystems vol 14. Albuquerque, NM: New Mexico Museum of Natural History and Science Bulletin.

Wu X-C., D.B., Brinkman, D.A., Eberth, D.R., Braman. 2007. A new ceratopsid dinosaur (Ornithischia) from the uppermost Horseshoe Canyon Formation (upper Maastrichtian), Alberta, Canada. Canadian Journal of Earth Sciences 44: 1243-1265.

Xu X., C.A. Forster, J.M. Clark, J. Mo. 2006. A basal ceratopsian with transitional features from the Late Jurassic of northwestern China. Proceedings of the Royal Society London B. 273(1598): 2135-2140.

APPENDIX A

SUPPLEMENTARY INFORMATION FOR CHAPTER 5

SI Text. Supporting information for: Evolutionary trends in *Triceratops* from the Hell Creek Formation, Montana

1) Variation in parietal-squamosal frill
2) Morphology of the rostrum
3) Other triceratopsin taxa
4) *Triceratops* biogeography
5) Stratigraphic placement of upper M3 specimens
6) Calculation of basal skull length
7) Details of cladistic analysis
8) Details of stratocladistic analysis
9) Character list and data matrix
10) References

Institutional Abbreviations

AMNH, American Museum of Natural History, New York, USA; BYU, Brigham Young University Museum of Paleontology, Provo, USA; MOR, Museum of the Rockies, Bozeman, USA; MPM, Milwaukee Public Museum, Milwaukee, USA; MWC, Museum of Western Colorado, Grand Junction, USA; OMNH, Oklahoma Museum of Natural History, Norman, USA; ROM, Royal Ontario Museum, Toronto, CA; RTMP, Royal Tyrrell Museum, Drumheller, Alberta, CA; SMP, State Museum of Pennsylvania, Harrisburg, USA; UCMP, University of California Museum of Paleontology, Berkeley, USA; USNM, National Museum of Natural History, Washington D.C., USA; YPM, Yale Peabody Museum, New Haven, USA.

Variation in Parietal-Squamosal Frill.

Scannella and Horner (2011) suggested that the number of epiossifications present in *Triceratops* may vary stratigraphically. Often, epiossifications are unpreserved or are

detached from the parietal-squamosal frill; which complicates testing of this hypothesis. Data currently available highlights variation in epiossification number and position; as the number and configuration can vary between the squamosals of a single individual [e.g. Museum of the Rockies (MOR) 1120]. Additionally, there may be an ontogenetic component to epiossification number and position in chasmosaurines (see, for example, Scannella and Horner, 2010; 2011; Mallon et al., 2011). Hell Creek Formation (HCF) specimens with the highest numbers of epiparietals (MOR 1122; MOR 3081) and episquamosals (MOR 1120; MOR 1122; MOR 3081) are found lower in the formation.

The development of fenestrae also varies within *Triceratops* (Scannella and Horner, 2010; 2011; but see Farke, 2011; Longrich and Field, 2012; Maiorino et al., 2013). A pronounced transition in thickness on the ventral surface of the parietal surrounding this area (Scannella and Horner, 2010) is noted in *Triceratops* from the upper unit of the HCF (U3) and at least one specimen from the upper part of the middle unit (M3)(MOR 3045), but lower in the formation there appears to be a more gradual transition in the thickness of the parietal (e.g. MOR 335; MOR 1120; MOR 2985). This finding may suggest that the fenestrae developed later, ontogenetically, in *Triceratops* found stratigraphically higher. Alternatively, if *Triceratops* and *Torosaurus* represent distinct but closely related taxa, *Triceratops* found stratigraphically lower may express more basal parietal features including eventual fenestration of the parietal.

The stratigraphically documented cranial morphological trends expressed in *Triceratops* are thus far consistent with the morphology of specimens referred to *Torosaurus latus* (however we note that the majority of specimens exhibiting the *Torosaurus* morphology were recovered from the lower half of the formation). Precise

locality data for MOR 981 is not available but it was collected in a mudstone located above the basal sandstone. Perhaps the stratigraphically highest known *Torosaurus* from the HCF of Montana, Milwaukee Public Museum (MPM) specimen VP6841 (which, based on study of topographic and geologic maps, appears to have been collected from the upper half of the formation), exhibits an incomplete yet relatively narrow epinasal morphology which is consistent with its stratigraphic position. The observation that a nasal boss morphology appears to occur in relatively mature specimens of *Triceratops* (*Torosaurus* morph; e.g. MOR 1122; MOR 981; Farke, 2007) suggests that development of the boss morphology was ontogenetic, as is seen in some centrosaurine ceratopsids (e.g. Sampson, 1995; Currie et al., 2008). The nasal boss morphology is not exhibited in all *Torosaurus* specimens [MOR 3081, MPM VP 6841,YPM 1830, Yale Peabody Museum (YPM) 1831], and thus the degree to which this feature is developed may vary individually or stratigraphically. UCMP 128561 exhibits a low nasal boss (Cobabe and Fastovsky, 1987; Forster, 1993), however due to the fragmentary nature of the specimen it is unclear if it represents the *Torosaurus* morphology.

Morphology of the Rostrum.

Forster (1996) recognized rostrum morphology as one of the features which distinguishes *T. horridus* from *T. prorsus*. *T. horridus* exhibits a low, elongate rostrum with a sinusoidal dorsal margin whereas in *T. prorsus* the rostrum is shorter and more convex. Longrich and Field (2010) noted that specimens of *T. prorsus* have a more vertically oriented nasal process (= ascending nasal process of the premaxilla sensu Horner and Goodwin (2008), here referred to as the nasal process of the premaxilla

[NPP]) when compared to *T. horridus*. Rostrum morphology appears to be tied to the orientation of the NPP, with a more posteriorly inclined NPP contributing to a low, sinusoidal rostrum in some specimens [e.g. MOR 1120; American Museum of Natural History (AMNH) 5116; National Museum of Natural History (USNM) 1201; YPM 1820].

The angle between the NPP and narial strut appears to increase stratigraphically in the HCF; specimens from the upper M3 and U3 exhibit a larger angle between the NPP and narial strut than specimens found lower in section (Fig. 5.2C).To quantify this shift in morphology, the angle between the NPP and narial strut (Fig. 5.S2) was measured using the Ruler tool in Adobe Photoshop. This angle was measured between the approximate midlines of each process, parallel to the direction representing the primary trend (results presented in Dataset S1; Fig. 5.2). We note that in some more basal taxa (e.g. *Anchiceratops* [Mallon et al., 2011]) the NPP can be oriented nearly perpendicular to the narial strut and as such give the rostrum a more convex appearance in lateral view.

The width of the NPP also affects the rostrum morphology, as a wider NPP reduces the apparent sinuosity of the anterior premaxilla. MOR 3027 and MOR 3045 (both recovered from upper M3) exhibit a more vertically inclined premaxillary articulation with the nasal than specimens found lower in the formation. MOR 3045 (collected ~ 2 m above MOR 3027) exhibits the further derived feature of an anteroposteriorly expanded NPP, contributing to a rostrum which appears even more convex in lateral view.

Rostrum length appears to vary both stratigraphically and ontogenetically. The largest specimens from U3 (e.g. MOR 004, MOR 1625) exhibit more elongate rostra

(Fig. 5.2E, Dataset S1); however even these large specimens do not exhibit the strongly posteriorly inclined NPP and sinusoidal dorsal margin of the rostrum exhibited in specimens referred to *T. horridus*. Evolutionary changes in rostrum morphology may reflect the development of an enlarged epinasal.

Other Triceratopsin Taxa.

Longrich (2011) referred Oklahoma Museum of Natural History (OMNH) specimen 10165, a large ceratopsid specimen recovered from Campanian deposits of New Mexico and previously diagnosed as a gigantic specimen of *Pentaceratops sternbergi* (1998), to the new taxon *Titanoceratops ouranos*. Longrich (2011) proposed that *Titanoceratops* represents the oldest member of the Triceratopsini, the clade which includes *Triceratops*, *Torosaurus*, *Nedoceratops*, and *Ojoceratops*. This specimen exhibits several features consistent with its stratigraphic position relative to HCF *Triceratops*. It has a relatively short epinasal, short arched nasals, a posteriorly inclined NPP, and elongate postorbital horn cores. Given the degree of ontogenetic transformation noted in several marginocephalians (e.g. Scannella and Horner, 2010; 2011; Horner and Goodwin, 2006; 2009), it is possible that many of the features considered to distinguish *Titanoceratops* from *Pentaceratops* (including large size, broad epiossifications, extensive cornual sinuses, strongly anteriorly curved postorbital horn cores, elongate premaxilla [Longrich, 2011]) may instead represent ontogenetic or individual variation within the latter taxon (Fowler et al., 2011; which would be consistent with the original diagnosis by Lehman [1998]). Further assessment of this specimen and its phylogenetic position is beyond the scope of the current study.

Triceratopsin material from the southern region of the western interior of North America includes specimens which have been referred to *Ojoceratops fowleri* and *Torosaurus utahensis* (Gilmore, 1946; Lawson, 1976; Hunt and Lehman, 2008; Longrich, 2011; Sullivan and Lucas, 2010; Sullivan et al., 2005). *Ojoceratops*, from the Ojo Alamo Formation of New Mexico, appears to be closely related to *Triceratops* (Sullivan and Lucas, 2010; Sampson et al., 2010; Mallon, 2011) and has been suggested to be synonymous with the latter taxon (Longrich, 2011). Material referred to *Ojoceratops* thus far consists of isolated or fragmentary elements. Due to the missing morphological information for much of this material, specimens of *O. fowleri* were not included in the current cladistic analysis of HCF *Triceratops*. A nasal horn referred to this taxon [State Museum of Pennsylvania (SMP) VP-1828] exhibits a morphology similar to that observed in several lower unit (L3)/lower M3 *Triceratops*, which is consistent with its stratigraphic position relative to the Hell Creek Formation of Montana. The holotype squamosal (SMP VP-1865) has a greatly reduced anterolateral projection of the squamosal, which has been used to distinguish it from *Torosaurus utahensis*. The degree to which this feature can distinguish *Ojoceratops* from other taxa is unclear; the HCF dataset demonstrates that the morphology of this projection varies within *Torosaurus* and *Triceratops*, and even within a single individual (MOR 2999). Variation in this feature has previously been noted by Hunt and Lehman (2008).

The incomplete or fragmentary nature of specimens which have been referred to *Torosaurus utahensis* has engendered debate regarding what material is referable to this taxon, its stratigraphic and biogeographic range, and which morphologic features, if any, distinguish it from other chasmosaurine taxa (see, for example, Sullivan et al., 2005;

Hunt and Lehman, 2008). This material was not included in the current study of HCF specimens.

Tatankaceratops sacrisonorum is represented by a fragmentary partial skull from the upper (~ 20 m below the K/Pg boundary) HCF in South Dakota (Ott and Larson, 2010). The specimen exhibits an enlarged nasal horn and very small postorbital horn cores. As noted by Longrich (2011), this specimen may represent *T. prorsus*, which would be consistent with its stratigraphic position.

Triceratops Biogeography.

Triceratops in the Frenchman Formation (Saskatchewan, Canada) and Laramie Formation (Colorado, USA) appear to exhibit morphologies consistent with those expressed by specimens in the Hell Creek Formation (HCF), Montana. The base of the Frenchman Formation occupies the uppermost C30n magnetozone, with the majority of the unit residing in C29r up to the K-Pg boundary (Lerbekmo, 1999; Lerbekmo and Braman, 2002), whichindicates the Frenchman Formation correlates largely to U3 of the HCF (Lerbekmo, 2009). Thus, we predict that most *Triceratops* skulls from the Frenchman Formation will exhibit *T. prorsus* morphologies. Diagnostic specimens published to date have been referred to *T. prorsus* (Tokaryk, 1986). Conversely, the uppermost Laramie Formation exhibits reversed magnetic polarity, aligning it with magnetochron C30R (Castle Pines core; Hicks et al., 2003; Raynolds and Johnson, 2003) and making it slightly older than the HCF (Lerbekmos, 2009). Thus, specimens from the Laramie Formation should exhibit cranial morphologies similar to L3 *Triceratops*, and to date this hypothesis remains unfalsified(Carpenter and Young, 2002). The Denver

Formation is partly coeval with the HCF of Montana (Hicks et al., 2002) and is predicted to yield a similar stratigraphically segregated *Triceratops* record. Thus far, specimens collected outside of Montana present morphologies which are consistent with their stratigraphic positions relative to the HCF sample. Increased stratigraphic resolution and sampling from the Lance Formation of Wyoming and other coeval formations will permit further testing of biogeographic hypotheses. The historical record remains unresolved and of limited utility.

Stratigraphic Correlations of
Specimens from Upper M3.

MOR 3027, MOR 3045, and UCMP 113697 were all recovered from high in the middle unit of the HCF. The localities which produced MOR 3027 and MOR 3045 (Fig. 5.S2) are within a mile of one another, which facilitates their relative stratigraphic placement. MOR 3027 was collected ~ 5.5 meters below the Apex Sandstone (the base of U3). MOR 3045 was collected from ~ 7.5 meters below this marker bed, thus initially it appeared that MOR 3045 was found stratigraphically lower than MOR 3027. However, the Apex Sandstone is thicker and cuts down further into the underlying strata just above the quarry which produced MOR 3027. There is a prominent organic-rich horizon which can be laterally traced above both quarries. MOR 3027 was found 5.3 m below this organic-rich bed whereas MOR 3045 was ~ 3.3 meters below. Thus, the quarry which produced MOR 3045 is higher stratigraphically relative to MOR 3027. UCMP 113697 was discovered 21.5 km to the east of these localities. Locally, the Apex Sandstone is ~ 6 meters above the base of the quarry which produced this specimen. An organic-rich horizon which may correlate with the organic-rich bed found above the two MOR

localities is ~ 3 meters above the quarry and thus UCMP 113697 appears to have been collected from roughly the same stratigraphic level as MOR 3045.

Estimation of Basal Skull Length.

In this study, basal skull length was considered the distance from the anteriormost point of the rostrum to the posterior surface of the occipital condyle (following previous researchers) (Forster, 1996; Farke, 2007). Skull length measurements for some specimens were taken from reconstructions (Dataset 5.S1). For some largely complete specimens which do not preserve the occipital condyle, or in which it is obscured (e.g. MOR 004), this distance was approximated by measuring the distance from the anteriormost point of the rostrum to the posterior margin of the lateral temporal fenestra (see Dataset 5.S1). For less complete, or disarticulated specimens, basal skull length was estimated using linear regressions of basal skull length against preserved cranial elements. Linear models relating basal skull length to dentary length (measured from the anteriormost point to the posterior surface of the coronoid process), maxilla length (measured along the lateral surface), occipital condyle area (following Anderson, 1999), and jugal length (measured from the base of the orbit to the distal tip) produced R^2 values of 0.995, 0.979, 0.944, and 0.980 respectively (Dataset 5.S1). The use of multiple elements allowed more specimens to be included in quantitative comparisons. If multiple elements were preserved in a specimen (for example, MOR 2982 has a dentary and jugal), the estimated values for basal skull length produced by the regression analyses were averaged.

Cladistic Analysis.

A cladistic analysis of cranial variation in HCF *Triceratops* initially employed the heuristic search strategy of the program PAUP* 4.0b10 (Swofford, 2003). Nexus files are available on MorphoBank (O'Leary and Kaufman, 2008) as project 1099. Analyses used the random addition sequence with tree-bisection-reconnection (TBR) branch swapping and 1,000 replicates; all most parsimonious trees were saved. Characters were unordered and unweighted. Maxtrees was set to 250,000. Analyses were initially performed using binary coding for morphological characters (see Pleijel, 1995; Frederickson and Tumarkin-Deratzian, 2014). Additional analyses were performed using multistate coding which combined binary characters 10 and 11 (development of the epninasal-nasal protuberance), 25 and 26 (development of the anterolateral projection of the squamosal), and 29 and 30 (number of epiparietals). Support for clades was determined using nonparametric bootstrap resampling (Felsenstein, 1985) in PAUP* 4.0b; 10,000 bootstrap replicates were analyzed with one tree retained per replicate. Application of bootstrap resampling to data in which multistate characters have been distilled to binary characters is problematic (Felsenstein, 1985) but was performed for comparative purposes. In addition, Bremer support indices were calculated using TreeRot.v3 (Sorenson and Franzosa, 2007) and PAUP* 4.0b10 (Swofford, 2003).

This analysis focused on features found to vary within the HCF *Triceratops* dataset. *Eotriceratops* was included in the analysis to test the hypothesis that it represents a taxon distinct from *Triceratops*. As such, characters found to distinguish *Eotriceratops* by Sampson et al. (2010) and characters describing the relative height of the narial process and the morphology of the epijugal (Wu et al., 2007) were examined. Forster

(1996) noted five cranial characters which vary within *Triceratops*. Four of these characters were included in this analysis (Forster's character 4, which describes rostrum shape, was modified in this analysis to reflect the influence of NPP orientation [see Longrich and Field, 2012]). Forster's character 1 (describing the postorbital, jugal, squamosal suture pattern) was not found to vary in the HCF data set. All coded specimens either exhibited the 'primitive' state of the jugal contributing to the dorsal margin of the lateral temporal fenestra, or sutural relationships of this region were unpreserved or were obscured by fusion.

Initially, specimens which were collected or stratigraphically relocated during the Hell Creek Project and which were largely complete or exhibited morphologies not otherwise found within their respective stratigraphic units (e.g. MOR 2552, UCMP 128561) were included in the cladistic analysis. Only post-juvenile stage specimens were included in the analyses (see Campione et al., 2013). MOR 981 exhibits the *Torosaurus* morphology, and was collected from a mudstone above the basal sand of the formation however detailed stratigraphic data is unavailable for this specimen.

The initial strict consensus tree produced using binary coding [most parsimonious trees (MPT) 250,000, 55 steps, consistency Index (CI) 0.7091, homoplasy Index (HI) 0.4000, retention Index (RI) .8400] produced a polytomy of all HCF specimens (Fig. 5.S5 A). The holotype of *Eotriceratops* [Royal Tyrrell Museum (RTMP) 2002.57.7] was recovered as being basal to the HCF dataset, consistent with the initial hypothesis proposed by Wu et al. (2007). The 50% majority tree revealed a succession of specimens which was consistent with stratigraphic position aside from some specimens which were missing a large portion of codeable characters (e.g., MOR 2552 and MOR 3010).

Specimens exhibiting the *Torosaurus* morphology clustered together as basal to the rest of the HCF dataset as these specimens exhibit several features (including a fenestrated parietal) that are observed in more basal taxa. MOR 3011, which preserves relatively thick sections of parietal-squamosal frill but is too fragmentary to be coded for features of these elements, was not distinguished from the *Torosaurus* group.

Re-running the analysis using multistate rather than binary characters produced a polytomy in the strict consensus tree (MPT 250,000, 54 steps, CI 0.7222, HI 0.3889, RI 0.8469), and the 50% majority-rule tree similarly produced a sequence of specimens consistent with stratigraphic position aside from the most fragmentary specimens (Fig. 5.S5B).

The analysis was next rerun after removing the most incomplete specimens (individuals which did not exhibit at least seven codeable features).This analysis resulted in a strict consensus (MPT 250,000, 55 steps, CI 0.7091, HI 0.4000, RI 0.8161) in which specimens were largely recovered in stratigraphic succession (except for MOR 3011 which, as noted above, grouped with *Torosaurus* specimens). MOR 1120 from L3 was found to be the most basal non-*Torosaurus* HCF specimen and MOR 2982 from the lower M3 was recovered as the next most basal. Above MOR 2982 is a large polytomy consisting of specimens from the upper half of the formation. The identical topology was recovered when the multistate matrix was analyzed (MPT 250,000, 54 steps, CI 0.7222, HI 0.3889, RI 0.8214; Fig. 5.3), however a bremer decay value of 2 was recovered for the upper M3-U3 polytomy when the binary matrix was used (as opposed to a value of 1 when the multistate matrix was employed).

The analysis was next run after removing specimens which could not be coded for features of the parietal-squamosal frill. A branch and bound search was used with the furthest addition sequence implemented. The strict consensus tree produced using the binary matrix (MPT 218972, 55 steps, CI 0.7091, HI 0.4000, RI 0.8000; Fig. 5.S5 C) recovered a polytomy of *Torosaurus* specimens as basal to other specimens. MOR 1120 and MOR 2982 from the lower half of the formation were recovered together as basal to a large polytomy of specimens from the upper half of the formation. The multistate analysis (MPT 189820, 54 steps, CI 0.7222, HI 0.3889, RI 0.8077; Fig. 5.S5 D) resulted in greater resolution; MOR 1120 was recovered as basal to the stratigraphically higher MOR 2982. MOR 1122 and MOR 981clustered together. These specimens both exhibit a nasal boss and do not exhibit an epiossification or crenulation spanning the parietal-squamosal margin whereas the third *Torosaurus* specimen (MOR 3081) possesses a narrow epinasal and a parietal-squamosal crenulation. As these features appear to exhibit a large degree of variation within *Triceratops* (Scannella and Horner, 2010), intraspecific variation appears more likely than these differences being taxonomic in nature. We note that in this analysis a midline epiparietal (character 32) was coded as absent in MOR 1122 as the element is not present and there does not appear to be a pronounced crenulation on the midline. Scannella and Horner (2011) suggested the presence of a midline epiparietal in this specimen based on vascular patterns observed on the parietal. The 50% majority tree for both analyses (Fig. 5.S5 E,F) found MOR 3045 to be more derived than MOR 3027. UCMP 113697 clusters with MOR 2924 (U3) in the binary analysis, and with MOR 2924 and MOR 2999 in the multistate analysis. This topology suggests that UCMP 113697 is more derived than other specimens from upper M3

however, we note that this result may be influenced by missing data. MOR 2924 (recovered from the sandstone at the base of U3) preserves a broader posterior surface of the epinasal than other specimens from U3, but does not preserve postorbital horn cores. The anteromedial processes of nasals of MOR 2924 are unobservable due to articulation with the premaxillae. The morphology of the anteromedial processes on the nasals of UCMP 113697 are currently obscured due to the mounting of the disarticulated skull elements for display.

When specimens which did not preserve at least 10 codeable features (in the multistate matrix) were removed from the analysis, the strict consensus trees (binary coding: MPT 7036; 54 steps; CI 0.7222; HI 0.3889; RI 0.8000; Fig. 5.S5 G; multistate coding: MPT 7036, 53 steps, CI 0.7358, HI 0.3774, RI 0.8082; Fig. 5.3B) exhibited an identical topology. *Torosaurus* specimens were recovered as basal to MOR 1120 and MOR 1982, and specimens from the upper half of the formation were again recovered in a large polytomy. When MOR 2924 was removed from the analysis, both analyses (binary coding: MPT 282; 53 steps; CI 0.7358; HI 0.3774; RI 0.8028; Fig. 5.S5 H; multistate coding: MPT 282; 52 steps; CI 0.7500; HI 0.3654; RI 0.8116; Fig. 5.3C) recovered MOR 3045 as basal to U3 specimens and as more derived than UCMP 113697 and MOR 3027, which cluster together.

Stratocladistic Analysis.

Stratocladistics incorporates stratigraphic data into cladistic analyses (see, for example, Fisher, 1994; 2008; Polly, 1997; Pardo et al., 2008; Campione and Reisz, 2010; Rook and Hunter, 2011). A stratocladistic analysis was performed using the program

StrataPhy, which produces trees that can indicate possible ancestor-descendant relationships (Marcot and Fox, 2008). The multistate dataset was used for the analysis, with the specimens MOR 981, MOR 1604, and MOR 2978 removed from the analysis due to ambiguity over their precise stratigraphic position. Rather than coding specimens separately, specimens from the lower M3, upper M3, lower U3, and upper U3 were combined into operational units based on stratigraphic position. MOR 3081 and MOR 3005 were considered separately from other specimens from the same stratigraphic zones due to the distinct ontogenetic (Scannella and Horner, 2010; or, alternatively, taxonomic [Farke, 2011; Longrich and Field, 2012; Maiorino et al., 2013]) morphological differences between these specimens. MOR 3005 is a fragmentary specimen, but preserves thin sections of frill and thus may represent the *Torosaurus* morphology. A single stratigraphic character was added [stratighraphic position: (position 0) stratigraphically below the HCF; (position 1) lower L3; (position 2) upper L3; (position 3) lower M3; (position 4) upper M3; (position 5) lower U3; (position 6) upper U3]. *Arrhinoceratops* (ROM 796) was designated the outgroup. MAXTREES was set to 250,000, and all other parameters were StrataPhy's default settings (Marcot and Fox, 2008).

The inital analysis produced 61 trees with nine topologies (total debt = 64) (Fig. 5.S6 A). Aside from one tree which suggests all operational units arose via cladogenesis, specimens from the upper half of the formation were consistently found to represent an anagenetic succession. The position of operational units from the lower half of the formation varied and were not always consistent with stratigraphic position. This result is likely influenced by the fact that specimens from the lower half of M3 do not preserve

features of the parietal-squamosal frill that would allow them to be distinguished from the *Torosaurus* morphology. MOR 2982 preserves an anterolateral projection of the squamosal, which is consistent with the morphology expressed in several other HCF specimens including the *Torosaurus* specimen MOR 3081. Incorporation of *Torosaurus* specimens into *Triceratops* operational units (total debt = 67, nine trees, three topologies; Fig. 5.S6 B) produced a single tree suggesting all operational units arose via cladogenesis and two additional topologies which include ancestor-descendant relationships. In four trees, all operational units were recovered within an anagenetic lineage except the lower M3 group. This operational unit was recovered as basal to the upper L3 operational unit, suggesting a cladogenetic event. The remaining four trees exhibit a bifurcation event in L3 giving rise to two lineages.

Given the lack of frill characters for the lower M3 operational unit, the influence of *Torosaurus* specimens on the results was examined by pruning all *Torosaurus* from the analysis. This pruning resulted in reduced total debt (57) and 12 trees (Fig. 5.S6 C). Four trees indicate that all HCF operational units represent a single anagenetic lineage with specimens exhibiting the *T. horridus* morphology evolving into *T. prorsus* (Fig. 5.4A). Eight trees recovered two lineages suggested to diverge at some point in L3 or prior to the deposition of the HCF. One lineage gives rise to lower M3 specimens and the other to U3 specimens. This result suggests that two anagenetic lineages, one comprised of specimens referable to *T. horridus* and the other giving rise to *T. prorsus*, coexisted in the HCF (for at least some time) (Fig. 5.4B).

Characters Incorporated in Cladistic
Analysis. First Use in a Cladistic Study is Cited.

1) Postorbital horn core length: (code 0) long (postorbital horn core/basal skull length ratio: ≥0.64 ; (code 1) short (postorbital horn core/basal skull length ratio: <.64 (1). [Forster, 1990 character 58 modified; Forster, 1996, character 2 modified]

2) Cross section of postorbital horn core: (code 0) circular to sub-circular; (code 1) narrow. The postorbital horn cores of some specimens of *Triceratops* (e.g. MOR 2702, MOR 2923) exhibit a markedly narrow morphology which does not appear to be a product of taphonomic distortion. MOR 2923 exhibits no evidence of lateral compression and yet the postorbital horn cores of this specimen have a pronounced ventral keel. Specimens for which apparently laterally compressed postorbital horn cores are likely a result of taphonomic processes (e.g. MOR 2982, MOR 3027) have been coded as '?'.

3) Rostrum shape: (code 0) primary axis of nasal process of premaxilla (NPP) is strongly posteriorly inclined; (code 1) NPP vertical or nearly vertical [Forster, 1990; Forster, 1996, character 4 modified; Longrich and Field, 2012; Fig. 5.S2]

4) Frontoparietal fontanelle: (code 0) open fontanelle; (code 1) closed or constricted due to fusion of frontals and parietals. [Forster, 1990, characters 49 and 50 modified; Forster, 1996, character 3 modified]

5) Epijugal: (code 0) comes to a pronounced peak; (code 1) low and blunt (Longrich, 2010, character 102 modified; Sampson et al., 2010 character 50 modified). Epijugal morphology has been used in phylogenetic studies of chasmosaurines (e.g. Sampson et

al., 2010; Longrich, 2011) and as a diagnostic feature of some taxa. In most specimens of *Triceratops*, the epijugal is a low, blunt element. Specimens exhibiting the *Torosaurus* morphology exhibit an epijugal which comes to a pronounced peak, similar to the condition noted in more basal taxa such as *Eotriceratops* (Wu et al., 2007). At least one large *Triceratops* with a non-fenestrated parietal (MOR 1625) also exhibits a peaked epijugal.

6) Quadratojugal notch: (code 0) present; (code 1) absent. [sensu Gates and Sampson, 2007, character 71 and McDonald et al., 2010, character 16]. The quadrates of *Triceratops* exhibit a pronounced ridge on the antero-lateral surface. In many specimens this ridge is interrupted by a pronounced notch, however in some specimens this notch is not present.

7) Nasal horn length: (code 0) short (length/width ratio < 1.85); (code 1) long (length/width ratio > 1.85). [Forster, 1990, character 28 modified; Forster, 1996, character 5 modified]

8) Dorsal surface of epinasal: (code 0) narrow to peaked; (code 1) broad. The posterior surface of the epinasal varies from being quite broad to nearly flat in some specimens, to being narrow and coming to a pronouned peak in others. The peaked condition is observed in the holotypes of *Arrhinoceratops* and *Eotriceratops*.

9) Nasal: (code 0) short, arched; (code 1) elongate, straight. A short, arched nasal is observed in the holotype of *T. horridus* (YPM 1820) and several other specimens referred

to this taxon. Specimens from U3 of the HCF exhibit a more elongate nasal morphology which lacks pronounced arching of the lateral margin.

10) Anterior nasals and posterior portion of epinasal fused to form a protuberance posterior to epinasal: (code 0) present; (code 1) subtle or absent. Forster (1996) noted a pronounced bump or boss posterior to the nasal horn in UCMP 113697. A similar structure is present in the holotype of *T. 'calicornis'* (USNM 4928) as noted by Ostrom and Wellnhofer (1986). The structure appears to be formed by a combination of the anterior nasals and the posterior portion of the epinasal. Forster (1996) suggested that this feature was due to the incomplete fusion of the epinasal to an underlying boss or horn core; disarticulated nasals reveal no underlying boss (see Horner and Goodwin, 2008) but the anterior nasal can be somewhat thickened relative to the middle segment of this element. Presence of a homologous structure in mature individuals (MOR 1122) suggest that its presence is not a result of incomplete fusion, though the degree to which this feature varies throughout ontogeny is currently unknown. Development of this feature may be tied to evolutionary elongation of the epinasal.

11) Epinasal-Nasal protuberance: (code 0) reduced or absent (code 1) developed into pronounced boss

12) Antero-medial process on nasal: (code 0) present, pronounced (code 1) reduced, constricted or absent (Fig. 5.S3). *Triceratops* from the lower half of the HCF appear to exhibit a distinct process on the antero-medial surface of the nasal, medial to the

rostroventral process (following the terminology of Fujiwara and Takakuwa [2011]). In specimens from U3 in which this process is visible, it is greatly reduced .

13) Posterior projection on epinasal: (code 0) present; (code 1) absent (Fig. 5.S4). The posterior surface of some epinasals exhibits a small but pronounced posterior projection or shelf. The projection appears to be absent in observed specimens from U3. The projection may contribute to formation of the epinasal-nasal protuberance (see character 9).

14) Nasal process of the premaxilla: (code 0) narrow; (code 1) expanded (Fig. 5.S2). In some specimens of *Triceratops* the NPP is narrow, exhibiting only slight antero-posterior expansion. The premaxilla of the holotype of *Eotriceratops* exhibits an extremely narrow NPP. In many specimens of *Triceratops* from relatively high in the HCF, this process is expanded into a wide, nearly square structure (Dataset 5.S1).

15) Midline peak on nasal process of the premaxilla: (code 0) absent; (code 1) present. The nasal process of MOR 3045 exhibits a pronounced dorsal peak anterior to its posterior margin (see Fig. 5.S2 E). This process appears to be absent or greatly reduced in other specimens, but is clearly present in juvenile specimens from U3 (MOR 1110, MOR 2951). The degree to which this feature varies ontogenetically in specimens from the lower half of the formation is currently unknown.

16) Prominence immediately anterior to or descending from the narial strut, directed into interpremaxillary fenestra: (code 0) absent (code 1) present (See Fig. 5.S7 A).

17) Premaxilla, accessory strut in septal fossa: (code 0) no accessory strut; (code 1) strut present [Sampson et al., 2010; character 12]. Many specimens of *Triceratops* appear to exhibit two prominences or struts directed into the interpremaxillary fenestra (characters 16 and 17; see Fig. 5.S7 A). The degree to which these features are developed varies between specimens.

18) Premaxilla, triangular process recess: (code 0) shallow; (code 1) deep [Dodson et al., 2004; character 12 (modified)]

19) Triangular ('narial' sensu Wu et al., 2007) process of premaxilla: (code 0) dorsal margin (at point of contact with narial strut) positioned roughly at or below the ventral margin of the interpremaxillary fenestra; (code 1) dorsal margin of narial process (at point of contact with narial strut) positioned well above ventral margin of interpremaxillary fenestra (see Wu et al., 2007).

20) Ventromedial foramina of the premaxilla positioned (code 0) close together; (code 1) far apart (more than 1.5 times the width of anterior foramen) [see Fig. S7 B]. The large anterior foramen was highlighted in the description of the holotype of *Eotriceratops* by Wu et al., (2007).

21) Posteroventral surface of the posterior 'prong' of premaxilla (sensu Wu et al., 2007): (code 0) comes to a narrow ridge (code 1) broad posterior surface. The prominent prong of the posteriormost premaxilla exhibits a narrow ridge on its posterior surface in some specimens of *Triceratops*. Specimens from U3, including juveniles (MOR 1110; MOR 2951) appear to exhibit a much broader posterior surface of this element. The degree to

which this feature might vary ontogenetically lower in the formation is currently unknown. (See Fig. S7).

22) Posterior prong of premaxilla: (code 0) broad surface for articulation with nasal; (code 1) exhibits a pronounced ridge on the lateral surface and a constricted area for articulation with the nasal (Fig. S6).

23) Episquamosal or squamosal crenulation number (Farke et al., 2011, character 55 modified): (code 0) seven or more; (code 1) six or fewer.

24) Convex margin of squamosal (code 0) absent; (code 1) present (see Longrich and Field, 2012). Longrich and Field (2012) noted that specimens of *T. prorsus* tend to exhibit a strongly convex margin of the squamosal. This study finds the shape of the squamosal to vary within *Triceratops* with some specimens which exhibit *T. horridus* morphologies (MOR 1120) possessing more convex squamosals than other specimens which exhibit *T. prorsus* morphologies (MOR 2702; Dataset 5.S1). This variation is likely tied to ontogenetic elongation of this element (see Scannella and Horner, 2010). Specimens from higher in the HCF appear to exhibit the convex morphology for a longer period of time, ontogenetically**.** In this study, specimens were coded as possessing a convex squamosal if the ratio of sqamosal length to the distance to the squamosal's lateral margin (measured from and perpendicular to the line representing length) was ≤ 4 (see Dataset 5.S1).

25) Anterolateral projection on squamosal (see Sullivan et al., 2005): (code 0) present; (code 1) greatly reduced or absent

26) Anterolateral projection on squamosal: (code 0) pronounced, forming strongly concave anterior margin of the squamosal; (code 1) reduced or absent (see Sullivan et al., 2005). Sullivan et al. (2005) noted that *Torosaurus latus* specimens exhibit a greatly pronounced projection of the anterolateral surface of the squamosal which causes the otic notch to become constricted. This projection is present to various degrees in many specimens of *Triceratops*, however in some it is greatly reduced (nearly absent).

27) Squamosal bar (code 0) present; (code 1) absent (Forster, 1990, character 90 modified; Sampson et al., 2010, character 64 modified)

28) Ventral surface of parietal in areas surrounding fenestrae/incipient fenestrae: (code 0) smooth transition in thickness; (code 1) thickness transitions in pronounced step from thicker to thinner bone. Scannella and Horner (2010) noted distinct thinning regions on the ventral surface of the parietal of many *Triceratops* specimens. This region is often rimmed by a pronounced transition in thickness, from thick bone posteriorly to far thinner bone within the depression ("incipient fenestra"; but see Farke, 2011; Longrich and Field, 2012; Tsuihiji, 2010). However, in some specimens of *Triceratops* the transition in thickness in these regions is more gradual and lacks the pronounced step between thicker and thinner bone. MOR 1122, a specimen with fenestrae, exhibits a trace of this step along the edge of a fenestra. The holotype of *'Nedoceratops hatcheri'* (USNM 2412) also appears to exhibit a slight step around its reduced parietal fenestra (Scannella and Horner, 2011). A distinct ventral parietal step appears to be more common in specimens found higher in section.

29) Number of epiparietals or epiparietal crenulations: (code 0) four or fewer; (code 1) five or more [Holmes et al., 2001, character 28 modified; Forster, 1990, character 46 modified]

30) Number of epiparietals or epiparietal crenulations: (code 0) 5 or fewer; (code 1) 6 or more [Holmes et al., 2001 character 28 modified; Forster, 1990, character 46 modified]

31) Parietal fenestrae: (code 0) present; (code 1) absent (Forster, 1990; character 84 modified)

32) Epiossification or crenulation on midline of parietal: (code 0) absent (code 1) present [(Forster, 1996; Sampson et al., 2010, character 95 modified)]. Scannella and Horner (2011) presented evidence suggesting the presence of a midline epiparietal on MOR 1122. For the purposes of the present analysis, epiossification positions were coded based either on presence of the element or a pronounced marginal crenulation indicating position on the parietal-squamosal frill.

33) Epiossification or crenulation spanning parietal-squamosal contact: (code 0) present; (code 1) absent [Farke et al., 2011; character 43 modified)].

Data Matrix.

Specimen codings for this analysis. ROM 796 is the holotype of *Arrhinoceratops brachyops*; RTMP 2002.57.7 is the holotype of *Eotriceratops xerinsularis*.

Matrix (Binary Coding)

ROM796	00010?00000??????00???00000(0 1)0000?
RTMP2002.57.7	0?0?0000????0000010?????????????0
MOR1122	10010001000????0?1?0??00000(0 1)11001
MOR3081	10??0?00?00?????????0??00010010000
MOR1120	1000?0010000?00111?100(0 1)(0 1)001000?10
MOR2552	00?01?????????????????????1?????1
MOR2985	??????????????????????????00110?????
MOR3005	????????0??0?????????0?????0????1
MOR2982	1?0?1?01?01??0?11????0??01???????
MOR3010	1?????01?000??????????????????????
MOR3011	??0???01???000?01????????????????
UCMP113697	0010??11?01??????????1?1011?00110
MOR3027	0?10?0??1??0000101?101?0011000?01
MOR3045	1010?0?1???00111???111100111001l0
UCMP128561	??????01????????1????????????????
MOR2574	101???101??1110111????????10???0?
MOR2702	?11??010?10??10?1???11?01111?????
MOR1625	??1?0?10?10????11101??111111?????
MOR2924	??1???111???11???1??11110111??1??
MOR2978	1??1??10110????????????11111??1??
UCMP136092	1??????????????????????11011???1??
MOR2936	?????01????11??0???11??11???????
MOR2979	11?1?0??????????????11??????????0
MOR2971	??1???10?10??1?11101????????????
UCMP137263	10??????1??1????????????????1?????0
MOR004	??111?10110????????????11?11?00110
MOR2999	10?0?1??1??1???????????1(0 1)(0 1)11100?10
MOR2923	11?1??101????????????????????0010?
MOR1604	1?1?1011110?????11??????11???????
MOR981	0?0???010????????????????????010001

Alternative Multistate Characters:

Character 10: Protuberance posterior to epinasal (code 0) very subtle or absent; (code 1) present, prominent (2) enlarged into a pronounced bump or boss (see Forster [1996] and Ostrom and Wellnhofer [1986])

Character 24: Anterolateral projection on squamosal: (code 0) present, projects anteriorly producing strongly concave anterior margin of the squamosal; (code 1) anterior

projection present but does not project strongly anteriorly; (code 2) greatly reduced or absent (see Sullivan et al., 2005)

Character 27: Number of epiparietals or parietal crenulations per side of parietal: (code 0) 4 or fewer; (code 1) 5; (code 2) 6 or more (Holmes et al., 2001, character 28 modified; Forster 1996,character 46 modified; Sampson et al., 2010, character 93 modified)

Matrix (Multistate)

ROM 796	00010?0001??????00???0000(0 1)000?
RTMP2002.57.7	0?0?0000????0000010??????????0
MOR1122	1001000101????0?1?0??0000(0 1)2001
MOR3081	10??0?00?1????????0??001001000
MOR1120	1000?001010?00111?100(0 1)(0 1)0100?10
MOR2552	00?01??????????????????1????1
MOR2985	??????????????????????0110????
MOR3005	????????0?0?????????0????0???1
MOR2982	1?0?1?01?2??0?11????0??1??????
MOR3010	1?????01?10????????????????????
MOR3011	??0???01??000?01?????????????
UCMP113697	0010??11?2??????????1?111?0110
MOR3027	0?10?0??1?0000101?101?01100?01
MOR3045	1010?0?1??00111???111101110110
UCMP128561	??????01???????1?????????????
MOR2574	101???101?1110111???????10??0?
MOR2702	?11??010?0??10?1???11?0211????
MOR1625	??1?0?10?0????11101??11211????
MOR2924	??1???111??11???1??1111111?1??
MOR2978	1??1??1010????????????1211?1??
UCMP136092	1??????????????????????1111??1??
MOR2936	?????01????11??0???11??2??????
MOR2979	11?1?0?????????????11????????0
MOR2971	??1???10?0??1?11101???????????
UCMP137263	10??????1?1?????????????1????0
MOR004	??111?1010????????????11?1?0110
MOR2999	10?0?1??1?1???????????1(0 1)(1 2)110?10
MOR2923	11?1??101?????????????????010?
MOR1604	1?1?101110?????11??????2??????
MOR981	0?0???010?????????????????01001

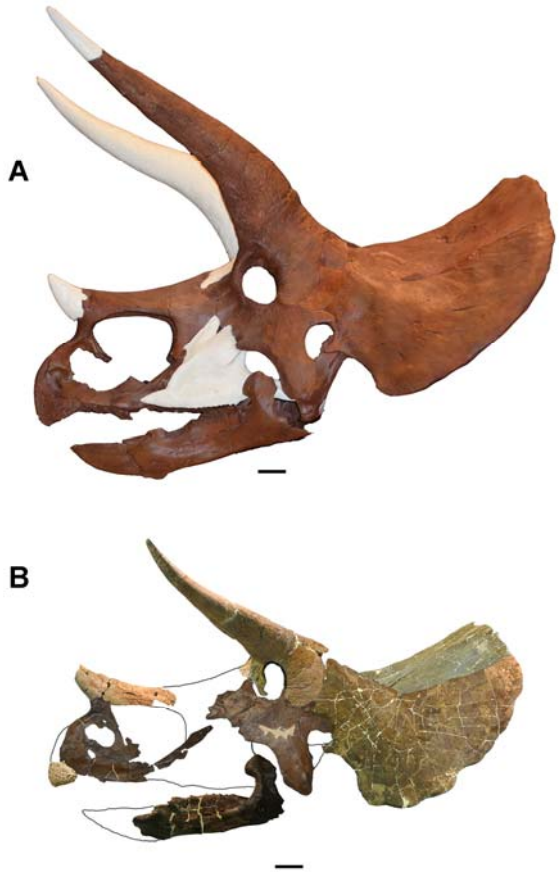


Figure 5.S1. *Triceratops* from upper M3. *(A)* MOR 3027 (cast), a large subadult. *(B)* MOR 3045, subadult recovered from ~ 2 m stratigraphically higher than MOR 3027. These specimens exhibit a combination of primitive and derived features. Both specimens exhibit a more convex rostrum than *Triceratops* found stratigraphically lower. MOR 3045 represents the lowest occurrence of a wide NPP in the HCF dataset. Parietal, squamosal, postorbital, nasal, and epinasal of MOR 3045 mirrored. Orbit is crushed. (Scale bars: 10 cm.)



Figure 5.S2. Variation in the nasal process of the premaxilla. *(A*) RTMP 2002.57.7, the holotype of *Eotriceratops*. *(B)* MOR 1120, collected from L3. *(C)* MOR 3011, collected from the lower part of M3. *(D)* MOR 3027, collected from upper M3. *(E)* MOR 3045, collected from upper M3. This specimen exhibits a pronounced peak on the nasal process (arrow) which is anterior to the posterior margin, a feature which is observed in juveniles from U3. *(F)* MOR 2574, collected from the lower U3. *(G)* MOR 2702, collected from the lower U3 (image mirrored for comparison). Specimens from U3 (F-G) exhibit a wider NPP; MOR 3045 represents the stratigraphically lowest occurrence of a wide NPP. MOR 2574 and MOR 2702 were collected from a multi-individual bone bed and exhibit variation in the morphology of the NPP. A trend towards an increased angle between the NPP and NS is noted in the HCF sample (Dataset 5.S1). NPP, nasal process of the premaxilla. NS, narial strut. (Scale bars: 10cm; *B*-*G* are to the same scale.)

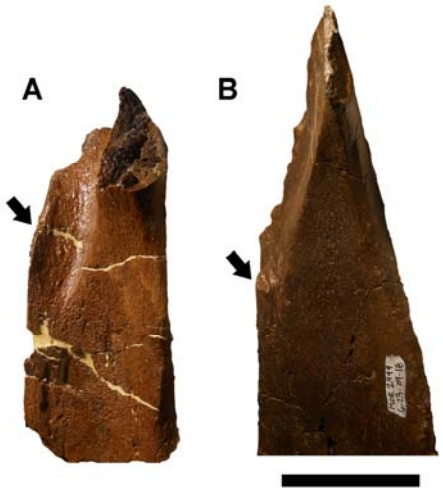


Figure 5.S3. Variation in the anteromedial process of the nasal. *(A)* MOR 3027 (from upper M3) expresses a prominent process on the anteromedial surface of the nasal. *(B)* MOR 2999 (from U3); this process is greatly reduced. (Scale bar: 5 cm.)

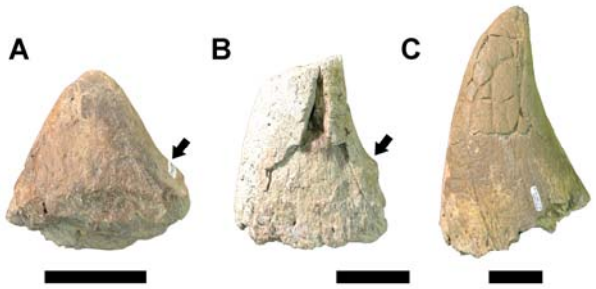


Figure 5.S4. Some specimens exhibit a pronounced shelf or projection on the posterior surface of the epinasal (indicated by arrow; character 13). *(A)* MOR 989, stratigraphic position to be determined. *(B)* MOR 3045 from upper M3. *(C)* MOR 2924 from U3. (Scale bars: 5 cm.)

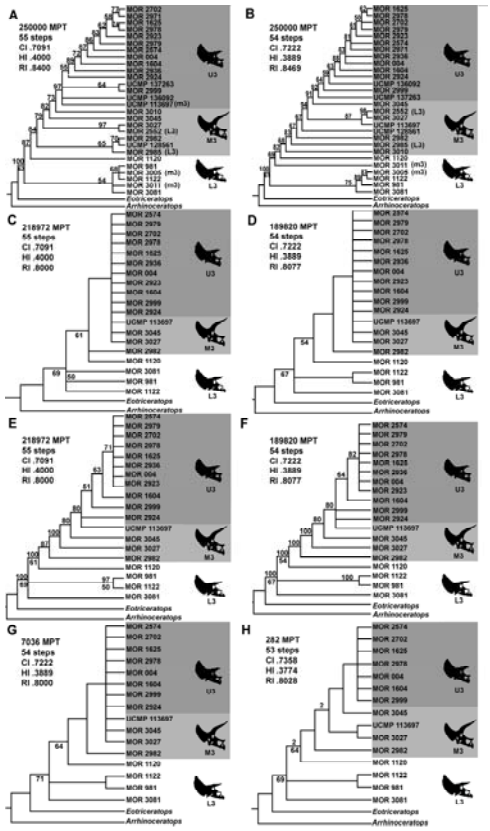


Figure 5.S5. Additional results of cladistic analyses of HCF *Triceratops*. (*A*) 50% majority-rule consensus tree produced by initial analysis using binary coding. Bootstrap support values below nodes. Percent occurrence for nodes are reported above horizontal lines. Specimens group according to relative stratigraphic position, however several fragmentary specimens are recorded in positions inconsistent with stratigraphic position. MOR 981, MOR 1122, MOR 3081, and MOR 3005 exhibit the *Torosaurus* morphology. *(B)* 50 % majority rule tree produced by initial analysis using multistate coding. *(C)* Strict consensus tree produced once specimens which could not be coded for characters of the parietal-squamosal frill are removed (binary coding, branch and bound search). Bremer decay values greater than one reported above nodes. (D) Strict consensus tree produced once specimens which could not be coded for characters of the parietal-squamosal frill are removed (multistate coding, branch-and-bound search). (E) 50% majority-rule consensus tree for analysis in which specimens which specimens which could not be coded for characters of parietal-squamosal frill are removed (binary coding, branch-and-bound search). (F) 50% majority-rule consensus tree for analysis in which specimens which specimens which could not be coded for characters of parietal-squamosal frill are removed (multistate coding, branch-and-bound search). *(G)* Strict consensus tree for analysis including only specimens exhibiting at least 10 cranial characters (in the multistate matrix); binary codings (branch-and-bound search). *(H)* Strict consensus tree for analysis after MOR 2924 is removed from the matrix; binary codings (branch-and-bound search).

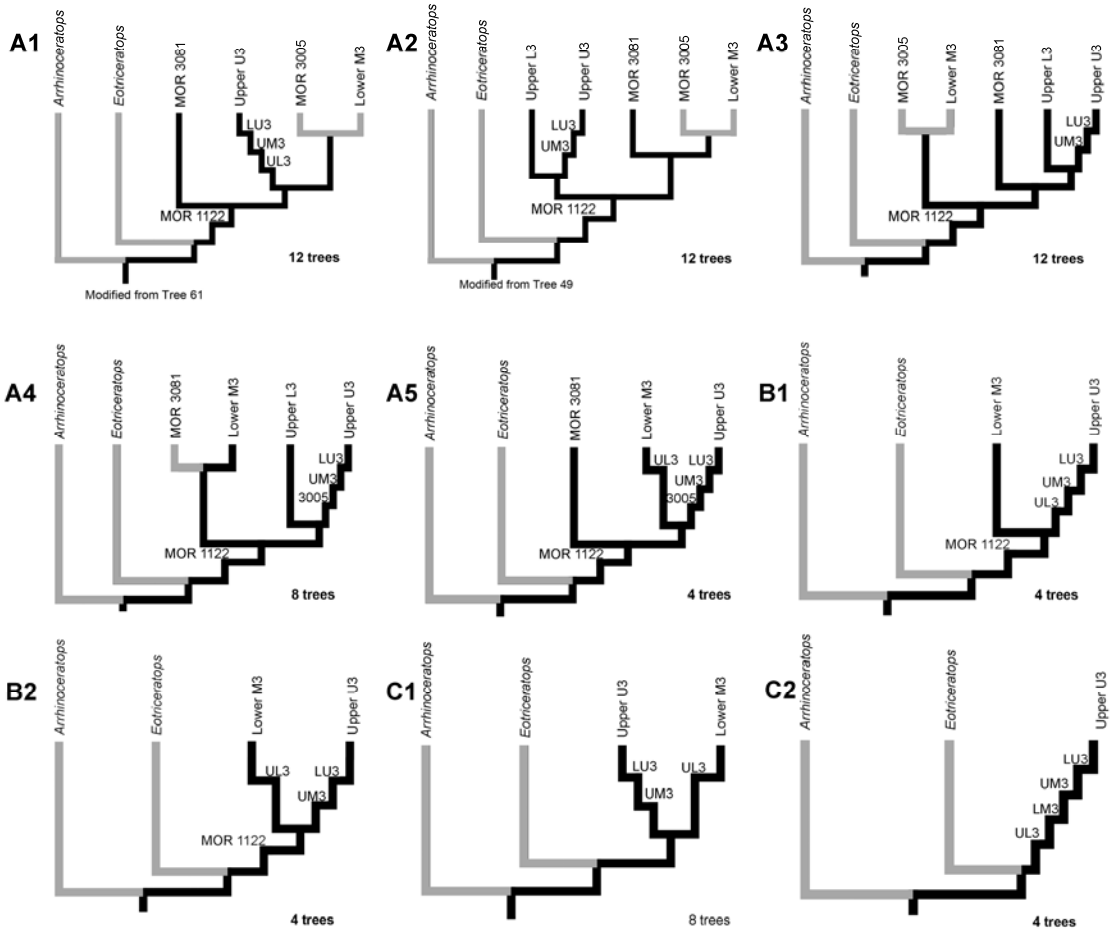


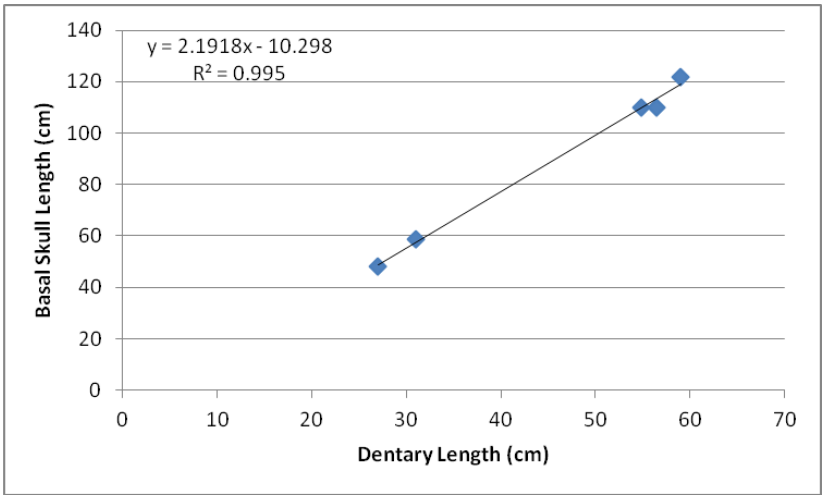
Figure 5.S6. Results of stratocladistic analyses. *(A)* Topologies produced in the initial analysis, in which specimens exhibiting the *Torosaurus* morphology are considered separately from other operational units (61 trees, nine topologies, Debt = 64). Nearly all topologies recover specimens from the upper half of the HCF in an anagenetic sequence, whereas positions for specimens from the lower half of the formation exhibit variation. Nexus file including all tree results are available on Morphobank as project 1099 (O'Leary and Kaufman, 2008). *(B)* Result when specimens exhibiting the *Torosaurus* morphology are incorporated into operational units (nine trees, three topologies, debt = 67). MOR 3081 and MOR 1120 are combined into an upper L3 operational unit; MOR 3005 is incorporated into the lower M3 operational unit. An additional topology suggesting a purely cladogenetic scenario was also recovered. *(C)* Results when *Torosaurus* specimens are pruned from the analysis. Twelve trees are produced and two topologies incorporating anagenesis are recovered (Debt = 57). Gray branches represent operational units which are also recovered as being ancestral in trees presenting the same topology.



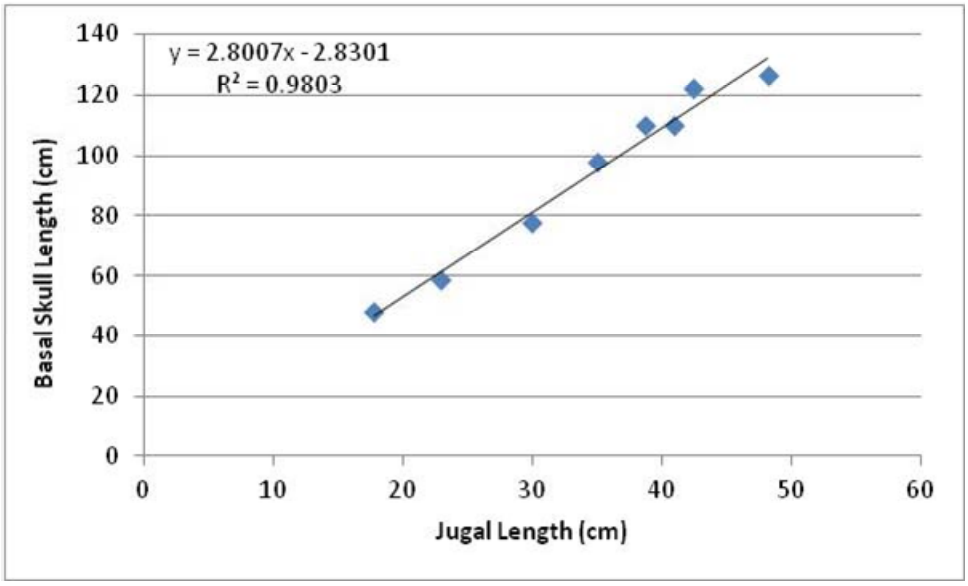
Figure 5.S7. Additional characters of the *Triceratops* premaxilla. *(A)* Rostrum of MOR 1625 (from U3). Black arrow indicates prominence anterior to the narial strut which projects into the interpremaxillary fenestra. White arrow indicates accessory strut in the septal fossa (Sampson et al., 2010, character 12). Scale bar, 5 cm. *(B)* Ventral view of the left premaxilla of MOR 1120. Arrows indicate primary ventro-medial foramina which penetrate the medial shelf. In this specimen these foramina are widely spaced, while in some they are positioned more closely together (≤ 1.5 x width of the anterior foramen). Scale bar, 10 cm. *(C-F)* Posterior prong of the premaxilla (characters 21-22). *(C)* Lateral view of the posterior prong of the left premaxilla of MOR 1120 (from L3). *(D)* Posteroventral surface of prong. *(E)* Lateral view of the posterior prong of the left premaxilla of MOR 2702 (from U3). *(F)* Posteroventral surface of premaxillary prong of MOR 2702. The posterior portion of the prong is narrow and comes to a sharp ridge (indicated by black arrows) in MOR 1120, which contrasts with the condition seen in specimens from U3 in which the posterior surface of the prong is broad. Juvenile specimens from U3 exhibit a broad posterior surface, similar to the condition observed in MOR 2702. Red arrows highlight the lateral surface of the prong; some specimens exhibit a more constricted lateral surface with a pronounced lateral ridge. (Scale bar, 10 cm.)

Dataset 5.S1 (Appendix 1)

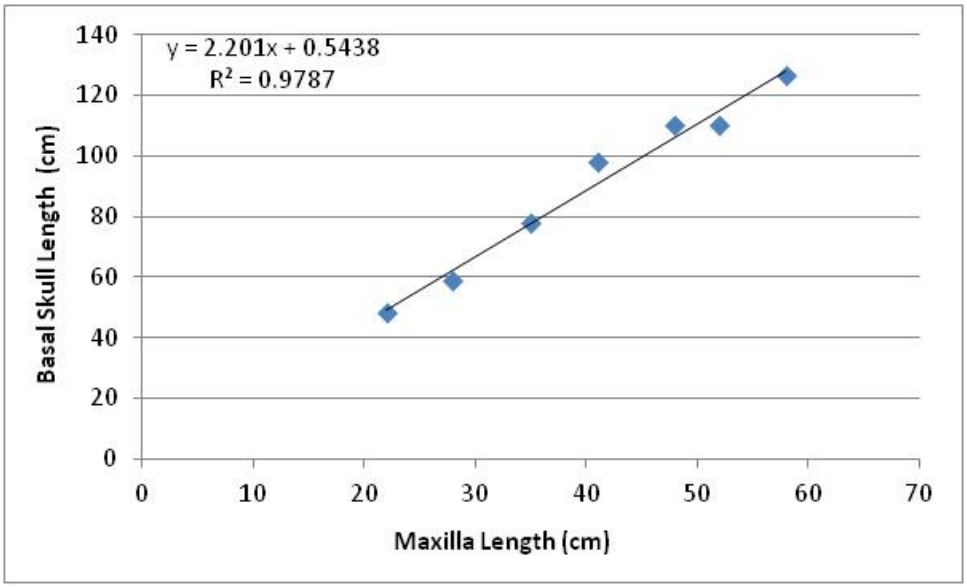
Basal Skull Length (BSL) Estimations			
Specimen No.	Unit	Dentary L. (cm)	BSL (cm)
MOR 1199	TBD	27	48.3
MOR 2951	U3	31	58.6
MOR 3027	M3	56.5	110
MOR 1604	TBD	54.8	110
MOR 004	U3	59	122
Estimates :			
UCMP 154452	U3	15.9	24.55162
MOR 2928	U3	40.5	78.4699
MOR 3081	L3	56.5	113.5387
MOR 2982	M3	50.5	100.3879
MOR 3010	M3	est. 50	99.292
MOR 3045	M3	51.5	102.5797
MOR 2702	U3	60	121.21
MOR 2574	U3	51	101.4838
MOR 2597	U3	46.6	91.83988
MOR 2999	U3	49.5	98.1961
MOR 3011	M3	est. 45	88.333
MOR 3046	U3	51	101.4838
MOR 8147	U3	57	114.6346
MOR 8148	U3	58.5	117.9223
MOR 3042	U3	52	103.6756
MOR 2945	TBD	54	108.0592



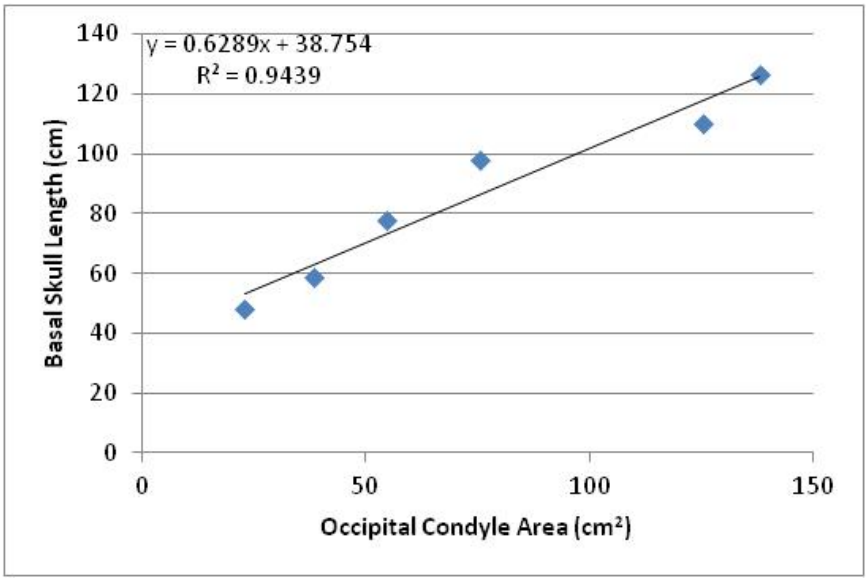
Specimen No.		Jugal L. (cm)	BSL (cm)
MOR 1199	TBD	17.8	48.3
MOR 2951	U3	22.9	58.6
MOR 1110	U3	30	77.6
MOR 3027	M3	38.8	110
MOR 1604	TBD	41	110
MOR 004	U3	42.5	122
MOR 1120	L3	35	98
MOR 1122	L3	48.2	126.4
Estimates:			
MOR 2569	M3	16	41.9811
UCMP 154452	U3	11.5	29.37795
MOR 3064	M3	20.4	54.30418
MOR 2982	M3	35	95.1944
MWC 8574	U3	50.5	138.60525
UCMP 113697	M3	39	106.3972
MOR 3045	M3	36	97.9951
UCMP 136092	U3	41	111.9986
UCMP 137263	U3	35.35	96.174645



Maxilla Length			
Specimen No.		Maxilla L. (cm)	BSL (cm)
MOR 2951	U3	27 (est. 28)	58.6
MOR 1110	U3	34.5 (est. 35)	77.6
MOR 1199	TBD	21.4 (est. 22)	48.3
MOR 1120	L3	37.8 (est. 41)	98
MOR 3027	M3	50 (est. 52)	110
MOR 1122	L3	58	126.4
MOR 1604	TBD	48	110
Estimates:			
MOR 2999	U3	42	92.9858
UCMP 113697	M3	50	110.5938
RTMP2002.57.7		60	132.6038



Occiptial Condyle Area					
		O.C. Width (cm)	**O.C. Height (cm)**	**O.C. Area (cm^2)**	**BSL (cm)**
MOR 1199	TBD	4.7	4.9	23.03	48.3
MOR 2951	U3	6.2	6.2	38.44	58.6
MOR 1110	U3	7.4	7.4	54.76	77.6
MOR 1120	L3	8.9	8.5	75.65	98
MOR 3027	M3	11.1	11.3	125.43	110
MOR 1122	L3	11.7	11.8	138.06	126.4
Estimates:					
UCMP 154452	U3	2.9	2.5	7.25	43.31353
MOR 2999	U3	9.1	9.1	82.81	90.83321
MOR 2979	U3	10.8	10.1	109.08	107.3544
MOR 2552	L3	10.7	10.3	110.21	108.0651
MOR 3081	L3	9.5	9.1	86.45	93.12241
MOR 3041	U3	9.4	9.4	88.36	94.3236
MOR 2551	TBD	9.8	9	88.2	94.22298
MOR 2936	U3	9.3	9.2	85.56	92.56268
MOR 1625	U3	11.9	11.2	133.28	122.5738
MOR 2972	U3	9.6	9.8	94.08	97.92091
UCMP 113697	M3	11.5	10.9	125.35	117.5866
MOR 2924	U3	9.3	9.1	84.63	91.97781
MOR 2570	U3	7.8	7.8	60.84	77.01628
MOR 699	TBD	7.3	7.7	56.21	74.10447
MOR 2959	?L3	9.8	9.6	94.08	97.92091



Note: Basal Skull Length measured from anteriormost point of rostrum to posterior surface of occipital condyle (following Forster, 1996). Values for MOR 004, MOR 1604, and MOR 3027 approximated using distance from anterior point of rostrum to posterior margin of lateral temporal fenestra. Rostra of MOR 1110 and MOR 1122 are reconstructed. Measurements taken from skull reconstructions at MOR (MOR 1199, MOR 1110, MOR 2951, MOR 3027) and from articulated specimens (MOR 004, MOR 1604).

	BSL (cm)	Distance from ant. rostrum to posterior margin of lateral temporal fenestra (cm)
MOR 1199	48.3	48.7
MOR 2951	58.6	57.8
MOR 1122	126.4	125.7

Dataset 5.S1 (Appendix 2)

HCF *Triceratops* nasal horns. TBD = to be determined. Red text indicates incomplete specimens. Green text indicates taphonomic distortion. Blue text indicates juvenile specimens. MOR 3011 is either a very large juvenile or a subadult. *RTMP2002.57.7 is the holotype of *Eotriceratops*, collected from the Horseshoe Canyon Formation of Alberta. Specimens highlighted in green were not included in Spearman's rank correlation test. Measurements are in cm.

Specimen no.	Locality Name	HCF Unit	Level	Length	Width	L/W	Mean	Std. Dev.	Std. Error
MOR 1122	TORO II	L3	lower	12	17.4	0.689655			
MOR 3081	JRH-008	L3	upper	13.9	est. 10.4	1.336538	1.088559	0.350696	0.2479795
MOR 1120	Getaway Trike	L3	upper	5.8	6.9	0.84058			
MOR 2982	3 Amigos	M3	lower	10	6.5	1.538462	1.209369	0.342027	0.1710135
MOR 3010	Golden Goose	M3	lower	6.5	8.6	0.755814	1.164553		
MOR 3011	Anky Breaky Heart	M3	lower	6.7	5.1(est. 6.8)	0.98529			
MOR 3055	Brown Nose	M3	lower	14.5	12.6	1.150794			
MOR 2570	Mark's Scavenged Trike	M3	lower	11	7.9	1.392405			
UCMP128561	Dave's Nose	M3	upper	13.6	14.2	0.9577	1.652774	0.613401	0.3541471
MOR 3045	Cliffhanger	M3	upper	12 (est. 16)	8.5	1.882353			
UCMP 113697	Ruben's Triceratops	M3	upper	24	11.33	2.11827			
MOR 2924	Lon's Trike	U3	lower	22.5	10	2.25	2.35038	0.145963	0.059589
MOR 2972	Supernasal	U3	lower	25	11.2	2.232143	2.145602	0.38882	
MOR 3008	American Beauty	U3	lower	26.5	10.1	2.623762	2.308763	0.142503	
MOR 2971	Crazy Trike	U3	lower	26.3	11	2.390909			
MOR 2936	Lazy Bones	U3	lower	19	9	2.111111			
MOR 2702	BAB	U3	lower	30	13	2.307692			
MOR 1625	Haxby Trike	U3	lower	30	13.5	2.222222			
MOR 2574	Quittin' Time	U3	lower	21	9.1	2.307692			
MOR 2965	TrkNas	U3	upper	14	6	2.333333			
MOR 1110	SG5	U3	lower	8.3	5.4	1.537037			
MOR 2951	DFJuvieTrike3	U3	lower	4.5	3.5	1.285714			
MOR 2923	Joe's Half Day Trike	U3	upper	29	13	2.230769	2.355036	0.39088	0.1381969
MOR 2576	Snap Creek	U3	upper	21.3	13.6	1.566176			
MWC 7584		U3	upper	36.6	12.6	2.904762			
MOR 004	MORT	U3	upper	28.5	13	2.192308			
MOR 2952	Homer's Nose	U3	upper	27	11.2	2.410714			
MOR 3048	Wednesday's Trike	U3	upper	19	7.2	2.638889			
MOR 2941	Nosy Nasal	U3	upper	24.8	10	2.48			
MOR 2938	Lauren's Trike	U3	upper	29	12	2.416667			
RTMP2002.57.7	'Dry Island Triceratops'	HCanyonFm		8	11.3	0.707			
MOR 2978	Greene Trike	U3	TBD	25.95	11.3	2.29646			
MOR 3049	Present	U3	TBD	21	10.5	2			
MOR 966		TBD		15.5	11.5	1.347826			
MOR 1604	Baker Trike	TBD		26.5	12	2.208333			
MOR 3058	JDExTrike2	M3		17	11	1.545455			
MOR 965	Mickey's Trike	TBD		24.9	17	1.464706			
MOR 2551	CSTrike2	TBD		22	14.3	1.538462			
MOR 2575		TBD		25	13.5 (est. >17)	<1.470589			
MOR 989	Pompey	TBD		8.1	8	1.0125			
MOR 981	TORO I	TBD		10	13	0.769231			

Dataset 5.S1 (Appendix 3)

Angle between nasal process of the premaxilla (NPP) and narial strut. Measurement taken between approximate midlines of each process, parallel to direction representing primary trend. Blue text indicates juvenile specimens. RTMP2002.57.7 is the holotype of *Eotriceratops*, collected from the Horseshoe Canyon Formation of Alberta.

Specimen no.	Locality Name	HCF Unit	Level	Angle	Mean	Std. Dev	Std. Error
MOR 1122	TORO II	L3	lower	125	124.5	0.707107	0.5
MOR 1122 7-22-00-1	TORO II	L3	lower	124			
MOR 1120	Getaway Trike	L3	upper	126			
MOR 3011	Anky Breaky Heart	M3	lower	127	127	2	1.15470054
MOR 6683	To the Premax	M3	lower	125			
MOR 2982	3 Amigos	M3	lower	129			
MOR 3027	Yoshi's Trike	M3	upper	141	140	2.645751	1.52752523
MOR 3045	Cliffhanger	M3	upper	142			
UCMP 113697	Ruben's Triceratops	M3	upper	137			
MOR 2924	Lon's Trike	U3	lower	144	141.4	5.639149	2.52190404
MOR 2574	Quittin' Time	U3	lower	136	139	6.271629	2.370453
MOR 2702	BAB	U3	lower	135			
MOR 1625	Haxby Trike	U3	lower	144			
MOR 2971	Crazy Trike	U3	lower	148			
MOR 2951	DFJuvieTrike3	U3	lower	135			
MOR 1110	SG5	U3	lower	131			
MOR 004	MORT	U3	upper	136	136		
RTMP 2002.57.7*	'Dry Island Triceratops'	HCanyonFm		114			
MOR 1604	Baker Trike	TBD		137			
MOR 981	TORO I	TBD		104			
MOR 1199	Sierra Trike	TBD		140			
MOR 2590	JRH7-2-05-2 Microsite	TBD		145			

Dataset 5.S1 (Appendix 4)

Nasal process of the premaxilla (NPP). Length measured from dorsalmost point of NPP to ventralmost point of NPP articulation with nasal. Width measured at narrowest point (waist). TBD = to be determined. Red text indicates incomplete specimens. Blue text indicates juvenile specimens. MOR 3011 is either a very large juvenile or a subadult. RTMP2002.57.7 is the holotype of *Eotriceratops*, collected from the Horseshoe Canyon Formation of Alberta. This specimen tapers to a point, width measured at approximate waist though there is some reconstruction in this area. *MOR 3045 exhibits a pronounced midline peak on the NPP; when measured to the base of this peak the length of NPP is 8.2 cm. **Length of the NPP of UCMP 113697 obscured by anterior nasals due to mounting of the skull. Measurements are in cm.

Specimen no.	Locality Name	HCF Unit	Level	Length	Width	L/W	Mean	Std. Dev.	Std. Error
MOR 1122 7-22-00-1	Toro II	L3	lower	14.9	4.9	3.040816			
MOR 1120	Getaway Trike	L3	upper	6.4	3.7	1.72973			
MOR 3011	Anky Breaky Heart	M3	lower	7.6	4.4	1.727273	1.65850816	0.097248	0.068765
MOR 2982	Three Amigos	M3	lower	5.89	3.705	1.589744			
MOR 3027	Yoshi's Trike	M3	upper	7.65	5.5	1.390909	1.42402597	0.046834	0.033117
MOR 3045	Cliffhanger	M3	upper	10.2*	7	1.457143			
MOR 2574	Quittin' Time	U3	lower	8.8	7	1.257143	1.15360747	0.163476	0.094383
MOR 2702	BAB	U3	lower	8.1	6.54	1.238532	1.24254978	0.217482	0.097261
MOR 2936	Lazy Bones	U3	lower	7.2	7.46	0.965147			
MOR 2951	DFJuvieTrike3	U3	lower	5.5	3.5	1.571429			
MOR 1110	SG5	U3	lower	5.69	4.82	1.180498			
RTMP2002.57.7	'Dry Island Triceratops'	HCanyonFm		15.6	est. 6	2.6			
MOR 1199	Sierra Trike	TBD		5.4	2.3	2.347826			
UCMP 113697	Ruben's Triceratops	M3	upper	8.43**	7.25	1.16			
MOR 6653	To the Premax	M3	lower	8.8	4.7	1.87234			

Dataset 5.S1 (Appendix 5)

HCF *Triceratops* nasals. Green text indicates taphonomic distortion. Blue text indicates juvenile specimens. Nasal length (NL) measured from anterior to the epinasal suture to the anteriormost point of the nasal-frontal suture. Basal Skull Length (BSL) measured from anterior of rostrum to posterior of occipital condyle. TBD = to be determined. Measurements are in cm.

Specimen no.	Locality Name	HCF Unit	Level	NL	BSL	NL/BSL	Mean	Std. Dev.	Std. Error
MOR 1122	Toro II	L3	lower	48	126.4	0.379747			
MOR 1120	Getaway Trike	L3	upper	32.3	98	0.329592			
MOR 3006	Antsy Trike	M3	lower	37					
MOR 3027	Yoshi's Trike	M3	upper	43.5	110	0.395455			
MOR 2574	Quittin' Time	U3	lower	39.1	101.48	0.385298	0.415523	0.042746	0.030226
MOR 2924	Lon's Trike U3	U3	lower	41	91.98	0.445749	0.390212	0.045312	0.022656
MOR 1625	Haxby Trike	U3	lower	51	122.57	0.416089	0.415712	0.030228	0.013518
MOR 2951	DFJuvieTrike3	U3	lower	19.9	58.6	0.33959			
MOR 1110	SG5	U3	lower	28.3	77.6	0.364691			
MOR 004	MORT	U3	upper	55.75	122	0.456967	0.435311	0.020568	0.010284
MOR 2999	Situ But Sad	U3	upper	38.8	94	0.412766			
MOR 2923	Joe's Half Day Trike	U3	upper	51.5	115	0.447826			
UCMP 137263	High Ceratopsian	U3	upper	40.75	96.18	0.423685			
MOR 1604	Baker Trike	TBD		46.5	110	0.422727			
MOR 2551	CSTrike2	TBD		54	94.22	0.573127			
MOR 1199	Sierra Trike	TBD		14.8	48.3	0.306418			

Dataset 5.S1 (Appendix 6)

HCF *Triceratops* postorbital horn cores. Red text indicates incomplete specimens. Blue text indicates juvenile specimens. *RTMP2002.57.7 is the holotype of *Eotriceratops*, collected from the Horseshoe Canyon Formation of Alberta. TBD = to be determined; BSL = basal skull length (measured from anterior point of the skull to the posterior surface of the occipital condyle). Measurements are in cm.

Specimen No.	Locality Name	HCF Unit	Level	P.O. Horn L	BSL	P.O./BSL	Mean	Std. Dev.	Std. Error
MOR 1122	Toro II	L3	lower	43 [est 60]	126.4	0.474684			
MOR 1120	Getaway Trike	L3	upper	49	98	0.5	0.574716	0.143592	0.0829031
MOR 2552	BOSH	L3	upper	78 [est 80]	108.07	0.740261			
MOR 3081	JRH-008	L3	upper	32[est 50]	103.33	0.483887			
MOR 2589	DK Site	L3	TBD	19.3					
MOR 1098	Fisk	L3	TBD	10.5					
MOR 2982	3 Amigos	M3	lower	40[est 50]	97.79	0.5113	0.49233	0.026827	0.0189694
MOR 3010	Golden Goose	M3	lower	43[est 47]	99.29	0.473361	0.433194	0.104168	0.0601415
MOR 2569	Afternoon Delight	M3	lower	13	41.28	0.314922			
MOR 3006	Warwick's Horn	M3	lower	43[est 51]					
MOR 3064	Little Horny Devil	M3	upper	25	54.3	0.460405	0.716357	0.121877	0.070366
MOR 3027	Yoshi's Trike	M3	upper	90	110	0.818182	0.652369	0.162113	0.0810564
UCMP 113697	Ruben's Triceratops	M3	upper	83.6	111.53	0.749574			
MOR 3045	Cliffhanger	M3	upper	58.3	100.29	0.581314			
MOR 2979	Seth's Trike	U3	lower	48.95	107.35	0.455985	0.451291	0.044987	0.0224933
MOR 2702	BAB	U3	lower	40.3[est 55]	121.21	0.453758	0.437942	0.157017	0.0593469
MOR 2574	Quittin' Time	U3	lower	51	101.48	0.502562			
UCMP 136092	Russell Basin Triceratops	U3	lower	44	112	0.392857			
MOR 2972	Supernasal	U3	lower	26.7	97.92	0.272672			
MOR 1110	SG5	U3	lower	50	77.6	0.64433			
UCMP 154452		U3	lower	4.15	32.41	0.128047			
MOR 2951	DFJuvieTrike3	U3	lower	28.6	58.6	0.488055			
MOR 2958	DFJuvieHornCore	U3	lower	42					
MOR 3047	Got the Horn	U3	lower	37.2					
MOR 3000	Ashes Trike	U3	lower	30					
MOR 2927	Trike Basin	U3	upper	30					
MOR 2923	Joe's Half Day Trike	U3	upper	55	115	0.478261	0.512576	0.043524	0.0194644
MOR 2597	Mark's Trike II	U3	upper	53.5	91.84	0.582535			
MOR 3041	Joey's Trike	U3	upper	42[est. 47]	94.32	0.498304			
MOR 2999	Situ But Sad	U3	upper	45	94	0.478723			
UCMP 137263	High Ceratopsian	U3	upper	50.5	96.18	0.525057			
MOR 2952	Homer's Nose	U3	upper	57[est 60]					
MOR 3053	PVU Trike	U3	TBD	53.5					
MOR 2988	Spike the Trike	U3	TBD	56					
MOR 539	Trumbo Ranch	TBD		18.35					
MOR 2579	Twitchell North	TBD		20.5					
MOR 1199	Sierra Trike	TBD		17	48.3	0.351967			
MOR 1604	Baker Trike	TBD		60.5	110	0.55			
MOR 2551	CSTrike 2	TBD		40.7[est. 50]	94.22	0.530673			
MOR 981	Toro I	TBD		83.5	129.5	0.644788			
RTMP2002.57.7	'Dry Island *Triceratops*'	HCanyonFm		74[est. 85]	132.6	0.641026			

Dataset 5.S1 (Appendix 7)

HCF *Triceratops* rostra. Blue text indicates juvenile specimens. Rostrum length measured from the anteriormost point of the rostrum to the narial strut. BSL = basal skull length. Measurement s for MWC 8574 and RTMP 2002.57.7 taken from photographs. Measurements are in cm.

Specimen no.	Locality Name	HCF Unit	Level	RL	BSL	RL/BSL	Mean	Std. Dev.	Std. Error
MOR 1120	Getaway Trike	L3	upper	28	98	0.285714			
MOR 3045	Cliffhanger	M3	upper	23	100.29	0.229335	0.239667	0.014612	0.0103325
MOR 3027	Yoshi's Trike	M3	upper	27.5	110	0.25			
MOR 1625	Haxby Trike	U3	lower	34	127.06	0.26759	0.244654	0.032436	0.0229358
MOR 2574	Quittin' Time	U3	lower	22.5	101.48	0.221719	0.245583	0.022992	0.013274
MOR 2951	DFJuvieTrike3	U3	lower	14.5	58.6	0.24744			
MOR 004	MORT	U3	upper	33	122	0.270492	0.260778	0.013737	0.0097138
MWC 8574		U3	upper	est. 34.8	138.61	0.251064			
RTMP 2002.57.7*	'Dry Island Triceratops'	HCanyonFm		47	132.604	0.354439			
MOR 1604	Baker Trike	TBD		24	110	0.218182			
MOR 1199	Sierra Trike	TBD		10.3	48.3	0.213251			
MOR 981	Toro I	TBD		47	129.5	0.362934			

Dataset 5.S1 (Appendix 8)

Squamosal Convexity. Squamosal length measured from parietal/squamosal contact to anterolateral projection. Distance to lateral margin of squamosal measured perpendicular to squamosal length measurement, from lateral margin to intersection with squamosal length measurement. In this study, specimens were coded as possessing a convex squamosal if SQL/DtLM was ≤4.

		Unit	SQ Length (cm)	Distance to lateral margin (cm)	SQ L/DtLM
UCMP 154452		U3	11	2.2	5
MOR 1199		TBD	33.5	5.8	5.77586207
MOR 2951		U3	39	10	3.9
MOR 1110	right:	U3	54	14	3.85714286
	left:		61.5	14.5	4.24137931
MOR 1120	left:	L3	78.5	21	3.73809524
	right:		82	19	4.31578947
MOR 3045		M3	76.5	17.8	4.29775281
MOR 3027		M3	84.5	19.8	4.26767677
UCMP 113697		M3	85.5	24.5	3.48979592
MOR 2924		U3	75.6	19.3	3.91709845
MOR 2999	right:	U3	72.5	17.6	4.11931818
	left:		75.5	19	3.97368421
MOR 1625		U3	87.2	22	3.96363636
UCMP 136092		U3	88	22	4
MOR 004		U3	est. 93	24	3.875
MOR 2985		L3	93	21	4.380952
MOR 2702		U3	100	19.5	5.12820513
MOR 3081		L3	108	12.5	8.64
MOR 1122	right:	L3	120	14	8.57142857

Supporting Material References

Anderson J. 1999. Occipital condyle in the ceratopsian dinosaur *Triceratops,* with comments on body size variation. Contributions from the Museum of Paleontology University of Michigan 30(8): 215-231.

Campione N.E., and R.R. Reisz. 2010. *Varanops brevirostris* (Eupelycosauria: Varanopidae) from the Lower Permian of Texas, with discussion of varanopid morphology and interrelationships. Journal of Vertebrate Paleontology 30(3):724-746.

Campione, N.E., K.S. Brink, E.A. Freedman, T. McGarrity, and D.C. Evans. 2013. '*Glishades ericksoni*', an indeterminate juvenile hadrosaurid from the Two Medicine Formation of Montana: implications for hadrosauroid diversity in the latest Cretaceous (Campanian-Maastrichtian) of western North America. Paleobiodiversity and Paleoenvironments 93: 65-75.

Carpenter K., and D.B. Young. 2002. Late Cretaceous dinosaurs from the Denver Basin, Colorado. Rocky Mountain Geology 37(2): 237-254.

Cobabe E.A., and D.E.Fastovsky. 1987. *Ugrosaurus olsoni*, a new ceratopsian (Reptilia: Ornithischia) from the Hell Creek Formation of eastern Montana. Journal of Paleontology 61(1): 148–154.

Currie PJ, Langston W, Tanke DH (2008) in A New Horned Dinosaur from an Upper Cretaceous Bone Bed in Alberta, NRC Research Press, (Ottawa, Ontario, Canada, NRC Research Press), pp 1–108.

Currie, P. J., W. Langston Jr, and D. H. Tanke. 2008. A new species of Pachyrhinosaurus (Dinosauria, Ceratopsidae) from the Upper Cretaceous of Alberta, Canada. A New Horned Dinosaur from an Upper Cretaceous Bone Bed in Alberta. Edited by PJ Currie, W. Langston, Jr., and DH Tanke. NRC Research Press, Ottawa 1–108.

Dodson, P., C. A. Forster, and S. D. Sampson. 2004. Ceratopsidae; pp. 494-513 in D. B. Weishampel, P. Dodson, and H. Osmólska (eds.), The Dinosauria. Univ. California Press, Berkeley.

Farke, A. A. 2007. Cranial osteology and phylogenetic relationships of the chasmosaurine ceratopsid *Torosaurus latus*; pp. 235-257 in K. Carpenter (ed.), Horns and Beaks: Ceratopsian and Ornithopod Dinosaurs. Indiana University Press, Bloomington and Indianapolis.

Farke A.A. 2011. Anatomy and taxonomic status of the chasmosaurine ceratopsid *Nedoceratops hatcheri* from the Upper Cretaceous Lance Formation of Wyoming, U.S.A. PLoS One 6(1): e16196.doi:10.1371/journal.pone.0016196.

Farke, A. A., M.J. Ryan, P.M. Barrett, D.H., Tanke, D. R. Braman, M.A. Loewen, and M.R. Graham. 2011. A new centrosaurine from the Late Cretaceous of Alberta, Canada, and the evolution of parietal ornamentation in horned dinosaurs. Acta Palaeontologica Polonica *56*(4): 691-702.

Felsenstein J. 1985. Confidence limits on phylogenies: an approach using the bootstrap. Evolution 39(4): 783-791.

Fisher D.C. 1994. Stratocladistics: morphological and temporal patterns and their relation to phylogenetic process pp. 133-171 in Interpreting the hierarchy of nature: from systematic patterns to evolutionary process theories, L. Grande, and O. Rieppel (eds.) Academic Press, San Diego, California.

Fisher D.C. 2008. Stratocladistics: integrating temporal data and character data in phylogenetic inference. Annual Revieve of Ecology, Evolution, and Systematics (39): 365-385.

Forster, C.A. 1990. The cranial morphology and systematics of *Triceratops* with a preliminary analysis of ceratopsid phylogeny. PhD dissertation. University of Pennsylvania.
Philadelphia. PA.

Forster C.A. 1993. Taxonomic validity of the ceratopsid dinosaur *Ugrosaurus olsoni* (Cobabe and Fastovsky). Journal of Paleontology 67(2): 316–318.

Forster C.A. 1996. Species resolution in *Triceratops*: cladistic and morphometric approaches. Journal of Vertebrate Paleontology 16(2): 259-270.

Fowler D.W., J.B. Scannella, and J.R. Horner. 2011. Reassessing ceratopsid diversity using unified frames of reference. Journal of Vertebrate Paleontology 31(5): 111A.

Frederickson J.A., and A.R. Tumarkin-Deratzian. 2014. Craniofacial ontogeny in *Centrosaurus apertus*. PeerJ 2:e252; DOI 10.7717/peerj.252

Fujiwara S., and Y. Takakuwa. 2011. A sub-adult growth stage indicated in the degree of suture co-ossification in *Triceratops*. Bulletin of Gumma Museum of Natural History 15: 1-17.

Gates T.A., and S.D. Sampson. 2007. A new species of *Gryposaurus* (Dinosauria: Hadrosauridae) from the Late Campanian Kaiparowits Formation, southern Utah, USA. Zoological Journal of the Linnean Society 151: 351-376.

Gilmore, C.W. 1946. Reptilian fauna of the North Horn Formation of central Utah. United States Geological Survey Professional Paper 210C: 29-51.

Hicks J.F., K.R. Johnson, J.D. Obradovich, L. Tauxe, and D. Clark. 2002. Magnetostratigraphy and geochronology of the Hell Creek and basal Fort Union Formations of southwestern North Dakota and a recalibration of the age of the Cretaceous-Tertiary boundary, pp. 35-55 in The Hell Creek Formation and the Cretaceous -Tertiary boundary in the northern Great Plains: an integrated continental record of the end of the Cretaceous, J.H. Hartman, K.R. Johnson, and D.J. Nichols (eds.) Geological Society of America Special Paper 361, Boulder, Colorado.

Hicks J.F., K.R. Johnson, J.D. Obradovich, D.P. Miggins, and L. Tauxe. 2003. Magnetostratigraphy of Upper Cretaceous (Maastrichtian) to lower Eocene strata of the Denver Basin, Colorado. Rocky Mountain Geology 38: 1-27.

Holmes R.B., C. Forster, M. Ryan, K.M. Shepherd. 2001. A new species of *Chasmosaurus* (Dinosauria:Ceratopsia) from the Dinosaur Park Formation of Southern Alberta. Canadian Journal of Earth Sciences 38: 1423-1438.

Horner J.R. and, M.B. Goodwin. 2006. Major cranial changes during *Triceratops* ontogeny. Proceedings of the Royal Society B 273: 2757-2761.

Horner J.R. and, M.B. Goodwin. 2008. Ontogeny of cranial epi-ossifications in *Triceratops*. Journal of Vertebrate Paleontology 28(1): 134–144..

Horner J.R., and M.B. Goodwin. 2009. Extreme cranial ontogeny in the upper Cretaceous dinosaur *Pachycephalosaurus*. PLoS ONE 4(10): e7626. doi.10.1371/journal.pone.0007626.

Hunt RK, Lehman, TM (2008) Attributes of the ceratopsian dinosaur *Torosaurus* and new material from the Javelina Formation (Maastrichtian) of Texas. *J Paleo* 82(6): 1127-1138.

Lawson, D.A. 1976. *Tyrannosaurus* and *Torosaurus*, Maestrichtian dinosaurs from Trans-Pecos, Texas. Journal of Paleontology 50(1): 158-164.

Lehman T.M. 1998. A gigantic skull and skeleton of the horned dinosaur *Pentaceratops sternbergi* from New Mexico. Journal of Paleontology 72(5): 894-906.

Lerbekmo J.F. 1999. Magnetostratigraphy of the Canadian continental drilling program Cretaceous-Tertiary (K-T) boundary project core holes, western Canada. Canadian Journal of Earth Sciences 36: 705-715.

Lerbekmo J.F. 2009. Glacioeustatic sea level fall marking the base of supercycle TA-1 at 66.5 Ma recored by the kaolinization of the Whitemud Formation and the Colgate Member of the Fox Hills Formation. Marine and Petroleum Geology 26: 1299-1303.

Lerbekmo J.F., and D.R. Braman. 2002. Magnetostratigraphic and biostratigraphic correlation of late Campanian and Maastrichtian marine and continental strata from the Red Deer Valley to the Cypress Hills, Alberta, Canada. Canadian Journal of Earth Sciences 39: 539-557.

Longrich N. R. 2010. *Mojoceratops perifania*, a new chasmosaurine ceratopsid from the Late Campanian of Western Canada. Journal of Paleontology 84(4): 681-694.

Longrich N. R. 2011. *Titanoceratops ouranos*, a giant horned dinosaur from the late Campanian of New Mexico. Cretaceous Research 32:264-276.

Longrich N. R., and D.J. Field. 2012. *Torosaurus* Is Not *Triceratops*: Ontogeny in Chasmosaurine Ceratopsids as a Case Study in Dinosaur Taxonomy. PLoS ONE 7(2): e32623.doi:10.1371/journal.pone. 0032623

Maiorino L., A. A. Farke, T. Kotsakis, and P. Piras. 2013. Is *Torosaurus Triceratops*? Geometric morphometric evidence of Late Maastrichtian ceratopsid dinosaurs. PLoS ONE 8(11): e81608: doi:10.1371/journal.pone.0081608

Mallon J. C., R. Holmes, D.A. Eberth, M. J. Ryan, J. S. Anderson. 2011. Variation in the skull of *Anchiceratops* (Dinosauria,Ceratopsidae) from the Horseshoe Canyon Formation (Upper Cretaceous) of Alberta. Journal of Vertebrate Paleontology 31(5): 1047–1071.

Marcot J. D., and D. L. Fox. 2008. StrataPhy: a new computer program for stratocladistic analysis. Palaeontologica Electronica 11:5A.

McDonald A. T., D. G. Wolfe, and J. I. Kirkland. 2010. A new basal hadrosauroid (Dinosauria: Ornithopoda) from the Turonian of New Mexico. Journal of Vertebrate Paleontology 3(3): 799–812.

O'Leary M. A., and S. G. Kaufman. 2008. MorphoBank 2.5: Web application for morphological phylogenetics and taxonomy, http://www.morphobank.org.

Ostrom J. H., and P. Wellnhofer. 1986. The Munich specimen of *Triceratops* with a revision of the genus. *Zitteliana* 14: 111-158.

Ott C. J., and P. L. Larson. 2010. A new, small ceratopsian dinosaur from the latest Cretaceous Hell Creek Formation, northwest South Dakota, United States: a preliminary description pp. 203-218 in New Perspectives on Horned Dinosaurs: The Royal Tyrell Museum Ceratopsian Symposium, M. J. Ryan, B. J. Chinnery-Allgeier, and D. A. Eberth (eds.) Indiana University Press, Bloomington and Indianapolis.

Pleijel F. 1995. On character coding for phylogeny reconstruction. Cladistics. 11:309-315.

Polly P. D. 1997. Ancestry and species definition in paleontology: stratocladistic analysis of Paleocene-Eocene Viverravidae (Mammalia, Carnivora) from Wyoming. Contributions from the Museum of Paleontology University of Michigan 30(1): 1-53.

Pardo J. D., A. K. Huttenlocker, and J. D. Marcot. 2008. Stratocladistics and evaluation of evolutionary modes in the fossil record: an example from the ammonite genus *Semiformiceras*. Palaeontology. 51(4): 767-773.

Raynolds R. G., and K. R. Johnson. 2003. Synopsis of the stratigraphy and paleontology of the uppermost Cretaceous and lower Tertiary strata in the Denver Basin, Colorado. Rocky Mountain Geology 38**:** 171-181.

Rook D. L., and J. P. Hunter. 2011. Phylogeny of the Taeniodonta: evidence from dental characters and stratigraphy. Journal of Vertebrate Paleontology 31(2): 422-427.

Sampson S. D. 1995. Two new horned dinosaurs from the Upper Cretaceous Two Medicine Formation of Montana; with a phylogenetic analysis of the Centrosauriane (Ornithischia: Ceratopsidae). Journal of Vertebrate Paleontology 15(4): 743-760.

Sampson S. D. , M. A. Loewen, A. A. Farke, E. M. Roberts, C. A. Forster, J. A. Smith, and A. L. Titus. 2010. New horned dinosaurs from Utah provide evidence for intracontinental dinosaur endemism. *PLoS ONE* 5(9): e12292. doi:10.1371/journal.pone.0012292.

Scannella J. B., and J.R. Horner. 2010. *Torosaurus* Marsh, 1891, is *Triceratops* Marsh, 1889 (Ceratopsidae: Chasmosaurinae): synonymy through ontogeny. Journal of Vertebrate Paleontology 30(4): 1157-1168.

Scannella J. B., and J. R. Horner. 2011. '*Nedoceratops*': An example of a transitional morphology. *PLoS ONE* 6(12): e28705. doi:10.1371/journal.pone.0028705

Sorenson, M. D. , and E. A. Franzosa. 2007. TreeRot, version 3. Boston University, Boston, MA.

Sullivan, R. M., and S. G. Lucas. 2010. A new chasmosaurine (Ceratopsidae, Dinosauria) from the Upper Cretaceous Ojo Alamo Formation (Naashoibito Member), San Juan Basin, New Mexico, pp. 169-180 in New Perspectives on Horned Dinosaurs: The Royal Tyrell Museum Ceratopsian Symposium, M. J. Ryan, B. J. Chinnery-Allgeier, and D. A. Eberth (eds.) Indiana University Press, Indiana University Press.

Sullivan, R. M., A. C. Boere, and S. G. Lucas. 2005. Redescription of the ceratopsid dinosaur *Torosaurus utahensis* (Gilmore, 1946) and a revision of the genus. Journal of Paleontology 79(3):564–582.

Swofford D. L. 2003. PAUP*. Phylogenetic Analysis Using Parsimony (*and Other Methods). Version 4. Sinauer Associates, Sunderland, Massachusetts.

Tokaryk T. T. 1986. Ceratopsian dinosaurs from the Frenchman Formation (Upper Cretaceous) of Saskatchewan. Canadian Field-Naturalist 100: 192-196.

Tsuihiji T. 2010. Reconstructions of the axial muscle insertions in the occipital region of dinosaurs: evaluations of past hypotheses on marginocephalia and tyrannosauridae using the Extant Phylogenetic Bracket approach. The Anatomical Record 293:1360–1386.

Wu X., D. B. Brinkman, D. A. Eberth, and D. R. Braman. 2007. A new ceratopsid dinosaur (Ornithischia) from the uppermost Horseshoe Canyon Formation (upper Maastrichtian), Alberta, Canada. Canadian Journal of Earth Sciences 44: 1243–1265.

APPENDIX B

SUPPLEMENTARY INFORMATION FOR CHAPTER 6

Appendix 6.1: Descriptions of linear measurements and geometric morphometric landmarks. L, length; Trans, transverse; Ant, anteriormost; Post, posteriormost; qj, quadratojugal; qu, quadrate; H, height

Linear Measurements

1: L from ant dentary to post rp
2: Transverse width at post rp
3: Transverse width at post contact of dentaries
4: Dentary depth at post contact
5: Basal Skull Length (rostrum to occipital condyle)
6: Ant rostrum to ventral jugal/maxilla contact
7: Trans width at jugal/maxilla contact
8: Trans width at ptyergoid/palatine contact
9: Tran width at dorsalmost point of orbits
10: L from dorsal pt of orbit to ventral pt of orbit
11: L from ant orbit to post orbit
12: L from ant jugal/maxilla contact to post qj/qu contact
13: Trans width at post qj/qu contact
14: L jugal/maxilla contact to pterygoid/palatine contact
15: qj/qu contact to qu/laterosphenoid contact
16: width of occipital condyle
17: height of occipital condyle
18: Basioccipital width
19: Vertical diameter of foramen magnum
20: Trans width of supraoccipital
21: L qj/qu to jugal projection
22: Height of jugal at projection
23: Total casque L
24: Basal casque L
25: L from casque contact with rostrum to posterodorsal point
26: Casque width dorsal to lachrymal suture
27: Casque width dorsal to ant contact with rostrum
28: L maxilla/jugal ventral contact to dorsal surface of casque
29: H of casque at ant contact with rostrum
30: Anteror contact of casque with rostrum to maxilla/jugal contact
31: L ant rostrum to ant casque
32: L ant rostrum to ant base of casque

Geometric Morphometric Landmarks

1: Ant point of rostrum
2: Ant contact of casque with rostrum
3: Anteriormost point of casque dorsal to contact with rostrum
4: Posterodorsal point of casque
5: Maxilla/jugal contact (ventral point)
6: Jugal/maxilla Contact at orbit margin
7: posteriormost point of jugal bar (quadratojugal contact with quadrate)
8: dorsal contact of quadrate with squamosal
9: dorsalmost point of fossa for *M. adductor mandibulae externus profundus*
10: anteriormost point of nares
11: dorsalmost point of orbit
12: dorsalmost point of jugal bar projection
13: ventralmost point of postorbital bar

Appendix 6.2 Linear measurements of hornbill skulls. Dark and light grey indicate male and female *C. atrata*, respectively. Blue and green indicate male and female *B. albotibialis*, respectively. Red and yellow indicate male and female *C. elata*, respectively.

	mes1	mes2	mes3	mes4	mes5	mes6	mes7	mes8
MOR-OST-259	165.1	38.4	29.6	23.6	167.9	130.1	41.845	7.35
MOR-OST-268	150.7	32.1	27	22.3	158.6	121.9	35.835	NA
MOR-OST-270	156.3	30.7	24.5	23.34	161.3	121.8	38.695	5.23
MOR-OST-269	147	29.6	23.7	20.52	154.4	115.6	37.255	5.79
MOR-OST-1635	157.08	36.075	29.36	23.395	163.365	125.625	38.015	4.665
MOR-OST-288	176.7	33.3	32.8	27.23	182.2	140.4	42.29	6.29
MOR-OST-285	165.5	38.5	30.6	24.2	173.8	131.85	40.445	8.43
MOR-OST-281	173.7	36.6	31.3	26.96	NA	142.3	41.61	7.28
MOR-OST-287	179.7	35.2	33.3	28.96	185.8	144.94	44.76	8.31
MOR-OST-275	171.1	24.4	26.5	27.1	180.5	141.6	41.395	5.03
MOR-OST-286	167.2	37.1	30.4	27.62	177.5	134.4	39.035	NA
MOR-OST-272	176.9	39.4	32.14	28.2	184.9	140.1	44.285	8.07
MOR-OST-278	182.4	36.3	31.1	26.02	188.5	144.7	41.56	7.5
MOR-OST-276	172.6	38.6	29.2	28.71	180.3	140.4	41.735	6.34
MOR-OST-279	203.2	29.1	32.9	27.93	203.5	157.6	40.645	6.28
MOR-OST-274	172.8	32.9	31.1	26.17	182.9	143.9	39.17	6.82
MOR-OST-273	182.77	34.3	27.6	27.39	191.7	149.6	40.9	7.98
MOR-OST-280	180.6	35.1	35.8	28.66	187	149.1	43.63	5.96
MOR-OST-277	181.6	37.1	31	31.01	187.6	149.2	39.55	6.23
MOR-OST-258	184.9	32.5	30.6	30.47	190.9	148.1	41.93	6.7
MOR-OST-289	170.4	36	28.02	25.1	182.2	142.3	42.99	6.42
MOR-OST-266	178.7	34.6	27.8	27.31	187.5	145.4	42.775	6.07
MOR-OST-267	165	33.2	31.5	27.75	177.9	137.8	39.445	6.69
MOR-OST-1625	163.435	33.155	25.825	26.625	174.925	131.17	38.07	4.425
MOR-OST-1626	175.34	33.72	29.98	28.05	186.08	146.625	38.935	6.39
MOR-OST-1627	165.095	36.645	30.91	27.28	176.08	136.465	42.335	6.325
MOR-OST-1628	181.05	40.79	27.44	27.445	187.975	148.73	39.94	5.935
MOR-OST-1629	173.515	37.79	31.695	28.645	182.875	143.6	39.125	7.565
MOR-OST-1630	177.14	34.935	31.645	28.015	185.64	145.72	39.677	7.675
MOR-OST-1631	177.28	37.05	32.065	26.92	187.695	147.98	42.895	7.65
MOR-OST-1632	170.38	39	28.87	26.73	178.11	138.225	37.19	6.16
MOR-OST-1622	155.82	29.9	30.1	23.5	163.02	123.03	41.59	5.9
MOR-OST-1621	167.6	32.4	29.8	24.8	176.89	135.84	43.565	6.335
MOR-OST-265	161.36	35.79	31.23	30.905	172.94	132.145	40.845	7.435
MOR-OST-1620	167.735	30.415	28.285	26.98	177.31	136.975	40.11	6.75
MOR-OST-1636	146.8	30.005	24.145	22.85	152.55	115.765	37.3	7.595

MOR-OST-1633	202.665	35.31	31.14	30.28	208.03	165.67	45.315	7.44
MOR-OST-290	215	41.89	31.54	29.33	213	171	42.41	6.65
MOR-OST-1634	178.4	36.745	28.485	24.265	184.345	147.045	43.065	7.195

mes9	mes10	mes11	mes12	mes13	mes14	mes15	mes16	mes17
45	23.57	25.625	32.04	53.76	21.905	17.43	6.195	3.695
42.2	22.175	24.115	31.12	49.245	NA	16.07	5.52	3.46
38.8	23.57	25.405	29.935	50.71	20.47	18.48	6.16	3.57
42.05	22.33	25.03	30.37	51.45	19.9	16.17	6.26	3.12
41.24	22.54	25.025	32.34	51.545	18.755	17.08	5.27	3.935
44.88	25.35	28.12	34.375	56.79	20.95	17.63	6.77	4.065
44.32	24.28	27.16	35.245	54.455	20.23	17.05	7.43	4.285
44.36	25.29	28.89	35.21	55.695	19.15	18.91	NA	NA
45.78	26.19	26.23	33.515	57.615	20.085	19.2	7.29	4.715
44.1	25.35	27.46	33.48	53.05	19.85	17.17	6.86	2.85
46.37	24.67	26.59	33.515	49.875	NA	18.78	6.405	3.8
49.13	25.08	27.785	36.83	58.175	22.125	18.52	7.095	4.07
48.51	26.48	28.365	34.69	54.615	20.09	19.87	6.2	3.91
46.66	26.795	27.205	33.1	56.315	18.88	19.63	6.54	4.38
44.12	27.575	27.89	36.435	56.375	19.825	19.27	6.84	4.395
43.04	25.07	26.595	34.23	52.99	18.995	18.37	6.57	3.9
46.19	25.815	27.26	32.84	54.92	20.33	20.04	6.955	3.95
47.63	26.915	27.71	32.95	54.595	19.72	18.98	6.845	3.925
45.27	26.755	26.11	33.935	55.01	19.37	18.8	7.425	4.535
50.11	24.875	26.175	31.765	55.795	20.285	18.93	6.975	4.18
46.22	26.585	27.17	34.285	53.505	21.81	18.34	6.41	3.68
44.85	26.565	27.99	33.32	55.01	22.38	19.04	7.11	3.745
46.35	24.4	25.565	32.68	NA	19.595	18.61	6.78	4.425
41.89	27.455	29.4	33.63	50.805	20.435	18.35	5.96	3.66
45.295	24.54	25.98	32.915	54.03	20.86	19.095	6.505	4.07
42.92	28.07	26.995	30.865	56.03	21.12	19.46	6.465	3.785
47.87	27.255	26.515	33.985	53.42	20.41	19.125	5.655	3.93
43.875	28.49	26.62	31.505	54.045	18.58	18.21	5.84	4.355
43.615	25.88	26.2	30.505	54.525	19.17	18.94	6.7	4.135
43.01	28.415	27.31	32.555	55.075	19.585	18.555	5.97	NA
42.225	26.715	27.305	33.26	51.685	18.93	18.11	6.38	3.71
43.87	28.07	28.01	34.24	52.12	28.2	18.71	6.62	3.84
45.035	27.215	27.015	32.98	54.72	20.835	19.585	5.865	4.06
42.425	23.115	26.51	32.67	NA	19.865	NA	5.735	4.305
41.425	22.45	25.85	32.915	46.015	20.665	16.075	5.35	3.795

36.8	21.255	23.385	29.42	44.92	20	15.34	4.595	3.61
53.26	25.455	28.01	38.135	60.5	21.325	20.775	6.785	4.235
51.3	26.62	28.805	38.065	53.99	22.41	21.26	6.64	4.065
44.255	25.02	26.315	29.46	55.565	19.1	17.87	6.61	3.88

mes18	mes19	mes20	mes21	mes22	mes23	mes24	mes25	mes26
12.085	6.42	23.45	10.9	7.73	99.145	96.56	96.69	32.73
11.515	6.02	21.79	9.89	7.01	87.24	87.63	88.135	31.26333
11.575	6.59	23.825	6.91	4.92	94.685	94.685	94.99	31.25333
11.55	6.51	22.385	9.48	5.87	80	76.97	80	29.14
11.175	7.42	21.97	9.89	6.825	90.99	88.14	88.91	26.93
12	7.57	25.165	10.42	6.79	163.67	111.885	140.905	54.905
15.115	7.11	25.855	9.73	7.21	116.01	92.555	114.315	43.28667
NA	8.32	25.29	12.81	8.95	167.695	108.66	139.44	62.40333
13.605	6.73	28.35	11.03	8.01	165.635	112.925	140.08	57.19
11.77	7.42	26.52	8.44	7.02	131.275	108.225	128.15	50.365
8.6	7.05	24.925	10.7	7.85	147.13	104.7	127.795	55.23333
13.975	8.06	30.575	13.14	9.54	156.57	111.86	137.845	58.655
13.53	7.81	27.295	10.29	7.16	178.045	115.975	144.515	50.32
12.66	7.65	27.16	11.37	8.28	168.125	105.14	134.195	56.54
12.935	7.93	24.445	12	9.3	193.915	121.265	149.215	58.04667
11.685	6.8	26.665	10.48	7.5	156.185	110.55	132.45	46.44
14.025	8.03	27.78	10.59	8.35	181.28	120.425	150.04	58.67
12.285	6.62	25.6	10.9	8.15	160.935	112.03	138	57.54333
12.855	NA	26.12	12.46	8.78	200.6	133.005	161.995	53.695
NA	7.3	26.83	10.46	6.67	143.025	113.495	136.41	52.59667
12.02	6.42	25.965	11.78	9.33	183.92	115.75	146.425	58.88
12.415	7.81	26.765	10.1	7.3	179.995	126.205	147.855	56.7
14.17	7.69	26.675	9.97	7.71	143.01	106.8	128.205	55.79667
12.155	7.985	24.7	13.35	5.4	148.585	100.735	130.61	51.665
12.8	7.81	24.81	12.465	8.55	154.92	111.225	134.445	47.77
12.9625	6.885	24	12.695	8.64	148.105	99.055	128.025	51.315
12.39	8.475	25.91	14.73	8.63	160.82	115.57	140.905	52.695
12.025	8.115	24.91	12.73	7.915	178.57	116.87	147.605	54.835
12.82	7.375	26.56	12.53	8.605	166.21	105.58	132.915	49.395
12.2625	7.515	26.275	11.105	8.77	163.975	112.91	139.6	52.115
12.245	8.005	25.295	10.655	7.18	162.28	108.795	138.975	48.37
12.45	8.055	25.91	8.845	5.615	121.82	108.56	121.82	45.07
12.725	NA	28.265	9.805	7.39	150.515	100.695	128.06	53.575
13.76	7.1	26.495	NA	7.835	177.645	107.32	124.155	37.7

10.7125	7.4	25.09	11.67	5.97	172.86	108.315	130.62	35.79
9.9675	7.01	19.81	9.39	5.205	40.815	39.62	40.815	26.39
13.78	8.72	29.325	16.62	10.335	112.065	92.06	123.785	55.335
12.61	8.78	28.43	12.68	8.56	141.87	90.54	122.955	59.315
12.24	8.75	25.79	13.91	7.62	62.855	55.9	62.855	26.85

mes27	mes28	mes29	mes30	mes31	mes32
3.645	40.34567	12.35	88.895	64.23	60.52
5.35	41.08	14.88333	77.635	72.78	64.85
8.345	38.51	15.205	84.18	56.92	57.71
4.845	37.055	11.41	71.74	61.14	61.4
8.115	37.505	13.77	81.395	67.13	61.43
32.79	82.025	46.225	100.68	72.63	63.55
11.19	71.145	28.865	87.75	76.82	71.8
33.385	79.045	45.54	99.53	86.62	69.99
27.95	82.68	46.5	102.515	86.37	74.58
21.155	73.465	29.88	96.66	75.57	67.8
28.37667	81.05	39.13	91.055	75.79	65.04
32.21	80.685	48.145	102.285	82.98	61.54
27.56333	84.47	52.28	102.4	81.69	65
31.745	87.105	49.65	95.3	86.41	73.55
40.45	81.07	41.695	104.415	83.76	79.31
16.205	76.21	41.79	100.785	88.55	73.8
30.47333	84.985	52.31	107.295	90.15	67.06
30.735	82.4	47.81	101.83	86.96	73.49
26.68	82.89	51.18	111.015	79.02	64.96
16.285	78.29	39.69	102.18	88.61	71.61
32.755	84.365	54.92	102.415	81.99	68.08
29.36	80.505	54.47	110.475	85.9	54.83
33.265	76.005	50.435	96.405	93.45	69.28
32.98	74.67	40.66	91.62	76.66	66.29
24.635	72.2	44.245	98.12	88.06	76.73
31.35	77.79	44.3	91.795	77.4	68.17
27.355	80.995	52.5	104.84	99	68.31
29.02	83.28	55.495	101.72	93.31	65.78
25.2	76.543	49.955	94.755	96.19	80.7
35.475	90.225	54.56	103.24	103.43	73.05
25.02	82.215	53.02	96.61	82.33	66.89
3.76	73.25	3.315	93.52	48.91	48.9
32.265	84.8	49.47	91.98	86.18	74.11

25.475	75.62	33.975	94.585	27.21	62.57
16.155	73.535	32.96	97.965	33.29	58.43
22.635	45.085	1.67	46.82	100.36	98.27
27.645	92.08	47.53	86.75	149.46	109.01
41.95	92.395	72.71	85.54	163.9	126.38
16.18	40.46	2.13	64.83	126	110.56

Appendix 6.3. SMA Results.

Black Casqued Hornbills

Mes	N	R^2	Slope	95% CI (Slope)	Intercept	95% CI (Intercept)	Allometry
1	32	0.949	1.078	0.9908312 - 1.172465	-0.195	- 0.4084942- 0.000854164	iso
2	32	0.0355	1.755	1.2265982 - 2.512187	-2.418	- 4.1239589 - - 1.226617	+
3	32	0.3202	1.475	1.089357 - 1.996004	-1.8502	- 3.025308 - - 0.9819903	+
4	32	0.7061	1.5071	1.2329213 - 1.842261	-1.974	- 2.728887 - - 1.3556126	+
5	32						
6	32	0.966	1.188	1.108936 - 1.272117	-0.534	- 0.7244892 - - 0.3567278	+
7	32	0.237	0.835	0.6094497 - 1.1438992	-0.256	- 0.9465754 - 0.2474257	iso
8	30	0.3999574	2.746	1.9391512 - 3.887440	-5.382	- 7.957747 - - 3.5631122	+
9	32	0.357	0.892	0.6643791 - 1.1978048	-0.3602	- 1.0492055 - 0.1529800	iso
10	32	0.3499	1.132	0.8419093 - 1.522674	-1.141	- 2.0213345 - - 0.4870901	iso
11	32	0.259	0.6899	0.5030731 - 0.9460819	-0.127	- 0.7042636 -0.2941488	-
12	32	0.248	0.792	0.5764007 - 1.088855	-0.266	- 0.93453141 - 0.2203913	iso
13	31	0.451	0.664	0.5030980 - 0.8768983	0.235	- 0.2447883 - 0.5976908	+
14	30	0.0584	-1.334	- 1.9263532 - -0.924017	4.319	3.3936870 - 5.654594	-
15	32	0.469	0.892	0.6817143 - 1.1662564	-1.362	- 1.3621386 - - 0.2701223	iso
16	32	0.207	1.385	0.9999011 - 1.919786	-2.311	- 3.515498 - - 1.4423467	iso
17	31	0.2606	1.688	1.2242754 - 2.326574	-3.2093	- 4.648663 - -2.1651052	+
18	31	0.1098	1.584	1.1153576 - 2.250936	-2.476	- 3.977223 - - 1.418956	+
19	30	0.239	1.4083	1.0107924 - 1.962170	-2.3073	- 3.555261 - - 1.4115618	+
20	32	0.388	1.2041	0.9030012 - 1.605482	-1.3046	- 2.209307 - - 0.6261205	iso
21	32	0.274	2.434	1.7808421 - 3.327375	-4.452	- 6.464766 - - 2.97933322	+
22	32	0.438	2.612	1.9822568 - 3.443001	-5.0106	- 6.882416 - - 3.590326	+
23	32	0.822	4.132	3.532850 - 4.833184	-7.152	- 8.732283 - - 5.801710	+
24	32	0.746	1.963	1.628733 - 2.366097	-2.396	-3.304218 - -1.6424134	+
25	32	0.80018	2.821	2.389741 - 3.330121	-4.2507	- 5.398063 - - 3.741488	+
26	32	0.687	3.628	2.949043 - 4.463710	-6.492	- 8.374858 - -4.961241	+
27	32	0.646	11.532	9.255086 -14.36801	-24.685	- 31.07767 - - 19.55464	+
28	32	0.651	4.454	3.579957 - 5.540648	-8.183	- 10.632626 - - 6.2138	+
29	32	0.619	10.639	8.469182 - 13.36598	-22.434	-28.57836 - -17.54242	+
30	32	0.8066	1.618	1.374099 - 1.904683	-1.664	- 2.310132 - - 1.1143508	+
31	32	0.446	2.0453	1.5548356 - 2.690563	-2.698	-4.152241 - -1.5926442	+
32	32	0.273	1.721	1.2588347 - 2.352790	-2.05101	-13.334900 - - 1.970324	+

White-thighed Hornbills

N	R^2	Slope	95% CI (Slope)	Intercept	95% CI (Intercept)	Allometry
3	0.983	0.851	0.2365102 - 3.060417	0.3081	- 4.604653 - 1.673871	iso
3	0.179	1.217	- 60.90662 - 1.387348	-1.2014	0.05277303 - 28.07088	iso
3	0.7295	1.6101	0.1211347 - 21.40067	-2.137	- 46.13814 - 1.173661	+
3	0.661	1.876	0.1262988 - 27.87332	-2.745	- 60.54542 - 1.145846	iso
3						
3	0.998	1.0992	0.6134885 - 1.969629	-0.337	- 2.272079 - 0.7430919	iso
3	0.885	0.596	0.06833259 -5.198606	0.2702	- 9.962938 - 1.44344	iso
3	0.564	-0.7798	- 13.137372 - - 0.04629	2.594	0.9632916 - 30.06931	-
3	0.0995	0.945	0.1189945 - 7.505512	-0.498	- 15.083780 - 1.339011	iso
3	0.766	0.528	0.04267299 - 6.541191	0.173	- 13.195813 - 1.252647	iso
3	0.885	0.823	0.09410514 -7.199283	-0.428	- 14.604902 -1.192374	iso
3	0.991	0.779	0.27900723 -2.173107	-0.231	- 3.331510 - 0.879732	iso
2	-	-	-	-	-	-
3	0.245	0.262	0.01183894 - 5.795170	0.722	- 11.579889 - 1.278463	iso
3	-	-	-	-	-	-
3	0.797	1.406	0.1219916 - 16.209567	-2.4101	- 35.32310 - 0.4451613	iso
3	0.364	1.126	0.05538946 - 22.87696	-1.913	- 50.27319 - 0.4670807	iso
3	0.3029	2.0995	0.09873281 - 44.64562	-3.612	- 98.20700 - 0.8361812	iso
3	0.6198	0.351	0.02231799 - 5.524943	0.0747	- 11.428463 - 0.805782	iso
3	0.893	1.918	0.2278456 - 16.138477	-2.8902	- 34.50825 - 0.8666033	iso
3	-	-	-	-	-	-
3	0.419	2.582	0.1329418 - 50.16366	-4.946	- 110.73575 - 0.4999023	iso
3	0.971	10.669	2.344022 - 48.560042	-21.693	-105.93780 - - 3.183554	+
3	0.978	7.1708	1.799798 - 28.569687	-14.0553	-61.63257 - - 2.113815	+
3	0.986	8.156	2.496074 - 26.65141	-16.194	-57.31508 - - 3.609373	+
3	0.918	2.3904	0.3221650 - 17.736350	-3.798	- 37.916879 - 0.8008962	iso
3	0.171	-2.932	- 67.97238 - - 0.126489	7.842	1.604298 - 152.44926	-
3	0.959	3.6084	0.6777867 - 19.210068	-6.223	- 40.910925 - 0.29276604	iso
3	0.973	21.472	4.900244 - 94.08584	-46.649	- 208.09485 - -9.804322	+
3	0.987	5.239	1.637645 - 16.76173	-9.771	-35.38948 - -1.763406	+
3	0.915	-8.936	- 67.399602 - - 1.18485	21.526	4.291695 - 151.510055	-
3	0.998	-3.723	- 6.145561 - - 2.255731	10.134	6.871534 - 15.51998	-

Yellow-casqued Hornbills

N	R^2	Slope	95% CI (Slope)	Intercept	95% CI (Intercept)	Allometry
3	0.974	1.231	0.2841663 - 5.328615	-0.538	- 9.980501 - 1.642139	iso
3	0.191	1.154	0.05035951 - 26.42254	-1.0794	- 59.30034 - 1.462372	iso
3	0.999	0.716	0.4511958 - 1.136589	-0.168	- 1.1364867 - 0.4426897	iso
3	0.9202	1.545	0.2111187 - 11.301346	-2.115	- 24.59434 - 0.9580555	iso
3						
3	0.998	1.0268	0.5805497 - 1.816204	-0.159	- 1.978054 - 0.8689505	iso
3	0.0217	0.448	0.0177761 - 11.265825	0.608	- 24.31770 - 1.598321	iso
3	0.139	-0.744	- 17.566645 - - 0.03147	2.564	0.9229883 - 41.32483	-
3	0.885	1.263	0.144853 - 11.01965	-1.217	- 23.69562 - 1.360412	iso
3	0.661	0.413	0.02777045 - 6.136412	0.459	- 12.728816 - 1.345772	iso
3	0.976	0.597	0.1440614 - 2.4754890	0.0664	- 4.261311 - 1.110404	iso
3	0.975	1.916	0.4496570 - 8.162408	-2.8704	- 17.262866 - 0.5076639	iso
3	0.0156	0.764	0.0302468 - 19.288089	-0.00689	- 42.68768 - 1.683267	+
3	0.976	1.0554	0.25306799 - 4.401442	-1.111	- 8.821001 - 0.7370412	+
3	0.999	1.217	0.8358360 - 1.772351	-1.505	- 2.7845 - - 0.626728	iso
3	0.289	0.1802	0.008217152 - 3.950326	0.4095	- 8.277092 - 0.8057071	iso
3	0.644	0.565	0.0371034 - 8.608801	-0.694	- 19.22682 - 0.5227606	iso
3	0.333	0.795	0.03822362 -16.552194	-0.723	- 37.02776 - 1.02118	+
3	0.0229	0.0442	0.001758238 - 1.112963	0.84008	- 1.6223128 - 0.9379553	iso
3	0.858	0.865	0.08938218 - 8.368197	-0.549	- 17.836552 - 1.238215	iso
3	0.00075	1.774	0.0697385 - 45.14209	-2.932	- 102.85375 - 0.9950118	iso
3	0.473	1.984	0.1072608 - 36.70906	-3.629	- 83.63644 - 0.6957793	iso
3	0.993	6.539	2.6347929 - 16.22961	-13.0896	-35.41669 - - 4.093598	+
3	0.964	2.7703	0.5496822 - 13.961716	-4.476	-30.261772 - 0.6401660	iso
3	0.974	4.922	1.138437 - 21.277441	-9.344	-47.02863 - - 0.6274464	+
3	0.995	5.663	2.4568340 - 13.05406	-11.3999	- 28.42879 - - 4.0122880	+
3	0.913	6.162	0.8091679 - 46.922740	-12.773	- 106.687692 - - 0.439917	iso
3	0.978	6.138	1.523719 - 24.729564	-12.298	- 55.13243 - - 1.665105	+
3	0.998	24.866	14.85242 - 41.63177	-56.0041	- 94.63251 - - 32.93167	+
3	0.963	2.185	0.42803276 - 11.153729	-3.142	- 23.805909 - 0.9065861	iso
3	0.961	1.723	0.3291515 - 9.015245	-1.8058	-18.60840 - 1.404755	iso
3	0.309	1.0527	0.04973908 - 22.28139	-0.365	- 49.27643 - 1.946313	iso

Appendix 6.4. Loadings for PCA.

	With casque			Without casque		
	PC1	PC2	PC3	PC1	PC2	PC3
R^2	**.6945**	**.1465**	**.0500**	**.4935**	**.1053**	**.0938**
1: L from ant dentary to post rp	-0.022792330	-0.0102581899	-0.0106870610	-0.0276661366	0.0084771445	0.0006829152
2: Transverse width at post rp	-0.016639484	-0.0058452600	-0.0147853749	-0.0265714994	-0.0111651040	-0.0086804188
3: Transverse width at post contact of dentaries	-0.021679385	-0.0008139522	-0.0036201938	-0.0271385006	-0.0016274122	0.0076730398
4: Dentary depth at post contact	-0.032059119	-0.0065571132	0.0040384805	-0.0297216305	0.0069936691	0.0001997448
5: Basal Skull Length (rostrum to occipital condyle)	-0.023581602	-0.0090214481	-0.0076829135	-0.0262447154	0.0075935246	0.0002531723
6: Ant rostrum to ventral jugal/maxilla contact	-0.026502191	-0.0113829572	-0.0106103653	-0.0308128559	0.0081285653	-0.0006631375
7: Trans width at jugal/maxilla contact	-0.009111216	-0.0048609480	-0.0022275809	-0.0146837568	0.0027612583	0.0062903811
8: Trans width at ptyergoid/palatine contact	-0.009657968	-0.0155876890	-0.0090508632	-0.0294793024	-0.0399934730	0.0166535875
9: Tran width at dorsalmost point of orbits	-0.017111181	-0.0022063468	-0.0135393338	-0.0226756215	0.0058054582	0.0032069464
10: L from dorsal pt of orbit to ventral pt of orbit	-0.019649469	-0.0033342732	-0.0010502631	-0.0175298959	0.0118310049	0.0012371758
11: L from ant orbit to post orbit	-0.012661079	-0.0010238013	0.0005856456	-0.0110533500	0.0093926794	0.0016125823
12: L from ant jugal/maxilla contact to post qj/qu contact	-0.015027382	0.0002592479	-0.0045147764	-0.0155701674	0.0071456563	0.0020179285
13: Trans width at post qj/qu contact	-0.013081484	-0.0026717102	-0.0108789293	-0.0187006339	0.0035108621	0.0061278926
14: L jugal/maxilla contact to pterygoid/palatine contact	0.005530707	0.0060690164	0.0006261750	0.0008310799	0.0070419148	0.0064152719
15: qj/qu contact to qu/laterosphenoid contact	-0.019833802	-0.0053113733	-0.0100414665	-0.0212015558	0.0096195270	0.0033823212
16: width of occipital condyle	-0.019397685	0.0045744736	-0.0117949375	-0.0228094263	0.0118367090	0.0191685680
17: height of occipital condyle	-0.019092878	-0.0067432158	-0.0014719180	-0.0270620362	-0.0079983330	0.0047268735
18: Basioccipital width	-0.016250054	0.0021536674	-0.0088499961	-0.0233786941	0.0004468901	0.0156645635
19: Vertical diameter of foramen magnum	-0.012242427	-0.0171076678	-0.0017344830	-0.0208626217	0.0110510995	-0.0081522754
20: Trans width of supraoccipital	-0.023768816	-0.0012534323	-0.0047375459	-0.0255712797	0.0077696240	0.0106299925
21: L qj/qu to jugal projection	-0.029255749	-0.0253481273	-0.0127302533	-0.0504439602	-0.0049857048	-0.0322893421
22: Height of jugal at projection	-0.047385613	-0.0146224428	-0.0240368873	-0.0633391925	-0.0073063829	-0.0048029510
23: Total casque L	-0.127130305	0.0443443338	0.0254291726			
24: Basal casque L	-0.070066693	0.0507943587	0.0049860638			
25: L from casque contact with rostrum to posterodorsal point	-0.099691924	0.0411699564	0.0048539998			
26: Casque width dorsal to lachrymal suture	-0.098257184	-0.0069188303	-0.0027424441			
27: Casque width dorsal to ant contact with rostrum	-0.225755847	-0.1531080682	0.0615815714			
28: L maxilla/jugal ventral contact to dorsal surface of casque	-0.104844150	-0.0141116482	0.0156580785			
29: H of casque at ant contact with rostrum	-0.371124583	0.0763289968	-0.0342954362			
30: Anteror contact of casque with rostrum to maxilla/jugal contact	054359572	0.0311310072	0.0031501231			
31: L ant rostrum to ant casque	-0.035272698	-0.0884882888	-0.0835037157			
32: L ant rostrum to ant base of casque	-0.004352704	-0.0619585562	-0.0305709840			

Appendix 6.5 TPS landmark data for hornbills

LM=31
43.00000 181.00000
230.00000 371.00000
52.00000 334.00000
829.00000 506.00000
668.00000 239.00000
664.00000 280.00000
810.00000 196.00000
842.00000 248.00000
879.00000 298.00000
621.00000 361.00000
754.00000 348.00000
750.00000 244.00000
776.00000 249.00000
42.00000 183.00000
89.00000 259.00000
156.00000 319.00000
229.00000 372.00000
232.00000 374.00000
174.00000 377.00000
111.00000 352.00000
51.00000 332.00000
49.00000 334.00000
105.00000 417.00000
186.00000 476.00000
272.00000 525.00000
359.00000 572.00000
456.00000 600.00000
554.00000 605.00000
652.00000 591.00000
746.00000 566.00000
829.00000 506.00000
IMAGE=MOR-OST-1620.tif
ID=0
SCALE=0.020492

LM=31
32.00000 172.00000
274.00000 418.00000
155.00000 560.00000
867.00000 551.00000

669.00000 242.00000
664.00000 281.00000
813.00000 202.00000
854.00000 257.00000
883.00000 312.00000
632.00000 361.00000
774.00000 362.00000
772.00000 245.00000
793.00000 255.00000
30.00000 171.00000
85.00000 275.00000
172.00000 356.00000
274.00000 416.00000
277.00000 419.00000
237.00000 465.00000
191.00000 508.00000
155.00000 559.00000
158.00000 565.00000
223.00000 616.00000
302.00000 645.00000
386.00000 658.00000
471.00000 662.00000
555.00000 662.00000
640.00000 652.00000
722.00000 633.00000
801.00000 602.00000
866.00000 552.00000
IMAGE=MOR-OST-1621.tif
ID=1
SCALE=0.020243

LM=31
21.00000 198.00000
188.00000 378.00000
220.00000 429.00000
770.00000 580.00000
642.00000 260.00000
629.00000 295.00000
803.00000 223.00000
835.00000 301.00000
858.00000 370.00000
578.00000 390.00000
728.00000 407.00000
753.00000 259.00000

772.00000 305.00000
20.00000 199.00000
63.00000 269.00000
122.00000 326.00000
187.00000 377.00000
188.00000 378.00000
197.00000 396.00000
210.00000 412.00000
221.00000 429.00000
224.00000 434.00000
280.00000 475.00000
337.00000 514.00000
395.00000 551.00000
452.00000 591.00000
513.00000 622.00000
580.00000 637.00000
649.00000 638.00000
716.00000 620.00000
770.00000 580.00000
IMAGE=MOR-OST-1622.tif
ID=2
SCALE=0.018726

LM=31
47.00000 179.00000
258.00000 384.00000
163.00000 524.00000
861.00000 508.00000
666.00000 237.00000
659.00000 270.00000
818.00000 205.00000
848.00000 267.00000
866.00000 338.00000
617.00000 355.00000
752.00000 379.00000
772.00000 233.00000
799.00000 273.00000
45.00000 179.00000
98.00000 264.00000
175.00000 328.00000
258.00000 384.00000
258.00000 384.00000
242.00000 433.00000
192.00000 469.00000

163.00000 523.00000
164.00000 525.00000
233.00000 568.00000
311.00000 593.00000
393.00000 602.00000
475.00000 604.00000
557.00000 601.00000
638.00000 590.00000
719.00000 576.00000
797.00000 550.00000
862.00000 508.00000
IMAGE=MOR-OST-1625.tif
ID=3
SCALE=0.020120

LM=31
30.00000 170.00000
274.00000 425.00000
178.00000 544.00000
875.00000 485.00000
687.00000 263.00000
694.00000 295.00000
823.00000 203.00000
867.00000 255.00000
893.00000 309.00000
658.00000 364.00000
784.00000 361.00000
799.00000 249.00000
815.00000 255.00000
28.00000 170.00000
85.00000 275.00000
174.00000 357.00000
275.00000 422.00000
277.00000 426.00000
244.00000 468.00000
201.00000 498.00000
179.00000 544.00000
179.00000 547.00000
245.00000 593.00000
326.00000 615.00000
409.00000 624.00000
493.00000 624.00000
576.00000 614.00000
658.00000 597.00000

738.00000 572.00000
816.00000 541.00000
875.00000 487.00000
IMAGE=MOR-OST-1626.tif
ID=4
SCALE=0.020920

LM=31
40.00000 174.00000
272.00000 402.00000
162.00000 519.00000
856.00000 534.00000
675.00000 244.00000
683.00000 268.00000
814.00000 196.00000
847.00000 256.00000
875.00000 319.00000
629.00000 359.00000
762.00000 374.00000
780.00000 250.00000
796.00000 255.00000
40.00000 174.00000
93.00000 270.00000
175.00000 344.00000
272.00000 400.00000
273.00000 404.00000
249.00000 451.00000
201.00000 481.00000
163.00000 519.00000
162.00000 523.00000
218.00000 573.00000
297.00000 597.00000
379.00000 609.00000
462.00000 614.00000
544.00000 613.00000
627.00000 606.00000
706.00000 584.00000
787.00000 574.00000
856.00000 534.00000
IMAGE=MOR-OST-1627.tif
ID=5
SCALE=0.020367

LM=31

29.00000 173.00000
239.00000 388.00000
142.00000 597.00000
845.00000 544.00000
688.00000 243.00000
683.00000 282.00000
829.00000 200.00000
859.00000 255.00000
889.00000 318.00000
646.00000 361.00000
780.00000 361.00000
783.00000 249.00000
799.00000 266.00000
27.00000 173.00000
78.00000 260.00000
155.00000 329.00000
239.00000 388.00000
242.00000 389.00000
213.00000 456.00000
169.00000 522.00000
144.00000 596.00000
144.00000 597.00000
218.00000 615.00000
298.00000 617.00000
378.00000 615.00000
458.00000 614.00000
538.00000 611.00000
618.00000 602.00000
697.00000 593.00000
776.00000 577.00000
844.00000 543.00000
IMAGE=MOR-OST-1628.tif
ID=6
SCALE=0.021276

LM=31
32.00000 176.00000
240.00000 397.00000
93.00000 588.00000
893.00000 528.00000
684.00000 250.00000
687.00000 282.00000
823.00000 204.00000
855.00000 252.00000

878.00000 320.00000
644.00000 371.00000
779.00000 371.00000
784.00000 245.00000
798.00000 260.00000
30.00000 175.00000
77.00000 268.00000
152.00000 341.00000
241.00000 397.00000
239.00000 397.00000
185.00000 452.00000
130.00000 514.00000
94.00000 589.00000
96.00000 593.00000
175.00000 629.00000
268.00000 630.00000
362.00000 632.00000
455.00000 636.00000
548.00000 637.00000
641.00000 624.00000
732.00000 605.00000
823.00000 582.00000
893.00000 530.00000
IMAGE=MOR-OST-1629.tif
ID=7
SCALE=0.020876

LM=31
28.00000 172.00000
296.00000 431.00000
155.00000 593.00000
905.00000 501.00000
696.00000 248.00000
699.00000 276.00000
830.00000 202.00000
874.00000 248.00000
908.00000 302.00000
654.00000 371.00000
791.00000 365.00000
797.00000 247.00000
812.00000 260.00000
26.00000 170.00000
83.00000 286.00000
180.00000 372.00000

295.00000 432.00000
296.00000 432.00000
243.00000 479.00000
194.00000 531.00000
156.00000 590.00000
156.00000 594.00000
229.00000 640.00000
318.00000 654.00000
407.00000 660.00000
497.00000 658.00000
586.00000 648.00000
674.00000 629.00000
759.00000 600.00000
838.00000 557.00000
905.00000 500.00000
IMAGE=MOR-OST-1630.tif
ID=8
SCALE=0.020661

LM=31
34.00000 174.00000
257.00000 404.00000
130.00000 625.00000
868.00000 566.00000
689.00000 249.00000
679.00000 285.00000
817.00000 202.00000
853.00000 245.00000
884.00000 302.00000
638.00000 362.00000
766.00000 378.00000
781.00000 251.00000
789.00000 253.00000
33.00000 174.00000
84.00000 270.00000
165.00000 344.00000
257.00000 403.00000
257.00000 406.00000
211.00000 476.00000
159.00000 545.00000
130.00000 623.00000
131.00000 626.00000
210.00000 645.00000
295.00000 648.00000

379.00000 648.00000
463.00000 645.00000
548.00000 642.00000
632.00000 635.00000
716.00000 624.00000
798.00000 606.00000
866.00000 566.00000
IMAGE=MOR-OST-1631.tif
ID=9
SCALE=0.021412

LM=31
41.00000 186.00000
257.00000 409.00000
136.00000 569.00000
890.00000 549.00000
685.00000 259.00000
678.00000 298.00000
830.00000 219.00000
859.00000 273.00000
890.00000 327.00000
643.00000 379.00000
778.00000 386.00000
787.00000 256.00000
808.00000 263.00000
39.00000 185.00000
90.00000 278.00000
168.00000 350.00000
256.00000 409.00000
257.00000 410.00000
224.00000 464.00000
175.00000 512.00000
136.00000 567.00000
136.00000 570.00000
204.00000 618.00000
291.00000 638.00000
379.00000 651.00000
468.00000 654.00000
557.00000 648.00000
646.00000 638.00000
734.00000 621.00000
820.00000 596.00000
890.00000 550.00000
IMAGE=MOR-OST-1632.tif

ID=10
SCALE=0.020408

LM=31
30.00000 155.00000
397.00000 403.00000
466.00000 589.00000
905.00000 459.00000
711.00000 224.00000
699.00000 264.00000
853.00000 183.00000
878.00000 243.00000
896.00000 302.00000
659.00000 344.00000
791.00000 335.00000
807.00000 233.00000
814.00000 254.00000
29.00000 155.00000
125.00000 271.00000
255.00000 349.00000
397.00000 403.00000
398.00000 404.00000
451.00000 448.00000
467.00000 517.00000
466.00000 588.00000
468.00000 591.00000
520.00000 615.00000
575.00000 629.00000
632.00000 633.00000
689.00000 625.00000
744.00000 609.00000
793.00000 581.00000
840.00000 548.00000
878.00000 506.00000
905.00000 459.00000
IMAGE=MOR-OST-1633.tif
ID=11
SCALE=0.023148

LM=31
17.00000 179.00000
457.00000 438.00000
514.00000 465.00000
739.00000 403.00000

680.00000 254.00000
682.00000 273.00000
816.00000 210.00000
844.00000 264.00000
883.00000 318.00000
617.00000 359.00000
763.00000 364.00000
768.00000 254.00000
791.00000 267.00000
15.00000 176.00000
130.00000 306.00000
285.00000 388.00000
455.00000 435.00000
457.00000 435.00000
475.00000 447.00000
495.00000 455.00000
514.00000 465.00000
514.00000 465.00000
541.00000 464.00000
567.00000 461.00000
593.00000 456.00000
620.00000 451.00000
646.00000 446.00000
671.00000 438.00000
697.00000 430.00000
717.00000 415.00000
740.00000 404.00000
IMAGE=MOR-OST-1634.tif
ID=12
SCALE=0.020790

LM=31
36.00000 191.00000
273.00000 401.00000
272.00000 454.00000
717.00000 423.00000
668.00000 260.00000
660.00000 296.00000
821.00000 221.00000
852.00000 279.00000
877.00000 341.00000
612.00000 375.00000
753.00000 378.00000
775.00000 262.00000

795.00000 270.00000
34.00000 193.00000
95.00000 279.00000
180.00000 346.00000
273.00000 401.00000
275.00000 402.00000
270.00000 419.00000
268.00000 437.00000
274.00000 454.00000
275.00000 457.00000
314.00000 488.00000
366.00000 495.00000
418.00000 496.00000
470.00000 492.00000
522.00000 488.00000
574.00000 480.00000
624.00000 469.00000
674.00000 453.00000
716.00000 423.00000
IMAGE=MOR-OST-1635.tif
ID=13
SCALE=0.018692

LM=31
36.00000 200.00000
512.00000 466.00000
526.00000 478.00000
723.00000 480.00000
657.00000 264.00000
645.00000 301.00000
799.00000 226.00000
835.00000 276.00000
866.00000 339.00000
589.00000 378.00000
742.00000 374.00000
750.00000 263.00000
764.00000 269.00000
35.00000 201.00000
166.00000 331.00000
332.00000 416.00000
512.00000 466.00000
515.00000 469.00000
519.00000 472.00000
522.00000 475.00000

525.00000 478.00000
528.00000 478.00000
550.00000 483.00000
571.00000 489.00000
592.00000 495.00000
614.00000 496.00000
637.00000 494.00000
659.00000 491.00000
681.00000 492.00000
703.00000 490.00000
722.00000 480.00000
IMAGE=MOR-OST-1636.tif
ID=14
SCALE=0.017699

LM=31
49.00000 177.00000
280.00000 402.00000
240.00000 514.00000
871.00000 505.00000
701.00000 242.00000
703.00000 274.00000
839.00000 207.00000
871.00000 260.00000
901.00000 322.00000
656.00000 360.00000
783.00000 363.00000
795.00000 240.00000
808.00000 257.00000
49.00000 176.00000
104.00000 270.00000
186.00000 343.00000
281.00000 399.00000
283.00000 403.00000
283.00000 441.00000
256.00000 474.00000
241.00000 514.00000
241.00000 517.00000
297.00000 567.00000
367.00000 597.00000
442.00000 614.00000
519.00000 617.00000
596.00000 611.00000
671.00000 598.00000

747.00000 581.00000
819.00000 556.00000
871.00000 507.00000
IMAGE=MOR-OST-258.tif
ID=15
SCALE=0.021691

LM=31
35.00000 193.00000
253.00000 395.00000
240.00000 419.00000
710.00000 417.00000
662.00000 257.00000
653.00000 293.00000
799.00000 223.00000
830.00000 278.00000
853.00000 334.00000
604.00000 372.00000
741.00000 373.00000
759.00000 266.00000
766.00000 277.00000
33.00000 193.00000
89.00000 277.00000
167.00000 341.00000
253.00000 393.00000
253.00000 397.00000
250.00000 405.00000
245.00000 412.00000
242.00000 418.00000
239.00000 417.00000
269.00000 461.00000
324.00000 476.00000
381.00000 478.00000
437.00000 474.00000
495.00000 471.00000
551.00000 467.00000
608.00000 459.00000
663.00000 446.00000
710.00000 416.00000
IMAGE=MOR-OST-259.tif
ID=16
SCALE=0.019802

LM=31

64.00000 189.00000
266.00000 397.00000
36.00000 307.00000
826.00000 513.00000
681.00000 240.00000
676.00000 273.00000
822.00000 202.00000
859.00000 246.00000
896.00000 286.00000
646.00000 360.00000
777.00000 349.00000
775.00000 244.00000
793.00000 247.00000
63.00000 189.00000
114.00000 272.00000
187.00000 340.00000
268.00000 397.00000
269.00000 401.00000
186.00000 400.00000
105.00000 360.00000
35.00000 304.00000
35.00000 308.00000
75.00000 401.00000
150.00000 475.00000
236.00000 536.00000
333.00000 578.00000
435.00000 604.00000
540.00000 613.00000
644.00000 606.00000
744.00000 573.00000
826.00000 513.00000
IMAGE=MOR-OST-265.tif
ID=17
SCALE=0.020366

LM=31
38.00000 180.00000
204.00000 366.00000
37.00000 559.00000
842.00000 562.00000
687.00000 241.00000
684.00000 271.00000
832.00000 216.00000
862.00000 271.00000

888.00000 332.00000
639.00000 352.00000
772.00000 371.00000
786.00000 249.00000
807.00000 265.00000
37.00000 179.00000
76.00000 253.00000
137.00000 313.00000
205.00000 365.00000
203.00000 365.00000
147.00000 426.00000
83.00000 486.00000
38.00000 557.00000
38.00000 560.00000
117.00000 597.00000
209.00000 607.00000
301.00000 618.00000
393.00000 622.00000
485.00000 626.00000
577.00000 622.00000
669.00000 612.00000
760.00000 596.00000
843.00000 561.00000
IMAGE=MOR-OST-266.tif
ID=18
SCALE=0.021141

LM=31
48.00000 184.00000
266.00000 420.00000
198.00000 616.00000
876.00000 547.00000
697.00000 266.00000
702.00000 297.00000
848.00000 217.00000
881.00000 266.00000
921.00000 324.00000
657.00000 389.00000
804.00000 377.00000
808.00000 259.00000
823.00000 272.00000
47.00000 184.00000
97.00000 281.00000
173.00000 360.00000

266.00000 419.00000
269.00000 420.00000
269.00000 493.00000
244.00000 563.00000
200.00000 617.00000
201.00000 621.00000
274.00000 653.00000
354.00000 669.00000
435.00000 679.00000
517.00000 684.00000
598.00000 679.00000
678.00000 665.00000
756.00000 641.00000
831.00000 607.00000
877.00000 547.00000
IMAGE=MOR-OST-267.tif
ID=19
SCALE=0.020000

LM=31
59.00000 198.00000
305.00000 413.00000
329.00000 476.00000
758.00000 434.00000
679.00000 269.00000
671.00000 307.00000
819.00000 220.00000
853.00000 274.00000
880.00000 330.00000
623.00000 384.00000
760.00000 380.00000
784.00000 265.00000
793.00000 281.00000
59.00000 200.00000
122.00000 290.00000
208.00000 360.00000
305.00000 413.00000
308.00000 415.00000
316.00000 435.00000
320.00000 457.00000
330.00000 477.00000
331.00000 481.00000
373.00000 508.00000
423.00000 516.00000

473.00000 515.00000
523.00000 510.00000
573.00000 505.00000
623.00000 496.00000
672.00000 485.00000
718.00000 466.00000
756.00000 434.00000
IMAGE=MOR-OST-268.tif
ID=20
SCALE=0.018657

LM=31
54.00000 211.00000
302.00000 409.00000
353.00000 486.00000
716.00000 449.00000
666.00000 280.00000
666.00000 309.00000
822.00000 247.00000
843.00000 308.00000
867.00000 367.00000
604.00000 393.00000
747.00000 405.00000
781.00000 281.00000
788.00000 308.00000
54.00000 211.00000
121.00000 295.00000
211.00000 355.00000
305.00000 410.00000
303.00000 410.00000
328.00000 430.00000
344.00000 456.00000
353.00000 487.00000
354.00000 490.00000
393.00000 506.00000
435.00000 515.00000
478.00000 517.00000
520.00000 514.00000
562.00000 509.00000
605.00000 503.00000
646.00000 494.00000
682.00000 474.00000
716.00000 449.00000
IMAGE=MOR-OST-269.tif

ID=21
SCALE=0.018083

LM=31
39.00000 208.00000
256.00000 413.00000
272.00000 483.00000
752.00000 442.00000
671.00000 276.00000
669.00000 308.00000
822.00000 239.00000
861.00000 304.00000
874.00000 372.00000
614.00000 392.00000
771.00000 398.00000
780.00000 269.00000
795.00000 310.00000
38.00000 209.00000
94.00000 292.00000
170.00000 357.00000
255.00000 411.00000
257.00000 415.00000
265.00000 436.00000
269.00000 459.00000
271.00000 482.00000
272.00000 486.00000
324.00000 506.00000
379.00000 515.00000
435.00000 518.00000
490.00000 516.00000
546.00000 509.00000
601.00000 501.00000
655.00000 489.00000
707.00000 470.00000
752.00000 440.00000
IMAGE=MOR-OST-270.tif
ID=22
SCALE=0.018315

LM=31
48.00000 171.00000
241.00000 380.00000
139.00000 555.00000
857.00000 534.00000

688.00000 239.00000
678.00000 277.00000
841.00000 203.00000
868.00000 262.00000
896.00000 330.00000
635.00000 359.00000
769.00000 365.00000
794.00000 256.00000
808.00000 256.00000
46.00000 170.00000
92.00000 255.00000
161.00000 323.00000
241.00000 379.00000
242.00000 382.00000
219.00000 442.00000
163.00000 487.00000
139.00000 554.00000
139.00000 559.00000
205.00000 599.00000
289.00000 604.00000
374.00000 607.00000
458.00000 608.00000
542.00000 607.00000
626.00000 600.00000
709.00000 591.00000
792.00000 574.00000
856.00000 533.00000
IMAGE=MOR-OST-272.tif
ID=23
SCALE=0.020833

LM=31
35.00000 179.00000
244.00000 392.00000
96.00000 574.00000
891.00000 552.00000
692.00000 238.00000
687.00000 276.00000
834.00000 206.00000
865.00000 264.00000
881.00000 324.00000
642.00000 355.00000
769.00000 360.00000
793.00000 248.00000

809.00000 254.00000
35.00000 179.00000
86.00000 264.00000
160.00000 331.00000
244.00000 386.00000
246.00000 389.00000
186.00000 443.00000
132.00000 501.00000
96.00000 573.00000
97.00000 577.00000
177.00000 611.00000
268.00000 613.00000
359.00000 619.00000
450.00000 617.00000
541.00000 626.00000
632.00000 623.00000
722.00000 608.00000
811.00000 588.00000
890.00000 551.00000
IMAGE=MOR-OST-273.tif
ID=24
SCALE=0.021552

LM=31
33.00000 177.00000
264.00000 427.00000
165.00000 556.00000
873.00000 510.00000
682.00000 254.00000
678.00000 284.00000
823.00000 208.00000
859.00000 258.00000
892.00000 310.00000
650.00000 369.00000
778.00000 365.00000
785.00000 246.00000
799.00000 247.00000
33.00000 177.00000
86.00000 278.00000
169.00000 360.00000
265.00000 425.00000
265.00000 425.00000
248.00000 474.00000
204.00000 512.00000

166.00000 554.00000
164.00000 558.00000
232.00000 602.00000
314.00000 618.00000
398.00000 627.00000
482.00000 628.00000
565.00000 621.00000
648.00000 606.00000
729.00000 585.00000
808.00000 557.00000
872.00000 509.00000
IMAGE=MOR-OST-274.tif
ID=25
SCALE=0.020833

LM=31
30.00000 181.00000
260.00000 406.00000
233.00000 466.00000
849.00000 500.00000
688.00000 246.00000
684.00000 278.00000
831.00000 208.00000
858.00000 261.00000
892.00000 317.00000
639.00000 364.00000
776.00000 367.00000
787.00000 241.00000
808.00000 273.00000
29.00000 182.00000
83.00000 276.00000
166.00000 348.00000
260.00000 404.00000
262.00000 406.00000
266.00000 432.00000
257.00000 454.00000
234.00000 465.00000
233.00000 468.00000
274.00000 533.00000
338.00000 578.00000
412.00000 603.00000
490.00000 608.00000
568.00000 604.00000
646.00000 592.00000

723.00000 574.00000
797.00000 550.00000
850.00000 501.00000
IMAGE=MOR-OST-275.tif
ID=26
SCALE=0.020450

LM=31
28.00000 190.00000
269.00000 429.00000
96.00000 574.00000
859.00000 595.00000
668.00000 262.00000
672.00000 296.00000
815.00000 219.00000
850.00000 272.00000
877.00000 332.00000
626.00000 388.00000
766.00000 387.00000
773.00000 265.00000
787.00000 280.00000
27.00000 190.00000
84.00000 290.00000
170.00000 369.00000
269.00000 429.00000
269.00000 430.00000
198.00000 464.00000
132.00000 506.00000
97.00000 574.00000
96.00000 576.00000
168.00000 622.00000
255.00000 645.00000
342.00000 665.00000
431.00000 678.00000
521.00000 681.00000
610.00000 677.00000
699.00000 664.00000
786.00000 640.00000
859.00000 594.00000
IMAGE=MOR-OST-276.tif
ID=27
SCALE=0.020661

LM=31

51.00000 167.00000
225.00000 377.00000
40.00000 511.00000
905.00000 503.00000
684.00000 243.00000
687.00000 276.00000
817.00000 192.00000
852.00000 242.00000
880.00000 302.00000
656.00000 364.00000
773.00000 358.00000
783.00000 243.00000
794.00000 253.00000
48.00000 167.00000
89.00000 251.00000
153.00000 320.00000
227.00000 378.00000
228.00000 378.00000
152.00000 400.00000
87.00000 446.00000
41.00000 510.00000
39.00000 513.00000
121.00000 566.00000
220.00000 588.00000
321.00000 604.00000
422.00000 611.00000
524.00000 612.00000
625.00000 601.00000
724.00000 580.00000
822.00000 551.00000
905.00000 504.00000
IMAGE=MOR-OST-277.tif
ID=28
SCALE=0.022124

LM=31
15.00000 182.00000
225.00000 389.00000
60.00000 551.00000
863.00000 540.00000
672.00000 248.00000
666.00000 286.00000
820.00000 213.00000
851.00000 271.00000

875.00000 337.00000
630.00000 367.00000
759.00000 371.00000
775.00000 247.00000
793.00000 266.00000
14.00000 183.00000
66.00000 267.00000
141.00000 334.00000
225.00000 388.00000
226.00000 392.00000
161.00000 435.00000
98.00000 484.00000
60.00000 552.00000
60.00000 555.00000
140.00000 598.00000
232.00000 623.00000
325.00000 641.00000
419.00000 652.00000
512.00000 653.00000
606.00000 643.00000
699.00000 623.00000
789.00000 593.00000
862.00000 538.00000
IMAGE=MOR-OST-278.tif
ID=29
SCALE=0.021052

LM=31
26.00000 152.00000
272.00000 378.00000
67.00000 505.00000
881.00000 505.00000
689.00000 219.00000
684.00000 253.00000
829.00000 185.00000
856.00000 235.00000
889.00000 289.00000
646.00000 332.00000
777.00000 340.00000
789.00000 226.00000
794.00000 231.00000
24.00000 151.00000
83.00000 249.00000
173.00000 321.00000

273.00000 378.00000
274.00000 380.00000
190.00000 391.00000
122.00000 443.00000
67.00000 504.00000
69.00000 508.00000
150.00000 547.00000
243.00000 550.00000
336.00000 552.00000
429.00000 555.00000
522.00000 554.00000
615.00000 551.00000
708.00000 544.00000
800.00000 529.00000
881.00000 506.00000
IMAGE=MOR-OST-279.tif
ID=30
SCALE=0.022573

LM=31
33.00000 175.00000
272.00000 415.00000
176.00000 545.00000
887.00000 525.00000
696.00000 247.00000
690.00000 283.00000
825.00000 203.00000
859.00000 252.00000
895.00000 321.00000
644.00000 378.00000
784.00000 373.00000
783.00000 247.00000
797.00000 256.00000
33.00000 176.00000
90.00000 275.00000
175.00000 352.00000
272.00000 414.00000
273.00000 417.00000
246.00000 460.00000
202.00000 495.00000
177.00000 544.00000
177.00000 547.00000
243.00000 594.00000
325.00000 615.00000

409.00000 628.00000
494.00000 636.00000
580.00000 636.00000
664.00000 625.00000
748.00000 608.00000
828.00000 581.00000
886.00000 524.00000
IMAGE=MOR-OST-280.tif
ID=31
SCALE=0.021097

LM=31
52.00000 174.00000
269.00000 401.00000
135.00000 551.00000
881.00000 532.00000
686.00000 243.00000
684.00000 277.00000
832.00000 208.00000
862.00000 264.00000
887.00000 322.00000
637.00000 360.00000
777.00000 362.00000
792.00000 259.00000
803.00000 259.00000
51.00000 174.00000
101.00000 266.00000
180.00000 339.00000
268.00000 399.00000
269.00000 403.00000
222.00000 452.00000
167.00000 492.00000
136.00000 550.00000
136.00000 553.00000
205.00000 592.00000
292.00000 601.00000
378.00000 609.00000
465.00000 612.00000
552.00000 611.00000
638.00000 604.00000
724.00000 591.00000
809.00000 572.00000
881.00000 533.00000
IMAGE=MOR-OST-281.tif

ID=32
SCALE=0.021186

LM=31
36.00000 189.00000
272.00000 419.00000
256.00000 478.00000
795.00000 518.00000
651.00000 258.00000
640.00000 292.00000
803.00000 224.00000
835.00000 281.00000
861.00000 353.00000
599.00000 366.00000
729.00000 381.00000
759.00000 258.00000
769.00000 278.00000
35.00000 189.00000
91.00000 285.00000
177.00000 358.00000
272.00000 418.00000
273.00000 420.00000
272.00000 440.00000
263.00000 458.00000
256.00000 476.00000
256.00000 479.00000
289.00000 538.00000
341.00000 585.00000
404.00000 612.00000
473.00000 620.00000
543.00000 616.00000
611.00000 603.00000
678.00000 584.00000
744.00000 560.00000
795.00000 520.00000
IMAGE=MOR-OST-285.tif
ID=33
SCALE=0.020202

LM=31
25.00000 185.00000
256.00000 387.00000
150.00000 529.00000
842.00000 557.00000

672.00000 237.00000
656.00000 276.00000
811.00000 201.00000
852.00000 258.00000
881.00000 324.00000
613.00000 355.00000
756.00000 366.00000
765.00000 245.00000
784.00000 260.00000
24.00000 185.00000
86.00000 268.00000
168.00000 334.00000
259.00000 387.00000
259.00000 391.00000
224.00000 434.00000
178.00000 475.00000
150.00000 527.00000
151.00000 527.00000
223.00000 560.00000
300.00000 582.00000
378.00000 600.00000
457.00000 610.00000
537.00000 618.00000
617.00000 617.00000
697.00000 608.00000
775.00000 594.00000
842.00000 557.00000
IMAGE=MOR-OST-286.tif
ID=34
SCALE=0.020080

LM=31
36.00000 176.00000
256.00000 419.00000
134.00000 561.00000
878.00000 534.00000
691.00000 249.00000
678.00000 287.00000
825.00000 210.00000
855.00000 268.00000
875.00000 333.00000
632.00000 382.00000
761.00000 379.00000
781.00000 255.00000

787.00000 274.00000
35.00000 177.00000
77.00000 280.00000
161.00000 360.00000
260.00000 420.00000
260.00000 424.00000
206.00000 458.00000
154.00000 498.00000
136.00000 560.00000
136.00000 563.00000
202.00000 612.00000
289.00000 628.00000
377.00000 639.00000
465.00000 645.00000
553.00000 645.00000
641.00000 631.00000
726.00000 609.00000
810.00000 582.00000
877.00000 534.00000
IMAGE=MOR-OST-287.tif
ID=35
SCALE=0.021052

LM=31
51.00000 171.00000
246.00000 376.00000
136.00000 500.00000
859.00000 528.00000
680.00000 240.00000
678.00000 278.00000
823.00000 198.00000
856.00000 254.00000
885.00000 312.00000
644.00000 360.00000
762.00000 366.00000
777.00000 238.00000
796.00000 257.00000
50.00000 170.00000
96.00000 253.00000
167.00000 321.00000
247.00000 375.00000
248.00000 376.00000
201.00000 405.00000
153.00000 442.00000

136.00000 500.00000
136.00000 502.00000
203.00000 552.00000
285.00000 577.00000
370.00000 593.00000
455.00000 602.00000
541.00000 608.00000
627.00000 609.00000
712.00000 600.00000
795.00000 578.00000
857.00000 527.00000
IMAGE=MOR-OST-288.tif
ID=36
SCALE=0.021052

LM=31
43.00000 170.00000
251.00000 397.00000
66.00000 550.00000
895.00000 538.00000
685.00000 241.00000
683.00000 272.00000
820.00000 191.00000
854.00000 241.00000
883.00000 296.00000
641.00000 362.00000
787.00000 358.00000
782.00000 242.00000
798.00000 249.00000
41.00000 170.00000
89.00000 263.00000
165.00000 336.00000
251.00000 397.00000
251.00000 398.00000
195.00000 456.00000
130.00000 505.00000
66.00000 550.00000
65.00000 552.00000
144.00000 598.00000
238.00000 620.00000
334.00000 638.00000
431.00000 647.00000
529.00000 646.00000
626.00000 639.00000

721.00000 618.00000
813.00000 587.00000
894.00000 537.00000
IMAGE=MOR-OST-289.tif
ID=37
SCALE=0.021141

LM=31
36.00000 148.00000
407.00000 417.00000
434.00000 660.00000
935.00000 406.00000
710.00000 226.00000
705.00000 263.00000
844.00000 174.00000
880.00000 222.00000
903.00000 278.00000
679.00000 330.00000
806.00000 323.00000
802.00000 220.00000
814.00000 229.00000
35.00000 149.00000
129.00000 275.00000
259.00000 363.00000
408.00000 417.00000
408.00000 418.00000
471.00000 480.00000
464.00000 573.00000
434.00000 660.00000
436.00000 663.00000
491.00000 695.00000
563.00000 695.00000
633.00000 680.00000
702.00000 657.00000
766.00000 625.00000
824.00000 583.00000
875.00000 531.00000
917.00000 473.00000
935.00000 406.00000
IMAGE=MOR-OST-290.tif
ID=38
SCALE=0.023980

Appendix 6.6 TPS Data for hornbills with casque landmarks removed

LM=10
43.00000 181.00000
668.00000 239.00000
664.00000 280.00000
810.00000 196.00000
842.00000 248.00000
879.00000 298.00000
621.00000 361.00000
754.00000 348.00000
750.00000 244.00000
776.00000 249.00000
IMAGE=MOR-OST-1620.tif
ID=0
SCALE=0.020492

LM=10
32.00000 172.00000
669.00000 242.00000
664.00000 281.00000
813.00000 202.00000
854.00000 257.00000
883.00000 312.00000
632.00000 361.00000
774.00000 362.00000
772.00000 245.00000
793.00000 255.00000
IMAGE=MOR-OST-1621.tif
ID=1
SCALE=0.020243

LM=10
21.00000 198.00000
642.00000 260.00000
629.00000 295.00000
803.00000 223.00000
835.00000 301.00000
858.00000 370.00000
578.00000 390.00000
728.00000 407.00000
753.00000 259.00000
772.00000 305.00000
IMAGE=MOR-OST-1622.tif

ID=2
SCALE=0.018726

LM=10
47.00000 179.00000
666.00000 237.00000
659.00000 270.00000
818.00000 205.00000
848.00000 267.00000
866.00000 338.00000
617.00000 355.00000
752.00000 379.00000
772.00000 233.00000
799.00000 273.00000
IMAGE=MOR-OST-1625.tif
ID=3
SCALE=0.020120

LM=10
30.00000 170.00000
687.00000 263.00000
694.00000 295.00000
823.00000 203.00000
867.00000 255.00000
893.00000 309.00000
658.00000 364.00000
784.00000 361.00000
799.00000 249.00000
815.00000 255.00000
IMAGE=MOR-OST-1626.tif
ID=4
SCALE=0.020920

LM=10
40.00000 174.00000
675.00000 244.00000
683.00000 268.00000
814.00000 196.00000
847.00000 256.00000
875.00000 319.00000
629.00000 359.00000
762.00000 374.00000
780.00000 250.00000
796.00000 255.00000

IMAGE=MOR-OST-1627.tif
ID=5
SCALE=0.020367

LM=10
29.00000 173.00000
688.00000 243.00000
683.00000 282.00000
829.00000 200.00000
859.00000 255.00000
889.00000 318.00000
646.00000 361.00000
780.00000 361.00000
783.00000 249.00000
799.00000 266.00000
IMAGE=MOR-OST-1628.tif
ID=6
SCALE=0.021276

LM=10
32.00000 176.00000
684.00000 250.00000
687.00000 282.00000
823.00000 204.00000
855.00000 252.00000
878.00000 320.00000
644.00000 371.00000
779.00000 371.00000
784.00000 245.00000
798.00000 260.00000
IMAGE=MOR-OST-1629.tif
ID=7
SCALE=0.020876

LM=10
28.00000 172.00000
696.00000 248.00000
699.00000 276.00000
830.00000 202.00000
874.00000 248.00000
908.00000 302.00000
654.00000 371.00000
791.00000 365.00000
797.00000 247.00000

812.00000 260.00000
IMAGE=MOR-OST-1630.tif
ID=8
SCALE=0.020661

LM=10
34.00000 174.00000
689.00000 249.00000
679.00000 285.00000
817.00000 202.00000
853.00000 245.00000
884.00000 302.00000
638.00000 362.00000
766.00000 378.00000
781.00000 251.00000
789.00000 253.00000
IMAGE=MOR-OST-1631.tif
ID=9
SCALE=0.021412

LM=10
41.00000 186.00000
685.00000 259.00000
678.00000 298.00000
830.00000 219.00000
859.00000 273.00000
890.00000 327.00000
643.00000 379.00000
778.00000 386.00000
787.00000 256.00000
808.00000 263.00000
IMAGE=MOR-OST-1632.tif
ID=10
SCALE=0.020408

LM=10
30.00000 155.00000
711.00000 224.00000
699.00000 264.00000
853.00000 183.00000
878.00000 243.00000
896.00000 302.00000
659.00000 344.00000
791.00000 335.00000

807.00000 233.00000
814.00000 254.00000
IMAGE=MOR-OST-1633.tif
ID=11
SCALE=0.023148

LM=10
17.00000 179.00000
680.00000 254.00000
682.00000 273.00000
816.00000 210.00000
844.00000 264.00000
883.00000 318.00000
617.00000 359.00000
763.00000 364.00000
768.00000 254.00000
791.00000 267.00000
IMAGE=MOR-OST-1634.tif
ID=12
SCALE=0.020790

LM=10
36.00000 191.00000
668.00000 260.00000
660.00000 296.00000
821.00000 221.00000
852.00000 279.00000
877.00000 341.00000
612.00000 375.00000
753.00000 378.00000
775.00000 262.00000
795.00000 270.00000
IMAGE=MOR-OST-1635.tif
ID=13
SCALE=0.018692

LM=10
36.00000 200.00000
657.00000 264.00000
645.00000 301.00000
799.00000 226.00000
835.00000 276.00000
866.00000 339.00000
589.00000 378.00000

742.00000 374.00000
750.00000 263.00000
764.00000 269.00000
IMAGE=MOR-OST-1636.tif
ID=14
SCALE=0.017699

LM=10
49.00000 177.00000
701.00000 242.00000
703.00000 274.00000
839.00000 207.00000
871.00000 260.00000
901.00000 322.00000
656.00000 360.00000
783.00000 363.00000
795.00000 240.00000
808.00000 257.00000
IMAGE=MOR-OST-258.tif
ID=15
SCALE=0.021691

LM=10
35.00000 193.00000
662.00000 257.00000
653.00000 293.00000
799.00000 223.00000
830.00000 278.00000
853.00000 334.00000
604.00000 372.00000
741.00000 373.00000
759.00000 266.00000
766.00000 277.00000
IMAGE=MOR-OST-259.tif
ID=16
SCALE=0.019802

LM=10
64.00000 189.00000
681.00000 240.00000
676.00000 273.00000
822.00000 202.00000
859.00000 246.00000
896.00000 286.00000

646.00000 360.00000
777.00000 349.00000
775.00000 244.00000
793.00000 247.00000
IMAGE=MOR-OST-265.tif
ID=17
SCALE=0.020366

LM=10
38.00000 180.00000
687.00000 241.00000
684.00000 271.00000
832.00000 216.00000
862.00000 271.00000
888.00000 332.00000
639.00000 352.00000
772.00000 371.00000
786.00000 249.00000
807.00000 265.00000
IMAGE=MOR-OST-266.tif
ID=18
SCALE=0.021141

LM=10
48.00000 184.00000
697.00000 266.00000
702.00000 297.00000
848.00000 217.00000
881.00000 266.00000
921.00000 324.00000
657.00000 389.00000
804.00000 377.00000
808.00000 259.00000
823.00000 272.00000
IMAGE=MOR-OST-267.tif
ID=19
SCALE=0.020000

LM=10
59.00000 198.00000
679.00000 269.00000
671.00000 307.00000
819.00000 220.00000
853.00000 274.00000

880.00000 330.00000
623.00000 384.00000
760.00000 380.00000
784.00000 265.00000
793.00000 281.00000
IMAGE=MOR-OST-268.tif
ID=20
SCALE=0.018657

LM=10
54.00000 211.00000
666.00000 280.00000
666.00000 309.00000
822.00000 247.00000
843.00000 308.00000
867.00000 367.00000
604.00000 393.00000
747.00000 405.00000
781.00000 281.00000
788.00000 308.00000
IMAGE=MOR-OST-269.tif
ID=21
SCALE=0.018083

LM=10
39.00000 208.00000
671.00000 276.00000
669.00000 308.00000
822.00000 239.00000
861.00000 304.00000
874.00000 372.00000
614.00000 392.00000
771.00000 398.00000
780.00000 269.00000
795.00000 310.00000
IMAGE=MOR-OST-270.tif
ID=22
SCALE=0.018315

LM=10
48.00000 171.00000
688.00000 239.00000
678.00000 277.00000
841.00000 203.00000

868.00000 262.00000
896.00000 330.00000
635.00000 359.00000
769.00000 365.00000
794.00000 256.00000
808.00000 256.00000
IMAGE=MOR-OST-272.tif
ID=23
SCALE=0.020833

LM=10
35.00000 179.00000
692.00000 238.00000
687.00000 276.00000
834.00000 206.00000
865.00000 264.00000
881.00000 324.00000
642.00000 355.00000
769.00000 360.00000
793.00000 248.00000
809.00000 254.00000
IMAGE=MOR-OST-273.tif
ID=24
SCALE=0.021552

LM=10
33.00000 177.00000
682.00000 254.00000
678.00000 284.00000
823.00000 208.00000
859.00000 258.00000
892.00000 310.00000
650.00000 369.00000
778.00000 365.00000
785.00000 246.00000
799.00000 247.00000
IMAGE=MOR-OST-274.tif
ID=25
SCALE=0.020833

LM=10
30.00000 181.00000
688.00000 246.00000
684.00000 278.00000

831.00000 208.00000
858.00000 261.00000
892.00000 317.00000
639.00000 364.00000
776.00000 367.00000
787.00000 241.00000
808.00000 273.00000
IMAGE=MOR-OST-275.tif
ID=26
SCALE=0.020450

LM=10
28.00000 190.00000
668.00000 262.00000
672.00000 296.00000
815.00000 219.00000
850.00000 272.00000
877.00000 332.00000
626.00000 388.00000
766.00000 387.00000
773.00000 265.00000
787.00000 280.00000
IMAGE=MOR-OST-276.tif
ID=27
SCALE=0.020661

LM=10
51.00000 167.00000
684.00000 243.00000
687.00000 276.00000
817.00000 192.00000
852.00000 242.00000
880.00000 302.00000
656.00000 364.00000
773.00000 358.00000
783.00000 243.00000
794.00000 253.00000
IMAGE=MOR-OST-277.tif
ID=28
SCALE=0.022124

LM=10
15.00000 182.00000
672.00000 248.00000

666.00000 286.00000
820.00000 213.00000
851.00000 271.00000
875.00000 337.00000
630.00000 367.00000
759.00000 371.00000
775.00000 247.00000
793.00000 266.00000
IMAGE=MOR-OST-278.tif
ID=29
SCALE=0.021052

LM=10
26.00000 152.00000
689.00000 219.00000
684.00000 253.00000
829.00000 185.00000
856.00000 235.00000
889.00000 289.00000
646.00000 332.00000
777.00000 340.00000
789.00000 226.00000
794.00000 231.00000
IMAGE=MOR-OST-279.tif
ID=30
SCALE=0.022573

LM=10
33.00000 175.00000
696.00000 247.00000
690.00000 283.00000
825.00000 203.00000
859.00000 252.00000
895.00000 321.00000
644.00000 378.00000
784.00000 373.00000
783.00000 247.00000
797.00000 256.00000
IMAGE=MOR-OST-280.tif
ID=31
SCALE=0.021097

LM=10
52.00000 174.00000

686.00000 243.00000
684.00000 277.00000
832.00000 208.00000
862.00000 264.00000
887.00000 322.00000
637.00000 360.00000
777.00000 362.00000
792.00000 259.00000
803.00000 259.00000
IMAGE=MOR-OST-281.tif
ID=32
SCALE=0.021186

LM=10
36.00000 189.00000
651.00000 258.00000
640.00000 292.00000
803.00000 224.00000
835.00000 281.00000
861.00000 353.00000
599.00000 366.00000
729.00000 381.00000
759.00000 258.00000
769.00000 278.00000
IMAGE=MOR-OST-285.tif
ID=33
SCALE=0.020202

LM=10
25.00000 185.00000
672.00000 237.00000
656.00000 276.00000
811.00000 201.00000
852.00000 258.00000
881.00000 324.00000
613.00000 355.00000
756.00000 366.00000
765.00000 245.00000
784.00000 260.00000
IMAGE=MOR-OST-286.tif
ID=34
SCALE=0.020080

LM=10

36.00000 176.00000
691.00000 249.00000
678.00000 287.00000
825.00000 210.00000
855.00000 268.00000
875.00000 333.00000
632.00000 382.00000
761.00000 379.00000
781.00000 255.00000
787.00000 274.00000
IMAGE=MOR-OST-287.tif
ID=35
SCALE=0.021052

LM=10
51.00000 171.00000
680.00000 240.00000
678.00000 278.00000
823.00000 198.00000
856.00000 254.00000
885.00000 312.00000
644.00000 360.00000
762.00000 366.00000
777.00000 238.00000
796.00000 257.00000
IMAGE=MOR-OST-288.tif
ID=36
SCALE=0.021052

LM=10
43.00000 170.00000
685.00000 241.00000
683.00000 272.00000
820.00000 191.00000
854.00000 241.00000
883.00000 296.00000
641.00000 362.00000
787.00000 358.00000
782.00000 242.00000
798.00000 249.00000
IMAGE=MOR-OST-289.tif
ID=37
SCALE=0.021141

LM=10
36.00000 148.00000
710.00000 226.00000
705.00000 263.00000
844.00000 174.00000
880.00000 222.00000
903.00000 278.00000
679.00000 330.00000
806.00000 323.00000
802.00000 220.00000
814.00000 229.00000
IMAGE=MOR-OST-290.tif
ID=38
SCALE=0.023980

APPENDIX C

SUPPLEMENTARY INFORMATION FOR CHAPTER 7

Appendix 7.1. SMA results.

	N	R^2	Slope	95% CI (Slope)	Intercept	95% CI (Intercept)	Allometry
Postorbital Horn Core Length	29	0.854	1.79	1.541042 - 2.082233	-1.85	- 2.416185 - -1.359890	+
U3 Postorbital Horn Cores	13	0.806	1.91	1.434036 - 2.551108	-2.106	- 3.338376 - -1.1816456	+
M3 Postorbital Horn Cores	7	0.936	1.75	1.309455 - 2.325455	-1.70095	- 2.814375 - - 0.8654290	+
L3 Postorbital Horn Cores	4	0.144	2.071	0.356820 - 12.014501	-2.45	- 22.68463 - 1.041392	iso
Epinasal Length	21	0.351	2.897	1.9856053 - 4.226378	-4.67	7.347761 - -2.83013783	+
U3 Epinasals	11	0.94	2.5	2.079996 - 3.004298	-3.71525	- 4.720554 - -2.878769	+
M3 Epinasals	4	0.634	9.46	2.404255 - 37.243693	-17.91	- 73.72187 - - 3.730746	+
L3 Epinasals	3	0.286	3.49	0.1619794 - 74.99595	-6.10008	- 151.67654 - 0.6654611	iso
Epinasal Width	21	0.854	1.74	1.449423 - 2.087715	-2.53	- 3.232410 - -1.944014	+
U3 Epinasal W	10	0.938	1.63	1.332094 - 1.994709	-2.296	- 3.022652 - -1.702193	+
M3 Epinasal W	5	0.828	3.48	1.7235819 - 7.034222	-6.068	13.22749 - -2.52417161	+
L3 Epinasal W	3	0.934	3.45	.5164384 - 23.0677879	-5.994	5.927718 - -0.01918698	iso
Squamosal Length	18	0.944	1.48	1.305993 - 1.677828	-1.062	- 1.443195 - -0.7253657	+
U3 Squamosal Length	10	0.952	1.54	1.285887 - 1.884766	-1.19	- 1.769087 - -.7088368	+
M3 Squamosal Length	4	1	1.304	1.231940 - 1.380954	-0.734	-0.8814831 - -0.5944162	+
L3 Squamosal Length	3	0.829	1.55	.1086925 - 22.13871	-1.15	- 43.06273 - 1.784505	iso
Squamosal Width	17	0.937	1.195	1.0414638 - 1.370671	-0.77468	- -1.113372 - -.4794569	+
U3 Squamosal Width	10	0.913	1.25	.9838062 - 1.583342	-0.888	- -1.533638 - -.3794041	iso
M3 Squamosal Width	4	1	1.14	1.097249 - 1.189055	-0.669	0.7595876 - - 0.5827284	+
Parietal Width	15	0.92	1.74	1.500712 - 2.143750	-1.44	- 2.052190 - -.9236849	+
U3 Parietal Width	6	0.934	1.62	1.1393906 - 2.298213	-1.25	- 2.499724 - -.36862918	+
M3 Parietal Width	4	0.992	1.45	1.111020 - 1.896759	-0.934	- 1.790974 - - 0.2772921	+
L3 Parietal Width	3	0.615	2.63	0.1662414 - 41.64271	-3.18	- 82.59265 - 1.842364	iso
Parietal Length	13	0.916	1.38	1.140594 - 1.671828	-0.8796	- 1.429746 - - .4252368	+
U3 Parietal Length	6	0.912	1.46	.9817222 - 2.185177	-1.062	- 2.387255 - - .1740813	iso
M3 Parietal Length	3	0.999	1.088	.6805902 - 1.737647	-0.341	- 1.567661 - .4260860	iso
Rostrum Length	12	0.886	1.35	1.0683824 - 1.713063	-1.29	- 2.016255 - -0.7214955	+
U3 Rostrum Length	5	0.961	1.097	.7683074 - 1.567154	-1.747	1.746645 - -0.13194623	iso
Nasal Length	13	0.955	1.356	1.177393 - 1.560808	-1.1105	- 1.514655 - - .07593756	+
U3 Nasal Length	9	0.979	1.376	1.209368 - 1.565013	-1.136	- 1.510563 - - .8057115	+
NPP Width	13	0.578	1.28	0.8436684 - 1.949228	-1.82	- 3.127175 - - 0.9553221	iso
U3 NPP Width	5	0.766	1.14	0.5126150 - 2.540603	-1.47	4.183829 - - 0.24381287	+
M3 NPP Width	5	0.385	3.059	0.957202 - 9.775215	-5.402	- 18.870523 - -1.187859	iso
Orbit Height	15	0.837	0.005	.003725043 - .006017333	0.70297	.5859700 - - .7950254	-
U3 Orbit Height	6	0.808	0.005	.002837332 - .008987055	0.695078	.3554069 - .8859333	-
M3 Orbit Height	3	0.911	0.006	.0007332934 - .04359110	0.627	- 1.9729713 - .9639312	-
Orbit Width	15	0.927	0.004	.003804853 - .005252000	0.6016	0.5302731 - .6622520	-
U3 Orbit Width	6	0.953	0.005	.003541640 - .006429651	0.578	.4345236 - .6836675	-
M3 Orbit Width	3	0.966	0.005	.001018971 - .02409876	0.586	- .7260424 - 1.5555718	-
Transv. Width at Orbit	14	0.985	1.22	1.137023 - 1.327455	-0.889	- 1.075481 - -.7160251	+
U3 Transv. Width at Orbit	10	0.988	1.28	1.171983 - 1.400009	-1.0071	- 1.238237 - - .7956506	+
M3 Transv. Width at Orbit	4	0.985	1.208	.8383291 - 1.740511	-0.857	- 1.883259 - -.1452552	iso

Appendix 7.2. Descriptions of linear measurements and geometric morphometric landmarks.

Linear Measurements

1. Postorbital Horn Length
2. Squamosal length (parietal-squamosal contact to anteroventral projection)
3. Squamosal width (anteroventral projection to inflection point of squamosal along medial margin
4. Epinasal length
5. Epinasal width
6. Parietal width
7. Parietal length (shortest distance between midline of posterior margin and anteriormost point)
8. Dentary length (posterior surface of cornoid process to anteriormost point)
9. Occipital condyle width
10. Occipital condyle height
11. Jugal length (ventralmost point of orbit to ventralmost point of jugal)
12. Orbit height
13. Orbit width
14. Nasal length (anteriormost point of contact with frontal to anterior contact with epinasal)
15. Rostrum length (anteriormost point to nasal process of the premaxilla)
16. Width of nasal process of the premaxilla
17. Transverse width of skull at orbits

Landmarks - skull in lateral view (modifed from Maiorino et al. 2013)

1. Dorsalmost point of orbit
2. Anteriormost point of orbit
3. Posteriormot point of orbit
4. Ventral tip of jugal
5. Maximum curvature point of anterior margin of jugal
6. Anteriormost contact of premaxilla and maxilla
7. Dorsalmost contact point of rostral and premaxilla
8. Anteroventralmost point of epinasal
9. Ventralmost posterior margin of anterolateral process of nasal
10. Posteriormost point of lateral margin of narial opening
11. Inflection point between postorbital horn core and margin of the orbit
12. Distalmost point of postorbital horn core
13. Tip of epinasal
14. Dorsalmost inflection point of otic notch
15. Anteroventral projection of squamosal
16. Contact of squamosal with parietal

17. Point of posteriormost contact of rostral with premaxilla along the oral margin
18.Posteriormost point of epinasal
19. Ventralmost point of orbit

Landmarks -epinasal
1. Anteroventral most point of epinasal
2. Tip of epinasal
3. Posteriormost point of epinasal

Landmarks -postorbital horn
1. Dorsalmost point of orbit
2. Inflection point between postorbtial horn core and margin of orbit
3. Tip of postorbital horn

Landmarks - squamosal (modified from Maiorino et al. 2013)
1. Dorsalmost inflection point of otic notch
2. Anteroventral projection
3. Midpoint between landmarks 2 and 4, along lateral margin
4. Posteriormost contact with parietal

Landmarks - parietal
1. Right posteriormost contact with squamosal
2. Midpoint of posterior margin (at peak of crenulation if present)
3. Left posteriormost contact with squamosal
4. Anteriormost point of parietal (posterior margin of frontoparietal fontanelle - if present)

Landmarks - nasal
1. Posterior margin of anterolateral process at ventralmost point
2. Posteriormost point of narial opening
3. Anteroventralmost contact with epinasal
4. Posterior contact with epinasal

Landmarks - NPP
1. Base of contact with anterolateral process of nasal
2. Posteriormost point of dorsal margin
3. Anteriormost point of dorsal margin

Appendix 7.3 Linear Measurments used in PCA and cluster analyses

Specimen	Locality Name	Ontog	HCF Unit	Level	PO	SQL
MOR 1122	Toro II	toro	L3	lower	60	120
MOR 1120	Getaway Trike	sub	L3	upper	49	80.3
MOR 3081	JRH-008	toro	L3	upper	50	108
MOR 2982	3 Amigos	sub	M3	lower	50	NA
MOR 3010	Golden Goose	ya	M3	lower	47	NA
MOR 2569	Afternoon Delight	juv	M3	lower	13	23.6
MOR 3064	Little Horny Devil	juv	M3	upper	25	NA
MOR 3027	Yoshi's Trike	sub	M3	upper	90	84.5
UCMP 113697	Ruben's Triceratops	ya	M3	upper	83.6	85.5
MOR 3045	Cliffhanger	sub	M3	upper	58.3	76.5
MOR 2924	Lon's Trike	sub	U3	lower	NA	75.6
MOR 2702	BAB	ya	U3	lower	55	100
MOR 2574	Quittin' Time	sub	U3	lower	51	NA
UCMP 136092	Russell Basin Triceratops	ya	U3	lower	44	88
MOR 1110	SG5	juv	U3	lower	50	57.8
UCMP 154452		baby	U3	lower	4.15	11
MOR 2951	DFJuvieTrike3	juv	U3	lower	28.6	39
MOR 1625	Haxby Trike	ya	U3	lower	NA	87.2
MOR 2923	Joe's Half Day Trike	ya	U3	upper	55	NA
MOR 2999	Situ But Sad	sub	U3	upper	45	74
MOR 004	MORT	ya	U3	upper	NA	93
MOR 1199	Sierra Trike	juv	TBD	TBD	17	33.5
MOR 1604	Baker Trike	ya	TBD	TBD	60.5	NA
MOR 981	Toro I	toro	TBD	TBD	83.5	NA
UCMP 136306		juv	U3	TBD	38	47

SQW	Epinasal L	Parietal W	Parietal L	Dentary L	OC Width	OC Height	Jugal L
55	12	197.4	125	NA	11.7	11.8	48.2
42.6	5.8	101.5	71	NA	8.9	8.5	35
NA	13.9	174	NA	NA	9.5	9.1	NA
NA	10	NA	NA	50.5	NA	NA	35
NA	6.5	NA	NA	50	NA	NA	NA
15	NA	26	26	NA	NA	NA	16
NA	NA	NA	NA	NA	NA	NA	20.4
45.5	NA	100	74	56.5	11.1	11.3	38.8
47	24	118.4	NA	NA	11.5	10.9	39
41.5	16	92	70	51.5	NA	NA	36
42	22.5	NA	68	NA	9.3	9.1	NA
46	30	NA	NA	60	NA	NA	NA
NA	21	NA	NA	51	NA	NA	NA
47	NA	NA	NA	NA	NA	NA	41
33	8.3	67.65	49	NA	7.4	7.4	30
8	NA	13.08	12	15.9	2.9	2.5	11.5
25.8	4.5	49.5	42	31	6.2	6.2	22.9
44	30	NA	NA	NA	11.9	11.2	NA
NA	29	NA	72.5	NA	NA	NA	NA
39.5	NA	83	73	49.5	9.1	9.1	NA
46	28.5	106	74	59	NA	NA	42.5
22	NA	39	38	27	4.7	4.9	17.8
NA	26.5	NA	NA	54.8	NA	NA	41
NA	10	210	116	NA	NA	NA	NA
28.5	7	59.5	46	NA	6.8	NA	NA

Orbit H	Orbit W	Nasal L	Rostrum L	NPP W	Epinasal W	Transverse width at orbit
15.9	13	48	NA	NA	17.4	47.3
17	11.3	32.3	28	3.7	6.9	35.6
NA	NA	NA	NA	NA	10.4	NA
NA	NA	NA	NA	3.7	6.5	NA
NA	NA	NA	NA	NA	8.6	NA
6.5	5.8	NA	NA	NA	NA	12.4
10.1	7.8	NA	NA	NA	NA	NA
16.8	13.2	43.5	27.5	5.5	10.4	37.4
NA	NA	NA	NA	7.25	11.33	41
NA	NA	NA	23	7	8.5	39.8
NA	NA	41	NA	NA	10	NA
NA	NA	NA	NA	6.54	13	NA
NA	NA	39.1	22.5	7	9.1	NA
17.9	11.4	NA	NA	NA	NA	NA
16.2	8.2	28.3	NA	4.82	5.4	25.4
6.1	5.4	NA	NA	NA	NA	8.1
11.7	7.9	19.9	14.5	3.5	3.5	19.8
NA	NA	NA	34	NA	13.5	NA
16.8	14.4	51.5	NA	NA	13	41.6
NA	NA	38.8	NA	NA	NA	33.5
17.5	15	55.75	33	NA	13	44.6
9.1	6.5	14.8	10.3	2.3	NA	17.1
18.6	14.5	46.5	24	NA	12	NA
18	15.1	NA	47	NA	13	NA
NA	NA	NA	NA	NA	5.2	NA

Appendix 7.4 Loadings of linear measurements on first three principal component axes.

With horns and frill

R^2	.8213	.1270	.0315
	PC1	PC2	PC3
1:Postorbital horn length	-0.25061934	0.0112385407	0.068401952
2: Squamosal length	-0.21579289	0.0195247837	-0.011331825
3: Squamosal width	-0.17440762	0.0253308072	0.002804012
4: Epinasal length	-0.08892715	-0.2454997802	0.012142261
5: Epinasal width	-0.10804655	-0.1054034502	-0.063401946
6: Parietal width	-0.23691068	0.0367228557	-0.035503524
7: Parietal length	-0.18801826	0.0393142038	-0.018168360
8: Dentary length	-0.13486352	-0.0055850679	0.005736973
9: occipital condyle width	-0.13638715	-0.0097075489	0.010888277
10: occipital condyle height	-0.14347083	-0.0007932122	0.013228710
11: Jugal length	-0.13710424	0.0022172003	0.001888082
12: Orbit Height	-0.11222536	0.0029714587	0.024526850
13: Orbit Width	-0.10618247	-0.0221230388	0.003936851
14: Nasal length	-0.1257615	-0.0695726647	-0.008153845
15: Rostrum length	-0.16315613	-0.0192194741	-0.052794904
16: NPP width	-0.06567606	-0.0929292957	0.049044815
17: Transverse width at orbit	-0.16913063	0.0056361606	0.004833355

Without horns and frill

	.9212	.04194	.0000
	PC1	PC2	PC3
8: Dentary length	-0.1242606	-0.0007939794	1.094358e-45
9: occipital condyle width	-0.1347737	-0.0067361378	-1.203298e-46
10: occipital condyle height	- 0.1421307	-0.0145393267	-5.087747E-46
11: Jugal length	-0.1269647	-0.0138449770	9.110301e-46
12: Orbit Height	-0.1060686	-0.0254960611	3.153692e-46
13: Orbit Width	-0.1007723	0.0007658239	4.505947e-46
14: Nasal length	-0.1382792	0.0490506481	-2.786528e-46
15: Rostrum length	-0.1081140	0.0614702608	3.817759e-45
16: NPP width	-0.1259680	0.0283308380	-5.707123e-45
17: Transverse width at orbit	-0.1586786	-0.0210058656	5.269606e-46

Appendix 7.5 Loadings for GM PCA of *Triceratops* skulls in lateral view

R^2	**.3412**	**.2029**	**.16587**	**.124661**	**.06223**
	PC1	PC2	PC3	PC4	PC5
[1,]	-0.1529929528	0.049443217	-0.2141167621	-0.0197546488	-0.109135985
[2,]	0.0294691721	-0.097819026	0.0383645326	0.1381143968	-0.020332020
[3,]	-0.1384006143	-0.021439861	-0.2078595827	0.0005829250	-0.085895978
[4,]	0.0392633231	-0.046333403	0.0704178409	0.1183063307	-0.038138423
[5,]	-0.1318849191	0.010550135	-0.1489647020	-0.0725308197	-0.059383696
[6,]	0.0354617253	-0.092076135	0.0696711757	0.1589514082	-0.012899238
[7,]	-0.0984762237	0.044763262	0.0436028526	-0.1254165753	0.014096718
[8,]	0.0017760943	0.040567842	0.1569177415	0.0900433577	-0.085422695
[9,]	-0.0494377089	0.053233221	0.0517572996	-0.0464376453	-0.127176172
[10,]	0.0221166558	-0.067224966	0.1251497158	0.0905687101	-0.064063662
[11,]	0.0925850098	-0.152105518	0.1547799255	0.1022324116	-0.159493272
[12,]	-0.0085519923	-0.177831590	0.1638080016	-0.0106017722	-0.083265863
[13,]	0.1112109896	-0.123267439	0.0808069458	0.0354502253	0.072887723
[14,]	-0.1521937028	-0.080947763	0.0084046132	-0.1575950966	-0.075882534
[15,]	0.0479194178	-0.098457120	-0.0003265912	0.0537308783	0.113444274
[16,]	-0.1615378648	-0.042533625	0.0246298997	-0.0912928530	0.182158192
[17,]	0.0719588953	-0.133493596	0.0105716438	0.0735172779	0.054202127
[18,]	-0.0674143285	-0.085160887	0.1012589804	-0.0805068614	-0.008156905
[19,]	-0.0742045201	-0.051354499	-0.0971009066	0.1280904130	-0.102543636
[20,]	-0.0798545975	-0.003098620	0.0782177958	0.1655952828	-0.003793241
[21,]	-0.1135557848	0.017459962	-0.1765835392	-0.0335763078	-0.099973983
[22,]	0.0532076855	-0.063974367	-0.0152625478	0.1907667366	-0.059503725
[23,]	0.2884130012	0.657821310	0.2531122982	-0.0562927124	-0.163621869
[24,]	0.4660773140	-0.046356482	-0.0252482375	-0.0680238179	0.240371508
[25,]	-0.0714868263	0.178686169	0.0017974534	0.0731261653	0.729974381
[26,]	-0.2773467216	0.161010285	-0.0571751701	0.0445169654	0.010772050
[27,]	-0.0708529256	0.046598264	-0.0563319891	-0.2316331817	-0.058292255
[28,]	0.0875774593	0.041609729	0.1908727355	-0.0910247208	0.013063877
[29,]	0.0666740907	-0.127250631	-0.0481453370	-0.2499923250	0.062940245
[30,]	0.0623701846	0.044874905	-0.0202317633	-0.3549940340	-0.083089155
[31,]	-0.1738435648	0.274004562	0.2794523331	0.1774192119	-0.060100703
[32,]	-0.2463975770	0.213415449	-0.0016446495	0.3507843940	0.126607878
[33,]	0.1910742779	-0.082083394	0.1107215484	0.1591457171	-0.203118213
[34,]	0.0005771591	0.003647273	-0.0181249873	-0.0351712302	-0.015865233
[35,]	0.0303744241	0.091845642	-0.0508984307	0.0786069203	0.059505046
[36,]	-0.0274978499	-0.029523254	0.0233626532	-0.0226323650	-0.049236848
[37,]	-0.0328817378	0.004019105	-0.0168716652	-0.0101548365	-0.044381419
[38,]	-0.0440330437	-0.026669446	-0.0074119925	-0.0080999992	-0.025495649

```
[39,]  0.0562209670  0.016938180 -0.0567833095  0.0516696092 -0.019039416
[40,] -0.0828060874  0.009790761  0.0612304206 -0.0620223693 -0.021148998
[41,]  0.0423212510 -0.031903186 -0.0882260033  0.0322834582 -0.037195411
[42,] -0.0617888092  0.038074608  0.0621719196 -0.0217570570  0.012076254
[43,] -0.0438251320 -0.071834385 -0.0862231681  0.0639528813 -0.059110404
[44,] -0.0060188081  0.007213677  0.0120632533 -0.0009323378 -0.013999530
[45,] -0.0171151196  0.017975081 -0.0595487751  0.0512346682 -0.069464281
[46,]  0.0477803308 -0.071798678 -0.2370364435  0.1580296920 -0.112348902
[47,]  0.0120134265  0.041328598 -0.1593375649  0.0730201493 -0.004736097
[48,]  0.1105926768  0.071802806 -0.3265619231  0.1363568780 -0.142123941
[49,]  0.0265857645  0.051764607 -0.0340862637  0.0138773522 -0.022274334
[50,]  0.2229173228  0.092514682 -0.3218645116  0.0941099719 -0.008041551
[51,]  0.0039696563  0.026854096 -0.0244573449  0.0024584634 -0.007519658
[52,]  0.3379526081  0.053879923 -0.1771397571 -0.0024729544  0.116373589
[53,]  0.0301106763  0.059777094 -0.0069732288 -0.0820172944  0.036181374
[54,] -0.0441054592  0.105969188 -0.0839177029 -0.2009957524 -0.017990277
[55,]  0.0130914545 -0.242104896  0.1721176229  0.0534455499  0.056114625
[56,] -0.0277261736  0.140432848 -0.0619007469 -0.0180448875  0.009961399
[57,] -0.0370873723 -0.124849154  0.2297690556  0.0504209295  0.042051965
[58,] -0.0232569929  0.008166115  0.0061115207  0.0039281416  0.042698203
[59,] -0.0078891569 -0.023058108  0.1351134478  0.0091458379 -0.039897412
[60,] -0.0299581484  0.023744005 -0.1228186580  0.0183163346  0.132845318
[61,] -0.0040226627 -0.077089591  0.0209714063 -0.0722945215  0.051624413
[62,] -0.0166009181 -0.042025178  0.0303576791  0.0396024173 -0.014444617
[63,]  0.0836265956 -0.116628558  0.0294369520  0.0556720368  0.098454509
[64,] -0.1535628317 -0.071271469  0.0206089532 -0.1272594024  0.040073673
[65,]  0.0711181580 -0.108158775  0.0083127042  0.0572459255  0.108678031
[66,] -0.1590545913 -0.061919813  0.0220601371 -0.1046382674  0.111826827
[67,] -0.0362923755  0.010549680 -0.0205413426 -0.1894855170 -0.003966292
[68,]  0.0776494346  0.036779747  0.1540068289 -0.1228521922 -0.030858670
[69,]  0.0149815411 -0.068533473 -0.0289469825 -0.2067426216  0.036165053
[70,]  0.0749173519  0.013070859  0.0566526927 -0.2170730468 -0.052727090
```

Appendix 7.6. Loadings for GM PCA of *Triceratops* skulls in lateral view when horns and frill are removed.

R^2	0.29619	0.56716	0.7146	0.83653	0.9094
	PC1	PC2	PC3	PC4	PC5
[1,]	-0.180446848	-0.1566603977	0.155225163	0.2151579475	0.014531233
[2,]	0.236099600	-0.3443810999	0.020792122	-0.0085682852	-0.177593131
[3,]	-0.179850547	-0.0946072523	0.262578835	0.1552506319	-0.017238587
[4,]	0.193767510	-0.2257810323	-0.125653958	-0.0022081389	-0.023176047
[5,]	-0.002889761	-0.0353858553	0.064696876	0.0863662238	-0.066179985
[6,]	0.100136857	-0.3110139814	-0.018471267	-0.1059692194	-0.072375539
[7,]	-0.027276294	0.4451802169	-0.299650338	-0.2074026778	-0.291524499
[8,]	-0.526956987	0.3095363061	0.036809031	-0.0144533746	-0.038907872
[9,]	0.121026023	0.3945463087	-0.075160269	0.0740594908	0.121260503
[10,]	-0.100447874	0.0002133947	-0.002269010	0.1120934417	-0.054853552
[11,]	0.248916443	0.0316994461	0.170724662	-0.5867841584	0.355476664
[12,]	0.125907409	0.1099378741	0.211652998	-0.1110265274	0.081223242
[13,]	0.083340790	0.0153304920	-0.090993711	-0.1372151967	-0.110542536
[14,]	-0.126590451	0.0860568376	0.253882752	-0.3271077192	-0.216536289
[15,]	-0.084952192	-0.0909114125	-0.270646757	0.1226557281	-0.065878801
[16,]	-0.082901305	-0.0029317458	-0.324124094	-0.0151019490	-0.016166685
[17,]	0.037968206	-0.1165184830	-0.117662026	-0.0445250964	-0.023732094
[18,]	0.218582973	-0.0007798965	-0.135565781	-0.0119640491	0.112059456
[19,]	-0.327227640	-0.1603980149	0.210349744	-0.1420966034	0.338261931
[20,]	-0.080373057	0.0203179960	-0.122426995	0.2707937354	0.445957465
[21,]	0.418918815	0.2424723746	0.329506388	0.4127184363	0.022858960
[22,]	0.138659010	0.1728225029	0.292285693	0.1200219038	-0.384373050

[23,] -0.001658613 -0.0351337396 0.116664904 0.0504098206 -0.004246833

[24,] -0.162623383 -0.1511922116 0.147881759 0.0818784825 -0.185493619

[25,] -0.114257987 -0.0846981493 0.034009777 -0.0090993502 -0.005833968

[26,] 0.055502263 0.0517980177 -0.024582813 -0.0386798984 0.013698828

[27,] -0.047912898 -0.0805815079 0.075151560 -0.0851900927 -0.076941584

[28,] 0.062292389 0.1388677946 -0.143609357 0.1330487201 0.171324102

[29,] -0.001592227 -0.0074810289 -0.003981919 0.0009006275 0.009649098

[30,] 0.011726760 0.0698550460 -0.016316751 0.1072613308 0.312144455

[31,] 0.067256700 -0.0610416360 -0.157430667 -0.0314994090 -0.041432037

[32,] -0.021197212 0.0278145347 0.036580448 -0.0747479967 0.004274415

[33,] 0.021096318 -0.0929690348 -0.175867460 0.0297522689 -0.073200644

[34,] -0.012333852 0.0335859467 -0.007525288 -0.0765357782 0.013834566

[35,] -0.030458288 -0.1128423260 -0.227514762 0.0965414091 -0.085286821

[36,] -0.029250649 0.0152737165 -0.079339489 -0.0387346784 0.014959253

Appendix 7.7. Loadings for individual elements examined in analyses. Note that images from the literature were used for the epinasal and parietal of UCMP 136306 (Goodwin and Horner, 2014) and the nasal of YPM 1820 (Hatcher et al., 1907).

Nasal Horns

R^2	.7944	.12958	.03032
	PC1	PC2	PC3
[1,]	0.438506390	-0.1545222177	0.26146383
[2,]	-0.160890976	-0.5030279182	0.10717356
[3,]	-0.091838705	0.4880836897	-0.12942348
[4,]	0.485298629	0.1446048654	-0.43614374
[5,]	-0.194615736	-0.5063977180	-0.36657373
[6,]	-0.417117465	0.2515533609	-0.23935157
[7,]	0.282513281	-0.0991351093	-0.05157357
[8,]	0.003983067	-0.0124476359	-0.11321789
[9,]	0.135431307	-0.0308061454	-0.20709894
[10,]	0.026422993	-0.0117477175	-0.04330402
[11,]	-0.018993533	0.0881622579	-0.25212256
[12,]	0.070046551	-0.0624418406	0.01710979
[13,]	-0.161497994	0.1595162998	-0.03242164
[14,]	0.162828955	-0.1341495335	-0.02260312
[15,]	0.023469807	0.1409491188	0.16924108
[16,]	0.178918899	0.1887027817	0.26127199
[17,]	-0.072132169	0.0358444801	0.32802344
[18,]	0.009260411	0.1131131669	0.26491605
[19,]	-0.144078273	-0.0469080661	0.24466334

[20,] -0.117708063 0.0264640557 0.24204238

[21,] -0.196764374 -0.0747865898 0.03582221

[22,] -0.241042999 -0.0006235849 -0.03789344

2. Postorbital Horn Cores

R^2	.8015	.11153	.05820
	PC1	PC2	PC3
[1,]	0.43768983	0.6912382631	-0.183724321
[2,]	0.29583144	-0.3056952249	-0.653987537
[3,]	0.17759802	-0.4772189857	0.087332911
[4,]	0.16052541	0.1627344748	0.332557828
[5,]	0.42030026	0.0009804044	0.279182849
[6,]	0.22131754	-0.2765292261	0.035427853
[7,]	0.02147870	-0.1695459645	0.210009837
[8,]	0.03117921	-0.0035052627	0.178567870
[9,]	-0.09873946	-0.1085953828	0.158959713
[10,]	-0.05270590	0.0409332485	0.186930758
[11,]	-0.19047297	-0.0428128582	0.097492741
[12,]	-0.12658823	0.0767263185	0.171434544
[13,]	-0.24496834	0.0131000342	0.004097226
[14,]	-0.17776793	0.0806971262	0.090536266
[15,]	-0.25582570	0.0200031024	-0.087412148
[16,]	-0.19614334	0.0847872734	-0.014748042

Appendix 7.7 (Continued)

[17,] -0.22394047 0.0440122583 -0.161503875

[18,] -0.17115527 0.1084414199 -0.084639637

[19,] -0.16635712 0.0406256071 -0.192092352

[20,] -0.11202185 0.0814300459 -0.124135403

[21,] -0.08706041 -0.0031754867 -0.179442898

[22,] -0.03504037 0.0434171038 -0.117785917

[23,] 0.03113121 -0.0056248268 -0.098159363

[24,] 0.05469265 0.0059703788 -0.047161005

[25,] 0.17916644 -0.0029861647 0.065259681

[26,] 0.10787663 -0.0994076763 0.047002423

3. Squamosals

R^2 .70093 .12683 .06865

PC1 PC2 PC3

[1,] -0.25150983 -0.624300668 0.381447976

[2,] 0.45161471 -0.251970573 -0.549464020

[3,] -0.08499859 0.250563396 -0.291498837

[4,] 0.23743446 0.070019170 0.300085606

[5,] 0.17523365 0.071548661 0.100073909

[6,] -0.11253410 -0.007065744 -0.080040848

[7,] -0.34567964 0.008267374 -0.147048785

[8,] 0.07830211 -0.157511620 0.138000854

[9,] -0.01513484 -0.111266000 0.023798894

[10,] 0.15040510 -0.359857883 -0.045322753

[11,] 0.02673223 -0.089885449 -0.011438930

[12,] 0.09936066 -0.132357307 0.029191906

[13,] -0.05107831 0.072458271 -0.070762575

[14,] 0.11813056 0.237637176 0.164445201

[15,] -0.03039095 -0.006604086 -0.110221952

[16,] 0.01644018 0.284926675 0.156485919

[17,] 0.03320191 0.024208197 -0.139767758

[18,] -0.07268594 0.221094362 0.163928832

[19,] 0.06370553 0.027829602 -0.141567522

[20,] -0.10608953 0.147531917 0.140631884

[21,] 0.09947865 0.041248617 -0.060706242

[22,] -0.13498080 0.093519509 -0.023382789

[23,] 0.13225626 0.037403321 -0.023070609

[24,] -0.16800555 0.079623708 -0.041834342

[25,] 0.15536084 0.025204010 -0.037616898

[26,] -0.17658574 0.057730925 -0.023464503

[27,] 0.16689830 0.049314106 0.059766980

[28,] -0.16658556 0.007451813 -0.067796939

[29,] 0.17779418 0.045011419 0.103693225

[30,] -0.14731594 0.016460774 -0.110402945

[31,] 0.13777761 0.031669673 0.157944342

[32,] -0.10257522 -0.018971023 -0.113666954

[33,] 0.13279849 0.040559348 0.177602423

[34,] -0.06929338 -0.021469012 -0.093295468

[35,] 0.09104674 0.097544981 0.089420848

[36,] -0.03613476 -0.067162582 -0.028780192

[37,] 0.04145696 0.039774822 0.103157125

[38,] -0.00211759 -0.040951298 -0.010728716

[39,] -0.01345264 0.013028040 0.073701704

[40,] 0.03232097 -0.021166703 0.001093049

[41,] -0.07602211 0.061050861 -0.038445179

[42,] 0.04487072 -0.041542291 0.038112002

[43,] -0.13400897 0.025040977 -0.080458678

[44,] 0.05546289 -0.021850685 0.049044420

[45,] -0.19541824 -0.079194604 -0.057100892

[46,] 0.03650260 -0.028106976 0.018362266

[47,] -0.23604723 -0.050474869 -0.060902568

[48,] -0.02594086 -0.046012333 -0.011201469

4. Parietal

R^2 .81010 .09525 .05701

PC1 PC2 PC3

[1,] 0.4392783875 -0.26889126 -0.42258136

[2,] 0.2996824544 0.35094760 0.19499931

[3,] -0.0007023885 0.09803984 0.46061291

[4,] -0.0001614155 -0.79772297 0.09215806

[5,] -0.4178436526 0.13861097 -0.51475220

[6,] 0.3489101288 0.36213741 -0.26457623

[7,] -0.0207323464 0.03224044 0.47672065

[8,] -0.6484311677 0.08463796 -0.02258114

5. Nasal

R^2 .6200 .25315 .05777

PC1 PC2 PC3

[1,] 0.005804609 0.019870602 0.62865523

[2,] -0.363579306 0.620990211 -0.04572734

[3,] -0.182930911 -0.001536377 -0.14843142

[4,] 0.123164192 0.195171964 -0.33951094

[5,] -0.110866690 -0.206566322 -0.03021705

[6,] -0.290244327 -0.631150508 -0.18543737

[7,] 0.612025928 0.028353185 -0.48378513

[8,] 0.546645711 0.070174255 0.39130570

[9,] -0.006132087 -0.106520815 0.09031442

[10,] -0.098256083 0.148433874 -0.01007480

[11,] -0.133314260 0.133273649 -0.04990545

[12,] 0.027554140 -0.096872500 0.09762223

[13,] -0.107792628 0.118377594 -0.02203917

[14,] 0.058786712 -0.213911870 0.14002842

[15,] -0.076793961 0.014748485 0.01540857

[16,] -0.004071039 -0.092835427 -0.04820591

6. NPP

R^2 .5252 .3426 .09639

PC1 PC2 PC3

[1,] -0.57171392 -0.120881778 -0.16676161

```
 [2,]  0.20166911 -0.532322570 -0.02475405
 [3,]  0.24232848 -0.393360257 -0.30730409
 [4,]  0.49638995  0.294515760 -0.24197406
 [5,]  0.13541569  0.540833182  0.16731908
 [6,] -0.25914793  0.376916773 -0.38778505
 [7,]  0.09588740 -0.107734937  0.02843854
 [8,]  0.16669524 -0.037101685  0.21001599
 [9,]  0.01355870  0.083168389  0.30094252
[10,] -0.21865360 -0.071913373  0.67248996
[11,]  0.08452364 -0.002024599 -0.02263443
[12,] -0.38695277 -0.030094905 -0.22799278
```

Appendix 7.8. MANOVA of linear measurements.

	Df	Sums of Sqs	Mean Sqs	F. Model	R^2	Pr(>F)	
Linear Measurements							
ontogeny	1	10.3333	10.3333	26.9171	0.56673	1.00E-04	***
stratigraphic level	1	1.3955	1.3955	3.6352	0.07654	0.05639	
ontogeny:stratigraphic level	1	0.3622	0.3622	0.9435	0.01986	0.39066	
Residuals	16	6.1423	0.3839		0.33687		
Total	19	18.2334			1		
Linear Measurements (w/o horns and frill)							
ontogeny	1	3.2979	3.2979	24.5141	0.72453	0.0007	***
stratigraphic level	1	0.0723	0.0729	0.5377	0.01589	0.50245	
ontogeny:stratigraphic level	1	-0.0293	-0.0293	-0.2175	-0.0064	0.9781	
Residuals	9	1.2108	0.1345		0.266		
Total	12	4.5518			1		

Appendix 7.9. MANOVA of skulls with and without cranial ornamentation.

	Df	Sums of Sqs	Mean Sqs	F. Model	R^2	Pr(>F)	
Skulls in Lateral View							
centroid size	1	0.014269	0.014269	3.9084	0.32497	0.01667	*
stratigraphic position	1	0.012761	0.012761	3.4955	0.29063	0.04167	*
centroid size:strat pos	1	0.013227	0.013227	3.6232	0.30125	0.025	*
Residuals	1	0.003651	0.003651		0.08315		
Total	4	0.043907			1		
centroid size	1	0.019776	0.019777	2.355	0.18017	0.0236	*
ontogenetic stage	1	0.01383	0.01383	1.6469	0.126	0.1113	
centroid size: ontogenetic stage	1	0.017374	0.017374	2.069	0.15829	0.0447	*
Residuals	7	0.058782	0.008398		0.53554		
Total	10	0.109763			1		
centroid size	1	0.018556	0.018556	2.2622	0.19865	0.0434	*
ontogenetic stage	1	0.010513	0.010513	1.2816	0.11255	0.25317	
centroid size (ctoro):ontogenetic stage	1	0.015123	0.015123	1.8437	0.16191	0.08589	
Residuals	6	0.049216	0.008203		0.52689		
Total	9	0.093407			1		
ontogenetic stage	1	0.020019	0.020019	3.9729	0.45593	0.04167	*
stratigraphic position	1	0.010152	0.010152	2.0148	0.23122	0.14167	
ontog:strat	1	0.008697	0.008698	1.7261	0.19809	3	
Residuals	1	0.005039	0.005039		0.11476		
Total	4	0.043907			1		
Horns and Frill Removed							
centroid size	1	0.0126187	0.012619	5.1469	0.47737	0.04167	*
stratigraphic position	1	0.0075493	0.007549	3.0792	0.28559	0.13333	
centroid size:strat pos	1	0.0038139	0.003814	1.5556	0.14428	0.325	
Residuals	1	0.0024517	0.002452		0.09275		
Total	4	0.0264337			1		
centroid size	1	0.018195	0.018195	2.53435	0.22278	0.008999	**
ontogenetic stage	1	0.009251	0.009251	1.2886	0.11327	0.257874	
centroid size: ontogenetic stage:	1	0.003971	0.003971	0.55311	0.04862	0.833417	
Residuals	7	0.050256	0.007179		0.61533		
Total	10	0.081673			1		
centroid size (ctoro)	1	0.015296	0.015296	2.02728	0.21201	0.0415	*
ontogenetic stage	1	0.007744	0.007744	1.02641	0.10734	0.4433	
centroid size (ctoro): ontogenetic stage	1	0.00385	0.003835	0.50834	0.05316	0.8867	
Residuals	6	0.04527	0.007545		0.62748		
Total	9	0.072145			1		
ontogenetic stage	1	0.0137905	0.013791	2.71974	0.5217	0.2	
stratigraphic level	1	0.0034379	0.003438	0.67802	0.13006	0.7167	
ontogenetic stage:stratigraphic level	1	0.0041348	0.004135	0.81545	0.15642	0.6667	
Residuals	1	0.0050705	0.005071		0.19182		
Totals	4	0.0264337			1		

Appendix 7.10. MANOVA results.

		Df	Sums of Sqs	Mean Sqs	F. Model	R^2	Pr(>F)	
Epinasal								
Ontogeny - numeric:		1	0.08743	0.087428	1.956	0.04895	0.1527	
	Residuals	38	1.69851	0.044698		0.95105		
	Total	39	1.78594			1		
Ontogeny(ctoro)		1	0.04491	0.044905	1.0531	0.03092	0.3258	
		33	1.40722	0.042643		0.96908		
		34	1.45212			1		
Stratigraphy- numeric:		1	0.44772	0.44772	26.098	0.50094	1.00E-04	***
	Residuals	26	0.44604	0.01716		0.49906		
	Total	27	0.89376			1		
centroid size		1	0.19314	0.193142	13.787	0.2161	1.00E-04	***
strat (numeric)		1	0.31262	0.312617	22.3155	0.34978	1.00E-04	***
c size:strat (numeric)		1	0.05179	0.051785	3.6966	0.05794	0.0363	*
Residuals		24	0.33622	0.014009		0.37618		
Total		27	0.89376			1		
centroid size (ctoro)		1	0.28052	0.280523	22.4525	0.44599	1.00E-04	***
strat		1	0.06378	0.063783	5.105	0.1014	0.0156	**
csize:strat		1	0.00982	0.009818	0.7858	0.01561	0.4307	
Residuals		22	0.27487	0.012494		0.437		
Total		25	0.62899			1		
P.O. Horn								
Ontogeny - numeric:		1	0.21169	0.211688	27.378	0.50348	1.00E-04	***
	Residuals	27	0.20876	0.007732		0.49652		
	Total	28	0.42045			1		
Ontogeny(ctoro)		1	0.23919	0.239185	36.649	5.94E-01	1.00E-04	***
	Residuals	25	0.16316	0.006526		0.40552		
	Total	26	0.40234			1		
Stratigraphy- numeric:		1	0.017888	0.017888	1.4163	0.0769	0.2409	
(include Eo as 0)	Residuals	17	0.214714	0.01263		0.9231		
	Total	18	0.232603			1		
centroid size		1	0.101569	0.101569	12.8746	0.43666	0.0004	***
strat (numeric)		1	0.004991	0.004991	0.6326	0.02416	0.5309	
c size:strat (numeric)		1	0.007706	0.007706	0.9768	0.03313	0.374	
Residuals		15	0.118337	0.007889		0.50875		
Total		18	0.232603			1		
Squamosal								
Ontogeny-numeric		1	0.060302	0.060302	15.312	0.32364	1.00E-04	***
	Residuals	32	0.126019	0.003938		0.67636		
	Total	33	0.186321			1		
Ontogeny(ctoro)		1	0.009365	0.009365	3.234	0.11063	0.0278	*
		26	0.075291	0.002896		0.88937		
		27	0.084657			1		
Stratigraphy-numeric		1	0.016091	0.016091	4.6943	0.22684	0.006399	**
	Residuals	16	0.054844	0.003428		0.77316		
	Total	17	0.070935			1		
centroid size		1	0.009499	0.0095	3.0533	0.13392	0.0461	*
strat (numeric)		1	0.010322	0.010323	3.3179	0.14552	0.0301	*
c size:strat (numeric)		1	0.007557	0.007557	2.4289	0.10653	0.09049	.
Residuals		14	0.043556	0.003111		0.61403		
Total		17	0.070935			1		
centroid size (ctoro)		1	0.001428	0.001428	0.68461	0.04277	0.6607	
strat		1	0.004753	0.004753	2.27878	0.14238	0.0473	*
csize:strat		1	0.002173	0.002173	1.04189	0.0651	0.4016	
Residuals		12	0.025027	0.002086		0.74975		

Parietal Dorsal								
Ontogeny - numeric		1	0.026706	0.026706	3.4939	0.25892	0.09091	.
	Residuals	10	0.076435	0.007644		0.74108		
	Total	11	0.103141			1		
Ontogeny (ctoro)		1	0.00774	0.00774	1.021	0.10189	0.3502	
	Residuals	9	0.068227	0.007581		0.89811		
	Total	10	0.075967			1		
Stratigraphy_numeric		1	0.009165	0.00916	1.1031	1.12118	0.2727	
	Residuals	8	0.066466	0.0083		0.87882		
	Total	9	0.07563			1		
centroid size		1	0.024218	0.024218	4.6786	0.32021	0.09091	.
strat (numeric)		1	0.008185	0.008185	1.5813	0.10822	0.63636	
c size:strat (numeric)		1	0.01217	0.01217	2.3512	0.16092	0.18182	
Residuals		6	0.031057	0.005176		0.41065		
Total		9	0.07563			1		
centroid size		1	0.004287	0.004287	0.983	0.08264	0.3997	
strat		1	0.007422	0.007422	1.7021	0.14308	0.2178	
csize:strat		1	0.018362	0.018362	4.2108	0.35397	0.09091	.
Residuals		5	0.021804	0.004361		0.42031		
Total		8	0.051876			1		
Nasal								
Ontogeny - numeric		1	0.09589	0.09589	7.1375	0.33767	0.0013	**
	Residuals	14	0.18809	0.013435		0.66233		
	Total	15	0.28397			1		
Ontogeny (ctoro)		1	0.034731	0.034731	3.3919	0.22037	0.0247	*
		12	0.122875	0.01024		0.77963		
		13	0.157606			1		
Stratigraphy-numeric:		1	0.032147	0.032147	1.3652	0.1632	0.2519	
	Residuals	7	0.164828	0.023547		0.8368		
	Total	8	0.196975			1		
centroid size		1	0.021566	0.021566	1.6966	0.10949	0.26127	
strat (numeric)		1	0.033301	0.033301	2.6198	0.16906	0.15148	
c size:strat (numeric)		1	0.078552	0.078552	6.1798	0.39879	0.07469	.
Residuals		5	0.063556	0.012711		0.32266		
Total		8	0.196975			1		
centroid size (ctoro)		1	0.010455	0.010455	0.93952	0.14571	0.4593	
strat		1	0.010259	0.010259	0.92194	0.14298	0.472	
csize:strat		1	0.006526	0.006526	0.58647	0.09095	0.6199	
Residuals		4	0.044511	0.011128		0.62035		
Total		7	0.071751			1		
NPP								
Ontogeny-numeric		1	0.054839	0.054839	1.2911	0.17708	0.2857	
	Residuals	6	0.254847	0.042475		0.82292		
	Total	7	0.309687			1		
Stratigraphy-numeric		1	0.22989	0.229891	5.3824	0.4022	0.0037	**
Eo as 0	Residuals	8	0.34169	0.042712		0.5978		
	Total	9	0.57158			1		
centroid size		1	0.18838	0.188375	4.0245	0.32957	0.0203	*
npp.strat (numeric)		1	0.08448	0.084478	1.8048	0.1478	0.1784	
centroid size:npp.strat (numeric		1	0.01789	0.017886	0.3821	0.03129	0.7923	
Residuals		6	0.28085	0.046808		0.49135		
Total		9	0.57158			1		

Appendix 7.11. Regression results for GM analyses.

	Epinasal	P.O. Horn	Squamosal	Parietal	NPP	Nasal	Skull	Skull_no orn
All								
n	47	30	35	12	11	17	11	11
R^2	0.285	0.429	0.0771	0.362	0.306	0.051	0.191	0.228
p-value	0.004	0.004	0.044	0.04	0.016	0.408	0.04	0.012
Remove specimens without Strat Data								
n	28	19	18	10	10	9	5	5
R^2	0.241	0.378	0.0568	0.311	0.306	0.13005	0.328	0.448
p-value	0.008	0.004	0.372	0.044	0.012	0.34	0.242	0.086
L3								
n	4	NA	5	NA	NA	NA	NA	
R^2	0.486	NA	0.733	NA	NA	NA	NA	
p-value	0.17	NA	0.018	NA	NA	NA	NA	
M3				NA				
n	5	5	4	NA	3	NA	NA	
R^2	0.586	0.686	0.443	NA	0.227	NA	NA	
p-value	0.074	0.136	0.418	NA	0.73	NA	NA	
U3								
n	20	11	9	6	4	5	NA	
R^2	0.299	0.363	0.128	0.221	0.377	0.295	NA	
p-value	0.008	0.008	0.44	0.286	0.35	0.35	NA	

Appendix 7.12. Fisher's Exact Tests

	Triceratops	*Torosaurus*		
Stratigraphic Level			p-value:	0.013
m3&u3	26	0		
l3	6	3		
Following criteria from Scannella and Honer (2010)				
Ontogenetic Stage			p-value:	0.022
juv or sub	23	0		
adult	34	9		
Using alternative ontogenetic stages from Longrich and Field (2012)				
Ontogenetic Stage			p-value:	0.071
juv or sub	26	1		
adult	31	8		

Appendix 7.13. Specimens included in Fisher's exact tests. Specimens included from or with differing ontogenetic designations in the study of Longrich and Field (2012) are noted. Specimens highlighted in red exhibit the "*Torosaurus*" morphology. TBD, to be determined.

Specimen	StratL1	Ontog	
AMNH FARB 5116	TBD	4	3 in Longrich and Field (2012)
CM 1221	TBD	4	*Longrich and Field
DMNH epv.48617	TBD	4	
FMNH P12003	TBD	4	
GMNH-PV 124	TBD	3	*Longrich and Field
LACM 59049	TBD	4	
MHNM 1912.20	TBD	4	*Longrich and Field
MOR 004	3	4	
MOR 1110	3	2	
MOR 1120	1	3	
MOR 1199	TBD	2	
MOR 136306	3	2	
MOR 1604	TBD	4	
MOR 1625	3	4	
MOR 2552	1	3	
MOR 2569	2	2	
MOR 2570	2	4	
MOR 2574	3	3	
MOR 2597	3	3	
MOR 2702	3	4	
MOR 2923	3	4	
MOR 2924	3	3	
MOR 2936	3	3	
MOR 2938	3	4	
MOR 2942	3	4	
MOR 2951	3	2	
MOR 2971	3	4	
MOR 2979	3	4	
MOR 2982	2	3	
MOR 2985	1	4	
MOR 2999	3	3	
MOR 3010	2	4	
MOR 3027	2	3	
MOR 3029	3	2	

MOR 3045	2	3	
MOR 3048	3	3	
MOR 8693	1	4	
OMNH 10170	TBD	4	*Longrich and Field
SMM P60.2.1	TBD	4	
UCMP 113697	2	4	*3 in Longrich and Field
UCMP 128561	2	4	*Longrich and Field
UCMP 154452	3	1	
USNM 1201	TBD	3	
USNM 1205	TBD	4	*Longrich and Field
USNM 2100	TBD	4	
USNM 2412	TBD	4	
USNM 4720	TBD	4	*Longrich and Field
USNM 4741	TBD	4	*Longrich and Field
USNM 4928	TBD	4	3 in Longrich and Field
USNM 5740	TBD	4	*Longrich and Field
YPM 1820	TBD	4	
YPM 1821	TBD	3	
YPM 1822	TBD	4	
YPM 1823	TBD	3	
YPM 1828	TBD	4	*Longrich and Field
MOR 335	1	3	
MOR 1186	1	4	
YPM 1831	TBD	4	*3 in Longrich and Field (2012)
YPM 1830	TBD	4	
MPM VP6841	TBD	4	
ANSP 15192	TBD	4	
MOR 1122	1	4	
SMM P97.6.1	TBD	4	
MOR 981	TBD	4	
MOR 2984	1	4	
MOR 3081	1	4	

Appendix 7.14. Skull factors. Stratigraphic levels: 1, L3; 2, M3; 3, U3; Ontogenetic stages: 1, baby; 2, juvenile; 3, subadult; 4, young adult; 5 toromorph

Specimen	StratL1	Ontog
AMNH FARB5116	NA	4
DMNH epv48617	NA	4
LACM 59049	NA	4
MOR 1110	3	2
MOR 1120	1	3
MOR 1122	1	5
MOR 1199	NA	2
MOR 2951	3	2
MOR 3027	2	3
USNM 4928	NA	4
YPM 1822	NA	4

Appendix 7.15. Nasal horn factors.

Specimen	StratL1	Ontog
AMNH FARB 5116	NA	4
ANSP 15192	NA	5
DMNH 48617	NA	4
FMNH P12003	NA	4
LACM 59049	NA	4
MOR 004	3	4
MOR 1110	3	2
MOR 1120	1	3
MOR 1604	NA	4
MOR 1625	3	4
MOR 2570	2	4
MOR 2574	3	3
MOR 2576	3	NA
MOR 2702	3	4
MOR 2923	3	4
MOR 2924	3	3
MOR 2936	3	3
MOR 2951	3	2
MOR 2952	3	NA
MOR 2965	3	3
MOR 2982	2	3
MOR 3008	3	NA
MOR 3010	2	4
MOR 3048	3	3
MOR 3055	2	NA
MOR 3073	3	NA
MOR 598	3	3
MOR 965	NA	4
MOR 966	NA	NA
MOR 989	NA	2
SMM P60.2.1	NA	4
UCMP 113697	2	4
USNM 1201	NA	3
USNM 2100	NA	4
USNM 2410	NA	NA
USNM 4805	NA	3
USNM 4928	NA	3
YPM 1820	NA	4
YPM 1822	NA	4
YPM 1830	NA	5
YPM 1831	NA	5
MOR 3081	1	5
MOR 1167	1	2
MOR 136306	3	2
MOR 2938	3	4
MOR 2971	3	4
MOR 1122	1	5

Appendix 7.16. Postorbital horn core factors.

Specimen	StratL1	Ontog
MOR 1110	3	2
MOR 1120	1	3
MOR 1199	NA	2
MOR 1604	NA	4
MOR 2552	1	3
MOR 2569	2	2
MOR 2574	3	3
MOR 2597	3	3
MOR 2923	3	4
MOR 2951	3	2
MOR 2958	3	2
MOR 2979	3	4
MOR 2999	3	3
MOR 3027	2	3
MOR 3045	2	3
MOR 3053	3	4
MOR 3064	2	2
MOR 981	NA	5
RTMP 2002.57.7	NA	NA
UCMP 113697	2	4
UCMP 136306	3	2
UCMP 154452	3	1
AMNH FARB 5116	NA	4
ANSP 15192	NA	5
DMNH 48617	NA	4
LACM 59409	NA	4
USNM 1201	NA	3
USNM 2100	NA	4
USNM 4928	NA	4
YPM 1822	NA	4

Appendix 7.17. Factors for squamosals.

Specimen	StratL1	Ontog
LACM 149538	NA	2
LACM 59049	NA	4
MOR 1110	3	2
MOR 1120	1	3
MOR 1122	1	5
MOR 1199	NA	2
MOR 2569	2	2
MOR 2702	3	4
MOR 2924	3	3
MOR 2942	3	4
MOR 2951	3	2
MOR 2985	1	4
MOR 2999	3	3
MOR 3027	2	3
MOR 3045	2	3
MPM VP 6841	NA	5
UCMP 113697	2	4
UCMP 136306	3	2
UCMP 154452	3	1
MOR 8693	1	4
AMNH FARB 5116	NA	4
ANSP 15192	NA	5
MOR 3081	1	5
SMM P971	NA	5
USNM 1201	NA	3
USNM 2100	NA	4
USNM 2412	NA	4
USNM 4928	NA	4
YPM 1821	NA	3
YPM 1822	NA	4
YPM 1823	NA	3
YPM 1831	NA	5
MOR 004	3	4
DMNH epv1018	NA	NA
DMNH epv48617	NA	4

Appendix 7.18. Parietal factors

Specimen	StratL1	Ontog
AMNH FARB 5116	NA	4
MOR 1110	3	2
MOR 1199	NA	2
MOR 2569	2	2
MOR 2999	3	3
MOR 3027	2	3
MOR 3029	3	2
UCMP 136306	3	2
MOR 2951	3	2
MOR 004	3	4
MOR 1122	1	5
MOR 1120	1	3

Appendix 7.19. Nasal factors

Specimen	StratL1	Ontog
MOR 3027	2	3
MOR 1110	3	2
MOR 1120	1	3
MOR 1122	1	5
MOR 1604	NA	4
MOR 2574	3	3
MOR 2999	3	3
MOR 3005	2	NA
AMNH FARB 5116	NA	4
DMNH epv.48617	NA	4
USNM 4928	NA	4
YPM 1820	NA	4
YPM 1822	NA	4
ANSP 15192	NA	5
MOR 004	3	4
MOR 1199	NA	2
MOR 2951	3	2

Appendix 7.20. NPP factors

Specimen	StratL1	Ontog
MOR 1110	3	2
MOR 1120	1	3
MOR 1122-7-22-00-1	1	NA
MOR 1199	NA	2
MOR 2574	3	3
MOR 2702	3	4
MOR 2951 L	3	2
MOR 3011	2	NA
MOR 3027 L	2	3
MOR 3045	2	3
RTMP 2002.57.7	NA	NA

Appendix 7.21. TPS landmark data for skulls in lateral view.

LM=35
-0.00380935182691885 0.0364690552962379
1.9527039230971e-05 0.00122432488493073
0.0270384095988638 0.030982776108885
0.134626942056235 -0.0440998417412715
0.0470464476539713 -0.0407855887566018
-0.0283854543666476 -0.129184971247625
-0.118848135149326 -0.105617333200917
-0.114502989991886 -0.0769892132672846
-0.107835000598103 -0.0983515077244039
-0.0279714076235171 -0.0585428847242958
-0.0263839663774785 0.0243798228462896
-0.256208865994814 0.0495240492889239
-0.128991835657293 -0.0451218236451268
0.142305590173547 0.0199044241132976
0.174969312262634 0.0257977384032226
0.23544091404417 0.294780600576054
-0.0718869832149507 -0.169107196645698
-0.118130665802395 -0.0652179557347732
0.0205231205476452 0.0171026986393657
-0.106693844543324 -0.074690759364651
-0.0859959726487836 -0.0610631218630937
-0.0528925550282707 -0.0573957593794901
-0.0702738096815073 0.0421035860652522
-0.107856702070171 0.0417311477755513
-0.141635423110468 0.0431133811545636
-0.168098109181868 0.0481931784911432
0.218629170678425 0.0717716694039725
0.242231477917124 0.118480006393024
0.260810646860524 0.176742471248025
0.252528094823686 0.234614754847917
-0.105940170006891 -0.121077114534113
-0.116110160984877 -0.0918481347728067
-0.11557360696539 -0.0846938196648464
0.153395011259147 0.0231916996685463
0.164460345909677 0.0236796410617975
ID= AMNH 5116 L.tif

LM=35
0.00083954640534062 2 0.035204523762227
-0.00567208419234254 0.00855639531590256

0.025606051642739 0.0303083822036665
0.139815408840608 -0.0494544307177166
0.0524716141186391 -0.0497147261829475
-0.0522572783654508 -0.161509962748433
-0.127398765020903 -0.122469259418445
-0.123134360542952 -0.101070428966984
-0.116546491250544 -0.120008445859529
-0.0390649223197095 -0.0757573375248543
-0.0204427808666012 0.0255915368472555
-0.179382950327193 0.100718202700935
-0.123272670422893 -0.084108574221095
0.146219693903951 0.029282667967433
0.180653528764049 0.0390347351285927
0.195021732489379 0.266933211445765
-0.0700489796824854 -0.161087225409479
-0.108193900709598 -0.0709335799245903
0.0229838551060987 0.0126649883624243
-0.095352477057051 -0.0884119476294649
-0.0790409829920613 -0.0695944560517306
-0.0601328476355855 -0.0587828339654761
-0.0665264817447558 0.0562595462286783
-0.0896850490382659 0.0842586023336362
-0.131222098131649 0.0943595571612361
-0.166732003441779 0.0956171393850835
0.225094180998695 0.0792703526154858
0.220949057964692 0.120668130108961
0.235332203623261 0.173930637934396
0.238792860608722 0.239811888832814
-0.110646233875801 -0.128341761506231
-0.123410453040712 -0.112318937883263
-0.122507763948379 -0.107265689599018
0.157758607425992 0.0328387996225746
0.169133232714545 0.0355202996521889
ID= DMNH epv48617.tif

LM=35
-0.0117489308525484 0.0516916826736035
-0.0108605900035301 0.0153265309391012
0.0124010137190661 0.0439315545412694
0.114582274056581 -0.0405363457372729
0.0447156719404041 -0.0408171915263189
-0.0119361177490051 -0.140801871970756

-0.116255595049752 -0.127093217437483

-0.122046412780723 -0.116482041818895
-0.106530888854607 -0.115679436070832
-0.0288381450537544 -0.0714015522627875
-0.0317002280058444 0.0491406986334234
-0.177573690725822 0.0919865762275305
-0.179012571600069 -0.0746783452334272
0.132022470390183 0.0257835920031072
0.175343028567464 0.0323977268186303
0.216703938321636 0.269335963903349
-0.0389784009882339 -0.168512192508821
-0.11142994691302 -0.0675475260457792
0.0202112906202458 0.0116275000623873
-0.092193816541134 -0.0896547354844342
-0.0719594413709696 -0.0739666455962466
-0.0534597817564988 -0.0577509091392161
-0.0605330893348541 0.0664964056555791
-0.0945948696069904 0.0805791561710265
-0.131911312911922 0.0841325923336045
-0.165494559453562 0.0865379331117857
0.219431344674949 0.0661978661939054
0.232691911396853 0.115421992452786
0.245147499753505 0.170904113986875
0.248420957647516 0.22664414971467
-0.114396181191709 -0.126805260965058
-0.117190811324631 -0.120966524086811
-0.119030774118832 -0.119155265192824
0.145672327595572 0.0320407268795361
0.160332427504038 0.031672298774794
ID= LACM 59049 R.tif

LM=35
-0.0331575873550951 0.057220566095906
-0.0227185522581664 0.0204145645424409
0.00094732212733937 0.0527550065224339
0.123358905479748 -0.032624029532762
0.0445763916196162 -0.0294063836707205
-0.00948380512793847 -0.12194777032085
-0.0962082280751126 -0.127764044871592
-0.10581062420986 -0.113441118895609
-0.0925573687208432 -0.117036395987991
-0.0344052865671861 -0.0610796777787861
-0.042776950107320 8 0.0464137398798681
-0.22554138388937 0.129735956370431
-0.14086420595486 -0.103843301901656

0.110671102946723 0.0348017774926922
0.165532841177353 0.0120322218855881
0.206393083829408 0.263458774917191
-0.0185776165165469 -0.16400077334722
-0.108971899545746 -0.0703207415713313
0.0158918408137986 0.0102508406068367
-0.0933870917197022 -0.0945414310292615
-0.0771067033729265 -0.0732388082312143
-0.0565628161317208 -0.0586198125081977
-0.070326601526217 7 0.052737897385085
-0.105745058528034 0.0607156966018124
-0.142410150376374 0.071577999786046
-0.170890185844706 0.0978433065077966
0.214399104336734 0.052607470547583
0.264435903031734 0.0989085090455623
0.272013557632154 0.173571652174711
0.255662058860368 0.225192387058213
-0.108286493837439 -0.117276941732477
-0.100154822370513 -0.12058643287729
-0.102764755292161 -0.117222550928182
0.131942508197285 0.0343522447742709
0.152884157190184 0.0283596029906703
ID= MOR 1110 L.tif

LM=35
-0.0192045853972409 0.065027257525604
-0.0237857622279619 0.0346036049785648
0.00602468657184146 0.0644380062471396
0.12915747820881 -0.0319271277982652
0.0439397980915307 -0.0254435613705056
-0.0152797999593017 -0.136708338390332
-0.115456042544729 -0.122325700603104
-0.115258672659826 -0.0912077426571177
-0.1028705032364 -0.10093961703563
-0.0280646922269759 -0.0505559043194051
-0.0419791242424795 0.0503209133149648
-0.203478886843812 0.0607038544883603
-0.132551013990557 -0.0833055397940258
0.122883132720418 0.0333250876491657
0.171115121565081 -0.00259853012694231
0.221263926827958 0.298912333815355
-0.0656748863818764 -0.171458705869071
-0.119864206662711 -0.0646599629016842
0.0222758949936166 0.0156098054572968

-0.101907707158908 -0.0815837061803049
-0.0829571014859886 -0.0654102726125595
-0.05364829265386 -0.0581141171348149
-0.0655329253715085 0.0522343388169279
-0.099855413953705 0.0483834160741232
-0.134134712795114 0.045982126384625
-0.169726384868668 0.0456667845501399
0.211280307612498 0.041622937381921
0.265165065388345 0.101850242603394
0.274586746948743 0.175015455050716
0.251980749924041 0.232373723899646
-0.107503652135966 -0.121457798682447
-0.112320976155869 -0.106145301109908
-0.11327637608478 -0.098312831891676
0.145652375945637 0.0318067599493841
0.159006434239718 0.0142781102904661
ID= MOR 1120 R.tif

LM=35
-0.00724418846606293 0.0430929629447321
-0.0110297853580184 0.0188658800266475
0.0139380936762442 0.0444224046877072
0.128738968112475 -0.0226564975711609
0.0564775427942217 -0.0332466787693605
-0.0253063415486313 -0.150413434806478
-0.125592685362419 -0.136683696708385
-0.123863709883186 -0.112487086399435
-0.113658473202351 -0.124901394970091
-0.0219425493313429 -0.0470927591487192
-0.0288889336969108 0.0401558544022617
-0.155609521869439 0.0723721287321341
-0.126645993410838 -0.0550404215486961
0.117930258816241 0.0249863099740447
0.13949956763737 -0.00289809250316432
0.26336625902268 0.325194631874396
-0.0461760424000255 -0.168449200954218
-0.0993815866629716 -0.0717030863612501
0.0199458836703093 0.0108193601900166
-0.0936484672608881 -0.0876351478764999
-0.0817928120113474 -0.064675435219141
-0.0558458486107733 -0.0572103173209096
-0.0638213696041795 0.0548436395409936
-0.0948338055723348 0.0787542183465508
-0.132246105986638 0.0803632763409041

-0.166172959348682 0.0786138952649839
0.219530609093372 0.0590285742187448
0.221437882947351 0.126830451261613
0.2451927675507 0.175200134092265
0.249784989043546 0.232833865547606
-0.124108227705874 -0.120032892962941
-0.123957998913222 -0.125869669564871
-0.123910941057345 -0.119691324255956
0.132881083569039 0.0243529947384489
0.136954441329932 0.00995655475722725
ID= MOR 1122 R.tif

LM=35
-0.0407356807305943 0.0414154773376686
-0.0415412833336513 0.0163783223181581
-0.00690362059872243 0.0392855193781666
0.119897065302209 -0.0302280647170894
0.0490084372484896 -0.0247022089669304
-0.0166491892001995 -0.137269044286029
-0.10089056384838 -0.14939823647892
-0.109533287884275 -0.11072450812495
-0.101317334398776 -0.108288087247924
-0.0560035723600957 -0.0646787335287474
-0.0595592060023396 0.0339003799923575
-0.146592851578504 0.122300449107111
-0.136256934717721 -0.10462772954689
0.130758616815513 0.0545460989125554
0.16725556557072 0.0364304766993845
0.237440548987658 0.258941836243855
-0.021336472947142 -0.168084529108284
-0.111508297402851 -0.0705679901870441
0.0176766621852852 0.00928512950420358
-0.0987029787234622 -0.0864336926954304
-0.0887863529147498 -0.0659580671469961
-0.0739495507942697 -0.0567020423558054
-0.0741049955625458 0.0426113494544541
-0.107172604740135 0.059813348870701
-0.131480119776818 0.0831334492352389
-0.16785031901677 0.0998229263140063
0.220635463870794 0.055811189471903
0.239453538437103 0.116943003111203
0.264810512596027 0.171531170351409
0.260990612233734 0.217686523307092
-0.110701745670663 -0.126138763777382

-0.10284863561381 -0.129385103114786
-0.105215470405185 -0.120404553377999
0.145507207523015 0.0511592481160427
0.156206837451111 0.0425954569356962
ID=MOR 1199 R.tif

LM=35
-0.0370704294074604 0.0492963502710116
-0.0347585183383092 0.0233517989986841
-0.00393600181110595 0.052091406865079
0.119217768180241 -0.0346719407895246
0.0406971261458143 -0.035065978973571
0.00172762031351186 -0.135368870995835
-0.101852965829937 -0.133663141990524
-0.114070117575435 -0.113507241987892
-0.0959788833978702 -0.115424436100342
-0.0353595668661457 -0.0727826533748856
-0.048779108369445 0.0398381658343816
-0.165603413739825 0.145554925933877
-0.140975678888902 -0.100158783421547
0.120104935313446 0.0398253079305731
0.197597232459042 0.0249032699512818
0.199053945994283 0.250299294745233
-0.0500054147856762 -0.171514113510589
-0.112619570868155 -0.0703326698140406
0.0130835558794327 0.00649795761931504
-0.0935828616704177 -0.0930400585001058
-0.0738545080676622 -0.0751472553018598
-0.0588585907514092 -0.0595246949195508
-0.0742310770203289 0.0469246318355573
-0.106172684980035 0.0595117215077807
-0.134526197377046 0.0789861665904195
-0.168198997151522 0.113004388990144
0.230516791372578 0.0567583819289349
0.246049092253082 0.111970840060892
0.244665375207775 0.172857467803234
0.246746910983452 0.23167495445749
-0.109303441440083 -0.122635233546714
-0.107138419263375 -0.123491026165206
-0.110272978073062 -0.119204879095646
0.146426948779575 0.0411995129455089
0.171262122790977 0.0309864342184364
ID= MOR 2951 R.tif

LM=35
-0.0119404102969078 0.0503299407391334
-0.00602353785957945 0.0234338396917455
0.0170025859287231 0.0509832197725458
0.121379131142251 -0.0361553248044784
0.0548812167307467 -0.0249272246431184
-0.00722875678357194 -0.130947638895397
-0.106861927332135 -0.128597277245593
-0.110888643176521 -0.106374318030525
-0.0937076032921065 -0.110174509033194
-0.0245581759258063 -0.0592188551130698
-0.0289654798459795 0.0438068643945962
-0.262418697560564 0.0897386260409697
-0.162781147770898 -0.0912061431100741
0.125641199866984 0.0226291695968427
0.176735449637063 0.0130679896858633
0.203252062388754 0.256482473061184
-0.0300230348631212 -0.166036162749427
-0.117740914922774 -0.0675300061277701
0.0220406259879414 0.016461048561661
-0.0960558404815922 -0.0909292179982665
-0.0766234909329347 -0.0737451529379718
-0.0498997096793242 -0.0584568456567786
-0.0692031541467002 0.0721510458835018
-0.0987982665538083 0.0808137165371529
-0.136901592167255 0.0849938970679381
-0.171002582535138 0.0821681872106982
0.214101938669396 0.0487526070395055
0.244518422695497 0.11055455448001
0.249659239976755 0.171642522991088
0.25241155238843 0.224517202318287
-0.109303945633898 -0.117668315258993
-0.105722027699414 -0.115994275571015
-0.107782633321062 -0.110722568834244
0.142588431017612 0.0245947652157884
0.16021971635094 0.0215621657214032
ID=MOR 3027 L.tif

LM=35
-0.0148224561977317 0.0550530420641008
-0.0122848994479059 0.0175815727357954
0.00747293005576278 0.0493858391063195
0.103233851175171 -0.0525872446151647
0.0256247357278219 -0.0397697359617984

-0.0242753574438086 -0.154318580872381
-0.105766475999247 -0.150593374619204
-0.100972773606538 -0.109689966522087
-0.0913597390762016 -0.122838879450468
-0.0262382107933269 -0.0650663642753418
-0.0386211443028778 0.0543922059131071
-0.216901014069524 0.122343536679148
-0.12142162431335 -0.090907748940193
0.11727707160733 0.0147678986385892
0.172046191469511 0.00547051396809057
0.190927988131333 0.287495922430519
-0.046366402336499 -0.171709433938648
-0.103116101659443 -0.0737808250888292
0.0167533031333502 0.00972627733519189
-0.0887577513948554 -0.0986185894046209
-0.0699514279162877 -0.0781171700956034
-0.0501888761700327 -0.0597450721377185
-0.0624873861259161 0.0850584091746444
-0.0814713424628276 0.0996593952814123
-0.129182492424657 0.117507296977618
-0.164697224472767 0.116328861979777
0.215898268671842 0.0493468344859355
0.237796181781464 0.115338159592472
0.242803443293072 0.172805538791068
0.238031340562413 0.245152707857561
-0.112928811755013 -0.126514133869956
-0.0989407054008453 -0.13055268183262
-0.0980463541913512 -0.119997823362976
0.136406848752473 0.0151788720848128
0.154526417199463 0.0122147398914479

ID= USNM 4928 L.tif

LM=35
-0.013318371220803 0.0505063301929347
-0.0155553106345763 0.0196921854132921
0.0116144437826333 0.0471186979031271
0.123979388630791 -0.0402860745253222
0.0427074039678406 -0.0287471430863721
-0.0124704558900478 -0.13149163379875
-0.110650229046445 -0.124264632062209
-0.110485196616488 -0.112679096505779
-0.0993893688308422 -0.10869537064567
-0.0247988657082467 -0.0634358403458126

-0.0348238555270732 0.0407876301621178
-0.201647088790995 0.10064233924762
-0.182773255931205 -0.108064658048155
0.13125231804231 0.0297801057614351
0.176487782691805 0.0221531170867926
0.18936909016933 0.262116019974161
-0.043518015848838 -0.167954687506482
-0.118902076833278 -0.0652695514719499
0.0205563316720361 0.0131580431053515
-0.0967102390701566 -0.0863029254908681
-0.0765571314178742 -0.0710023725787046
-0.049974366918352 -0.0581564812862498
-0.0648651994273325 0.0663659526129167
-0.0967495566499938 0.0766050963869807
-0.132867669673261 0.0827535640309936
-0.166659712259165 0.089352691977561
0.215041282057265 0.0552334830459739
0.253635042493005 0.104674178144787
0.259178406353409 0.17059201953911
0.246318170618194 0.231007627059357
-0.10905469260943 -0.121501030974179
-0.108890244923231 -0.118203275309639
-0.108680220731179 -0.115734670669431
0.147132538714131 0.0317175410701456
0.162068925366065 0.0275328215909172
ID= YPM1822_R.tif

Appendix 7.22. TPS landmark data for skulls with cranial ornamentation removed.

LM=18
0.112567946875936 0.262572607101888
0.12290541833037 0.167286586985137
0.195945441713202 0.247652301706407
0.48631002344398 0.0447619034469926
0.249581640875898 0.0538501631356437
0.0454349170312669 -0.184546833515369
-0.198875092229167 -0.120471473076065
-0.18698265184835 -0.0430547525857
-0.169061940958625 -0.101019728246929
0.0469189622344819 0.00621265727382337
-0.0691818300065109 -0.266428030171855
0.192985659214671 0.176040581544116
-0.144341755029579 -0.0207819889509901
-0.0875796979971973 0.0193184114406811
-0.020846681308679 0.0377836671669426
-0.192471394423556 -0.107862826084968
-0.191810411021121 -0.0933647791842025
-0.191498554897019 -0.0779484679855518
ID= AMNH 5116 L.tif

LM=18
0.137035908554955 0.269947915909222
0.118680803069888 0.20472784044382
0.197742921919049 0.255748607227457
0.472827927063541 0.0491965231166313
0.257227795621283 0.0559487830054726
-0.0108187774121716 -0.211151650719829
-0.192970281414697 -0.108322333832861
-0.180608861778198 -0.0558629460327472
-0.165945562618146 -0.103197258023927
0.0290630213121894 -0.000563754550691766
-0.0685942018528029 -0.243147987811522
0.196694294770064 0.185661294711903
-0.129775818487489 -0.0328991425793342
-0.0816883130670178 0.00362215979426108
-0.0231088329700987 0.0150908896698115
-0.19070670299196 -0.109303061495068
-0.184925168785491 -0.0956272132285204
-0.180130150932897 -0.0798686656040798

ID= DMNH epv48617.tif

LM=18
0.141529147823367 0.297194273682269
0.127777170513083 0.205250835648403
0.198923420738073 0.267040041502175
0.419049897597948 0.00944325089613482
0.243019151213333 0.0394604901780026
0.0564173622765188 -0.187367151012062
-0.200196278788913 -0.106988144839496
-0.210104537754805 -0.0777138911495598
-0.17068966975593 -0.0825220178746223
0.0443806903906684 -0.00519714529435004
-0.025288566679887 -0.250271077423463
0.205081349488783 0.182542283028935
-0.134224792834744 -0.0296472586251481
-0.0772247685500386 -0.00100767874607492
-0.0213115154089311 0.0318644654037043
-0.198338595905774 -0.107328355758758
-0.197493493013541 -0.096024508956525
-0.201305971349212 -0.0887284106595643
ID=LACM 59049R.tif

LM=18
0.111924550572253 0.313002220370603
0.112330226473947 0.210314358439823
0.196851478700622 0.276817488346793
0.451572374947453 -0.0322718487327704
0.250280808295976 0.0329426331924174
0.0437556659268403 -0.167184926599459
-0.184600144825789 -0.119612002902003
-0.199095348219883 -0.0756624066096273
-0.167428400110079 -0.0945241071557632
0.0232674473116861 0.00812414742364069
-0.0105035314074644 -0.243930212031307
0.19582222953099 0.1638790583475
-0.142889291688631 -0.0254862114054146
-0.0871120854893898 0.0124278272666186
-0.0226611919421507 0.0341487652024801
-0.18634263264885 -0.11110295205492
-0.189914433536519 -0.097347751523574
-0.195257721891012 -0.084534079575037

ID= MOR 1110 L.tif

LM=18
0.121201516229234 0.295217213994787
0.0974637607120626 0.22181086659536
0.183370311039526 0.283520236314014
0.44890595187747 -0.00505636900996083
0.240648919049771 0.0456493784471197
0.0489296815266895 -0.205620490031071
-0.193127936669987 -0.129271754218965
-0.179965603687435 -0.052310637819923
-0.153265861918103 -0.0814450230849423
0.0523277506792637 0.0128057812782804
-0.0906830178367798 -0.279729992309647
0.194666305123439 0.164016348716066
-0.129994175775897 -0.0298621450046967
-0.0806080563228342 0.00901994854128342
-0.0197546607990229 0.0337969450239412
-0.183096870747506 -0.110165464262882
-0.179291870169816 -0.0943930644051897
-0.177726142310076 -0.0779817787635757
ID= MOR 1120 R.tif

LM=18
0.143340520989634 0.253252390535425
0.125005886868041 0.19786587070281
0.193571281205395 0.248166363775311
0.437130647043684 0.0460791796083968
0.263320354441303 0.0492087062156779
0.0255507374126938 -0.194237584240726
-0.20469867809939 -0.122955088751134
-0.191201630931653 -0.0667960962821497
-0.17206963127139 -0.0999562903164579
0.0737573993905821 0.0472834390195336
-0.0617895254619948 -0.280950548725191
0.196406084850285 0.171678073734456
-0.129514886276898 -0.032142660167453
-0.088701497205607 0.0183952628591066
-0.0227056324867355 0.0470764541998613
-0.198027832971896 -0.108074337899938
-0.195982636751807 -0.0944072171453067
-0.193391028229293 -0.0794859171222216

ID= MOR 1122 R.tif

LM=18

0.108592778237023 0.284350400518508
0.0873804503351253 0.220434395706674
0.194132603619862 0.252970860988996
0.467692980727941 -0.0231990994696332
0.289238276714934 0.0452427432410007
0.0339451133597659 -0.194601313210438
-0.192479199099188 -0.161384672704155
-0.185132734973486 -0.0551357854526323
-0.16206629737509 -0.0551621501885611
-0.0118954078000075 0.0226154659268799
-0.000171667681118828 -0.251470244035835
0.192619502886939 0.148603955124928
-0.154757352629449 -0.0196519699625332
-0.100764211051056 0.0378836166718408
-0.0216804501543305 0.0438927506151351
-0.18164720273269 -0.115250703526023
-0.181502093545302 -0.0981536565325748
-0.181505088839872 -0.0819845937115772
ID= MOR 1199 R.tif

LM=18
0.109246217827685 0.30068272455049
0.0972626750600084 0.23377502736594
0.194626942012828 0.284970770969692
0.445168143466191 -0.0181108917397873
0.24717112702147 0.0348099026051426
0.0802434329036931 -0.191025659411126
-0.179458118673387 -0.11559897409994
-0.196414971139044 -0.0564471838808112
-0.15214473030333 -0.0736954278725778
0.0297400485439594 -0.00795692887332018
-0.0733448805018732 -0.275244884489137
0.193177173204284 0.164826883871985
-0.140284451773208 -0.0239455484359649
-0.0815593212108642 0.00233146319381818
-0.023362022734282 0.0181599360281591
-0.177834794790102 -0.106873848115797
-0.183407464122135 -0.0918089441090979
-0.188825004791894 -0.0788484175576685

ID= MOR 2951 R.tif

LM=18
0.125041262403753 0.281720741180186

0.127227215447402 0.20978719150353
0.199703169323563 0.269379967812982
0.425471441955845 -0.00503646869779814
0.260195184859245 0.05606904030182
0.0492813442934114 -0.186116887329327
-0.205510923183409 -0.131799968865895
-0.205088103329916 -0.0727779926946682
-0.162771193596656 -0.0908579866390612
0.0395259116069423 0.00648987346971271
-0.0275754536739871 -0.231331395075124
0.210152410571152 0.175147510050502
-0.138764095675506 -0.0273167511766958
-0.0841700636107869 0.00894970539078787
-0.0218064553995839 0.0311922289509243
-0.195100927493925 -0.110222197818538
-0.196548500471956 -0.0980071514337174
-0.199262224025589 -0.0852694589296207
ID= MOR 3027 L.tif

LM=18
0.15154050361415 0.324131464851786
0.136210542970836 0.225747723359848
0.205931715744362 0.29645713253153
0.39415593318001 -0.0231843622925987
0.200886356386214 0.0552600514903237
0.00482920075042342 -0.21187198702156
-0.203867522516932 -0.154604095666395
-0.167608731461859 -0.0516677620535512
-0.150401357894331 -0.0912710971923683
0.0518234212168284 0.0201067503801873
-0.0720068002323049 -0.283021875662986
0.201291747765049 0.198522571868918
-0.130696582719055 -0.0329903288478984
-0.0806530742230582 0.00382785356013511
-0.02069998640009 0.0286840234249629
-0.181253202270454 -0.117211973374469
-0.17297186979699 -0.103410962747788
-0.166510294112801 -0.0835031266080768

ID= USNM 4928 L.tif

LM=18
0.132595346776126 0.289055684120418
0.112587401754148 0.210216356982282

0.195653966591892 0.268781391698057
0.446611368703972 -0.009573742485279
0.241268610031606 0.0578143662927547
0.0509096677750094 -0.183066164173362
-0.200256076293716 -0.119081456122097
-0.194487386383547 -0.0891553158450475
-0.163886301276965 -0.083919502524814
0.0503213770022256 -0.00099954063904051
-0.0473746608757715 -0.239804359089597
0.198118701627897 0.181660062380547
-0.141259084329931 -0.0246907204629107
-0.0831069051556533 0.00803446207216975
-0.0211870445017613 0.0255358270644642
-0.19495524140522 -0.109342825065497
-0.190076682945891 -0.0967332692575202
-0.191477057094421 -0.0847312549455281
ID= YPM1822_R.tif

Appendix 7.23. TPS landmark data for nasal horns.

LM=11
-0.299290225679355 -0.39331901067024
-0.0594433805883122 0.253498170099928
0.435509341040632 -0.0743794451162406
-0.232592558510677 -0.254739806662509
-0.207019580065879 -0.114650720887139
-0.190347341233102 0.0300288161227816
-0.15147222050155 0.168547533486218
0.0345216318552173 0.222883569403654
0.120703518397913 0.129134212030484
0.221005018016523 0.0494935687187904
0.32842579726859 -0.0164968865257277
ID= AMNH5116

LM=11
-0.354247567775576 -0.393238194919291
0.00220087186620675 0.174936606655507
0.464581951388555 0.0254847747156938
-0.328954683373383 -0.253011822814301
-0.278397766142408 -0.0901967682173829
-0.183366236570824 0.0158267732886778
-0.095799169983862 0.103133595044884
0.0277100315142802 0.16705534661042
0.135513760880704 0.130287937065061
0.251078925077386 0.0794549656648385
0.35967988311892 0.0402667869058924
ID= ANSP15192

LM=11
-0.414929841902093 -0.383131295860746
0.00176846278264857 0.141253769731386
0.490856675425781 0.0553539324303114
-0.347853605612251 -0.235392580880764
-0.266563849043896 -0.103798816171948
-0.180149514253834 0.00306640105231461
-0.0977082116281525 0.0857760967104163
0.0475081594973115 0.139018232968737
0.140400977788922 0.125705603397591
0.254410752227912 0.0926267586539815
0.372259994717651 0.0795218979687206

ID= DMNHepv48617

LM=11
-0.395262175929612 -0.411736216188882
0.0131214961641528 0.168636820161026
0.436860140086055 0.0291404372796806
-0.332938997637397 -0.234653660055786
-0.24112670891927 -0.118532144624268
-0.172848871725436 0.0065566164870936
-0.103337521108681 0.104589675962511
0.0334396069104969 0.176119344813669
0.137351712609403 0.139250749907737
0.25246375136087 0.0869447068925792
0.372277568189419 0.05368366936464
ID= FMNHP12003

LM=11
-0.136120681171553 -0.37135021785988
-0.107805956638838 0.346392859496092
0.460967692769248 -0.191060807898753
-0.18962905562855 -0.2338537616418
-0.211228869463986 -0.0981670499812952
-0.225574372769705 0.0491066591891673
-0.205488510263607 0.212283710918215
0.0174037794995218 0.216969179798653
0.0994741749787328 0.11447149813824
0.199213492484368 0.0224124837653042
0.29878830620437 -0.0672045539239426
ID= LACM59049

LM=11
-0.169690068334279 -0.420288587224949
-0.10105420319707 0.365660374529789
0.396604797641662 -0.190926466973865
-0.188152054724507 -0.246492782683603
-0.19685134296146 -0.103108402497811
-0.19307950815691 0.043333476123727
-0.183479810545605 0.19322527520785
0.040701194291684 0.246775052777394
0.11605937702606 0.139975529797846
0.195988339431223 0.0348631415296894
0.282953279529201 -0.0630166105860686

ID= MOR004

LM=11
-0.212126252848049 -0.3945887399377
-0.100590936765173 0.278839303304448
0.409778843405379 -0.159411108251376
-0.210599958113979 -0.253041047478318
-0.201761480833261 -0.109223605764811
-0.204374957348426 0.0357476573714618
-0.181070390327457 0.184826912566849
0.0487605740699631 0.263391184414706
0.137664883807778 0.150828323205059
0.213276753676757 0.0474688053521612
0.301042921276467 -0.0448376847824793
ID= MOR1110

LM=11
-0.24554600901783 -0.323005438278144
-0.124777104446972 0.216161430289539
0.504576915329289 -0.096675245506093
-0.261937458393403 -0.258247600966419
-0.23933112670407 -0.107473148129984
-0.196759399227669 0.0331605867789727
-0.155534373826424 0.173747303544795
0.0312504515289619 0.198535016001029
0.129506992708717 0.134358826758456
0.226797720814644 0.048028329549744
0.331753391234756 -0.0185900600418964
ID= MOR1120

LM=11
-0.147719922069409 -0.406257996524776
-0.106223232206343 0.40385374339819
0.450392335875288 -0.198815634625715
-0.170797569977896 -0.236422543203514
-0.178878971564388 -0.0916443444879924
-0.184278946782542 0.0572241860523608
-0.200876885072457 0.211047959186217
0.00385779083195561 0.228986482932208
0.0742886609535388 0.110061725413803
0.177030045499175 0.00741059209730755
0.283206694513078 -0.0854441702380891
ID= MOR1604

LM=11
-0.176825046994284 -0.375412566910508
-0.127607820798538 0.343982643339211
0.456658593286838 -0.188255990986778
-0.184502659898821 -0.241987486348674
-0.19418194038775 -0.0972081508603093
-0.200476878628451 0.0484294962918572
-0.194121625329907 0.200760943684904
0.0186501193614278 0.218696626647634
0.102352239265312 0.121247691664329
0.198788928587475 0.0270450966797791
0.301266091536697 -0.0572983032014454
ID= MOR1625

LM=11
-0.21896687598849 -0.299774786675061
-0.169891427832093 0.260351701263812
0.524834360553905 -0.1562923006983
-0.223146131648184 -0.250296015622891
-0.204812104082528 -0.104447827508763
-0.201004135469416 0.0428147316813288
-0.193149713503648 0.190540227103465
0.0179846879404165 0.183104212084475
0.114525537988254 0.115763302992764
0.223397376542588 0.0466324971592158
0.330228425499197 -0.0283957417800454
ID= MOR2570

LM=11
-0.133286289734403 -0.4741516580416
-0.040278532157367 0.421440111736949
0.370171575870172 -0.179940921088294
-0.187098445497247 -0.243082163969003
-0.200267230795713 -0.0997128860561268
-0.199845889569555 0.0501524971303984
-0.169819773262832 0.199129872148656
0.0504389237821621 0.26128787035847
0.0829204253501427 0.137830007845206
0.161373344479567 0.0138498730542981
0.265691891535072 -0.0868026031189536
ID= \MOR2574

LM=11
-0.182907880430693 -0.372620879584223

-0.116717928397377 0.310233224207791
0.443882011326925 -0.169984060565427
-0.21394656153762 -0.246444162078639
-0.216107499942536 -0.103282240157313
-0.199554085829721 0.0421748578659418
-0.182622616051307 0.190995410122447
0.0277281856059352 0.219344127646786
0.118524455705272 0.1325359561393
0.213137610286777 0.0425241331140999
0.308584309264345 -0.0454763667107644
ID= MOR2576

LM=11
-0.206430860839913 -0.516380828759044
-0.0232971696083905 0.424866550918209
0.319735144249465 -0.152477446601115
-0.175555795323757 -0.261876865605509
-0.171774126893427 -0.105621070418034
-0.167976081804582 0.0467287441122218
-0.15743700142255 0.19177039869181
0.0639038609758439 0.273264815617955
0.099738507988226 0.15067585771424
0.166117866750874 0.0298935584383298
0.252975655928209 -0.0808437141090642
ID= MOR2702

LM=11
-0.151272211536328 -0.421037809279947
-0.145644247418711 0.408697557025565
0.404548463168466 -0.238781047756969
-0.165021697483185 -0.247281525656561
-0.169992024470244 -0.0983448003959499
-0.175239818191668 0.0526563266323946
-0.181433717800346 0.200338543168002
0.0282645235289731 0.24895394158148
0.102602121710656 0.138728542445361
0.187592379707761 0.0327188009740178
0.265596228784626 -0.0766485287373951
ID= MOR2923

LM=11
-0.133351114268949 -0.452854249160452
-0.0595278021992673 0.408388059879122
0.383234548675415 -0.192759848340901

-0.183702329839424 -0.240665553082259
-0.194209870405055 -0.0983877668002655
-0.198668270107869 0.0501282181766912
-0.191958397118098 0.207758801510724
0.0390959647560538 0.250394721756658
0.0915845593584857 0.130633945714633
0.17726783341698 0.0192589355152077
0.270234877731726 -0.0818952651691585
ID= MOR2924

LM=11
-0.155819587882758 -0.442652325713784
-0.115444194622356 0.39190287760558
0.373174771256982 -0.215828872935374
-0.17970489558312 -0.250281140359823
-0.183582304584483 -0.104290214392213
-0.18409685048918 0.0446417098034892
-0.172284718839584 0.192850966071783
0.0583270041129677 0.274823691670763
0.110558742620473 0.145570568104145
0.185156021784494 0.0343074227434971
0.263716012226564 -0.0710446825980627
ID= MOR2936

LM=11
-0.194333466612734 -0.379612412984397
-0.0882369583579272 0.262712650539593
0.410945301907494 -0.154389127318163
-0.215146483077998 -0.251044808458619
-0.237265025054357 -0.110886794550486
-0.236235863822211 0.0452562536916401
-0.170314873355265 0.186131166446736
0.0409957262249598 0.233897498705299
0.135461345456119 0.14549528463575
0.228868005105999 0.0556708462466127
0.325262291585919 -0.0332305569539665
ID= MOR2951

LM=11
-0.138581521128352 -0.49494717698603
-0.0332432777540171 0.424403324000324
0.335077439929018 -0.196588807961868
-0.182227974454903 -0.248657720901099
-0.184003769046866 -0.101615027794746

-0.187899033804829 0.050841754674021
-0.191648110901861 0.209184231897232
0.0585458929735945 0.267092935615395
0.0983513640934056 0.143669545201368
0.174274229891945 0.0275204106818443
0.251354760202866 -0.0809034684264401
ID= MOR2952

LM=11
-0.15118306222905 -0.445974012406018
-0.0680876581786436 0.366376773761457
0.37894866350213 -0.18264277174219
-0.185444940113356 -0.243360000314189
-0.200662527515471 -0.101207128335857
-0.202182565336084 0.0458676434870892
-0.201024487148042 0.207098010108595
0.0628964407158375 0.263592565307283
0.106190910028316 0.13634522535526
0.188834137101857 0.0293651676421477
0.271715089172507 -0.0754614728635785
ID= MOR2965

LM=11
-0.203348632167517 -0.413241857013223
-0.0556659593989739 0.311365812619186
0.413001545041319 -0.0910991897799881
-0.262774780303064 -0.257244103537392
-0.229071071273278 -0.104881196299742
-0.186937711660901 0.0326189910760091
-0.147488625538886 0.170317825364295
0.0457772203933621 0.239035636543336
0.122334954879914 0.134762101962281
0.202469004269044 0.0328845637679462
0.301704055758981 -0.054518584702708
ID= MOR2982

LM=11
-0.187162542704503 -0.413756696232602
-0.0934939084075518 0.350874247127574
0.410471441722552 -0.161657364331561
-0.204765613697606 -0.247938058094981
-0.202401730913224 -0.104204781648065
-0.201185993490146 0.0421631487597192
-0.160762959151016 0.183581852543073

0.0370305144370192 0.238871967171218
0.113331199731567 0.135281276634836
0.196216216811747 0.0330392563068973
0.292723375661162 -0.0562548482361089
ID= MOR3008

LM=11
-0.264041405655629 -0.291417408156858
-0.113004460220573 0.160732466977372
0.553670591792343 -0.0574360467560259
-0.294556308556256 -0.263011067619636
-0.25615041710997 -0.106328033789602
-0.228178928036425 0.050308439765081
-0.141367835568829 0.16693812670108
0.0310372196683964 0.156423464300334
0.12303209511805 0.113771933605396
0.237578659179374 0.0603369626065367
0.351980789389518 0.00968116236632086
ID= MOR3010

LM=11
-0.156929015962071 -0.451537837608454
-0.0678289247192431 0.371150183456972
0.366350382432322 -0.176469403472862
-0.203701123328885 -0.250285141818694
-0.195172424192291 -0.106116826243905
-0.192645476212927 0.0425234057854793
-0.186094895356815 0.195531360314849
0.0654983940733008 0.270777197298014
0.117566587657126 0.144900514061767
0.184113960539083 0.0319102325837726
0.2688425350704 -0.0723836843569391
ID= MOR3048

LM=11
-0.214153580439986 -0.346026105753693
-0.132338491280105 0.288285825311045
0.482182270074106 -0.144003781868306
-0.225790557776182 -0.24874590615537
-0.20977121649887 -0.10424428277438
-0.196407352190022 0.0414992739500234
-0.173534632241697 0.18736126908086
0.0187537552887726 0.198265184383284
0.115006989980124 0.12231523436116

0.216286503422086 0.0413867367711675
0.319766311661773 -0.0360934473057904
ID= MOR3055

LM=11
-0.131790553666888 -0.457082960324216
-0.0858390761836844 0.430197220727935
0.382315572412185 -0.218888172881432
-0.169073272407437 -0.243836978548941
-0.175058036830045 -0.0970913291843765
-0.184418535036107 0.0541798371601686
-0.189196119924992 0.207761863131349
0.036818051458129 0.258086355698039
0.0894401414707347 0.13683618463898
0.168929492508464 0.0198702250445115
0.257872336199641 -0.0900322454620182
ID= MOR3073

LM=11
-0.158750133365616 -0.463228388267734
-0.0751406091824491 0.379594912597161
0.355340993556589 -0.187443766245742
-0.18565464297065 -0.249327874596941
-0.191998656719272 -0.103975613231844
-0.194535561457047 0.0441271988333134
-0.183489092850221 0.196196891649763
0.0739157785426268 0.280957667783034
0.117749093874365 0.146940163445625
0.178810892482843 0.030245068035071
0.263751938088832 -0.0740862600017068
ID= MOR598

LM=11
-0.214126108255758 -0.395916743507253
-0.104120127835146 0.330098181175941
0.428546078920111 -0.160548739743958
-0.191036888605903 -0.250431617953807
-0.193386440188986 -0.103176727647351
-0.196474939877944 0.0415180727366793
-0.176922673990175 0.188890161385816
0.0307030187489246 0.229655791604464
0.113155579658566 0.132368158839661
0.204506967745039 0.0385030573870238
0.299155533681272 -0.0509595942772158

ID= MOR965

LM=11
-0.322838510089775 -0.376885159503486
-0.0851817048508002 0.234750764535644
0.453889280151173 -0.0701345673255642
-0.280493864704461 -0.233796490483862
-0.178881554015283 -0.138552124738224
-0.165488230094014 0.019457986568231
-0.142974728148999 0.159166332232624
0.0223936897810841 0.203678688877967
0.123849208863759 0.1360743524112
0.233278345988829 0.0683223251782956
0.342448067118488 -0.00208210775282443
ID= MOR966

LM=11
-0.256370473063837 -0.411039532085163
-0.0507159202035005 0.256841672973049
0.406696302980008 -0.0861259537829131
-0.251941229054746 -0.25310547371714
-0.225505239574857 -0.109675596957469
-0.194346797294525 0.0313552279791029
-0.148086785077325 0.165126708743718
0.0371930030483395 0.231548824788505
0.138412203010913 0.15135743664589
0.226062835981249 0.0543876559267111
0.31860209924828 -0.030670970514291
ID= MOR989

LM=11
-0.175516640113704 -0.434306230863176
-0.0834158375586393 0.364358791382249
0.390372229598137 -0.179637825302675
-0.189757730681031 -0.248043429273895
-0.191376616517219 -0.102739445393483
-0.193149532465139 0.0441339765015681
-0.183619522057114 0.195147134020273
0.0490577224658599 0.256213887035713
0.108555887377752 0.138263356619984
0.190314407514792 0.0327807206421764
0.278535632436304 -0.0661709353687346
ID= SMMP60.2.1

LM=11
-0.146548788959709 -0.478598392701684
0.00644162649803016 0.394044472855415
0.368499948347455 -0.112095863598961
-0.224509441115724 -0.247287445350764
-0.220534108118895 -0.100234906704733
-0.203300392699746 0.0480070002710884
-0.167839080794027 0.194545758538505
0.0607468624239375 0.252618138734147
0.0876602833395042 0.136047189931472
0.151381335027481 -0.00243226908619048
0.288001756051692 -0.0846136828882934
ID= UCMP113697

LM=11
-0.331877066460749 -0.35481931652902
-0.0754418550235409 0.184388129284258
0.490395623914124 -0.0392167936236162
-0.293211244976039 -0.246065822372579
-0.235769377251083 -0.115891902473615
-0.184478198895931 0.0184772055758768
-0.114197264064066 0.138821193641074
0.0265796588482167 0.187177685458588
0.127475473443085 0.135482080144847
0.237264171457616 0.0701470186868456
0.353260079008368 0.0215005222073411
ID= USNM1201

LM=11
-0.401528553834531 -0.352725403859214
-0.0774471885319869 0.169295687379827
0.501684841502256 -0.000720221499002319
-0.305277182989315 -0.230222796332965
-0.222112799267884 -0.139452273304567
-0.150942936327459 -0.0061842440897794
-0.104542616264496 0.142374379932355
0.0228436801778922 0.162941786915308
0.125871600556327 0.131594275588111
0.247533435630113 0.0881104562481927
0.363917719349084 0.0349883530217342
ID= USNM2100

LM=11
-0.295043430759071 -0.352418754433767

-0.0955783452889509 0.218039072298567
0.485885385864254 -0.0759858031084359
-0.250154688520518 -0.249739636013456
-0.210510220335355 -0.114737846639035
-0.186780282378233 0.0296140222888269
-0.162595740687579 0.17628292091705
0.0294169928232509 0.200750877103511
0.124594488300497 0.128710290415965
0.226637589782291 0.050582066064819
0.334128251199414 -0.0110972088940449
ID= USNM2410

LM=11
-0.275976640804656 -0.4503534795006
-0.0479923375592707 0.288618826066708
0.359805427067065 -0.083801568310631
-0.243601227506645 -0.25817956833579
-0.209714946302816 -0.118340813908817
-0.170330325770091 0.0188594304279657
-0.122896293426295 0.150424420176457
0.0529830855276932 0.279476136114661
0.144980041491593 0.162478866077673
0.216422316547776 0.0552454267859759
0.296320900735648 -0.0444276755936024
ID= USNM4805

LM=11
-0.31333081162926 -0.397632494237579
-0.0359640745912946 0.272041932505431
0.474430598025678 -0.0182603285169084
-0.264472285727612 -0.247286163701271
-0.21687775039174 -0.112193439780741
-0.176283428209928 0.027895786604821
-0.12507090480086 0.160531642958908
0.0231452015124505 0.206575403105808
0.102147802030721 0.101773910165182
0.20774830808728 -0.00376516859415307
0.324527345694565 0.0103189194905028
ID= USNM4928

LM=11
-0.284429371546581 -0.343044878780796
-0.0675775671869178 0.196356538422934
0.504702090279496 -0.0480729293897446

-0.285127746500516 -0.254825695392024
-0.253784357869864 -0.103761577008964
-0.211459995147615 0.0442380176634233
-0.131025456301112 0.15920150926747
0.0178705999469386 0.16672464675755
0.120728691264528 0.104440014111763
0.235453715197154 0.0611823199092379
0.354649397864489 0.0175620344391508
ID= YPM1820

LM=11
-0.0951237512219381 -0.425414453365177
-0.118237511514145 0.447023392184814
0.413690557029206 -0.266424748630747
-0.144560853310865 -0.231027537705409
-0.164975442648015 -0.084119191754762
-0.200423474881288 0.0596560996763993
-0.221706855789992 0.221144483652148
0.00582403968420436 0.239184486964136
0.0855055763384596 0.123793847578474
0.173615142006803 0.0104299235920649
0.266392574307571 -0.0942463021919405
ID= YPM1822

LM=11
-0.309684982978968 -0.348481350042473
-0.076365300941751 0.185148091721166
0.491000029781366 -0.0564555370455933
-0.277237925378655 -0.251536498878862
-0.248791354173036 -0.106179050958364
-0.19373173566699 0.0312935409447212
-0.135488012309708 0.159618903617285
0.0231446313938901 0.161624311061527
0.126154509114823 0.126591450966931
0.240321919768002 0.0778517141832878
0.360678221391027 0.0205244244303738
ID= YPM1830

LM=11
-0.215537423607663 -0.415526317020956
-0.0711045869022268 0.323276681834917
0.418795487280793 -0.123447557065099
-0.21981677875787 -0.248154173285948
-0.20723421784188 -0.104756464214964

-0.192205900364809 0.0395655254154664
-0.163413951370449 0.183121793864929
0.0386708926534533 0.234400884518291
0.108836075714851 0.12705416141455
0.204028521435511 0.0369871751522565
0.29898188176029 -0.0525217106134438
ID= YPM1831

LM=11
-0.321876228587731 -0.435730084606874
0.000751022341720281 0.230008087311996
0.394284734153887 -0.0194901496887924
-0.29413484045958 -0.251073000385861
-0.245401061397555 -0.104295193483988
-0.165034219198289 0.00967574218173906
-0.114297475187694 0.135392649921862
0.0324936250924588 0.221297073749445
0.134442521399896 0.145263972361685
0.234730624345461 0.0642959173600399
0.344041297497426 0.00465498527874787
ID= MOR3081

LM=11
-0.277484389337349 -0.400785735495151
-0.0342559784958406 0.195589529725486
0.400458260709648 -0.0697521178783661
-0.287313567554104 -0.255954117360607
-0.249959848421611 -0.105695493200164
-0.207310429713956 0.0364286526596582
-0.126133209184731 0.1347452750449
0.03050765423944 0.211257226117088
0.140993258161812 0.173757433147778
0.257735070629517 0.0905377139479331
0.352763178967175 -0.010128366708554
ID= MOR1167

LM=11
-0.169784484765748 -0.430705517064283
-0.0575135699642247 0.298171413904957
0.335718236681484 -0.162962158852871
-0.227700316509803 -0.260045357879121
-0.23556841208301 -0.113519404344871
-0.226733125530206 0.0401433171304903
-0.162138349258582 0.174652887979093

0.0581605149190794 0.274747839294218
0.154340537758731 0.165613745524256
0.235305618534965 0.0597100093299223
0.295913350217315 -0.0458067750217906
ID= ucmp136306 (image from Goodwin and Horner, 2014)

LM=11
-0.183003204753657 -0.423436382182104
-0.0898689184724642 0.38386334097955
0.402652440438788 -0.193636926356171
-0.154935939557259 -0.2505239565055
-0.180062938572832 -0.0959733734386305
-0.198557475217456 0.0470021040537639
-0.198706594268908 0.203658755343833
0.0326063346654183 0.24270809878718
0.100865984806263 0.13137409278347
0.186402420082172 0.0243840007219759
0.282607890849935 -0.0694197541873666
ID= MOR2938

LM=11
-0.12039779206016 -0.44717003557764
-0.111650742423119 0.450207164222027
0.401705830581274 -0.247388471672726
-0.141739345417789 -0.23910388289702
-0.163979311657608 -0.087304578885992
-0.183338994648429 0.0616833799089509
-0.199126517420192 0.215338438753943
0.018344845555339 0.251679926681392
0.0782434781982715 0.129978028056618
0.16356741683421 0.010615282482909
0.258371132458201 -0.0985352510724616
ID= MOR2971

LM=11
-0.37560385730379 -0.38357985996977
-0.00736285353939035 0.165872618404681
0.462897303620897 0.014011505701401
-0.316218482797509 -0.251150549782988
-0.283186546383583 -0.0921921697828035
-0.187796842281554 0.0162031299503886
-0.0918653839894047 0.0906846844775785
0.0294796334863957 0.145153188544805
0.132465772979773 0.137564831840922

0.255166355039824 0.109027536066853
0.382024901168341 0.0484050845489315
ID= MOR1122

Appendix 7.24. TPS landmark data for postorbital horn cores.

LM=13
0.31506087204339 -0.279169574971949
0.253376291813153 -0.298398041388381
-0.226094373474971 0.385750424713879
0.187335371087053 -0.232181825621717
0.1366996446547 -0.18144520934385
0.084404394463049 -0.12901181276063
0.0320944791262998 -0.0745025379496539
-0.0208964130675529 -0.0193282411428843
-0.0731771967709713 0.0397947690415432
-0.114166459693702 0.104109640924575
-0.158211220028324 0.164685960445358
-0.194383180581419 0.228658677736916
-0.222042209570704 0.291037770316794
ID= MOR1110

LM=13
0.349835059852834 -0.314471885516863
0.210189319001719 -0.290794988411315
-0.226389391946333 0.370301124173464
0.184853762249247 -0.226572004885099
0.139120245814797 -0.168923871292192
0.0889195309967597 -0.116117506932327
0.0356054898408285 -0.0648777625339787
-0.0168253970457384 -0.0105131474954989
-0.06550446796707 0.0469957176222761
-0.114194050089877 0.10323514753597
-0.161315879032752 0.161204532975155
-0.202178215086874 0.222953225891077
-0.22211600658754 0.287581418869331
ID= MOR1120

LM=13
0.427301614332573 -0.244584900455591
0.219012694749698 -0.274823636515632
-0.21586047903876 0.380949152414819
0.166967677272204 -0.245036021861109
0.112450234736304 -0.199864277086088
0.0574436477063221 -0.148800623630885
0.00292380647092162 -0.0907960328841899
-0.0456305631582591 -0.0242391328754124

-0.0790242173924813 0.0437558082961389
-0.114556552780555 0.106501591110116
-0.145777424726116 0.171352396230755
-0.180608151792459 0.233201638622378
-0.204642286379392 0.292384038634702
ID= MOR1199

LM=13
0.271504150193797 -0.365197172828189
0.180429359407 -0.315253018380341
-0.299979713742802 0.327684739040477
0.171619188215787 -0.23703028027436
0.156234330674873 -0.169087443554888
0.125716229299004 -0.0995646133140377
0.0839345026076142 -0.0321437083497879
0.0325758658704665 0.0295240591753582
-0.0242601295987774 0.0853906653687999
-0.0849754228285412 0.132139554644801
-0.144781514134656 0.173295044402154
-0.202835106290633 0.212688154208371
-0.265181739673132 0.257554019861643
ID= MOR1604

LM=13
0.331601179336219 -0.32468095940607
0.221817762807374 -0.28695970140196
-0.25001809982468 0.355992369953622
0.177046774690405 -0.232289339135189
0.133276972129937 -0.175340770634073
0.086169269017537 -0.119061468985227
0.0408444623730898 -0.0601891405181484
-0.0070469559289471 -0.00293842534321973
-0.0525887125704168 0.0562064834401213
-0.101172249585768 0.11222393198061
-0.14752059170232 0.16965644401601
-0.195232522023375 0.22455963350871
-0.237177288719055 0.282820942524813
ID= MOR2552

LM=13
0.383545696311482 -0.255506846590173
0.20829338382458 -0.305535803914372
-0.219789894518994 0.378122726481777
0.177833009469455 -0.23613447466437

0.130985459568999 -0.182133998508864
0.0774537633053304 -0.132980209044395
0.0230526126154259 -0.0790247878733996
-0.0273087847609123 -0.0202930942054217
-0.0763109838520012 0.0398402712880451
-0.117861846425343 0.103348537778765
-0.157855119995232 0.166232916733168
-0.187473969540759 0.231621373322532
-0.214563326002031 0.292443389196709
ID= MOR2569

LM=13
0.341095515462394 -0.299705310794112
0.222206361843966 -0.297804891328325
-0.230658405774202 0.371929729107365
0.18126581225723 -0.23110353777524
0.136348582945484 -0.17412110410886
0.0883354403911121 -0.118525173686081
0.0382432532329295 -0.0637606454232064
-0.0145295953851487 -0.0107298496730219
-0.0670065400629358 0.044060901830954
-0.116882534658718 0.101253669205182
-0.161945029323337 0.162115534909762
-0.196793338601651 0.226275796982321
-0.219679522327123 0.290114880753262
ID= MOR2574

LM=13
0.322040323142354 -0.301720052410249
0.228140063055669 -0.299767188610281
-0.249832041244965 0.367961132028933
0.180018007218312 -0.234475660792178
0.135063644630391 -0.177578668468613
0.092024092453258 -0.117665980957547
0.0419789078560767 -0.0627111128091597
-0.0092169322510 4609 -0.0077159482039 2813
-0.0599559088566776 0.048205637983 1687
-0.109233995906258 0.105075420849682
-0.153409982024048 0.165194598906143
-0.19323401427414 0.2261885730772
-0.224382163798928 0.289009249406828
ID= MOR2597

LM=13

0.300116197084051 -0.372318590773229
0.183291608344786 -0.301003870539713
-0.302515891166391 0.318279181793773
0.16924259747461 -0.233661053430896
0.146321678019309 -0.167069235246117
0.110892608821905 -0.102249482575489
0.0708910013074054 -0.0383984731544017
0.0240693912732435 0.0229267697442703
-0.0281745662363895 0.0795271172062136
-0.0828659816494362 0.132529496035785
-0.140853459416044 0.178357357813988
-0.197204793299154 0.220719006619312
-0.253210390557895 0.262361776506503
ID= MOR2923

LM=13
0.350635632894574 -0.243620695685123
0.276600959988447 -0.274726659805905
-0.184979154413904 0.404695918788297
0.18819091253762 -0.231955684317165
0.130172618961817 -0.19996811034734
0.0674369110500712 -0.154568422505674
0.00788590255346981 -0.0966280478498189
-0.0450034129824217 -0.0331909759312767
-0.0915223545003517 0.0314346884285311
-0.13738245821728 0.0976717403817722
-0.168879738381418 0.169106996608185
-0.189898902422743 0.23672996073463
-0.203256917067881 0.295019291500888
ID= MOR2951

LM=13
0.358949280032887 -0.269695634855891
0.240528679739769 -0.290648885671402
-0.205548131960955 0.385749483891378
0.182978433957108 -0.231664129845029
0.131067048787718 -0.183168047999914
0.077370414815837 -0.132875561155437
0.0231495579352421 -0.0798725130523138
-0.0308396536220535 -0.0238354352784514
-0.0806165552924595 0.0363368500818042
-0.128390035655994 0.0982125627772339
-0.165799632768805 0.165628211609122
-0.189470161169354 0.232877025909364

-0.213379244798939 0.292956073589535
ID= MOR2958

LM=13
0.316844632425073 -0.326231768581522
0.179314122001046 -0.320178943790718
-0.294431491432834 0.335275634312541
0.162343651771033 -0.240097169612309
0.14073759604369 -0.174175382197948
0.108490829866799 -0.108321793265013
0.0675695074283109 -0.0448284831312318
0.0217420742880057 0.0164810900623098
-0.0297330392910665 0.0747869263315674
-0.0863732255925046 0.124955720436427
-0.141165443770798 0.173853549074399
-0.195832581558443 0.220351626148312
-0.249506632178313 0.268128994213187
ID= MOR2979

LM=13
0.339479219463814 -0.285754027671126
0.230635011665163 -0.300230514974495
-0.22262611369213 0.377897292163033
0.187057467453203 -0.229192961748578
0.138571876922077 -0.174599076514
0.082061988135631 -0.128049028406165
0.0298586909901357 -0.0714307413688166
-0.0175345376128739 -0.0136729634526064
-0.0734182388694316 0.0387389426629299
-0.119721042622992 0.101653814109859
-0.159466742295401 0.165091616163685
-0.194807798407916 0.22859725696924
-0.220089781129279 0.290950392067039
ID= MOR2999

LM=13
0.254217939772006 -0.342114503504793
0.195792606313356 -0.325331379787217
-0.307513452496991 0.335120713771127
0.178607728837339 -0.240222987162937
0.156447051736807 -0.172827985224195
0.130878941316115 -0.0996377227994306
0.0799706505470095 -0.0350834775234065
0.0270019458608247 0.0249934776569528

-0.0342698216864445 0.0727900787584616
-0.090240171578814 0.120151011900956
-0.142430381543182 0.173179576177652
-0.19843074585424 0.219759985738573
-0.250032291223785 0.269223211998257
ID= MOR3027

LM=13
0.344058506438124 -0.325719391970222
0.222750789084488 -0.2805891810294
-0.227421652071937 0.368005645584426
0.187026312926357 -0.222410014667392
0.139863179223434 -0.166711681391599
0.0864327082176474 -0.118275390037429
0.0297777525271298 -0.0693219057372738
-0.0190736703715808 -0.010969207240048
-0.0688698181115353 0.0446271478594562
-0.117879320793428 0.101821572555498
-0.161081617270659 0.16327710079937
-0.19419994726477 0.227237070220168
-0.221383222533271 0.289028235054444
ID= MOR3045

LM=13
0.337049346203719 -0.354923548081431
0.192760298873718 -0.284534332616107
-0.261216679924728 0.345017045719593
0.176983306660468 -0.22792355871498
0.142205543738352 -0.164669997917279
0.0997985476767724 -0.104445855021961
0.0500071921718777 -0.0495293253661039
-0.0021056594461343 0.00281962598515407
-0.052336024237749 0.0572346539228132
-0.102170466224804 0.111242712166183
-0.15066511072605 0.165975239774273
-0.195089437388446 0.222738110807097
-0.235220857376996 0.280999229342748
ID= MOR3053

LM=13
0.375333152771564 -0.305905903600136
0.225402007555749 -0.272481958288779
-0.211116152280968 0.372836113562147
0.186746060658678 -0.21894805104085

0.128078147030663 -0.180923063975506
0.073102952428284 -0.131541397158653
0.0191588820220595 -0.0773486119250333
-0.0307083323802536 -0.0184362005823538
-0.0777302468189213 0.0420380205693937
-0.120095000952345 0.104343750733331
-0.158043628316019 0.167318366638448
-0.196616771017093 0.22859277236435
-0.213511070701396 0.290456162703642
ID= MOR3064

LM=13
0.2939034373593 -0.335876047133963
0.182950217032704 -0.324000339562675
-0.321568598872517 0.31084104233014
0.164093246220027 -0.243185293112228
0.140184221683435 -0.17694555835886
0.111653498451614 -0.109720902213035
0.076301375302968 -0.0423775177991827
0.0315893423736955 0.0243443844133497
-0.0237845439855463 0.0817220517698177
-0.0776272893929172 0.135275623287199
-0.133573856822934 0.188061107950631
-0.193757023600279 0.22909959189104
-0.250364025749549 0.262761856537767
ID= MOR981

LM=13
0.311871387057166 -0.278175941414466
0.179524579031847 -0.349538721925403
-0.292256253846616 0.342001656852708
0.159979356352825 -0.249205338368802
0.13788590154385 -0.183181014187889
0.108103366555705 -0.115905312171445
0.0687298916504142 -0.0505580043321101
0.0244753283965086 0.0130819085981254
-0.0250873529809772 0.0737911410180285
-0.0788591378125335 0.130920632630421
-0.137418450755478 0.180806785950835
-0.196433049718424 0.222085638552218
-0.260515565474288 0.263876568797779
ID= RTMP2002.57.7

LM=13

0.257717319549157 -0.367449031533349
0.197156795390568 -0.307048953278885
-0.282252302433269 0.343608589424502
0.194452341207613 -0.231857566675731
0.168154545720766 -0.159728647721201
0.125043366043546 -0.0920421529250865
0.0709699147032195 -0.0346973703869035
0.0151240008525215 0.0175750946917826
-0.0437099447134481 0.0641638224919271
-0.100784428668025 0.110725734789077
-0.152470540218359 0.163731417323495
-0.203419904823033 0.216791520044121
-0.245981162611258 0.276227543756253
ID= UCMP113697

LM=13
0.356126506551176 -0.262771001627146
0.267740339083819 -0.275570560805914
-0.172390398643075 0.399973297099213
0.190281314190002 -0.223446813848714
0.13406235909431 -0.185560716697279
0.075236696663577 -0.142499848255888
0.0149159661378002 -0.0941081114894953
-0.0446108576601242 -0.039540190173184
-0.103927407391887 0.0242802512833194
-0.145873767375399 0.0984259601465582
-0.17583643892203 0.169719301249469
-0.192406479202928 0.237666824082558
-0.203317832525241 0.293431609036502

ID= UCMP136306

LM=13
0.511918275824139 -0.330175915137793
0.16280516482957 -0.236447309252134
-0.160313075089153 0.348703569544417
0.16119783648266 -0.225213949700593
0.111921875134 -0.174607925232049
0.0645680907260949 -0.12023344749843
0.0117948934370237 -0.0722268551862925
-0.0471334554907415 -0.0213718373376562
-0.0980713392841651 0.0414720697225199
-0.140887170536977 0.104256526890018
-0.182633378829083 0.169794825633845

-0.197017495644891 0.236971428180053
-0.198150221558479 0.279078819374096
ID= UCMP154452

LM=13
0.297731119194928 -0.334872736785915
0.210062541019786 -0.305026087174522
-0.282356117162124 0.344158080629595
0.181152814206879 -0.2330904785821
0.144653499832244 -0.169967118077269
0.102480325146593 -0.108937622203852
0.0548487443556559 -0.0512629392926931
0.00679469840428129 0.00673328159267226
-0.0469459890767541 0.0591087467411472
-0.0941523894026613 0.116335431689657
-0.143752559333019 0.171317093618186
-0.191365578249527 0.226426256004962
-0.239151108936281 0.279078091840131
ID= AMNH5116

LM=13
0.355026040837511 -0.298833409339033
0.194408395474218 -0.307749816084052
-0.255354397307616 0.355470391121401
0.163395591111559 -0.240565735820088
0.136495247984938 -0.174517960595599
0.0910263687957753 -0.117162813120701
0.0453669005730135 -0.0583492570962635
-6.10301459738038e-05 0.0010014067075758
-0.0508329730738562 0.0561654368583321
-0.10278352945597 0.109435685844423
-0.150561686436397 0.166058703477265
-0.193787818868326 0.224677795823578
-0.232337109488876 0.284369572223161
ID= ANSP15192

LM=13
0.294075222458711 -0.335861920964037
0.183279252552322 -0.32449986836831
-0.319714594737259 0.312717669148835
0.169121160065977 -0.240658651994018
0.139310505532401 -0.176419064824721
0.107624696139633 -0.110581424444351
0.0734706534427297 -0.0439290628695094

0.0308029446872848 0.0223930741393395
-0.0214351314439729 0.0823285164605083
-0.0763537922198348 0.138381736383964
-0.136139452380955 0.185487702082124
-0.194022138323694 0.227408332487438
-0.250019325773342 0.263232962762738
ID= DMNHepv.48617

LM=13
0.288155571853564 -0.342944454331023
0.193726100715437 -0.311755083752398
-0.297980203263436 0.335584964791573
0.179931756688638 -0.235361786747064
0.14634280692649 -0.171036736079485
0.1107907516357 -0.106139290908179
0.0673915119161475 -0.0432072535346801
0.0168988070754293 0.014600183488825
-0.0353597415035074 0.0690749053886535
-0.0869294036415107 0.123530972277072
-0.141496638062765 0.174123470510889
-0.195928075474076 0.221405324575925
-0.245543244866111 0.272124784319891
ID= LACM59409

LM=13
0.257919593265899 -0.386314477849651
0.181721600940909 -0.312678080633468
-0.31746436736576 0.305961548211481
0.170048285838777 -0.236903367612774
0.154079341627112 -0.169622307942314
0.130900461900821 -0.0995073412085372
0.0944992948213591 -0.0269146281455765
0.0422877127042306 0.0400293977481729
-0.0188786827012476 0.098233812036196
-0.0840665924882201 0.140504849298913
-0.144410192524486 0.179261303994302
-0.203300059472765 0.215853774421829
-0.263336396546629 0.252095517681427
ID= USNM1201

LM=13
0.256136155737522 -0.353136369183957
0.203376769449385 -0.310925720997619
-0.281184699025169 0.347103071365795

0.196940133168839 -0.232718253725901
0.161590777487317 -0.164304089376502
0.121293589551745 -0.0979756697694774
0.0683267594787673 -0.0399715684993493
0.0139229150748035 0.0130191960775531
-0.0406114465782502 0.0655312482438991
-0.0964154170598742 0.115347210684949
-0.151537780310403 0.164661364430338
-0.205825546321046 0.215507590351947
-0.246012210653636 0.277861990398325
ID= USNM2100

LM=13
0.25005054793987 -0.370273628828815
0.166812492792182 -0.327064749310198
-0.325016667991222 0.310726781867693
0.173114123705218 -0.239226458563138
0.161903116666988 -0.171690084078258
0.135339917653774 -0.101631027567694
0.102146650930436 -0.0271718934677168
0.0475583252648047 0.0430116682229208
-0.0168956457128008 0.0994292289068913
-0.0821372935320168 0.141834024218337
-0.144068788407566 0.178640435029049
-0.20441752599192 0.212249220440834
-0.264389253317748 0.251166483130095
ID= USNM4928

LM=13
0.289516756431488 -0.337646104124752
0.183745791956283 -0.315136198482045
-0.284295015059873 0.345857531558672
0.183933031827805 -0.236005595282523
0.159523419434561 -0.16568739946879
0.115824585070759 -0.101472181236871
0.0666301420024697 -0.0424607342092827
0.0131447064322987 0.0117543867849516
-0.0413745479487502 0.0638926390087654
-0.0960249727036957 0.114298268691047
-0.148206141739134 0.166651604414888
-0.198233761601035 0.219952838601195
-0.244183994103177 0.276000943744745
ID= YPM1822

Appendix 7.25. Landmark data for squamosals.

LM=24
-0.310645646631906 -0.0831336609562579
-0.204855567677597 -0.141867389286381
0.0799879647766935 -0.0142493118136883
0.107623992180434 0.285846269783616
-0.250089145332549 -0.0884214993283235
-0.21547020207234 -0.117525097279658
-0.168483528489293 -0.151966672126408
-0.139970241149909 -0.159250097963742
-0.108453513919697 -0.153002021189437
-0.0807925095354263 -0.13490319032086
-0.0494917883212411 -0.130701520706912
-0.0154722561054085 -0.115852217000876
0.00967878855762592 -0.0903557883972024
0.0327382856970578 -0.0692061183520927
0.0612918193716017 -0.0475207727602653
0.0987217232960242 0.010962648700917
0.120317312867408 0.039608266531625
0.1287813425246 0.0725788465640736
0.143036292637554 0.102362623841954
0.151651252433097 0.134928895234544
0.152377545503561 0.167338783654147
0.155225628412153 0.200080993223815
0.158766128558202 0.231239411212317
0.143526322419355 0.253008618735096
ID=LACM 149538 L

LM=24
-0.29004514379306 -0.111213821440491
-0.196435449510034 -0.157609123282623
0.0611535640051715 -0.00225746866471458
0.154292215885257 0.282048556124076
-0.252955511076646 -0.117019572045786
-0.225583149502623 -0.134688821390756
-0.165445664795562 -0.162656148299712
-0.13569682878707 -0.15632181672328
-0.107959981523634 -0.143185227935611
-0.0785728973933524 -0.129630870031444
-0.0485772008653549 -0.119788105343123
-0.0276981447127048 -0.095711471373970 8
-0.00258330714449217 -0.0746623425128154

0.0212035987678788 -0.0548765638732393
0.0399660958735801 -0.02981454900399
0.0875857394317506 0.0184609407001278
0.106421486822511 0.0440814609938259
0.118598970967247 0.0738653565700666
0.135105633609487 0.10191157009605
0.149010723726833 0.130775087545038
0.166059651882226 0.159939922638095
0.163722663121961 0.193980792981869
0.165568156417664 0.225968316233403
0.162864778592965 0.258403898039005
ID=LACM 59049 R_

LM=24
-0.29272181369374 -0.0593100129409147
-0.208345181135516 -0.14434618810134
0.0761425294714963 -0.0149838043713521
0.124989366445744 0.291594428339101
-0.245355857696074 -0.0899705213845139
-0.221625245827397 -0.122608343959316
-0.170081326862333 -0.155467214691385
-0.140774811681209 -0.162234560764899
-0.106593137478487 -0.162452633789777
-0.0766808138095426 -0.144976988711739
-0.0458861241353907 -0.135608662261849
-0.0135050665931095 -0.117171357318812
0.00997966013711919 -0.0927496542756843
0.0377771037453247 -0.0740159083482432
0.0612929970838345 -0.044862773561029
0.0935815696412297 0.0150479720926308
0.106167225679671 0.0457431583928006
0.124529500758433 0.0731166372362507
0.13429597411113 0.104080838491914
0.139682832318882 0.136533910429443
0.150643940534526 0.167446035420875
0.15559258582256 0.198716488165558
0.157227625526901 0.229877208926105
0.149666467635949 0.258601946986176
ID=MOR 1110_L_

LM=24
-0.272448152945215 -0.0587899110542558
-0.216252196821102 -0.130699318576074
0.0767912727006227 -0.0132089827675461

0.110276020359712 0.298283567222456
-0.237699992727386 -0.0746575136506192
-0.210210314378677 -0.117834008904312
-0.185118142675832 -0.173160353702625
-0.143822128138801 -0.180762483818485
-0.11014476714596 -0.164250739169919
-0.0770873608623322 -0.155094385166296
-0.0452663218543745 -0.134538659333547
-0.0222704110751533 -0.11043018922197
0.00502364546500114 -0.092465542565807
0.0318742096815689 -0.0697484961508224
0.0531974041158135 -0.0424998851038926
0.100600753946941 0.00793975303897581
0.118946465719231 0.0407848750287032
0.128184907903041 0.0731117933581903
0.141399145613783 0.103424101812153
0.154938446655145 0.135484699040448
0.152839735183642 0.168461218625546
0.150792294683628 0.201812595341241
0.1549818268398 0.232887641723507
0.140473659756905 0.255950223994949
ID=MOR 1120 _L_

LM=24
-0.233789323150989 -0.123744387599752
-0.200956089288633 -0.195173353306509
0.0412399924805983 0.00361547139346508
0.177002828299958 0.288413162326747
-0.247388115635003 -0.0938347108224686
-0.206100816574796 -0.130918519136031
-0.1636989872672 -0.191346710986221
-0.131751888796232 -0.177200400320393
-0.113190364813859 -0.153971215098752
-0.0884726745172585 -0.132130128783424
-0.0654557503608451 -0.112938943842384
-0.0454050985084804 -0.0869614995648094
-0.0177637213349484 -0.06450892963837
0.00448327973376541 -0.0442524760745963
0.0239118854257263 -0.0227333843712501
0.0731632481569359 0.0313332400113924
0.0933407277883502 0.0513056512148141
0.108709945627387 0.0812942899538818
0.133161681887414 0.103684553170602
0.151798382910203 0.129282882477833

0.161523046501527 0.160564212723837
0.177550712778457 0.18898075410142
0.186921447066335 0.226982852612809
0.181165651591585 0.26425758955816
ID=MOR 1122_R_

LM=24
-0.27493962229433 -0.0779488620608103
-0.205623715997076 -0.148524420235757
0.066091352297691 -0.0070403160379422
0.136363691480902 0.286552582198214
-0.246185079344726 -0.09393449586043
-0.222065228757623 -0.125122717110466
-0.173985395859743 -0.17181635716317
-0.136879723881577 -0.175343530132692
-0.105447599572638 -0.159793965141203
-0.0733884839428354 -0.148157444915003
-0.0471539015167685 -0.125968740701697
-0.0236382923593082 -0.103750462866544
-0.000416619010864443 -0.0811380744415236
0.0192453065299821 -0.0552822162550246
0.0447098180187946 -0.0344905831039849
0.0878094958858017 0.0177436095186505
0.109770205501533 0.0427807429507588
0.119568021979817 0.0743378793764279
0.137078223433948 0.102560195806115
0.150522772182309 0.132568961398499
0.155272654179801 0.164992031931018
0.163343497672687 0.196689605216756
0.164617548889456 0.229523154252209
0.155331074484767 0.260563423377601
ID=MOR 1199_R_

LM=24
-0.259514288243996 -0.0839912448258301
-0.212282138294593 -0.147044283198639
0.0680587330962674 -0.017607150340116
0.138330897705655 0.300136471283062
-0.244241940808985 -0.0913139802621398
-0.218861547652828 -0.12404576086331
-0.175561056135656 -0.177395359828275
-0.141509885400175 -0.162209495110983
-0.111452851515407 -0.151561306002684
-0.0823655308591353 -0.136916627802841

-0.0546168783970525 -0.120232272935405
-0.0256384796939629 -0.105626758226729
0.0032985358797561 -0.0905852137398893
0.0343462085452446 -0.0736324375536368
0.0565944777883925 -0.0434215949377243
0.0948252699969462 0.0114598610721582
0.111266477897176 0.042032060308907
0.11966165756196 0.0736451206057612
0.132506639446502 0.104200305570352
0.142510533848072 0.135179224974667
0.150130100028967 0.166733224877069
0.156365386354832 0.198502718516887
0.159099885697698 0.230518370384786
0.15904979315432 0.263176128034555
ID=MOR 2569_R_

LM=24
-0.311845886751745 -0.0555799042945324
-0.185870572021409 -0.159269414344987
0.0648935619981325 -0.00667688228191976
0.132332912085223 0.282519589603347
-0.251136425121628 -0.103639691184649
-0.222029119215152 -0.126617166153512
-0.168277277655558 -0.172202998381265
-0.134547835940604 -0.166203706752361
-0.102129749572893 -0.160759095613538
-0.0696029254819294 -0.145534679038547
-0.0460466212958721 -0.121960929332105
-0.0237147413946804 -0.0995595470781858
0.00435996020838143 -0.0828592161123408
0.0267836836371964 -0.0596370082996048
0.0493486211847555 -0.0360948418943157
0.0853249076940795 0.0205317330596095
0.104864466767887 0.0469717159968764
0.124252619599676 0.0724982174832909
0.140552749880515 0.100698987929161
0.152061314165728 0.131446893473301
0.161032793044043 0.163140551993458
0.161304968700867 0.195577886527082
0.15802164327015 0.226887244642272
0.150066952214837 0.256322260053465
ID=MOR 2702 R_

LM=24

-0.2675254298977 -0.08898846313333
-0.215070180733248 -0.150647484360912
0.0765191343821273 -0.0220115681067443
0.123422748142161 0.296588921953363
-0.250051987811918 -0.0999217519087825
-0.228909085219776 -0.131149721378447
-0.171088882868467 -0.156268290535249
-0.141590166682806 -0.149234001258559
-0.1103914127258 -0.146740914537444
-0.0810923428949864 -0.135675509882342
-0.053648084706134 -0.118757842216226
-0.0238899829374652 -0.106111132860069
0.00501590074410936 -0.0892580476041793
0.0317465575907653 -0.0684297398468885
0.0535554277607618 -0.043302425981323
0.102349753294352 0.00766930443929524
0.117879164449338 0.0399832492866595
0.128528218645029 0.0711359003564531
0.140236341429571 0.102048062897784
0.147500311884592 0.1341181481492
0.1534811639509 0.166133203772899
0.157384755333889 0.198138347416941
0.15450188098185 0.229927891576831
0.151136197888855 0.260753863761071
ID=MOR 2924 L_

LM=24
-0.316727143510481 -0.07699478287441
-0.188542652871928 -0.15664574629386
0.0805994325810035 -0.0151307614691772
0.134258169404157 0.275174475103235
-0.256740017200602 -0.114249567890044
-0.228357860233802 -0.139301188481886
-0.165260557929165 -0.158807177935019
-0.136942538225615 -0.15002089026661
-0.10737451065328 -0.138756437589691
-0.0768217443963983 -0.130758515443841
-0.0478402050050896 -0.119156118615682
-0.0184481354032837 -0.104327154353651
0.00435210114885371 -0.0806279984763647
0.0293761820916865 -0.0612748001646604
0.0547095839879703 -0.0411313165563346
0.0917362216444009 0.0168603276256476
0.109621652223409 0.0443396595550443

0.134061052489711 0.0683266195846351
0.137718980873738 0.102302879922147
0.143085656904972 0.134710888997874
0.157434299080616 0.163851796349079
0.159904255494293 0.195342092907326
0.148711325004479 0.227138110301486
0.157486452500356 0.259135606064759
ID=MOR 2942_R_

LM=24
-0.302688497533326 -0.0365009044471119
-0.20369065879339 -0.153797610276051
0.0753017133158295 -0.0142549013404883
0.117867734202693 0.293320590731539
-0.244508698294756 -0.0929052161062737
-0.227304170319891 -0.127071928347824
-0.170380317874919 -0.158093379705958
-0.138998688341878 -0.155711813710142
-0.10804379638987 -0.16220692635623
-0.0706356484721184 -0.152122072670871
-0.0442124466223021 -0.128647673011928
-0.0183123789688691 -0.112692509380658
0.012457045433169 -0.0976766200891405
0.0414213585751933 -0.073266170326915
0.0618098567189899 -0.0426929012411999
0.0974955153064405 0.01210950199445
0.118900970805872 0.040297760448048
0.12914494255317 0.0730773321366349
0.135165460686714 0.104952881580482
0.145335258667808 0.136282947058858
0.154091252485766 0.167122492431785
0.153568172263491 0.197838923473513
0.14705469241207 0.227322901133975
0.139161328184111 0.255315296021507
ID=MOR 2951_L_

LM=24
-0.293039748012633 -0.0666749290682953
-0.204244507748666 -0.154675052069834
0.0735191325886649 -0.0148748232557531
0.135182754197894 0.290740208436936
-0.245605659547581 -0.0920027831435237
-0.217898517464174 -0.122525671095375
-0.169507440287269 -0.160436743993976

-0.139260735396339 -0.16954939429581
-0.103336618560432 -0.163553390215925
-0.0744343334195729 -0.143832564595485
-0.0466602777271775 -0.126880650580517
-0.0214080943248939 -0.105805158339288
0.00398501195160175 -0.085357751853197
0.0289054663798912 -0.0648279154090392
0.0540441631695328 -0.042395877552407
0.0940796458611376 0.0137153508225249
0.108067499099505 0.0438667499412821
0.119784913600053 0.0737035525875505
0.128003585258683 0.106153706738129
0.144873452642304 0.134745134477013
0.154488787059163 0.16494793146732
0.157436837156625 0.196863212197518
0.158369177320965 0.228740901527685
0.154655506202719 0.259915957272466
ID=MOR 2985_R_

LM=24
-0.329316866545172 -0.0532003529700688
-0.187796770391021 -0.155646128462416
0.0757085214975481 -0.0133744743576389
0.128194620078501 0.280508395436388
-0.254973672699163 -0.109161258897214
-0.22730937742884 -0.135294799645274
-0.165246674633354 -0.160347172645826
-0.137404922617566 -0.149534213774931
-0.106037350238694 -0.137688266997191
-0.0749394963025159 -0.139037107806722
-0.0414949129087043 -0.127314715971159
-0.0196176960969202 -0.101473506961672
0.00590127963729479 -0.0849056643494369
0.0426639529744748 -0.0779027297783244
0.0634155516897358 -0.041121592173879
0.101344337146065 0.0106114003790948
0.11718282035896 0.0421519041702913
0.126415667483603 0.0730516272407698
0.141562564122693 0.101960972992789
0.150881945216659 0.133294364418574
0.150499194283386 0.163916302134361
0.145036957157681 0.196048371110473
0.148856578786267 0.228939261695727
0.146473749429083 0.255519385213285

ID=MOR 2999 R_

LM=24
-0.280937393528505 -0.072703375319425
-0.21107204929855 -0.151370433515706
0.0746901748570616 -0.0139200408537378
0.128575399169017 0.29084186270737
-0.248310565133655 -0.0964321652760961
-0.224372192261002 -0.126458883467229
-0.170629486778485 -0.165043611817385
-0.138656953767521 -0.162615196854066
-0.106168475128876 -0.157165914331629
-0.0771270884364022 -0.140111861394194
-0.0492438152115953 -0.123934919354934
-0.0214656216397407 -0.106490837272858
0.00575547347227402 -0.0864720634728313
0.0271254462158314 -0.0618318043187106
0.0514982353982334 -0.0401247776509115
0.0933357376850484 0.0146352707039335
0.111115855496792 0.0428055233597405
0.127674845967385 0.0713118440022984
0.141187181778526 0.101670464502586
0.151770437396471 0.133191669768524
0.15535047841644 0.165536092342916
0.156483006801299 0.197645360764957
0.155702513644125 0.229029081601025
0.147718854885827 0.258008715146363
ID=MOR 3027_L_

LM=24
-0.298552724990538 -0.053339952926464
-0.203828146769928 -0.156777658305834
0.0698203552647972 -0.0142165143871998
0.125372967505755 0.288310924164717
-0.242094000201806 -0.0897870301814417
-0.220045620513685 -0.124077186974185
-0.170023178902464 -0.167379646654638
-0.138173287504083 -0.16251035087537
-0.105892748401143 -0.163028041438674
-0.0701484093967747 -0.151299061435515
-0.045122631793708 -0.12862995301495
-0.016391343354597 -0.115372785309342
0.0170748280114541 -0.0925309383996676

0.0249346129505719 -0.0591258609605289
0.0416781673256587 -0.0300858581458437
0.0928067585567568 0.0147825823341473
0.109867478767755 0.0435383860195852
0.122077639679806 0.0737976943006855
0.137822171610072 0.102578980563908
0.147047194174753 0.133581289829915
0.147784507345293 0.166804935614739
0.160867894955948 0.197151953189759
0.160592201227802 0.228908602417568
0.152525314451965 0.258705490574629
ID=MOR 3045_R_

LM=24
-0.271675241160417 -0.127672267224606
-0.18736505657211 -0.183131836903674
0.0447350497883546 0.00221757339799
0.161515149965667 0.276402313685897
-0.248670138568221 -0.117248548734925
-0.222926903597858 -0.133591058647161
-0.158083250334248 -0.181038741960633
-0.134530033502896 -0.161298510717802
-0.107630001034996 -0.148318229789899
-0.0877120425988067 -0.12410310659828
-0.0598313072498853 -0.106239655492715
-0.0380362025407615 -0.0867413368133277
-0.014219435794424 -0.0617432384864254
0.0116417984642508 -0.0460405768626747
0.0262311363368882 -0.0225498730789467
0.0752620567271151 0.0289686402831919
0.0946781431156184 0.054142494673292
0.117588523718016 0.0761319859577131
0.137411552984659 0.0994291934370142
0.1534095957333 0.126939578340901
0.16974504858362 0.155238550723248
0.180170888202804 0.189602449332671
0.181740888098902 0.225840961034911
0.17654978123543 0.26480324044424
ID=MPM VP6841_R_

LM=24
-0.285544959609424 -0.0902010923670226
-0.213224658237432 -0.136183490154004
0.076723732618634 -0.0136402566573628

0.130650139753423 0.291192722324755
-0.251763268413419 -0.0944695625721124
-0.220503559390838 -0.120546543620688
-0.169378780812479 -0.155615568043713
-0.140323942210375 -0.161455513321752
-0.108226054619284 -0.155786517573917
-0.077872649689466 -0.143384081544484
-0.0457752391086277 -0.132015349960336
-0.0177136148834234 -0.109279346456659
0.00291020651930108 -0.0841628776145705
0.0297384784032447 -0.0661648229630187
0.0533378408181212 -0.0416548540929565
0.0958275427698002 0.0128918119748521
0.11291714932157 0.0419991361569974
0.127856016616425 0.0714440847484025
0.141657707887735 0.101835708652138
0.14975671203909 0.133922436426453
0.152905185847245 0.166125094623322
0.156101788167647 0.198058964768425
0.153913772203231 0.228919551453114
0.146030454009301 0.258170365814136
ID=UCMP 113697_R_

LM=24
-0.294252354657734 -0.0540313259741865
-0.21217446437225 -0.135395408715412
0.0839161465419084 -0.0255595266873635
0.101006493742373 0.289745350523299
-0.242469249909913 -0.0854371653302385
-0.221725538432843 -0.122411572341099
-0.170043665680327 -0.153892440322783
-0.142606034126279 -0.1631942147664
-0.105640404190597 -0.165951223062733
-0.0789495389672559 -0.140073093946273
-0.0520902861724286 -0.129566429877483
-0.0151413346677468 -0.126266023008913
0.0181876715652099 -0.0964871484209046
0.0338345482140473 -0.0687981221784873
0.061100928099579 -0.0524376806368387
0.0965714054975911 0.0142739922452762
0.119765587496169 0.0380925964082204
0.136064926499058 0.0718945197062114
0.138268526146463 0.105276673080204
0.151823014140735 0.136098813026043

0.148263832042325 0.167578425430297
0.144288137520192 0.202291152747994
0.153160289270391 0.234398792008316
0.148841364401334 0.259851060093253
ID=UCMP 136306 L_

LM=24
-0.314716914963073 -0.0842043055840042
-0.188882671831267 -0.153565140029904
0.0765176662985254 -0.0172690917997695
0.148886815129917 0.285119803997924
-0.247513691931569 -0.101883897937664
-0.223393372038353 -0.130040906140698
-0.163472910079848 -0.155615656320152
-0.136597987147437 -0.172038130945826
-0.0952920825655194 -0.165769281029262
-0.0723518676774061 -0.136618266891844
-0.0572856894851923 -0.105793370814093
-0.022324591236969 -0.103084959655311
0.0156307964610209 -0.0925245779661152
0.0212110291647412 -0.057051047290091
0.0413365005380868 -0.0263570847153499
0.0831806465396701 0.0179299506361284
0.0968912253346972 0.0528729057274483
0.12638443138689 0.0696883134401671
0.130436744328761 0.101021146981598
0.130485545457163 0.139673086803709
0.158928948342742 0.160056893700412
0.172453655401681 0.192752166719777
0.164576036889442 0.226331042539571
0.154911737683296 0.256370406573348
ID=UCMP 154452_R_

LM=24
-0.280914187651885 -0.0863501060367587
-0.209035764442053 -0.152833702851424
0.069353754312355 -0.0124872364388625
0.132861214581121 0.296008195674719
-0.250169374643991 -0.099317313347693
-0.22399414332135 -0.127374958318357
-0.169181108983437 -0.158171206422676
-0.138824493993666 -0.15803868238956
-0.109467604590759 -0.147433758211452
-0.079540203465 -0.135709763923344

-0.0486568129428411 -0.125328056305135
-0.0232282040460568 -0.103885380534458
0.00391954071229678 -0.0859015609501388
0.0299396101132103 -0.0658146633407675
0.053356375534603 -0.040889109853535
0.096015837461807 2 0.00969892012901862
0.11949286714887 0.0370172427967782
0.131198889524092 0.0702945155096362
0.1362834595876 0.102256630498235
0.14375647842524 0.133745867111627
0.149110168746538 0.165826540504081
0.156726818985738 0.197189874552017
0.158960519407499 0.228538497008449
0.152036363541211 0.25895921513962
ID=MOR 8693_R_

LM=24
-0.283196472868668 -0.145678425849946
-0.189625113183197 -0.162135499863103
0.0589552335237114 -0.00218993749375063
0.164361357298631 0.278956859794752
-0.251998408347882 -0.143106706045501
-0.227079227857441 -0.153986019888288
-0.166210948267674 -0.157649630935758
-0.143465553435635 -0.142158420501053
-0.114049307710862 -0.127991446426162
-0.0849391212450273 -0.1151172767781
-0.0579189187894446 -0.101897439303663
-0.0329141061942006 -0.0865018831053634
-0.00934874134846966 -0.0659748876589848
0.0153327072925055 -0.0469952922883664
0.0371928169508116 -0.0256104187610714
0.0832533671654005 0.0219375859507932
0.104275923241803 0.0457608759222816
0.123387070159957 0.0707771871045025
0.139120356330139 0.0987535170910329
0.153980915485977 0.127691925590809
0.163505222799635 0.15927515675101
0.168923671550297 0.191086222659278
0.176277880154285 0.223748998806441
0.172179397295349 0.259004955228211
ID= AMNH FARB 5116_R

LM=24

-0.255700158143955 -0.127041089433666
-0.193544630501058 -0.182331950305687
0.0496488567208239 0.00134999641353615
0.1838562412974 0.277160744893768
-0.251981177293839 -0.117269067619166
-0.228152713069585 -0.14058357192988
-0.161984392182005 -0.175561472662856
-0.131544768605664 -0.167136079842114
-0.108046375043735 -0.147948544834871
-0.0826701837341974 -0.130188366917774
-0.0611165935139056 -0.106238342242061
-0.0331173578322006 -0.0885865657785262
-0.0119675045342501 -0.0679133974177739
0.0080523412422135 -0.0464374252913586
0.0271062327976253 -0.0185298936229572
0.0728822286561331 0.028973505143822
0.0914627799366414 0.0549945292783131
0.10979811952464 0.0805770417494321
0.126301692745845 0.10800222040024
0.143964656638321 0.133742497693883
0.155523147913911 0.163018343990514
0.170882800775955 0.188721437727841
0.188149652540849 0.218628524392151
0.192197103664036 0.26059692621519
ID= ANSP15192_R

LM=24
-0.246882062276677 -0.112905936272019
-0.192213955926661 -0.190370639958576
0.0461593658829024 -0.000874296447852934
0.162248249547713 0.279881417256416
-0.249150517636205 -0.109290085034741
-0.222614429699412 -0.135907905365692
-0.159585144710336 -0.190749185060857
-0.13135547316078 -0.170852367736499
-0.114321099745063 -0.148142084651186
-0.0890143054577963 -0.127078942411054
-0.0660027653378388 -0.106306349160223
-0.0414776827468045 -0.0833974947688216
-0.0142265403593109 -0.0629949238562375
0.00971750824195102 -0.0443434201950827
0.0302147946308608 -0.0242607719959154
0.0805581924331439 0.0225379926565052
0.0922606543639287 0.0502675159321991

0.111901446582456 0.0789876590139313
0.132173682137629 0.104954765540497
0.155393901567517 0.125891947718401
0.169948625008535 0.158639866492961
0.173449502167188 0.191725550492195
0.185562842771303 0.225791705199271
0.177255211721758 0.26879598261238
ID= MOR 3081_L

LM=24
-0.253186934194833 -0.111502242523671
-0.195890898900651 -0.18573711276227
0.0513932654166661 0.00279946567258684
0.176164500060475 0.280500655060004
-0.249509241336221 -0.109664045313018
-0.231745242267643 -0.141727661739296
-0.161450120464603 -0.17752784069821
-0.13265396207728 -0.166686110039698
-0.103849524567671 -0.154346419525976
-0.0806651110422595 -0.133984273808643
-0.0601494436683304 -0.110769663023563
-0.0358647957151104 -0.0885637067431931
-0.0135013653691906 -0.0684731243751227
0.00520955940221751 -0.043245207457068
0.0295220870908097 -0.0189233892097526
0.0741992243186995 0.0281764409861679
0.0941506008143009 0.0537528820053291
0.114802399803164 0.0781440519713098
0.134162832528102 0.102176482199738
0.148208424187446 0.130821672564447
0.162413642856345 0.15978740823265
0.171018537740523 0.191548532364058
0.179326560261436 0.224595318052549
0.17789500512361 0.258847888110643
ID= SMMP97.6.1_L

LM=24
-0.291516682651787 -0.0702848427013592
-0.208721275413592 -0.144228025904102
0.0752972278798989 -0.0153275421860658
0.123555532490927 0.294550754645298
-0.245973575649366 -0.0886969246708725
-0.218789884072916 -0.121527931430215
-0.17142465172678 -0.161617496415832

-0.140058794532616 -0.163493992482264
-0.107845788421663 -0.156722882401184
-0.0773235675523265 -0.143255329898038
-0.0480281211716724 -0.128553745728157
-0.019310631253085 -0.111394725758943
0.0084104961045028 -0.0914408755555372
0.0330091408062947 -0.0688283344931769
0.0576408521024922 -0.0443097794435862
0.096774781937476 0.0122034394911369
0.113328839554409 0.0418999014938021
0.128533151593685 0.0713551107316883
0.140771648124312 0.102574913381036
0.145512421990341 0.134836760099775
0.150777545315483 0.167069038730111
0.156438413228406 0.198588915504442
0.153910629709813 0.229140222090341
0.145032291607764 0.257463372901703
ID= USNM1201_L

LM=24
-0.298494317699637 -0.0979937230302869
-0.207793497736578 -0.13716553278821
0.0745947964318223 -0.0125204929933051
0.12831182459081 0.284712509805449
-0.255346273446922 -0.109922029632069
-0.222087837596982 -0.121445235012527
-0.167332317385103 -0.148827069462013
-0.138258640024354 -0.14957210276722
-0.10813284594434 -0.150445590198098
-0.0791595882447608 -0.136063260562061
-0.0477446570336127 -0.127169931530134
-0.0204288338471929 -0.106852548548161
0.00589491390809956 -0.0873920480412775
0.0324592522634409 -0.0670963698610884
0.0540333181132388 -0.0407004879770617
0.098055419999891 0.0107183793749553
0.115589096336863 0.040623500714168
0.130208741274449 0.0702502846221188
0.144024205964051 0.100794644626012
0.151850395714293 0.13338340518861
0.149840577849461 0.165109541837427
0.151053546759537 0.198617940578619
0.156979409848102 0.22982470601276
0.151883309905424 0.259131509643393

ID= USNM2100_R

LM=24
-0.337985343911202 -0.095247606120045
-0.17652252954462 -0.156191960273869
0.0677859068370924 -0.00874585773214841
0.146350918696639 0.278618313436169
-0.249997296004221 -0.114129856125558
-0.223353522785389 -0.13464982148022
-0.165371138353289 -0.151449975419643
-0.133716577741291 -0.148484335533086
-0.103449791215373 -0.147099265875991
-0.0726969907326016 -0.13833803657764
-0.0473764061693381 -0.118213529274986
-0.0247266681596414 -0.0958798786531059
0.00163368212762554 -0.0769202983397543
0.0269511183674619 -0.0583627655494733
0.0483938615305745 -0.034632996470087
0.0917378705290235 0.015842155368975 9
0.111083085489554 0.0422562552734757
0.127056724694501 0.0707079085366443
0.131660538571155 0.10319239021973
0.148800105728058 0.13130279262612
0.157095743453884 0.162155319227917
0.16469314930547 0.193663052351792
0.160447385648854 0.225240829963108
0.151506173637072 0.255367166421675
ID= USNM2412_R

LM=24
-0.295774108289585 -0.0836315451195929
-0.194628660970363 -0.164162929902767
0.06295231066958 -0.0100350858870513
0.133693449733522 0.285014764485996
-0.250399492150633 -0.104411010636534
-0.221692896672672 -0.127637059752059
-0.166724123043026 -0.170223378802254
-0.134323012716702 -0.164287029856393
-0.105505321134347 -0.150777235127573
-0.0784855623780199 -0.133429948697324
-0.0515689047100417 -0.116429318779548
-0.0247653984623326 -0.0989434930594244
-0.000180908199504669 -0.0783505141091278
0.0219452227177639 -0.0559029730159908

0.042866410571507 -0.0313332949275941
0.0901056068054122 0.0164108021239924
0.111411632356704 0.0415388494662559
0.128273071425307 0.0698504561674814
0.141466206465118 0.100176013280072
0.150969491897433 0.131549304782613
0.157944994638155 0.163219317549684
0.16326236958798 0.195230873427469
0.164713182437078 0.227965634876765
0.154444439421668 0.258598801512904
ID= USNM4928

LM=24
-0.268277547436509 -0.0778466100284033
-0.202253922162901 -0.169873812479347
0.059793124349505 -0.00662942999030617
0.140303661217782 0.291330184638067
-0.242428394192552 -0.0966262494508106
-0.224907561221213 -0.130439064826666
-0.169736706265678 -0.178783055644216
-0.133589673746783 -0.173154645388554
-0.107021718028473 -0.153841988406509
-0.0790538308749997 -0.137579557410546
-0.0520916777082283 -0.120345545110048
-0.0285023240702395 -0.0988911840690054
-0.0055933271089752 -0.0756354360512408
0.0189634716259181 -0.0551389677421044
0.0399904385568743 -0.03139548398847
0.0851748270908484 0.0190524319503801
0.104780874918833 0.0451905130050385
0.124342155890497 0.0709573240508613
0.139108637099575 0.100391985441537
0.149990402295604 0.131478063366885
0.157770388487927 0.163142513040242
0.166312367572399 0.194751679757526
0.169891389375752 0.229227829485976
0.157034944335036 0.260658505849715
ID= YPM1821 L

LM=24
-0.291385107997398 -0.0565796565040677
-0.217622910484368 -0.134352757783285
0.0823409195814348 -0.0208140958977246
0.109266825827362 0.304481542352095

-0.24433585368861 -0.087313685503379
-0.223890014150701 -0.123359024130781
-0.169889779673521 -0.151684642443504
-0.142516199371488 -0.162041216308546
-0.108535865465987 -0.159042804107875
-0.0792935039461955 -0.141092830174874
-0.0506271478170082 -0.129444219648339
-0.0187531019020474 -0.119551367404611
0.0148579827713634 -0.100315630647282
0.0399861005313235 -0.0735625799876915
0.0628190113764812 -0.0478259395148862
0.10918681012422 0.00383970500198863
0.127348065029097 0.0398859236568444
0.132818317888494 0.0723840710758221
0.149088832527557 0.102791692307427
0.149065116148072 0.136807539309495
0.148190081990012 0.168991382822629
0.15106620958894 0.200712553466604
0.14563367005946 0.225338322551311
0.125181541053508 0.251747717512627
ID= YPM1822_R

LM=24
-0.296163859767964 -0.0730788107749522
-0.204664039716372 -0.145733286861623
0.0780186886717922 -0.0158126493831347
0.115438554228901 0.293065788989929
-0.252266833471944 -0.0995886641098327
-0.222099387640835 -0.123220825133532
-0.169987969550961 -0.160827817372411
-0.138733935353155 -0.16136344763432
-0.109899895774076 -0.147205261857794
-0.078744654420831 -0.13817217121718
-0.0489978507979371 -0.123416800204284
-0.0250473729659311 -0.10097201203835
0.00526722830888115 -0.089653534801468
0.035453426901452 -0.0705133459245424
0.0562447637299837 -0.0421465545176885
0.10254541040192 0.00776826912350933
0.120385992861402 0.0389477424308866
0.134873579165862 0.0696340502918696
0.145432027518997 0.101560947381328
0.154302121082389 0.133743182874097
0.157774322021971 0.166456651585105

0.152433084146269 0.197179089538943
0.147996694603956 0.228175526356898
0.140439905816229 0.255173933258548
ID= YPM1823_R

LM=24
-0.236803733419771 -0.184359122390093
-0.193719304539087 -0.187564074495307
0.04506708504777 0.00690590453869932
0.199065143380678 0.274679474466003
-0.225198946391841 -0.125318194998958
-0.236747521155386 -0.145400509937076
-0.163206495417616 -0.176827033935797
-0.13825595272788 -0.16443969097024
-0.122880567649211 -0.140274840550077
-0.0939243110276995 -0.119793579042385
-0.0736682531683147 -0.100779618157059
-0.051354664757375 -0.0763176428504123
-0.0255265127258332 -0.0536356514841973
-0.00113791984379774 -0.0304430891619572
0.0254479300179587 -0.0094991092966176
0.0709194279258596 0.0335164633104855
0.0922766945882365 0.057385431752755
0.112334944253706 0.0809773439166006
0.130407007916494 0.106795716007371
0.148556327041789 0.132644820233686
0.164614592271236 0.159542347009288
0.179528914125986 0.187373681763111
0.193853900273373 0.219034742582163
0.200352215980728 0.255796231690014
ID= YPM1831 R

LM=24
-0.2997916015566 -0.0956633468257914
-0.201594439941626 -0.143401947600019
0.0700155324631042 -0.0154468156672123
0.130252245634977 0.289386074507756
-0.254270110729615 -0.109963984863343
-0.223170032402214 -0.126987823047375
-0.166933143886568 -0.152171519766773
-0.137551057416402 -0.151257585095072
-0.107275252755387 -0.149401944175838
-0.079235298783089 -0.133834587551708
-0.0505797205924586 -0.119702766973686

-0.0213168558295677 -0.105633603903566
0.00570269153138411 -0.0859200590297468
0.0299871895459558 -0.0637122679467987
0.0508937984844621 -0.0383015594581755
0.0961336664718658 0.0119368225073106
0.115053607006291 0.0402423735667128
0.131823933346583 0.0696008711648538
0.141153984527458 0.101794101580229
0.147818181066094 0.133696562723616
0.161477119672128 0.16359466982027
0.165016962629537 0.197654310020524
0.150082393948985 0.225637723469527
0.146306207564704 0.257856302544304
ID= MOR 004_R

LM=24
-0.277830896113084 -0.111614983715877
-0.205728002339263 -0.151369604980676
0.0701801705394234 -0.013920745160008
0.138286812922227 0.292067623175323
-0.253135888132206 -0.107241845737325
-0.222729845720249 -0.126563113355319
-0.168930729633939 -0.159871699150084
-0.139576821309128 -0.153669774138788
-0.109611041372901 -0.146095208739337
-0.081070852491693 9 -0.132232474052982
-0.052663069816113 4 -0.118022793679829
-0.026081135743717 -0.0999478810061988
-0.000346122703202765 -0.0801850903718728
0.0234141035835655 -0.0588213235031691
0.0460429040070514 -0.0355916492117113
0.0935569368174577 0.012955767098451
0.110617641021785 0.0418322985640989
0.12627617799603 0.0705437093191188
0.140447212113609 0.100236352810047
0.152787534162395 0.131061965091205
0.158812566123692 0.16345155835806
0.162755214760544 0.195869920174629
0.160993633856978 0.228097091313076
0.153533497470739 0.259031900899169
ID=DMNH epv1018_R

LM=24
-0.304593005772676 -0.1308045646155

-0.184023254320154 -0.159215993088177
0.0630673547864819 -0.00721429707575422
0.137545604361247 0.276336245837494
-0.249425977122804 -0.125144507379876
-0.225939439365342 -0.138605679274396
-0.164776634459723 -0.162714618808685
-0.140720312997726 -0.146429394702683
-0.110111874582634 -0.135040030176524
-0.0818043855670934 -0.123495297875555
-0.056775265590396 9 -0.108124200984629
-0.033030379350412 -0.0867386869780812
-0.0054729093267476 -0.0688110144869811
0.0180486910681262 -0.0503452624532921
0.0396295654746747 -0.0267452182646594
0.0880431747643218 0.0181404140345024
0.107635917075436 0.0440341491565976
0.128105130045452 0.0686912894340938
0.144766331176695 0.097020772559797
0.158985038624814 0.127086370993654
0.169002055817336 0.158881371987076
0.176988675221151 0.193780783606844
0.169668296132245 0.228486806692698
0.155187603907728 0.256970561862037
ID=DMNHepv48617_R

Appendix 7.26. TPS landmark data for parietals.

LM=4
-0.549608548173721 0.156228998638078
0.0472865001003224 0.323874559695535
0.517263200656481 0.0648061985871996
-0.0149411525830829 -0.544909756920813
ID= AMNH FARB 5116

LM=4
-0.521105411559113 0.125482300167359
0.017424465432821 0.322802999371989
0.565158431113634 0.0840322673386385
-0.0614774849873424 -0.532317566877986
ID= MOR 1110

LM=4
-0.442426435660848 0.207692522097316
0.0115973632304767 0.315254067780509
0.471566769913847 0.141294614872178
-0.0407376974834756 -0.664241204750003
ID= MOR 1199

LM=4
-0.454474782747541 0.180118552171834
0.0312733452234496 0.353276193211203
0.462315106162117 0.117544410547343
-0.0391136686380257 -0.65093915593038
ID= MOR 2569

LM=4
-0.493076198766151 0.193897237609203
0.0196412906813706 0.286890126061141
0.510109154577864 0.123820435206326
-0.036674246493084 -0.604607798876669
ID= MOR 2999

LM=4
-0.521042556076109 0.182551310531457
0.0343417734520436 0.310367816555578
0.502417383767499 0.0888948184228066
-0.0157166011434335 -0.581813945509842
ID= MOR 3027

LM=4
-0.518532502461989 0.186623515845445
0.0197634027597265 0.304721071444089
0.513332025573389 0.0859631726885644
-0.0145629258711263 -0.577307759978098
ID= MOR 3029

LM=4
-0.552632931584803 0.149390481613056
0.00192670889346551 0.313595832951596
0.56900597042806 0.0443859276252103
-0.0182997477367222 -0.507372242189863
ID= UCMP136306 (from Goodwin and Horner, 2014)

LM=4
-0.520122834865488 0.162764876533881
0.0482918030282582 0.32609592595589
0.500354451715792 0.0908159967520861
-0.0285234198785621 -0.579676799241858
ID= MOR 2951

LM=4
-0.550382788598035 0.159922297166415
0.0587597770614486 0.277566145113959
0.532779613600374 0.108687480188064
-0.0411566020637881 -0.546175922468437
ID= MOR 004

LM=4
-0.582954627758614 0.11085833324903
0.0235895183540203 0.321889588264671
0.592322160920826 0.0316999310595729
-0.0329570515162331 -0.464447852573274
ID= MOR1122

LM=4
-0.527554535403903 0.128582501357696
0.0293231795207941 0.363470017936744
0.528949965667025 0.0502185282880361
-0.0307186097839164 -0.542271047582476
ID= MOR1120

Appendix 7.27. TPS landmark data for nasals.

LM=8
-0.225946682500294 -0.260572080577546
0.556786436603206 0.0587553246130142
-0.352238513726738 -0.170172943485302
-0.3756709444237 0.155085964062874
-0.165230385769767 -0.0966746854762472
-0.0101151087357413 0.0362714480323697
0.184647820079852 0.114111624141657
0.387767378473181 0.163195348689181
ID= MOR 3027_left

LM=8
-0.260003094081715 -0.274271673334426
0.572455738409264 0.0536536101939981
-0.348685665894769 -0.14828458440143
-0.326011917902058 0.103277300199627
-0.187196056235678 -0.083914527021154
-0.016700057551153 0.0423200285809283
0.177303947307455 0.1306967859609
0.388837105948652 0.176523059821556
ID= MOR1110nasal_left

LM=8
-0.254027574565381 -0.269895364439097
0.582828350753981 0.0324416230408607
-0.331359058353519 -0.126038184729274
-0.364296450751423 0.0775830298629765
-0.180339588011168 -0.0882349273652748
-0.0214332964945018 0.0548811615349249
0.175913634344295 0.152762741117169
0.392713983077716 0.166499920977715
ID= MOR1120nasal_left

LM=8
-0.268817121020601 -0.362710914915737
0.497680814622416 0.114596697666867
-0.383590352872182 -0.330648124365433
-0.0898987708366793 0.338817627447058
-0.198038867291 -0.116245417945097
-0.0617410556943402 0.0494870825457032
0.142954387458539 0.145909214982552

0.361450965633848 0.160793834584087
ID= MOR1122nasal_left

LM=8
-0.23456874758876 -0.246172181913936
0.555939760116449 0.0796917273535586
-0.392836400689317 -0.268756336131894
-0.244462893962669 0.177565605563138
-0.209403223808622 -0.0707253239148034
-0.0259092016153756 0.0498516816088667
0.173823196272986 0.116634626184311
0.377417511275307 0.161910201250758
ID= MOR1604nasal_left

LM=8
-0.249013072099317 -0.234219067369396
0.577230966191236 0.06584328803366
-0.355908338226146 -0.197394150395858
-0.330006774235286 0.11722441376974
-0.197895716295624 -0.0690527278312411
-0.0128104816370145 0.03846760494019
0.182580756909617 0.116762219967846
0.385822659392535 0.162368418885059
ID= MOR2574nasal_right

LM=8
-0.258934840059057 -0.230731546921146
0.567979757103118 0.0631002631213217
-0.347783856432544 -0.211885023924494
-0.330489236078654 0.129420147310958
-0.195799380586874 -0.0686230288052675
-0.00773780764263095 0.0304178529127188
0.183997134712066 0.119516882726935
0.388768228984576 0.168784453578975
ID= MOR2999

LM=8
-0.253582313808892 -0.369768237330807
0.555413511688416 0.0710080017826588
-0.365918664937676 -0.136695414143142
-0.237833461203607 0.173044111305815
-0.1727905131596 -0.111215860796975

-0.0470409283152608 0.0530611883619763

0.151941194970511 0.155447714993945
0.369811174766108 0.165118495826528
ID= MOR3005nasal_left

LM=8
-0.237052152501941 -0.388276916705399
0.546633677582101 0.0446859670771663
-0.330939751844968 -0.144144812423202
-0.255207026291037 0.193921058164023
-0.195225573771818 -0.103536906020613
-0.0524549858698044 0.0588594357317484
0.149955814387236 0.159878344132393
0.374289998310231 0.178613830043884
ID= AMNH FARB 5116

LM=8
-0.285598236071756 -0.345813464635284
0.557188409896736 0.0767684317032628
-0.337070689897957 -0.160910692497685
-0.240910041408004 0.174875497111395
-0.184365261277333 -0.104246071732506
-0.0394244542422395 0.0471404373717326
0.158079140891482 0.134623803468932
0.372101132109071 0.177562059210153
ID= DMNHepv. 48617

LM=8
-0.269784652064947 -0.315039240011654
0.567473417771883 0.0909632344883946
-0.335654886442692 -0.151869331761286
-0.291523266728276 0.161234088115157
-0.190111704323243 -0.0940991107962502
-0.0259815124544422 0.0356889052454532
0.17111882039486 0.109405660090859
0.374463783846857 0.163715794629326
ID= USNM4928_nasal

LM=8
-0.203933425486177 -0.369426018540952
0.528183945599287 0.0659101377645775
-0.401513296078665 -0.191022727419232
-0.232686155250854 0.24091692224434
-0.157621582916918 -0.114638045762219
-0.0496038839471036 0.0536355761478172

0.151038198524996 0.149882835909149
0.366136199555436 0.164741319656519
ID= ypm1820nasal_(from hatcher et al. 1907)

LM=8
-0.221677747917637 -0.233997433602748
0.568300526134384 0.0414497147706381
-0.33949660713741 -0.227648840123714
-0.353477642529357 0.151891301572119
-0.197373435977016 -0.0738385142374083
-0.0196162012617358 0.052472301758351 8
0.178045497368348 0.134919733667177
0.385295611320424 0.154751736195584
ID= YPM1822_right

LM=8
-0.248665430301531 -0.363449941919116
0.53356540743914 0.0223341919300345
-0.333327694406633 -0.165886746170251
-0.270528735579049 0.19104313420881
-0.16971792002192 -0.108981165482762
-0.0478759972408594 0.0594012487017729
0.150930135911704 0.170349722160807
0.385620234199148 0.195189556570705
ID= ansp15192 nasal

LM=8
-0.241318933561666 -0.239045118883641
0.54491114141855 0.109929059151629
-0.415791312193798 -0.253072807333509
-0.254545578002921 0.189165611791611
-0.187350004545026 -0.0822758326651142
-0.00882333718253336 0.0178657083813482
0.183796294299077 0.0970666357207756
0.379121729768319 0.1603667438369
ID= MOR004nasal_right

LM=8
-0.294708055841295 -0.252128284456456
0.570224194629698 0.0767112966174629
-0.351277290199359 -0.191234401381974
-0.290174498520512 0.120029240455765
-0.178114219228961 -0.0915125463843212
-0.0186406345952628 0.0441192190802157

0.176946855412981 0.127600556057244
0.385743648342711 0.166414920012063
ID= MOR1199nasal_left

LM=8
-0.265781463615221 -0.275810446988668
0.564991861809238 0.0591010078584131
-0.370284223747052 -0.150658087216034
-0.302945413926363 0.10540412742858
-0.177759699897522 -0.0907221371544125
-0.0140164255203809 0.0380709955437363
0.176831650440517 0.13061855111528
0.388963714456784 0.183995989413105
ID= MOR2951_right

Appendix 7.28. TPS landmark data for NPP.

LM=6
-0.259397294066568 -0.590929594981311
0.473755069294439 -0.0279579684084878
-0.398075901725317 0.0541697096734752
0.257267143478228 0.131116689671282
0.0775242519246342 0.236898176377957
-0.151073268905415 0.196702987667085
ID=MOR 1110 npp left

LM=6
-0.283916823578617 -0.623022772189013
0.475265799357676 0.0441778804810498
-0.362274983210282 0.0999770543164201
0.254611706124364 0.117819375183061
0.0613372921705175 0.156305409983516
-0.145022990863659 0.204743052224967
ID=MOR 1120 npp left

LM=6
-0.441326175053859 -0.748339250652195
0.360770950083513 0.182171066924646
-0.156623595191689 0.140239977088171
0.264510726095816 0.20359537654983
0.110047693473607 0.142208746095188
-0.137379599407388 0.0801240839943604
ID=MOR 1122-7-22-00-1 npp right

LM=6
-0.228358218286498 -0.785645368061482
0.301354506870867 -0.0310098418029526
-0.235880449150734 0.164673612966796
0.205737709412727 0.111708260972741
0.112115710540172 0.289622383536602
-0.154969259386533 0.250650952388295
ID=MOR 1199 npp left

LM=6
-0.303057967864507 -0.494768755319953
0.525284882159799 -0.0533579883593968
-0.455101280578633 -0.0449011195666785
0.312486326471382 0.216870217377656
0.0701244410222735 0.209642749611094

-0.149736401210314 0.166514896257278
ID=MOR 2574 npp left

LM=6
-0.153398110936702 -0.640047809974445
0.465251570950717 -0.0679874017650657
-0.419475675350844 0.155934394771926
0.228707334449895 0.0903193395627678
0.0359143968974732 0.163522707251585
-0.15699951601054 0.298258770153232
ID=MOR 2702 npp right

LM=6
-0.1326972825909 -0.695519873970274
0.323821372952999 -0.158150112911038
-0.388670541647212 0.122683314851575
0.234037985905272 0.125467336405752
0.131588049545932 0.348977296528784
-0.168079584166092 0.256542039095202
ID=MOR 2951 npp left

LM=6
-0.375129659386037 -0.560581993127639
0.510458435312511 0.0451376590006122
-0.3465283421525 -0.0266668417837151
0.270107185559935 0.160427692483118
0.0691237545331075 0.236806602510503
-0.128031373867017 0.14487688091712
ID=MOR 3011 npp left

LM=6
-0.22931955295671 -0.703592711840865
0.404589690933868 0.0306636186457497
-0.339196865720462 0.201349888598919
0.250991090895544 0.115715637973248
0.0490271543110182 0.134451316087151
-0.136091517463259 0.221412250535798
ID=MOR 3027 npp left

LM=6
-0.257826748075668 -0.587334797445666
0.456820038194782 -0.0306248332769107

-0.430571851414456 0.0802521102349132
0.281517112260161 0.159121891071978
0.0736842747158105 0.247960941612826
-0.123622825680629 0.130624687802859
ID=MOR 3045 npp left

LM=6
-0.480383729530141 -0.563676707702316
0.523487279575468 0.195973055038245
-0.327212527850499 -0.00382393217083084
0.271341617163262 0.18789025049763
0.11202815228622 0.143458745671477
-0.0992607916443093 0.0401785886657946
ID= RTMP 2002.57.7